

UNIVERSITY OF STRATHCLYDE  
Strathclyde Institute of Pharmacy and Biomedical Sciences

**MICROFLUIDICS TECHNOLOGY FOR THE FORMULATION DESIGN AND  
PRODUCTION OF LIPOSOMAL PRODUCTS.**

MARYAM TABASSUM HUSSAIN  
DOCTOR OF PHILOSOPHY

2019

## Declaration of Authorship

This thesis is the result of the author's original research. It has been composed by the author and has not been previously submitted for examination which has led to the award of a degree.

The copyright of this thesis belongs to the author under the terms of the United Kingdom Copyright Acts as qualified by University of Strathclyde Regulation 3.50. Due acknowledgement must always be made of the use of any material contained in, or derived from, this thesis.

Signed: M. Hussain

Date: 17.04.2019

## Abstract

In recent years, microfluidics technology has been researched as an alternative liposome manufacturing technique to improve batch-to-batch consistency and overall production costs. Whilst previous research has shown microfluidics parameters such as the flow rate ratio (FRR) adopted in the microfluidic process is important, there is a lack of defined operating parameters and designed space for liposome production. To this end, this thesis focuses on microfluidics technology for the production of a range of liposomal formulations containing proteins or small molecular drugs, as well as defining the optimal manufacturing parameters.

Investigation of the microfluidics system shows the process is rapid and reliable, in comparison to traditional methods. For the first time through collective analysis, both the formulation composition and microfluidics manufacturing parameters were shown to impact liposomal characteristics. Analysis of the parameters (using design of experiments) allowed the identification of the design space with the ability to adjust microfluidics parameters to meet formulation specifications. In particular, a high FRR (3:1 FRR) and initial lipid concentration of above 3 mg/mL were shown to be the two most important factors when producing small homogenous liposomes (< 100 nm). Also, a scalable manufacturing model was developed without the need for bespoke equipment, using readily available instruments. The model is able to manufacture liposomes in a single step, followed by purification of liposomes using tangential flow filtration. A key feature, shown for the first time is the ability to monitor the quality of the liposomes produced at-line (in real time). The model developed enables quality assurance, with problematic batches easily identified therefore reducing waste and improving the overall efficiency of the manufacturing process.

Moreover, to the best of knowledge, the studies in this thesis are the first to show the production of protein loaded liposomes using microfluidics. Results show microfluidics technology is able to produce protein and drug loaded formulations without further downsizing requirements. The encapsulation of protein (approximately 34%) and drug loading (approximately 40%) is significantly ( $p < 0.05$ ) more than formulations produced by thin film lipid hydration followed by sonication. Analytical methods to quantify encapsulation of protein were developed; the results from the two different quantification approaches were equally comparable. The quantification methods are efficient and reliable, allowing for rapid screening of liposomal formulations. In addition, the stability and characteristics of the liposomes was preserved by developing a high-throughput freeze drying method using 96 well plates. In conclusion, the results from this thesis indicate microfluidics technology is a viable option for the production of a vast range of liposomal formulations for therapeutic use.

**Keywords:** microfluidics technology, liposomal formulations, rapid high-throughput manufacturing, scalable production, design of experiments and protein encapsulation.

## **Acknowledgements**

I would like to thank my supervisor Professor Yvonne Perrie for her continuous guidance and support throughout the last three years. Working with Yvonne has been an excellent experience; thank you for the opportunities (including the option to attend conferences worldwide, collaborate with other researchers and companies) and for always providing quick feedback. I would also like to extend my thanks to everyone in the research group, for making this a fun experience and motivating me when things weren't going quite to plan.

Furthermore, I would like to thank Professor Nicolas Szita (based at University College London, London, UK) for his input. I would also like to thank Dr. Paul Matejtschuk for all your help with freeze drying and inviting me into your laboratory based at the National Institute for Biological Standards and Control (NIBSC, Hertfordshire, UK). Working with you, Kiran Malik and Chinwe Duru was a great experience, whereby I learnt so much about freeze drying analytical techniques.

Many thanks to the Engineering and Physical Sciences Research Council for funding this project, and introducing me to the field of biochemical engineering by allowing me to partake in UCL accredited short courses.

Last but not least, I would like to thank my family and friends for their ongoing support and motivation, in particular to my parents to whom this thesis is dedicated.

## Own Publications

HUSSAIN, M. T., FORBES, N. & PERRIE, Y. 2019. Comparative Analysis of Protein Quantification Methods for the Rapid Determination of Protein Loading in Liposomal Formulations. *Pharmaceutics*, 11, 39.

FORBES, N., HUSSAIN, M. T., BRIUGLIA, M. L., EDWARDS, D. P., HORST, J. H. T., SZITA, N. & PERRIE, Y. 2019. Rapid and scale-independent microfluidic manufacture of liposomes entrapping protein incorporating in-line purification and at-line size monitoring. *International Journal of Pharmaceutics*, 556, 68-81.

DIMOV, N., KASTNER, E., HUSSAIN, M. T., PERRIE, Y. & SZITA, N. 2017. Formation and purification of tailored liposomes for drug delivery using a module-based micro continuous-flow system. *Scientific reports*, 7, 12045.

JOSHI, S., HUSSAIN, M. T., ROCES, C. B., ANDERLUZZI, G., KASTNER, E., SALMASO, S., KIRBY, D. J. & PERRIE, Y. 2016. Microfluidics based manufacture of liposomes simultaneously entrapping hydrophilic and lipophilic drugs. *International journal of pharmaceutics*, 514, 160-168.

## Conference Abstracts

Hussain M. T., Szita N, Perrie Y (2015). Engineering liposomes using microfluidics; the effect of transition temperature on liposomes. International liposome society. UCL school of Pharmacy, London, England.

Hussain M. T., Szita N, Perrie Y (2016). Microfluidics process analysis and production of high throughput of liposomes encapsulating protein. UKPharmSci, SIPBS, Glasgow, Scotland.

Hussain M. T., Szita N, Perrie Y (2016). Microfluidics-based manufacture of protein-loaded liposomes. 43<sup>RD</sup> Annual Meeting & Exposition of the Controlled release society. Seattle, Washington, USA.

Hussain M. T., Szita N, Perrie Y (2016). Microfluidics process analysis and production of protein encapsulated liposomes. Strathclyde Institute of Biomedical Sciences research day, Glasgow, Scotland.

Hussain M. T., Szita N, Perrie Y (2017). Small-scale microfluidics manufacturing model for liposome production. UKICRS, Glasgow, Scotland.

Hussain M. T., Szita N, Perrie Y (2017). Production of protein encapsulated liposomes by microfluidics for therapeutic use. CDT Research day, UCL London, England.

Hussain M. T., Szita N, Perrie Y (2017). High-throughput manufacturing of ovalbumin loaded liposomes using microfluidics. International liposome society, Athens, Greece.

Hussain M. T, Szita N and Perrie Y (2018). Engineering protein loaded liposomes by microfluidics for therapeutic use. APS @FIP (Glasgow, UK).

Hussain M. T, Szita N and Perrie Y (2018). Identification of key parameters influencing liposome encapsulation of protein using microfluidics. UKICRS 2018 symposium (Belfast, UK).

Hussain M. T, Matejtschuk P, Szita N and Perrie Y (2019). High throughput production, processing and strategies for freeze drying protein loaded liposomes. 29<sup>th</sup> ESACT conference (Drayton Manor Hotel, UK).

## **Conference Presentation**

UCL Biochemical engineering Research day: 22<sup>nd</sup> April 2016. UCL, London, UK.

Strathclyde Institute of Pharmacy and Biomedical Sciences (SIPBS) Research day: 18<sup>th</sup> August, 2016. University of Strathclyde, Glasgow, UK.

UKICRS Symposium 2017: 30-31st May, 2017. University of Strathclyde, Glasgow, UK.

WP1 TuBerculosis Vaccine Initiative (TBVAC2020) meeting: 6-7th July 2017. Pasteur Institute, Brussels, Belgium.

International liposome society: 16- 18th September, 2017. Royal Olympic Hotel, Athens, Greece.

SMI's 6th Annual Lyophilisation Conference: 13-14<sup>th</sup> June, 2018. Holiday Inn Kensington Forum, London, UK.

<b><i>Declaration of Authorship</i></b> .....	<b>1</b>
<b><i>Abstract</i></b> .....	<b>2</b>
<b><i>Acknowledgements</i></b> .....	<b>3</b>
<b><i>Own Publications</i></b> .....	<b>4</b>
<b><i>Conference Abstracts</i></b> .....	<b>4</b>
<b><i>Conference Presentation</i></b> .....	<b>5</b>
<b><i>List of Figures</i></b> .....	<b>15</b>
<b><i>List of Tables</i></b> .....	<b>28</b>
<b><i>Chapter 1</i></b> .....	<b>34</b>
<b><i>Introduction</i></b> .....	<b>34</b>
<b><i>1.1 Background</i></b> .....	<b>35</b>
<b><i>1.2 Liposome manufacturing techniques</i></b> .....	<b>38</b>
1.2.1 Conventional techniques used to produce liposomes .....	38
<b><i>1.2.3 Novel liposome production methods</i></b> .....	<b>40</b>
1.2.3.1 Supercritical reverse phase evaporation (SPER) method.....	40
1.2.3.2 Dual asymmetric centrifugation (DAC) .....	40
1.2.3.3 Microfluidics.....	41
<b><i>1.3 Liposomal medicines</i></b> .....	<b>45</b>
1.3.1 Protein loaded liposomal formulations .....	46
1.3.2 Biodistribution and targeting of liposomes .....	47
1.3.3 Clearance of liposomes.....	49
<b><i>1.4 Lipid Selection</i></b> .....	<b>51</b>
<b><i>1.4 Aim and Objectives</i></b> .....	<b>54</b>
<b><i>Chapter 2</i></b> .....	<b>55</b>
<b><i>Characterisation of liposomes</i></b> .....	<b>55</b>
<b><i>2.1 Introduction</i></b> .....	<b>56</b>
<b><i>2.1.1 Liposome manufacturing techniques</i></b> .....	<b>56</b>
2.1.1.1 Thin film lipid hydration method to produce liposomes .....	56
2.1.1.2 Microfluidics method to produce liposomes.....	57
<b><i>2.1.2 Liposome size</i></b> .....	<b>57</b>
<b><i>2.2 Aim and Objectives</i></b> .....	<b>58</b>

<b>2.3</b>	<b><i>Methods and Materials</i></b> .....	<b>58</b>
2.3.1	<b>Materials</b> .....	<b>58</b>
2.3.2	<b>Methods</b> .....	<b>59</b>
2.3.2.1	Liposome manufacturing techniques .....	59
2.3.2.2	Downsizing techniques .....	59
2.3.2.3	Purification techniques .....	60
2.3.2.4	Dynamic light scattering .....	60
2.3.2.5	Lipid quantification .....	61
2.3.2.6	Flame ionised detector (FID) gas chromatography .....	62
2.3.2.7	Design of experiments .....	62
2.3.2.8	Statistical package .....	62
<b>2.4</b>	<b><i>Results and discussion</i></b> .....	<b>63</b>
2.4.1	<b>Liposome production techniques</b> .....	<b>63</b>
2.4.1.1	Comparison of thin film lipid hydration (with sonication) and microfluidics for the production of liposomes .....	63
2.4.1.2	The effect of formulation components on liposome physicochemical properties produced by microfluidics .....	66
2.4.1.3	Stability of liposomes produced by microfluidics .....	69
2.4.1.4	The effect of cholesterol amount on liposome physicochemical properties .....	73
2.4.1.5	Determining normal operating ranges and parameters for liposomes produced by microfluidics .....	75
2.4.2	<b>Effect of microfluidics parameters</b> .....	<b>79</b>
2.4.2.1	Investigating the use of temperature during the production of liposomes by microfluidics .....	79
2.4.2.2	Testing the effect of flow rate ratio on liposomal physicochemical properties .....	82
2.4.2.3	Establishing the optimal operating ranges for liposomes using design of experiments .	88
2.4.3	<b>Lipid recovery of liposomal formulations</b> .....	<b>90</b>
2.4.4	<b>Measuring residual solvent for purified liposomes</b> .....	<b>96</b>
<b>2.5</b>	<b><i>Conclusion</i></b> .....	<b>98</b>
	<b><i>Chapter 3</i></b> .....	<b>100</b>
	<b><i>Continuous manufacturing of liposomes</i></b> .....	<b>100</b>
<b>3.1</b>	<b><i>Introduction</i></b> .....	<b>101</b>
3.1	High throughput manufacturing .....	101
3.2	Scalable manufacturing of liposomes .....	102
<b>3.2</b>	<b><i>Aim and Objectives</i></b> .....	<b>103</b>
<b>3.3</b>	<b><i>Materials and Methods</i></b> .....	<b>104</b>
3.3.1	<b>Materials</b> .....	<b>104</b>
3.3.2	<b>Methods</b> .....	<b>104</b>
3.3.2.1	Liposome manufacturing methods .....	104
3.3.2.2	Measuring the physicochemical properties of liposomes .....	104
3.3.3	Tangential flow filtration .....	106



3.3.4 Calculating liposome recovery.....	107
3.3.5 Headspace gas chromatography .....	107
3.3.6 Investigating liposome morphology .....	107
3.3.7 Statistical tests.....	108
<b>3.4 Results and Discussion.....</b>	<b>108</b>
<b>3.4.1 Purification of empty liposomes by Tangential Flow Filtration (TFF).....</b>	<b>108</b>
3.4.1.1 Characterisation of liposomes purified by Tangential flow filtration .....	108
3.4.1.2 Comparing liposome physiology after dialysis and TFF purification .....	111
3.4.1.2 Liposome recovery after TFF purification.....	113
3.4.1.3 Measuring residual solvent using headspace gas chromatography .....	115
3.4.1.4 Morphology of liposomes by transmission electron microscopy.....	118
3.4.1.5 Concentration of liposomes using Tangential Flow Filtration (TFF) .....	119
<b>3.4.2 Purification of protein loaded liposomes .....</b>	<b>121</b>
3.4.2.1 The purification of protein loaded liposomes .....	121
3.4.2.2 Determining morphology of liposomes by transmission electron cryomicroscopy (CryoTEM).....	123
<b>3.4.3 Scalable production of liposomes .....</b>	<b>124</b>
3.4.3.1 Large scale manufacturing using Zetasizer AT.....	124
3.4.3.2 The use of the Zetasizer APS to measure the physicochemical properties of liposomes .....	129
<b>3.5 Conclusion .....</b>	<b>131</b>
<b>Chapter 4.....</b>	<b>133</b>
<b><i>Rapid protein quantification techniques using High Performance Liquid Chromatography (HPLC) for the determination of protein loading in liposomal formulations.....</i></b>	<b>133</b>
<b>4.1 Introduction.....</b>	<b>134</b>
4.1.1 High throughput quantification techniques for protein loaded liposomes.....	134
4.1.2 High performance liquid chromatography (HPLC) techniques to quantify protein .....	136
<b>4.2 Aim and Objectives .....</b>	<b>138</b>
<b>4.3 Materials and Methods.....</b>	<b>138</b>
<b>4.3.1 Materials .....</b>	<b>138</b>
<b>4.3.2 Liposome manufacturing methods.....</b>	<b>139</b>
4.3.2.1 The NanoAssemblr® Benchtop.....	139
4.3.2.2 Removal of non-incorporated protein and solvent.....	139
<b>4.3.3 Solubilisation of liposomes .....</b>	<b>139</b>
4.3.5 Protein quantification using Reverse phase- high performance liquid chromatography (RP- HPLC) .....	139
4.3.6 Protein quantification using high performance liquid chromatography- evaporative light scattering detector (HPLC- ELSD) .....	140
4.3.7 Method Validation.....	140
4.3.8 Statistical tests.....	141

<b>4.4 Results and Discussion</b> .....	<b>141</b>
<b>4.4.1 Solubilisation of liposomal formulations</b> .....	<b>141</b>
<b>4.4.2 Methods to quantify the amount of encapsulated ovalbumin by liposomal formulations</b> .....	<b>144</b>
4.4.2.1 Reverse phase- high performance liquid chromatography (RP-HPLC) .....	144
4.4.2.2 High performance liquid chromatography- Evaporative light scattering detectors (HPLC-ELSD).....	148
<b>4.4.3 Comparison of the analytical techniques used to quantify encapsulated ovalbumin</b> .....	<b>152</b>
<b>4.5 Conclusion</b> .....	<b>157</b>
<b>Chapter 5</b> .....	<b>158</b>
<b>Rapid microfluidics manufacture of liposomes encapsulating protein</b> .....	<b>158</b>
<b>5.1 Introduction</b> .....	<b>159</b>
<b>5.1.1 Manufacturing protein loaded liposomes with high encapsulation efficiency</b> ....	<b>159</b>
5.1.1.2 Factors effecting protein stability.....	161
<b>5.1.2 Manufacturing protein loaded liposomes using microfluidics</b> .....	<b>162</b>
<b>5.2 Aim and Objectives</b> .....	<b>163</b>
<b>5.3 Materials and Methods</b> .....	<b>163</b>
<b>5.3.1 Materials</b> .....	<b>163</b>
<b>5.3.2 Methods</b> .....	<b>164</b>
5.3.2.1 Production of ovalbumin loaded liposomes.....	164
5.3.2.2 Removal of organic solvent .....	164
<b>5.3.2.3 Quantification of protein and drugs encapsulated in liposomes</b> .....	<b>165</b>
5.3.2.3.1 Quantification of ovalbumin loaded liposomes using reverse-phase high performance liquid chromatography .....	165
5.3.2.3.2 Quantification of ovalbumin loaded liposomes using high performance liquid chromatography-evaporative light scattering detector .....	165
<b>5.3.2.4 Protein release studies</b> .....	<b>165</b>
<b>5.3.2.5 Circular dichroism</b> .....	<b>165</b>
<b>5.3.2.6 Statistical analysis</b> .....	<b>166</b>
<b>5.4 Results and Discussion</b> .....	<b>166</b>
<b>5.4.1 Encapsulation of protein within liposomes</b> .....	<b>166</b>
5.4.1.1 Comparison of ovalbumin encapsulation by liposomes produced by microfluidics and sonication .....	166
5.4.1.2 Encapsulation of protein using various neutral lipids .....	168
5.4.1.3 Encapsulation of protein at varying protein concentrations.....	171
5.4.1.4 Encapsulation of protein across a range of lipid concentrations .....	172
5.4.1.5. Effect of protein encapsulation efficiency on flow rate ratio.....	175
5.4.1.6 Circular dichroism of to confirm protein stability. ....	177

5.4.1.7 Stability of OVA loaded liposomes .....	181
5.4.1.8 Release of ovalbumin from ovalbumin loaded liposomes .....	184
<b>5.5 Conclusion .....</b>	<b>187</b>
<b>Chapter 6.....</b>	<b>188</b>
<b>High throughput microfluidics manufacture of liposomes loaded with small molecular drugs.....</b>	<b>188</b>
<b>6.1 Introduction .....</b>	<b>189</b>
6.1.1 Liposomal delivery systems for poorly soluble drugs .....	189
6.1.1 Manufacturing small molecular drug loaded liposomes using microfluidics.....	190
6.1.1.1. Manufacturing small drug loaded liposomes .....	190
6.1.1.2 The manufacture of anticancer liposomes loaded with the novel SU1349 small drug molecule .....	191
<b>6.2 Aim and Objectives .....</b>	<b>192</b>
<b>6.3 Materials and Methods .....</b>	<b>193</b>
6.3.1 Materials .....	193
6.3.2 Methods .....	193
6.3.2.1 Production of liposomes.....	193
6.3.2.1.1 Production of propofol loaded liposomes using thin film lipid hydration .....	193
6.3.2.1.2 Production of propofol loaded liposomes using microfluidics .....	193
6.3.2.1.3 Production of SU1349 drug loaded liposomes .....	194
6.3.3 Removal of organic solvent .....	194
6.3.3.1 Removal of solvent and non- incorporated propofol using a syringe pump diafiltration system .....	194
6.3.3.2 Removal of solvent and non- incorporated SU1349 drug from DMPC:Chol liposomes	194
6.3.4 Quantification of protein and drugs encapsulated in liposomes.....	195
6.3.4.1 Quantification of propofol drug loaded in PC:Chol liposomes .....	195
6.3.5 CryoTEM microscopy of propofol loaded liposomes .....	195
6.3.6 Polyvar microscope images for SU1349 loaded DMPC:Chol liposomes .....	196
6.3.7 Statistical analysis.....	196
<b>6.4 Results and discussion .....</b>	<b>196</b>
6.4.1 Production of bilayer drug-loaded liposomes .....	196
6.4.1.1 Characterisation of Propofol loaded liposomes produced by microfluidics and post- extrusion.....	196
6.4.2. Morphology of Propofol loaded liposomes.....	200
6.4.2 Production of SU149 incorporated liposomes .....	201
6.4.2.1 Morphology of SU1349 incorporated liposomes .....	205
6.4.2.2 Optimisation of the SU1349 incorporated DMPC:Chol liposomes .....	206
<b>6.5 Conclusion .....</b>	<b>211</b>

<b>Chapter 7.....</b>	<b>212</b>
<b><i>Strategies for the high throughput production of liposomes in a freeze- dried format.....</i></b>	<b>212</b>
<b>7.1 Introduction .....</b>	<b>213</b>
7.1.1 Stability of liposomes .....	213
7.1.2 Approaches for improving the storage stability of liposomes.....	215
<b>7.2 Aim and Objectives .....</b>	<b>218</b>
<b>7.3 Materials and Methods.....</b>	<b>218</b>
7.3.1 Materials .....	218
7.3.2 Methods .....	218
7.3.2.1 Production and purification of Ovalbumin loaded liposomes using microfluidics .....	218
7.3.2.2 Dynamic light scattering.....	219
7.3.2.3 Quantification of encapsulated Ovalbumin.....	219
7.3.2.4 Freeze- thawing of liposomes.....	220
7.3.2.5 Freeze dried microscopy .....	220
7.3.2.6 Modulated Differential scanning calorimetry (MDSC) .....	221
7.3.2.7 Dynamic Mechanical Analysis (DMA) .....	221
7.3.2.8 Freeze drying cycle .....	222
7.3.2.9 Measuring moisture content using the automated Karl Fisher .....	223
7.3.2.10 Design of Experiments.....	223
<b>7.4 Results and Discussion.....</b>	<b>224</b>
7.4.1 Characterization of liposomes before freeze drying.....	224
7.4.2 Analytical experiments to develop the freeze drying cycle.....	227
7.4.2.1 Freeze-thaw .....	227
7.4.2.2 Freeze drying microscopy.....	229
7.4.2.3 Modulated Differential scanning calorimetry .....	235
7.4.3 Freeze drying cycles .....	240
7.4.3.1 Real time analysis of the freeze drying cycle 1 .....	241
7.4.4 High throughput production of freeze dried liposomes.....	243
.....	248
.....	248
7.4.5 Design of Experiments.....	250
7.4.6 Freeze dried cycle 2 and Freeze dried cycle 3.....	253
.....	255
7.4.7 Residual moisture content .....	256
<b>7.5 Conclusion .....</b>	<b>258</b>
<b>Chapter 8.....</b>	<b>259</b>
<b><i>Developing rapid in vitro screening tools to investigate liposomal formulations</i></b>	<b>259</b>

<b>8.1 Introduction</b> .....	<b>260</b>
<b>8.1.1 Consideration of factors influencing the interactions between cells and liposomal formulations</b> .....	<b>260</b>
8.1.1.1 Impact of liposomal formulation characteristics on cells.....	260
8.1.1.2 Consideration of cell lines for investigation of liposomal interactions .....	261
<b>8.1.2 Cells on a chip</b> .....	<b>264</b>
<b>8.2 Aim and Objectives</b> .....	<b>265</b>
<b>8.3 Materials and Methods</b> .....	<b>266</b>
<b>8.3.1 Materials</b> .....	<b>266</b>
<b>8.3.2 Methods</b> .....	<b>266</b>
8.3.2.1 THP-1 cells .....	266
8.3.2.2 RAW264.7 cells .....	267
8.3.2.3 Cell counting .....	267
8.3.2.4 Cell imaging .....	267
8.3.2.5 Viability assays.....	268
8.3.2.6 Uptake studies .....	268
8.3.2.7 Determining THP-1 cell differentiation.....	269
8.3.2.8 Investigating protein integrity using DQ-OVA.....	269
8.3.2.9 Statistical packages .....	270
<b>8.4 Results</b> .....	<b>270</b>
8.4.1 Morphological analysis of cells .....	270
8.4.2 Cell viability of cells exposed to liposomal formulations.....	272
8.4.3 Uptake of liposomal formulations by macrophage cells.....	277
8.6 DQ-OVA processing by macrophages .....	281
8.7 Passing THP-1 cells through a microfluidics cartridge. ....	282
<b>8.5 Conclusion</b> .....	<b>286</b>
<b>Chapter 9</b> .....	<b>287</b>
<b><i>Evaluating the addition of co-polymers to liposomal formulations produced by microfluidics</i></b> .....	<b>287</b>
<b>9.1 Introduction</b> .....	<b>288</b>
9.1.1 Long circulating liposomes .....	288
9.1.2 Co-polymers as delivery vehicles .....	290
<b>9.2 Aim and Objectives</b> .....	<b>291</b>
<b>9.3 Materials and Methods</b> .....	<b>291</b>

9.3.1 Materials .....	291
9.3.2 Methods .....	291
9.3.2.1 Production of co-polymer liposomes using microfluidics .....	291
9.3.2.2 Quantification of entrapped protein .....	292
9.3.2.3 Stability of the co- polymer liposomal formulations .....	292
9.3.2.4 In-vitro studies.....	292
9.3.2.5 Statistical analysis .....	292
<b>9.4 Results and Discussion.....</b>	<b>292</b>
9.4.1 Evaluating the ideal amount of co-polymer required for stealth liposomal formulations .....	292
9.4.2 The effect of varying co-polymer chain length on DMPC:Chol formulation characteristics .....	301
9.4.3 Protein encapsulation of co-polymer DMPC:Chol liposomal formulations .....	303
9.4.4 The viability of THP-1 cells exposed to co-polymer DMPC:Chol liposomal formulations .....	305
9.4.5 The uptake of co-polymer DMPC:Chol liposomal formulations by THP-1 cells ...	307
.....	309
.....	309
.....	310
9.4.6 Processing of co-polymer DMPC:Chol formulations.....	311
<b>9.5 Conclusion .....</b>	<b>312</b>
<b>Chapter 10.....</b>	<b>313</b>
<b>Conclusion .....</b>	<b>313</b>
<b>10.1 Summary of the findings .....</b>	<b>314</b>
<b>10.2 Characterisation of liposomal formulations produced by microfluidics .....</b>	<b>314</b>
<b>10.3 Continuous manufacturing and scale- out of liposomal formulations .....</b>	<b>314</b>
<b>10.4 Rapid protein quantification techniques for determining the protein loading in liposomal formulations .....</b>	<b>315</b>
<b>10.5 Rapid microfluidics manufacture of protein loaded liposomes.....</b>	<b>316</b>
<b>10.6 High throughput manufacture of liposomes loaded with small molecular drugs.....</b>	<b>316</b>
<b>10.7 Strategies for the high throughput production of liposomes in a freeze dried format.....</b>	<b>317</b>
<b>10.8 Screening of cell cultures for liposomal formulation investigation .....</b>	<b>317</b>

<b>10.9 Evaluating the addition of co-polymers to liposomal formulations produced by microfluidics.....</b>	<b>318</b>
<b>10.10 Overall conclusion .....</b>	<b>319</b>
<b>Chapter 11.....</b>	<b>321</b>
<b>References.....</b>	<b>321</b>

## List of Figures

### Chapter 1

**Figure 1.1.** The basic structural components of liposomes. The lipids are representative of phosphatidylcholine, which has a hydrophilic phosphate head group and two hydrophobic hydrocarbon tails. Hydration of lipids causes special rearrangement of the lipids into bilayer structures so that the hydrophobic tails avoid contact with the aqueous environment, as a results a spherical liposome vesicles. .... 35

**Figure 1.2.** The structural layout of a staggered herringbone mixer section found inside a microfluidics chip. The herringbone grooves are added as sets, with the centre points offset from one another enabling changes in the flow of fluid therefore improving mixing. .... 44

**Figure 1.3.** Image of the commercially available NanoAssemblr® Benchtop (Precision Nanosystems, Canada), alongside a schematic representation of the accompanying microfluidics chip to the device. Fluid enters through two inlet ports and mixing occurs via the chaotic mixing principle, with liposomes produced. .... 45

### Chapter 2

**Figure 2.1.** The thin film lipid hydration method for the production of liposomes. Lipids dissolved in solvent is evaporated in a round bottom flask using a rotary evaporation, forming a dry film. The film is then hydrated to produce liposomes forming multi-lamellar vesicles. The multilamellar vesicles are then down sized using probe sonication at a set time. .... 56

**Figure 2.2.** Image of the commercially available NanoAssemblr® Benchtop (Precision Nanosystems Inc, Vancouver, Canada). .... 57

**Figure 2.3.** Comparison of liposome attributes produced by either thin film lipid hydration followed by sonication (A) or microfluidics (B). The physicochemical properties for liposomal formulations (PC:Chol, DMPC:Chol, DPPC:Chol and DSPC:Chol) was investigated, with liposomal physicochemical properties measured using dynamic light scattering. The results represent mean  $\pm$  SD, n=3 independent batches. .... 65

**Figure 2.4.** Testing parameters for the 3:1 FRR. Liposomes composed of PC, DMPC, DPPC, DSPC and cholesterol were prepared by microfluidics. The Physicochemical properties of liposomes produced by methanol with PBS (A) or Tris buffer (B), and ethanol with PBS (C) or Tris buffer (D) were investigated. Results represent mean  $\pm$  SD, n=3 independent batches. 68

**Figure 2.5.** Stability of empty DMPC:Chol liposomes produced by microfluidics over 48 hours. The formulations were kept under three different test conditions (5°C, 25°C and 37°C), with changes to liposome size (A), PDI (B) and zeta potential (C) measured using dynamic light scattering. Measurements were taken at set time points over 48 hours. Results represent n= 3  $\pm$  SD. .... 71



**Figure 2.6.** Stability of empty DSPC:Chol liposomes produced by microfluidics over 48 hours. The formulations were kept under three different test conditions (5°C, 25°C and 37°C), with changes to liposome size (A), PDI (B) and zeta potential (C) measured using dynamic light scattering. Measurements were taken at set time points over 48 hours. Results represent n= 3 ± SD. .... 72

**Figure 2.7.** The effect of cholesterol on DMPC:Chol liposome physicochemical properties. The DMPC:Chol liposomes were produced with varying amount of cholesterol to lipid, by microfluidics at a 3:1 FRR and 15 mL/ min TFR. The size, PDI and zeta potential of the liposomes was measured using dynamic light scattering (A) with the size intensity plots shown (B). Results represent mean ± SD, n=3 independent batches..... 74

**Figure 2.8.** The size of liposome formulations made at concentrations ranging from 0.3- 10 mg/mL of the initial lipid concentration. The four liposome formulations were made using microfluidics at a 3:1 flow rate ratios (FRR) and 15 mL/min flow rate (TFR). Results represent mean ± SD, n=3 independent batches. .... 77

**Figure 2.9.** The effect of liposomal formulation on physicochemical characteristics. Four liposome formulations (PC:Chol, DMPC:Chol, DPPC:Chol and DSPC:Chol) with increasing hydrocarbon tail length (and transition temperature) were manufactured using microfluidics at a 3:1 FRR and 15 mL/min TFR. The effect of transition temperature on liposomes size (A) and PDI (B) was investigated. (Note: PC is a mixture of lipids so the value is for illustration purposes). Results represent mean ± SD, n=3 independent batches..... 78

**Figure 2. 10.** The effect of heating DMPC:Chol liposomes during the production process of microfluidics was tested. DMPC:Chol liposomes was made at room temperature and 70°C. The size (A), PDI (B), zeta potential (C), and intensity plots (D) were obtained using dynamic light scattering. Results represent mean ± SD, n=3 independent batches..... 81

**Figure 2.11.** The physicochemical properties of PC:Chol liposomes produced by microfluidics at varying flow rate ratios (FRRs) and total flow rates (TFR) (mL/min). The size (A), PDI (B) and zeta potential (C) was measured using dynamic light scattering. Results represent mean ± SD, n=3 independent batches. .... 84

**Figure 2.12.** The physicochemical properties of DMPC:Chol liposomes produced by microfluidics at varying flow rate ratios (FRRs) and total flow rates (TFR) (mL/min). The size (A), PDI (B) and zeta potential (C) was measured using dynamic light scattering. Results represent mean ± SD, n=3 independent batches. .... 85

**Figure 2.13.** The physicochemical properties of DPPC:Chol liposomes produced by microfluidics at varying flow rate ratios (FRRs) and total flow rates (TFR) (mL/min). The size (A), PDI (B) and zeta potential (C) was measured using dynamic light scattering. Results represent mean ± SD, n=3 independent batches. .... 86

**Figure 2.14.** The Physicochemical properties of DSPC:Chol liposomes produced by microfluidics at varying flow rate ratios (FRRs) and total flow rates (TFR) (mL/min). The size

(A), PDI (B) and zeta potential (C) was measured using dynamic light scattering. Results represent mean  $\pm$  SD, n=3 independent batches. .... 87

**Figure 2.15.** Establishing the design space for PC:Chol liposomes produced by microfluidics. Size (A) and PDI (B) contour plot for PC:Chol liposomes. The results were combined to form a sweet spot contour plot (C). Results represent mean  $\pm$  SD, n=3 independent batches..... 89

**Figure 2.16.** ELSD-HPLC detected chromatogram of DMPC (0.1 mg/mL), Cholesterol (0.1 mg/mL), DPPC (0.1 mg/mL) and DSPC (0.1 mg/mL). .... 91

**Figure 2.17.** ELSD-HPLC detected chromatogram of PC lipids (0.1 mg/mL)..... 92

**Figure 2.18.** Standard calibration curves for PC (A), DMPC (B), DPPC (C), DSPC (D) and cholesterol (E) used to determine the lipid recovery of the liposomal formulations. The LOD and LOQ for each lipid is shown in E. Results represent mean  $\pm$  SD, n=3 independent batches. .... 94

**Figure 2.19.** The effect of dialysis time on liposome physicochemical properties. The PC:Chol formulations were produced using microfluidics at a 3:1 FRR and 15 mL/min. The PC:Chol formulations underwent dialysis for 1, 2, 4 and 24 hours after which the size, PDI and zeta potential of PC:Chol was determined using dynamic light scattering. Results represent mean  $\pm$  SD, n=3 independent batches. .... 97

### **Chapter 3**

**Figure 3.1.** Flow diagram illustrating the ability to produce high throughput liposomes in a continuous process using commercial instruments available. For the production of liposomes, the microfluidics NanoAssemblr<sup>®</sup> Benchtop (Precision Nanosystems Inc., Canada) was coupled to the Krosflo Research Iii tangential flow filtration system (Spectrum Inc., Breda, The Netherlands). .... 103

**Figure 3.2.** The user software interface for the Zetasizer AT (Malvern Panalytical Ltd, Malvern, UK)..... 105

**Figure 3.3.** The user interface for the Zetasizer APS (Malvern Panalytical Ltd, Malvern, UK). .... 106

**Figure 3.4.** The characterisation of DPPC:Chol (A) and DSPC:Chol (B) liposomes produced post- microfluidics production and post- purification by tangential flow filtration. The liposomes were characterised in terms of their size and PDI by dynamic light scattering, with the size- intensities also plotted. The results represent mean  $\pm$  SD, n=3 independent batches, meanwhile the size- intensity plots are representative plots taken from one reading. .... 110

**Figure 3.5.** The physicochemical properties of DMPC:Chol and DSPC:Chol liposomes post dialysis or TTF purification. The liposomes were produced at a 3:1 FRR and 15 mL/min TFR,

with the initial lipid concentration of either 4 or 10 mg/mL. The results represent mean  $\pm$  SD, n=3 independent batches. .... 112

**Figure 3.6.** The liposomes recovery of fluorescently labelled DiIc DPPC:Chol liposomes before post microfluidics manufacture and post-TFF purification. The liposomes were made at a 3:1 FRR and 15 mL/min TFR. The results represent mean  $\pm$  SD, n=3 independent batches. .... 114

**Figure 3.7.** The liposome recovery of DiIc labelled DPPC:Chol and DSPC:Chol liposomes post-TFF. The effect of manufacturing liposomes using microfluidics at either a 3:1 or 5:1 FRR was investigated. The results represent mean  $\pm$  SD, n=3 independent batches. .... 114

**Figure 3.8.** Calibration curve for methanol containing the solvent isopropyl alcohol as an internal control. The solvent was measured by headspace gas chromatography, with the peak area ratio of methanol to isopropyl alcohol plotted against the percentage of methanol present. The results represent mean  $\pm$  SD, n=3 independent batches, with the LOD (0.28% methanol) and LOQ (0.86) calculated. .... 116

**Figure 3.9.** The use of tangential flow filtration to establish the amount of buffer needed to remove methanol, which was used to produce liposomes. The DPPC:Chol liposomes were purified by TFF with a total of 20 mL permeate collected (in 1 mL aliquots). The amount of methanol was measured using headspace gas chromatography, and plotted as the percentage of solvent remaining in the aliquots against the amount of wash cycle. The results represent mean  $\pm$  SD, n=3 independent batches. .... 116

**Figure 3.10.** The headspace gas chromatography plots for the amount of methanol present within the permeate after being washed with a set amount of phosphate buffered saline (A) and the liposome sample (B). The results show the amount of methanol detected decreases as the wash cycle progresses. The samples were spiked with isopropanol alcohol as an internal control; the concentration of which remains the same throughout the wash cycle. .... 117

**Figure 3.11.** The morphology of the DPPC:Chol liposomes was investigated by transmission electron microscopy. Liposomes purified by tangential flow filtration were tested to see if this purification technique effected the morphology and characteristic of the DPPC:Chol liposomal formulation. .... 118

**Figure 3.12.** Characterisation of DSPC:Chol liposomes that underwent a TFF wash and were concentrated one, two and four times. The size, polydispersity index and zeta potential of the DSPC:Chol liposomes was measured (A). The bars represent size and the circles represent PDI. The size- intensity peaks of the DSPC:Chol liposomes at the various test conditions was also plotted (B). The characterisation results represent the mean  $\pm$  SD, with an n=3, meanwhile (B) are representative plots taken from one reading. .... 120

**Figure 3.13.** The amount of OVA present in permeate over 20 mL of phosphate buffered saline washes was calculated, and subtracted from the original starting concentration to work out the amount of OVA remaining. The DPPC:Chol liposomes were made using

microfluidics at a 3:1 FRR and 15 mL/min. The results represent three independent batches.

..... 122

**Figure 3.14.** The physicochemical properties of DPPC:Chol liposomes before and after purification with tangential flow filtration. The liposomes were produced at a 3:1 FRR and 15 mL/min TFR, with 0.25 mg/mL initial ovalbumin added into the aqueous buffer. Dynamic light scattering was used to determine the size, polydispersity index and zeta potential of the liposomal formulations. The results represent mean  $\pm$  SD, n=3 independent batches. .... 122

**Figure 3.15.** The morphology of OVA loaded DMPC:Chol liposomes post microfluidics production (A), purification by dialysis (B) and purification by tangential flow filtration (C). The morphology of the liposomal formulation was investigated by cryoTEM..... 123

**Figure 3.16.** The process flow for the lab scalable model for liposome manufacture. Liposomes are manufactured by microfluidics and purified by tangential flow filtration, with the ability to check the quality of the liposomes produced in real- time by using the Zetasizer AT (Malvern Panalytical Ltd). ..... 125

**Figure 3.17.** The physicochemical properties of empty DPPC:Chol liposomes made using microfluidics (at a 3:1 FRR and 15 mL/ min TFR). The ability to characterise liposomes at-line (Zetasizer AT) and offline (Zetasizer NanoZS) was compared post microfluidics production in terms of size (A) and polydispersity (PDI) (B). After purification of the liposomes, the size (C) and PDI (D) was investigated both at-line and offline. All results represent the mean  $\pm$  SD, with an n=3 independent batches. .... 127

**Figure 3.18.** The size- intensity plots measured at-line (Zetasizer AT) and offline (Zetasizer NanoZS) for empty DPPC:Chol liposomes produced at a 3:1 FRR (A) and 5:1 FRR (B), as well as for DSPC:Chol liposomes produced at a 3:1 FRR (C) and 5:1 FRR (D). The size- intensity plots are representative plots taken from one reading..... 128

**Figure 3.19.** The Malvern Zetasizer APS (Malvern Panalytical Ltd, Malvern, UK) and the software that controls the machine ..... 129

**Figure 3.20.** A comparison of the physicochemical properties of liposomes measured using the Zetasizer APS and Zetasizer NanoZS. The size (A) and PDI (B) of DPPC:Chol and DSPC:Chol liposomes produced at either a 3:1 or a 5:1 flow rate ratio (FRR) and 15 mL/ min total flow rate (TFR). The results represent mean  $\pm$  SD, n=3 independent batches..... 131

#### **Chapter 4**

**Figure 4.1.** The process involved in quantification of protein by reverse phase- high performance liquid chromatography (RP-HPLC)..... 136

**Figure 4.2.** The process involved in quantification of protein by high performance liquid chromatography coupled with an evaporative light scattering detector (HPLC-ELSD)..... 137

**Figure 4.3.** Solubilisation of ovalbumin (OVA) loaded liposomes labelled with DiIc. Three approaches were used to solubilise the OVA loaded liposomal formulations by isopropanol alcohol:phosphate buffered saline (50/50 V/V) (A), 1% Triton X-100 in PBS (B) and 10% Triton X-100 (C). The liposomal formulations were added to the solubilising agent at a 1:1 volume ratio..... 143

**Figure 4. 4.** Chromatographic peaks of OVA loaded liposomes dissolved in IPA:PBS (50:50 v/v) (A), OVA loaded liposomes dissolved in 1% Triton X-100 (B) and OVA loaded liposomes dissolved in 10% Triton X-100 (C). ..... 144

**Figure 4.5.** Ovalbumin calibration curves solubilised in PBS, to establish LOD and LOQ values using UV- HPLC (A). Intraday curves were generated (B) within the same day, while Interday curves were generated over 3 separate days (C). Accuracy was determined at three concentrations, each in replicate (D), while intraday and interday precision was calculated across three different concentrations with %RSD shown (E-F)..... 146

**Figure 4.6.** RP- HPLC chromatographs for (A) PBS only, (B) 400 µg/ mL of ovalbumin in PBS, (C) empty liposomes, (D) empty liposomes mixed with 100 µg/mL protein ovalbumin, (E) OVA loaded liposomes without solubilisation and, (F) OVA loaded liposomes containing 56 µg/mL of protein encapsulated, solubilised in IPA:PBS (50:50 v/v). All liposomes were produced using microfluidics at a 3:1 FRR and 15 mL/min TFR (initial lipid concentration of 4 mg/ mL and initial lipid concentration of 0.25 mg/ mL). ..... 147

**Figure 4.7.** Ovalbumin calibration curves solubilised in PBS, to establish LOD and LOQ values using HPLC- ELSD (A). Intraday curves were generated (B) within the same day, while Interday curves were generated over 3 separate days (C). Accuracy was determined at three concentrations, each in replicate (D), while intraday and interday precision was calculated across three different concentrations with %RSD shown (E-F)..... 150

**Figure 4.8.** HPLC- ELSD chromatographs for (A) PBS only, (B) 100 µg/ mL of ovalbumin in PBS, (C) empty liposomes, (D) empty liposomes mixed with 100 µg/mL ovalbumin, (E) DSPC:Chol liposomes containing ovalbumin (~ 56 µg/mL) without solubilisation and, (F) DSPC:Chol liposomes containing ovalbumin (~ 56 µg/mL) solubilised in IPA:PBS (50:50 v/v). All liposomes were produced using microfluidics at a 3:1 FRR and 15 mL/min TFR (initial lipid concentration of 4 mg/ mL and initial OVA concentration of 0.25 mg/ mL)..... 151

**Figure 4.9.** Comparative study between two protein quantification techniques, RP-HPLC and HPLC- ELSD. The DSPC:Chol liposomes were made at an initial lipid concentration of 4 mg/mL and 0.25 mg/ mL initial ovalbumin concentration, using microfluidics at a 3:1 flow rate ratio (FRR) and 15 mL/min total flow rate (TFR). The results represent the mean ± SD, n= 3 independent batches. .... 154

**Figure 4.10.** Bland and Atlman plot analysis for the comparison of two analytical techniques. Plot of differences between the RP-HPLC and HPLC-ELSD analytical techniques on the y-axis, versus the mean of the two analytical techniques for the ovalbumin loaded DSPC:Chol liposomal formulations. The mean 0.418 (horizontal solid line), with the bias represented by

the gap between the mean and the dashed lines. The ovalbumin loaded DSPC:Chol liposomal formulations were measured six independent times to quantify the encapsulation efficiency, with each measurement plotted. .... 155

**Figure 4.11.** Comparative study between three protein quantification techniques, UV-HPLC, HPLC- ELSD and BCA assay. All three liposomal formulations were made using microfluidics. The DSPC:Chol and DSPC:Chol:PS formulations were made at a 3:1 FRR and 15 mL/ min TFR (4 mg/ mL initial lipid and 0.25 mg/ mL initial ovalbumin concentration). The DSPC:Chol:DOTAP formulation was produced at a 1:1 FRR, the ovalbumin was adsorbed onto the surface by passing pre-made DSPC:Chol:DOTAP formulation through the microfluidics nanoassemblr. All results were measured three times, with the average encapsulation and ovalbumin loading calculated. .... 155

**Figure 4.12.** Bland and Atlman plot analysis for the comparison of three analytical techniques. Plot of differences between three analytical techniques (RP-HPLC, HPLC-ELSD and BCA assay) on the y-axis, versus the mean of the three analytical techniques for the three formulations (DSPC:Chol, DSPC:Chol:PS and DSPC:Chol:DOTAP). The calculated mean is -8.8 (horizontal solid line), with the bias represented by the gap between the mean and the dashed lines. All formulations were measured three times for the encapsulation efficiency, with each measurement plotted. .... 156

## **Chapter 5**

**Figure 5.1.** Comparison of manufacturing techniques using OVA loaded DSPC:Chol liposomes. The encapsulation efficiency and liposome physicochemical (size and polydispersity (PDI)) properties were investigated, using microfluidics and lipid-film hydration (followed by sonication). The DSPC:Chol liposomes were made using 4 mg/mL and 0.25 mg/mL ovalbumin. The bars represent encapsulation efficiency (%), and the square dots represent size (d. nm). The results represent mean  $\pm$  SD, n=3 independent batches. .... 167

**Figure 5.2.** The characterisation of liposomes produced using microfluidics. The PC:Chol, DMPC:Chol, DPPC:Chol and DSPC:Chol liposomes were produced using 4 mg/mL initial lipid concentration and 0.25 mg/mL initial OVA concentration (at a 3:1 FRR and 15 mL/min TFR). The encapsulation efficiency was calculated using RP-HPLC, whilst the liposome physicochemical characteristics were obtained using dynamic light scattering (Bars= encapsulation efficiency (%) and square dots= size (d. nm)). The results represent mean  $\pm$  SD, n=3 independent batches. .... 168

**Figure 5.3.** The encapsulation efficiency of OVA loaded PC:Chol, DMPC:Chol, DPPC:Chol and DSPC:Chol liposomes made using microfluidics (at a 3:1 FRR and 15 mL/min TFR). Initial lipid concentration of 4 mg/mL and initial OVA concentration of either 0.1 or 0.25 mg/mL was used. The encapsulation efficiency was calculated using HPLC, with the results represent mean  $\pm$  SD, n=3 independent batches. .... 169

**Figure 5.4.** The intensity plots of 0.25 (A) and 0.1 (B) mg/mL initial OVA loaded (PC:Chol, DMPC:Chol, DPPC:Chol and DSPC:Chol) neutral formulations made by microfluidics at a 3:1 FRR and 15 mL/min TFR. The results represent three independent batches, mean  $\pm$  SD... 169

**Figure 5.5.** Comparison of manufacturing techniques using OVA loaded PC:Chol, DMPC:Chol, DPPC:Chol and DSPC:Chol liposomes (using 4 mg/mL initial lipid and 0.25 mg/mL initial OVA). The encapsulation efficiency and liposome physicochemical (size and polydispersity (PDI)) properties were investigated, using microfluidics and lipid-film hydration (followed by sonication). The results represent mean  $\pm$  SD, n=3 independent batches..... 170

**Figure 5.6.** The effect of increasing ovalbumin concentration on neutral DMPC:Chol liposomes (2:1 wt/wt) produced by microfluidics at a 3:1 FRR and 15 mL/min. Increasing initial ovalbumin concentration on entrapment efficiency and loading was quantified. The results represent mean  $\pm$  SD, n=3 independent batches..... 171

**Figure 5.7.** The effect of increasing ovalbumin concentration on neutral DMPC:Chol liposomes (2:1 wt/wt) produced by microfluidics at a 3:1 FRR and 15 mL/min. The physicochemical properties (including size, polydispersity index and zeta potential) were determined by dynamic light scattering. (Bars= size and round dots= polydispersity index). The results represent mean  $\pm$  SD, n=3 independent batches..... 172

**Figure 5.8.** The physicochemical properties of OVA loaded liposomes (0.25 mg/mL initial ovalbumin) produced at varying lipid concentrations (0.3- 10 mg/mL initial lipid) by microfluidics at 3:1 FRR and 15 mL/min TFR. The size, polydispersity (PDI) and zeta potential (ZP) of PC:Chol, DMPC:Chol, DPPC:Chol and DSPC:Chol using dynamic light scattering. The results represent mean  $\pm$  SD, n=3 independent batches..... 174

**Figure 5.9.** Investigating the relationship between log lipid concentration on the log encapsulation efficiency of four liposomal formulations (PC:Chol, DMPC:Chol, DPPC:Chol and DSPC:Chol). The liposomal formulations were prepared using microfluidics at varied lipid concentration and 0.25 mg/mL initial ovalbumin concentration. All formulations were produced at a 3:1 FRR and 15 mL/min TFR. The results represent mean  $\pm$  SD, n=3 independent batches..... 175

**Figure 5.10.** Characterisation of OVA loaded DMPC:Chol liposomes produced by microfluidics at a 3:1 FRR and 5:1 FRR. The liposomes were produced at a 4 mg/mL initial lipid concentration with an initial ovalbumin concentration of 0.188 mg/mL. The physicochemical properties (size and polydispersity index) was determined by dynamic light scattering (A), and the encapsulation efficiency calculated (B). The results represent mean  $\pm$  SD, n=3 independent batches. .... 176

**Figure 5.11.** The structural integrity of ovalbumin loaded into the liposomes was tested by circular dichroism (CD). The CD spectra was identified for empty DSPC:Chol liposomes (A), OVA solubilised in 100% methanol (B) and OVA dissolved phosphate buffered saline (PBS) as well as OVA entrapped within DSPC:Chol liposomes. The results are representative of the samples. .... 179

**Figure 5.12.** The effect of flow rate ratio (FRR) on the integrity of ovalbumin (OVA) encapsulated inside liposomes. OVA loaded DSPC:Chol liposomes were produced at either a 1:1 FRR, 3:1 FRR or 5:1 FRR (at 15 mL/min speed) using microfluidics. The formulations were inspected visually (A) as well as by circular dichroism. The results are representative of the samples. .... 180

**Figure 5.13.** The stability of OVA loaded liposomes produced by microfluidics (at a 3:1 FRR and 15 mL/min TFR), with regards to liposome size (A), polydispersity index (B) and zeta potential (C). Four liposomal formulations (PC:Chol, DMPC:Chol, DPPC:Chol and DSPC:Chol) were produced and kept three different test conditions (5°C, 25°C and 37°C) to determine the stability. Measurements were taken at set time points over seven days using dynamic light scattering. The results represent mean  $\pm$  SD, n=3 independent batches..... 182

**Figure 5.14.** Peak intensity of OVA loaded PC:Chol (A), DMPC:Chol (B), DPPC:Chol (C) and DSPC:Chol made by microfluidics (3:1 FRR and 15 mL/ min TFR) and kept at 4°C for 7 days. The plots are representative of one measurement of the liposomal formulations. .... 183

**Figure 5.15.** The release profile of ovalbumin from OVA loaded (PC:Chol, DMPC:Chol, DPPC:Chol and DSPC:Chol) liposomes produced by microfluidics (3:1 FRR and 15 mL/min TFR) and purified by TFF. The formulations were kept at 37°C in buffer, with samples collected at specific time points. Direct measurement of the encapsulated OVA was performed, to establish the release rate of the protein. The results represent mean  $\pm$  SD, n=3 independent batches..... 186

**Figure 5.16.** The release profile of OVA loaded DMPC:Chol liposomes produce at either a 3:1 or a 5:1 FRR (with a 15 mL/min TFR) and purified by TFF. The formulations were kept at 37°C in buffer, with samples collected at specific time points. Direct measurement of the encapsulated OVA was performed, to establish the release rate of the protein. The results represent mean  $\pm$  SD, n=3 independent batches. .... 186

## **Chapter 6**

**Figure 6.1.** Representation of a liposomal formulation with cholesterol, and loaded with a lipophilic drug. .... 189

**Figure 6.2.** The bespoke TFF set up designed and built by Professor Nicolas Szita (University College London, UK)..... 197

**Figure 6.3.** The calibration curve established to determine the amount of loading for propofol loaded PC:Chol liposomes. The results represent mean  $\pm$  SD, n=3 independent batches. . 200

**Figure 6.4.** The morphology of Propofol loaded PC:Chol liposomes by cryoTEM. Images are taken by x1200 magnification..... 201

**Figure 6.5.** The morphology of SU1349 loaded DMPC:Chol liposomes. The images were taken by a light microscope. .... 205



**Figure 6.6.** The physicochemical properties of SU1349 drug loaded DMPC:Chol liposomes. The size (d. nm), polydispersity index (PDI) and zeta potential (mV) is measured by dynamic light scattering. The results represent mean  $\pm$  SD, n=3 independent batches..... 207

**Figure 6.7.** Identification of the SU1349 drug using mass spectroscopy ran at positive (A) and negative (B) parameters. The peaks are representative of one SU1349 loaded liposomal sample..... 209

**Figure 6.8.** Quantifying the amount of SU1349 using liquid chromatography, with the chromatograph scan of the SU1349 drug loaded into the liposomes..... 210

## **Chapter 7**

**Figure 7.1.** The effect of freezing and thawing on the size and PDI of ovalbumin loaded DMPC:Chol (A) and DSPC:Chol (B) liposomes. The physicochemical properties were measured after the samples were frozen at varying temperatures. Results represent three independent batches,  $\pm$  SD..... 229

**Figure 7.2.** Freeze dried microscopy of DSPC:Chol (4 mg/ml initial) with an initial concentration of 0.25 mg/mL OVA entrapped inside. The formulation was added at a 1:1 v/v ratio to sucrose, producing a final concentration of 7.5% sucrose in the formulation..... 232

**Figure 7.3.** Freeze dried microscopy of empty DMPC:Chol (10 mg/mL initial). The formulation was added at a 1:1 v/v ratio to sucrose, producing a final concentration of 7.5% sucrose in the formulation..... 233

**Figure 7.4.** Freeze dried microscopy of DMPC:Chol (10 mg/mL initial) with an initial concentration of 0.25 mg/mL OVA entrapped inside. The formulation was added at a 1:1 v/v ratio to sucrose, producing a final concentration of 7.5% sucrose in the formulations. .... 234

**Figure 7.5.** Modulated differential scanning calorimetry results for DMPC:Chol (10 mg/mL) with (A) and without (B) ovalbumin, and DSPC:Chol (4 mg/mL) liposomes with OVA (C ) encapsulated inside the aqueous core (0.25 mg/mL initial). The sample contained a final concentration of 7.5% sucrose. .... 237

**Figure 7.6.** Dynamic mechanical analysis results for DMPC:Chol (10 mg/mL) with (A) and without (B) ovalbumin, and DSPC:Chol (4 mg/mL) liposomes with OVA (C ) encapsulated inside the aqueous core (0.25 mg/mL initial). The sample contained a final concentration of 7.5% sucrose. .... 239

**Figure 7.7.** Process flow sheet for three freeze drying cycles including the freezing procedure for liposome formulations. .... 241

**Figure 7.8.** Real time analysis of liposomes frozen using freeze drying cycle 1. .... 243

**Figure 7.9.** DMPC:Chol freeze dried in either a microplate (A) or a conventional vial (B). . 244

**Figure 7.10.** Characterising DMPC:Chol (4 and 10 mg/mL ) liposomes loaded with and without OVA (0.25 mg/mL) before and after freeze drying. The samples contained different amounts of sucrose and were freeze dried in either vials (A) or in microplates (B). Results represent three independent batches,  $\pm$  SD. .... 247

**Figure 7.11.** Characterising DSPC:Chol (4 and 10 mg/mL ) liposomes loaded with and without OVA (0.25 mg/mL) before and after freeze drying. The samples contained different amounts of sucrose and were freeze dried in either vials (A) or in microplates (B). Results represent three independent batches,  $\pm$  SD. .... 248

**Figure 7.12.** Design of experiments plots predicting the outcomes in terms of size (A), PDI (B) and encapsulation efficiency (C) of OVA loaded DMPC:Chol liposomes. .... 251

**Figure 7.13.** Design of experiments graphs predicting the outcomes in terms of size (A), PDI (B) and encapsulation efficiency (C) of OVA loaded DSPC:Chol liposomes. .... 252

**Figure 7.14.** The cakes formed after testing different freezing and freeze drying conditions. The DMPC:Chol liposomes were either ramp frozen (A) or snap frozen (C) . The DSPC:Chol formulations were also subjected to ramp (B) and snap freezing (D), after which the cakes were inspected visually for any deformations..... 253

**Figure 7.15.** The physicochemical properties of OVA loaded DMPC:Chol and DSPC:Chol liposomes before and after freeze drying. The liposomes were subjected to two freeze drying options; a ramp freeze cycle or a snap freeze cycle, with liposome suspensions (before freeze drying) used as a control. All samples were freeze dried in the presence of the cryoprotectant sucrose (10% v/v at a 1:1 ratio). Results represent three independent batches,  $\pm$  SD. .... 255

## **Chapter 8**

**Figure 8.1.** Exposing cells in aqueous media to pre-formed liposomes (produced by microfluidics) to encourage mixing, study uptake and interactions. .... 265

**Figure 8.2.** Metabolic reaction that causes a visual change in the cell culture solution allowing detection of cell viability..... 268

**Figure 8.3.** Morphology of undifferentiated THP-1 cells (A) and RAW264.7 cell line (B). After THP-1 cells are stimulated with Vitamin D3, images of the cells were taken every 24 hours for 2 days to observe any morphological change due to differentiation (C). The results are representative of the sample..... 272

**Figure 8.4.** THP-1 cells that have not been differentiated are shown by the histogram (A), while the histogram on the right shows the positive cell population which had differentiated (B). .... 272

**Figure 8.5.** Cell viability of DMPC:Chol and DSPC:Chol liposomes exposed to RAW264.7 cells (A) and differentiated THP-1 cells (B). The DMPC:Chol and DSPC:Chol were produced by

microfluidics at a 3:1 FRR and 15 mL/min TFR. Varying concentrations of the lipid were exposed to the cells plated in 96 well plates and left for 24 hours. The cell viability was then calculated using the cell titre blue assay. The results represent mean  $\pm$  SD, n=3 independent batches..... 275

**Figure 8.6.** RAW264.7 cells were exposed to four neutral formulations containing OVA. The four formulations were made at a 3:1 FRR and 15 mL/min TFR. The aqueous phase contained 0.25 mg/ mL of OVA. The formulations were purified using TFF. The cells were exposed to 100  $\mu$ g/ mL of each formulation and cell viability was determined using cell titre blue. Results represent mean  $\pm$  SD, n=3 independent batches. .... 276

**Figure 8.7.** Uptake of empty and OVA loaded DMPC:Chol and DSPC:Chol formulations by RAW264.7 cells at 37°C (A) and 4°C (B) and stimulated THP-1 cells at 37°C (C) and 4°C (D). All formulations were made using microfluidics at a 3:1 FRR and 15mL/min TFR, with 0.25 mg/mL of OVA added into the aqueous phase. Removal of untrapped OVA was by tangential flow filtration at 27 mL/min. The formulations were added to RAW264.7 cells for varying amounts of time after which uptake was determined using the BD FACSCanto. The results represent mean  $\pm$  SD, n=3. .... 280

**Figure 8.8.** The percentage of DQ-OVA cleaved in three hours was compared to the amount of OVA loaded liposomes taken up by RAW264.7 (A) and THP-1 cells (B). Results represent three independent batches,  $\pm$  SD. .... 282

**Figure 8.9.** The morphology of THP-1 cells before after being passed through the microfluidics chip at varying flow rates. The cells were analysed using a light microscope using an x10 objective lens. .... 284

**Figure 8.10.** The uptake of DiIC labelled DMPC:Chol (1 mg/mL final concentration) by THP-1 monocytes. The pre-formed DiIC labelled liposomes were passed through the microfluidics chip alongside the THP-1 cells at a 1:1 FRR and 5 mL/ min. After this, the cells were then plated onto a 96 well plate and fluorescence was measured using a plate reader, to quantify the amount of liposome uptake. The results represent three independent batches, each shown individually  $\pm$  SD. .... 285

## **Chapter 9**

**Figure 9.1.** The size (A) and polydispersity index (B) measurements of empty and DMPC:Chol liposomes loaded with varying amounts of Co-polymer 1 (CP1) or Co-polymer 5 (CP5) before and after purification. The liposomal formulations were produced using microfluidics at a 3:1 FRR and 15 mL/min TFR. The results represent mean  $\pm$  SD, n=3 independent batches. .... 294

**Figure 9.2.** The stability of co-polymer loaded DMPC:Chol formulations kept at 37°C for seven days. The formulation were made using microfluidics (at a 3:1 FRR and 15 mL/min TFR) using either 1% or 4% co-polymer 1 or 5. Samples were taken every day for seven days with the size (A), polydispersity index (B) and zeta potential (mV) measured using dynamic light scattering. The results represent mean  $\pm$  SD, n=3 independent batches..... 297

**Figure 9.3.** The size- intensity plots of co-polymer DMPC:Chol liposomes at 37°C. The co-polymer 1 was added to DMPC:Chol liposomes during production at 1 % (A) or 4 % (B), with co-polymer 5 also added at either 1 % (C) or 4 % (D). The size-intensity plots were analysed every day for up to seven days, with each plot representative of one measurement of the sample..... 298

**Figure 9.4.** The stability of co-polymer loaded DMPC:Chol formulations kept at 4°C for seven days. The formulation were made using microfluidics (at a 3:1 FRR and 15 mL/min TFR) using either 1% or 4% co-polymer 1 or 5. Samples were taken every day for seven days with the size (A), polydispersity index (B) and zeta potential (mV) measured using dynamic light scattering. The results represent mean  $\pm$  SD, n=3 independent batches..... 299

**Figure 9.5.** The size- intensity plots of co-polymer DMPC:Chol liposomes at 4°C. The co-polymer 1 was added to DMPC:Chol liposomes during production at 1 % (A) or 4 % (B), with co-polymer 5 also added at either 1 % (C) or 4 % (D). The size-intensity plots were analysed every day for up to seven days, with each plot representative of one measurement of the sample..... 300

**Figure 9.6.** The physicochemical properties of DMPC:Chol liposomes containing varying lengths of co-polymers chains. The liposomal formulations were produced using microfluidics at a 3:1 FRR and 15 mL/min TFR. The size (A), polydispersity index (B) and zeta potential (C) were measured using dynamic light scattering. The results represent mean  $\pm$  SD, n=3 independent batches. .... 302

**Figure 9.7.** The cell viability of THP-1 cells exposed to empty DMPC:Chol liposomes with varying lengths of co-polymer (co-polymers 1-5). The THP-1 cells were exposed to 100  $\mu$ g/mL of the formulations for 24 hours after which the viability was determined by cell titre blue assay. The results represent mean  $\pm$  SD, n=3 independent batches..... 306

**Figure 9.8.** The cell viability of THP-1 cells exposed to OVA loaded DMPC:Chol liposomes with varying lengths of co-polymer (co-polymers 1-5). The THP-1 cells were exposed to 100  $\mu$ g/mL of the formulations for 24 hours after which the viability was determined by cell titre blue assay. The results represent mean  $\pm$  SD, n=3 independent batches..... 306

**Figure 9.9.** The uptake of empty co-polymer (CP1- 5) liposomal DMPC:Chol formulations compared to DMPC:Chol formulations. All formulations were produced by microfluidics at a 3:1 FRR and 15 mL/min TFR. The cells were exposed to the formulations for up to three hours (with samples collected at 0.5, 1 2, and 3 hours) at either 37°C or 4°C. After a set amount of time the formulations were removed and the uptake was measured using flow cytometry. The results represent mean  $\pm$  SD, n=3 independent batches..... 309

**Figure 9.10.** The uptake of ovalbumin (OVA) loaded co-polymer (CP1- 5) liposomal DMPC:Chol formulations compared to OVA loaded DMPC:Chol formulations. All formulations were produced by microfluidics at a 3:1 FRR and 15 mL/min TFR. The cells were exposed to the formulations for up to three hours (with samples collected at 0.5, 1 2, and 3 hours) at either 37°C or 4°C. After a set amount of time the formulations were removed and the uptake

was measured using flow cytometry. The results represent mean $\pm$ SD, n=3 independent batches.....	310
<b>Figure 9.11.</b> The processing of DQ-OVA in relation to uptake over 48 hours. THP-1 cells were exposed to OVA loaded CP4 (4%) DMPC:Chol liposomes for a set amount of hours (3- 48 hours), after which the formulations were removed and the amount of OVA processing was quantified by flow cytometry. The results represent mean $\pm$ SD, n=3 independent batches. ....	311

## List of Tables

### Chapter 1

<b>Table 1.1.</b> List of approved liposome medicines on the market. ....	36
<b>Table 1.2.</b> Representation of the range of liposomes sizes that can be manufactured.....	37
<b>Table 1.3.</b> An overview of some of the traditional methods used to produce liposomes (Dua et al., 2012, Laouini et al., 2012).....	39
<b>Table 1.4.</b> The microfluidics devices available for the development of formulations. ....	42
<b>Table 1.5.</b> Structural and general information about the lipids used to produce neutral liposomes .....	53

### Chapter 2

<b>Table 2.1.</b> Liposomes size parameters for the Malvern Zetasizer Nano ZS.....	61
<b>Table 2.2.</b> Comparing the predicted liposome physicochemical properties (Size, polydispersity (PDI) and zeta potential (ZP) to the actual values obtained for liposomes produced by microfluidics using the predicted optimal parameters. Dynamic light scattering was used to determine the size, PDI and ZP. Results represent mean $\pm$ SD, n=3 independent batches.....	90
<b>Table 2.3.</b> The lipid recovery of PC:Chol, DMPC:Chol, DPPC:Chol and DSPC:Chol liposomes produced by microfluidics and rotary evaporation. The effect of additional downstream processes like solvent removal (dialysis and Sephadex® G-75 columns) and sonication on lipid recovery was also quantified. Results represent mean $\pm$ SD, n=3 independent batches. ....	95
<b>Table 2.4.</b> The quantification of DMPC lipid and cholesterol formed with varying production parameters. The DMPC:Chol liposomes were produced at a 3:1 FRR, with the total flow rate varied. The effect of changing the lipid and cholesterol ratio was also investigated, with	

recovery calculated by HPLC- ELSD. Results represent mean  $\pm$  SD, n=3 independent batches..... 95

**Table 2.5.** The effect of dialysis time on solvent removal. The amount of solvent remaining in PC:Chol liposomes was quantified. Results represent mean  $\pm$  SD, n=3 independent batches..... 97

**Table 2.6.** Quantifying remaining solvent post dialysis. All four liposome formulations underwent dialysis for one hour, with the amount of solvent remaining calculated. Results represent mean  $\pm$  SD, n=3 independent batches. .... 98

### **Chapter 3**

**Table 3.1.** Summary of the range of liposome that can be produced by Y-shaped chips... 102

### **Chapter 5**

**Table 5.1.** The amount of protein encapsulated within neutral and anionic liposomes by traditional manufacturing methods..... 160

**Table 5.2.** Factors that can cause denaturation of ovalbumin during the manufacturing of this protein inside liposomes..... 162

### **Chapter 6**

**Table 6.1.** The characteristics of small molecule drug propofol (Formulary, 2018, Database, 2018)..... 190

**Table 6.2.** The characteristics of the novel small molecular drug SU1349..... 192

**Table 6.3.** The high performance liquid chromatography elution gradient to quantify the amount of propofol drug. .... 195

**Table 6.4.** The physicochemical characteristics of propofol loaded PC:Chol liposomes manufactured as multilamellar vesicles (MLVs) by thin film lipid hydration, and downsized to small unilamellar vesicles (SUVs). The liposomes were purified by tangential flow filtration cycles, with the size and polydispersity index measured by dynamic light scattering. The amount of propofol loaded was calculated using HPLC. The results represent mean  $\pm$  SD, n=3 independent batches. .... 199

**Table 6.5.** The physicochemical characteristics of propofol loaded PC:Chol liposomes manufactured by microfluidics. The liposomes were purified by tangential flow filtration cycles (TFF), with the size and polydispersity index measured by dynamic light scattering. The amount of propofol loaded was calculated using HPLC. The results represent mean  $\pm$  SD, n=3 independent batches. .... 199

<b>Table 6.6.</b> Characterising SU1349 DMPC:Chol formulations in terms of size, PDI and zeta potential.....	204
<b>Table 6.7.</b> The quantification of loading amount and ratio of SU1349 by DMPC:Chol liposomes produced by microfluidics.....	210
 <b>Chapter 7</b>	
<b>Table 7.1.</b> Degradation mechanisms accounting for the reduced stability of liposome formulations.....	213
<b>Table 7.2.</b> Liposome products currently on the market. ....	214
<b>Table 7.3.</b> Comparison of the three drying technologies available for the stabilisation of liposomes in a dry state. ....	216
<b>Table 7.4.</b> Theories of freeze drying. ....	217
<b>Table 7.5.</b> The HPLC gradient used to detect the OVA protein. ....	220
<b>Table 7.6.</b> The physicochemical properties of DMPC:Chol liposomes produced with and without ovalbumin.....	226
<b>Table 7.7.</b> The physicochemical properties of DSPC:Chol liposomes produced with and without ovalbumin.....	226
<b>Table 7.8.</b> Determining the freezing and collapse temperatures of liposome formulations using freeze dried microscopy. ....	231
<b>Table 7.9.</b> Comparing techniques used to determine the glass transition temperature for liquid samples. ....	240
<b>Table 7.10.</b> Ovalbumin encapsulation of DMPC:Chol liposomes before and after freeze drying with different sucrose concentrations. Results represent n of three independent batches, $\pm$ SD. ....	249
<b>Table 7.11.</b> Ovalbumin encapsulation of DSPC:Chol liposomes before and after freeze drying with different sucrose concentrations. Results represent n of three independent batches, $\pm$ SD. ....	249
<b>Table 7.12.</b> The encapsulation of OVA before and after freeze drying using two different cycles. Results represent three independent batches, mean $\pm$ SD.....	255
<b>Table 7.13.</b> The residual moisture content of liposomes freeze dried under different conditions, containing the cryoprotectant sucrose.....	257

<b>Table 7.14.</b> The optimal freeze drying cycle for the preservation of protein loaded liposomes. ....	258
---	-----

## **Chapter 8**

<b>Table 8.1.</b> Comparison of monocyte/ macrophage cell lines. ....	263
---	-----

<b>Table 8.2.</b> The advantages and disadvantages of microfluidics cell culture and macroscopic cell cultures. ....	264
--	-----

<b>Table 8.3.</b> Cell viability of RAW264.7 cells when exposed to empty and Ovalbumin (OVA) loaded DMPC:Chol and DSPC:Chol liposomes. The DMPC:Chol liposomes containing a different starting concentration of OVA were produced using microfluidics at a 3:1 FRR and 15 mL/min TFR. Similarly, empty and OVA loaded DSPC:Chol liposomes, using 0.25 mg/mL initial OVA were produced at a 3:1 FRR and 15 mL/min TFR. The liposomes were added to RAW264.7 cells and left for 24 hours, with the cell viability measured using the cell titre blue assay. The results represent mean $\pm$ SD, n=3 independent batches. ....	276
--	-----

<b>Table 8.4.</b> The physicochemical properties of empty and OVA loaded DMPC:Chol and DSPC:Chol formulations. The size, polydispersity and zeta potential was measured using dynamic light scattering. The results represent mean $\pm$ SD, n=3 independent batches. ....	279
--	-----

<b>Table 8.5.</b> The percentage of DQ-OVA (which was loaded into either DMPC:Chol and DSPC:Chol liposomes) processed over a 48 hour period. ....	<b>Error! Bookmark not defined.</b>
---	-------------------------------------

<b>Table 8.6.</b> The percentage of viable cells after passing through the microfluidics chip at various speeds. The results represent three independent batches, $\pm$ SD. ....	284
--	-----

## **Chapter 9**

<b>Table 9.1.</b> The properties of functionalised polyethylene glycol attached to varying lengths of polylysine. ....	290
--	-----

<b>Table 9.2.</b> Characterisation of ovalbumin loaded DMPC:Chol liposomes containing 4% of all five co-polymers. The size, polydispersity index and zeta potential was determined by dynamic light scattering. The amount and encapsulation efficiency of the protein ovalbumin by co-polymer DMPC:Chol liposomes of varying lengths. The formulations were produced by microfluidics (at a 3:1 FRR and 15 mL/min TFR). The results represent mean $\pm$ SD, n=3 independent batches. ....	304
---	-----



## Abbreviations

ANOVA	Analysis of variance
APS	Antigen presenting cells
CF	Carboxyfluorescein
Chol	Cholesterol
CryoTEM	Cryogenic Transmission electron microscopy
DAC	Dual Asymmetric Centrifugation
DDA	Dimethyldioctadecylammonium
DilC	Dil Stain (1,1'-Dioctadecyl-3,3,3',3'- Tetramethylindocarbocyanine Perchlorate ('Dil'; DilC18 (3))
DLS	Dynamic light scattering
DMEM	Delbecco's modified eagles medium
DoE	Design of experiments
DMPC	1,2-dimyristoyl-sn-glycero-3-phosphocholine (DMPC)
DPPC	1,2-dipalmitoyl-sn-glycero-3-phosphocholine
DSPC	1,2-distearoyl-sn-glycero-3-phosphocholine
ELSD	Evaporative light scattering detector
EPR	Enhanced permeability and retention
FACS	Fluorescence activated cell sorting
FBS	Foetal bovine serum
FD	Freeze drying
FRR	Flow rate ratio
GC	Gas chromatography
GUV	Giant Unilamellar Vesicles
HS	Headspace
HPLC	High performance liquid chromatography
LOD	Limit of detection
LOQ	Limit of quantification
LUV	Large Unilamellar Vesicles
MHC	Major Histocompatibility complex
MLV	Multilamellar vesicles
MPS	Mononuclear phagocyte system

OFAT	One factor at a time
OVA	Ovalbumin
PBS	Phosphate buffer saline tablets
PC	Phosphatidylcholine
PDI	Polydispersity index
PEG	poly-(ethylene glycol)
QbD	Quality by design
RP	Reverse phase
RPMI 1640	Roswell park memorial institute medium 1640
SHM	Staggered herringbone micromixer
SUV	Small unilamellar vesicles
TFA	Trifluoroacetic acid
TFF	Tangential flow filtration
TFR	Total flow rate
TMP	Transmembrane pressure

# **Chapter 1**

## **Introduction**

## 1.1 Background

Liposomes are defined as spherical vesicles at the microscopic level, containing an aqueous core with a bilayer structure. First described by Alec. D. Bangham in the 1960s (Bangham and Horne, 1964) whilst studying cell membranes, they were subsequently shown to be an effective delivery system by Gregoriadis (Gregoriadis, 1973). The nature of liposomes makes them ideal for therapeutic use; the bilayer of liposomes consists of lipids, such as phosphatidylcholines, which are amphiphilic in nature (containing both a hydrophobic and a hydrophilic region). Due to this attribute, lipids placed in an aqueous environment spatially reorganise to minimise the unfavourable interactions between the hydrophobic acyl chains and the aqueous environment, thus forming liposomes (Laouini *et al.*, 2012) (see Figure 1.1). The interactions between the lipids are enhanced by hydrogen bonds, Van der Waals forces and electrostatic interactions (Pattni *et al.*, 2015). The lipids generally used are non-toxic and biodegradable as they are readily taken up by cells. The structure of the liposomes containing an enclosed aqueous environment, protects the active pharmaceutical ingredient (API) from breakdown. The amphiphilic nature of lipids allows both hydrophobic and hydrophilic drugs to be incorporated, enhancing bioavailability of otherwise poorly soluble therapeutics. Currently, there are many liposomal formulations available on the market for clinical use (Table 1.1). A wide range of liposome sizes can be produced as required for the given clinical application. Liposomal formulation characteristics such as morphology, size (Table 1.2), encapsulation efficiency and drug release profiles can be adjusted according to the formulation specification.

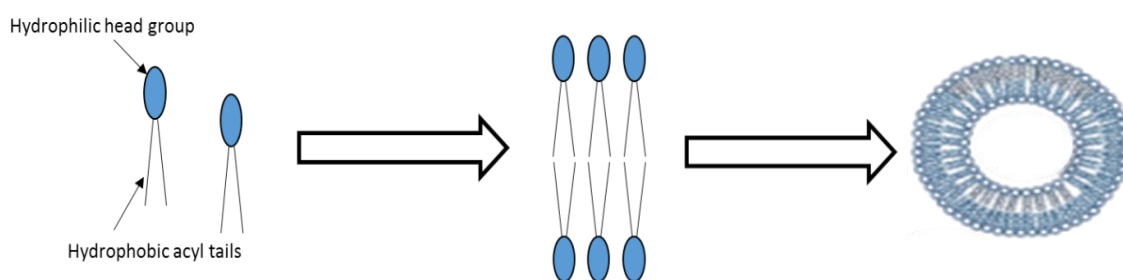




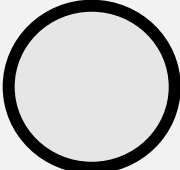
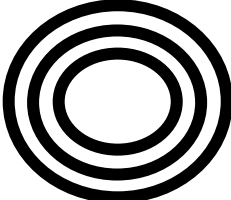
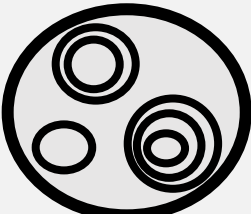
**Figure 1.1.** The basic structural components of liposomes. The lipids are representative of phosphatidylcholine, which has a hydrophilic phosphate head group and two hydrophobic hydrocarbon tails. Hydration of lipids causes spatial rearrangement of the lipids into bilayer structures so that the hydrophobic tails avoid contact with the aqueous environment, resulting in a spherical liposome vesicles.

**Table 1.1.** List of approved liposome medicines on the market.

**Abbreviations:** L- $\alpha$ -phosphatidylcholine, hydrogenated (Soy) (HSPC), 1,2-distearoyl-*sn*-glycero-3-phospho-(1'-*rac*-glycerol) (sodium salt) (DSPG), Egg phosphatidylcholine (EPC), 1,2-distearoyl-*sn*-glycero-3-phosphoethanolamine-N-[amino(polyethyleneglycol)-2000] (ammonium salt) (DSPE- PEG).

PRODUCT NAME	DRUG	LIPID COMPOSITION	LIPOSOME ROLE	TREATMENT	DRUG MECHANISM OF ACTION	REFERENCES
<b>AMBISOME®</b>	Amphotericin B	HSPC, DSPG and cholesterol	Increase tolerability, reduce nephrotoxicity, and works by passive targeting.	Fungal infections	Binds ergosterol; disruption of fungal membrane	(Walsh <i>et al.</i> , 1998, Boswell <i>et al.</i> , 1998)
<b>MYOCET®</b>	Doxorubicin	EPC and cholesterol	Reduces cardiotoxicity, nausea and works by passive targeting	Metastatic breast cancer	Inserts into DNA. Stops transcription and translation from taking place	(Leonard <i>et al.</i> , 2009)
<b>DOXIL®/ CAELYX®</b>	Doxorubicin	HSPC, cholesterol and DSPE-PEG2000	Prolonged circulation time, increased loading and works by passive targeting	Breast cancer, ovarian cancer	Inserts into DNA/topoisomerase 2 inhibitor.	(Barenholz, 2012, Birngruber <i>et al.</i> , 2014)
<b>LIPODOX®</b>	Doxorubicin	DSPC, cholesterol and DSPE-PEG2000	Generic version of Doxil, and works by passive targeting	Breast cancer, ovarian cancer	Inserts into DNA/topoisomerase 2 inhibitor.	(Burade <i>et al.</i> , 2017)
<b>DAUNOXOME®</b>	Daunorubicin	DSPC and cholesterol	Enhanced drug delivery, reduces toxicity, passive targeting	Myeloid leukaemia	Intercalation into DNA	(Forssen, 1997)

**Table 1.2.** Representation of the range of liposomes sizes that can be manufactured.

NAME	SIZE RANGE	SCHEMATIC
<b>SMALL UNILAMELLAR VESICLES (SUV)</b>	< 100 nm	
<b>LARGE UNILAMELLAR VESICLES (LUV)</b>	100- 1000 nm	
<b>GIANT UNILAMELLAR VESICLES (GUV)</b>	>1000 nm	
<b>MULTI-LAMELLAR VESICLES (MLV)</b>	Varied	
<b>MULTI- VESICULAR VESICLE (MVV)</b>	Varied	

## **1.2 Liposome manufacturing techniques**

To produce liposomal products currently on the market and those in clinical trials a range of production techniques have arisen to meet manufacturing demands. These can be broadly defined into two groups: the “top- down” approach whereby large liposomes undergo various downsizing procedures to decrease the vesicle size and, the “bottom- up” approach. The majority of production techniques have adapted the thin film liposome production method first described by Bangham (Bangham and Horne, 1964).

### **1.2.1 Conventional techniques used to produce liposomes**

The thin film lipid hydration is good for small scale production of liposomes, but use in manufacturing for industrial purposes is difficult due to problems in scalability and batch to batch uniformity. As a result, other techniques have been developed (including reverse phase evaporation, ether injection and ethanol injection), however, these methods also have limitations as outlined in Table 1.3.

**Table 1.3.** An overview of some of the traditional methods used to produce liposomes (Dua et al., 2012, Laouini et al., 2012).

<b>METHOD</b>	<b>DESCRIPTION</b>	<b>ADVANTAGES</b>	<b>DISADVANTAGES</b>
<b>THIN FILM LIPID HYDRATION</b>	The original way of producing liposomes. It involves dissolving a mixture of lipid and drug in an organic solvent and evaporating it to remove the solvent, forming a thin film. The film is then hydrated with an aqueous solution to form liposomes.	Cheap Easy to do	Large heterogeneous liposomes are formed so down-sizing processes are required. Hard to upscale
<b>REVERSE PHASE EVAPORATION</b>	Lipids dissolved in an organic solvent are evaporated so that the solvent is removed. The contents are then reconstituted with another aqueous buffer and organic solvent such as diethyl ether, before the organic solvent is removed under low pressure.	High encapsulation efficiency	Drugs or proteins are exposed to solvent Heterogeneous liposomes that are in the micron range
<b>ETHER INJECTION</b>	Lipids dissolved in ether are injected into heated aqueous buffer. Upon contact with the aqueous phase the ether vaporizes and liposomes are formed.	Easy removal of the solvent	Heterogeneous population of liposomes
<b>ETHANOL INJECTION</b>	Lipids dissolved in ethanol are injected into a large volume of buffer with MLVs formed.	Quick	Hard to remove solvent Heterogeneous population Possibility of the solvent reacting with the biologically active molecules
<b>DETERGENT METHOD</b>	Lipids dissolved in detergent form micelles. Removal of the detergent via dialysis causes the micelles to change and form liposomes.	Good for large scale processing	Large liposomes Difficult to remove all the detergent-chance of residual detergent



### **1.2.3 Novel liposome production methods**

Whilst traditional methods outlined in Table 1.3 are capable of producing liposomes, the manufacturing processes are often lengthy and expensive. Furthermore, batch to batch consistency of therapeutic liposomes is difficult, therefore novel approaches have been developed to combat these problems.

#### **1.2.3.1 Supercritical reverse phase evaporation (SRPE) method**

The rapid production of liposomes is possible using a modified version of the reverse phase evaporation method, called the supercritical reverse phase evaporation method (SRPE). As part of this method, the organic solvent used in the traditional reverse phase evaporation is substituted for a supercritical fluid. A supercritical fluid is a fluid where there is no distinct liquid to gas phase. An example of a supercritical fluid is supercritical carbon dioxide (scCO<sub>2</sub>) which is non-toxic. The method, described by Otake and his colleagues (Otake *et al.*, 2001), has the ability to produce phosphatidylcholine liposomes in a single step. The technique does not require solvent removal which is advantageous for clinical use, and produces liposome dispersions by emulsion. The encapsulation efficiency of glucose was five times more using the SPER method compared to thin film lipid hydration. Whilst this technique enables single step production, the process mainly produces large unilamellar vesicles (LUVs). The liposomes produced are heterogonous with a size range of between 0.1- 1.2 µm possible, therefore batch to batch consistency as well as producing liposomes of less than 100 nm using this process is not possible.

#### **1.2.3.2 Dual asymmetric centrifugation (DAC)**

Liposomes can also be prepared using dual asymmetric centrifugation. Dual asymmetric centrifugation is a high speed mixing centrifuge. It is able to rotate samples around its own axis (vertical rotation), alongside the normal rotating motion of the centrifuge (horizontal rotation). During DAC, the horizontal rotation pushes samples towards the walls of the vials, meanwhile vertical rotation pushes the sample in the opposite direction. Unlike the SPER method, DAC is able to produce liposomes of around 60 nm, such as phosphatidylcholine

liposomes containing cholesterol (55:45 mol %) (Massing *et al.*, 2008). However, the DAC technique is a multiple step process. Post centrifugation liposomes require diluting as the highly concentrated liposomes form highly viscous phospholipid gels, thus this technique may not be the most efficient and ideal for large scale manufacture.

### 1.2.3.3 Microfluidics

Microfluidics is a lab-on-a-chip approach used to produce liposomes. It can be defined as the study of systems, whereby manipulation of small volumes in a controlled microchannel environment can occur to encourage mixing (Whitesides, 2006). Microfluidics, unlike the thin film lipid hydration method, produces liposomes in a single step process, and is described as a “bottom- up” approach (Akbarzadeh *et al.*, 2013). Formation of small liposomes from individual lipid monomers can occur so additional size reduction techniques needed for the “top- down” approach are unnecessary. The use of microfluidics, offers ease of scale-up as well as high throughput screening capability (as small volumes are sufficient), whilst maintaining high resolution and sensitivity. The increased efficiency of the process along with the fact it can decrease production cost has led to microfluidics becoming increasingly popular in the pharmaceutical industry.

In microfluidics chips, fluid streams converge due to the design of the chip; the organic phase (lipids dissolved in alcohol) flows through one channel whilst the aqueous phase (buffer) flows through the other. Formation of liposomes occurs by diffusion at the liquid interface, which is where the two fluid streams meet. At the interface, the mixing of the organic phase with the aqueous phase causes a decrease in the concentration of alcohol, due to diffusion and dilution (Capretto *et al.*, 2013). As such, the low concentration of alcohol causes the lipids to increase in polarity and precipitate to form lipid discs at the interface. The discs curve and assemble into vesicles with a lipid bilayer and aqueous core, due to the surface area of the lipids in the presence of decreasing alcohol concentration (Jahn *et al.*, 2010, Zook and Vreeland, 2010). Assembly can be controlled by varying the speed fluid flows through the channels, known as the Total Flow Rate (TFR) and by changing the ratio of buffer to lipid (referred to as the Flow Rate Ratio) (Jahn *et al.*, 2007).

The material used to make the chip is also an important parameter; early microfluidics systems used a range of materials including polydimethylsiloxane (PDMS), silicon, glass and steel but this was not good for biological research. Unlike the silicon chip, the PDMS polymer is a cheaper material for producing microfluidics chips. An extensive study of 30 typically used solvents has shown alcohols such as methanol do not cause damage to the chip (Lee *et al.*, 2003). However, the chip is also heat sensitive and can only be heated to a maximum of 60°C (Whitesides, 2006). At present there are a range of lab-on-a-chip microfluidics designs, with some specifically targeted for formulation development; as illustrated in Table 1.4 different approaches have been used to achieve this.

**Table 1.4.** The microfluidics devices available for the development of formulations.

<b>TYPE OF MIXING</b>	<b>DESCRIPTION</b>	<b>TYPE</b>	<b>REFERENCES</b>
<b>DIFFUSION</b>	<ul style="list-style-type: none"> <li>Multiple inlets and 1 outlet.</li> <li>Mixing occurs at the solvent boundary: controlled by channel length and speed.</li> <li>Diffusion is enhanced by adding a staggered herringbone structure.</li> </ul>	<ul style="list-style-type: none"> <li>T and Y shaped channels</li> <li>Can also contain the staggered herringbone structure</li> </ul>	(Gobby <i>et al.</i> , 2001, Damiani <i>et al.</i> , 2018)
<b>DROPLET GENERATOR</b>	<ul style="list-style-type: none"> <li>Encapsulation of molecules into droplets</li> <li>Droplets produced by electric fields, microinjections or needles</li> <li>Size of droplet depends on the chip geometry and flow focusing</li> </ul>	<ul style="list-style-type: none"> <li>T and Y shaped chips</li> <li>Co-flow junction</li> <li>Flow focusing junction</li> </ul>	(Quevedo <i>et al.</i> , 2005, Kim and Martin, 2006, Damiani <i>et al.</i> , 2018)
<b>CHAOTIC MIXING</b>	<ul style="list-style-type: none"> <li>improve mixing more than 2 fold</li> <li>addition of structures causes a change in the flow and induce whirls as it introduces more interface boundary interactions</li> </ul>	<ul style="list-style-type: none"> <li>slanted groove micromixer</li> <li>staggered herringbone structures</li> </ul>	(Stroock <i>et al.</i> , 2002)
<b>AUTOMATED MICROFLUIDICS MIXING</b>	<ul style="list-style-type: none"> <li>Computer controlled system; size, shape and formulation of droplets is pre-set</li> </ul>		(Riahi <i>et al.</i> , 2015)

### 1.2.3.3.1 Fluid dynamics of microfluidics systems

Two key factors that influence the production of liposomes during the microfluidics process are the Peclet's number (Pe) and Reynold's number (Re). The Peclet's number is used to calculate the nature and strength of diffusion. It is used to calculate the dimensions of the micro channels so diffuse mixing can take place. The Re is the number of inertial forces over viscous ones, hence low Re (< 2000) causes laminar flow whilst a number of > 3000 causes turbulent flow. Due to the small lengths in microchannels, Re is always less than 100 (Capretto *et al.*, 2011) therefore laminar flow always occurs.

$$Re = \frac{\rho u L_0}{\mu} = \frac{\rho u D_h}{\mu} = \frac{u D_h}{\nu}$$

$L_0$  = Characteristic length  
 $u$  = Fluid velocity  
 $D_h$  = Hydraulic channel diameter  
 $\nu$  = Kinematic viscosity  
 $\mu$  = Dynamic viscosity  
 $\rho$  = Fluid density

Equation 1.1 Reynold's Equation

$$Pe = \frac{u L_0}{D} = \frac{v w}{D}$$

$L_0$  = Characteristic length  
 $u$  = Fluid velocity  
 $w$  = Channel diameter  
 $D$  = Diffusion coefficient

Equation 1.2 Peclet's number

The volume of aqueous stream affects mixing and can ultimately influence the production of liposomes. At small volumes there is no turbulence; when the two liquids in separate micro-channels converge they flow in parallel. Mixing only occurs as a result of diffusion at the interface between the two liquids. The mixing of fluids by diffusion takes a long time, so to overcome this, various strategies have been developed. The two approaches can be classified as active or passive micromixers (Capretto *et al.*, 2011). The active micromixers require energy to aid the diffusion process, which can be achieved by ultrasound, pressure-driven or by electrowetting amongst other techniques. The active micromixers are not cost effective; they require a large amount of energy to aid mixing (Nguyen and Wu, 2004, Hessel *et al.*, 2005).

In contrast, passive micromixers do not require added energy to aid diffusion. The process is facilitated by the addition of strategically placed and designed microstructures that enhance the diffusion and advection process (Nguyen and Wu, 2004, Hessel *et al.*, 2005). Modifications to the chip include changing the microchannel lengths, splitting multiple flow streams, changing the chip geometry (T or Y-shaped), or even adding a staggered herringbone structure. Stroock *et al.* (Stroock *et al.*, 2002) developed the Staggered Herringbone Mixer (SHM) (Figure 1.2). The SHM has grooves on the base of the micro channels which aids diffusion by increasing mixing of fluids (Stroock *et al.*, 2002, Whitesides, 2006). This allows multiple fluid layers to flow on top of each other encouraging mixing (Stroock *et al.*, 2002). The incorporation of passive micromixers is a lot easier to implement into liposome manufacturing techniques as it requires less energy.

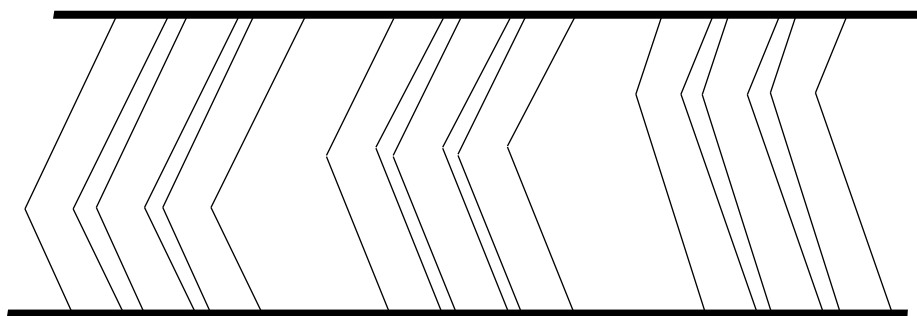


**Figure 1.2.** The structural layout of a staggered herringbone mixer section found inside a microfluidics chip. The herringbone grooves are added as sets, with the centre points offset from one another enabling changes in the flow of fluid therefore improving mixing.

In addition, one example of a commercial microfluidics device is the Microfluidics Nanoassemblr™ (Precision Nanosystems) (Figure 1.3). The chip is Y-shaped, with two inlet ports and micro-channels that converge. The liquid flows continuously through micro-channels and forms liposomes by the chaotic mixing principle, aided by the presence of staggered herringbone structures within the chip. The channels are 300  $\mu\text{m}$  in width and 130  $\mu\text{m}$  in height. Lipid(s) dissolved in an appropriate solvent (e.g. ethanol or methanol) are injected into one port whilst buffer is injected into the other. Assembly of liposomes is an automated process and unlike the thin film hydration process, it is possible to scale up microfluidics as multiple chips can be run in parallel.

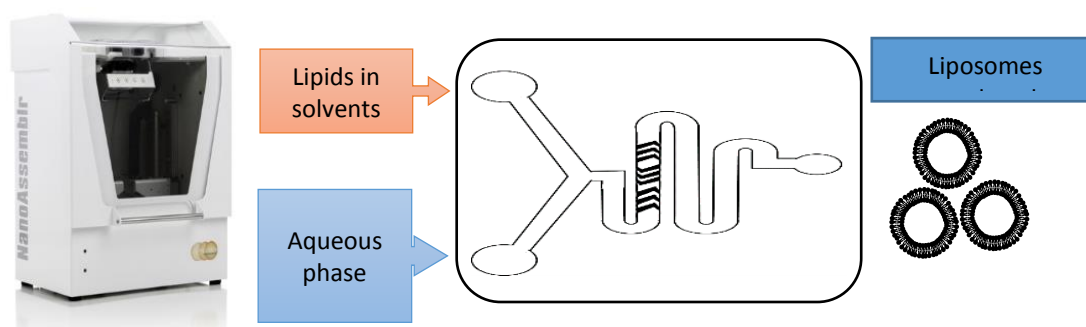


**Figure 1.3.** Image of the commercially available NanoAssemblr® Benchtop (Precision Nanosystems, Canada), alongside a schematic representation of the accompanying microfluidics chip to the device. Fluid enters through two inlet ports and mixing occurs via the chaotic mixing principle, with liposomes produced.

### 1.3 Liposomal medicines

There is a wealth of research into using liposomes for the delivery of drugs and proteins (including antigens), with some already on the market (Table 1.1). Most commonly, liposomal formulations (drugs and vaccines) are administered intravenously or intramuscularly (Wilkhu *et al.*, 2011). In the case of vaccines, liposomes are used because of their dual functionality; not only can they deliver material but they can elicit an immune response as they have adjuvant capabilities. This adjuvant capability was first described by Gregoriadis (Allison and Gregoriadis, 1974) and has subsequently led to the investigation of liposomes, and their ability to deliver a whole host of drugs and proteins (Christensen *et al.*, 2012). The adjuvant ability of liposomes is particularly important when developing subunit vaccines. Often, the protein used will be unable to invoke a strong immune response without the addition of immunomodulatory compounds such as lipids (Schwendener *et al.*, 2014). Second, despite liposomal vaccines being relatively expensive, they are good delivery vehicles for antigens including proteins, peptides, DNA or RNA. The range of moieties they can carry, as well as their functional ability, make them a good delivery choice. For instance, positively charged cationic liposomes can interact with negatively charged nucleic acids (DNA, RNA and mRNA), proteins and peptides. Due to the opposite charges they can be adsorbed onto the surface as well as entrapped inside the liposome (Henriksen-Lacey *et al.*, 2010b). Compared to neutral liposomes and anionic liposomes, positively charged liposomes are able to entrap protein (particularly anionic in nature) more efficiently and promote a depot effect at the site of injection (Kaur *et al.*, 2012). Studies have shown OVA (ovalbumin) or cationic OVA mixed

with either neutral, anionic or cationic liposomes produces different antibody responses (Yan and Huang, 2009).

For instance, cationic liposomes are good immune stimulators and are extensively studied for use in liposomal vaccines. Liposome formulation consisting of dimethyldioctadecylammonium (DDA) and trehalose 6,6-dibehenate (TDB) has been shown to improve the immune responses for a range of sub-unit antigens. DDA is a synthetically derived quaternary ammonium lipid. It is an amphiphilic molecule with a positively charged head group and two hydrophobic tails, and was first described as immunostimulatory by Gall (Gall, 1966). When DDA is placed in an aqueous environment it forms cationic liposomes and due to its cationic nature it is able to bind a range of proteins. DDA alone is able to produce a moderate T- helper cell 2 (Th2) response and a strong Th1 response (Lindblad *et al.*, 1997). The addition of TDB, an immunostimulatory compound derived from the mycobacterial cell wall, enhances the immunostimulatory capability of liposomes. TDB allows the activation of antigen presenting cells (APCs) via the mucosa-associated-lymphoid-tissue lymphoma-translocation gene 1 (MALT1) pathway (Werninghaus *et al.*, 2009). This DDA:TDB formulation, known as CAF01, can be used to promote a strong Th1 response against Ag85B-ESAT-6 fusion sub-unit antigen (H1) (Henriksen-Lacey *et al.*, 2010b). However, at times the cationic liposomal formulations can trigger a strong immune response when it is not required.

### **1.3.1 Protein loaded liposomal formulations**

The physicochemical properties of drugs, DNA and protein are all susceptible to clearance and breakdown from the body. In particular, proteins are large in size, highly hydrophilic and susceptible to degradation (explained further in Chapter 5.1.1.2 and 5.1.2), which in turn impacts the pharmacology (pharmacokinetics and pharmacodynamics) of these active pharmaceutical ingredients (APIs). The main hindrance of using proteins as therapeutics is that they are extremely fragile; susceptible to denaturation by many environmental conditions (such as solvent and heat) and aggregation (Crommelin, 2016, Salmaso *et al.*, 2006, Lu *et al.*, 2006). The addition of surfactant can improve the stability of proteins, limiting unfolding of the protein so that structural integrity is maintained. Alternatively, other approaches such as the addition of polyethylene glycol (PEG) chains to the protein to improve

stability, clearance and uptake have been used (Veronese and Mero, 2008). Examples of PEGylated proteins currently on the market include Neulasta® (Amgen Ltd, Cambridge, UK), a PEGylated recombinant human granulocyte colony-stimulating factor analog filgrastim, used to improve white blood cell count (Neulasta, September 2018). Another example of a PEGylated biologic is Cimzia® (UCB, Brussels, Belgium) the Fab portion of the antibody, used to treat a variety of conditions including Crohn's disease and rheumatoid arthritis (Dozier and Distefano, 2015). However, modifications to the protein are not always possible and so alternative methods are needed for the biologics to reach the target site. One such way is the use of nanoparticles as delivery vehicles; these can include polymeric particles, lipoplexes and liposomes. Based on the fragility of proteins, the ability to encapsulate protein within liposomes was investigated, with production of these formulations needing to overcome a unique set of challenges (highlighted in Chapter 5.4). As a result, the production of protein loaded liposomes by microfluidics was investigated in this thesis.

### **1.3.2 Biodistribution and targeting of liposomes**

The biodistribution of liposomes can be controlled by a range of factors, and whether uptake of the liposome is passive or active. Passive targeting is the non-specific trafficking of liposomes to the therapeutic site. In order for the liposomes to reach their target site, they must avoid the mononuclear phagocytic system (MPS) (Sawant and Torchilin, 2012). To avoid uptake by the MPS, strategies have been developed to allow for long circulation time of liposomes. One such strategy is to coat liposomes with polyethylene glycol (PEG); a hydrophilic compound that occupies the space surrounding the surface of the liposome. The PEG layer acts as a protective coating around the liposomes and stops macromolecules and other physiological proteins from binding, thus avoiding detection by the MPS (Immordino *et al.*, 2006). Due to PEGylation, liposomes can avoid the MPS cells and are able to circulate for longer. This long circulating ability of PEGylated liposomes is exploited for drug delivery, particularly for anticancer drugs. These systems rely on the enhanced permeability and retention (EPR) effect to deliver drugs at the desired therapeutic concentration.

The EPR effect is the retention of large molecules at the tumour site due to physiological changes such as increased angiogenesis, defective vasculature, decreased lymphatic drainage and wider fenestrations between cells (Fang *et al.*, 2011). As a result, liposomes can accumulate at the tumour site passively through a process known as extravasation. Drugs on



the market that take advantage of this include the anti-cancer drug Caelyx® (Eloy *et al.*, 2014). The size and charge of the liposomes can determine functionality, with larger and charged liposomes more likely to be picked up by MPS cells. MPS cells can also be the target of passive drug delivery, if an immune response is desired (Eloy *et al.*, 2014).

In addition, specific targeted release liposomes are being investigated so that cargo is only released as a response to a certain trigger. There are many triggered release systems under investigation including light, temperature and pH sensitive liposomes (Torchilin, 2005). For instance, pH sensitive liposomes have been developed as possible anti-cancer treatments. Research by Simões and group (Simões *et al.*, 2001), developed formulations that exploit the difference in pH for release of cargo. Initially the difference in pH at the tumour interstitial fluid (pH = 6.5) and the blood (pH = 7.4) was investigated, however the small pH difference (of 0.9) did not cause sufficient destabilisation of liposomes and promote drug release. Instead a strategy that causes the disruption of the liposomal formulations at pH 5, the pH inside the cell cytoplasm, has been developed (Simões *et al.*, 2001). These particular liposomes are made of fusogenic lipids such as 1,2-Dioleoyl-sn-glycero-3-phosphoethanolamine (DOPE). The lipids when exposed to acidic conditions undergo a formation change; protonation of the weakly ionized head-group causes destabilisation of the liposomes (Litzinger and Huang, 1992) releasing the drug contents into the cell.

Other strategies include immunoliposomes and thermal sensitive liposomes that often use lipids with high transition temperature such as 1,2-dipalmitoyl-sn-glycero-3-phosphocholine (DPPC) (41°C) and 1,2-distearoyl-sn-glycero-3-phosphocholine (DSPC) (55°C). Immunoliposomes are liposomes that have antibody or fragments of antibody attached either directly or indirectly on the surface, to allow direct targeting to specific sites. Production of immunoliposomes relies on an understanding of the physiological components present in the disease and how it differs from the norm (Bazak *et al.*, 2015). For instance, ED-B fibronectin is an isoform of fibronectin specific to tumour sites so a single chain antibody (which is a fragment of antibody) has been added to liposomal formulations to direct cell targeting (Marty and Schwendener, 2005). All the active targeting strategies have the potential for efficient delivery of pharmaceutical compounds. These strategies need further exploring as they all have advantages and disadvantages associated with them. Hence it depends on the target site and disease condition as to what type of targeting is picked, or perhaps a combination strategy would be more useful (Bazak *et al.*, 2015).

### 1.3.3 Clearance of liposomes

Therapeutic liposomal formulations need to avoid clearance; there are many mechanisms that aid clearance that need to be avoided or limited for the formulations to be effective. Factors such as size, play a huge role in this. Previous research has shown liposomes that are 500 nm or larger in size, are more likely to be cleared by the immune system, compared to liposomes less than 150 nm in size, which are not as readily recognised by the MPS system (Kraft *et al.*, 2014) . The small size allows the formulations to pass through fenestrated capillaries entering into a tumour microenvironment (Kraft *et al.*, 2014). Research has shown there are three main ways clearance can occur; (1) by cells of the MPS, (2) the complement system, and (3) binding of LDLs (low density lipoproteins) and HDLs (high density lipoproteins) to liposomes (Immordino *et al.*, 2006).

Liposomes are readily coated in plasma proteins and complement proteins, facilitating the opsonisation of the vesicles (Immordino *et al.*, 2006). The MPS cells (macrophages, neutrophils and monocytes) recognise and remove liposomes associated with plasma protein from the blood circulation (Scherphof *et al.*, 1985).

#### 1.3.3.1 Liposomal targeting of antigens

Liposome can be designed to trigger an immune response (with the aim of producing antibodies) to treat specific conditions. This is achieved by targeting antigen specific cells such as macrophages. In general, there are two ways in which an immune response can be triggered; by triggering the major Histocompatibility complex 1 (MHC 1) or Major Histocompatibility complex 2 (MHC 2) system (Janeway *et al.*, 2005). Uptake of liposomal formulations containing therapeutics (such as proteins or peptides) can occur by endocytosis depending on the size of the formulations, with receptor mediated uptake also possible. Upon uptake of the formulations, processing of the formulations occurs. Briefly, the formulations with cargo, are broken down by proteosomes. A protein called Transporter associated with antigen processing (TAP), found in the membrane of the endoplasmic reticulum (ER), transports the peptides to the lumen of the rough endoplasmic reticulum. Also found in the ER is the MHC1 complex in association with  $\beta$ 2 microglobulin. Through a series

of interactions, the peptide binds to the cleft of the MHC1 molecule and is subsequently transported to the cell surface by the golgi apparatus. Some crossover between the MHC1 and MHC2 pathway is possible, with peptides displayed on MHC2. As a result, displaying these peptides can trigger the intended immune responses required (Allen and Cullis, 2004).

#### 1.3.3.2 Cellular pathways involved in liposome uptake

Liposomes and many other nanoparticles have been investigated in order to understand how they illicit their therapeutic effect (He *et al.*, 2010). Depending on the therapeutic effect desired it is possible to target different uptake routes of liposomes into cells. The most common uptake route for liposomes is by endocytosis; either via Clathrin mediated endocytosis or caveolae mediated endocytosis. The clathrin pathway involves the use of the cytosol protein clathrin, which has a three- legged triskelion structure (Rejman *et al.*, 2004). Endocytosis occurs when clathrin forms pits, causing an invagination in the cell membrane of about 150 nm allowing for small sized molecules to be taken up. The alternative caveolae endocytosis pathway is characterised by flask like invaginations. These invaginations are a result of the dimeric protein caveolin binding to cholesterol and sphingolipids in the cell membrane. It has been reported that endothelial cells such as Caco-2 cells contain 10- 20% more of this protein.

The endocytosis pathway used by the cells is dependent on the size, shape and charge of the liposomes. In a study by Andar and colleagues (Andar *et al.*, 2014), the uptake mechanisms of liposomes ranging from 40.6 nm to 276.6 nm was investigated in Caco-2 cells. Results show uptake via clathrin mediated endocytosis was size dependent; liposomes 97.8 nm and 162.1 nm in size underwent clathrin mediated endocytosis. Larger molecules around 500 nm in diameter are subjected to caveolin mediated endocytosis (Rejman *et al.*, 2004). The shape also greatly influences uptake, with spherical nanoparticles 500 % more likely to be taken up then rod shaped particles, which can be explained by the greater wrapping time required for the uptake of rod-like structures (Jiang *et al.*, 2008). The liposomal charge also influences uptake by cells, with cationic liposomes taken up at a better rate compared to neutral liposomes due to cells having a slightly negative charge, therefore aiding interaction and internalization (Mao *et al.*, 2005).

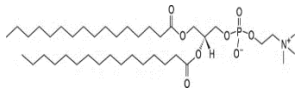
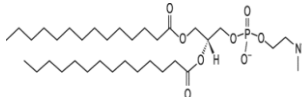
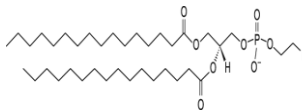
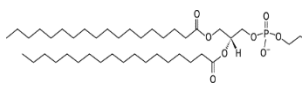
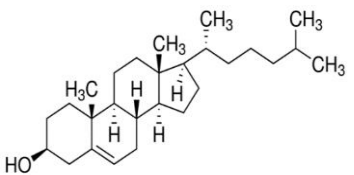
Alternatively, other uptake routes include phagocytosis by MPS cells (macrophages, neutrophils and dendritic cells) and macropinocytosis. Phagocytosis usually occurs for liposomes around 500 nm upwards. The process involves three key stages; (a) opsonisation in the blood by complement proteins (b) recognition by receptors on the phagocytic cells and (c) internalization of the liposomes. The new formed phagosome will then fuse with a lysosome (containing enzymes) for the break-down and release of contents. Depending on the nature of the therapeutic compound it may be further processed or affect the cells directly, causing toxicity and subsequent cell death. It is important to note, the maximum liposome size a cell can internalize varies depending on the cell type and even subtype. For instance, alveolar macrophages can phagocytose liposomes as big as 3- 6  $\mu\text{m}$  in diameter whilst peritoneal macrophages have a range between 0.3- 1  $\mu\text{m}$  in size (Hirota and Terada, 2012).

#### **1.4 Lipid Selection**

The properties of lipids influence the functional capability of liposomes. The majority of liposomal therapeutic formulations on the market consist of simple lipids. For instance, the liposomal formulation Myocet<sup>®</sup> used to treat breast cancer, consists of egg phosphatidylcholine together with cholesterol. Keeping this in mind, four neutral phosphatidylcholine (PC) derivatives similar in molecular weight and structure to PC but with varying hydrocarbon tail length were investigated (Table 1.5). The transition temperatures of these four lipids varies as a result of the hydrocarbon tail length, and is the temperature at which lipids go from an ordered gel phase to the liquid crystalline phase. Cholesterol (Chol), an abundant molecule found in bio-membranes, was added to these formulations as it is important for membrane stability, organisation, dynamics and function (Allen and Cullis, 2013). It decreases rotational freedom of the phospholipid hydrocarbon chains, therefore cholesterol stabilises the bilayer and smaller amounts of hydrophilic compounds are able to permeate through the bilayer of liposomes (Eloy et al, 2014). Not surprisingly, cholesterol can be found in many of the current liposomal formulations on the market including Doxil<sup>®</sup> (see Table 1.1). For instance, research looking into the impact of lipid type on doxil loading has found saturated lipids (such as egg phosphatidylcholine) without cholesterol take up very little of the drug. In contrast, the presence of cholesterol in these formulations significantly increases loading of doxil (Farzaneh *et al.*, 2018) thus highlighting the importance of this lipid.

The inclusion of cholesterol also improves the stability of formulations, with better controlled drug release at 1:1 or 2:1 lipid to cholesterol ratios (Briuglia *et al.*, 2015), therefore cholesterol was added to the formulations manufactured throughout this thesis.

**Table 1.5.** Structural and general information about the lipids used to produce neutral liposomes.

Name	Structure	Mw	Tc (°c)	Additional information
<b>Phosphatidylcholine (PC)</b>		770	0	Mixture of neutral lipids. Abundantly found in cell membranes. Generally obtained from natural sources such as soy beans or egg yolk.
<b>1,2-dimyristoyl-sn-glycero-3-phosphocholine (DMPC)</b>		678	24	A neutral lipid with a 14 hydrocarbon tail length.
<b>1,2-dipalmitoyl-sn-glycero-3-phosphocholine (DPPC)</b>		734	41	A neutral lipid with a 16 hydrocarbon tail length.
<b>1,2-distearoyl-sn-glycero-3-phosphocholine (DSPC)</b>		790	55	A neutral lipid with an 18 hydrocarbon tail length.
<b>Cholesterol</b>		386	-	A neutral lipid obtained from sheep's wool. Although, it is referred to as a 'sterol' due to its physical structure consisting of four hydrocarbon rings typical to a steroid structure, as well as a hydrocarbon tail and a hydroxyl group. The hydroxyl group is able to form H bonds with phospholipids and thus is a key regulator of fluidity for liposomes and other phospholipid structures.

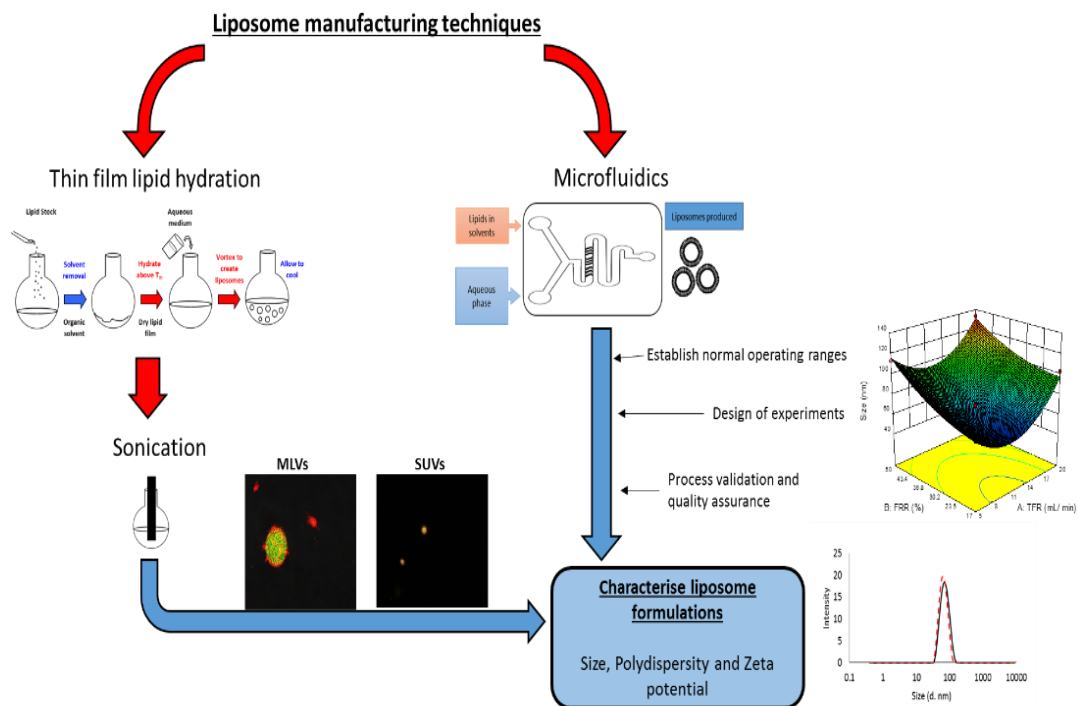
## 1.4 Aim and Objectives

Given the growing interest in liposomal research for therapeutic use, there is a need for efficient manufacturing processes for the production of these formulations. Increasingly, microfluidics technology is an approach that is being considered for the manufacture of these products, however the scalability and process parameters for optimal liposomal formulations are not well defined. As a result, the overall aim of this thesis was to investigate microfluidics technology (with particular emphasis on defining optimal parameters) for the production of a range of liposomal formulations. The objectives of this thesis are to:

1. Compare and characterise liposomal formulations produced by different manufacturing methods (sonication and microfluidics).
2. Identify the ideal parameters and normal operating ranges for different formulations types, as well as using statistical processes such as design of experiments (DoE).
3. Investigate a scalable method for the manufacture of liposome formulations, with the ability to monitor the process so that the product remains within designed specification.
4. Develop rapid high-throughput protein quantification methods using high-performance liquid chromatography.
5. Determine the ability of microfluidics technology to encapsulate proteins and small molecular drugs, as well as long circulating liposomal formulations. Compare and contrast the physicochemical properties of these formulations with traditional manufacturing methods.
6. Investigate the parameters associated with liposomal formulation uptake and processing.
7. Identify formulation components and parameters that allow for the stable freeze-drying of liposomal formulations, with consideration to high-throughput freeze drying using various freeze drying vessels. The experimental design space and optimal freeze-drying method will be determined using DoE.

# Chapter 2

## Characterisation of liposomes



Work presented in this chapter has been published in:

1. JOSHI, S., HUSSAIN, M. T., ROCES, C. B., ANDERLUZZI, G., KASTNER, E., SALMASO, S., KIRBY, D. J. & PERRIE, Y. 2016. Microfluidics based manufacture of liposomes simultaneously entrapping hydrophilic and lipophilic drugs. *International journal of pharmaceutics*, 514, 160-168.
2. FORBES, N., HUSSAIN, M. T., BRIUGLIA, M. L., EDWARDS, D. P., HORST, J. H. T., SZITA, N. & PERRIE, Y. 2019. Rapid and scale-independent microfluidic manufacture of liposomes entrapping protein incorporating in-line purification and at-line size monitoring. *International Journal of Pharmaceutics*, 556, 68-81.



## 2.1 Introduction

### 2.1.1 Liposome manufacturing techniques

At present, a range of liposomal manufacturing techniques exist to produce liposomal drugs on the market or in clinical trials. In general, the majority of these products are manufactured using the “top- down” approach, with the majority of techniques having adapted the thin film liposome production technique (Bangham and Horne, 1964).

#### 2.1.1.1 Thin film lipid hydration method to produce liposomes

The thin film lipid hydration method is a traditional production technique and is associated with producing liposomes using the “top- down” approach. The method involves dissolving a mixture of lipid in an organic solvent and evaporating it to remove the solvent, forming a thin film (Figure 2.1). The film is then hydrated with an aqueous solution to form liposomes. The large multi-lamellar vesicles produced are then downsized using a range of techniques such as sonication. Whilst this thin film lipid hydration is good for the small scale production of liposomes in the laboratory setting, its use in manufacturing for industrial purposes is limited due to problems in scalability and batch to batch uniformity. As a result, other techniques have been developed.

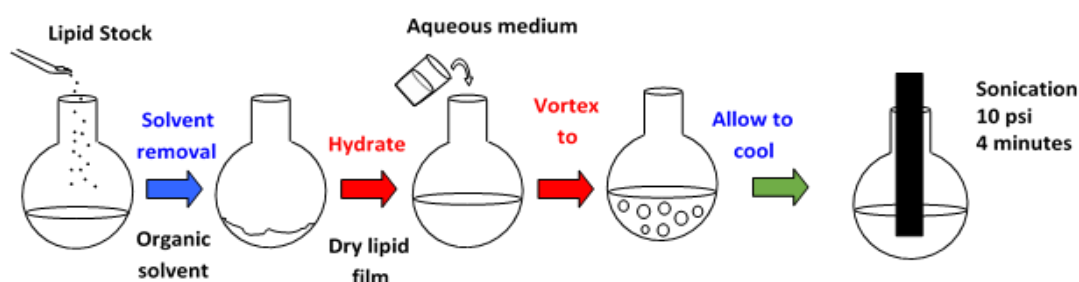


**Figure 2.1.** The thin film lipid hydration method for the production of liposomes. Lipids dissolved in solvent is evaporated in a round bottom flask using a rotary evaporation, forming a dry film. The film is then hydrated to produce liposomes forming multi-lamellar vesicles. The multilamellar vesicles are then down sized using probe sonication at a set time.

### 2.1.1.2 Microfluidics method to produce liposomes

Microfluidics is a lab-on-a-chip approach used to produce liposomes. It has the ability to produce liposomes in a single step process, and is described as a “bottom- up” approach (Akbarzadeh *et al.*, 2013). Formation of small liposomes from individual lipid monomers can occur so additional size reduction techniques are need for the “top- down” approach are unnecessary. The use of microfluidics, offers ease of scale-up as well as use for high throughput screening (as small volumes are sufficient), whilst maintaining high resolution and sensitivity. The increased efficiency of the process along with the fact it can decrease production costs has led to microfluidics becoming increasingly popular in the pharmaceutical industry. One microfluidics device commercially available is the microfluidics Nanoassemblr® Benchtop (Precision Nanosystems, Inc.) (Figure 2.2), which is able to produce liposomes in a single step (as described in Chapter 1.2.3.3.1).



**Figure 2.2.** Image of the commercially available NanoAssemblr® Benchtop (Precision Nanosystems Inc, Vancouver, Canada).

### 2.1.2 Liposome size

Liposomes have been extensively researched for their use as drug delivery vehicles. For liposomal drug formulations to be useful they have to avoid clearance by the reticuloendothelial system (RES). There are many mechanisms that aid clearance which need to be avoided or limited if the liposomal drugs are to be effective. In order to achieve this, the size of liposomes is key; with previous research having shown the rate of clearance is proportional to the size (Harashima and Kiwada, 1996). Liposomes that are 500 nm or larger are likely to be cleared by the immune system. Small liposomes, less than 150 nm in size are

less likely to be recognised by APCs, and can reach the target site (Kraft *et al.*, 2014). Adding to this, the uptake of liposomes is dependent on several liposomal characteristics including size. Small liposomes (less than 150 nm) are more easily and readily taken up by a wide range of cells. The most common uptake route for liposomes less than 150 nm is by endocytosis; either via Clathrin mediated endocytosis or caveolae mediated endocytosis (Andar *et al.*, 2014). Liposomes that are larger in size, can be taken up by phagocytosis from phagocytic cells (macrophages, monocytes, neutrophils and dendritic cells) and by micropinocytosis (Hirota and Terada, 2012). Depending on the desired therapeutic effect, it is possible to target different uptake routes and cells by changing the size of liposomes. As a result, this important liposomal characteristic is investigated thoroughly, and is clearly defined when developing liposomal formulations (ICH (Guideline, 2005b)).

## **2.2 Aim and Objectives**

The aim of the work within this chapter was to characterise liposome formulations produced by microfluidics. Liposomes were produced by various techniques and the effect on the physicochemical properties were investigated. To achieve this aim, the objectives of this chapter were to:

- 1) Compare liposome production methods
- 2) Establish a design space for liposomes produced by microfluidics
- 3) Investigate the optimal working parameters for liposomes produced by microfluidics.

## **2.3 Methods and Materials**

### **2.3.1 Materials**

Phosphatidylcholine (PC), 1,2-dimyristoyl-sn-glycero-3-phosphocholine (DMPC), 1,2-dipalmitoyl-sn-glycero-3-phosphocholine (DPPC), and 1,2-distearoyl-sn-glycero-3-phosphocholine (DSPC) from Avanti Polar Lipids Inc., Alabaster, USA. Cholesterol, trifluoroacetic acid, Sephadex® G-75 and, D9777-100ft dialysis tubing cellulose was obtained from Sigma Aldrich Company Ltd., Poole, UK. Disposable macro sized optical polystyrene

cuvettes (634-0677BTU) were used to determine the size and polydispersity of liposomes (VWR International., Pennsylvania., USA). To measure the zeta potential, the DTS1070 Zeta cuvettes were used (Malvern Panalytical., Malvern., UK). For purification of untrapped protein by dialysis, a Biotech CE Tubing MWCO 300 kD was used (Spectrum Inc., Breda, The Netherlands). Purification by Tangential flow filtration (TFF), a modified polyethersulfone (mPES) 750 kD MWCO hollow fibre column was used (Spectrum Inc., Breda, The Netherlands). A Luna column (C18 (2), 5  $\mu\text{m}$ , dimensions 4.60 X 150 mm, pore size 100 Å) was used for lipid quantification and purchased from Phenomenex., Macclesfield, UK. HPLC grade Methanol and 2-propanol were purchased from Fisher Scientific., Loughborough, England, UK.

## **2.3.2 Methods**

### **2.3.2.1 Liposome manufacturing techniques**

#### *2.3.2.1.1 Thin film lipid hydration*

To produce liposomes using the lipid-film hydration method, lipids were dissolved at specific concentrations in a chloroform:methanol mixture (v/v 9:1). Lipids dissolved in solvent were then placed under a vacuum rotatory evaporation for 6 minutes at 200 rpm in a heated water bath (20- 60°C) to remove solvent. Hydration of the lipid film was achieved by the addition of phosphate buffered saline (PBS) (pH 7.3).

#### *2.3.2.1.2 Microfluidics production of liposomes*

Lipids were either dissolved in ethanol or methanol, at the appropriate concentrations. Tris (10 mM, pH 7.4) or phosphate buffered saline (PBS) (10 mM, pH 7.3) were used to form the aqueous medium. A range of parameters were tested including changing the speed of flow through the chip, referred to as the Total Flow Rate (TFR) and the Flow Rate Ratio (FRR).

### **2.3.2.2 Downsizing techniques**

#### *2.3.2.2.1 Sonication*

Multilamellar vesicles (MLVs), produced by thin film lipid hydration, can undergo size reduction by probe sonication. A 9.5 mm titanium probe sonicator (Soniprep 150, MSE Labs, UK) was used to produce SUVs. The tip of the sonication probe was placed on the surface of the mixture and sonicated for 4 minutes at 10 Hz. To remove any possible metal debris from the tip, the samples were centrifuged for 10 minutes at 500 x g.

### **2.3.2.3 Purification techniques**

#### *2.3.2.3.1 Dialysis to remove solvent*

Liposomes prepared by microfluidics require the solvent to be removed. To do this, D9777-100ft dialysis tubing cellulose was prepared by boiling the membrane at 80°C for 2 hours in 2% bicarbonate buffer and 1 mM EDTA in 1 L of water. After this, the membrane was washed with deionised water and cut into approximately 6 cm strips. Dialysis clips were used to tie one end, after which 1 mL of the liposome sample was added. The membrane was then sealed and placed into 200 mL beaker containing 200 mL of either Tris or PBS buffer (10 mM, pH 7.3) for a set amount of time to remove residual solvent present.

#### *2.3.2.3.2 Sephadex® G-75 columns*

Sephadex® G-75 columns were used for removal of solvent and unbound protein. For purification of liposome formulations, 1 mL of liposomes and 0.5 mL of PBS buffer was added. The first 1.5 mL of permeate was discarded, and 3 mL of buffer was added to the column. This causes the elution of the liposomes, which are collected and can be further tested.

### **2.3.2.4 Dynamic light scattering**

Dynamic light scattering (DLS) was used to analyse the size of liposomes, (ideally between 0 - 1000 nm), with the Z-average and polydispersity index (PDI) given, using the Malvern Zetasizer Nano ZS (Malvern Panalytical Ltd, Malvern, UK). Liposome sample was added into PBS diluted to 1:300 to measure the size and PDI. The zeta potential was also measured using DTS1070 Zeta cells (Malvern Panalytical, Malvern, UK). The settings used for the dynamic light scattering are shown below (Table 2.1).

**Table 2.1.** Liposomes size parameters for the Malvern Zetasizer Nano ZS.

INFORMATION	MATERIAL	SIZE & POLYDISPERSITY	ZETA POTENTIAL
	Refractive index	1.45	1.45
	Absorption	0.001	0.001
<b>SAMPLE</b>	<b>Dispersant</b>	Water	Water
	Temperature	25°C	25°C
	Viscosity	0.8872 cP	0.8872 cP
	Refractive index	1.330	1.330
<b>GENERAL</b>	Equilibrium time	30s	30s
<b>OPTIONS</b>	Cell type	634-0677BTU (VWR)	DTS1070
<b>MEASUREMENT</b>	Angle	173° Backscatter	
	Number of runs	Automatic	Automatic
	Number of measurements	3	3
	Delay between measurements	10s	Between 10s
	Data Processing	General purpose (normal resolution)	General purpose (normal resolution)

### 2.3.2.5 Lipid quantification

HPLC- ELSD (high performance liquid chromatography- evaporative light scattering detector) was used to quantify the lipid recovery within liposomes. To detect the lipids, a Luna column (C18 (2), 5 µm, dimensions 4.60 X 150 mm, pore size 100 Å) was used, at a flow rate of 2 mL/min. A twenty minute elution gradient, composed of solvent A (0.1% TFA in water) and solvent B (100% methanol) was used. During the first six minutes the gradient was 15:85 (A:B), at 6.1 minutes 0: 100 (A:B) and then back to the initial gradient of 15:85 (A:B) from 15.1 to 20 minutes. Standard calibration curves were established for each lipid, and the lipid recovery was calculated as a peak area of the sample in relation to the standards.

### **2.3.2.6 Flame ionised detector (FID) gas chromatography**

The presence of solvent in samples was quantified using the Ellutia 200 series gas chromatography (Elluita, Cambridgeshire, UK). The detection column used was TRACE 15m x 0.25 mm x 0.25  $\mu$ m TR-5, with the Clarity DataApex version 2.4.1.9.1 software used. The gas chromatography (GC) was turned on 30 minutes prior to use. The injection temperature was 200°C, the detector temperature was 230°C, with Helium as the carrier gas (flow rate of 100 mL/sec). Samples of 1  $\mu$ L were injected directly into the column and detected via flame ionization. All samples contained Propan-1-ol as an internal control to account for any variations in injection volume. A calibration curve was established using varying concentration of solvent, with the concentration of unknown solvent calculated using the peak area of analyte in relation to the standards.

### **2.3.2.7 Design of experiments**

The statistical software package, Design Expert 10 (Stat-Ease) was used to plan and implement the design of experiments looking at the ideal parameters needed to produce the smallest liposome size, PDI and zeta potential. Results are represented as mean  $\pm$  SD with n=3 independent batches.

### **2.3.2.8 Statistical package**

Results are represented as mean  $\pm$  SD with n=3 independent batches. ANOVA and T-tests tests were used to assess statistical significance, with a Tukey's post adhoc test (p value of less than 0.05).

## 2.4 Results and discussion

### 2.4.1 Liposome production techniques

#### 2.4.1.1 Comparison of thin film lipid hydration (with sonication) and microfluidics for the production of liposomes

Despite advances in our understanding of liposomes for drug delivery, there is a lack of clinical translation of liposome drug delivery systems. In particular there is a bottle neck in the production which is due to a combination of problems related to manufacturing (including quality assurance and costs), government relations and issues with intellectual property (Narang *et al.*, 2013, Allen and Cullis, 2004). Quality assurance (QA) are procedures put in place for the maintenance of manufactured products to a high standard. Liposome manufacture has many problems related to QA manufacturing process including (a) scalability, (b) reliability and reproducibility, (c) lack of equipment and expertise, (d) denaturation or chemical instability of the encapsulated compound during manufacture and (e) stability (Narang *et al.*, 2013, Sercombe *et al.*, 2015). Whilst large scale manufacture of conventional liposomes products seen on the market can be achieved (Jaafar-Maalej *et al.*, 2012, Kraft *et al.*, 2014), the cost of manufacturing is expensive. Producing more complex liposomes (with modifications) is very difficult, therefore the production of four neutral liposomal formulations with different production techniques was evaluated.

To investigate the production of liposomes using various methods, the efficiency of liposome production by microfluidics was compared to a conventional production technique involving thin film hydration, followed by sonication to down-size four liposome formulations (2:1 wt/wt) with varying hydrocarbon tail length (PC:Chol, DMPC:Chol, DPPC:Chol and DSPC:Chol). The results in Figure 2.3 show that microfluidics produces liposomes are smaller than those made by sonication, irrespective of the hydrocarbon tail length (Figure 2.3). Across all 4 formulations tested, the difference in size between the two production techniques is statistically significant ( $p < 0.0001$ ), with microfluidics producing liposomes between 48 – 68 nm compared to 176- 221 nm for sonicated liposomes (Figure 2.3). Indeed, the liposome produced by sonication were more than triple the size of liposomes produced by microfluidics (Figure 2.3A). Similarly, the PDI of the liposomes produced via microfluidics was very small ( $< 0.2$ ; Figure 2.3B), illustrating a narrow liposome range compared to sonicated liposomes (from 0.34- 0.44; figure 2.3A). The results show sonication is not ideal

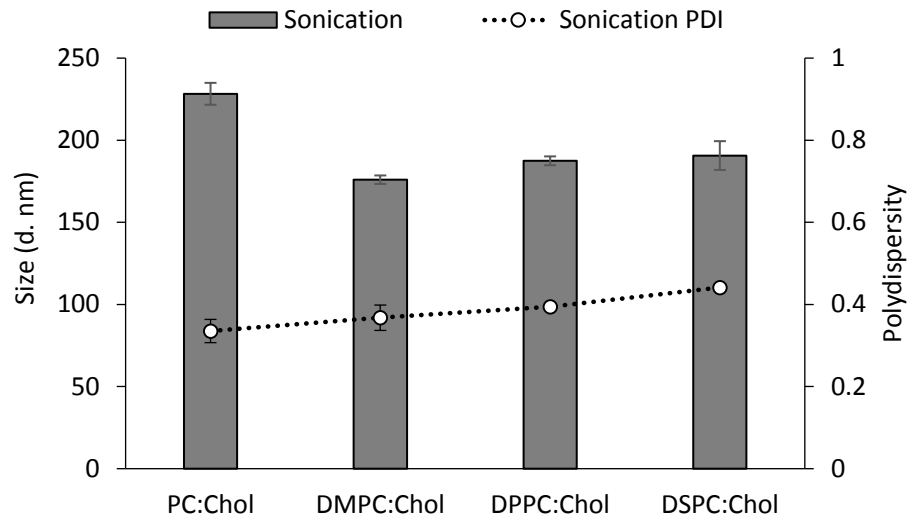


for the production of liposomes. Although sonication is widely used to break down MLVs by acoustic energy (Mendez and Banerjee, 2017), there is little process control. The temperature is often hard to regulate and often batch to batch inconsistencies occur.

In contrast, microfluidics offers the ability to fine – tune liposomes by regulating the rate of mixing and the ratio of lipid to buffer. Studies using similar microfluidics chip dimensions have found the microfluidics offers greater process control (Jahn *et al.*, 2007). Previous studies by Jahn *et al* have shown the ability of microfluidics to produce liposomes ranging from 50 -200 nm in size by changing process controls (Jahn *et al.*, 2004), but these studies lacked comparison to traditional manufacturing techniques, with the results from Figure 2.3 addressing this issue.

In addition, the production of liposomes by microfluidics is quicker as it is a single step process, whilst producing small unilamellar vesicles (SUVs) by thin film hydration/sonication is a multistep method. These multiple stages increase the likelihood for batch to batch variation. The hydration phase in the thin film lipid hydration method relies on self-assembly of liposomes by reconstitution with buffer. During this process, it is possible not all lipids are exposed to the same amount of hydration buffer, thus accounting for variations in liposomes sizes and the formation of multilamellar vesicles (Akbarzadeh *et al.*, 2013). Further downsizing such as sonication, compounds this problem, producing liposomes with varying internal volumes and encapsulation efficiency. This harsh downsizing technique can also cause degradation of phospholipids in an uncontrolled manner, accounting for the larger liposomes sizes seen for the sonication method (Akbarzadeh *et al.*, 2013).

A



B

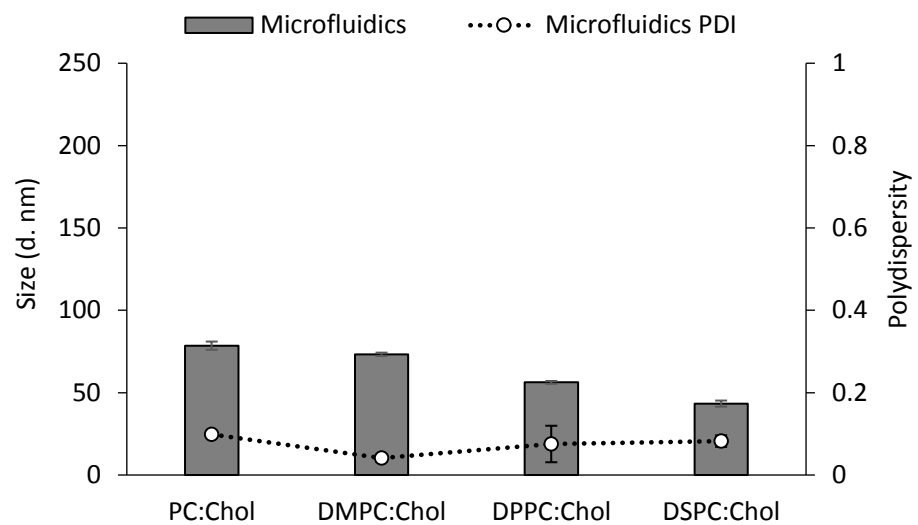


**Figure 2.3.** Comparison of liposome attributes produced by either thin film lipid hydration followed by sonication (A) or microfluidics (B). The physicochemical properties for liposomal formulations (PC:Chol, DMPC:Chol, DPPC:Chol and DSPC:Chol) was investigated, with liposomal physicochemical properties measured using dynamic light scattering. The results represent mean  $\pm$  SD, n=3 independent batches.

#### **2.4.1.2 The effect of formulation components on liposome physicochemical properties produced by microfluidics**

The microfluidics production technique is more efficient at producing liposomes in comparison to traditional techniques. Besides the production techniques, the type of materials (including lipid type, concentration and buffer type) can influence the physicochemical characteristics of liposomes to varying degrees. The aqueous buffer is an essential component of all liposome formulations. Many types of buffer including Tris, citrate and phosphate buffered saline (PBS) can be used, which all have different ionic compositions (Mozafari, 2010). For instance, PBS is an ionic buffer commonly used in liposome formulations, consisting of sodium chloride, sodium phosphate and (potassium chloride in some formulations) (Morris *et al.*, 2001). The effect of Tris and PBS buffer (at pH 7.3), alongside changes to the solvent phase (ethanol or methanol), were investigated. Particular attention was paid to the changes in liposomes physicochemical properties of four neutral liposomes produced by microfluidics.

Results from Figure 2.4 show the type of solvent (ethanol or methanol) and buffer (PBS or Tris) has minimal effects on liposome physicochemical characteristics. Figures 2.4A and 2.4B show similar results for the liposomes made with methanol, despite the aqueous buffer differing. Liposomes produced with PBS (Figure 2.4A) and Tris (Figure 2.4B) follow the same trend; as the hydrocarbon tail of the lipid gets longer the sizes of the liposomes decreases. This is evident in both Figure 2.4A and 2.4B where DSPC:Chol liposomes are the smallest liposomes out of the four neutral formulations, at  $50 \pm 2$  and  $49 \pm 3$  nm respectively. The largest liposomes formed for both aqueous conditions were the PC:Chol liposomes with a size of  $69 \pm 3$  nm for PBS buffer and  $77 \pm 8$  nm for Tris buffer. As evident, there is no significant difference in the liposomes produced with either Tris or PBS. The formulations are all homogenous with a PDI of less than 0.2 and a zeta potential between -5 to 0 mV (Figure 2.4).

When considering the effect of solvent, liposomes produced by ethanol (Figures 2.4C and 2.4D) are below 100 nm in size. Figure 2.4C (ethanol with PBS buffer) follows the same trend as seen with Figure 2.4A-B; PC:Chol liposomes (shown in Figure 2.4C) are the largest in size ( $99 \pm 1$  nm) with the size decreasing as the hydrocarbon tail length of the lipids increases. Once again, the DSPC:Chol liposomes form the smallest liposomes at around 68 nm (Figure 2.4C). Whilst a trend can be observed, the difference in liposome sizes across all four formulations in Figure 2.4C is not significant. In comparison, Figure 2.4D (ethanol with Tris

buffer) does not show the trend seen for Figure 2.4A-C. The smallest liposomes produced at this condition are PC:Chol liposomes with a size of  $54 \pm 11$  nm, with the other three formulations below 100 nm too (Figure 2.4D). All formulations produced using ethanol with Tris buffer (Figure 2.4D), were homogenous with a PDI of below 0.2 and have neutral zeta potentials (-5 to 0 mV).

The results show the solvent choice has minimal effect on liposome physicochemical properties, with removal of solvent necessary as both ethanol and methanol are toxic to humans. Of more importance is how effective the solvents are at dissolving lipid as the initial lipid concentration is known to influence liposome size. The alcohol methanol can dissolve lipids at higher concentrations in comparison to ethanol, so this was an important consideration when selecting the solvent to use. Also, the ion composition of the buffer does not significantly affect liposome physicochemical properties (as shown by the use of PBS and Tris buffer). The similar sizes, despite the difference in solvent and buffer can be attributed to the fluid mixing process that occurs during microfluidics manufacturing. During microfluidics, the aqueous and solvent stream (containing the lipids) meet at the solvent-buffer interface. At this point the concentration of solvent changes causing the lipids to precipitate and form bilayer discs, to form liposomes. As all the liposomes are produced using the same manufacturing conditions (a 3:1 flow rate ratio and 15 mL/min TFR), it is likely the fluid mixing has a greater influence on the liposome size than the solvent and buffer choice. The results show both methanol and ethanol can be used for these systems as they offer suitable lipid solubility. Also, the PBS buffer is commonly used and preferred for the production of liposomes. It has an ion compositions and osmolality closely match that of humans (Dulbecco and Vogt, 1954), thus this was selected for all further work (unless stated otherwise).

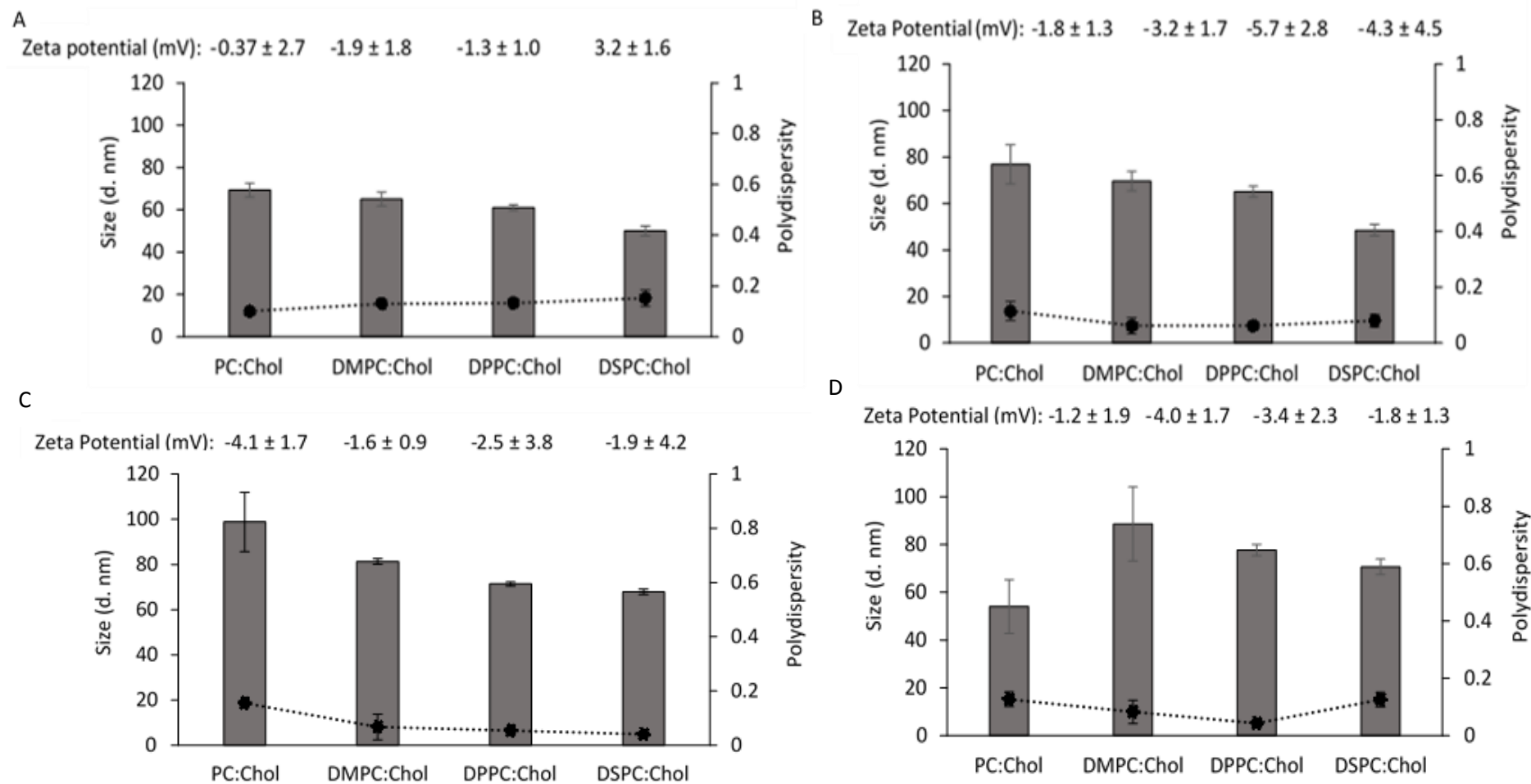


**Figure 2.4.** Testing parameters for the 3:1 FRR. Liposomes composed of PC, DMPC, DPPC, DSPC and cholesterol were prepared by microfluidics. The Physicochemical properties of liposomes produced by methanol with PBS (A) or Tris buffer (B), and ethanol with PBS (C) or Tris buffer (D) were investigated. Results represent mean  $\pm$  SD, n=3 independent batches.

### 2.4.1.3 Stability of liposomes produced by microfluidics

The stability of liposomes is important as changes to liposomes size (due to aggregation or fusion) as well as loss of encapsulated compounds from leakage (Crommelin *et al.*, 1994, Kettenes-van den Bosch *et al.*, 2000), can impact the overall functionality of the formulations. Destabilisation of the liposomes can occur by oxidation of the lipids or by hydrolysis of ester bonds and, can impact storage as well as shelf life of liposomes (Kettenes-van den Bosch *et al.*, 2000). Given microfluidics is a relatively new technique, the effect of this manufacturing process on liposome stability is not well understood. Therefore, the thermal stability of liposomes produced by microfluidics was investigated. To test this, lipids with transition temperatures above (DSPC ( $T_c = 55^\circ\text{C}$ )) and below (DMPC ( $T_c = 23^\circ\text{C}$ )) physiological temperature were selected. The thermal stability of DMPC:Chol and DSPC:Chol liposome formulations produced by microfluidics were tested across different temperatures. The temperatures chosen ( $5^\circ\text{C}$ , room temperature and  $37^\circ\text{C}$ ) were in accordance with the International conference on harmonisation guidelines ((ICH) (Guideline, 2016)). The  $5^\circ\text{C}$  was used to reflect long term stability. Room temperature was also tested for storage conditions and  $37^\circ\text{C}$  to reflect physiological temperature.

The results from Figure 2.5 and 2.6 shows both formulations are stable across a range of temperatures, with no significant changes in size observed after 48 hours. Despite some fluctuations in size for DMPC:Chol liposomes, the changes are not significant with the formulation remaining around 60 nm after 48 hours (Figure 2.5A). This is reflective in the low PDI (Figure 2.5B) and zeta potential above -10 mV (Figure 2.5C). Similarly, the DSPC:Chol liposomes are also stable over 48 hours at all three temperatures. There is no significant changes in size, with the formulation remaining around 57 nm in size (Figure 2.6A). The PDI remains low (Figure 2.6B), and the zeta potential remains between -5 and 0 mV (Figure 2.6C), suggesting the formulation is stable.

Furthermore, results from Figures 2.5 and 2.6 show the manufacturing technique does not adversely impact the liposomal formulations. The stability data of DMPC:Chol and DSPC:Chol liposomes produced by microfluidics, is similar to literature where neutral liposomes produced by traditional methods are stable over 48 hours (Anderson and Omri, 2004). Work by Anderson *et al* comparing lipids with varying hydrocarbon tails (DMPC, DPPC, and DSPC) found the lipid composition to be the most important factor affecting lipid stability. The DSPC liposome formulation was the most stable at around 85 nm over a 48 hour period (Anderson

and Omri, 2004). In general, liposomes containing lipids with higher transition temperatures (DSPC,  $T_c = 55^\circ\text{C}$ ) are more stable; however, no difference in stability between DMPC:Chol (Figure 2.5) and DSPC:Chol (Figure 2.6) is observed over 48 hours. This is due to the high cholesterol content of 50:50 mol% lipid to cholesterol present in the formulations, compared to the 21% cholesterol used by Anderson and Omri. It is well documented that cholesterol provides stability to liposomes (Raffy and Teissie, 1999, Kirby *et al.*, 1980), thus the results from Figures 2.5 and 2.6 suggest microfluidics is a good alternative for the production of liposomes, with the formulation composition the determining factor of liposome stability.

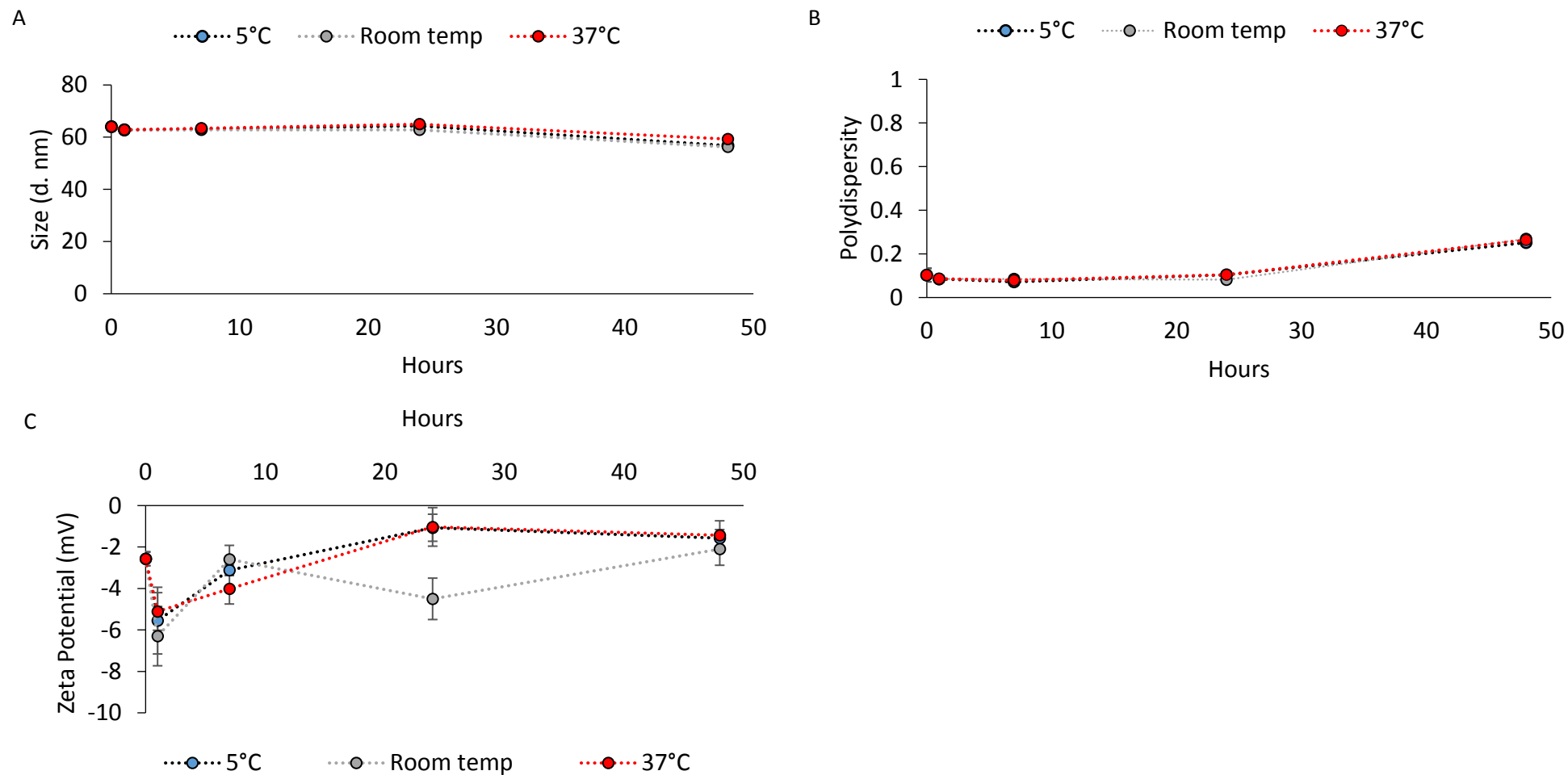


**Figure 2.5.** Stability of empty DMPC:Chol liposomes produced by microfluidics over 48 hours. The formulations were kept under three different test conditions (5°C, 25°C and 37°C), with changes to liposome size (A), PDI (B) and zeta potential (C) measured using dynamic light scattering. Measurements were taken at set time points over 48 hours. Results represent  $n = 3 \pm \text{SD}$ .



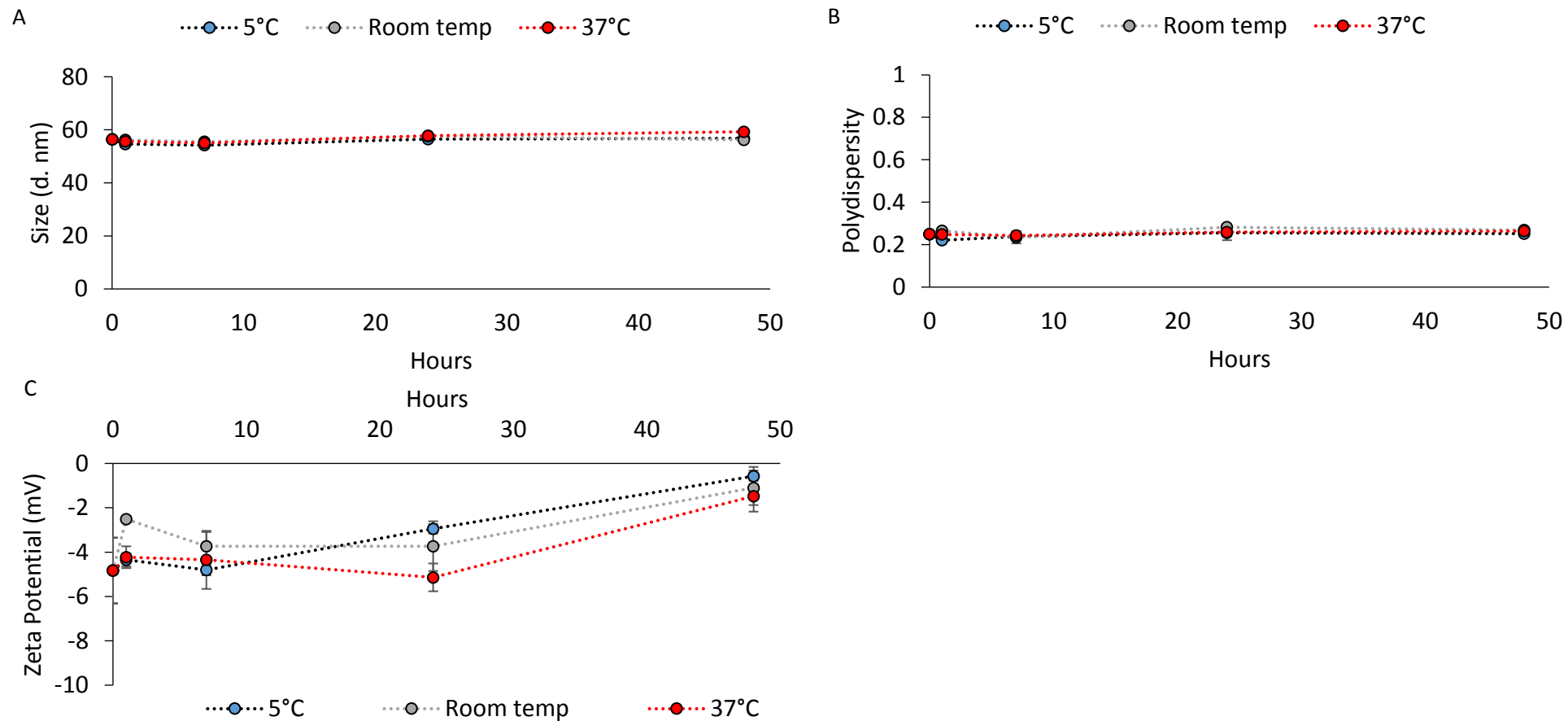


**Figure 2.6.** Stability of empty DSPC:Chol liposomes produced by microfluidics over 48 hours. The formulations were kept under three different test conditions (5°C, 25°C and 37°C), with changes to liposome size (A), PDI (B) and zeta potential (C) measured using dynamic light scattering. Measurements were taken at set time points over 48 hours. Results represent  $n = 3 \pm \text{SD}$ .

#### 2.4.1.4 The effect of cholesterol amount on liposome physicochemical properties

As mentioned, the addition of cholesterol into liposomal formulations is well documented to enhance stability, by integrating into the lipid bilayer. Cholesterol improves stability by increasing the packing densities of the phospholipids (Semple *et al.*, 1996), as cholesterol packs into the molecular cavities formed by the rearrangement of lipid molecules into bilayers (Devaraj *et al.*, 2002). Thus, this space-filling action of cholesterol results in a more compact bilayer (Epand *et al.*, 2003). It reduces drug leakage and membrane permeability (Gregoriadis and Davis, 1979) which has been shown by many researchers, using a multitude of manufacturing techniques.

The DMPC:Chol formulation was selected to investigate the effect of different cholesterol to lipid ratios on physicochemical characteristics, and to determine whether the microfluidics production technique has any impact (Figure 2.7). Results from Figure 2.7 show a trend of increasing cholesterol content decreases liposome size. At a ratio of 1:1 (50:50 mol%) lipid to cholesterol, the smallest DMPC:Chol liposomes were produced at around 80 nm (Figure 2.7A). A decrease in cholesterol content to 3:1 (75:25 mol%) lipid results in an increase in liposome size; the liposome size is around 100 nm (Figure 2.7). Further decreasing the cholesterol content further to a 7:1 (87.5: 12.5 mol%) ratio resulted in the largest liposome size of  $122 \pm 3$  nm (Figure 2.7A). The PDI values are reflective of the increase in size, with the 7:1 ratio having the highest PDI of 0.26 (Figure 2.7A). The zeta potentials for all three DMPC:Chol formulations was above -10 mV, which is within the expected range for neutral liposomes and did not notably change over the time period. The intensity plots (Figure 2.7B) along with the PDI, show that all three formulations are homogenous.

The results indicate the ability of microfluidics to form liposomes irrespective of the amount of cholesterol. The ratio of cholesterol to lipid influences the size of the liposomes produced which may be useful when wanting to produce liposomes of a particular size range. The cholesterol content is a key formulation attribute; cholesterol up to 50:50 mol% can readily dissolve and integrate into the bilayer, whilst anything higher than this leads to the formation of crystals (Epand *et al.*, 2003). The ratio of cholesterol in liposomal formulations also affects release rates. Liposomes consisting of a 1:1 ratio of lipid to cholesterol are the most stable. Research in mice using PC liposomes has found a lower ratio of cholesterol to PC lipid results in a faster release of 6- carboxyfluorescein (Kirby *et al.*, 1980). The effect of

cholesterol is observed irrespective of the charge of liposomes, thus illustrating the importance of cholesterol for release profiles as well as stability (Kirby *et al.*, 1980). In addition, the presence of 50:50 mol% cholesterol is known to negate the gel-to-liquid phase transition temperature of liposomes (Moghaddam *et al.*, 2011). The removal of the transition temperature coupled with the single step production of liposomes from lipids, removes the requirement of heat for production irrespective of the lipids used.

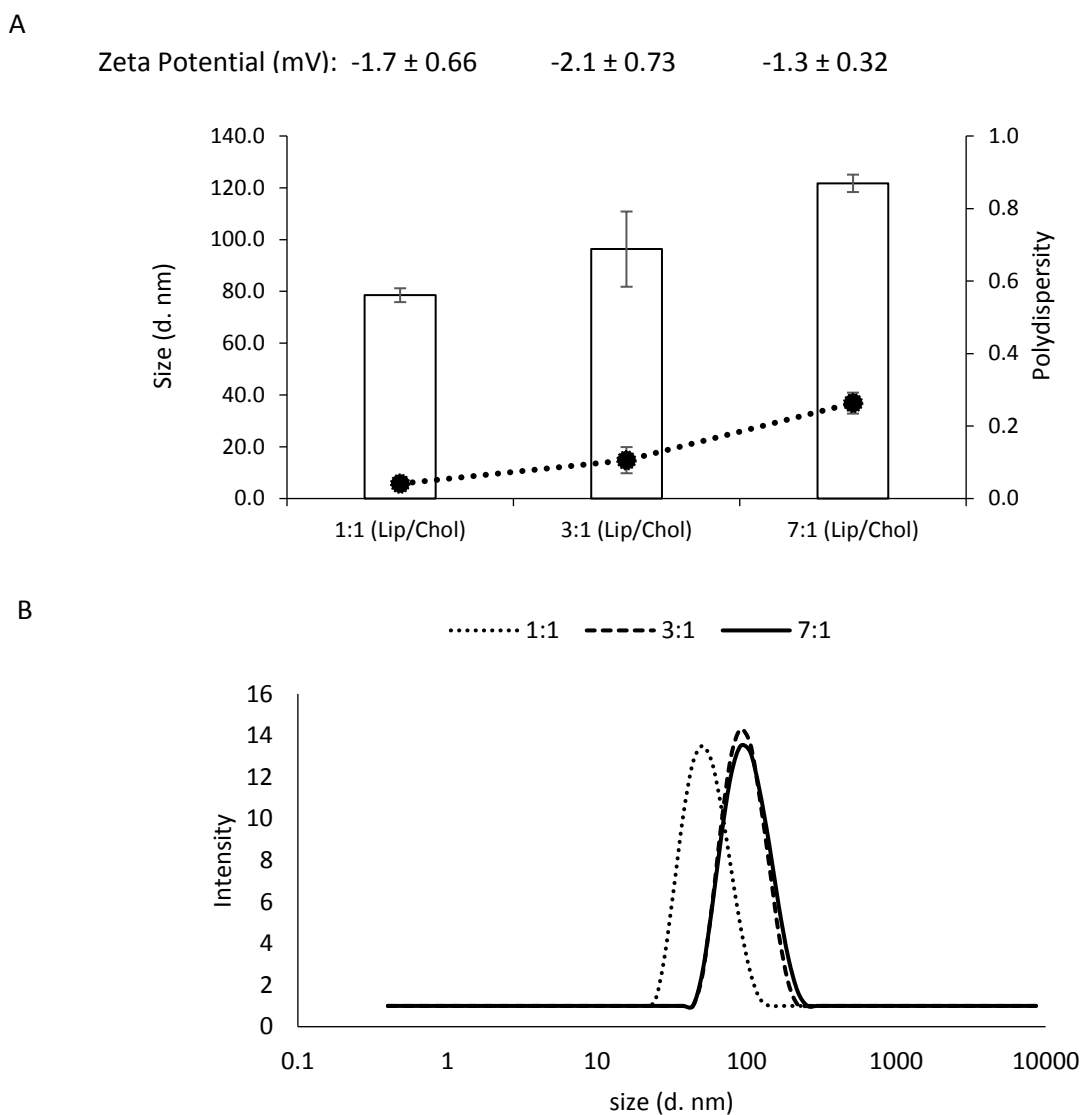


**Figure 2.7.** The effect of cholesterol on DMPC:Chol liposome physicochemical properties. The DMPC:Chol liposomes were produced with varying amount of cholesterol to lipid, by microfluidics at a 3:1 FRR and 15 mL/ min TFR. The size, PDI and zeta potential of the liposomes was measured using dynamic light scattering (A) with the size intensity plots shown (B). Results represent mean  $\pm$  SD, n=3 independent batches.

#### 2.4.1.5 Determining normal operating ranges and parameters for liposomes produced by microfluidics

To support the application of microfluidics for the manufacture of liposomes there is a need to establish standardised operating ranges and parameters. Whilst the effect of lipid concentration has briefly been investigated with PC liposomes (Joshi *et al.*, 2016), to further production control and understanding, lipid concentration as a process parameter of four neutral liposome formulations was investigated. To achieve this, four liposome formulations were prepared using phospholipids with increasing hydrocarbon tail length (and transition temperature) i.e. PC:Chol, DMPC:Chol, DPPC:Chol and DSPC:Chol. The results from Figure 2.8 show at lipid concentrations below 2 mg/mL, lipid concentration is an influencing factor in vesicle size with liposome size reducing with increasing concentration (Figure 2.8A). Above 2 mg/mL initial lipid concentration, the concentration has no significant impact on liposome size with all liposomes ranging between 52- 114 nm (depending on the lipid composition), with a PDI of  $\leq 0.2$  (Figure 2.8B). As expected, the zeta potential was approximately -10 mV for all four formulations (Figure 2.8C). This trend was observed irrespective of the lipid hydrocarbon tail length. These results help identify the lipid concentration as an important parameter that must be considered when developing a design space for liposome production using microfluidics. This is in line with previously reported studies (Joshi *et al.*, 2016) where we investigated PC:Chol liposomes and Figure 2.8 demonstrates this effect applies to a range of liposome formulations.

Furthermore, whilst establishing the normal operating ranges and parameters, a trend was spotted. The size was plotted against the hydrocarbon tail length of the four lipids (Figure 2.9), at varying initial lipid concentrations (0.3 - 10 mg/mL). The effect of the hydrocarbon tail length of the PC on the resulting liposomes size and PDI was investigated post solvent removal (Figure 2.9). The lipids have the following hydrocarbon tail length: PC (a mixture of lipids, so it was taken as 12 hydrocarbon tail length), DMPC (14 hydrocarbon tail length), DPPC (16 hydrocarbon tail length), and DSPC (18 hydrocarbon tail length). Results from Figure 2.9 in general show the longer alkyl chain (higher transition temperature) lipids formed smaller liposomes at any given concentration in comparison to lower transition temperature lipids (Figure 2.9). As the phospholipid alkyl chain length (PC up to DSPC) is increased, a trend of decreasing vesicle size from around 100 nm down to 60 nm in the case of the lowest lipid concentration tested (0.3 mg/mL initial concentration) is observed. This trend of decreasing

liposome size with increasing alkyl chain length is evident across all concentrations tested (from 0.3 mg/mL to 10 mg/mL; Figure 2.9). The decrease in vesicle size as lipids with longer lipids are used can be attributed to two factors: the length of the hydrocarbon tail and the presence of cholesterol. In terms of bilayer structure, the surface curvature of SUVs differs from that of MLVs (Huang and Mason, 1978). The curvature can heavily influence the molecular packing of phospholipids in the bilayer; the outer bilayer of SUVs tend to have loosely packed head groups and tightly packed hydrocarbon chains. The reverse is observed for the inner bilayer phospholipid packing (Komatsu *et al.*, 2001). Previous research has found increasing the hydrocarbon tail length of saturated lipids from 14 (DMPC) to 16 (DPPC) and 18 (DSPC), causes an increase in the bilayer thickness of liposomes produced. The positive linear relationship is reflected by DSPC liposome bilayers which are thicker than the DMPC bilayer (Lewis and Engelman, 1983). The increasing hydrophobic layer thickness of DMPC, DPPC and DSPC liposomes (at 29.6 Å, 32.2 Å, and 38.6 Å at 50°C respectively) (Kučerka *et al.*, 2011) may influence the curvature of the liposomes, resulting in smaller vesicles (Israelachvili *et al.*, 1977). In addition, using neutron scattering and solid state <sup>2</sup>H NMR, Marquardt *et al.* found the presence and position of cholesterol is influenced by the thickness of the liposome bilayers (Marquardt *et al.*, 2016). In thinner bilayers, the cholesterol tilts and can be found in the bilayer centre, whilst in thicker bilayers the cholesterol is in an upright position (Marquardt *et al.*, 2016). The upright position of cholesterol in DSPC:Chol liposomes allows for greater interactions with the lipids, thus DSPC:Chol liposomes are smaller in size compared to PC:Chol liposomes.

In addition, the degree of lipid saturation can also influence the position of cholesterol. To test this, recent research comparing two lipids with the same alkyl chain length but different transition temperatures, DSPC (T<sub>m</sub> of 55°C) and DOPC (T<sub>m</sub> of -17°C) (Forbes *et al.*, 2019) were investigated. The DOPC:Chol liposomes were 40 nm larger (85 ± 4.3) in comparison to DSPC:Chol liposomes (42 ± 0.18 at 1 mg/mL). The results suggest the amount of saturation impacts the packing ability of liposomes, thus all factors influencing liposome size must be considered. Furthermore, Figure 2.9B shows all liposome formulations produced have a low PDI (less than 0.2). This is achieved irrespective of the lipid concentration, the lipid transition temperature or lipid alkyl chain length, demonstrating the highly homogenous nature of the liposomal products produced via microfluidics.

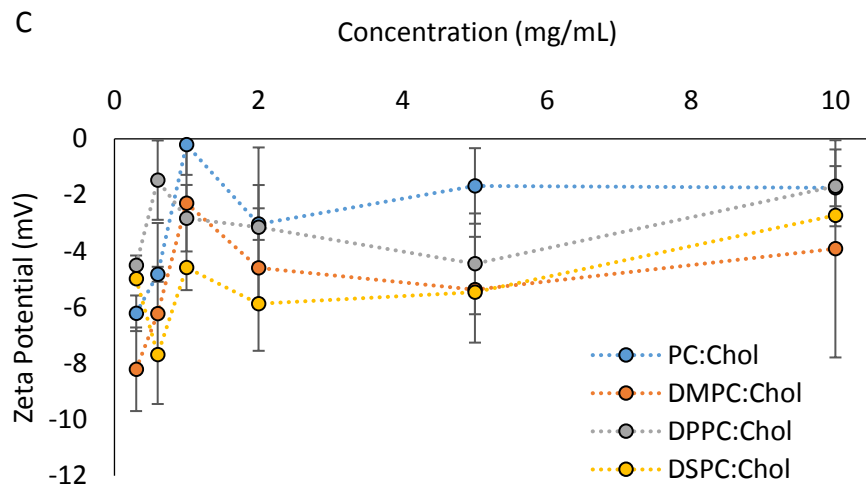
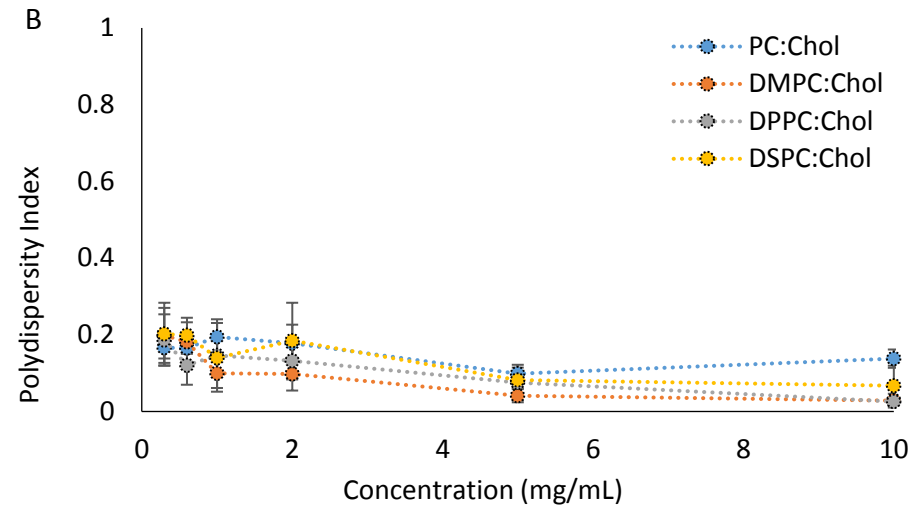
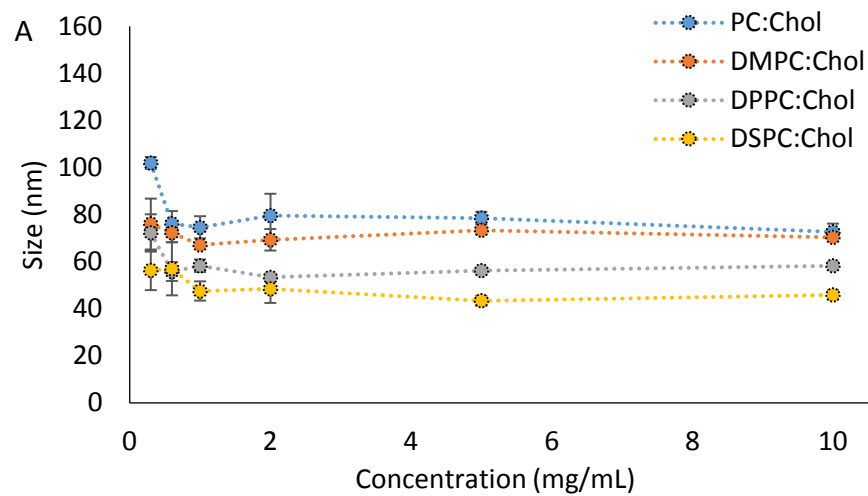


**Figure 2.8.** The size of liposome formulations made at concentrations ranging from 0.3- 10 mg/mL of the initial lipid concentration. The four liposome formulations were made using microfluidics at a 3:1 flow rate ratios (FRR) and 15 mL/min flow rate (TFR). Results represent mean  $\pm$  SD, n=3 independent batches.

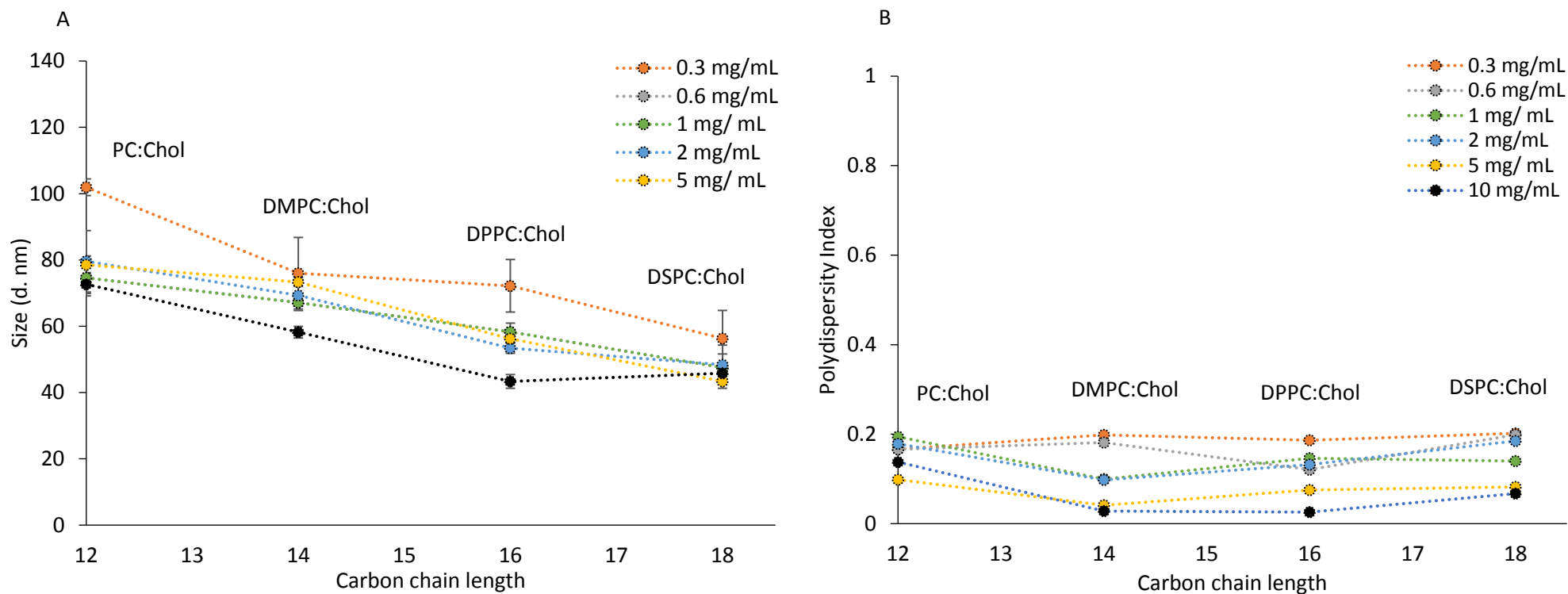


**Figure 2.9.** The effect of liposomal formulation on physicochemical characteristics. Four liposome formulations (PC:Chol, DMPC:Chol, DPPC:Chol and DSPC:Chol) with increasing hydrocarbon tail length (and transition temperature) were manufactured using microfluidics at a 3:1 FRR and 15 mL/min TFR. The effect of transition temperature on liposomes size (A) and PDI (B) was investigated. (Note: PC is a mixture of lipids so the value is for illustration purposes). Results represent mean  $\pm$  SD, n=3 independent batches.

## 2.4.2 Effect of microfluidics parameters

### 2.4.2.1. Investigating the use of temperature during the production of liposomes by microfluidics

The heating block is a feature of the NanoAssemblr® Benchtop that allows lipids and buffer to be heated whilst being manufactured. Generally for the production of liposomes using lipid-hydration methods, liposomes must be formed above their transition temperature (Szoka Jr and Papahadjopoulos, 1980). To investigate if this was required for liposome production using microfluidics, DMPC:Chol liposomes at a final concentration of 2 mg/mL were formulated (at 3:1 FRR and 15 mL/ min TFR) at either room temperature or at 70°C. The results from Figure 2.10 show increasing the manufacturing temperature does not influence the liposome attributes. The size remains around 65 nm for DMPC:Chol liposomes formulated at both temperatures (Figure 2.10A). The liposomes formed are homogenous, illustrated with a PDI below 0.2 (Figure 2.10B). The zeta potential remains above -10 mV (Figure 2.10C) and the size distribution illustrated by the single intensity peak remains the same (Figure 2.10D). The results show the manufacturing temperature does not significantly impact liposomal physicochemical properties.

The results from Figure 2.10 suggest liposome formulations can be made without the heating block. Heating during microfluidics manufacture does not impact the DMPC:Chol liposome physicochemical properties, thus suggesting heating is not required during liposome manufacture. The key component in controlling liposome physicochemical properties, is the cholesterol content. Differential scanning calorimetry (DSC) and neutron scattering have shown the addition of cholesterol of 50 mol % to DMPC liposomes, can lead to the suppression of the main phase transition (Peters *et al.*, 2017, McElhaney, 1982). This is reflected in Figure 2.10, whereby DMPC:Chol liposomes containing 50 mol% cholesterol do not require heat, and confirm the liposomal properties are independent of heat used during microfluidics manufacturing. Similar findings were also presented by Forbes *et al.*; DSPC:Chol liposomes produced by microfluidics (at a 50:50 lipid to cholesterol mol%) over a range of process temperatures (room temperature to 60°C) showed no impact on DSPC:Chol liposome (Forbes *et al.*, 2019). The size remained around 50 nm, whilst changing the ratio of DSPC lipid to cholesterol (from 16- 50 mol%) impacted liposomes size (Forbes *et al.*, 2019). At 16 mol% cholesterol, the largest sized DSPC:Chol liposomes were produced at around 150 nm. All



DSPC:Chol liposomes (with differing cholesterol ratios) could be prepared at room temperature with no effect on liposomes size (Forbes *et al.*, 2019). The formulation composition influences liposome characteristics (shown by Figure 2.10), and is not transition temperature dependent. As a result, microfluidics can be used to formulate a range of liposomes of varying lipid temperatures and combinations. It can be argued the single step microfluidics production technique is more cost effective compared to traditional production techniques (Hood *et al.*, 2014), especially when producing liposomes containing cholesterol.

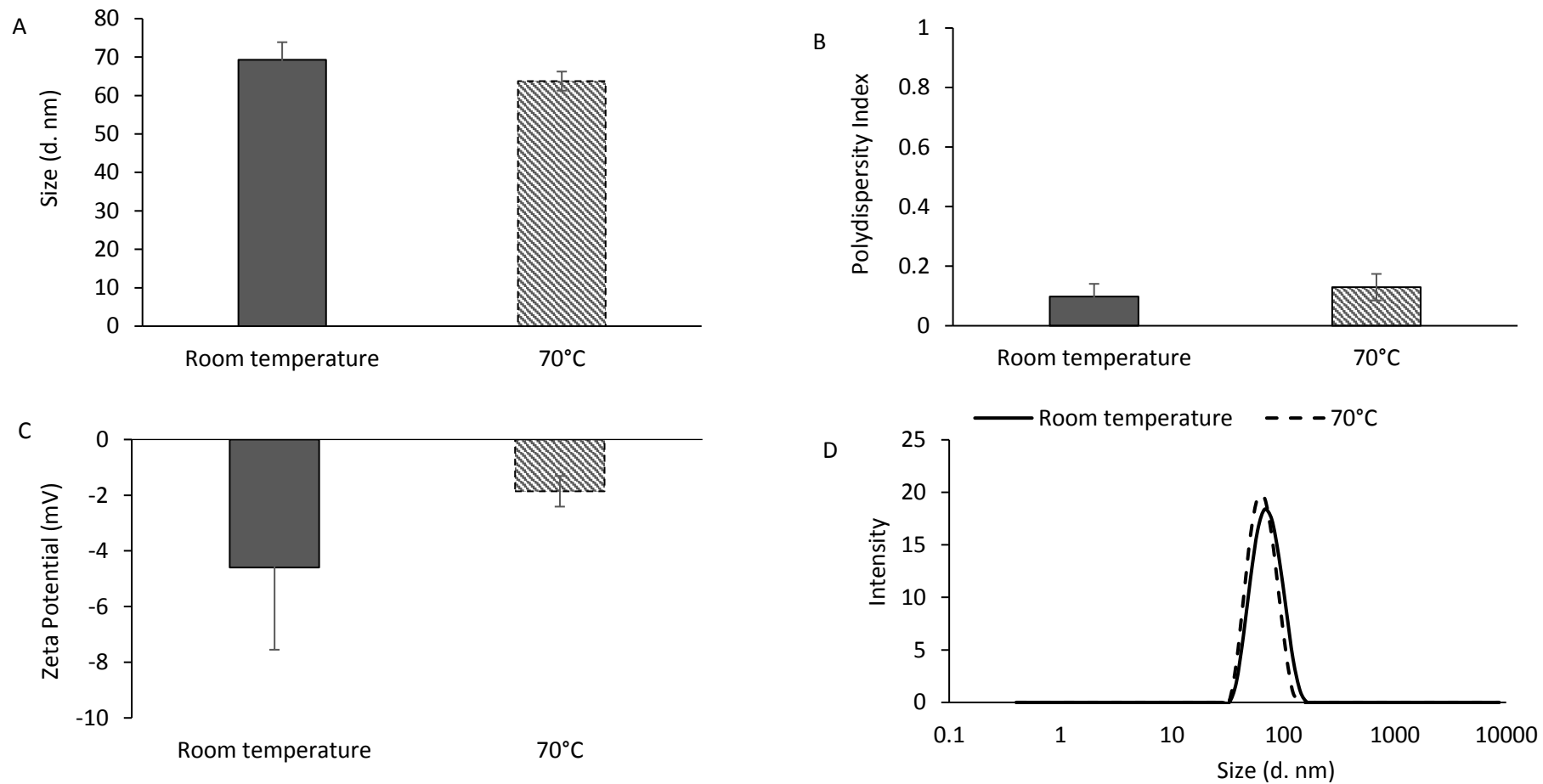


**Figure 2. 10.** The effect of heating DMPC:Chol liposomes during the production process of microfluidics was tested. DMPC:Chol liposomes was made at room temperature and 70°C. The size (A), PDI (B), zeta potential (C), and intensity plots (D) were obtained using dynamic light scattering. Results represent mean  $\pm$  SD, n=3 independent batches.

#### 2.4.2.2 Testing the effect of flow rate ratio on liposomal physicochemical properties

The results from the previous sections (Sections 2.4.1.1- 2.4.2.1) demonstrate both the lipid concentration and lipid choice affect the size of liposomes formed. Besides this, microfluidics parameters can influence liposome characteristics, which was investigated by determining the impact of the flow rate ratio (FRR) on formulations. The FRR is the ratio of aqueous to solvent stream present during liposome production. The effect of FRR and speed of mixing was determined for all four formulations (PC:Chol, DMPC:Chol, DPPC:Chol and DSPC:Chol) (Figure 2.11- 2.14).

As can be seen from Figure 2.11A, a 1:1 FRR can be used to form large liposomes (113- 133 nm) for PC:Chol liposomes, in comparison to below 100 nm for liposomes produced at either a 3:1 or 5:1 FRR. Although all three FRR produce small liposomes, the difference between the FRR with particular emphasis on the 15 mL/ min TFR is statistically significant ( $p < 0.05$ ). The difference in liposomes size produced at a 1:1 FRR compared to the 3:1 and 5:1 FRR is more noticeable for DMPC:Chol in Figure 2.12 ( $p < 0.0001$ ) and DSPC:Chol formulations observed in Figure 2.14 ( $p < 0.0001$ ). The size of these formulations produced at a 1:1 FRR is between 95- 320 nm in contrast to sizes below 150 nm, for formulations produced at a 3:1 or a 5:1 FRR. Unlike the other three formulations, DPPC:Chol liposomes do not show this trend (Figure 2.13). The 5:1 FRR produces the largest sized liposomes across all flow rate speeds (referred to as the total flow rate (TFR)), meanwhile the 3:1 and 1:1 FRR produce liposomes below 100 nm ( $p < 0.001$ ). The PDI for all four formulations were low regardless of the FRR or the TFR tested (Figure 2.11 - 2.14B), with the zeta potential within the range expected for neutral liposomes (-10 to 0 mV) (Figure 2.11 - 2.14C). The results from Figure 2.11 - 2.14 show the TFR has little impact on the liposomes physicochemical properties. Given these results, the 3:1 FRR and 15 mL/min TFR was selected for all future work.

Furthermore, the 3:1 FRR was found to be the optimal ratio of aqueous to solvent phase irrespective of the lipid hydrocarbon length. The results show liposome size is influenced by the manufacturing control parameters, in addition to the formulation composition. Whilst previous research has identified the FRR to be the most important manufacturing parameter that influences size (Jahn *et al.*, 2010, Zook and Vreeland, 2010), Figures 2.11 - 2.14 provide an in depth investigation, comparing the impact of FRR and TFR on varying neutral liposome formulations. The results show smaller liposomes are produced at higher FRR (of 3:1), with

the TFR having a minimal impact on liposome physicochemical properties. Similar findings reported by Kastner et al showed positively charged liposomes made at a higher FRR are between 50 - 75 nm, in comparison to 175 - 200 nm produced at a 1:1 FRR (Kastner *et al.*, 2014). The difference between the liposomes produced by the three FRR can be explained by changes that occur during the microfluidics manufacturing process. At higher FRR, where the solvent stream is smaller, the amount of time lipids are exposed at the solvent-buffer interface is reduced. The exposure time at the solvent-buffer interface directly impacts liposomes. The lipids exposed at the interface (which bends to form liposomes), does not expand as much at a 3:1 and 5:1 FRR resulting in smaller sized liposomes (Zizzari *et al.*, 2017). There is also a reduced opportunity for Ostwald ripening to take place (Ramana *et al.*, 2010). Ostwald ripening, otherwise known as secondary particle growth, is a phenomenon whereby large vesicles gradually become larger in size. The increase in size is due to the diffusion and lipid exchange of smaller vesicles, typically 20 nm in diameter.

Furthermore, liposome production by microfluidics is modulated by changes in lipid polarity (Zook and Vreeland, 2010). Previous research has shown FRR can impact polarity (Zhigaltsev *et al.*, 2012); at high FRRs (3:1 and 5:1) the final concentration of the solvent is reduced, therefore an increase in polarity is achieved at a faster rate. This coupled with the fast mixing time (TFR of 15 mL/ min) reduces the chance of Ostwald ripening, and so smaller sized particles are produced. The results highlight although FRR is important, the microfluidics device parameters can be adapted to form a wide variety of liposomes (Joshi *et al.*, 2016). Also, as the speed has little impact on production this allows the quicker manufacture of liposomes using microfluidics.

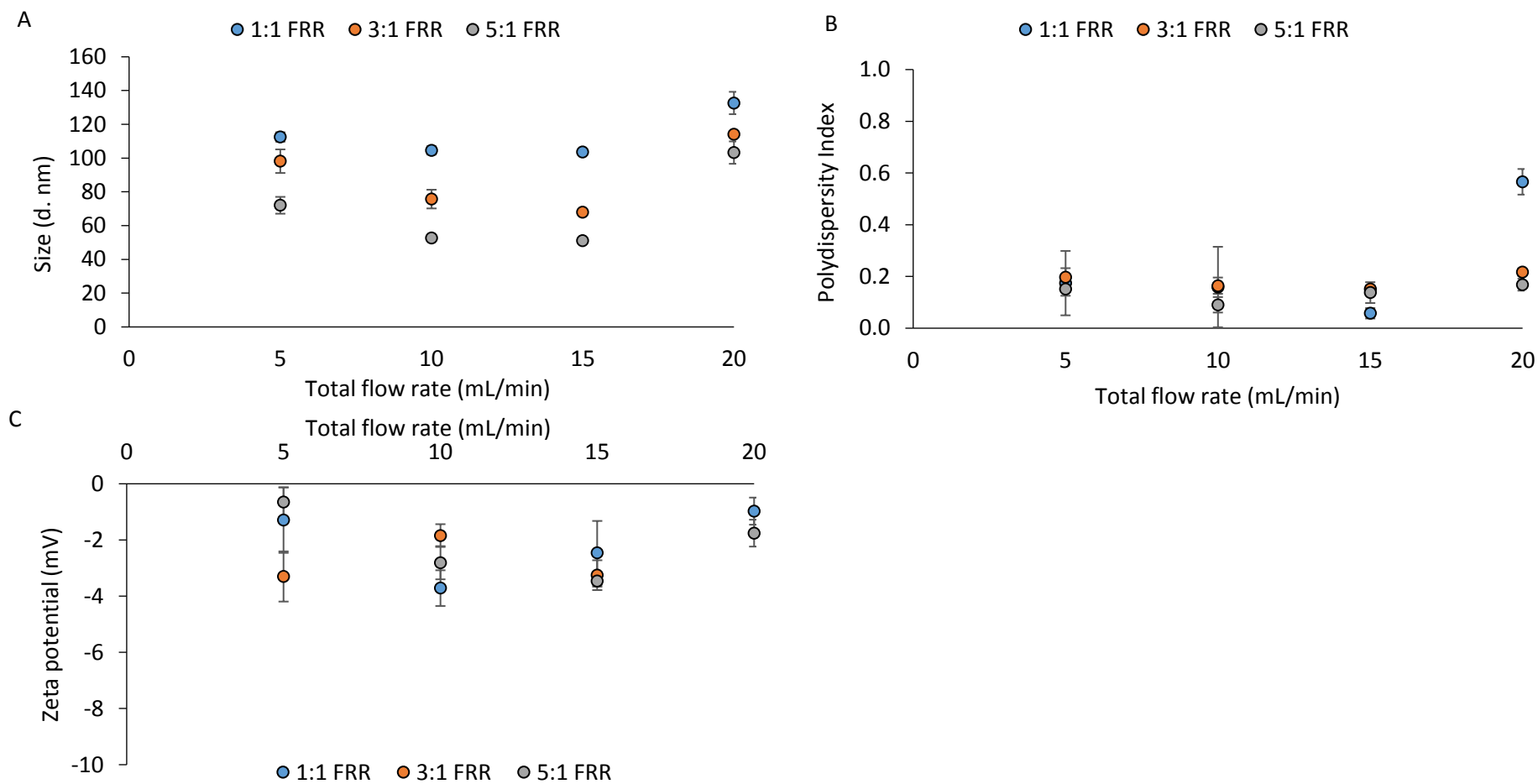


**Figure 2.11.** The physicochemical properties of PC:Chol liposomes produced by microfluidics at varying flow rate ratios (FRRs) and total flow rates (TFR) (mL/min). The size (A), PDI (B) and zeta potential (C) was measured using dynamic light scattering. Results represent mean  $\pm$  SD, n=3 independent batches.

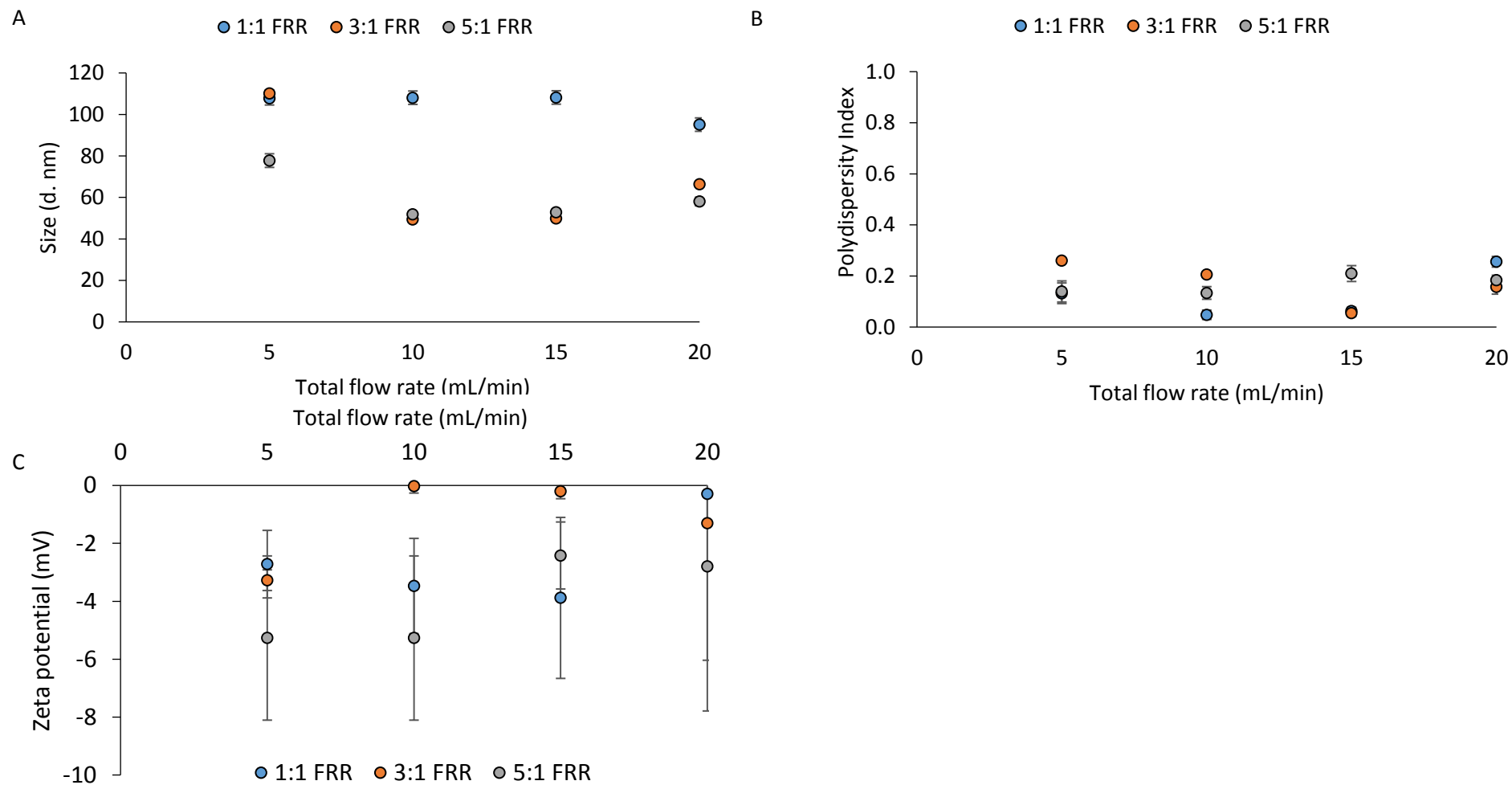


**Figure 2.12.** The physicochemical properties of DMPC:Chol liposomes produced by microfluidics at varying flow rate ratios (FRRs) and total flow rates (TFR) (mL/min). The size (A), PDI (B) and zeta potential (C) was measured using dynamic light scattering. Results represent mean  $\pm$  SD, n=3 independent batches.

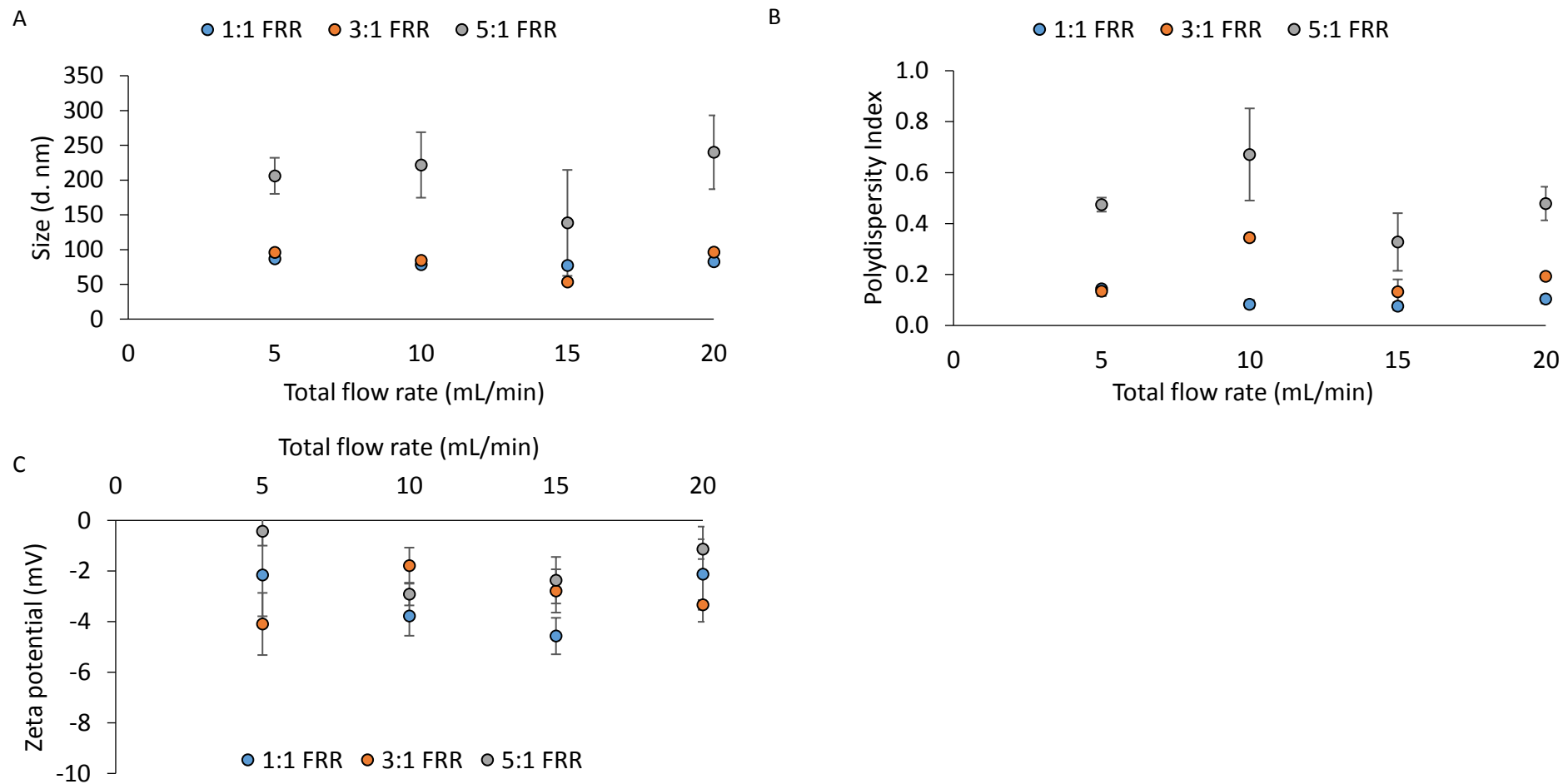


**Figure 2.13.** The physicochemical properties of DPPC:Chol liposomes produced by microfluidics at varying flow rate ratios (FRRs) and total flow rates (TFR) (mL/min). The size (A), PDI (B) and zeta potential (C) was measured using dynamic light scattering. Results represent mean  $\pm$  SD, n=3 independent batches.

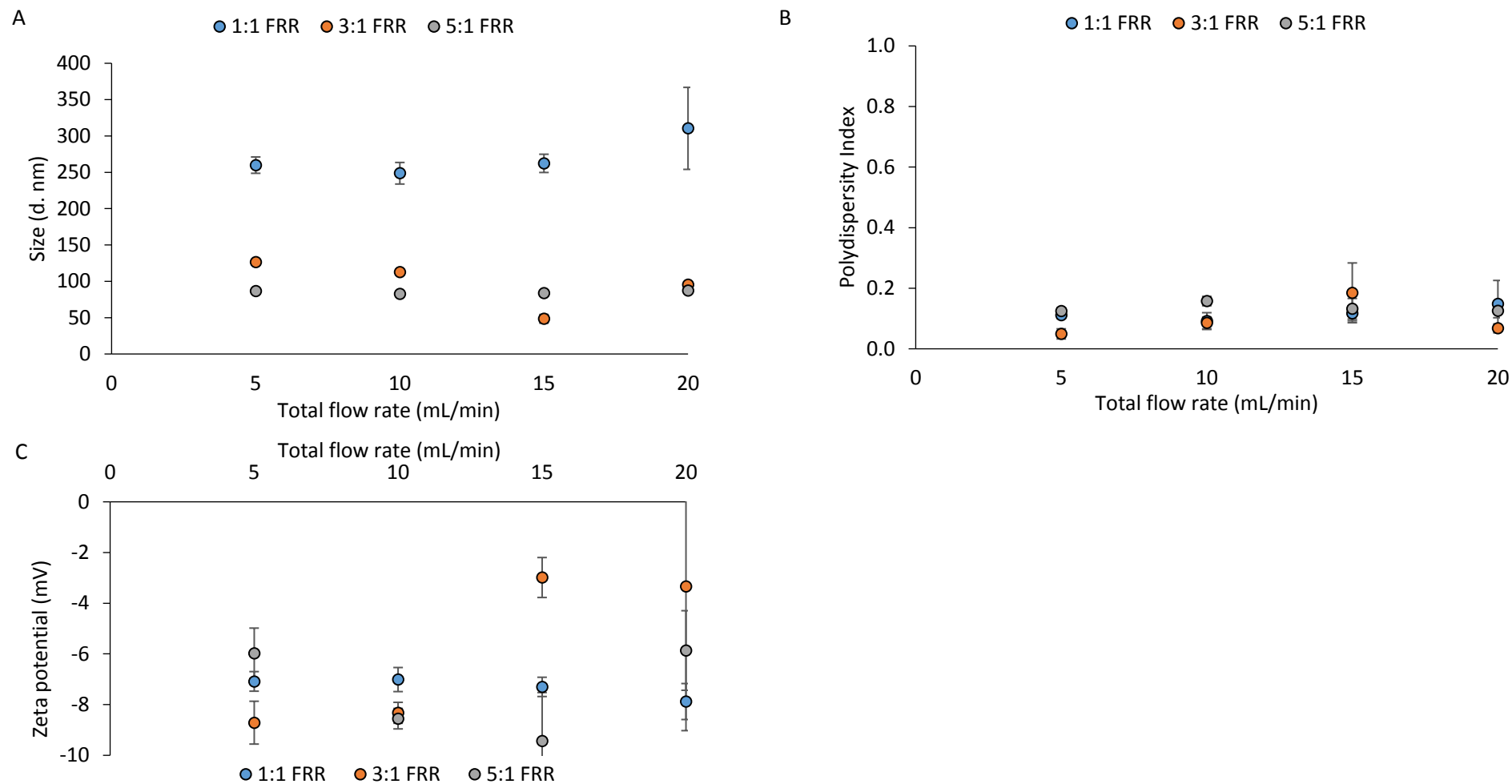


**Figure 2.14.** The Physicochemical properties of DSPC:Chol liposomes produced by microfluidics at varying flow rate ratios (FRRs) and total flow rates (TFR) (mL/min). The size (A), PDI (B) and zeta potential (C) was measured using dynamic light scattering. Results represent mean  $\pm$  SD, n=3 independent batches.



### 2.4.2.3 Establishing the optimal operating ranges for liposomes using design of experiments

Design of Experiments (DoE) is a method used to determine the relationship between several factors affecting the process and output. It is used to identify the key parameters required for the desired outputs more efficiently in comparison to the traditional one factor at a time methods (OFAT). DoE helps broaden design spaces, allowing identification of relationships and trends that may not have been easily spotted. The statistical software, Design Expert 10, was used to identify the relationship between concentration, FRR and TFR on the size, PDI and zeta potential of liposome formulations. The desired outcome for this particular DoE was the smallest sized liposomes (below 100 nm), a PDI of less than 0.2 and a zeta potential above -10 mV. For neutral liposomes, the surface charge of liposomes is known to be between -10 and +10 mV (Clogston and Patri, 2011); the slight negative charge of the zeta potentials is due to the liposomes dispersed in water. Deviations from this range would suggest that the liposome composition has changed (possibly due to chemical degradation), thus measuring the zeta potential of neutral liposomes above -10 mV is important.

A central composite design was used with two centre points; 10 different input combinations were tested in triplicate, with surface plots used to visualise any relationship. Figure 2.15 are representative plots that are used to establish the parameters needed to obtain the desired results. Figure 2.15A shows a surface plot for the effect of FRR and TFR on PC:Chol liposome size. Based on the curvature, it suggests that both the FRR has an effect on the size. Figure 2.15B shows the effect on PDI caused by varying the FRR and TFR, meanwhile no relationship is seen between the FRR and TFR on the zeta potential. This information was pooled to create a sweet spot contour plot (Figure 2.15C). The results suggest that a 3:1 FRR and 15 mL/ min TFR are the ideal parameters for producing the smallest sized DMPC:Chol liposomes. Similar parameters were identified for PC:Chol, DMPC:Chol and DSPC:Chol liposomes shown in Table 2.2. In addition to identifying parameters to run, the DoE gives predicted size, PDI and zeta potential values if the ideal parameters are run. To validate this, the ideal parameters were run and the size, PDI and zeta potential was checked and compared to the predicted values. With the exception of the DSPC:Chol liposomes, the statistical software package

was able to predict the size of the liposomes with a 86% accuracy (Table 2.2). It performed better for DMPC:Chol liposomes (91.5% accuracy) and DPPC:Chol liposomes (94.5% accuracy). For DSPC:Chol liposomes the predicted size is 27 nm which was not achieved using the predicted DoE parameters (Table 2.2), despite 25 nm being the smallest theoretical liposome size that can be achieved (Lasic, 1993). The difference in size between the actual and predicted may be due to the instability of the DSPC:Chol liposomes. Very small liposomes tend to be unstable and may fuse together during production (Toh and Chiu, 2013), thus producing DSPC:Chol liposomes which are  $47.3 \pm 0.31$ . The results suggest that while DoE is good at identifying relationships and defining design space, there are some limitations, thus the results should be analysed critically.

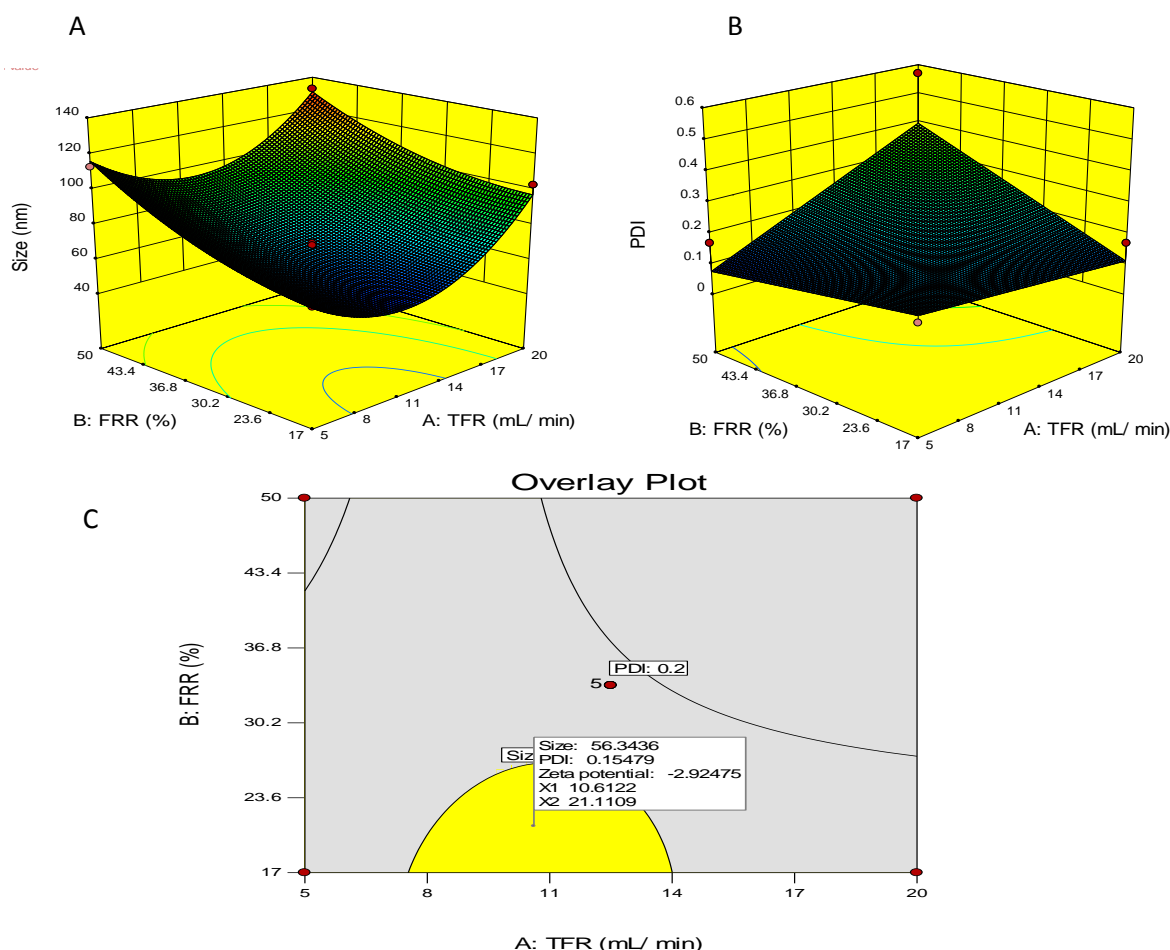


**Figure 2.15.** Establishing the design space for PC:Chol liposomes produced by microfluidics. Size (A) and PDI (B) contour plot for PC:Chol liposomes. The results were combined to form a sweet spot contour plot (C). Results represent mean  $\pm$  SD, n=3 independent batches

**Table 2.2.** Comparing the predicted liposome physicochemical properties (Size, polydispersity (PDI) and zeta potential (ZP) to the actual values obtained for liposomes produced by microfluidics using the predicted optimal parameters. Dynamic light scattering was used to determine the size, PDI and ZP. Results represent mean  $\pm$  SD, n=3 independent batches.

FORMULATIONS	PREDICTED PARAMETERS	PREDICTED SIZE, PDI AND ZETA POTENTIAL	ACTUAL SIZE AND PDI
<b>PC:CHOL</b>	FRR: 4:1	Size: 56 nm	Size: 64.2 $\pm$ 0.44 nm
	TFR: 10 mL/ min	PDI: 0.15 ZP: -2.92 mV	PDI: 0.209 $\pm$ 0.015 ZP: -1.69 $\pm$ 0.758 mV
<b>DMPC:CHOL</b>	FRR: 3:1	Size: 43 nm	Size: 47.2 $\pm$ 0.44 nm
	TFR: 15 mL/ min	PDI: 0.07 ZP: -0.46 mV	PDI: 0.209 $\pm$ 0.015 ZP: -1.69 $\pm$ 0.758 mV
<b>DPPC:CHOL</b>	FRR: 2:1/ 3:1 TFR: 15 mL/ min	Size: 54 nm	<u>2:1 FRR</u> Size: 56.6 $\pm$ 0.63 nm
		PDI: 0.10 ZP: -2.25 mV	PDI: 0.130 $\pm$ 0.011 ZP: -0.94 $\pm$ 0.060 mV
			<u>3:1 FRR</u> Size: 51.3 $\pm$ 0.42 nm
			PDI: 0.119 $\pm$ 0.009 ZP: -2.07 $\pm$ 1.23 mV
<b>DSPC:CHOL</b>	FRR: 3:1	Size: 27 nm	Size: 47.3 $\pm$ 0.31 nm
	TFR: 15 mL/ min	PDI: 0.11 ZP: -3.07 mV	PDI: 0.102 $\pm$ 0.002 ZP: -1.94 $\pm$ 1.22 mV

### 2.4.3 Lipid recovery of liposomal formulations

When considering the manufacture of the liposomes, the importance of lipid composition for liposomes in terms of drug incorporation, release properties and their stability have to be thoroughly explored. Given the majority of liposomes products approved for clinical use are a combination of phosphatidylcholine and cholesterol, including Caelyx<sup>®</sup> and Myocet<sup>®</sup>, identifying the different components and quantifying lipids is necessary. Whilst rapid manufacturing productions have been developed, there is a lack of rapid high throughput quantification techniques available for the analysis of lipids. Various high performance liquid chromatography (HPLC) methods have been developed for the rapid separation of liposome components (Lesnefsky *et al.*, 2000, Holland *et al.*, 2003, Lin and McKeon, 2000, Mazzella *et al.*, 2004); however, the quantification of lipids remains challenging. This is in part due to a

lack of easily detectable functional groups, such as chromophores on most lipids. To overcome this, evaporative light scattering detectors (ELSD) can be used alongside HPLC to rapidly quantify the concentration of lipids within liposomes (Christie, 1985). Work by Roces et al (2016) outlined a HPLC-ELSD method to quantify range of lipids including the neutral lipid DMPC, as well as the cationic lipid dimethyldioctadecylammonium (DDA) bromide from liposomes (Roces *et al.*, 2016). This method was adapted to quantify the lipid concentration of four formulations (PC:Chol, DMPC:Chol, DPPC:Chol and DSPC:Chol) using HPLC-ELSD.

The ELSD detector can be used to quantify volatile and non-volatile components. In this HPLC-ELSD method, the ELSD component works after the sample has passed through the HPLC column. As the eluent passes the column, it enters a heated nebulizing chamber whereby it mixes with the inert nitrogen gas. The heat in this chamber causes evaporation of the solvent, meanwhile the non-volatile analytes form droplets that are carried to the detector region by the compressed nitrogen. The particles pass through an optical cell, and cross the path of a laser beam light causing scattering. The intensity of the scattered light is measured by a detector which is measured and translated into a signal (Mourey and Oppenheimer, 1984). Distinct peaks are produced for all four lipids and cholesterol, with the time each lipid elutes shown by the HPLC-ELSD chromatograms (Figure 2.16 and Figure 2.17). The DMPC (11.9 minutes), DPPC (14.1 minutes), DSPC (18 minutes) and Cholesterol (13.9 minutes) appear as single peaks (Figure 2.16). As seen from Figure 2.17, the PC lipid has multiple peaks as it is made up of a mixture of lipids. The peaks appear at 13, 15 and 16.5 minutes.

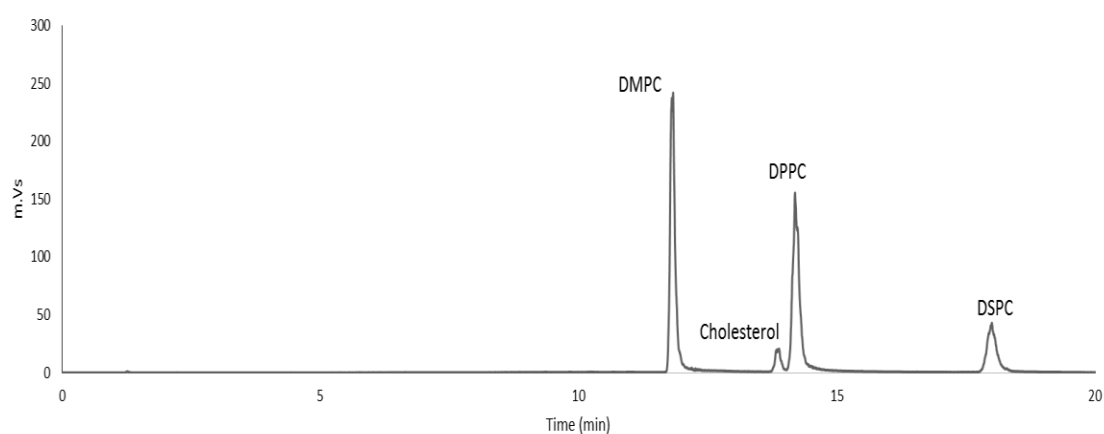


**Figure 2.16.** ELSD-HPLC detected chromatogram of DMPC (0.1 mg/mL), Cholesterol (0.1 mg/mL), DPPC (0.1 mg/mL) and DSPC (0.1 mg/mL).

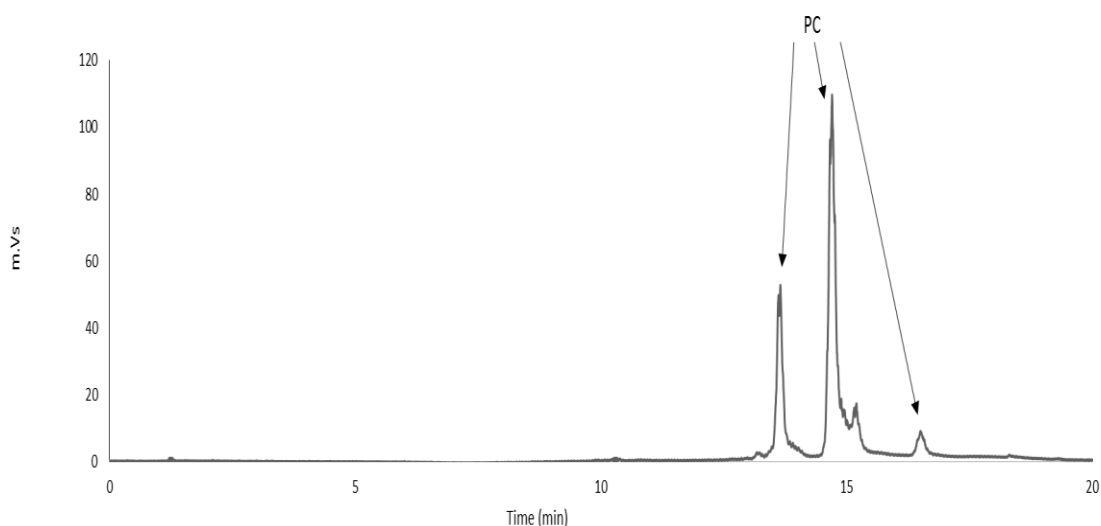


**Figure 2.17.** ELSD-HPLC detected chromatogram of PC lipids (0.1 mg/mL).

To quantify the amount of lipid recovery, standard calibration curves were produced for all four formulations; PC lipid (Figure 2.18A), DMPC lipid (Figure 2.18B), DPPC lipid (Figure 2.18C), DSPC lipid (Figure 2.18D) and cholesterol (Figure 2.18E), with the LOD and LOQ values also given (Figure 2.18F). Using the calibration curves, the lipid recovery of the four formulations (PC:Chol, DMPC:Chol, DPPC:Chol and DSPC:Chol) produced by different manufacturing and purification methods was investigated. The manufacturing methods of thin film lipid hydration, and downsizing by sonication were compared to the microfluidics production technique. The amount of lipid quantified after production by thin film lipid hydration and post sonication was above 95% for all four formulations. The amount of cholesterol measured was also above 95% and was reflective of the 50:50 mol% of lipid to cholesterol (Table 2.3), therefore no lipid is lost during the production and downsizing of these techniques. Similarly, the lipid recovery of all four formulations post microfluidics production was above 95 % with the cholesterol ratio remaining the same, thus all three methods are suitable for liposome production.

In addition, liposomes produced by microfluidics need to undergo purification steps to remove residual solvent present. Two purification techniques (dialysis) and the use of Sephadex® G-75 columns were investigated to determine whether these steps caused a loss of lipid. As shown by Table 2.4, the dialysis purification method agree with the previous findings of the microfluidics manufacturing, as well as previous literature (Roces *et al.*, 2016). There is a high lipid recovery near 100% with little to no lipid being lost during the production

process. The amount of lipid to cholesterol being recovered is in keeping with the 50:50 mol% of lipid to cholesterol used. Meanwhile, the lipid recovery for the Sephadex® G-75 columns was poor. Between 62- 78% of lipid was recovered, with around 20% lost in the purification step. The amount of cholesterol recovered was in the same range, therefore indicating that liposomes are getting stuck.

Furthermore, as the microfluidics parameters allows fine- tuning to produce optimal sized liposomes, these parameters need to be investigated with respect to the lipid recovery. The DMPC:Chol liposomal formulation was selected as the model formulation. The liposomes were produced at a 3:1 FRR with the speed of flow (TFR) at either 15 or 20 mL/min. Higher TFRs were chosen as previous experiments in section 2.4.2.2 have shown the speed of production does not influence liposome physicochemical properties. The results from Table 2.5 show the TFR has minimal effect on the lipid recovery of liposomes. The lipid recovery for DMPC:Chol liposomes is above 90% for liposomes produced at either 15 or 20 mL/min. Previous research has shown a high recovery rate of lipids is also observed across FRRs; lipid recovery values of above 87% were reported for positively charged liposomes (produced at 1:1, 3:1 and 5:1 FRRs) (Kastner *et al.*, 2014) and propofol loaded PC:Chol liposomes (1:1 and 3:1 FRRs) (Kastner *et al.*, 2015). This is further investigated with results from Table 2.5; a high lipid recovery of above 95% for neutral formulations (PC:Chol, DMPC:Chol, DPPC:Chol and DSPC:Chol) produced at a 3:1 FRR.

As previously mentioned, the physicochemical properties of liposomes are heavily influenced by the presence and ratio of cholesterol (sections 2.4.1.3 and 2.4.1.4). Using DMPC:Chol liposomes, the impact of cholesterol ratio on lipid recovery was tested. Results from Table 2.5 show a lipid recovery of above 90% for both DMPC and cholesterol liposomes irrespective of the cholesterol ratio (1:1, 3:1 and 7:1). The amount of DMPC lipid recovered is in proportion to the amount of cholesterol, suggesting the liposomes are still intact and maintain their lipid formulation ratio. The high retention of lipids post microfluidics irrespective of the formulation components or manufacturing parameters is highly advantageous; minimal loss of lipid suggests the microfluidics manufacturing process is highly efficient and cost effective.

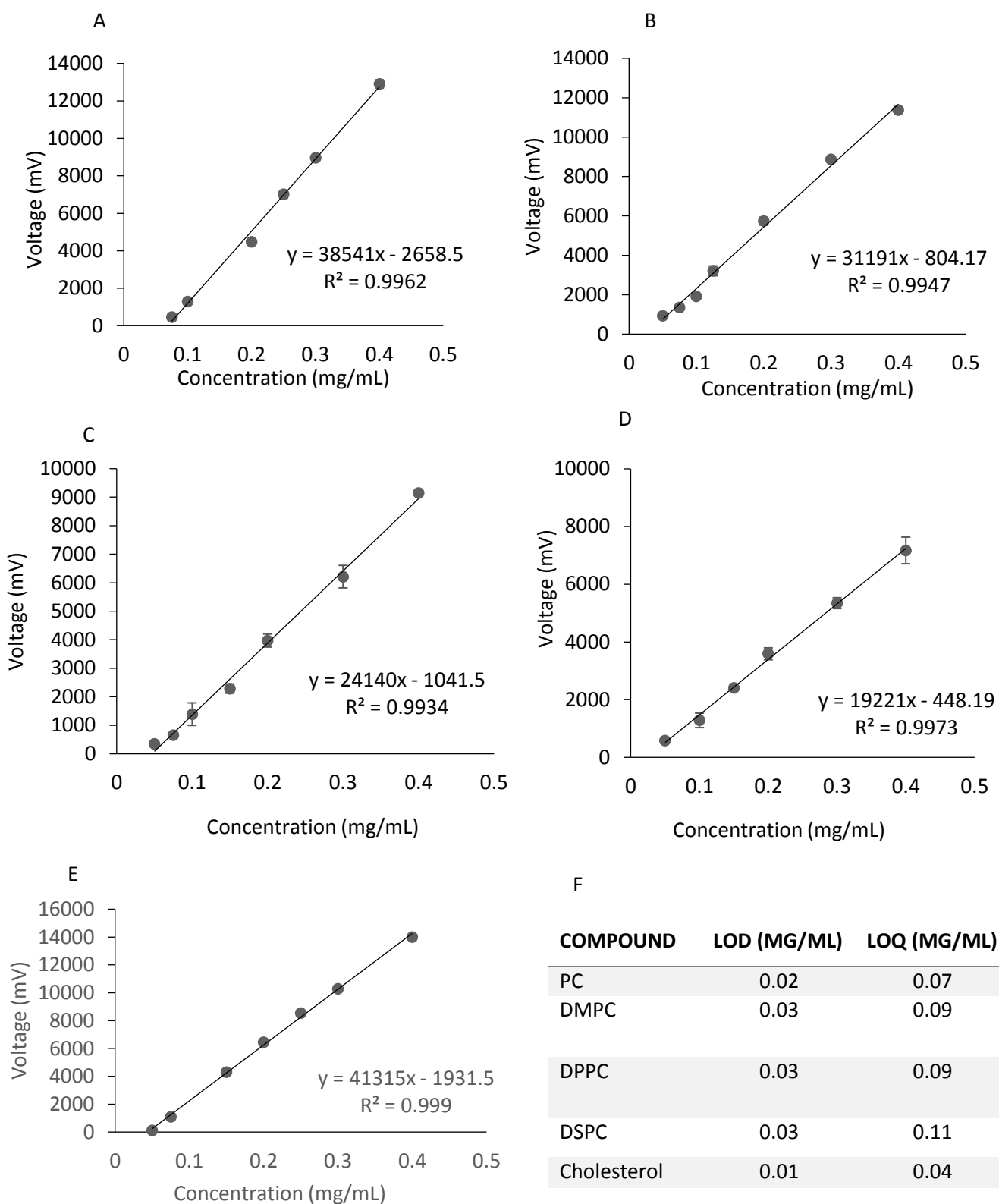


**Figure 2.18.** Standard calibration curves for PC (A), DMPC (B), DPPC (C), DSPC (D) and cholesterol (E) used to determine the lipid recovery of the liposomal formulations. The LOD and LOQ for each lipid is shown in E. Results represent mean  $\pm$  SD, n=3 independent batches.

**Table 2.3.** The lipid recovery of PC:Chol, DMPC:Chol, DPPC:Chol and DSPC:Chol liposomes produced by microfluidics and rotary evaporation. The effect of additional downstream processes like solvent removal (dialysis and Sephadex® G-75 columns) and sonication on lipid recovery was also quantified. Results represent mean  $\pm$  SD, n=3 independent batches.

	<b>PC:CHOL</b>		<b>DMPC:CHOL</b>		<b>DPPC:CHOL</b>		<b>DSPC:CHOL</b>	
	PC	Chol	DMPC	Chol	DPPC	Chol	DSPC	Chol
Rotary Evaporation	95 $\pm$ 3.3	96 $\pm$ 6.4	101 $\pm$ 3.2	100 $\pm$ 7.3	97 $\pm$ 4.2	96 $\pm$ 2.3	104 $\pm$ 9.4	97 $\pm$ 3.7
Sonicated (Rotary evaporation)	97 $\pm$ 2.7	95 $\pm$ 1.4	98 $\pm$ 2.2	99 $\pm$ 9.4	103 $\pm$ 1.3	97 $\pm$ 0.7	100 $\pm$ 3.9	96 $\pm$ 1.5
Microfluidics	95 $\pm$ 5.0	95 $\pm$ 2.3	95 $\pm$ 1.6	96 $\pm$ 1.0	96 $\pm$ 1.2	97 $\pm$ 2.7	98 $\pm$ 5.7	97 $\pm$ 3.8
Dialysis (Microfluidics)	95 $\pm$ 5.0	95 $\pm$ 2.3	95 $\pm$ 1.6	96 $\pm$ 1.0	96 $\pm$ 1.2	97 $\pm$ 2.7	98 $\pm$ 5.7	97 $\pm$ 3.8
Sephadex® G-75 (Microfluidics)	69 $\pm$ 0.5	62 $\pm$ 3.9	76 $\pm$ 3.6	78 $\pm$ 1.8	70 $\pm$ 3.8	78 $\pm$ 3.0	69 $\pm$ 7.8	55 $\pm$ 3.1

**Table 2.4.** The quantification of DMPC lipid and cholesterol formed with varying production parameters. The DMPC:Chol liposomes were produced at a 3:1 FRR, with the total flow rate varied. The effect of changing the lipid and cholesterol ratio was also investigated, with recovery calculated by HPLC- ELSD. Results represent mean  $\pm$  SD, n=3 independent batches.

	<b>Test Conditions</b>	<b>DMPC:Chol</b>	
		DMPC	Chol
<i>Effect of flow rate (mL/ min)</i>	15	95 $\pm$ 5.7	96 $\pm$ 10.8
	20	93 $\pm$ 6.9	93 $\pm$ 10.3
<i>Effect of changing the ratio of lipid to cholesterol</i>	1:1	93 $\pm$ 10.9	93 $\pm$ 7.0
	3:1	92 $\pm$ 3.5	99 $\pm$ 2.7
	7:1	93 $\pm$ 2.8	91 $\pm$ 13.5



#### 2.4.4 Measuring residual solvent for purified liposomes

The need to have rapid and quantifiable methods to measure solvent is imperative given the lipids are dissolved in solvent for microfluidics manufacture. For traditional methods such as thin film lipid hydration this is not a problem as the solvent is removed before the formation of liposomes. However, the microfluidics method produces liposomes in the presence of solvent, and depending on the FRR selected the maximum solvent present in a formulation can be as high as 50 %. Whilst purification techniques such as dialysis can remove the majority of solvent, it is important to identify any possible residual solvent remaining. This is necessary as many solvents are inherently toxic. The residual solvent, present as a result of microfluidics manufacturing must be below the threshold set by the International Council on Harmonisation of Technical Requirements for Registration of Pharmaceuticals for Human Use (ICH) guidelines (ICH (Guideline, 2016)). Solvents can be separated into three classes according to their toxicity:

**Class 1.** Solvents to be avoided; these include solvents such as benzene (a known carcinogen) and carbon tetrachloride (harmful to the environment).

**Class 2.** Solvents should be limited in their use as they have inherent toxicity. These include; methanol (3000 ppm), hexane (290 ppm) and acetonitrile (410 ppm).

**Class 3.** Solvents whereby no obvious link to toxicity has been established, but the daily limit exposure must not exceed 5000 ppm.

Gas chromatography is a rapid analysis technique that can be used to ensure all the solvent is removed post dialysis, and to check the residual amount is at a bio-safe level for administration. The solvent methanol was selected for the microfluidics manufacturing process as it is compatible with a host of lipids (including PC, DMPC, DPPC and DSPC), as well as cholesterol. Standard curves containing an internal control were established to determine the unknown amount of methanol present in the liposome sample. A range of dialysis times were tested using PC:Chol as the model liposomes, to determine the minimum time required for the sample to be safe for administration (Table 2.5). To remove solvent, liposomes underwent dialysis for 1, 2, 4 and 24 hours respectively to determine the minimum time needed to remove the most solvent to the safe level specified by ICH.

The results from Table 2.5 show that one hour dialysis was sufficient to remove the solvent to a safe level below 3000 parts per million (ppm) for methanol as stipulated by the ICH guidelines (Guideline, 2016). After one hour of dialysis the amount of residual methanol drops to  $708 \pm 28$  ppm ( $0.7 \pm 0.03\%$ ), which is below the 3000 ppm threshold specified by ICH. The size of PC:Chol liposome formulations post dialysis was also measured. The liposomes remained below 100 nm after 24 hours of dialysis (Figure 2.19), with a size of  $84 \pm 0.8$  nm. The PC:Chol liposomes remained homogenous with PDI value of less than 0.2 over 24 hours. The dialysis time did not affect the zeta potential, with the formulations remaining neutral (a zeta potential -5 to 0 mV measured) (Figure 2.19).

**Table 2.5.** The effect of dialysis time on solvent removal. The amount of solvent remaining in PC:Chol liposomes was quantified. Results represent mean  $\pm$  SD, n=3 independent batches.

DIALYSIS TIME (HOURS)	REMAINING SOLVENT (%)	PARTS PER MILLION (PPM)
1	$0.7 \pm 0.03$	$708 \pm 28$
2	$0.7 \pm 0.03$	$659 \pm 33$
4	$0.4 \pm 0.02$	$353 \pm 23$
24	$0.1 \pm 0.01$	$37 \pm 3$

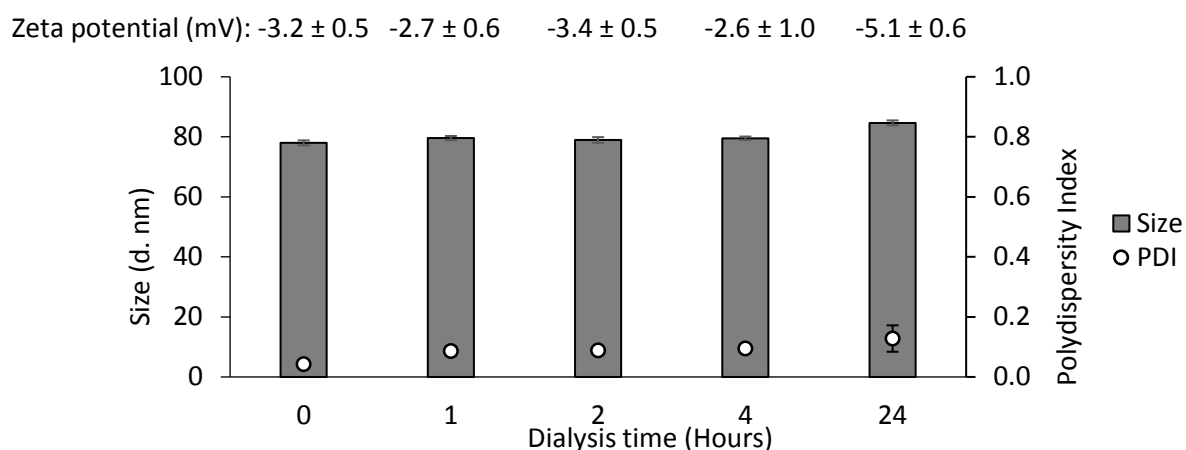


**Figure 2.19.** The effect of dialysis time on liposome physicochemical properties. The PC:Chol formulations were produced using microfluidics at a 3:1 FRR and 15 mL/min. The PC:Chol formulations underwent dialysis for 1, 2, 4 and 24 hours after which the size, PDI and zeta potential of PC:Chol was determined using dynamic light scattering. Results represent mean  $\pm$  SD, n=3 independent batches.

Following on from this, the residual solvent content was measured for four formulations (PC:Chol, DMPC:Chol, DPPC:Chol and DSPC:Chol) post one hour dialysis (Table 2.6). One hour dialysis was sufficient to remove residual solvent to below the 3000 ppm required. The removal of the solvent is independent of the lipid selected, therefore a one hour time was selected for the rapid and efficient removal of residual solvents.

**Table 2.6.** Quantifying remaining solvent post dialysis. All four liposome formulations underwent dialysis for one hour, with the amount of solvent remaining calculated. Results represent mean  $\pm$  SD, n=3 independent batches.

LIPOSOMES	REMAINING SOLVENT (%)	PARTS PER MILLION (PPM)
PC:CHOL	0.7 $\pm$ 0.05	733 $\pm$ 45
DMPC:CHOL	0.8 $\pm$ 0.06	790 $\pm$ 61
DPPC:CHOL	0.7 $\pm$ 0.06	713 $\pm$ 56
DSPC:CHOL	0.8 $\pm$ 0.01	812 $\pm$ 10

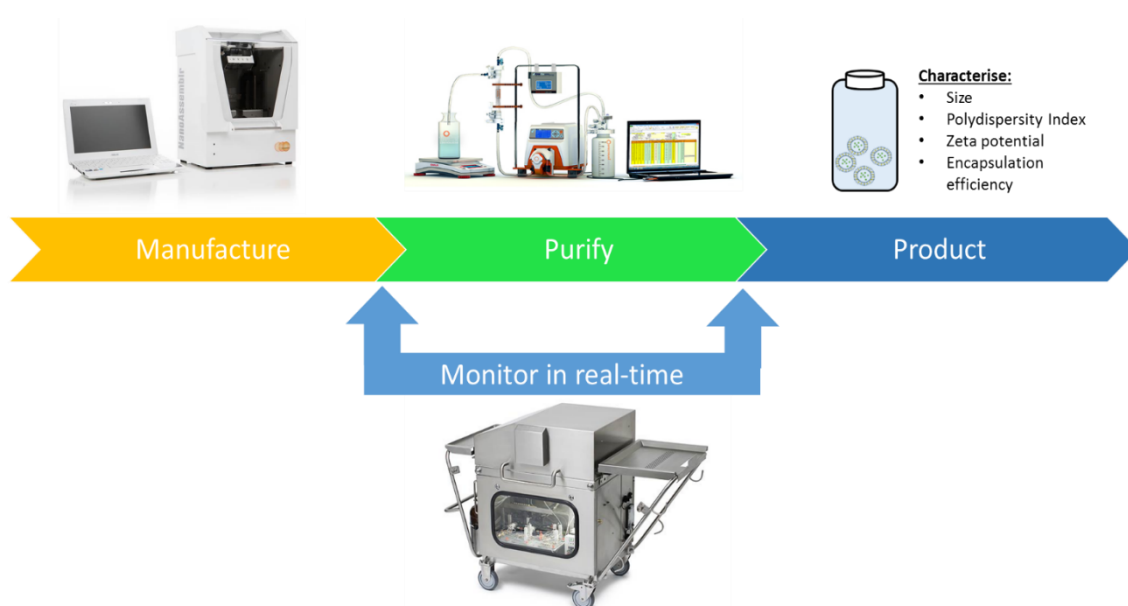
## 2.5 Conclusion

The research presented in this chapter evaluated the manufacturing techniques of liposomes produced by either thin film lipid hydration followed by sonication or by microfluidics. The two manufacturing approaches to liposome production were thoroughly investigated and compared. The lipid recovery by both approaches was investigated alongside differences in the physicochemical properties of liposomes. Whilst there was no difference in liposome recovery for both approaches (with lipid recoveries above 95%), the liposome physicochemical properties were influenced by the manufacturing method. This chapter has identified microfluidics is a better choice for producing smaller in size (less than 100 nm), with batch to batch uniformity (PDI less than 0.2).

In addition, the four neutral liposomes (PC:Chol, DMPC:Chol, DPPC:Chol and DSPC:Chol) were characterised in depth. The normal operating ranges and parameters for the four liposomal formulation, in terms of formulation concentration was determined to be above 2 mg/mL. Other formulation parameters such as cholesterol content was also shown to be important for producing stable liposomes. Added to this, the design of experiment (DoE) models were successfully used to identify and establish the ideal work space for liposomes produced by microfluidics. A 3:1 FRR alongside a fast flow rate (15 mL/min TFR) was identified as the optimal manufacturing parameters for producing small homogenous liposomes. The successful predictions and application of microfluidics parameters by DoE, show microfluidics is a robust technique, with clearly defined design space. The microfluidics system is capable of producing liposomes for clinical use, which meet the quality assurance guidelines. Based on the capability of microfluidics system to produce liposomes quickly and efficiently, the microfluidics method was selected for all further work.

# Chapter 3

## Continuous manufacturing of liposomes



Work presented in this chapter has been published in:

1. FORBES, N., HUSSAIN, M. T., BRIUGLIA, M. L., EDWARDS, D. P., HORST, J. H. T., SZITA, N. & PERRIE, Y. 2019. Rapid and scale-independent microfluidic manufacture of liposomes entrapping protein incorporating in-line purification and at-line size monitoring. *International Journal of Pharmaceutics*, 556, 68-81.
2. DIMOV, N., KASTNER, E., HUSSAIN, M., PERRIE, Y. & SZITA, N. 2017. Formation and purification of tailored liposomes for drug delivery using a module-based micro continuous-flow system. *Scientific reports*, 7, 12045.

## 3.1 Introduction

### 3.1 High throughput manufacturing

Microfluidics devices have gained popularity for the use of handling small volumes in controlled settings, which has the ability to accelerate production and screening times of pharmaceuticals. The small microliter scale handling exploits the fluid flows which occur at small volumes. The microscale environment does not experience turbulence, surface effects, interfacial effects and capillary pressures experienced at the macroscale, which can be used to develop scaled down biochemical processes (Whitesides, 2006). Since the ability to use soft lithography to engineer complex microfluidics chips and designs at the microscale (Sackmann *et al.*, 2014, Whitesides *et al.*, 2001), there has been a huge rise in the use of microfluidics to manufacture delivery vehicles such as liposomes. A broad range of chip designs and geometry have been produced, that have shown the ability to produce high throughput liposomes (Table 3.1). For instance, Joshi *et al.* showed the ability to simultaneously encapsulate glipizide and metformin drugs (lipophilic and hydrophilic drugs respectively) using a Y-shaped microfluidics chip (Precision Nanosystems Ltd, Vancouver, Canada). High encapsulation was achieved for metformin (20- 24% of initial drug) and glipizide (40- 42% of initial drug loaded), with co-loading having no impact on encapsulation efficiency (Joshi *et al.*, 2016). Despite the highly efficient microfluidics production method, dialysis was used to purify and remove non- incorporated drug, thus the overall liposome manufacturing process is not streamlined. Whilst many research papers have shown the ability to produce liposomes quickly using microfluidics, the manufacturing process ability is still limited due to the purification steps (in order to remove solvent and untrapped drugs). Research by Dimov *et al.*, addressed this issue by using a small scale tangential flow filtration system to purify liposomes (remove solvent and drug) post microfluidics production. The continuous process flow allowed the production, modification (including concentration) as well as purification of liposomes. The process showed more than 95% solvent removal can be achieved, in addition to a 95% reduction of non-incorporated propofol in PC:Chol liposomes within four minutes (Dimov *et al.*, 2017). Whilst the results are promising, the use of bespoke and specialised equipment means the results are not easily comparable. Monitoring liposome production during manufacturing (referred to as at-line) was not possible, with the physicochemical properties of the liposomes measured manually.

**Table 3.1.** Summary of the range of liposome that can be produced by Y-shaped chips.

CHIP TYPE	LIPOSOMES	LIPID SOLVENT AND BUFFER	EXPERIMENTS	REFERENCE
<b>Y-shaped chip (available from Precision Nanosystems Ltd, Vancouver, Canada).</b>	DOPE:DOTAP	Ethanol & Tris (10 mM, pH= 7.4)	Effect of FRR and TFR	(Kastner <i>et al.</i> , 2014)
	PC:Chol	Ethanol Tris (10 mM, pH= 7.4)	Propofol loading at varying FRR and TFRs	(Kastner <i>et al.</i> , 2015)
	PC:Chol	Methanol & PBS (10 mM, pH= 7.3)	Effect of lipid concentration on physicochemical properties	(Joshi <i>et al.</i> , 2016)
	DSPC:Chol	Methanol & PBS (10 mM, pH= 7.3)	Co- loading of glipizide and metformin	(Joshi <i>et al.</i> , 2016)
	PC:Chol, DMPC:Chol, DPPC:Chol & DSPC:Chol	Methanol & PBS (10 mM, pH= 7.3)	Ovalbumin loading of liposome: effect of FRR & TFR	(Forbes <i>et al.</i> , 2019)
	DSPC:Chol:PS	Methanol & PBS (10 mM, pH= 7.3)	Encapsulation efficiency of ovalbumin	(Forbes <i>et al.</i> , 2019)
<b>Cross flow microfluidics chip (3 inlets &amp; one outlet)</b>	PC:Chol, PC:DDAB	Ethanol, water	Effect of FRR	(Carugo <i>et al.</i> , 2016)
<b>T- shaped microfluidics chip</b>	DMPC:Chol:DCP	Isopropanol alcohol	Effect of flow conditions. Investigating chip geometry	(Jahn <i>et al.</i> , 2007)

### 3.2 Scalable manufacturing of liposomes

The microfluidics system is able to produce a high volume of liposomes; however, scalability of the microfluidics continuous process is challenging. Scaling microfluidics for the production of litre volumes has been challenging, as often scale-up compromises the precision possible with microfluidics. As a result, alternative techniques such as scale-out

have been developed rather than scale-up to meet production demands. The process involves running microfluidics chips in parallel. Whilst this new technologies can accommodate production demand, the downstream steps are often neglected. The ability to monitor the quality of the liposomes produced during manufacturing is another important factor when investigating manufacturing techniques. As a result, using commercial equipment available, a continuous microfluidics production process was developed at a laboratory scale, with the ability to scale up or down as necessary.

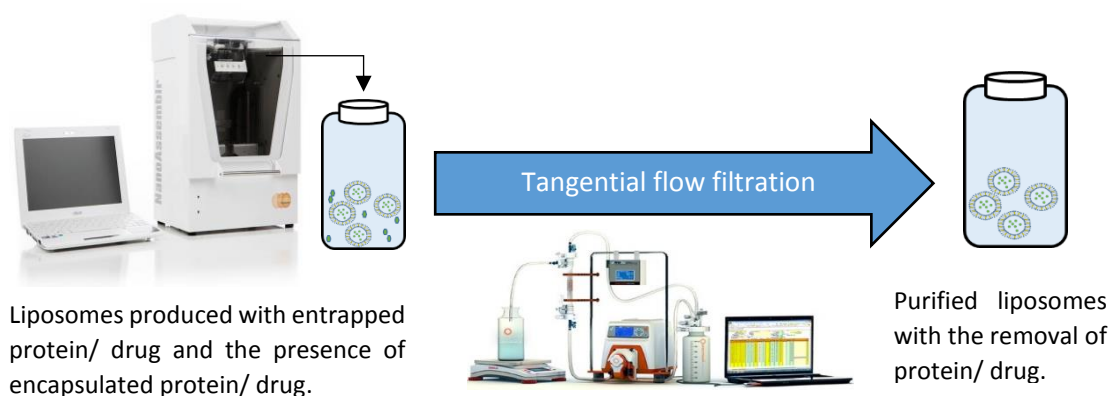


**Figure 3.1.** Flow diagram illustrating the ability to produce high throughput liposomes in a continuous process using commercial instruments available. For the production of liposomes, the microfluidics NanoAssemblr® Benchtop (Precision Nanosystems Inc., Canada) was coupled to the Krosflo Research tangential flow filtration system (Spectrum Inc., Breda, The Netherlands).

### 3.2 Aim and Objectives

The aim of this chapter is to determine a scalable method for the manufacture of liposome formulations. To do this the following objectives were considered:

- 1) Identification of the critical process parameters within the microfluidics process.
- 2) Development of high throughput manufacturing alternatives instead of traditional methods.
- 3) Development of a scale independent technique for producing high throughput liposomes.
- 4) Assessment of liposome physicochemical properties after high throughput production.



### 3.3 Materials and Methods

#### 3.3.1 Materials

Phosphatidylcholine (PC), 1,2-dimyristoyl-sn-glycero-3-phosphocholine (DMPC), 1,2-dipalmitoyl-sn-glycero-3-phosphocholine (DPPC), and 1,2-distearoyl-sn-glycero-3-phosphocholine (DSPC) from Avanti Polar Lipids Inc., Alabaster, USA. Cholesterol and, D9777-100ft dialysis tubing cellulose was obtained from Sigma Aldrich Company Ltd., Poole, UK. For purification of untrapped protein by dialysis, a Biotech CE Tubing MWCO 300 kD was used (Spectrum Inc., Breda, The Netherlands). Purification by Tangential flow filtration (TFF), a modified polyethersulfone (mPES) 750 kD MWCO hollow fibre column was used (Spectrum Inc., Breda, The Netherlands). A Luna column (C18 (2), 5  $\mu$ m, dimensions 4.60 X 150 mm, pore size 100 Å) was used for lipid quantification and purchased from Phenomenex., Macclesfield, UK. Dil Stain (1,1'-Dioctadecyl-3,3,3',3'- Tetramethylindocarbocyanine Perchlorate ('Dil'; DilC18 (3)), HPLC grade methanol and 2-propanol were purchased from Fisher Scientific, Loughborough, England, UK, in addition to the use of HPLC grade water.

#### 3.3.2 Methods

##### 3.3.2.1 Liposome manufacturing methods

The ability to produce liposomes at different scales was investigated using the NanoAssemblr<sup>®</sup> Benchtop two microfluidics (Precision Nanosystems Inc., Canada). Lipids were dissolved in methanol at the appropriate concentrations, with phosphate buffered saline (PBS) (10 mM, pH 7.3) used to form the aqueous medium. A 3:1 flow rate ratio (FRR) was selected alongside a total flow rate (TFR) of 15 mL/min.

##### 3.3.2.2 Measuring the physicochemical properties of liposomes

To measure liposome physicochemical properties dynamic light scattering was used. To determine the scalability of the manufacturing process, three instruments from Malvern Panalytical (Malvern, UK) varying in the amount that can be tested were investigated.

###### 3.3.2.2.1 *The Zetasizer NanoZS*

Dynamic light scattering (DLS) was used to analyse the size of liposomes, (ideally between 0 - 1000 nm), with the Z-average and polydispersity index (PDI) given, using the Malvern

Zetasizer Nano ZS (Malvern Panalytical, Malvern, UK). To measure size and PDI, 100  $\mu\text{L}$  of liposomes was added to 900  $\mu\text{L}$  of diluted phosphate buffered saline (1:300 deionized water, 10 mM, pH= 7.3). Also, the zeta potential was measured using zeta cuvettes with liposomes diluted 1:100 in water.

### 3.3.2.2.2 The Zetasizer AT

The Zetasizer AT was run as part of a continuous manufacturing process. The instrument runs in an automated fashion, with the user control interface which can control speed shown in Figure 3.2. Two inlet streams (for buffer and liposome samples) and outlet streams for waste. The Zetasizer AT measured liposome size and PDI at a 1:10 dilution (liposomes to buffer), with adjustments to the automated mixing possible. The buffer (5 mL/min) and liposome formulation (0.5 mL/min) are taken up by the instrument, there is a 90 second delay before the diluted sample can enter the flow cell, to allow for sufficient mixing. Once the sample enters the flow cell, the size can be measured. A total of 1 mL is required for each size measurement. The cleaning procedure in between repeat samples involved running buffer through lines. A more vigorous cleaning between different formulations involved flushing 10% ethanol (diluted with deionised water) through the system to remove any possible residual lipids present.

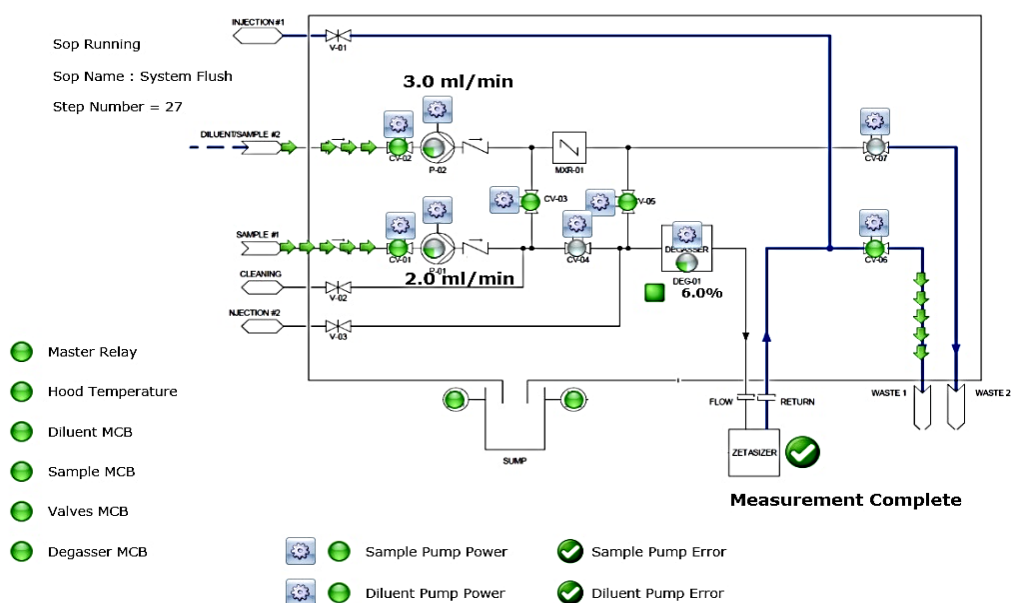


**Figure 3.2.** The user software interface for the Zetasizer AT (Malvern Panalytical Ltd, Malvern, UK).

### 3.3.2.2.3 The Zetasizer APS

The Zetasizer APS is a dynamic light scattering instrument. It is an automated process able to measure sizes in 96 and 384- well plates. The plate layout is entered into the software (Figure 3.3) with the size and PDI measured in the order assigned to the wells. The manual dilution of liposomes into PBS at a 1:10 to measure size and PDI required for the Zetasizer NanoZS is done by a robotic arm instead. The ratio of liposomes to PBS is maintained, but a smaller volume is required. For the 96 well plates, 20  $\mu\text{L}$  of liposomes are mixed with 180  $\mu\text{L}$  of buffer.

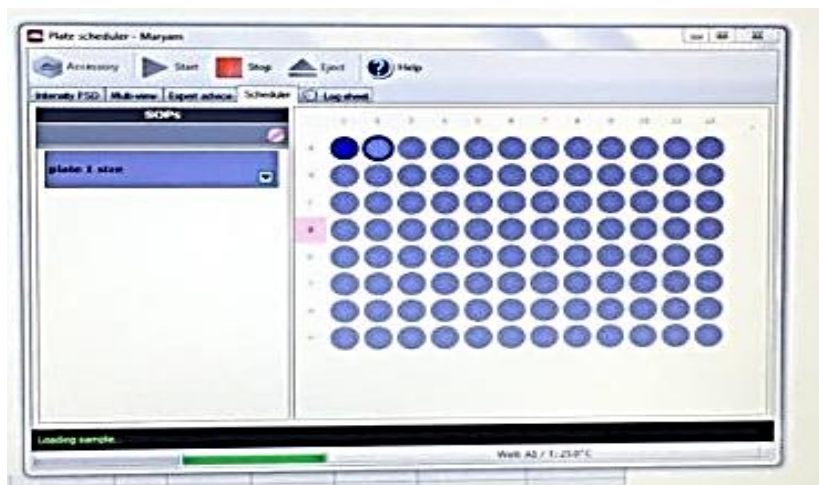


**Figure 3.3.** The user interface for the Zetasizer APS (Malvern Panalytical Ltd, Malvern, UK).

### 3.3.3 Tangential flow filtration

Liposome samples were purified using the Krosflo Research Iii tangential flow filtration system (Spectrum Inc., Breda, The Netherlands) fitted with an mPES (modified polyethersulfone) column with a pore size of 750 kD (Spectrum Inc., Breda, The Netherlands). Tangential flow filtration (TFF) was used to remove solvent and the protein ovalbumin (OVA). For the removal of solvent and protein, the liposomal formulations were run through the column with solvent and untrapped protein removed by difiltration. Fresh PBS was added at the same rate as the permeate leaving the column. For 1 mL of liposome sample (containing solvent and protein) approximately 12 mL of wash buffer is required. To concentrate the sample, TFF can be run in a closed loop without buffer added, allowing concentration to the desired volume.

### **3.3.4 Calculating liposome recovery**

Liposome recovery post TFF was calculated by incorporating the hydrophobic dye Dil Stain (1,1'-Dioctadecyl-3,3',3'- Tetramethylindocarbocyanine Perchlorate ('Dil'; DiIC18 (3)) (DiIC) at 0.2 mol% into the bilayer of the liposomes. During purification of DiIC labelled liposomes by TFF, 1 mL aliquots of permeate were collected with 100  $\mu$ L added to 96 well plates. The amount of fluorescence within permeate waste was then measured to determine liposome recovery.

### **3.3.5 Headspace gas chromatography**

Headspace gas chromatography (Agilent 7697A, Agilent Technologies, USA) was used to measure residual solvent content for liposomes produced by microfluidics. Solvent was measured by isothermal approach using an Agilent 122-1334 column (30m x 250 $\mu$ m x 1.4  $\mu$ m). The sample was held at 60°C for a minute before the temperature was ramped up to 80°C, with a total run time of 6 minutes. A calibration curve was established for solvents, containing an internal control (propan-1-ol), with the residual solvent present in samples calculated using the peak area of analyte in comparison to solvent.

### **3.3.6 Investigating liposome morphology**

#### *3.3.6.1 Transmission Electron microscopy*

Transmission electron microscopy was used to investigate the morphology of liposomes produced by microfluidics (as described in section 3.3.2.1). Approximately 10  $\mu$ L of liposome formulation was placed onto a 3.05 copper grid containing numerous hexagonal pores. The sample was left for around 30 seconds, after which 10  $\mu$ L of uranyl acetate (UA) stain was placed on top of the grid. Images of the liposome sample were then taken using transmission electron microscopy. The pictures were taken by David McCarthy, DM Microscopy, Suffolk, UK.

#### *3.3.6.2. Cryogenic transmission electron microscopy (CryoTEM)*

The morphology of liposome formulations were determined by cryogenic transmission electron microscopy (CryoTEM). Images were taken on a Jeol 2011 with a 200kv beam using minimal dose protocol, scanned at low magnification and jumped to high magnification without exposing the sample to the beam first. The camera used was a Gatan ultrascan (2k by 2k pixels). Grids were lacey carbon, 200 mesh and were prepared by adding 8  $\mu$ L of sample to a glow discharged grid, blotting from both sides for approximately 5 seconds then plunging into nitrogen cooled ethane propane mix (70% ethane). CryoTEM pictures were taken at

Warwick University, UK by Dr Saskia Bakker, Advanced Bioimaging Platform, and University of Warwick. Evaluation was performed at 15000x magnification.

### **3.3.7 Statistical tests**

Results are represented as mean  $\pm$  SD with n=3 independent batches. ANOVA and T-tests tests were used to assess statistical significance, with a Tukey's post adhoc test (p value of less than 0.05).

## **3.4 Results and Discussion**

### **3.4.1 Purification of empty liposomes by Tangential Flow Filtration (TFF)**

#### **3.4.1.1 Characterisation of liposomes purified by Tangential flow filtration**

The majority of liposomes made by microfluidics require further downstream processes to remove solvent and non-incorporated molecules. The purification of liposomes can be achieved in a number of ways, of which dialysis is the simplest. However, it is not practical at large scale and so tangential flow filtration (TFF) was considered as an alternative. The TFF system is a technique that can easily be incorporated into a continuous manufacturing process, saving time and expenditure (on costs of goods and smaller facility required) as well as improving the quality and quantity of the product produced (Kleinebudde, 2017). For instance, the demand for biologics such as monoclonal antibodies has led to the successful implementation of TFF into the process chain to remove media (Pollock, 2013). The TFF system works by flowing fluid material in a parallel direction to the membrane, causing a separation of desired and unwanted material. For this to be achieved successfully, the membrane selected has to be compatible with the sample and have a set molecular weight (Mw) cut off value. In the case of liposome purification, the liposome samples along with fresh media flow in parallel to the membrane, in this case a membrane with a 750 kD Mw cut off weight was selected. This membrane is large enough for the removal of solvent, buffer and some untrapped protein, but the liposomes are too big to get through. As a result, the permeate contains the waste material whilst the purified liposomes remain within the retentate.

To test the ability of TFF to purify liposomes, the physicochemical properties of DPPC:Chol (Figure 3.4A) and DSPC:Chol (Figure 3.4B) liposome formulations were compared before and after purification by TFF. The results show, TFF does not affect the size with no significant increase in size or PDI for both DPPC:Chol (Figure 3.4A) post production ( $84 \pm 5.0$  nm) and post TFF ( $88 \pm 0.1$  nm). The same is observed for DSPC:Chol liposomes; no significant increase in size is observed post TFF ( $49 \pm 0.3$  nm) when compared to post- production ( $43 \pm 0.3$  nm) (Figure 3.4B). The results show the TFF system is capable of purifying neutral liposomes irrespective of the lipid type, with the formulations remaining homogenous, shown by a single peak in the intensity plots and the PDI below 0.2 for both formulations (Figure 3.4A and B). The results from Figure 3.4 demonstrate the ability of TFF to purify liposomes less than 150 nm in size. The results are similar to the bespoke TFF model used by Dimov et al to purify liposome formulations that are more than 120 nm in size; using a specially designed lab-scale TFF system it was shown purification of neutral (PC:Chol liposomes, 150 nm), anionic (DPPC:Chol:DPPG, approximately 120 nm) and cationic liposomes (DDA:TDB, approximately 120 nm) can be achieved without significant loss of liposomes (Dimov *et al.*, 2017). The results from Figure 3.4 illustrate the ability to purify a range of neutral liposomes, irrespective of size and the lipid used, thus highlighting the versatility of using a TFF system to for post- production changes to liposomal formulations.

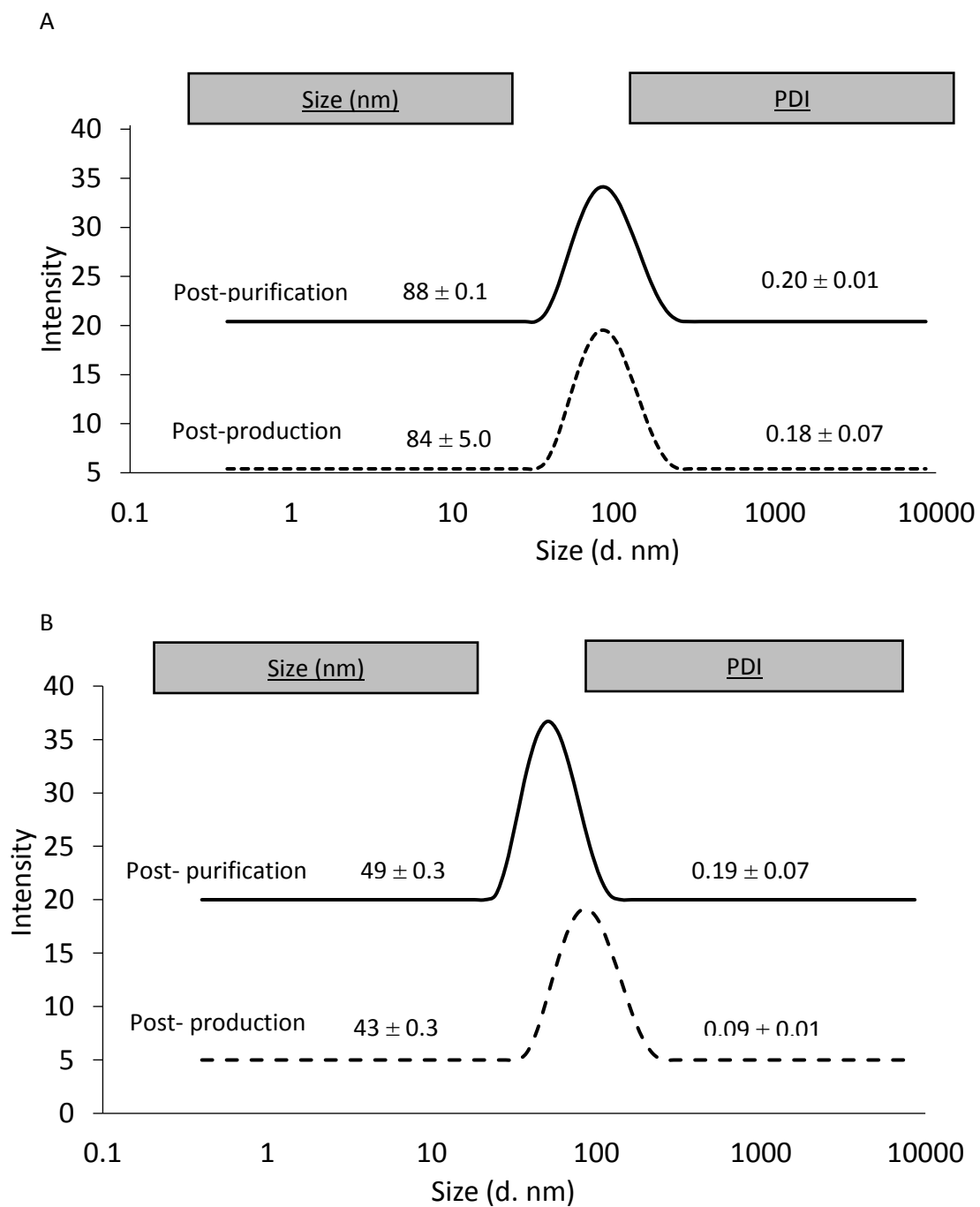


**Figure 3.4.** The characterisation of DPPC:Chol (A) and DSPC:Chol (B) liposomes produced post-microfluidics production and post-purification by tangential flow filtration. The liposomes were characterised in terms of their size and PDI by dynamic light scattering, with the size-intensities also plotted. The results represent mean  $\pm$  SD,  $n=3$  independent batches, meanwhile the size-intensity plots are representative plots taken from one reading.

### 3.4.1.2 Comparing liposome physiology after dialysis and TFF purification

The purification of liposomes by TFF is achievable for neutral liposomes. The ability of TFF was compared to the dialysis method to identify any changes in physicochemical properties, and to identify the best method. Empty DMPC:Chol and DSPC:Chol liposomes were investigated by comparing the dialysis and TFF method. The results show the two purification methods do not alter the physicochemical properties of liposomes, regardless of the concentrations used (Figure 3.5). The DMPC:Chol liposomes produced at 4 mg/mL and 10 mg/mL post- dialysis were  $73 \pm 1.3$  nm and  $70 \pm 1.3$  nm respectively, compared to  $69 \pm 1.7$  nm and  $66 \pm 2$  nm post- TFF (Figure 5.3A). Similarly, no change in size is observed between DSPC:Chol liposomes purified by either dialysis or TFF;  $47 \pm 2.1$  nm and  $46 \pm 2.0$  nm at 4 and 10 mg/mL respectively post- dialysis and  $50 \pm 0.5$  nm and  $46 \pm 0.3$  nm post- TFF (Figure 5.3A). The polydispersity of the DMPC:Chol and DSPC:Chol liposomes is not affected by either dialysis or TFF purification, with the PDI remaining below 0.2 (Figure 5.3B). The purification processes does not impact the charge of the liposomes, with the charge of DMPC:Chol and DSPC:Chol liposomes remaining above -10 mV at both concentrations (4 or 10 mg/mL) (Figure 5.3C). Whilst dialysis and TFF give similar results, the TFF system is more advantageous in that it can be easily integrated into large scale manufacturing system, with the ability to incorporate process analytical tools when producing liposomes at the large scale. Multiple microfluidics chips can be run in parallel alongside a larger TFF system, with the possibility to change the TFF column and size accordingly, thus the TFF system offers both scalability and flexibility (Ball, 2000).



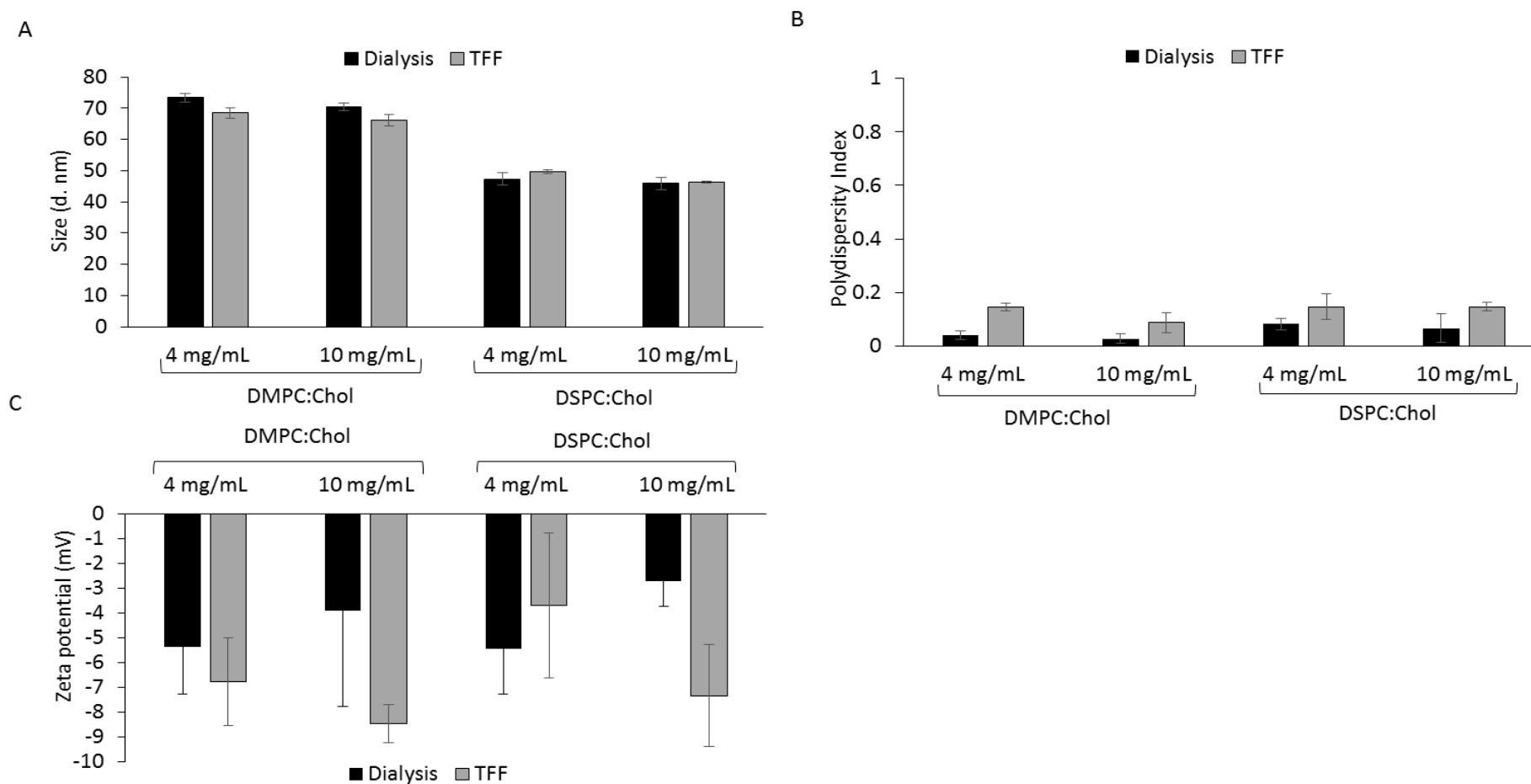


**Figure 3.5.** The physicochemical properties of DMPC:Chol and DSPC:Chol liposomes post dialysis or TTF purification. The liposomes were produced at a 3:1 FRR and 15 mL/min TFR, with the initial lipid concentration of either 4 or 10 mg/mL. The results represent mean  $\pm$  SD, n=3 independent batches.

### 3.4.1.2 Liposome recovery after TFF purification

In addition to purification of liposomes post TFF, it is important to ensure a full recovery of liposomes. Loss of liposomes can alter the concentration and thus the overall functionality of the formulation, in addition to causing a loss of material from a manufacturing perspective. To test for this, DiIC liposomes underwent purification by TFF to remove solvent. A total of 20 mL permeate was collected in 1 mL aliquots. The aliquots were then measured for any trace of fluorescence, which would indicate the presence of liposomes. As Figure 3.6 shows, DPPC:Chol liposomes are not lost during purification with the recovery of liposomes above 95% post- TFF. Although the TFF purification did not result in a loss of liposomes, the effect of FRR was tested to determine whether this influenced liposome recovery. As a result, DiIC labelled DPPC:Chol liposomes were formulated at a 5:1 FRR, alongside DiIC labelled DSPC:Chol liposomes made at both a 3:1 and a 5:1 FRR. The results from Figure 3.7 show the FRR does not affect the liposome recovery post-TFF purification. Liposomes remain in the retentate, with recovery values of between 99 -102% calculated for all formulations. The liposome recovery is not influenced by the lipid type, with both DPPC:Chol and DSPC:Chol liposomes recovery measured above 95% post-TFF.

Moreover, the pressure of the TFF system can influence the retention of liposomes, with a backpressure of more than 75 psi causing a loss of neutral liposomes in the permeate waste (Dimov et al., 2017). This impacts the concentration of the liposomal formulations and may subsequently have adverse therapeutic effects or the liposomal formulation may not be able to function at full capacity. Other factors that influence the purification and downstream modification of the liposome system is the size of the membrane, concentration and ratio of the liposomes, the presence of cholesterol, the flow rate and choice of buffer, amongst other things (Fayolle et al., 2018, Peschka et al., 1998).

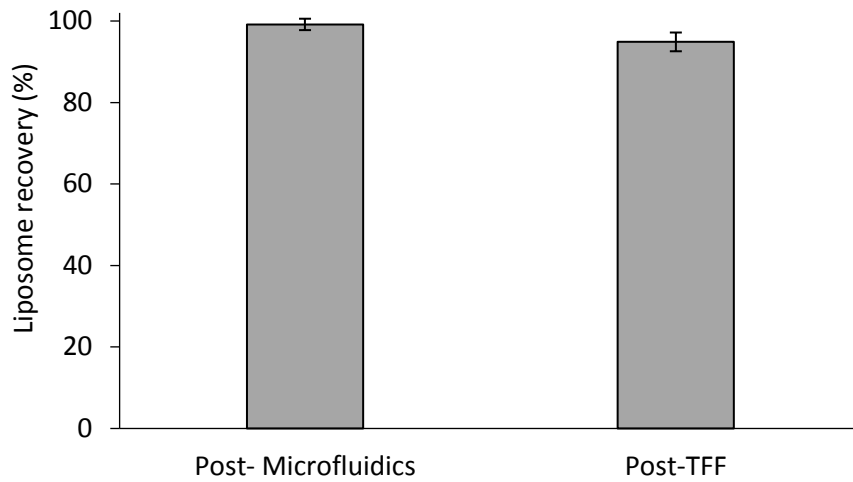


**Figure 3.6.** The liposomes recovery of fluorescently labelled DiIC DPPC:Chol liposomes before post microfluidics manufacture and post-TFF purification. The liposomes were made at a 3:1 FRR and 15 mL/min TFR. The results represent mean  $\pm$  SD, n=3 independent batches.

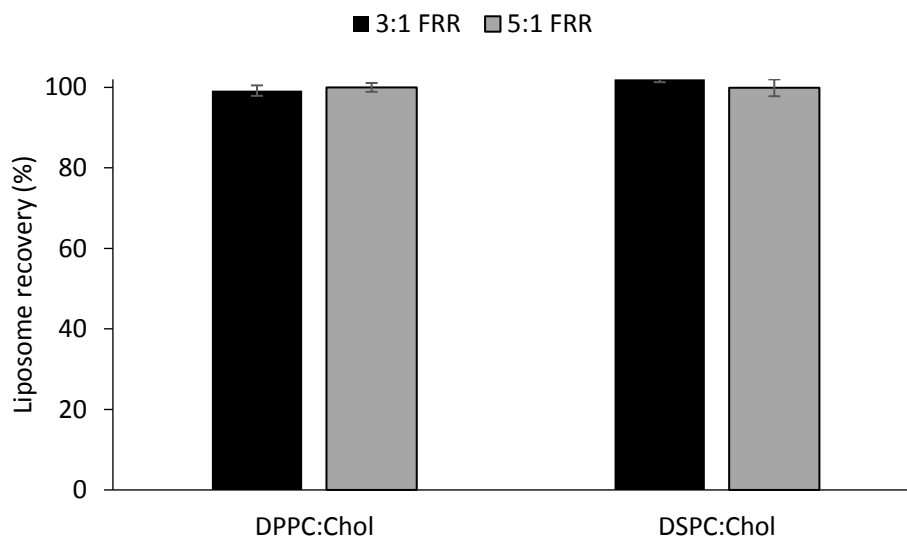


**Figure 3.7.** The liposome recovery of DiIC labelled DPPC:Chol and DSPC:Chol liposomes post-TFF. The effect of manufacturing liposomes using microfluidics at either a 3:1 or 5:1 FRR was investigated. The results represent mean  $\pm$  SD, n=3 independent batches.

### 3.4.1.3 Measuring residual solvent using headspace gas chromatography

In general, gas chromatography is the most common widely used for the quantification of solvent, and organic impurities. The technique is highly sensitive and can achieve a high degree of separation of similar compounds, with low detection limits of organic solvents achieved. The system is highly versatile with the possibility of using different columns to suit needs. The gas chromatography can involve sample analysis in two ways; direct or non-direct. The direct analysis is a simple technique whereby the sample is injected directly into the column to be analysed by gas chromatography. In cases whereby samples are a mixture of compounds, containing analytes that can stick and remain on the column causing fouling, headspace gas chromatography (H-GC) can be used (Witschi and Doelker, 1997). The H-GC can be used for substance containing a mixture of compounds, it can separate volatile substances from the non-volatile substances in order to quantify the amount of solvent present.

To confirm the TFF system is able to purify the formulations (to remove solvent and protein), the solvent content was measured using H-GC. A calibration curve, containing an internal control isopropanol alcohol was established to determine the amount of residual methanol post-TFF purification of liposome formulations (Figure 3.8), with a high degree of linearity ( $> 0.99$ ). The results show twelve cycles are sufficient to remove the methanol levels to below 0.3% (3000 part per million (ppm)) as stated by the International conference in Harmonisation (ICH), 2016 guidelines (Figure 3.9). The chromatographs also show a gradual decrease in the amount of methanol detected by the H-GC as the purification of liposomes by TFF progresses (Figure 3.10A) with no methanol detected within the sample after purification with TFF (Figure 10.B). The appropriate quantification of residual solvent is not only important for toxicity reasons, but the presence of solvent can also affect the physicochemical properties of liposomes including size and release rate (Devotta et al., 1995). The results from Figure 3.10 show the H-GC is a rapid and highly efficient technique for the quantification of the residual solvent content within the liposomal formulations. It shows the TFF system is able to refine liposomes (by removal of solvent), thus the H-GC is a good analytical technique to measure the quality of the liposomal formulations produced.

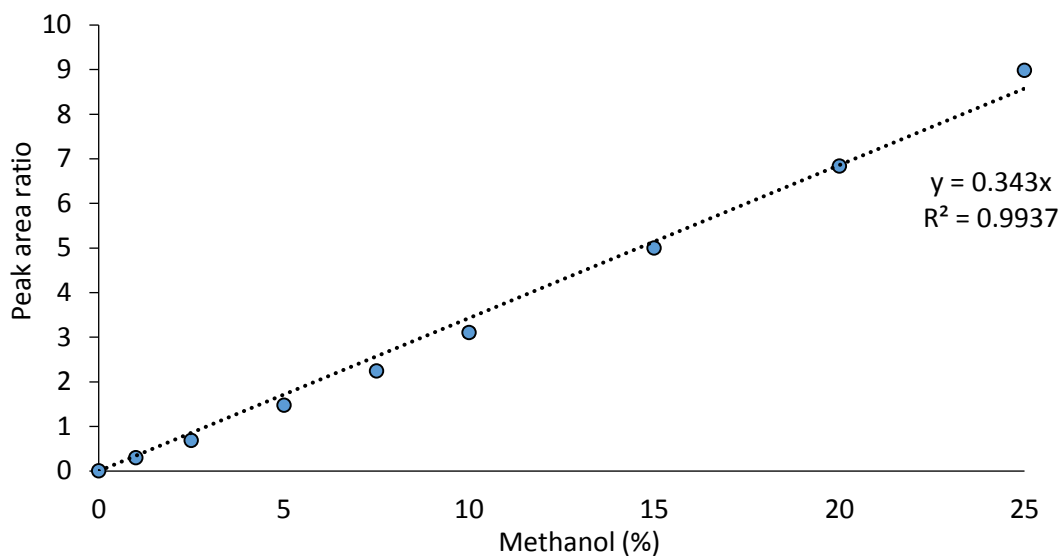


**Figure 3.8.** Calibration curve for methanol containing the solvent isopropyl alcohol as an internal control. The solvent was measured by headspace gas chromatography, with the peak area ratio of methanol to isopropyl alcohol plotted against the percentage of methanol present. The results represent mean  $\pm$  SD, n=3 independent batches, with the LOD (0.28% methanol) and LOQ (0.86) calculated.

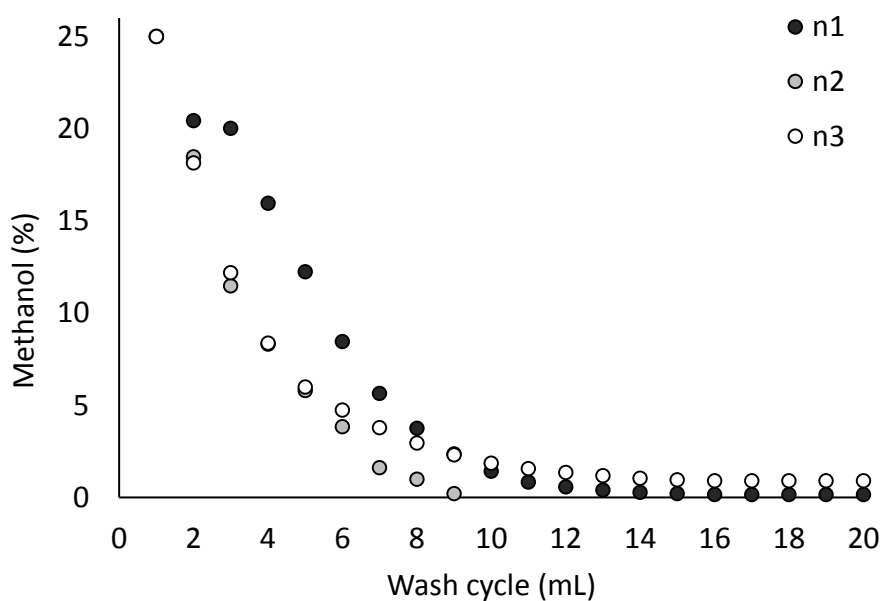


**Figure 3.9.** The use of tangential flow filtration to establish the amount of buffer needed to remove methanol, which was used to produce liposomes. The DPPC:Chol liposomes were purified by TFF with a total of 20 mL permeate collected (in 1 mL aliquots). The amount of methanol was measured using headspace gas chromatography, and plotted as the percentage of solvent remaining in the aliquots against the amount of wash cycle. The results represent mean  $\pm$  SD, n=3 independent batches.

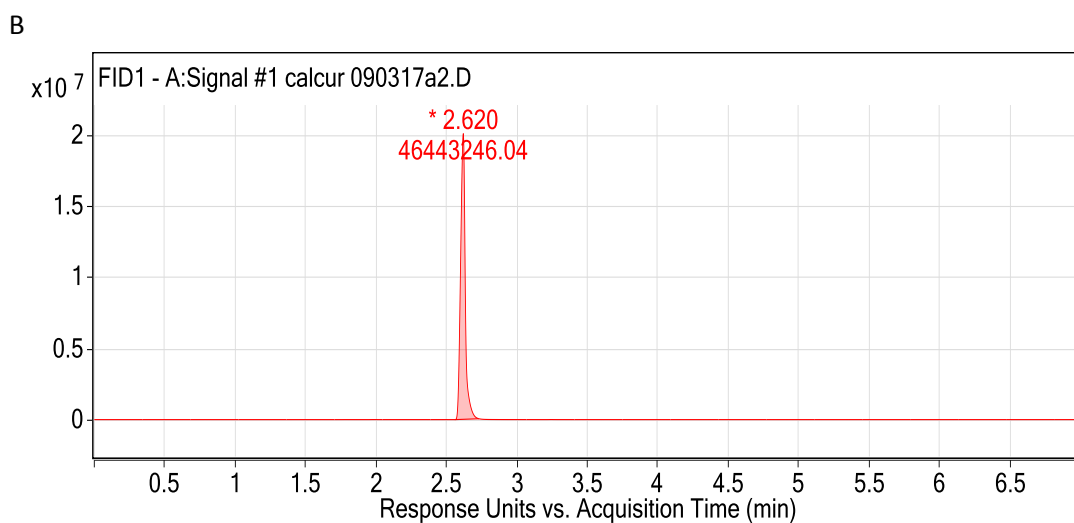
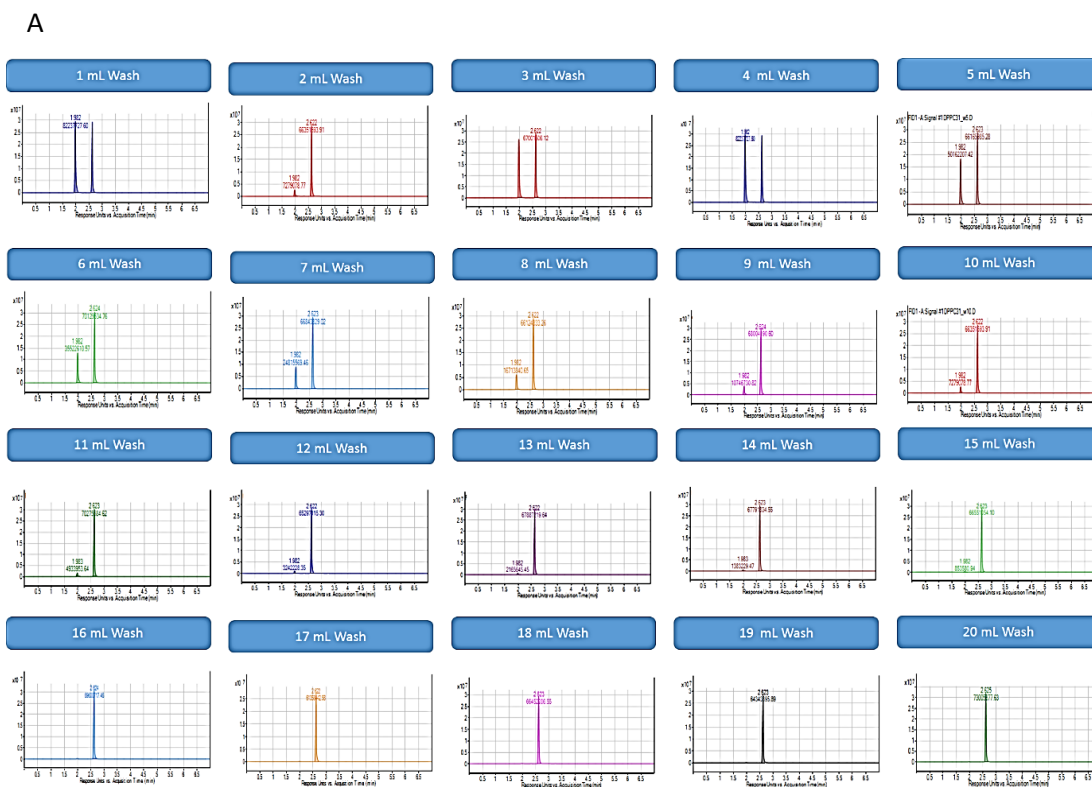


**Figure 3.10.** The headspace gas chromatography plots for the amount of methanol present within the permeate after being washed with a set amount of phosphate buffered saline (A) and the liposome sample (B). The results show the amount of methanol detected decreases as the wash cycle progresses. The samples were spiked with isopropanol alcohol as an internal control; the concentration of which remains the same throughout the wash cycle.

#### 3.4.1.4 Morphology of liposomes by transmission electron microscopy

The morphology of the liposomes post TFF purification was investigated, with empty DPPC:Chol liposomes as model liposomes. Figure 3.11 shows the liposome morphology is not affected by the TFF purification, with the DPPC:Chol liposomal formulations retaining the spherical structure associated with liposomes. The DPPC:Chol liposomes retaining the aqueous core and lipid bilayer which is visible in Figure 3.11. The images show the TFF purification technique does not impact the morphology; in general the purification technique should not influence the morphology or loading of the liposomal formulations. For instance, Joshi et al showed the ability to manufacture dual loaded (metformin and glipizide drugs) DSPC:Chol liposomes with no changes in morphology observed post dialysis (Joshi et al., 2016). The cryoTEM images of the DSPC:Chol liposomes remained spherical in nature post dialysis. Furthermore, research by Dimov et al using a bespoke TFF system showed no changes in propofol loaded PC:Chol liposomes post-TFF purification, with the expected morphology shown by cryoTEM imaging (Dimov et al., 2017). Thus the results from Figure 3.11 show the morphology of liposomes is not influenced by the TFF purification system, which is a versatile system that can purify a wide range of liposome formulations.

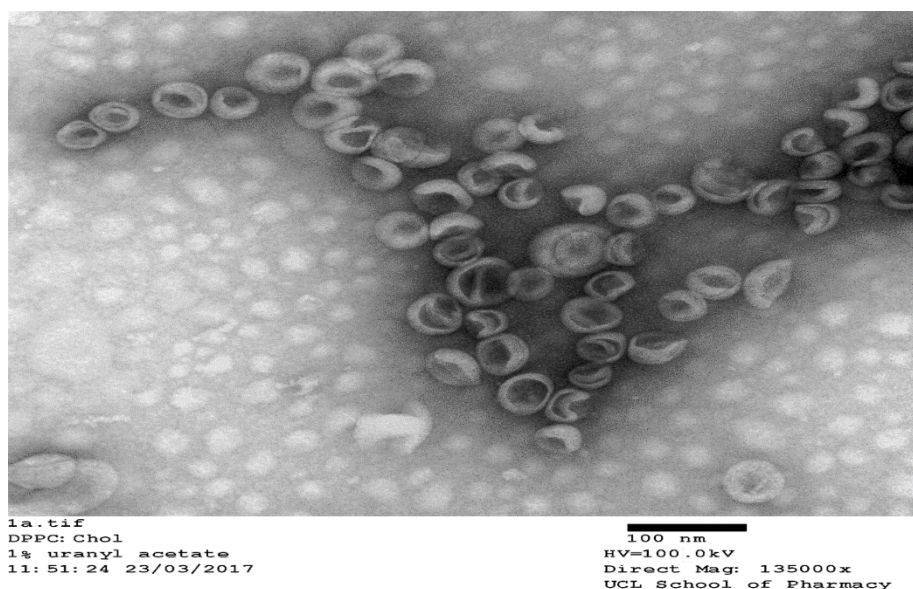


**Figure 3.11.** The morphology of the DPPC:Chol liposomes was investigated by transmission electron microscopy. Liposomes purified by tangential flow filtration were tested to see if this purification technique effected the morphology and characteristic of the DPPC:Chol liposomal formulation.

### 3.4.1.5 Concentration of liposomes using Tangential Flow Filtration (TFF)

The TFF system has the ability to concentrate samples in addition to purifying and removing unwanted products. This can be achieved by running the liposomal samples through the hollow fibre column without replenishing the buffer lost in the waste permeate stream. As the liposomal formulations are recirculated in a closed loop, buffer and solvent can leave into the waste stream, allowing for the concentration of the liposome formulations to a desired level. To test this ability, DSPC:Chol formulations underwent purification and were concentrated up to four times. The results from Figure 3.12A shows the TFF system is good for concentrating samples. The size of the DSPC:Chol liposomes does not increase remaining at around 43 nm post TFF, and after x1, x2 and x4 concentration. The PDI post- TFF is  $0.09 \pm 0.14$  with the PDI post concentration still below 0.2 (Figure 3.12A). The PDI for the x1, x2 and x4 concentrations are  $0.11 \pm 0.02$ ,  $0.11 \pm 0.01$  and  $0.15 \pm 0.002$  respectively, suggesting the liposomes remain a homogenous population despite up to x4 concentration of the formulations. There is no change in the population of liposomes, with a single peak observed for the size intensity plots (Figure 3.12B). Also, the zeta potential is not affected by the TFF and concentration step, with the measured zeta potential above -10 mV (Figure 3.12A). The ability to purify liposome formulations in a scalable format is an important feature of any manufacturing process. Furthermore, the lipid solubility of some lipids within suitable solvents can be limited and thus TFF can allow the concentration of liposome formulations to required doses. These studies demonstrate the ability to purify and concentrate liposome formulations in a scalable format.

Furthermore, the concentration of liposomes without replenishing the lost buffer, does not lead to a loss of lipid retention. The physicochemical liposomal properties of liposomes is maintained throughout the concentration steps (Figure 3.12). The formulations were first purified and then concentrated, with research having shown this way is preferred as it results in fewer changes to the liposomal formulations (Pattnaik, 2009). However, if the buffer to be exchanged is expensive, then it may be more cost effective to concentrate the formulations before purifying; thus illustrating the TFF system is flexible and can be adapted to meet specific needs.



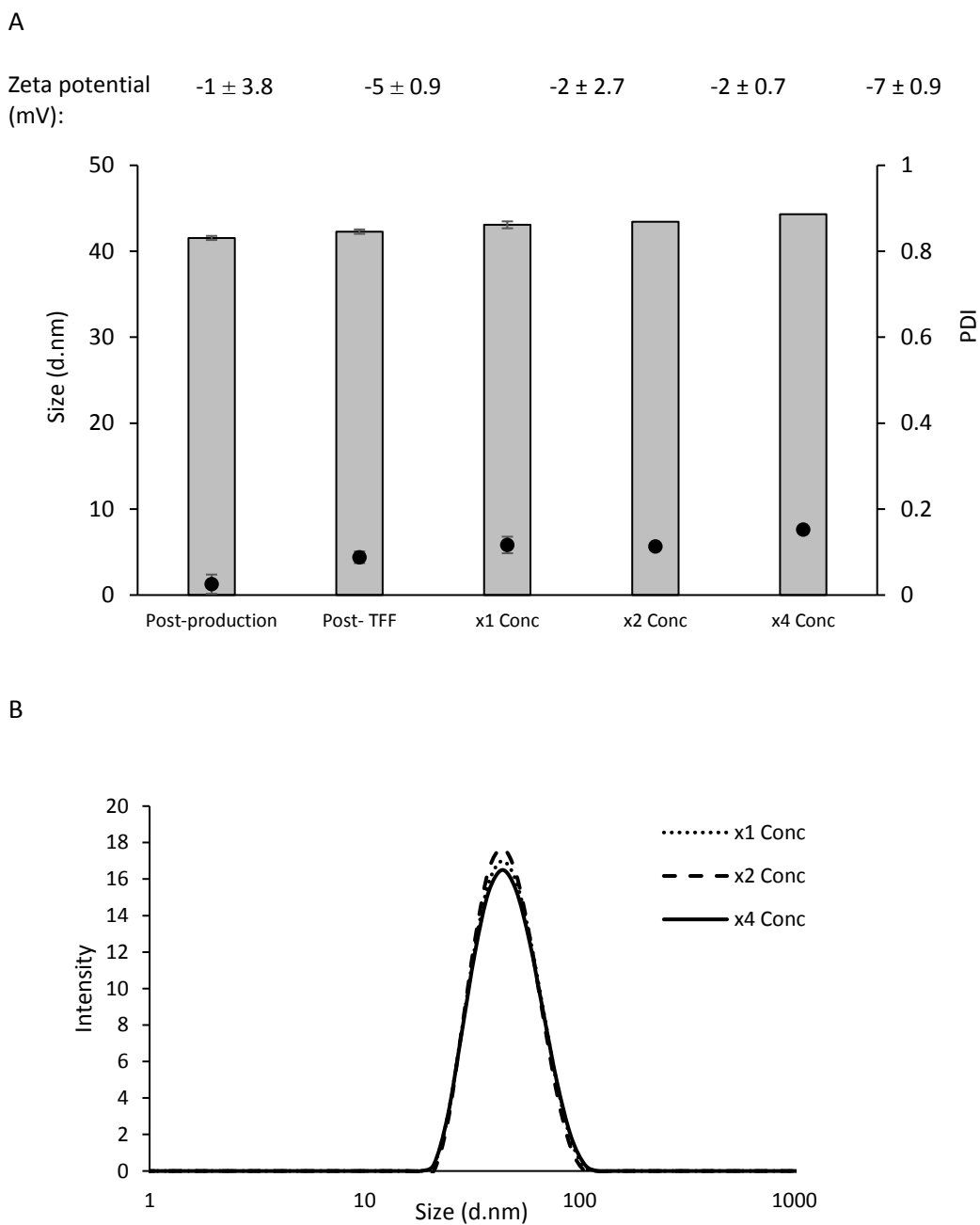


**Figure 3.12.** Characterisation of DSPC:Chol liposomes that underwent a TFF wash and were concentrated one, two and four times. The size, polydispersity index and zeta potential of the DSPC:Chol liposomes was measured (A). The bars represent size and the circles represent PDI. The size- intensity peaks of the DSPC:Chol liposomes at the various test conditions was also plotted (B). The characterisation results represent the mean  $\pm$  SD, with an  $n=3$ , meanwhile (B) are representative plots taken from one reading.

### **3.4.2 Purification of protein loaded liposomes**

#### **3.4.2.1 The purification of protein loaded liposomes**

In addition to the removal of solvent, the TFF system must be able to remove non-incorporated drugs and protein. To test this, the ability of the TFF system to remove the protein ovalbumin (OVA) was determined by mixing 1 mg/mL of non-incorporated OVA with empty DPPC:Chol liposomes. The results from Figure 3.13 show the TFF is able to simultaneously remove untrapped OVA, as well as solvent in the same amount of wash cycles (12 mL). It suggests the purification of OVA is efficient, with no significant change in liposome size observed before and after purification of OVA loaded DPPC:Chol liposomes by TFF (Figure 3.14). The OVA loaded DPPC:Chol liposomes are  $75 \pm 2.8$  and  $79 \pm 4.1$  nm before and after TFF respectively, with the PDI remaining below 0.2 after TFF suggesting a homogenous population. Furthermore, the zeta potential remains above -10 mV after TFF, with the neutral charge retained (Figure 3.14).

Previous research has coupled the ethanol injection method with a TFF system to produce high throughput manufacturing methods for protein loaded liposomes. For instance, the ethanol injection method was adapted to form a crossflow injection method to produce protein loaded liposomes, with 7.5% residual ethanol content. Removal of solvent and protein involved a two-step process involving long ultrafiltration cycle, followed by diafiltration to remove untrapped protein and solvent (Wagner *et al.*, 2002). The removal of high concentrations of protein concentration is difficult, due to the possibility of membrane fouling due to protein to membrane interactions (O'Sullivan *et al.*, 2012). In comparison, the results from Figure 3.13 show the possibility to remove both protein and solvent simultaneously. The results suggest TFF is a quicker alternative for the removal of non-incorporated OVA.

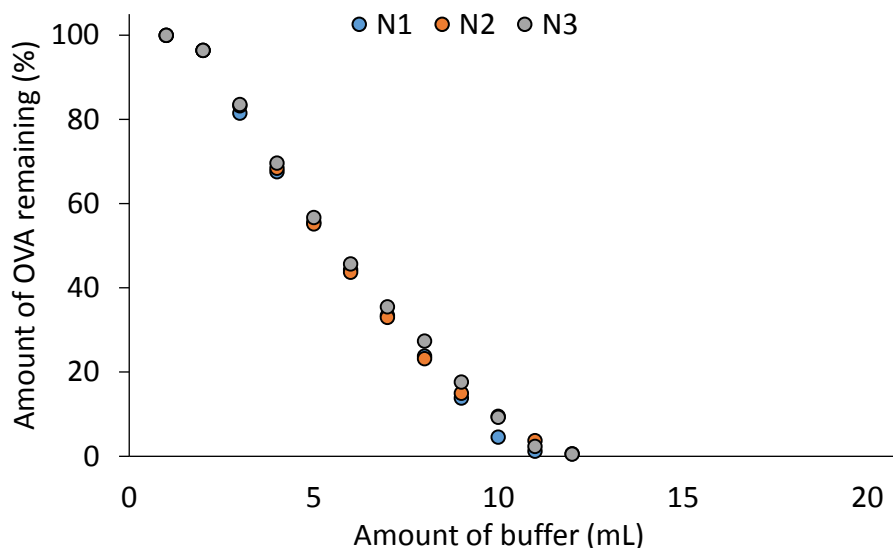


**Figure 3.13.** The amount of OVA present in permeate over 20 mL of phosphate buffered saline washes was calculated, and subtracted from the original starting concentration to work out the amount of OVA remaining. The DPPC:Chol liposomes were made using microfluidics at a 3:1 FRR and 15 mL/min. The results represent three independent batches.

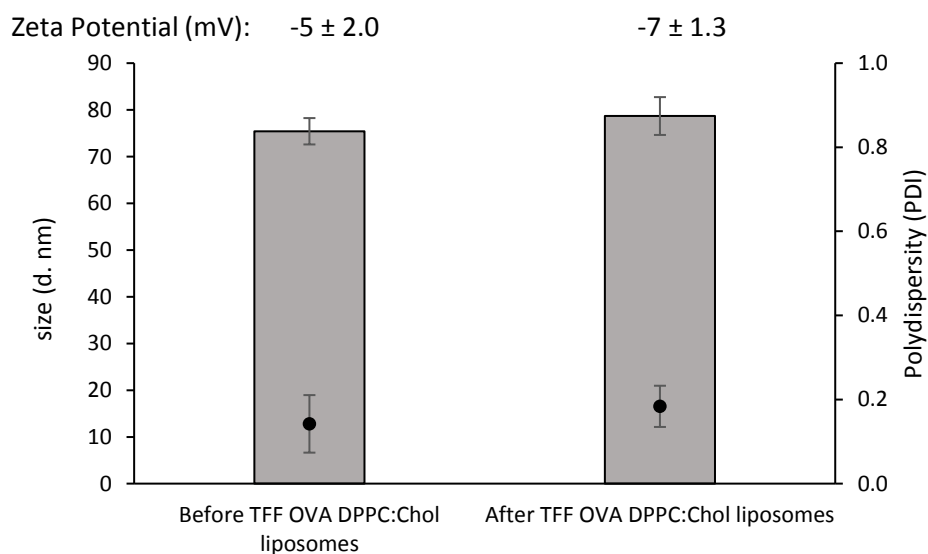


**Figure 3.14.** The physicochemical properties of DPPC:Chol liposomes before and after purification with tangential flow filtration. The liposomes were produced at a 3:1 FRR and 15 mL/min TFR, with 0.25 mg/mL initial ovalbumin added into the aqueous buffer. Dynamic light scattering was used to determine the size, polydispersity index and zeta potential of the liposomal formulations. The results represent mean  $\pm$  SD, n=3 independent batches.

### 3.4.2.2 Determining morphology of liposomes by transmission electron cryomicroscopy (CryoTEM)

The morphology of OVA loaded liposomes purified by TFF was investigated in comparison to the dialysis purification technique. As with the empty liposomes, Figure 3.15 shows the addition of OVA protein does not affect the morphology of the OVA loaded DMPC:Chol liposomes. Spherical OVA loaded DMPC:Chol liposomes are produced by microfluidics (Figure 3.15A), the morphology was retained throughout purification by dialysis (Figure 3.15B) or TFF (Figure 3.15C). The liposomes also remained below 100 nm, and the size was not significantly different post- TFF compared to the post-production of OVA loaded DMPC:Chol liposomes. Upon visual inspection, the liposome appear homogenous after purification by either dialysis or TFF, which corresponds with the low PDI values (less than 0.2) measured after purification of liposomal formulations. The results illustrate the purification process does not influence the morphology of the liposomal formulations produced, with TFF the preferred method for removal of untrapped protein. Unlike dialysis, the TFF system uses a pump to actively pump sample across a membrane, thus reducing the time taken for the purification of liposomes to occur and so this method is more economically viable.

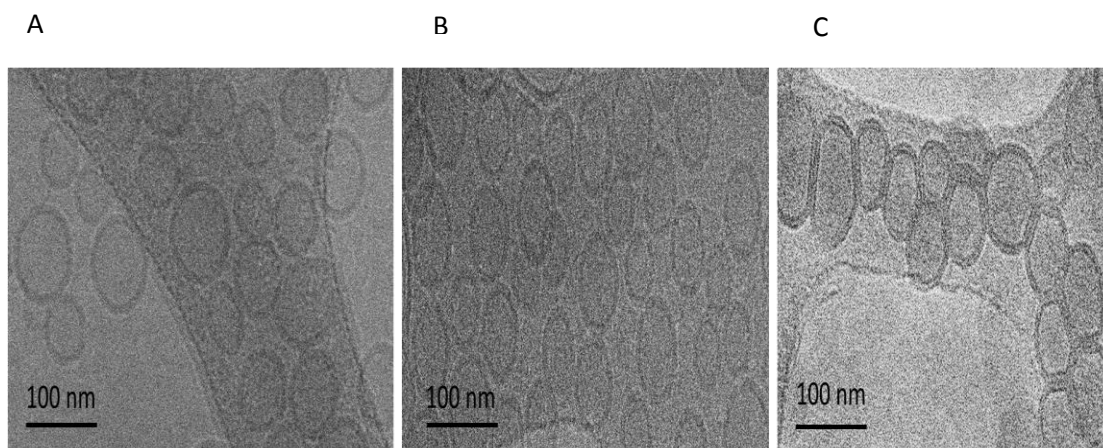


**Figure 3.15.** The morphology of OVA loaded DMPC:Chol liposomes post microfluidics production (A), purification by dialysis (B) and purification by tangential flow filtration (C). The morphology of the liposomal formulation was investigated by cryoTEM.

### 3.4.3 Scalable production of liposomes

#### 3.4.3.1 Large scale manufacturing using Zetasizer AT

The introduction of microfluidics technology for the production of liposomal medicines shows promise in overcoming problems associated with process control, heterogeneity and batch-to-batch uniformity associated with the manufacturing of liposomal medicines. Whilst microfluidics has been thoroughly investigated for the high throughput production of liposomes (Jahn *et al.*, 2010, Kastner *et al.*, 2014, Joshi *et al.*, 2016, Dimov *et al.*, 2017), challenges remain with the liposome refinement (solvent and non-incorporated active pharmaceutical ingredients (API) removal) needed downstream of the production process. Having highlighted the use of TFF to purify liposomes efficiently, this was coupled with microfluidics to set up a scalable liposome manufacturing model. The robustness and accuracy of the model is investigated alongside the quality of the liposomes produced, by using process analytical tools (PATs). For this model, microfluidics was connected to a TFF system, with the Zetasizer AT monitoring the quality of liposomes produced throughout production (post microfluidics production and post purification) (Figure 3.16). To test this two liposome formulations DPPC:Chol and DSPC:Chol were made at both a 3:1 and 5:1 FRR (with the TFR was kept constant at 15 mL/ min).

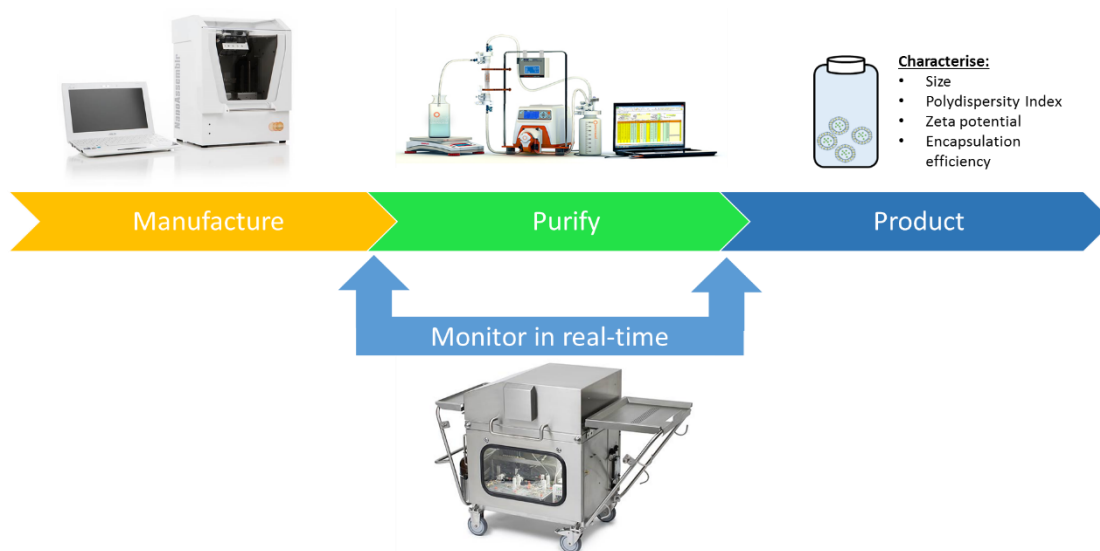


**Figure 3.16.** The process flow for the lab scalable model for liposome manufacture. Liposomes are manufactured by microfluidics and purified by tangential flow filtration, with the ability to check the quality of the liposomes produced in real-time by using the Zetasizer AT (Malvern Panalytical Ltd).

Initially, using the scale-up method the DPPC:Chol and DSPC:Chol liposome physicochemical properties were measured post production, and compared to off-line manual measurements (using the Zetasizer NanoZS). The effect of FRR on the scalable model was also compared to investigate if this influenced the characteristics of the liposomes produced, so DPPC:Chol and DSPC:Chol liposomes were produced at a 3:1 and a 5:1 FRR. The results from Figure 3.17 show the scalable model has the ability to measure liposomal characteristic in real time. The size of DPPC:Chol liposomes measured at-line or off-line post-production remained the same irrespective of the FRRs used; DPPC:Chol liposomes are around 60 nm when produced at a 3:1 FRR and at 54 nm when produced at a 5:1 FRR (Figure 3.17A). Equally, the type of lipid used did not adversely impact the ability of the at-line measuring system; DSPC:Chol liposomes were measured to be around 49 nm in size using both dynamic light scattering systems and at different FRRs post- microfluidics production. The scaleable model did not impact the heterogeneity of the liposomal formulations (DPPC:Chol and DSPC:Chol), with both formulations having a measured PDI of less than 0.2. The at-line and off-line measurements gave similar values at both FRRs tested (Figure 3.17B).

Furthermore, the scalable model was also tested after purification of liposomes by TFF. Once again the results were measured both at-line and off-line, with the size of the DPPC:Chol and DSPC:Chol liposomes remaining the same for both measurement techniques (Figure 3.17C). This was observed irrespective of the FRR tested, and the PDI remained below 0.2 (Figure

3.17D). The liposomal formulations remained homogenous throughout the manufacturing process (from production to purification), illustrated by the single peak for the size-intensity plots (Figure 3.18). The results show that the scale-up process is suitable for the large scale manufacture of liposomes; with commercial equipment available to increase manufacturing quantities as well as having quality control measures in place to ensure the product meets specification. The results show the model is able to facilitate the complete removal of unwanted active pharmaceutical ingredients (APIs) and solvents, which was previously only achievable using dialysis techniques (Hood et al., 2014, Kastner et al., 2015). Also, as the liposome model is made up of commercial equipment, with larger versions of the systems available, the liposome production method is translatable to a commercial setting (Ball, 2000) and economically viable. Research by Worsham et al has found running a liposome manufacturing model for 24 hours in a continuous manner would lead to 8.4 times more liposomal drug product produced (with the same overhead costs) compared to batch production in the same amount of hours (Worsham et al., 2018). Given the scalable model (Figure 3.17) can be used to produce liposomes in a batch or continuous manner (with minor adjustments), the flexibility of this model depending on the units of liposomal formulations required, makes it a good model for the production of liposomal formulations.

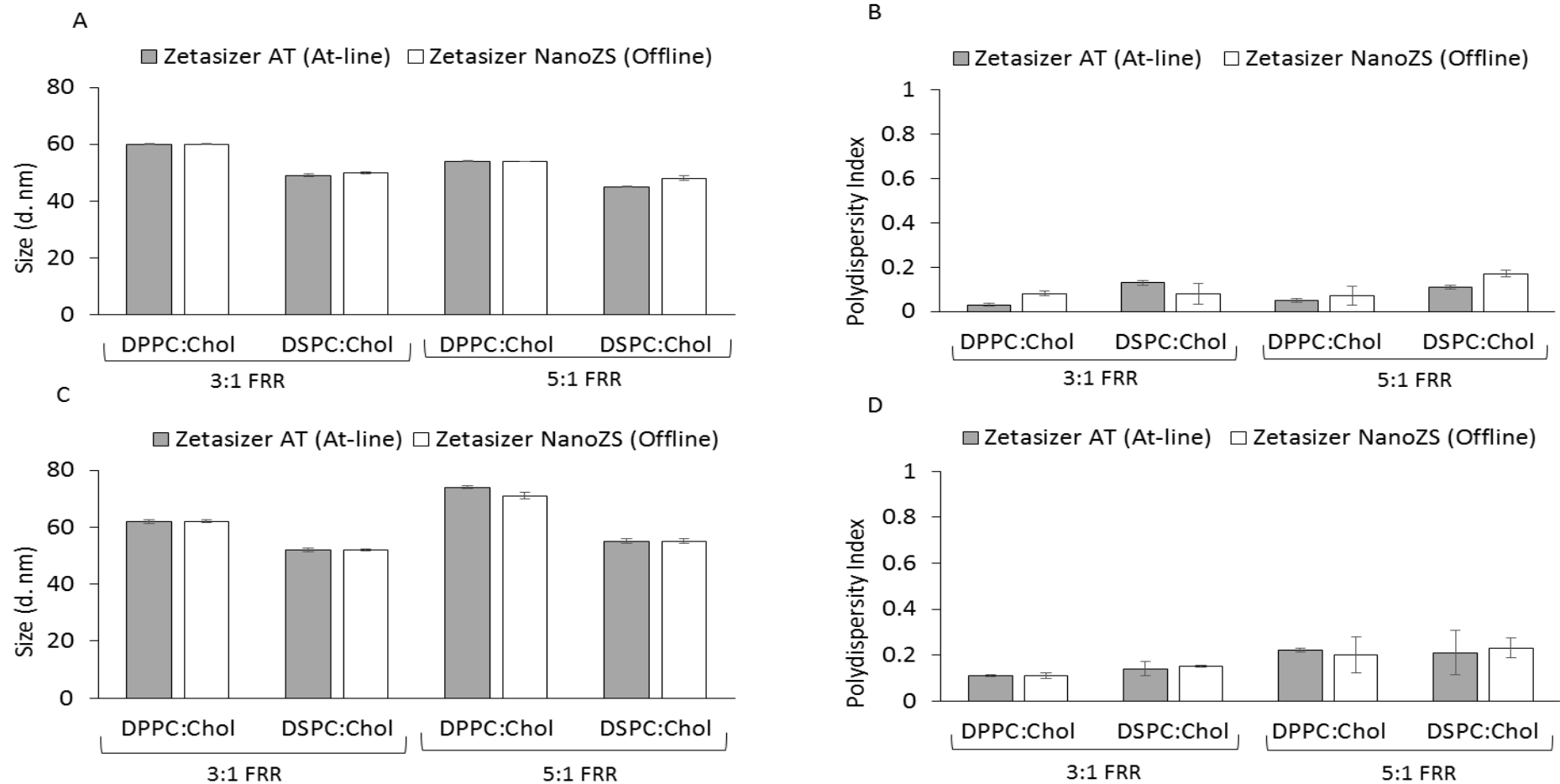


**Figure 3.17.** The physicochemical properties of empty DPPC:Chol liposomes made using microfluidics (at a 3:1 FRR and 15 mL/ min TFR). The ability to characterise liposomes at-line (Zetasizer AT) and offline (Zetasizer NanoZS) was compared post microfluidics production in terms of size (A) and polydispersity (PDI) (B). After purification of the liposomes, the size (C) and PDI (D) was investigated both at-line and offline. All results represent the mean  $\pm$  SD, with an n=3 independent batches.



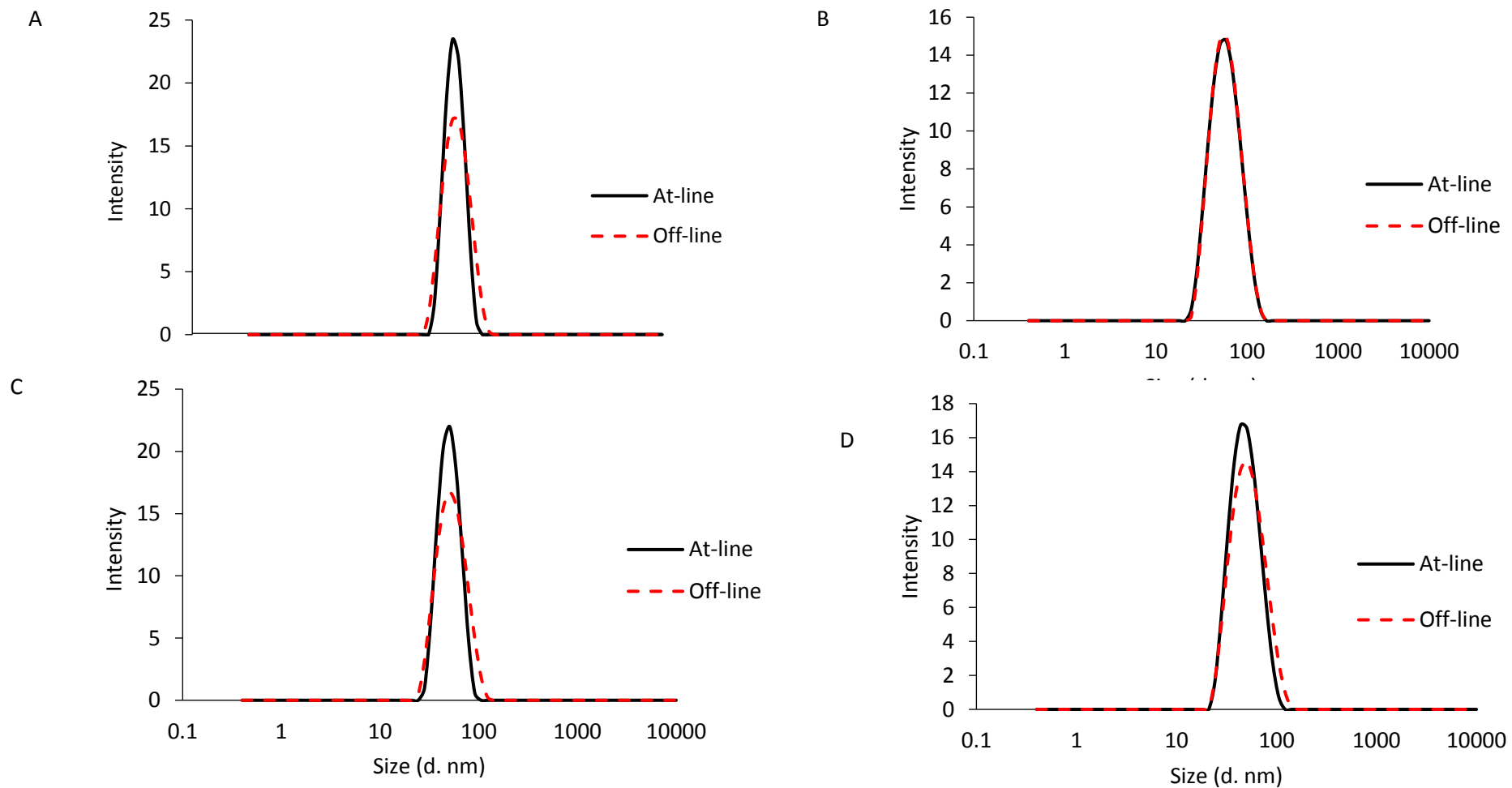


**Figure 3.18.** The size- intensity plots measured at-line (Zetasizer AT) and offline (Zetasizer NanoZS) for empty DPPC:Chol liposomes produced at a 3:1 FRR (A) and 5:1 FRR (B), as well as for DSPC:Chol liposomes produced at a 3:1 FRR (C) and 5:1 FRR (D). The size- intensity plots are representative plots taken from one reading.

### 3.4.3.2 The use of the Zetasizer APS to measure the physicochemical properties of liposomes

In addition to increasing the efficiency and production of liposomes, high throughput screening of test formulations is important in order to identify and select the right liposomal formulation quickly. This saves resources such as time and money which can be used elsewhere. Current methods to characterise liposomes are often labour intensive; for instance the Zetasizer NanoZS requires an operator to measure each liposomal formulation to be characterised. In contrast, the Zetasizer APS (Malvern Panalytical Ltd) is a simple to operate automated dynamic light scattering instrument which is able to measure sizes in 96 and 384- well plates; Figure 3.19 shows images of the instruments and software.

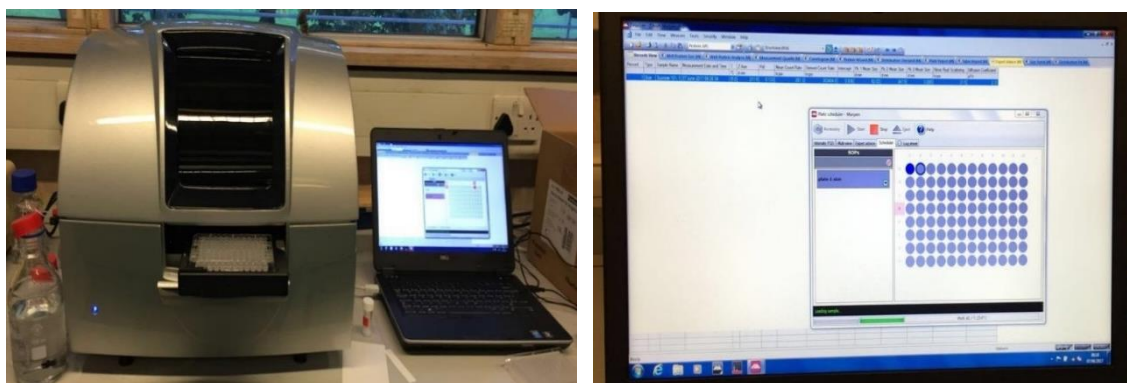
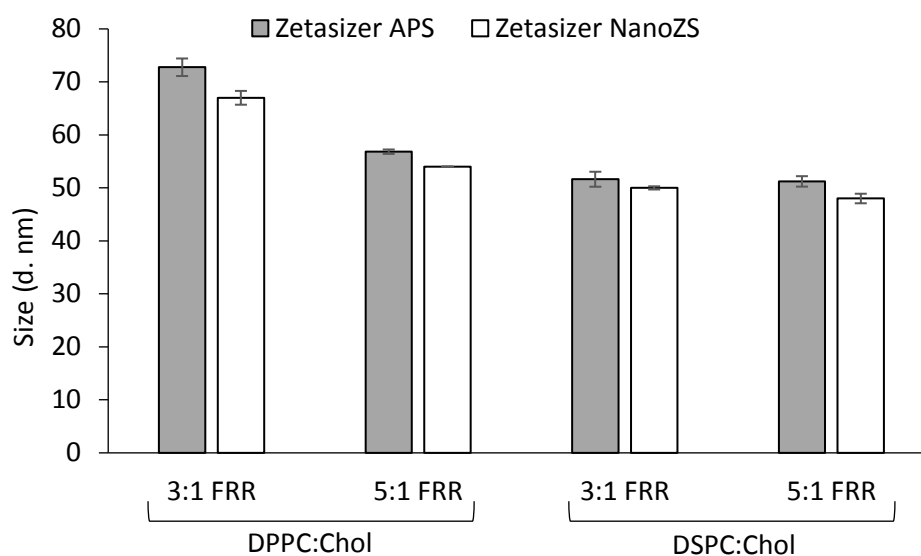


**Figure 3.19.** The Malvern Zetasizer APS (Malvern Panalytical Ltd, Malvern, UK) and the software that controls the machine

The ability of the Zetasizer APS to characterise liposomes was compared to manual measurements by the Zetasizer NanoZS. The DPPC:Chol and DSPC:Chol liposomes were produced at both a 3:1 FRR and at a 5:1 FRR, with 100  $\mu\text{L}$  of the samples pipetted into a 96 well plate. Like with the Zetasizer NanoZS, the dilution factor for the liposomes was kept at 1:10 (liposomes: PBS), but at a smaller volume. The injection volume of the Zetasizer APS was set at 20  $\mu\text{L}$  of liposome sample mixing automatically with 180  $\mu\text{L}$  of phosphate buffered saline (PBS, 10 mM, pH= 7.3). The plate layout was input into the software and multiple samples were run in sequence, with a cleaning procedure added in between each sample to remove any possibility of contamination. Results from Figure 3.20A show the Zetasizer APS is equally capable of characterising liposomes compared to manual measurements using the

Zetasizer NanoZS. There is no significant difference in the sizes measured for both DPPC:Chol and DSPC:Chol liposomes at both FRRs. For instance, the measured size for DSPC:Chol produced at a 3:1 FRR by the Zetasizer APS is  $52 \pm 1.4$  nm, which is similar to the measurement obtained from the Zetasizer NanoZS ( $50 \pm 0.3$  nm) (Figure 3.20A). Both instruments (Zetasizer APS and Zetasizer NanoZS) also show the liposome formulations are homogenous, with measured PDI values of less than 0.2 for DPPC:Chol and DSPC:Chol irrespective of the FRR used (Figure 3.20B). The results are encouraging as they suggest the Zetasizer APS can be used in early stage research for the rapid screening and selection of liposomes that fit the formulation specifications required for a particular liposomal drug formulation. Time and money can be saved by the earlier screening and elimination of unsuccessful candidates (Worsham *et al.*, 2018), therefore earlier characterisation screening of liposomal formulations using automated systems such as the Zetasizer APS may make the liposomal drug formulations more streamlined.

A



Continued on the next page

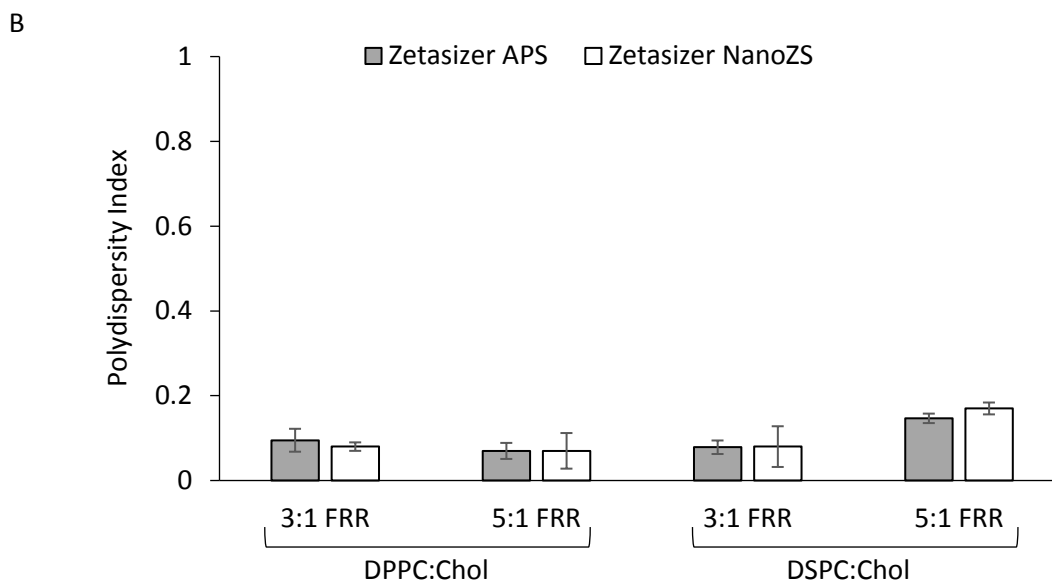


**Figure 3.20.** A comparison of the physicochemical properties of liposomes measured using the Zetasizer APS and Zetasizer NanoZS. The size (A) and PDI (B) of DPPC:Chol and DSPC:Chol liposomes produced at either a 3:1 or a 5:1 flow rate ratio (FRR) and 15 mL/ min total flow rate (TFR). The results represent mean  $\pm$  SD, n=3 independent batches.

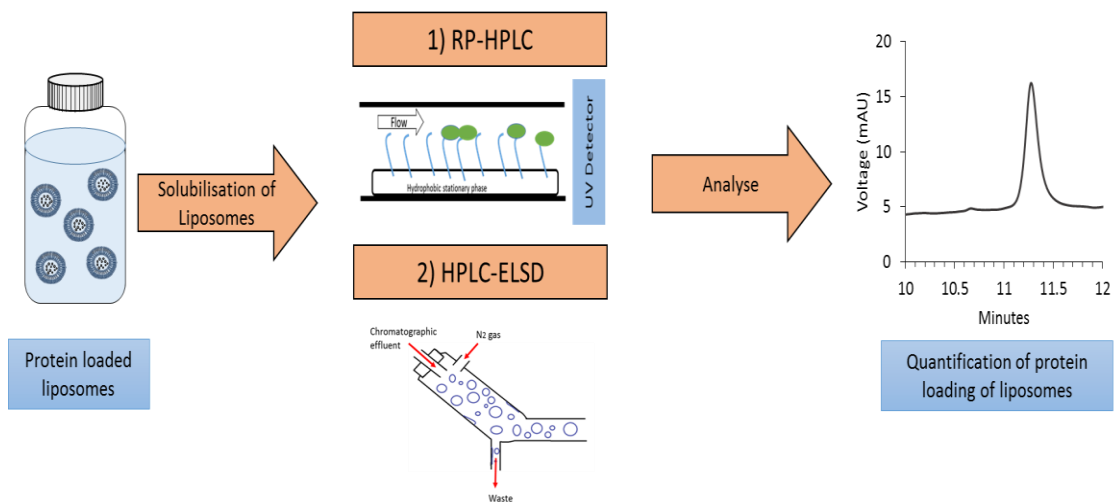
### 3.5 Conclusion

The high- throughput production of liposomes is important to overcome the current bottlenecks associated with liposome manufacture. In this chapter, the main stages needed for the manufacture of liposomes were identified, with microfluidics coupled with TFF downstream a viable option for the rapid manufacture of liposomal formulations. The TFF system was investigated as an alternative to the traditional methods for liposome refinement (removal of solvent and non- incorporated APIs) such as dialysis. The research in this chapter shows the TFF maintains liposome characteristics post- TFF, with the size and polydispersity remaining the same. Given the importance of the size of liposomes on drug loading, release and biodistribution, having effective ways to measure liposomal characteristics is key. A number of process analytical tools were used to monitor the liposomal formulations during development. The successful monitoring of liposomes at-line (in real time) was shown using the Malvern Zetasizer AT (Malvern Instruments, Malvern, UK) both for in-process monitoring and for product validation. The results obtained in real-time were directly compared to off-line measurements (Zetasizer NanoZS), with the same results obtained for both irrespective of the liposomal formulations used. Rapid at-line particle size analysis can be incorporated

(post- liposome production and post- TFF) within a scalable-independent process for monitoring liposomal formulation quality in real-time. As a result, a scale independent process for the manufacturer, purification and monitoring of liposomes was successfully identified, and thoroughly investigated with the possibility of using this model for commercial manufacturing of liposomal formulations.

# Chapter 4

## Rapid protein quantification techniques using High Performance Liquid Chromatography (HPLC) for the determination of protein loading in liposomal formulations



Work presented in this chapter has been published in:

1. HUSSAIN, M. T., FORBES, N. & PERRIE, Y. 2019. Comparative Analysis of Protein Quantification Methods for the Rapid Determination of Protein Loading in Liposomal Formulations. *Pharmaceutics*, 11, 39.
2. FORBES, N., HUSSAIN, M. T., BRIUGLIA, M. L., EDWARDS, D. P., HORST, J. H. T., SZITA, N. & PERRIE, Y. 2019. Rapid and scale-independent microfluidic manufacture of liposomes entrapping protein incorporating in-line purification and at-line size monitoring. *International Journal of Pharmaceutics*, 556, 68-81.

## 4.1 Introduction

### 4.1.1 High throughput quantification techniques for protein loaded liposomes

The use of proteins as therapeutics and preventatives for a wide range of diseases has become increasingly popular, with a lot of interest in the field of vaccine development (Carter, 2011, Leader *et al.*, 2008). The bioavailability of protein subunit antigens or recombinant proteins can be enhanced by the use of suitable delivery systems for administration routes that impact the stability of free proteins (such as oral and pulmonary administration routes) (Gupta *et al.*, 2013). Liposomes are one such delivery system that are well-established drug, RNA and DNA carriers. The use of liposomes for protein and peptides carriers is promising, with liposomes able to adsorb or encapsulate the protein of interest (Chonn and Cullis, 1995). Until recently, the manufacture of liposomal formulations has been a barrier in translating the therapeutics from research into a marketed product. Existing liposomal therapeutics such as Doxil/Caelyx require multi-stage procedures for manufacturing which can cause problems with batch to batch uniformity in addition to incurring high economic costs (Abraham *et al.*, 2005). In recent years, the use of microfluidics technology to produce liposomes in a single step (the “bottom-up” approach) has been investigated (Joshi *et al.*, 2016, Jahn *et al.*, 2007, Kastner *et al.*, 2014), with microfluidics allowing for high throughput production of liposomal formulations. Given this rise in high-throughput manufacturing techniques for liposomal delivery vehicles, it is critical that suitable, rapid analytical techniques are established in order to quantify the protein loading capacity of liposomes as delivery systems (Perrie *et al.*, 2008).

Currently, there are a range of techniques and methods available to quantify loading capacities of liposomes (Table 4.1) and this includes the bicinchoninic acid assay (BCA), Bradford protein assay, variations of high-performance liquid based chromatography (HPLC), fluorescent labelled protein and radio-chemically labelled protein. Other methods including the Kjeldahl method which determines the nitrogen content in organic substances (Haidar *et al.*, 2008, Huang *et al.*, 2015, Li *et al.*, 2011, Lutsiak *et al.*, 2002, Xu *et al.*, 2012, Henriksen-Lacey *et al.*, 2010a, Schiltz *et al.*, 1977).

**Table 4.1.** Methods that can be used to quantify the amount of protein loaded in liposomal formulations (*Abbreviations:* reverse-phase high performance liquid chromatography (RP-HPLC), high performance liquid chromatography (HPLC) and bicinchoninic acid assay (BCA assay)).

PROTEIN LOADED	LIPOSOME FORMULATION	LIPOSOME PRODUCTION TECHNIQUE	METHOD OF PROTEIN QUANTIFICATION	REF
<b>BOVINE SERUM ALBUMIN (BSA)</b>	PC:Chol:Tween:Vit E	Lipid film hydration.	Kjedahl Method	(Liu <i>et al.</i> , 2015)
<b>HEPATITIS B CORE PEPTIDE (HBCAG126-140)</b>	DPPC:Chol:DMPG	Modified Freeze-Thaw method	RP-HPLC	(Lutsiak <i>et al.</i> , 2002)
<b>SUPEROXIDE DISMUTASE (SOD)</b>	DPPC:Chol:SA DSPC:Chol:SA DSPC:DPPC:Chol:SA DPPC:Chol:DPTAP	Lipid film hydration.	HPLC	(Xu <i>et al.</i> , 2012)
<b>ACETYLCHOLINESTERASE</b>	EggPC	Lipid film hydration.	Acetylcholinesterase activity	(Colletier <i>et al.</i> , 2002)
<b>BOVINE SERUM ALBUMIN (BSA)</b>	DPPC:Chol:DDAB	Lipid film hydration.	BCA Assay	(Haidar <i>et al.</i> , 2008)
<b>INSULIN</b>	HPC:Chol	Lipid film hydration.	BCA Assay	(Huang and Wang, 2006)
<b>OVALBUMIN (OVA)</b>	Phospholipid S, Chol	Lipid film hydration.	BCA Assay	(Li <i>et al.</i> , 2011)



#### 4.1.2 High performance liquid chromatography (HPLC) techniques to quantify protein

High performance liquid chromatography (HPLC) is a commonly used analytical tool for a range of purposes including detection and quantification of drugs, small molecules, amino acids, peptides and proteins. Due to the versatility of HPLC there are a range of variations available (Awade and Efstathiou, 1999), including ultra violet (UV) HPLC which is commonly used for protein analysis. In brief, UV-HPLC works by passing a sample through a HPLC column where separation of the analytes occurs (Figure 4.1). The analyte then passes through a single light source set at a fixed wavelength whereby, the absorbance is measured and compared to a reference beam to quantify the concentration of analytes present.

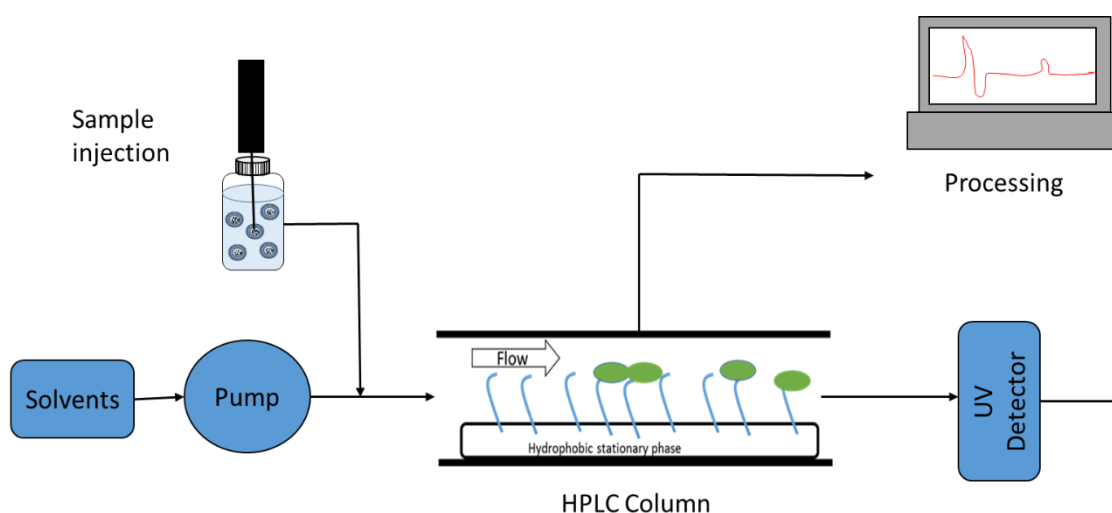


**Figure 4.1.** The process involved in quantification of protein by reverse phase- high performance liquid chromatography (RP-HPLC).

The reverse phase-HPLC (RP-HPLC) method is an analytical method that relies on UV-HPLC; in this method the stationary phase is hydrophobic. Separation of the samples occurs on the basis of hydrophobicity; the binding of samples in the mobile phase to the hydrophobic stationary phase with elution facilitated by the addition of an organic solvent (or a moderately polar mixture) in either an isocratic or gradient fashion. This technique is used for the analysis of peptides and proteins due to the high degree of method versatility, sensitivity, and efficiency of the RP-HPLC process (Aguilar, 2004). In addition, the RP-HPLC method is easily available in most analytical laboratories (Bartolomeo and Maisano, 2006) in

comparison to other HPLC techniques such as HPLC coupled with evaporative light scattering detector (HPLC-ELSD). The HPLC-ELSD is a technique that can be used to analyse pharmaceutical ingredients that do not have a chromophore, or for impurity analysis (Vervoort *et al.*, 2008). It uses a universal detector which is able to detect analytes at very low concentrations (Figure 4.2); analytes are passed through the HPLC column followed by a nebuliser which converts the analyte into fine spray. The analytes are then passed through a detection unit with a light source, the scattering of light is then converted into a signal which corresponds to a concentration (Douville *et al.*, 2006). Previous papers by our group have shown the ability to quantify lipids using an HPLC-ELSD system to a high degree of sensitivity and versatility (Roces *et al.*, 2016).

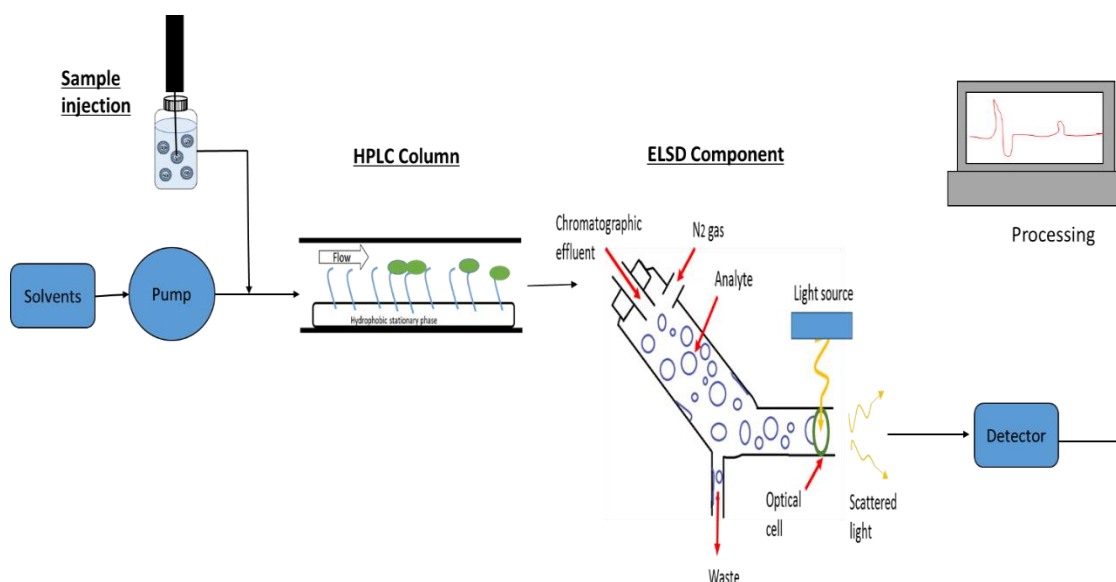


**Figure 4.2.** The process involved in quantification of protein by high performance liquid chromatography coupled with an evaporative light scattering detector (HPLC-ELSD).

The quantification of protein loading in liposomes is important, especially for achieving the appropriate pharmaceutical concentration. Routinely, encapsulated protein is measured indirectly, by measuring the free non-encapsulated protein which is then subtracted from the original amount to quantify the amount of entrapped protein. Issues arise with measuring encapsulated protein in this manner, as the method assumes all the remaining protein is associated with the delivery system. It does not take into account the possible loss of protein during the production or manufacturing process, therefore direct measurement

of the encapsulated protein is needed. Taking this into account, the ability of two HPLC techniques (RP-HPLC and HPLC-ELSD) to quantify the entrapped protein in liposomal delivery systems was investigated and compared.

## 4.2 Aim and Objectives

The aim of the work within this chapter was to determine comparable methods for the quantification of protein encapsulated by liposome formulations. To do this the following objectives were considered:

1. Direct quantification of protein encapsulated by liposomal formulations.
2. Development and validation of assays for the rapid quantification of encapsulated protein.
3. Cross method validation of protein quantification.

## 4.3 Materials and Methods

### 4.3.1 Materials

Phosphatidylcholine (PC), 1,2-dimyristoyl-sn-glycero-3-phosphocholine (DMPC), 1,2-dipalmitoyl-sn-glycero-3-phosphocholine (DPPC), and 1,2-distearoyl-sn-glycero-3-phosphocholine (DSPC) from Avanti Polar Lipids Inc., Alabaster, USA. Cholesterol and, D9777-100ft dialysis tubing cellulose was obtained from Sigma Aldrich Company Ltd., Poole, UK. For purification of untrapped protein by dialysis, a Biotech CE Tubing MWCO 300 kD was used (Spectrum Inc., Breda, The Netherlands). Purification by Tangential flow filtration (TFF), a modified polyethersulfone (mPES) 750 kD MWCO hollow fibre column was used (Spectrum Inc., Breda, The Netherlands). A Luna column (C18 (2), 5  $\mu\text{m}$ , dimensions 4.60 X 150 mm, pore size 100 Å) was used for lipid quantification and purchased from Phenomenex., Macclesfield, UK. Ovalbumin (OVA), Dil Stain (1,1'-Dioctadecyl-3,3,3',3'-Tetramethylindocarbocyanine Perchlorate ('DiI'; DiIC18 (3)), HPLC grade methanol and 2-propanol were purchased from Fisher Scientific, Loughborough, England, UK, in addition to the use of HPLC grade water.

### **4.3.2 Liposome manufacturing methods**

#### **4.3.2.1 The NanoAssembl<sup>®</sup> Benchtop**

Lipids were dissolved in methanol at the appropriate concentrations, with phosphate buffered saline (PBS) (10 mM, pH 7.3) containing 0.25 mg/ mL ovalbumin used to form the aqueous medium. A 3:1 flow rate ratio (FRR) was selected alongside a total flow rate (TFR) of 15 mL/min.

#### **4.3.2.2 Removal of non-incorporated protein and solvent**

Liposome samples were purified using the Krosflo Research lli tangential flow filtration system (Spectrum Inc., Breda, The Netherlands) fitted with an mPES (modified polyethersulfone) column with a pore size of 750 kD (Spectrum Inc., Breda, The Netherlands). Tangential flow filtration (TFF) was used to remove solvent and protein. For the removal of solvent and protein, the liposomal formulations were run through the column with solvent and untrapped protein removed by difiltration. Fresh PBS was added at the same rate as the permeate leaving the column. For 1 mL of liposome sample (containing solvent and protein) approximately 12 mL of wash buffer is required. To concentrate the sample, TFF can be run in a closed loop without buffer added, allowing concentration to the desired volume.

#### **4.3.3 Solubilisation of liposomes**

To directly quantify the amount of entrapped ovalbumin by liposomal formulations, the liposomes need to be solubilised. A previously published protocol was followed (Fatouros and Antimisiaris, 2002), whereby 500  $\mu$ L of IPA:PBS (50:50 v/v) was added to 500  $\mu$ L of liposome formulations after which the mixture underwent a quick vortex for thorough mixing. The samples were then run by high performance liquid chromatography (HPLC) to quantify the amount of OVA encapsulated within the liposomes.

#### **4.3.5 Protein quantification using Reverse phase- high performance liquid chromatography (RP-HPLC)**

A reverse phase–high performance liquid chromatography (RP- HPLC) method for quantifying the protein ovalbumin was developed using a universal ultra violet detector (Hewlett Packard 1100 Series., California, USA). All samples were run at a 280 nm wavelength, using a C18 column (i.d. 150 X 4.6 mm) from Phenomenex (Macclesfield, UK). A 1 mL/min flow rate was used with a twenty minute elution gradient, composed of solvent A (0.1% TFA in water) and solvent B (100% methanol). During the first ten minutes the gradient was 100: 0 (A: B), at 10.1 minutes 0: 100 (A: B) and then back to the initial gradient of 100: 0 (A: B) from 15.1 to

20 minutes. The injection volume for the sample is 20  $\mu$ L. A standard calibration curve for OVA was established using various concentrations with an OVA peak appearing at 11.6 minutes; the amount of encapsulated OVA in liposomes produced by microfluidics and sonication was calculated using the peak area of the sample in relation to the standards.

#### **4.3.6 Protein quantification using high performance liquid chromatography- evaporative light scattering detector (HPLC- ELSD)**

The encapsulated ovalbumin (OVA) was also measured using high performance liquid chromatography- evaporative light scattering detector (HPLC- ELSD). The HPLC was run in conjunction with a SEDEX 90LT ELSD (Sedex sedere, Alfortville, France) for OVA quantification. A Jupiter A100 column was used to detect the OVA protein. The flow rate used was 1 mL/ min, with a 20  $\mu$ L injection volume and a gain of 8. A twenty minute elution gradient, composed of solvent A (0.1% TFA in water) and solvent B (100% methanol). During the first ten minutes the gradient was 100: 0 (A: B), at 10.1 minutes 0: 100 (A: B) and then back to the initial gradient of 100: 0 (A: B) from 15.1 to 20 minutes. A standard calibration curve for OVA was established using various concentrations with an OVA peak appearing at 11.8 minutes; the amount of encapsulated OVA in liposomes produced by microfluidics and sonication was calculated using the peak area of the sample in relation to the standards.

#### **4.3.7 Method Validation**

The RP-HPLC and HPLC-ELSD methods were validated by a range of methods. First, the linearity was determined by using the established calibration curve across a range of OVA concentrations. The signal output (Area (mAU) and Area (mV) for RP-HPLC and ELSD-HPLC respectively) was plotted against known concentrations to determine the equation of the straight line and regression coefficient ( $R^2$ ). In addition, the limit of detection (LOD) and limit of quantification (LOQ) were calculated using the following equations (4.1 and 4.2). The standard deviation calculated ( $\sigma$ ) is divided by the gradient of the slope, and multiplied by 3.3 or 10 (LOD and LOQ respectively).

$$LOD = \left( 3.3 * \left( \frac{\sigma}{S} \right) \right) \quad \text{(Equation 4.1)}$$

$$LOQ = \left( 10 * \left( \frac{\sigma}{S} \right) \right) \quad \text{(Equation 4.2)}$$

Furthermore, the accuracy (trueness) of the results was calculated by comparing experimental values to theoretical values. The difference between theoretical and experimental values was calculated; taken at 3 separate concentrations across the calibration curve in triplicate using low, medium and high concentration values (equation 4.3) (Umrethia *et al.*, 2010, Guideline, 2005a). The accuracy can be defined as the closeness of agreement between the mean and the accepted true value together with confidence values (Guideline, 2005a). Repeatability of the measurements was explored by calculating the intraday precision; a measure of the closeness of values taken over a short period of time (usually the same day) under the same experimental conditions, whilst interday precision is determined over three days. Three concentrations (low, medium and high) were selected, with the results expressed as % RSD using a minimum of nine values (equation 4.4).

$$\text{Accuracy} = \frac{\text{Measured Value}}{\text{True Value}} \times 100 \quad (\text{Equation 4.3})$$

$$\% \text{RSD} = \left( \frac{\text{Std}}{\text{mean}} \right) * 100 \quad (\text{Equation 4.4})$$

#### 4.3.8 Statistical tests

Results are represented as mean  $\pm$  SD with n=3 independent batches. ANOVA and T-tests tests were used to assess statistical significance, with a Tukey's post adhoc test (p value of less than 0.05). The Bland and Altman method was used to compare the two analytical techniques; the agreeability was assessed by establishing the mean difference, limits of agreement (LOA) and standard deviations at a 95% confidence interval.

## 4.4 Results and Discussion

### 4.4.1 Solubilisation of liposomal formulations

In order to directly quantify the amount of protein encapsulated inside neutral liposomes produced by microfluidics, the liposomal formulations had to be first solubilised. This can be

achieved in several ways including the use of detergents or organic solvents. There are a number of methods to solubilise liposomes by varying the concentration and temperature of the detergent or organic solvent used (Lichtenberg *et al.*, 2005, Fatouros and Antimisiaris, 2002). It is well documented solubilisation of liposomes can be achieved using Triton X-100 or by using a previously validated method involving IPA:PBS (50:50 v/v), and generally follows three stages (partitioning, disintegration of the bilayer and, solubilisation) (Helenius and Simons, 1975). To solubilise the protein OVA entrapped in DSPC:Chol liposomes three approaches were considered to determine how efficient these approaches are; 1) using a previously validated method involving Isopropanol alcohol (IPA): phosphate buffered saline (PBS) (50:50 v/v) (Fatouros and Antimisiaris, 2002), 2) using 1% Triton X-100 and 3) using 10% Triton X-100. Visual inspection after adding the solubilising reagents to Ovalbumin (OVA) loaded DiIc DSPC:Chol liposomes show there is no obvious visual separation of the lipids and protein, post solubilisation of liposomes after adding the reagent and vortexing (Figure 4.3).

The rapid solubilisation of the liposomes, can be attributed to the methods used. For detergents such as Triton X-100, the curvature of the detergents aids the solubilising process; phospholipids have zero spontaneous curvature whilst detergent prefer to adopt a curved structure (Kozlov *et al.*, 1997). As a result, when placed into a liposomal suspension, the detergent accumulates around the outer bilayer, and insert into the bilayer as well as causing flip- flopping of the phospholipids (Pantaler *et al.*, 2000). Consequently, the liposomes develop transient structural defects in the membrane causing leakage of the active pharmaceutical ingredients such as protein. The rate of flip- flop of the phospholipids often dictates the rate of solubilisation, with the inner bilayer flip-flop largely determined by the type of detergent used (Stuart and Boekema, 2007). Triton X-100 allows for rapid solubilisation (Kragh-Hansen *et al.*, 1998, Alonso *et al.*, 1987) so it is often used for the extraction of protein from eukaryotic cells. Despite this, the use of Triton X-100 as a liposomal solubilising agent is highly influenced by the type of lipids (the interactions of the polar head groups can influence this) as well as the presence of cholesterol which is known to cause inefficient solubilisation (Toro *et al.*, 2009). As the DSPC:Chol liposomes contained 50 mol% cholesterol, the formulation was tested using HPLC-ELSD (Figure 4.3) using all three solubilisation techniques (IPA:PBS, 1% Triton X-100 and 10% Triton X-100).

The samples run in the HPLC-ELSD show all three methods are capable of solubilising liposomes and exposing protein, with the OVA peak for liposomes solubilised in IPA:PBS

appearing at the same time and height observed for free OVA in PBS. This indicated the lipids do not interfere with the quantification, and that the IPA:PBS solubilisation technique is a quick and efficient approach for measuring protein directly. In contrast, for liposomes solubilised in Triton X-100 multiple peaks appears close to the OVA peak, and increases in area as the concentration of Triton X-100 is increased from 1 to 10%. The results indicate the Triton X-100 interferes with the quantification of OVA, and that the results obtained are not reliable. As the concentration of Triton X-100 is increased above a certain concentration, there is some evidence showing it can cause turbidity of the sample (Lichtenberg *et al.*, 1979, Ahyayauch *et al.*, 2012), which could explain the multiple peaks and unreliable data obtained from HPLC-ELSD. In contrast, only a single peak corresponding to the OVA peak was observed for the IPA:PBS solubilising method, with the intensity of the peak matching that of a known OVA concentration. Based on these results, the IPA:PBS method was selected for the solubilisation of all future protein loaded liposomal formulations.

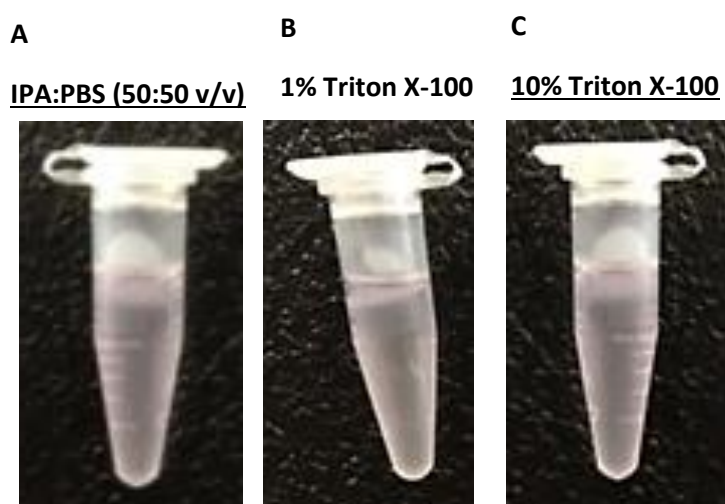


**Figure 4.3.** Solubilisation of ovalbumin (OVA) loaded liposomes labelled with DiIC. Three approaches were used to solubilise the OVA loaded liposomal formulations by isopropanol alcohol:phosphate buffered saline (50/50 V/V) (A), 1% Triton X-100 in PBS (B) and 10% Triton X-100 (C). The liposomal formulations were added to the solubilising agent at a 1:1 volume ratio.



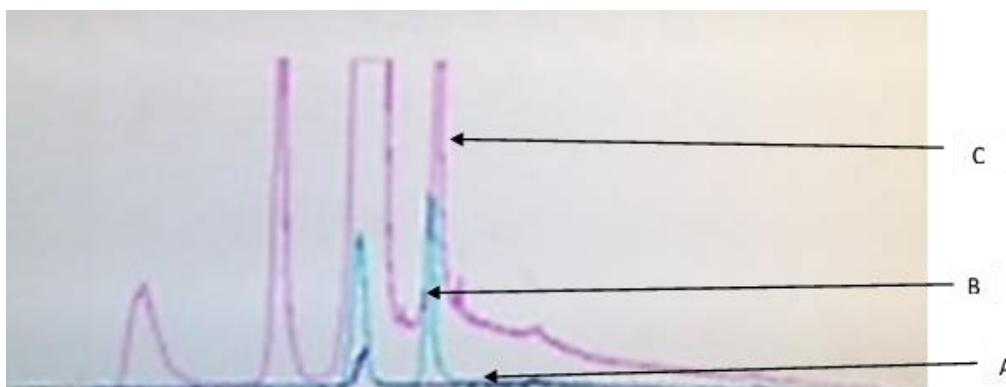


**Figure 4. 4.** Chromatographic peaks of OVA loaded liposomes dissolved in IPA:PBS (50:50 v/v) (A), OVA loaded liposomes dissolved in 1% Triton X-100 (B) and OVA loaded liposomes dissolved in 10% Triton X-100 (C).

#### 4.4.2 Methods to quantify the amount of encapsulated ovalbumin by liposomal formulations

There are a wide range of protein quantification techniques available. Robust testing for protein loading liposomes is limited because it is well known lipids can interfere with some assays such as the bicinchoninic acid (Kessler and Fanestil, 1986). Over coming this is difficult so a better understanding of the advantages and limitations is required. This is particularly important for formulation development, where small quantities of liposomes containing protein are produced, thus analytical techniques require a high degree of sensitivity. As a result, HPLC techniques (RP-HPLC and HPLC-ELSD) were investigated for their ability to quantify protein.

##### 4.4.2.1 Reverse phase- high performance liquid chromatography (RP-HPLC)

To quantify the amount of encapsulated ovalbumin (OVA) inside liposomes by reverse phase-high performance liquid chromatography (RP-HPLC), a gradient method was used to establish an OVA calibration curve (from 5- 400  $\mu\text{g}/\text{mL}$ ) (Figure 4.5A). Further validation involved repeating the measurements for intraday and interday measurements to determine the precision and repeatability of the results obtained (Figure 4.5B and C). The limit of detection (LOD) and limit of quantification (LOQ) values of 2.43  $\mu\text{g}/\text{mL}$  and 7.37  $\mu\text{g}/\text{mL}$  respectively were determined (Figure 4.5D). The results show all the curves have regression values of greater than 0.99. The accuracy of the RP-HPLC method was measured across a range of concentrations (25, 200 and 400  $\mu\text{g}/\text{mL}$ ) respectively, with the accuracy remaining above 95% for all three concentrations tested (Figure 4.5E and F).

Furthermore, visual inspection of the RP-HPLC chromatograms was referred to determine any issues such as contamination of the run. The chromatographs provide good visual inspection of the run, indicating any changes in pressure, the solvent gradient or injection volume amongst other things that can occur within the twenty minute run time. Initially, blank runs containing phosphate buffered saline (PBS, 10 mM and pH= 7.3) were run to ensure this does not interfere with the quantification (Figure 4.6A). Samples containing OVA at set concentrations were ran with the OVA protein eluting at approximately 11.2 minutes (Figure 4.6B). Empty liposomes (Figure 4.6C) and empty liposomes mixed with a known amount of OVA were ran to ensure the lipids do not interfere with the quantification (Figure 4.6D). In order to quantify the amount of entrapped OVA, solubilisation is necessary. Running OVA loaded liposomes without solubilisation resulted in the absence of a peak at 11.2 minutes, so the amount of encapsulated OVA could not be quantified (Figure 4.6E). The mixture was then solubilised and the samples were run using the RP-HPLC method, illustrating the solubilisation technique does not interfere with the quantification. Second, the presence of the lipids does not impact the quantification of OVA with the intensity of the peak remaining the same with and without the presence of lipid and solubilising agents (Figure 4.6f). The results show that the solubilising agents (IPA:buffer 50:50 v/v) is effective for the quantification of the protein OVA, and can be successfully used alongside RP-HPLC. The validation of the RP-HPLC method has ensured the amount of OVA encapsulated quantified will be an accurate measurement of the amount of encapsulated OVA by liposomes. The RP-HPLC results are in keeping with previous methods that have shown this analytical method is a robust technique, with low LOD values calculated (of less than 15 µg/mL) (Grotefend et al., 2012).

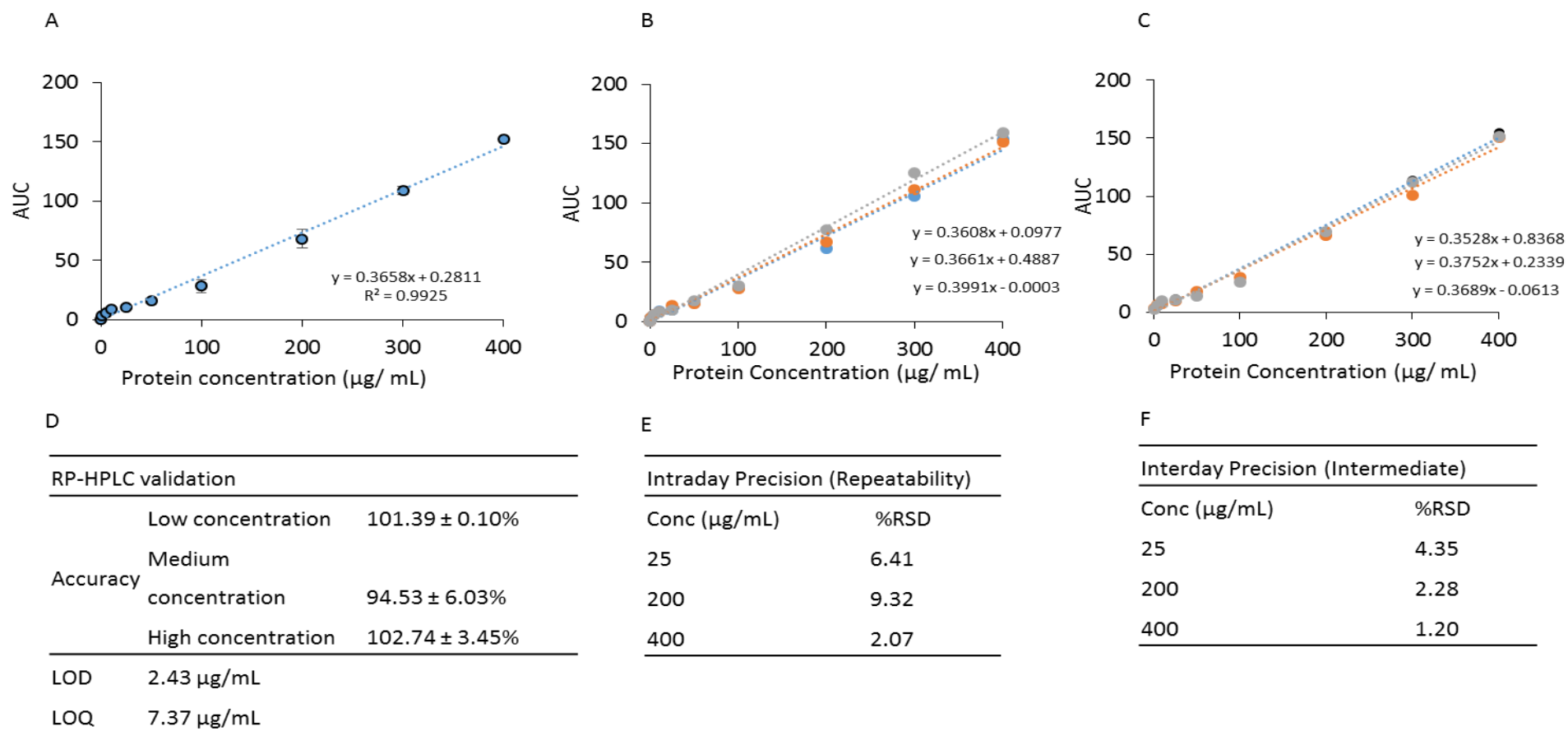


**Figure 4.5.** Ovalbumin calibration curves solubilised in PBS, to establish LOD and LOQ values using UV- HPLC (A). Intraday curves were generated (B) within the same day, while Interday curves were generated over 3 separate days (C). Accuracy was determined at three concentrations, each in replicate (D), while intraday and interday precision was calculated across three different concentrations with %RSD shown (E-F).

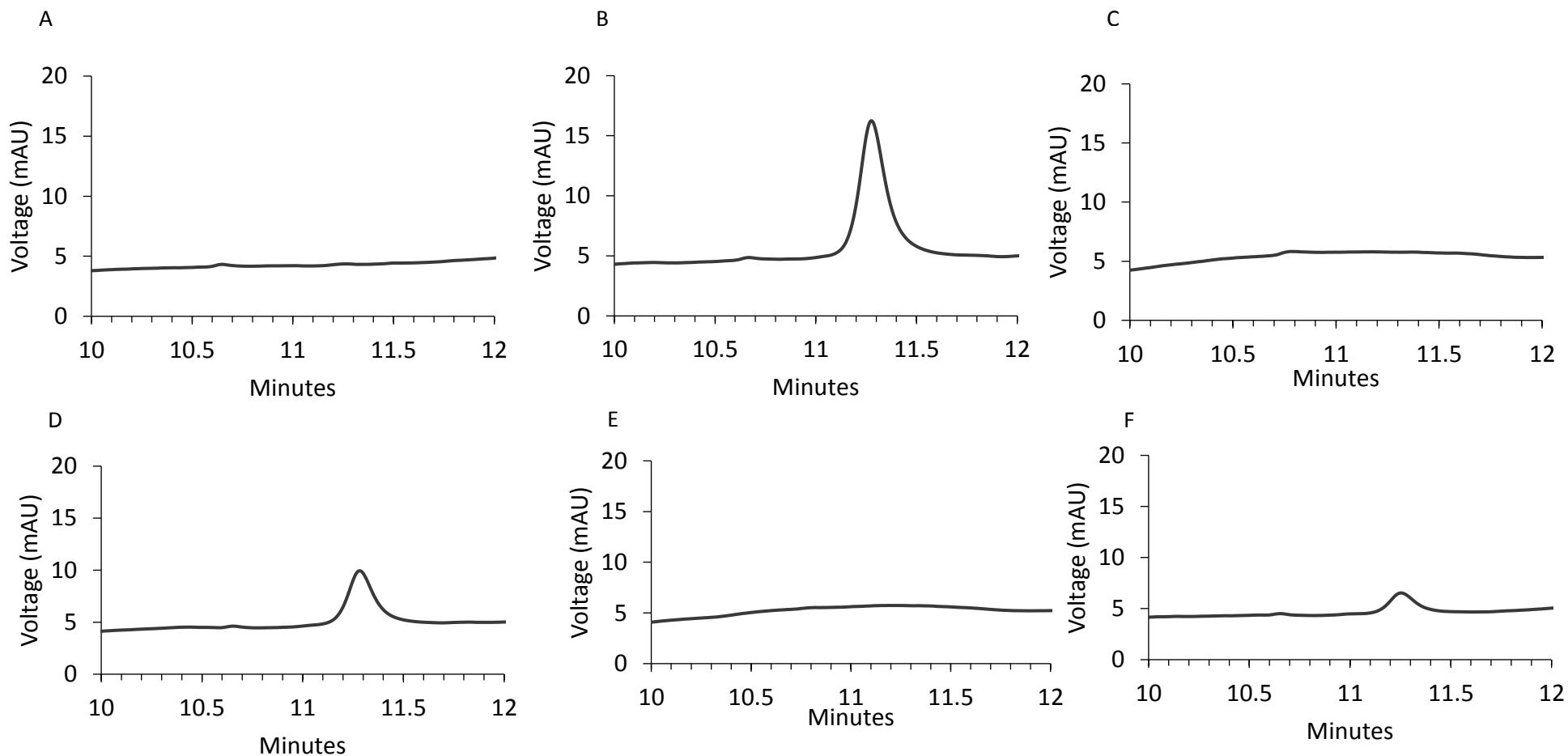


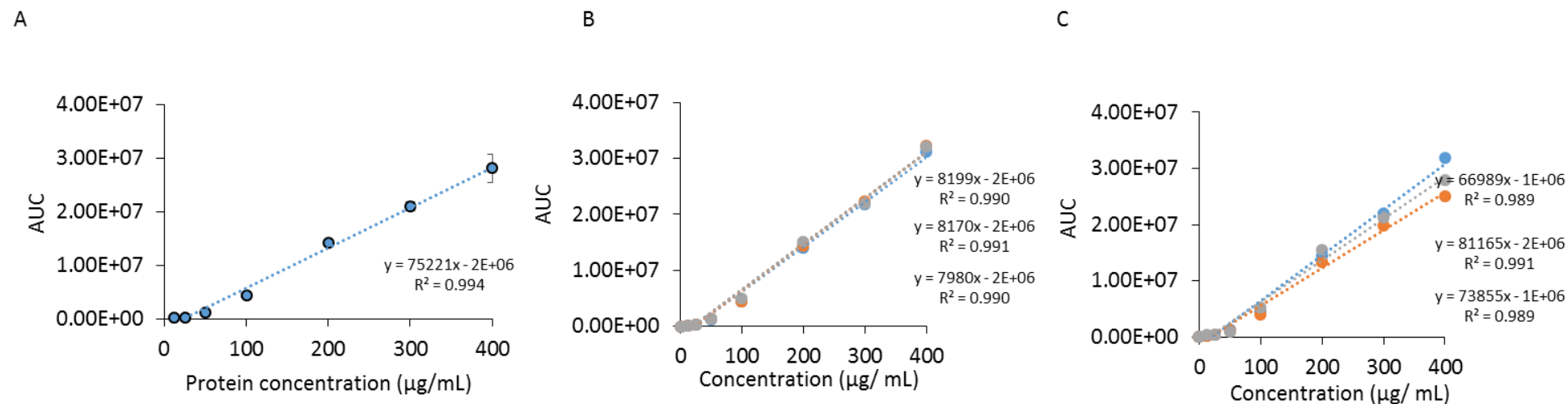
**Figure 4.6.** RP- HPLC chromatographs for (A) PBS only, (B) 400 µg/ mL of ovalbumin in PBS, (C) empty liposomes, (D) empty liposomes mixed with 100 µg/mL protein ovalbumin, (E) OVA loaded liposomes without solubilisation and, (F) OVA loaded liposomes containing 56 µg/mL of protein encapsulated, solubilised in IPA:PBS (50:50 v/v). All liposomes were produced using microfluidics at a 3:1 FRR and 15 mL/min TFR (initial lipid concentration of 4 mg/ mL and initial lipid concentration of 0.25 mg/ mL).

#### 4.4.2.2 High performance liquid chromatography- Evaporative light scattering detectors (HPLC- ELSD)

A number of HPLC methods and assays that can be used to quantify the amount of OVA encapsulated inside liposomes. As well as RP-HPLC, an evaporative light scattering detector (ELSD) can be run alongside a HPLC to quantify the analyte of interest or identify impurities within a sample. The ELSD is a universal detector that has the ability to quantify volatile compounds in addition to other compound products such as protein. The ELSD was coupled and used with the HPLC to determine if this technique is comparable to RP-HPLC. As with the RP-HPLC method, a gradient elution method was developed with each sample run lasting 20 minutes. Calibration curves were established in order to quantify the amount of encapsulated OVA (with a concentration range of 12- 400  $\mu\text{g}/\text{mL}$ ) (Figure 4.7A). The intraday (Figure 4.7B) and interday (Figure 4.7C) calibration curves have been established. As evident by the calibration curves shown, the regression coefficient was above 0.99 for all curves, with the average calibration curve used to determine the LOD (0.65  $\mu\text{g}/\text{mL}$ ) and LOQ (2  $\mu\text{g}/\text{mL}$ ) (Figure 4.7D). The precision and accuracy of the results was also determined by intraday and interday curves, with the %RSD below 6 and 11% respectively (Figure 4.7E) and (Figure 4.7F). The accuracy of the assay across at medium and high concentrations remained within the acceptance criteria, although at the lower concentration of 100  $\mu\text{g}/\text{mL}$  the accuracy dropped to  $93.37 \pm 4.41\%$ .

In addition, the chromatograms were analysed to determine the elution time of OVA protein using this method. A blank run of PBS only (10 mM, pH= 7.3) was run to observe any possible interference and background noise; as shown by Figure 4.8A PBS buffer does not interfere with the assay. Free OVA in PBS was eluted at approximately 11.8 minutes (Figure 4.8B). Once again, the presence of lipids did not adversely impact the OVA quantification, with the same peak appearing at the expected time and intensity (Figure 4.8C and D). As the HPLC-ELSD method involves turning samples into droplets (and can measure volatile and non-volatile analytes) the impact of the solubilisation technique was investigated. The results show OVA loaded liposomes can be quantified with or without solubilising as the sample is nebulised during the quantification process (Figure 4.8E and F). This allows the quantification of the 'neat' liposomal samples, without the need to expose the product to chemicals for degradation, and so is a good alternative to traditional HPLC techniques (such as RP-HPLC) to measuring active pharmaceutical ingredients (APIs) that are highly sensitive to solvent.

Overall, both RP-HPLC and HPLC-ELSD methods are highly sensitive, with the ability to quantify protein at low concentrations. This is reflected by the LOD values of less than 3  $\mu\text{g}/\text{mL}$  and LOQ values of less than 10  $\mu\text{g}/\text{mL}$ . An added feature of the HPLC-ELSD is the ability to change the gain of the system, allowing the analytical process to become more sensitive and optimised depending on the requirements. The HPLC techniques can analyse samples quickly, in addition to possessing the ability to process a large amount in an automated fashion thus offering an ease of quantification (as lipids do not interfere with the ovalbumin quantification). The HPLC-ELSD performed to a higher degree of accuracy (of more than 90%) and is the most sensitive (LOD of 2.33  $\mu\text{g}/\text{mL}$ ). Unlike RP-HPLC, the liposomal formulations do not require solubilisation in order to quantify the amount of encapsulated OVA, with the sample nebulised into droplets which is advantageous.



ELSD-HPLC validation		
Accuracy	<b>Low concentration</b>	93 ± 4.41%
	<b>Medium concentration</b>	102 ± 13.8%
	<b>High concentration</b>	99 ± 5.59%
LOD	0.77 µg/mL	
LOQ	2.33 µg/MI	

Intraday Precision (Repeatability)	
Conc (µg/mL)	%RSD
<b>100</b>	5.89
<b>200</b>	3.09
<b>400</b>	1.42

Interday Precision (Intermediate)	
Conc (µg/mL)	%RSD
<b>100</b>	11.44
<b>200</b>	4.19
<b>400</b>	9.84

**Figure 4.7.** Ovalbumin calibration curves solubilised in PBS, to establish LOD and LOQ values using HPLC- ELSD (A). Intraday curves were generated (B) within the same day, while Interday curves were generated over 3 separate days (C). Accuracy was determined at three concentrations, each in replicate (D), while intraday and interday precision was calculated across three different concentrations with %RSD shown (E-F).

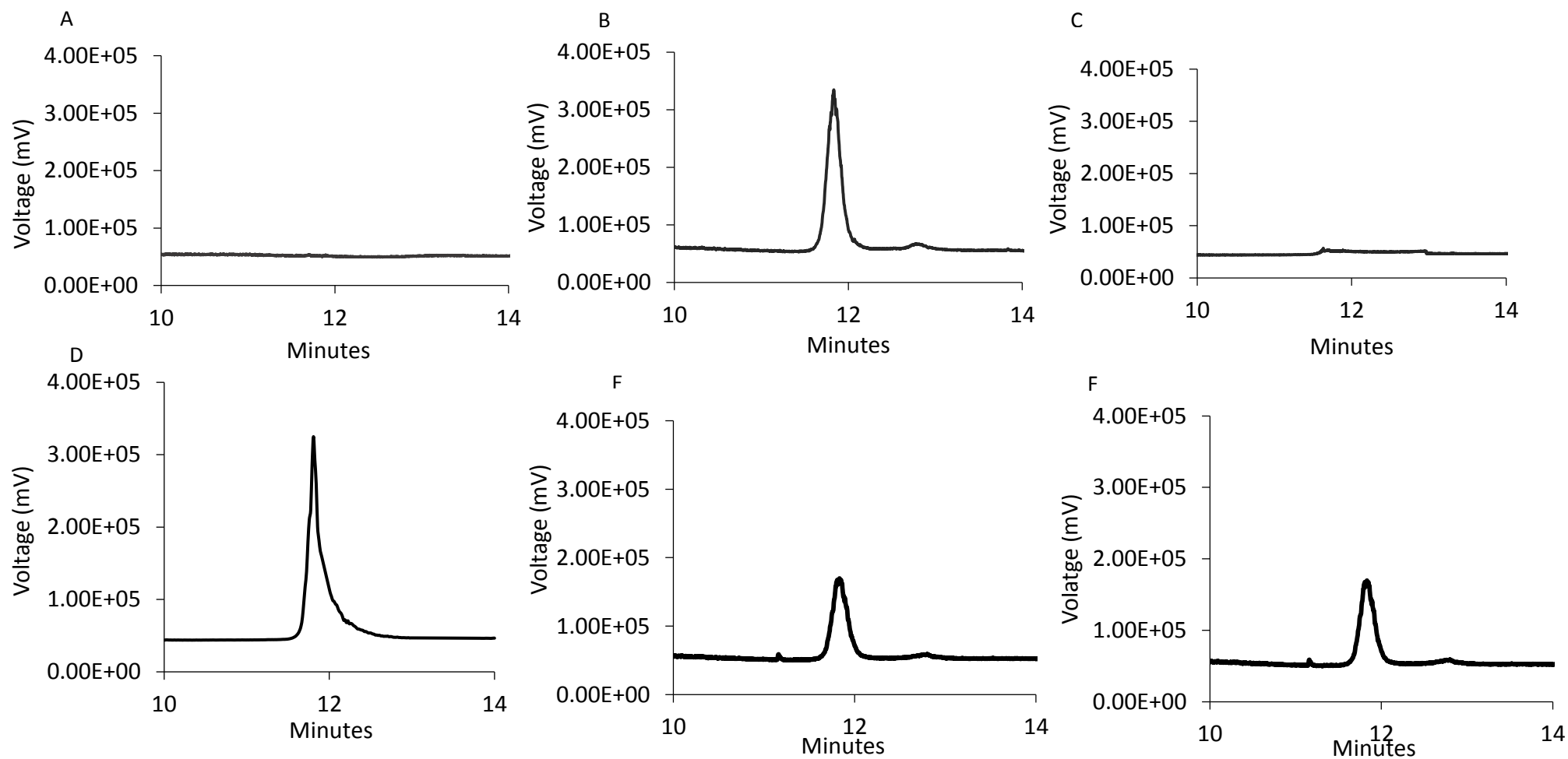


**Figure 4.8.** HPLC- ELSD chromatographs for (A) PBS only, (B) 100 µg/ mL of ovalbumin in PBS, (C) empty liposomes, (D) empty liposomes mixed with 100 µg/mL ovalbumin, (E) DSPC:Chol liposomes containing ovalbumin (~ 56 µg/mL) without solubilisation and, (F) DSPC:Chol liposomes containing ovalbumin (~ 56 µg/mL) solubilised in IPA:PBS (50:50 v/v). All liposomes were produced using microfluidics at a 3:1 FRR and 15 mL/min TFR (initial lipid concentration of 4 mg/ mL and initial OVA concentration of 0.25 mg/ mL).



#### 4.4.3 Comparison of the analytical techniques used to quantify encapsulated ovalbumin

The ability of two HPLC techniques (RP-HPLC and HPLC-ELSD) to quantify the amount of entrapped OVA was analysed. The OVA loaded DSPC:Chol liposome formulation was investigated in triplicate, with both methods (RP-HPLC and HPLC-ELSD) able to quantify the amount of OVA encapsulated (Figure 4.9). The RP-HPLC and HPLC-ELSD gave similar results; the amount entrapped is between 52 - 56  $\mu\text{g}/\text{mL}$  for OVA with an encapsulation efficiency of 34 - 38% for neutral DSPC:Chol liposomes highlighting the accuracy of the results (Table 4.2). Use of different methods to quantify the amount of encapsulated OVA shows both methods are comparable to one another. The two methods were further analysed by considering statistical analysis results; the ANOVA tests showed there is no significant difference between the two analytical techniques. This was further confirmed by determining the agreeability between the two techniques using the Bland and Altman plot analysis method. Comparability was determined by calculating the mean difference, and identifying the standard deviations of this (referred to as limits of agreement (LOA)). The upper LOA of +2.269 and lower LOA of -1.434 were calculated along with a mean of 0.418 (Figure 4.10). There is no obvious trend, with an equal distribution of points above and below the mean, highlighting a good degree of agreeability between the two methods.

In addition, this was further tested by investigating the impact of charged liposomal formulations on OVA quantification by using negatively charged DSPC:Chol:PS and positively charged DSPC:Chol:DOTAP (Figure 4.11). Once again, the results show both methods (RP-HPLC and HPLC-ELSD) are able to quantify the amount of entrapped OVA with both methods giving the same encapsulation efficiency of  $20 \pm 0.82\%$  (Table 4.3). Similarly, the amount of OVA entrapped by DSPC:Chol:DOTAP by the RP-HPLC and HPLC-ELSD are the same;  $82 \pm 3\%$  and  $80 \pm 3\%$  for RP-HPLC and HPLC-ELSD respectively (Table 4.3). Statistical analysis were also conducted for DSPC:Chol:PS and DSPC:Chol:DOTAP liposomal formulations, with ANOVA results showing no significant difference between the two formulations and analytical techniques (Figure 4.12). Collated Bland and Altman plot analysis were also conducted for the anionic and cationic liposomes. The plots shows, in comparison to DSPC:Chol liposomes, the DSPC:Chol:DOTAP liposomal formulations plots are more variable (Figure 4.12). There is

a wider distribution which highlights the variability of the formulation, as the OVA protein is adsorbed onto the liposomes. Overall, the results from Figure 4.10 and Figure 4.12 show the RP-HPLC and HPLC-ELSD analytical techniques are comparable.

Furthermore, analysis of the two techniques shows a great degree of agreeability irrespective of the formulations used (DSPC:Chol, DSPC:Chol:PS and DSPC:Chol:DOTAP). The ANOVA analysis showed the results between the two techniques are not significant; similar encapsulation efficiency values were calculated by both analytical techniques. Due to the inherent error associated with measuring variables such as encapsulation efficiency, the Bland and Altman methodology was used to determine agreeability. In general, when a relationship between two variables is explored, linear regression analysis is among the first to be analysed. However, linear regression models are not favoured when interested in the relationship between methodologies, as it studies the linear relationship rather than differences between the methodologies of interest (Twomey and Kroll, 2008). Unlike linear regression, the Bland and Altman approach is based on the degree of confirmation between methods by studying the position of individual results (Eksborg, 1981, Altman and Bland, 1983). A scatter plot is established at a 95% confidence interval (within  $\pm 2$  standard deviations); how far away data points are from the calculated mean, and whether or not the values are within the established LOA provides a good indication of the agreeability between analytical techniques. The results highlight the versatility of the analytical techniques as they are all able to quantify the encapsulation efficiency of protein for neutral, anionic and cationic liposomes (Megoulas and Koupparis, 2005, Grotefend et al., 2012).

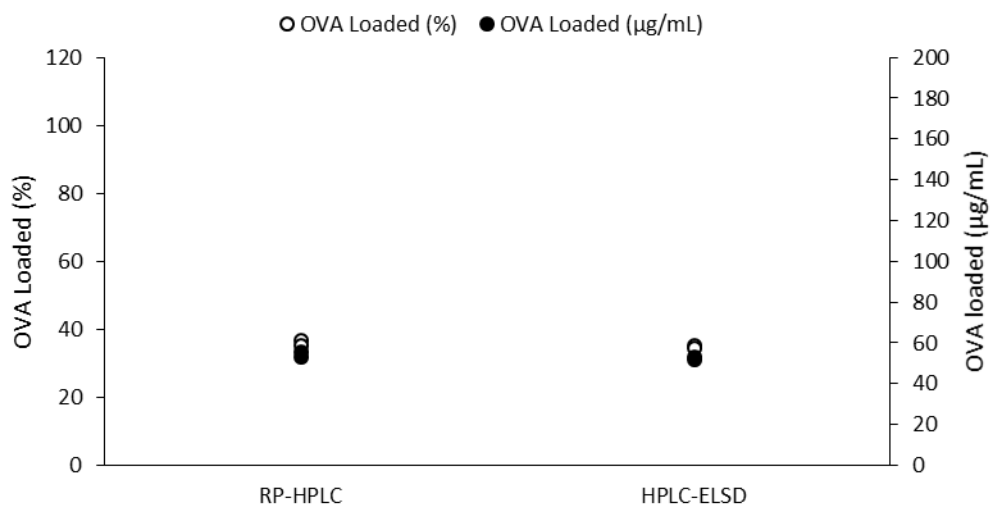


**Figure 4.9.** Comparative study between two protein quantification techniques, RP-HPLC and HPLC-ELSD. The DSPC:Chol liposomes were made at an initial lipid concentration of 4 mg/mL and 0.25 mg/mL initial ovalbumin concentration, using microfluidics at a 3:1 flow rate ratio (FRR) and 15 mL/min total flow rate (TFR). The results represent the mean  $\pm$  SD, n= 3 independent batches.

**Table 4.2.** The encapsulation efficiency and concentration ( $\mu\text{g/mL}$ ) of the ovalbumin entrapped in DSPC:Chol liposomal formulations was quantified using either RP-HPLC and HPLC-ELSD. The results represent the mean  $\pm$  SD, n= 3 independent batches.

<u>DSPC:CHOL</u>		
Method	<i>RP-HPLC</i>	<i>ELSD-ELSD</i>
%	$36 \pm 1$	$35 \pm 0.5$
$\mu\text{g/mL}$	$54 \pm 1$	$52 \pm 0.5$

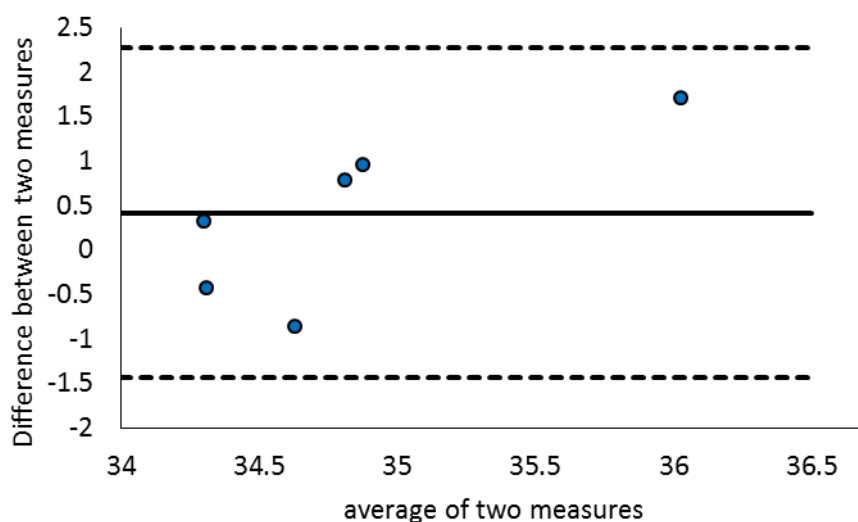


**Figure 4.10.** Bland and Altman plot analysis for the comparison of two analytical techniques. Plot of differences between the RP-HPLC and HPLC-ELSD analytical techniques on the y-axis, versus the mean of the two analytical techniques for the ovalbumin loaded DSPC:Chol liposomal formulations. The mean 0.418 (horizontal solid line), with the bias represented by the gap between the mean and the dashed lines. The ovalbumin loaded DSPC:Chol liposomal formulations were measured six independent times to quantify the encapsulation efficiency, with each measurement plotted.

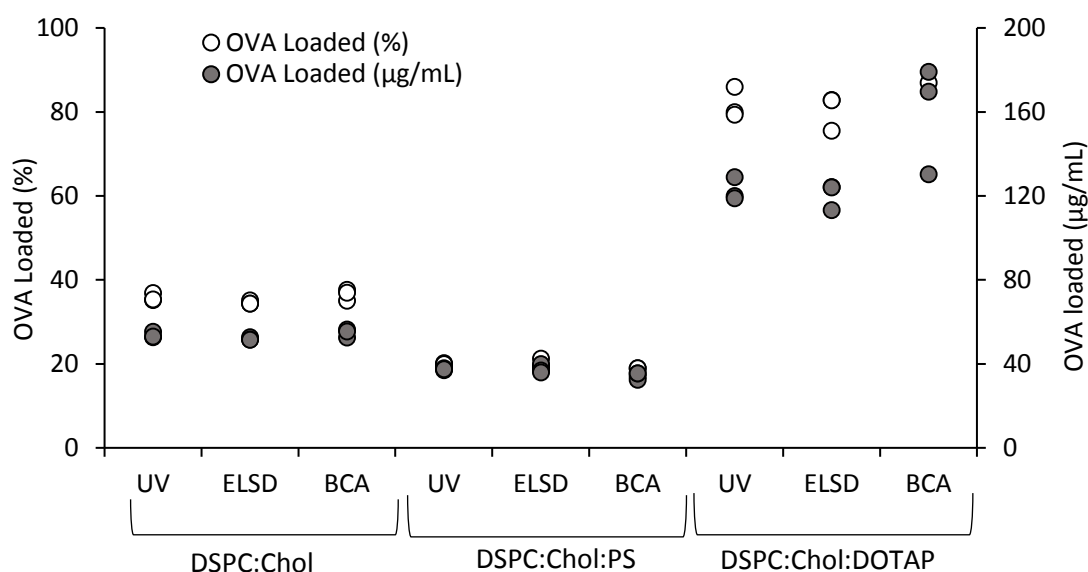


**Figure 4.11.** Comparative study between three protein quantification techniques, UV-HPLC, HPLC-ELSD and BCA assay. All three liposomal formulations were made using microfluidics. The DSPC:Chol and DSPC:Chol:PS formulations were made at a 3:1 FRR and 15 mL/ min TFR (4 mg/ mL initial lipid and 0.25 mg/ mL initial ovalbumin concentration). The DSPC:Chol:DOTAP formulation was produced at a 1:1 FRR, the ovalbumin was adsorbed onto the surface by passing pre-made DSPC:Chol:DOTAP formulation through the microfluidics nanoassemblr. All results were measured three times, with the average encapsulation and ovalbumin loading calculated.

**Table 4.3.** The encapsulation efficiency and concentration ( $\mu\text{g}/\text{mL}$ ) of the ovalbumin protein entrapped in liposomal formulations. Three formulations with differing charges were investigated; neutral DSPC:Chol, anionic DSPC:Chol:PS, and cationic DSPC:Chol:DOTAP formulations. The results represent the mean  $\pm$  SD,  $n=3$  independent batches.

Method	DSPC:CHOL			DSPC:CHOL:PS			DSPC:CHOL:DOTAP		
	RP	ELSD	BCA	RP	ELSD	BCA	RP	ELSD	BCA
%	36 $\pm$ 1	35 $\pm$ 0.5	36 $\pm$ 1	20 $\pm$ 0.0	20 $\pm$ 1	18 $\pm$ 1	82 $\pm$ 3	80 $\pm$ 3	106 $\pm$ 12
$\mu\text{g}/\text{mL}$	54 $\pm$ 1	52 $\pm$ 0.5	54 $\pm$ 1	38 $\pm$ 0.5	38 $\pm$ 2	34 $\pm$ 1	123 $\pm$ 5	121 $\pm$ 5	160 $\pm$ 21

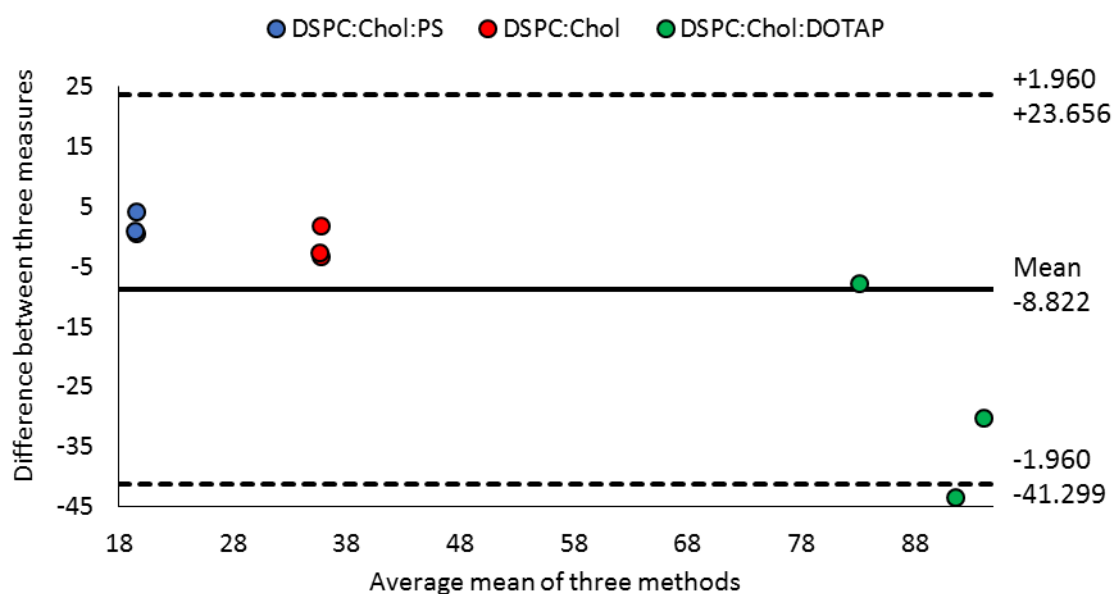


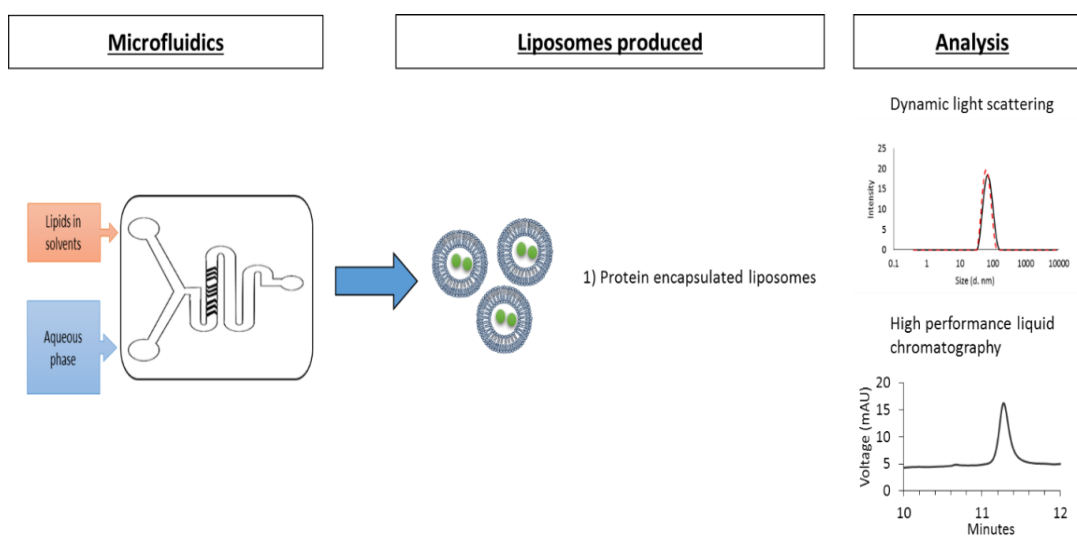
**Figure 4.12.** Bland and Altman plot analysis for the comparison of three analytical techniques. Plot of differences between three analytical techniques (RP-HPLC, HPLC-ELSD and BCA assay) on the y-axis, versus the mean of the three analytical techniques for the three formulations (DSPC:Chol, DSPC:Chol:PS and DSPC:Chol:DOTAP). The calculated mean is -8.8 (horizontal solid line), with the bias represented by the gap between the mean and the dashed lines. All formulations were measured three times for the encapsulation efficiency, with each measurement plotted.

## 4.5 Conclusion

The ability to quantify active pharmaceutical ingredients (APIs) such as protein encapsulated by liposomal formulations is important. Accurate quantification of protein is needed as it can impact the pharmacokinetic properties of the liposomal formulations. In this chapter, methods to directly determine the amount of entrapped protein OVA was developed and validated. The IPA:PBS solubilisation technique was an effective approach for exposing OVA entrapped within liposomes. It enabled direct measurement of protein encapsulation within liposomal formulations, with no impact on the HPLC analytical techniques. The IPA:PBS solution did not interfere, or over quantify the amount of OVA observed by chromatography approaches. Two HPLC analytical techniques (RP-HPLC and HPLC-ELSD) were developed and validated; both analytical techniques are highly sensitive with LOD values of less than 2  $\mu\text{g}/\text{mL}$  and an LOQ value of less than 10  $\mu\text{g}/\text{mL}$ . Both approaches enabled rapid and reproducible quantification of OVA. The results show both analytical techniques are comparable, the amount of OVA quantified for neutral, anionic and cationic liposomes are the same. A particular advantage of the HPLC-ELSD is that the method can be further optimised, by changing the gain (sensitivity of the detector) so this can be ideal for detecting API present at very low concentrations, and adjusted accordingly. Also, for OVA quantification using the HPLC-ELSD, the liposomal formulations did not require solubilisation further shortening the process time. Overall, the results show we have developed easily transferable methods for the direct quantification of protein irrespective if the liposomal formulation characteristics.

# Chapter 5

## Rapid microfluidics manufacture of liposomes encapsulating protein



Work presented in this chapter is published in:

1. FORBES, N., HUSSAIN, M. T., BRIUGLIA, M. L., EDWARDS, D. P., HORST, J. H. T., SZITA, N. & PERRIE, Y. 2019. Rapid and scale-independent microfluidic manufacture of liposomes entrapping protein incorporating in-line purification and at-line size monitoring. *International Journal of Pharmaceutics*, 556, 68-81.

## 5.1 Introduction

### 5.1.1 Manufacturing protein loaded liposomes with high encapsulation efficiency

The manufacture of liposomal delivery systems is incredibly important to overcome any issues related to drug and protein toxicity. In recent years, the amount of protein and peptides therapeutics such as anti-cancer agents has increased with approximately 240 currently approved by the FDA (Usmani et al., 2017, Fosgerau and Hoffmann, 2015, Lu et al., 2014). Whilst this is advantageous, many of these proteins and peptides often cannot reach the target site. Degradation by the immune system, over stimulating the immune system, and avoiding toxic doses are some of the many challenges when developing pharmaceutical formulations. One solution of this would be to use delivery systems such as liposomes, which are able to deliver peptides and protein to the target site, protect the payload, offer high biocompatibility and low toxicity (Torchilin and Lukyanov, 2003). These liposomal formulations are versatile and can be used for diagnostic purposes, as part of vaccines, or for the treatment of a range of diseases (Carter, 2011). Despite this, manufacturing protein and peptide loaded liposomes is difficult; the macromolecules are prone to physical and chemical degradation as a result of changes in temperature or the presence of chemicals. The loss of structural or chemical integrity therefore affects the overall functionality of the formulation, including low bioavailability and short half-life after *in vivo* administration (Lee and Yuk, 2007) so ensuring protein integrity is important.

Furthermore, the manufacturing methods used for the production of liposomes introduces a fresh set of problems for protein loading liposomes. Changes in temperature, high pressure, non-aqueous solvents, metal ions, detergents, incompatible pH and/or ionic strength, and shearing can all impact on the chemical and physical stability of proteins. In addition to this, achieving high loading is difficult (as illustrated in Table 5.1), and there are multiple manufacturing steps and procedures required which can lead to a loss of protein or peptides. Strategies to overcome this include introducing freeze-thaw cycles to improve encapsulation efficiency. This was shown by Colletier et al (Colletier et al., 2002), who achieved approximately 26% encapsulation efficiency of the enzyme acetylcholinesterase after 20 freeze-thaw cycles. However, this is a laborious process that requires many steps from



production of liposomes by thin film lipid hydration, followed by freeze-thaw cycles and extrusion. The overall process time is long with little process control, inability to fine-tune parameters and can lead to formulations that are heterogeneous (Szoka and Papahadjopoulos, 1978). Added to this, the liposome formulation can also influence protein encapsulation; the type of lipid(s) used, the amount of cholesterol and protein concentration all have been shown to effect the amount of protein encapsulation (Xu et al., 2012).

**Table 5.1.** The amount of protein encapsulated within neutral and anionic liposomes by traditional manufacturing methods.

<b>PROTEIN LOADED</b>	<b>LIPOSOME FORMULATION</b>	<b>PRODUCTION TECHNIQUE</b>	<b>PROTEIN LOADING</b>	<b>REFERENCE</b>
<b>BOVINE SERUM ALBUMIN</b>	soyabean PC/DSPC, cholesterol, phosphatidylglycerol	Lipid hydration.	0.1 mg/mL	(Ramaldes et al., 1996)
<b>BOVINE SERUM ALBUMIN</b>	PC:Chol	Dehydration-rehydration method.	28%	(Chan et al., 2004)
<b>BOVINE SERUM ALBUMIN</b>	PC:Chol:Tween:Vitamin E	Lipid hydration.	34 ± 9%	(Liu et al., 2015)
<b>BOVINE SERUM ALBUMIN</b>	Soybean PC:Chol	Thin film lipid hydration.	22-32%.	(Vila-Caballer et al., 2016)
<b>OVALBUMIN</b>	PC:Chol	Thin film lipid hydration.	10%	(Habjanec et al., 2006)
<b>OVALBUMIN</b>	Phospholipid S, Chol (very high lipid concentration, 200 mg)	Thin film lipid hydration.	48% ± 9%	(Li et al., 2011)
<b>AMYLOGLUCOSIDASE, ALBUMIN</b>	PC:Chol:Dicetylphosphate	Lipid film hydration	4 - 6.5%, 6.8 - 10.6%	(Gregoriadis et al., 1971)
<b>SUPEROXIDE DISMUTASE</b>	DPPC:Chol DSPC:Chol	Unilamellar vesicles mixed with freeze-thaw cycling	50%	(Xu et al., 2012)
<b>ACETYLCHOLINESTERASE</b>	Egg PC	Thin film lipid hydration.	35%	(Colletier et al., 2002)
<b>INSULIN</b>	Hydrogenated PC:Chol	Thin film lipid hydration.	28% (4°C) 30% (25°C) and 50% (40°C)	(Huang and Wang, 2006)

### 5.1.1.2 Factors affecting protein stability

Proteins are of particular interest to the biopharmaceutical industry due to their ability to act as antigens. Encapsulation of proteins inside particles have become an interesting research area for vaccines. The protein OVA used as a model protein antigen is a fairly stable protein. It is a disulfide protein and is part of the serpin family (Huntington *et al.*, 1995, Takahashi and Hirose, 1992). Unlike the other members it is unable to inhibit serine proteinases. It is 45 kDa in size and exists as a tetramer containing four subunits (each consisting of 386 amino acids). The four subunits are non-identical (Stein *et al.*, 1991, Yamasaki *et al.*, 2003):

1. Subunit A: 32% alpha-helices, 32% beta sheets and 36% random coils.
2. Subunit B: 30% alpha-helices, 32% beta sheets and 38% random coils.
3. Subunit C: 28% alpha helices, 31% beta sheets and 41% random coils.
4. Subunit D: 31% alpha-helices, 31% beta sheets and 38% random coils.

The increase in protein encapsulation research has led to much debate considering the effect the bioprocessing methods have on the proteins. Often these processes involve using heat or shear stress that can denature the protein. Denaturation can be described as changes to the shape of the protein which result in a loss of functionality. The protein can become denatured at the secondary (loss of alpha helical and beta pleated sheets), tertiary (van der Waal's interactions and covalent interactions) and quaternary levels (dissociation of subunits and changes in spatial arrangements) (Tanford, 1968). For instance, for the production of OVA encapsulated liposomes produced by microfluidics, the OVA is exposed to heat, organic solvent and possible shear by the TFF system. Of particular concern, is the exposure to organic solvent in the microfluidics chip (the principal production step). It is important to note that some denaturation can be reversible and the extent of reversible and irreversible denaturation is dependent on the protein studied. There are a number of chemical and physical processes that can cause denaturation of protein. Table 5.2 focuses on the types of denaturation OVA encapsulated inside liposomes is subjected to. As a result, the effect of solvent on OVA structure was investigated.

**Table 5.2.** Factors that can cause denaturation of ovalbumin during the manufacturing of this protein inside liposomes.

<b><u>TYPE OF DENATIURATION</u></b>	<b><u>CONSIDERATIONS</u></b>	<b><u>REF</u></b>
<b>HEAT</b>	Causes partial unfolding of Ovalbumin. The heat increases kinetic energy leading to the disruption to H-bonds and non-polar hydrophobic interactions. An increase in beta-sheets and decrease in alpha helical structure is observed.	(Takahashi and Hirose, 1992, Kato and Takagi, 1988)
<b>ORGANIC SOLVENT</b>	Causes irreversible conformational changes to the protein structure at the secondary and tertiary level. The solvent breaks side chain H bonds with new H bonds forming between the alcohol and side chains.	(Clark and Smith, 1989, Sah, 1999)
<b>SHEAR STRESS</b>	Damages Ovalbumin.	(Clark and Smith, 1989)

### **5.1.2 Manufacturing protein loaded liposomes using microfluidics**

Microfluidics is an alternative technology that allows the production of liposomes, but unlike other methods, the liposomes are produced in a ‘bottom-up’ approach (Akbarzadeh et al., 2013). Small unilamellar vesicles (SUVs) are formed from individual monomers without the need to down-size, as the liposomes are formed from individual lipid monomers. This technique allows the rapid production of liposomes with the ability to scale-up (as shown in Chapter 3). Fine tuning is possible, with the production of liposomes of varying sizes and the encapsulation of different materials possible (Dimov et al., 2017). Although microfluidics has been shown as a viable alternative, the use of microfluidics to produce protein loaded liposomes has not been investigated. The nature of the microfluidics system, whereby the solvent stream (containing lipids) mixes with the aqueous phase (containing protein) leaves the protein susceptible to changes or degradation as the protein comes into contact with the organic solvent (Capretto et al., 2011, Jahn et al., 2004, Jahn et al., 2007, Zook and Vreeland, 2010). As a result, the use of microfluidics to produce high throughput protein loaded liposomes with high encapsulation efficiency was investigated.

## 5.2 Aim and Objectives

The aim of this chapter is to determine the ability of microfluidics to encapsulate proteins in liposomal formulations. To do this the following objectives were considered:

1. Identification of the critical process and formulation parameters that enable high protein loading using microfluidics.
2. Determining the integrity of protein loaded inside liposomal formulations.
3. Establishing the release profiles of protein loaded liposomal formulations.

## 5.3 Materials and Methods

### 5.3.1 Materials

Phosphatidylcholine (PC), 1,2-dimyristoyl-sn-glycero-3-phosphocholine (DMPC), 1,2-dipalmitoyl-sn-glycero-3-phosphocholine (DPPC), and 1,2-distearoyl-sn-glycero-3-phosphocholine (DSPC) from Avanti Polar Lipids Inc., Alabaster, USA. Cholesterol, Ovalbumin and, D9777-100ft dialysis tubing cellulose was obtained from Sigma Aldrich Company Ltd., Poole, UK. For purification of untrapped protein by dialysis, a Biotech CE Tubing MWCO 300 kD was used (Spectrum Inc., Breda, The Netherlands). For purification by Tangential flow filtration (TFF), a modified polyethersulfone (mPES) 750 kD MWCO hollow fibre column was used (Spectrum Inc., Breda, The Netherlands). A Luna column (C18 (2), 5  $\mu\text{m}$ , dimensions 4.60 X 150 mm, pore size 100 Å) was used for lipid quantification and purchased from Phenomenex., Macclesfield, UK. Dil Stain (1,1'-Dioctadecyl-3,3,3',3'-Tetramethylindocarbocyanine Perchlorate ('Dil'; DilC18 (3)), HPLC grade methanol, 2-propanol and dimethyl sulfoxide (DMSO) were purchased from Fisher Scientific, Loughborough, England, UK, in addition to the use of HPLC grade water.

## **5.3.2 Methods**

### **5.3.2.1 Production of ovalbumin loaded liposomes**

The microfluidics system was used to produce OVA loaded liposomes. The lipids were dissolved at the appropriate concentration (0.3- 10 mg/ mL) in methanol and injected into the aqueous phase, with ovalbumin (OVA) dissolved in phosphate buffered saline (10 mM, pH 7.3) at the desired concentration (0 - 2 mg/mL) injected into the aqueous phase. Four neutral formulations composed of egg phosphatidylcholine (PC), 1,2-dimyristoyl-sn-glycero-3-phosphocholine (DMPC), 1,2-dipalmitoyl-sn-glycero-3-phosphocholine (DPPC), 1,2-distearoyl-sn-glycero-3-phosphocholine (DSPC), with cholesterol added at a 2:1 wt/ wt ratio were produced. The flow rate ratio (FRR) used was 3:1 with the speed (referred to as total flow rate (TFR)) kept constant at 15 mL/min.

To produce OVA liposomes using the lipid-film hydration method, lipids were dissolved at specific concentrations in a chloroform:methanol mixture (v/v 9:1). Lipids dissolved in solvent were then placed under a vacuum rotatory evaporation for 6 minutes at 200 rpm in a heated water bath (20- 60°C) to remove solvent. Hydration of the lipid film was achieved by the addition of phosphate buffered saline (PBS, 10 mM, and pH 7.3) containing OVA (0- 0.25 mg/mL). The liposomes then underwent probe sonication for 4 minutes at 10 Hz (as previously optimized (results not shown)) to produce liposomes under 100 nm. The liposomes were then centrifuged at 300  $xg$  to remove any debris. Liposomal formulations produced by microfluidics and traditional methods were characterised by dynamic light scattering as previously described in Chapter 2.3.2.4.

### **5.3.2.2 Removal of organic solvent**

Liposome samples (both empty and loaded) were purified to remove solvent and protein using the Krosflo Research lli tangential flow filtration system (Spectrum Inc., Breda, The Netherlands) as previously described (Section 3.3.4). The mPES (modified polyethersulfone) column with a pore size of 750 kD (Spectrum Inc., Breda, The Netherlands) was used to do this. In brief, purification of 1 mL of solvent required 12 mL of buffer, with the ability to concentrate the sample.

### **5.3.2.3 Quantification of protein and drugs encapsulated in liposomes**

#### **5.3.2.3.1 Quantification of ovalbumin loaded liposomes using reverse-phase high performance liquid chromatography**

The solubilisation of liposomes was achieved using IPA:PBS (50:50 v/v) as previously described (Fatouros and Antimisiaris, 2002), with the release OVA protein quantified by reverse phase-high performance liquid chromatography (RP-HPLC) (Agilent 1100 Series HPLC, California, USA). In brief, a C18 column (i.d. 150 X 4.6 mm) (from Phenomenex, Macclesfield, UK) was used to quantify the protein at a flow rate of 1 mL/min at 280 nm as previously described in chapter 4. The sample run time was twenty minutes.

#### **5.3.2.3.2 Quantification of ovalbumin loaded liposomes using high performance liquid chromatography-evaporative light scattering detector**

Quantification of OVA encapsulated by liposomal formulations was investigated using HPLC coupled with an evaporative light scattering detector (SEDEX 90LT, Sedex sedere, Alfortville, France) as previously described (in chapter 4.3.6).

### **5.3.2.4 Protein release studies**

The release profiles of ovalbumin loaded liposomes (PC:Chol, DMPC:Chol, DPPC:Chol and DSPC:Chol) in 20 mL of PBS was determined. The liposomal formulations were produced using microfluidics (4 mg/mL initial lipid and 0.25 mg/mL Ovalbumin) at a 3:1 or 5:1 FRR and a speed of 15 mL/min total flow rate (TFR). The liposomes were purified for residual solvent and unentrapped OVA by 12 mL of TFF, after which 1 mL of liposomal formulations were placed into 300 kD dialysis bag in the presence of 25 mL PBS. The samples were then left in an agitated water bath, set at 37°C for 0.5, 1, 3, 6, 18, 24, 48, 72, 96 and 120 hours. After the allocated time the liposomal formulations were collected, and analysed directly to quantify the amount of OVA remaining.

### **5.3.2.5 Circular dichroism**

The structural integrity of protein ovalbumin (OVA) was investigated after microfluidics and TFF, using circular dichroism (Chiroscan™- plus CD spectrometer, Applied Photophysics Limited, UK). The controls consisted of free OVA (0.3 mg/mL) dissolved in PBS, OVA dissolved

in methanol and empty DSPC:Chol liposomes (3:1 FRR and 15 mL/min TFR). The integrity of encapsulated OVA was tested for DSPC:Chol liposomes made using an initial lipid concentration of 8 mg/mL and an initial OVA concentration of 8 mg/mL. The liposomes were then purified using TFF to remove non-encapsulated OVA, before 20 µL of the respective samples were placed in between two microscope slides and placed into a Suprasil® quartz absorption cuvette (Hellma, Germany: path length of 1 mm). All sample measurements were performed at 25 °C and spectra recorded from 180-260 nm range.

### **5.3.2.6 Statistical analysis**

Results are represented as mean ± SD with n=3 independent batches. ANOVA and T-tests were used to assess statistical significance, with a Tukey's post adhoc test (p value of less than 0.05). The F2 similarity test was performed in accordance to the FDA guidelines (Appendix II of the "Note for Guidance on the investigation of bioavailability and bioequivalence" (CPMP/EWP/QWP/1401/10)" which states that a single mean value of > 85% release for any formulation should be tested, therefore the 96 hour time point was selected.

## **5.4 Results and Discussion**

### **5.4.1 Encapsulation of protein within liposomes**

#### **5.4.1.1 Comparison of ovalbumin encapsulation by liposomes produced by microfluidics and sonication**

The effect of manufacturing techniques for the encapsulation of OVA by liposomal formulations was investigated. With the normal operating ranges established as 3:1 FRR and 15 mL/min TFR, these optimised parameters were selected for the production of OVA loaded liposomes. As a result, OVA loaded DSPC:Chol liposomes were manufactured by microfluidics and sonication (post production of multi-lamellar vesicles produced by thin film lipid hydration). The manufacturing methods were compared for differences in physicochemical properties (size and polydispersity), and the amount of encapsulation efficiency (EE %) was determined. The liposome production method is shown to impact on the liposomal

characteristics including protein loading (Figure 5.1). Liposomes produced by microfluidics, achieves higher encapsulation efficiency of around  $34 \pm 5\%$  in comparison to  $5 \pm 3\%$  produced by sonication. The liposomes produced by microfluidics are homogenous small vesicles ( $73 \pm 9$  nm; PDI  $0.21 \pm 0.001$ ) compared to sonicated liposomes ( $194 \pm 16$  nm; PDI  $0.45 \pm 0.027$ ). The poor encapsulation of protein by probe sonication is well documented: it is hard to achieve encapsulation efficiency above 10% (Lapinski et al., 2007). Sonication is largely used to break MLVs by acoustic energy (Mendez and Banerjee, 2017), however the processes offers little control or batch variations. The breakdown of MLVs produces heat; this can be detrimental for OVA loaded liposomes as the heat can cause denaturation of the OVA protein. Depending on the probe sonication system, the need to remove contamination post sonication is a necessary additional step in production (Philippot and Schuber, 2017). Similarly, extrusion also results in poor encapsulation efficiency in comparison to microfluidics (Forbes *et al.*, 2019), therefore, the lab on the chip microfluidics enables the rapid encapsulation efficiency, allows for one step production, fine-tuning and is scale independent.

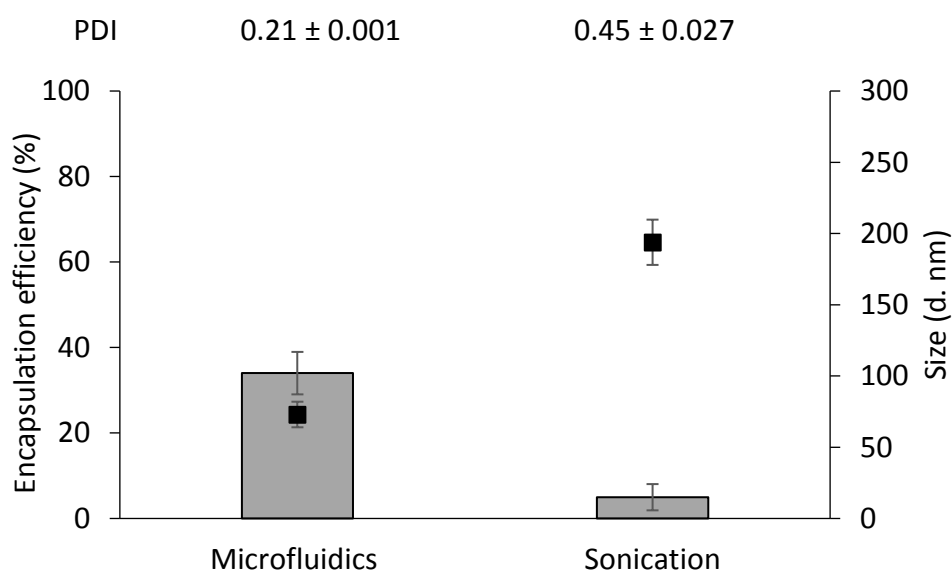


**Figure 5.1.** Comparison of manufacturing techniques using OVA loaded DSPC:Chol liposomes. The encapsulation efficiency and liposome physicochemical (size and polydispersity (PDI)) properties were investigated, using microfluidics and lipid-film hydration (followed by sonication). The DSPC:Chol liposomes were made using 4 mg/mL and 0.25 mg/mL ovalbumin. The bars represent encapsulation efficiency (%), and the square dots represent size (d. nm). The results represent mean  $\pm$  SD, n=3 independent batches.



#### 5.4.1.2 Encapsulation of protein using various neutral lipids

To test if the high encapsulation efficiency achieved by microfluidics is dependent on lipid type, other neutral formulations were used. Three additional phospholipid derivatives were used alongside a 2:1 wt/wt cholesterol (PC, DMPC and DPPC). The results for all four OVA loaded protein liposomes (using 0.25 mg/mL initial OVA) show the lipid type had no significant impact on the encapsulation efficiency Figure 5.2. The protein loading of all four liposomes PC:Chol, DMPC:Chol, DPPC:Chol and DSPC:Chol show equally high protein loading between (30-40%). This is achieved when either 0.1 mg/mL or 0.25 mg/mL initial OVA was used (Figure 5.3). The sizes of all four liposomes remained below 100 nm, with microfluidics producing homogenous liposomes at both OVA concentrations with PDI values of below 0.2 (Figure 5.2) and illustrated by the intensity plots (Figure 5.4). The results show the encapsulation efficiency of OVA liposomes is independent of the lipid type for formulations produced by microfluidics.

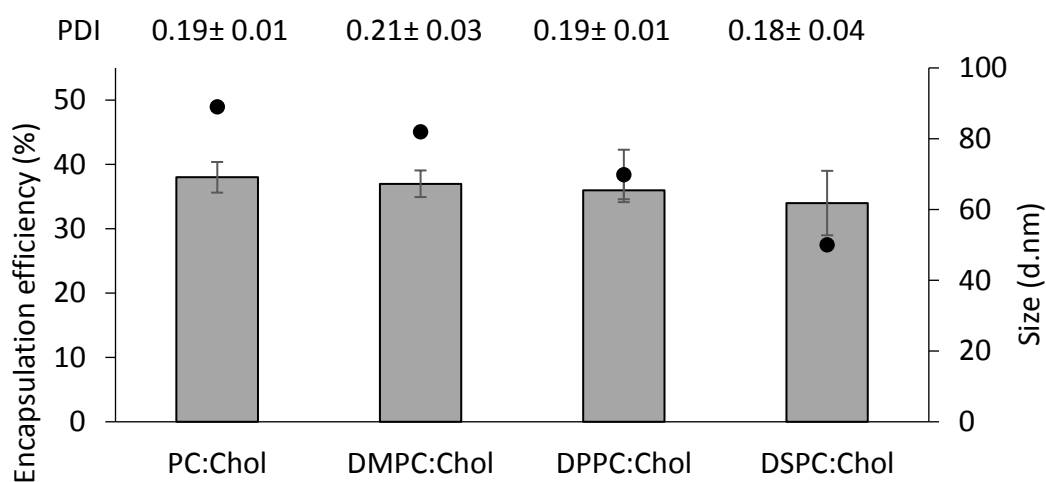


**Figure 5.2.** The characterisation of liposomes produced using microfluidics. The PC:Chol, DMPC:Chol, DPPC:Chol and DSPC:Chol liposomes were produced using 4 mg/mL initial lipid concentration and 0.25 mg/mL initial OVA concentration (at a 3:1 FRR and 15 mL/min TFR). The encapsulation efficiency was calculated using RP-HPLC, whilst the liposome physicochemical characteristics were obtained using dynamic light scattering (Bars= encapsulation efficiency (%) and square dots= size (d. nm)). The results represent mean  $\pm$  SD, n=3 independent batches.

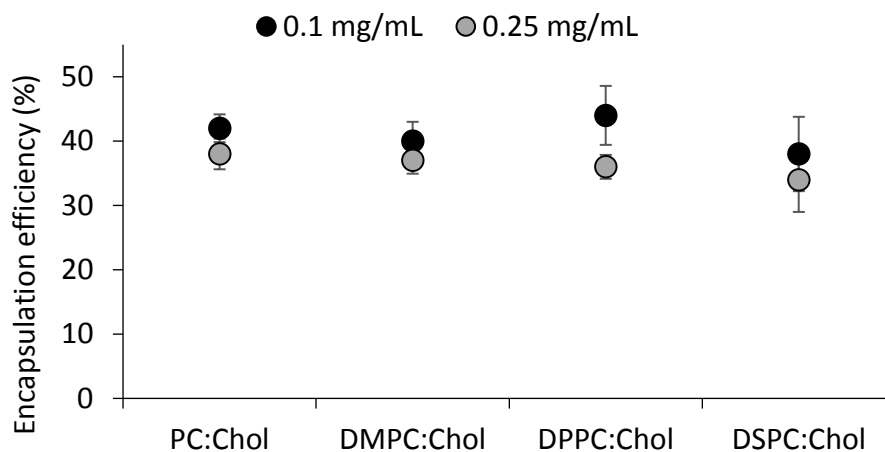


**Figure 5.3.** The encapsulation efficiency of OVA loaded PC:Chol, DMPC:Chol, DPPC:Chol and DSPC:Chol liposomes made using microfluidics (at a 3:1 FRR and 15 mL/min TFR). Initial lipid concentration of 4 mg/mL and initial OVA concentration of either 0.1 or 0.25 mg/mL was used. The encapsulation efficiency was calculated using HPLC, with the results represent mean  $\pm$  SD, n=3 independent batches.

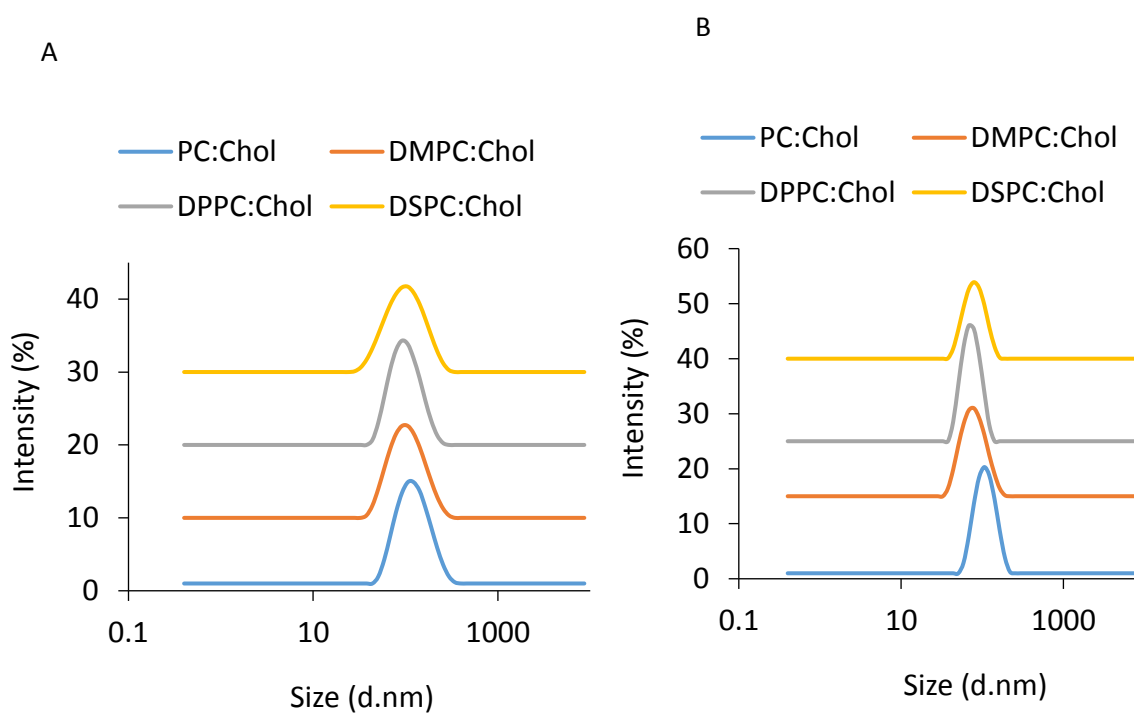


**Figure 5.4.** The intensity plots of 0.25 (A) and 0.1 (B) mg/mL initial OVA loaded (PC:Chol, DMPC:Chol, DPPC:Chol and DSPC:Chol) neutral formulations made by microfluidics at a 3:1 FRR and 15 mL/min TFR. The results represent three independent batches, mean  $\pm$  SD.

Furthermore, the four formulations were also produced by sonication for comparison with the microfluidics technique. The results show sonication did not result in a significant difference between the formulations with encapsulation efficiency between 5 - 10% (Figure 5.5). The sizes of liposomes produced by sonication are much larger (between 176- 221 nm) in comparison to those produced by microfluidics (less than 100 nm). The sonication process provides less process control as evident by the heterogeneous population of liposomes, shown by the PDI values of more than 0.25 in comparison to microfluidics. The results from Figure 5.5 show the production of OVA loaded liposomes with high encapsulation efficiency is for the most part influenced by the manufacturing method.

PDI Microfluidics:	$0.19 \pm 0.004$	$0.21 \pm 0.003$	$0.26 \pm 0.009$	$0.21 \pm 0.010$
Sonication:	$0.33 \pm 0.040$	$0.37 \pm 0.060$	$0.40 \pm 0.050$	$0.45 \pm 0.080$

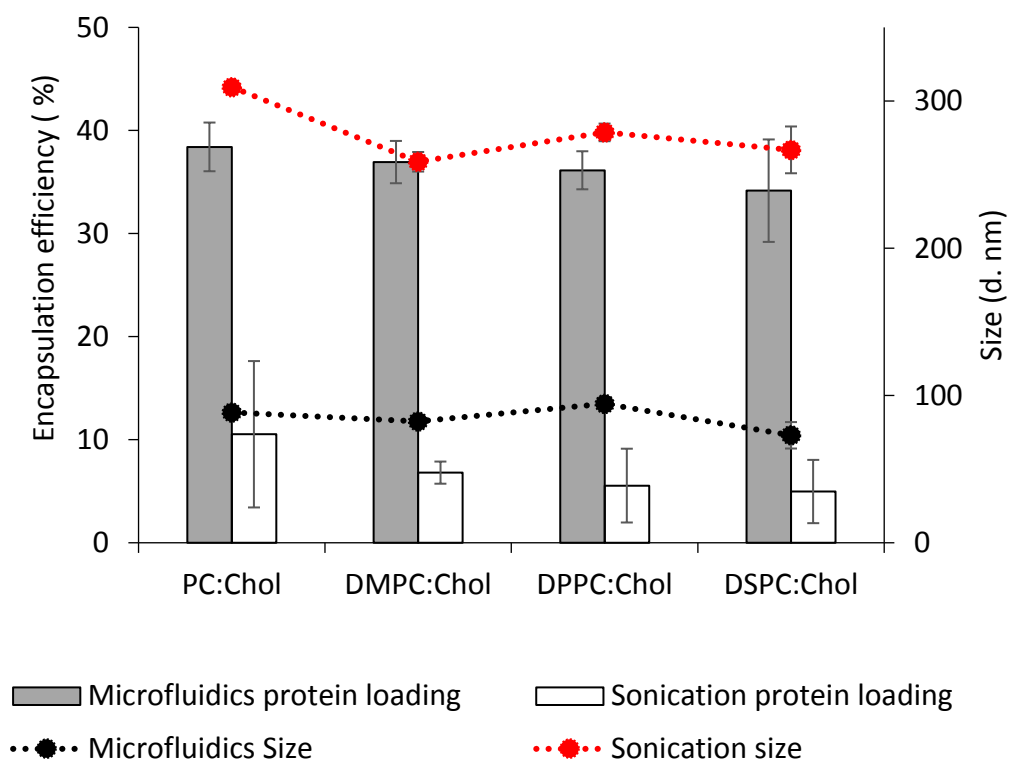


**Figure 5.5.** Comparison of manufacturing techniques using OVA loaded PC:Chol, DMPC:Chol, DPPC:Chol and DSPC:Chol liposomes (using 4 mg/mL initial lipid and 0.25 mg/mL initial OVA). The encapsulation efficiency and liposome physicochemical (size and polydispersity (PDI)) properties were investigated, using microfluidics and lipid-film hydration (followed by sonication). The results represent mean  $\pm$  SD, n=3 independent batches.

#### 5.4.1.3 Encapsulation of protein at varying protein concentrations

The protein loading efficiency of DMPC:Chol liposomes was further investigated by increasing the amount of initial OVA concentration from 0.1 to 1 mg/mL. Figure 5.6 show that as the initial OVA concentration increases, the amount of entrapped OVA increases from  $31 \pm 2.4$   $\mu\text{g}/\text{mL}$  (using 0.1 mg/mL initial OVA) to  $110 \pm 2.4$   $\mu\text{g}/\text{mL}$  (when using 1 mg/mL initial OVA). In keeping with this, the calculated encapsulation efficiency decrease from  $41 \pm 3.2$  % to  $15 \pm 0.3$  % at 1 mg/mL of initial OVA. Despite the difference in loading observed, the size of DMPC:Chol liposomal formulations produced at increasing OVA concentration remained below 100 nm (Figure 5.7). The formulations produced with microfluidics are homogenous (with a PDI of below 0.2) and the zeta potential (above -10 mV) indicates the liposomes remain neutral in charge (Figure 5.7). The OVA does not interfere with the charge of the liposomal formulations. To ensure the lipid concentration does not influence the encapsulation, this was kept constant at 4 mg/mL initial lipid with the concentration of OVA increased. The results from Figure 5.6 and Figure 5.7 show the encapsulation efficiency is minimally influenced by the initial OVA concentration.

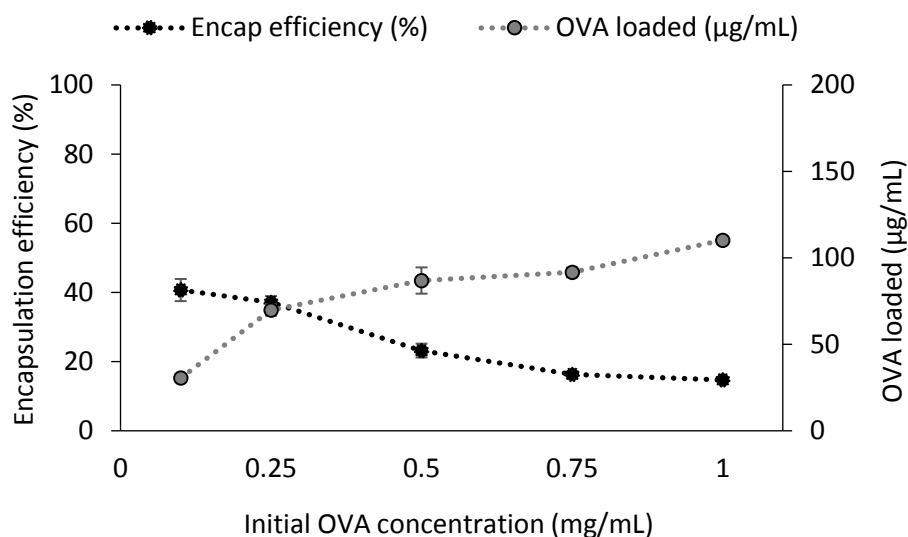


**Figure 5.6.** The effect of increasing ovalbumin concentration on neutral DMPC:Chol liposomes (2:1 wt/wt) produced by microfluidics at a 3:1 FRR and 15 mL/min. Increasing initial ovalbumin concentration on entrapment efficiency and loading was quantified. The results represent mean  $\pm$  SD, n=3 independent batches.

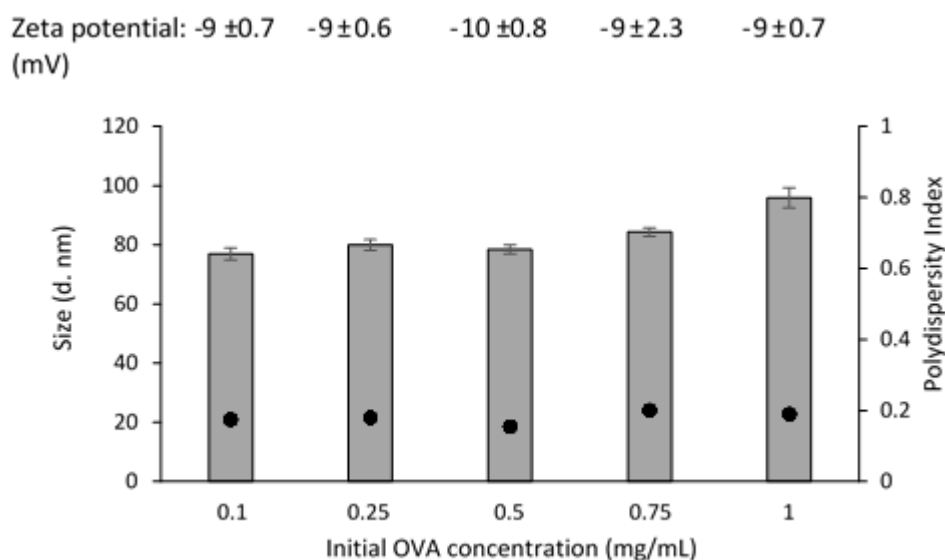


**Figure 5.7.** The effect of increasing ovalbumin concentration on neutral DMPC:Chol liposomes (2:1 wt/wt) produced by microfluidics at a 3:1 FRR and 15 mL/min. The physicochemical properties (including size, polydispersity index and zeta potential) were determined by dynamic light scattering. (Bars= size and round dots= polydispersity index). The results represent mean  $\pm$  SD, n=3 independent batches.

#### 5.4.1.4 Encapsulation of protein across a range of lipid concentrations

Factors impacting encapsulation efficiency were further explored by investigating the effect of lipid concentration in relation to OVA protein encapsulation. Four liposomal formulations were tested; a range of PC, DMPC, DPPC and DSPC liposomes (from 0.5 to 10 mg/mL initial lipid concentration) was used, whilst the encapsulation efficiency of OVA (250  $\mu$ g/mL) tested. The physicochemical characteristics (size, PDI and zeta potential) of the four formulations across the range of liposome concentrations was measured Figure 5.8. The size of the liposomal formulations changed significantly ( $p < 0.05$ ) with increasing initial lipid concentration, for all four formulations ( $p < 0.05$ ). For example, at 0.5 mg/mL initial lipid concentration the size measured for PC:Chol liposomes was  $491 \pm 76$  nm and decreased to below 100 nm at initial lipid concentrations of 4 mg/mL or above (Figure 5.8A). The same trend was observed for DMPC:Chol, DPPC:Chol and DSPC:Chol liposomes, with the formulations becoming more homogenous as the initial lipid concentration increases (Figure 5.8B). The liposome formulations remain neutral across all four formulations with the zeta potential measured above -10 mV for all formulations irrespective of the initial lipid concentrations (Figure 5.8C). Whilst the initial lipid concentration influences the size, the effect on protein encapsulation is not as clear.

Furthermore, the data produced was adjusted to determine the relationship between lipid concentration and encapsulation; a double logarithmic plot of log encapsulation versus log lipid concentration was plotted as previously shown by Colletier et al (Colletier et al., 2002) (Figure 5.9). In doing so, it provides a clearer insight into the parameters being tested as the total liposome surface area is proportional to the lipid concentration, whilst the encapsulated inner volume is proportional to the lipid concentration to the power  $3/2$ . Figure 5.9, shows all four formulations have a good linear relationship with an  $R^2$  value of more than 0.9. The gradient value is important as values close to 1 suggest encapsulation is proportional to the number of lipids and the surface area, whilst values above 1.5 suggests the encapsulation is related to internal volume. From Figure 5.9, the results show all four formulations have gradients at 1 (DMPC:Chol) or below (PC:Chol, DPPC:Chol and DSPC:Chol), thus suggesting the high incorporation of OVA by microfluidics manufacture is not influenced by the initial lipid concentration. These results suggest the manufacturing methods plays a greater role in the encapsulation efficiency and that microfluidics is a good method for the production of liposomal formulations with high encapsulation efficiency.

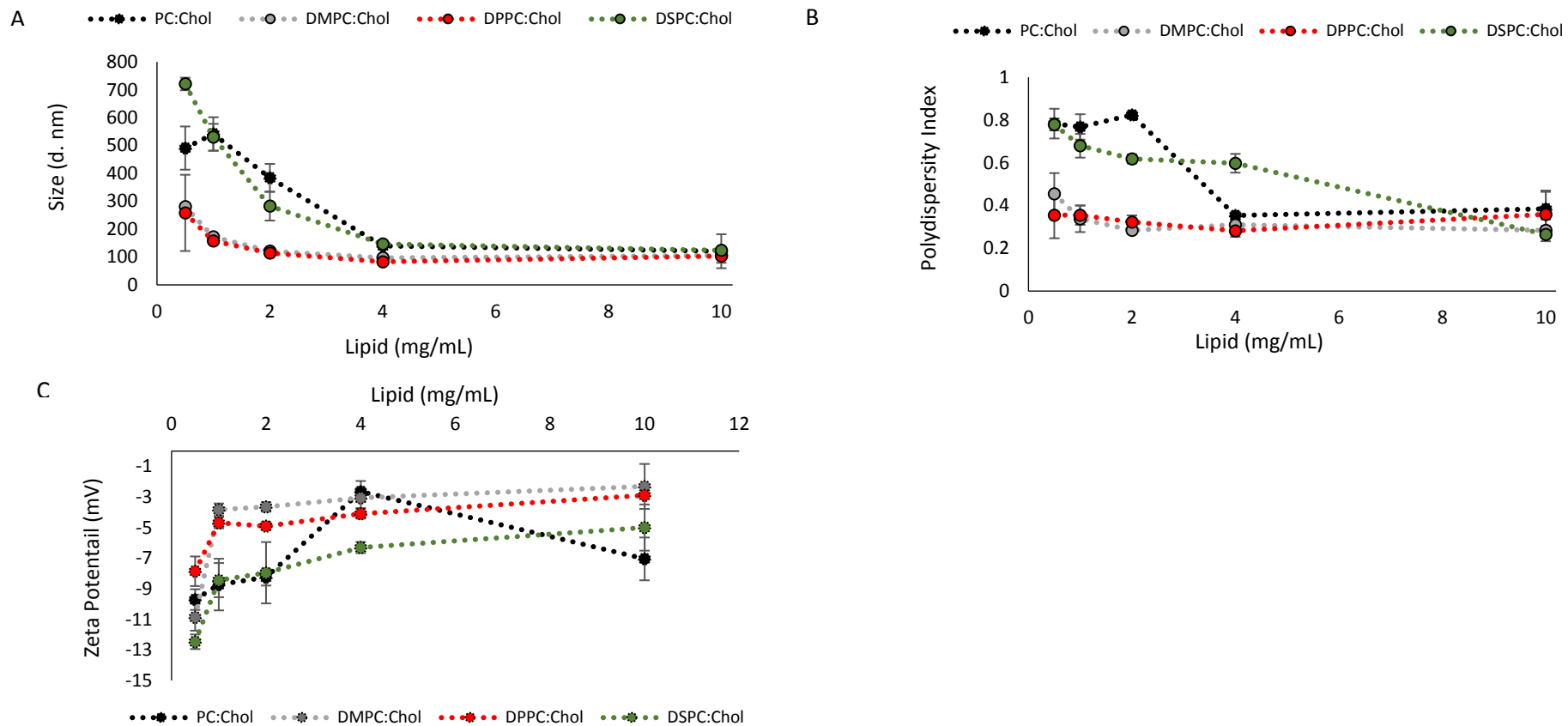


**Figure 5.8.** The physicochemical properties of OVA loaded liposomes (0.25 mg/mL initial ovalbumin) produced at varying lipid concentrations (0.3- 10 mg/mL initial lipid) by microfluidics at 3:1 FRR and 15 mL/min TFR. The size, polydispersity (PDI) and zeta potential (ZP) of PC:Chol, DMPC:Chol, DPPC:Chol and DSPC:Chol using dynamic light scattering. The results represent mean  $\pm$  SD, n=3 independent batches.

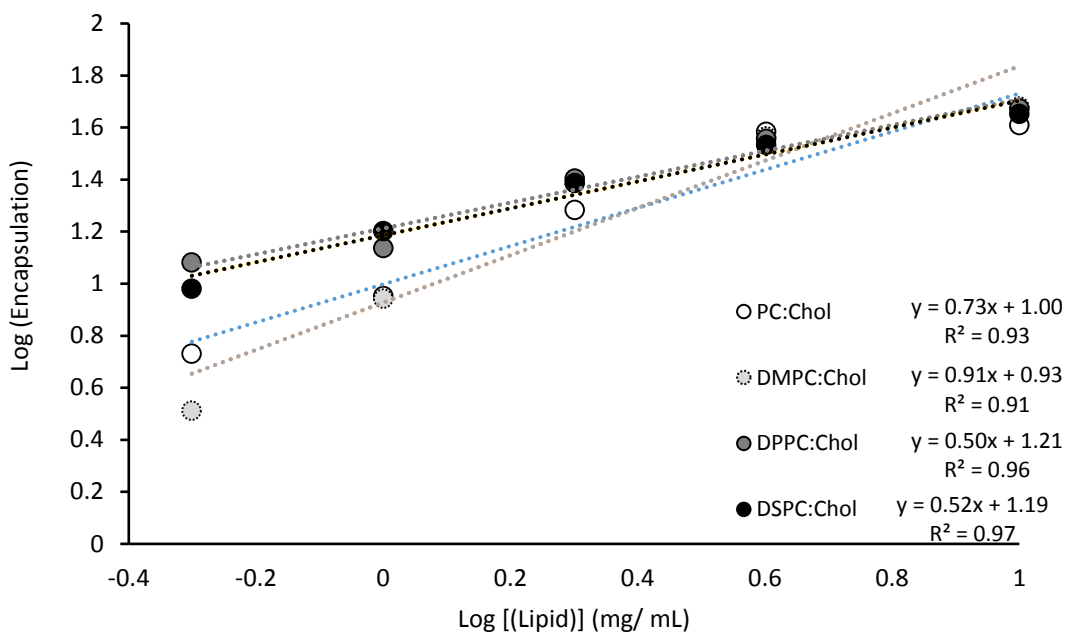


**Figure 5.9.** Investigating the relationship between log lipid concentration on the log encapsulation efficiency of four liposomal formulations (PC:Chol, DMPC:Chol, DPPC:Chol and DSPC:Chol). The liposomal formulations were prepared using microfluidics at varied lipid concentration and 0.25 mg/mL initial ovalbumin concentration. All formulations were produced at a 3:1 FRR and 15 mL/min TFR. The results represent mean  $\pm$  SD, n=3 independent batches.

#### 5.4.1.5. Effect of protein encapsulation efficiency on flow rate ratio

To further develop understanding of the microfluidic manufacturing process, the effect of FRR on the encapsulation efficiency of OVA by DMPC:Chol liposomes was investigated. The liposomes were produced at either a 3:1 or 5:1 FRR to investigate possible changes in encapsulation efficiency or physicochemical properties (size, PDI and zeta potential). The initial OVA concentration was matched (0.188 mg/mL) alongside the initial lipid concentration (4 mg/mL) to determine the impact of FRR. The liposomes measured by dynamic light scattering show no significant difference between liposomes size of formulations produced at a 3:1 FRR ( $78 \pm 2.7$  nm) or at a 5:1 FRR ( $82 \pm 1.8$  nm) (Figure 5.10A). The formulation produced at both FRR are homogenous with a measured PDI of less than 0.2 (Figure 5.10A), showing this is an effective production technique. The liposomes were further characterised with respect to the amount of OVA loading and encapsulation efficiency. Both formulations are able to encapsulate OVA at a high rate with the 3:1 FRR ( $37 \pm 0.2\%$ ,  $69 \pm 0.5$   $\mu$ g/mL) encapsulating significantly ( $p < 0.05$ ) more OVA in comparison to the 5:1 FRR ( $29 \pm$



0.6%,  $55 \pm 1.1 \mu\text{g/mL}$ ) (Figure 5.10B). The 8% difference in encapsulation efficiency can be attributed to the difference in the manufacturing; the position of mixing at the solvent- buffer interface is shifted alongside a smaller amount of solvent stream causes the difference in encapsulation. As a result, the 3:1 FRR was the preferred FRR for producing OVA loaded DMPC:Chol liposomes.

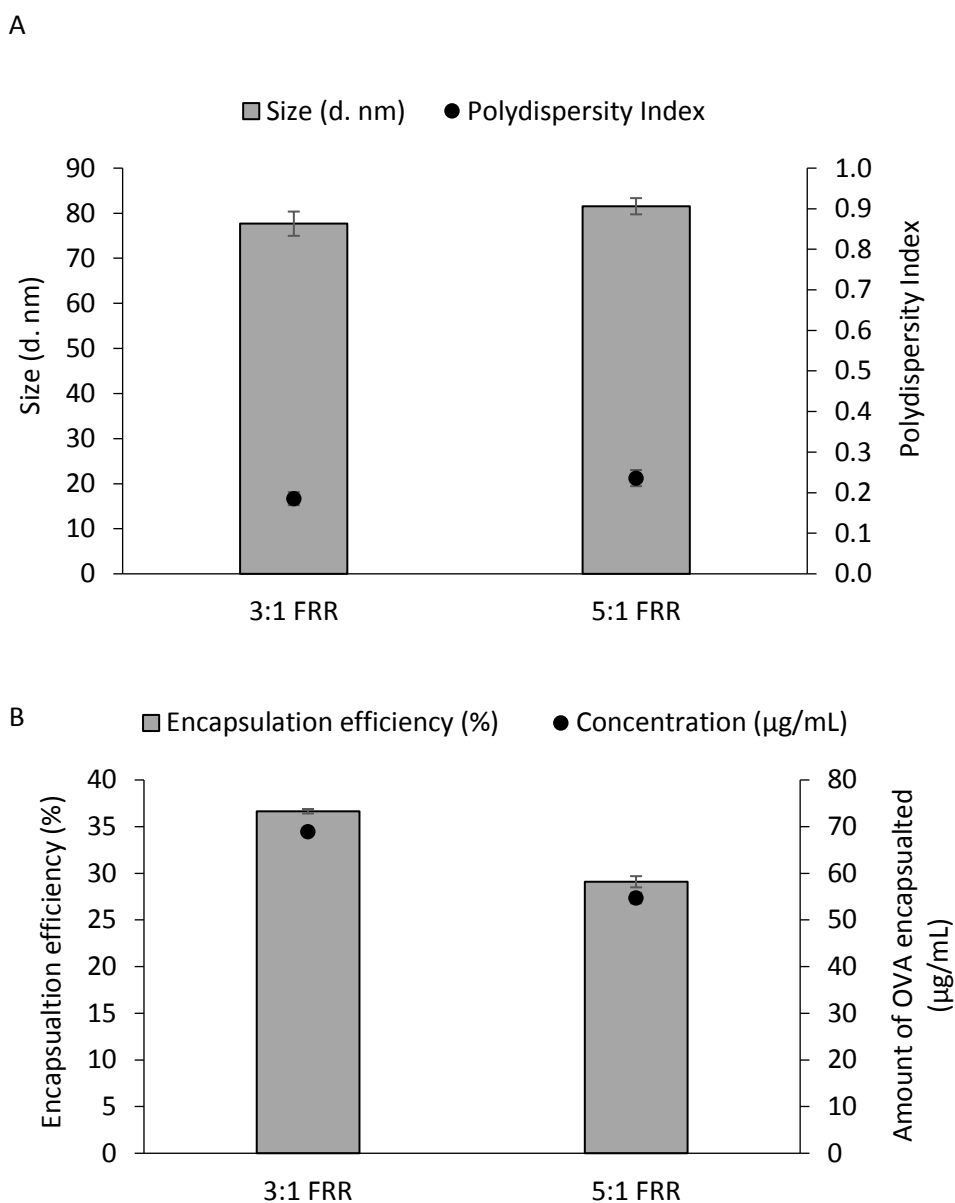


**Figure 5.10.** Characterisation of OVA loaded DMPC:Chol liposomes produced by microfluidics at a 3:1 FRR and 5:1 FRR. The liposomes were produced at a 4 mg/mL initial lipid concentration with an initial ovalbumin concentration of 0.188 mg/mL. The physicochemical properties (size and polydispersity index) was determined by dynamic light scattering (A), and the encapsulation efficiency calculated (B). The results represent mean  $\pm$  SD, n=3 independent batches.

#### 5.4.1.6 Circular dichroism of OVA to confirm protein stability.

Despite the microfluidics method being able to produce high loaded protein liposomes, due to the manufacturing process (whereby the solvent stream and aqueous stream converge), in this case methanol (as the lipids are dissolved in methanol), it is possible the protein may come into contact with the solvent causing denaturation. To check the structural integrity of proteins encapsulated into liposomes by microfluidics, OVA was used as a model protein to determine the protein integrity post microfluidics by circular dichroism.

Empty liposomes (Figure 5.11A) were tested to determine any background influence on detection. Figure 5.11A shows the empty DSPC:Chol liposomes do have some background interference and so this was subsequently blanked from all OVA protein runs. Equally, OVA protein dissolved in 100% methanol causes aggregation and precipitation of the protein; the sample was hard to measure with no distinct curvature associated with protein structural measurements (including alpha helix and beta sheets) using circular dichroism (Figure 5.11B). The results (Figure 5.11C) show protein encapsulated into liposomal formulations does not undergo denaturation, with the OVA encapsulated within DSPC:Chol liposomes produced by microfluidics production purification by TFF maintaining structural integrity. Both the native and OVA found in the liposomes follow a similar curve pattern (Figure 5.11C), the short exposure of the protein to solvent does not significantly impact proteins to be encapsulated. The structure of OVA is known; it has nine alpha helical structures and two beta sheets (Stein et al., 1990). Figure 5.11C shows that the OVA has alpha helical structures seen between 190-205 nm, and the dip representing beta sheets is also observed, which is in keeping in literature (Paolinelli et al., 1997). The results from both native and OVA from DSPC:Chol liposomes show this, confirming the microfluidics is a good method for manufacturing OVA loading liposomes.

In addition, the FRR selected in relation to the denaturation of protein was investigated using OVA as the model protein. The FRR is important as it not only impacts the size of liposomes, but also during the manufacturing process differing amounts of solvent is used. At a 1:1 FRR, the maximum amount of solvent (50% methanol) is used and mixed with 50% of the aqueous buffer (which can contain the protein OVA). As the FRR is increased, the amount of solvent decreases with OVA loaded liposomes produced at a 3:1 FRR exposed to 25% methanol,

whilst production at a 5:1 FRR exposes the OVA to 16.7% solvent. To investigate if the varying amounts of solvent has a detrimental effect on the OVA encapsulated, OVA loaded DSPC:Chol liposomes were produced at three FRRs (1:1, 3:1 and 5:1 FRRs). Figure 5.12A shows the production of OVA loaded DSPC:Chol liposomes causes an opaque cloudy suspension to be formed. In contrast, the OVA loaded DSPC:Chol liposomes produced at a 3:1 or a 5:1 FRR are clear. Testing the FRR using circular dichroism revealed the 1:1 FRR caused significant denaturation of the OVA entrapped within the liposomes leading to an exaggeration of the beta sheet amount detected (as shown in Figure 5.12B). Unlike the higher FRR, the denaturation of the protein at a 1:1 FRR is caused due to the protein exposed to the most methanol (50%) during manufacture. As a result, the OVA protein aggregates, with structural changes evident by a larger amount of beta sheets detected by circular dichroism. The integrity of OVA protein encapsulated within liposomes produced at a 3:1 or a 5:1 FRR remains (Figure 5.12B); the smaller volume of methanol does not impact the formulations with the OVA maintaining distinct alpha helical and beta sheet structures. The results from circular dichroism confirm that the 3:1 FRR (as well as the 5:1 FRR) are preferable for the production of OVA loaded liposomes. As a result, the 3:1 FRR parameter was selected for the production of OVA loaded liposomes.

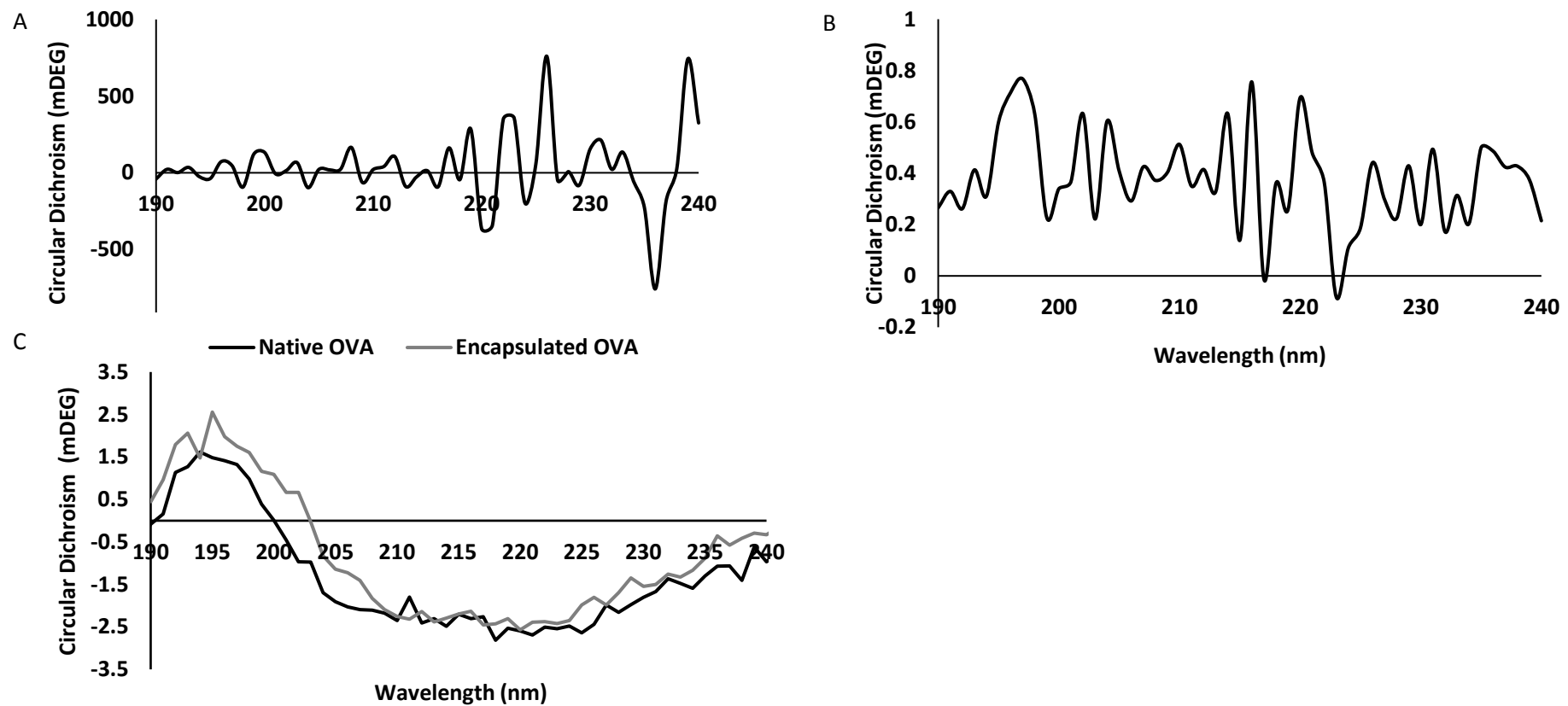
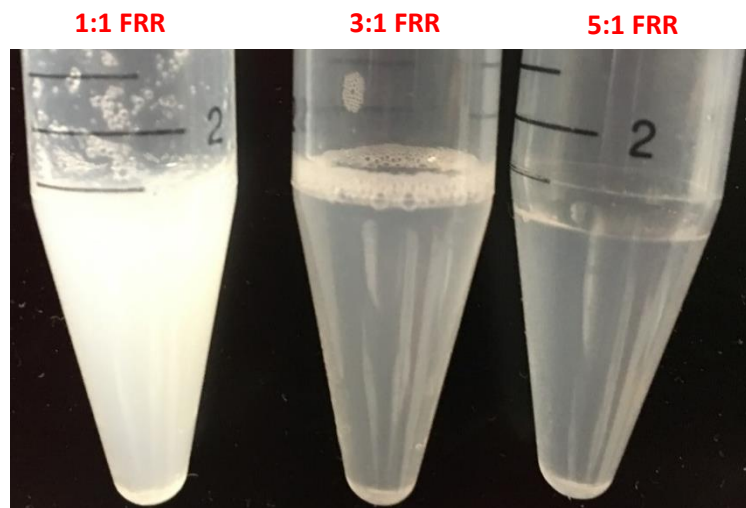


**Figure 5.11.** The structural integrity of ovalbumin loaded into the liposomes was tested by circular dichroism (CD). The CD spectra was identified for empty DSPC:Chol liposomes (A), OVA solubilised in 100% methanol (B) and OVA dissolved phosphate buffered saline (PBS) as well as OVA entrapped within DSPC:Chol liposomes. The results are representative of the samples.

A



B

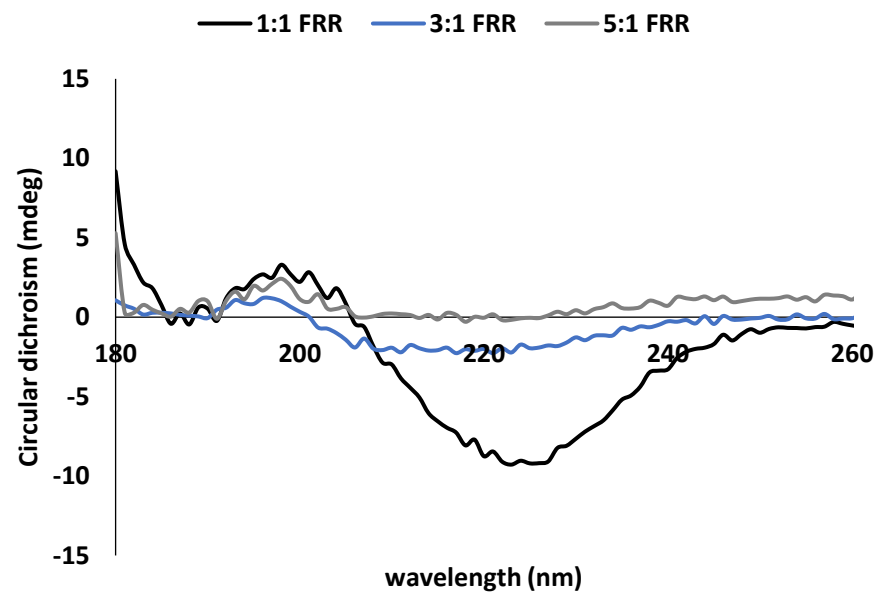


**Figure 5.12.** The effect of flow rate ratio (FRR) on the integrity of ovalbumin (OVA) encapsulated inside liposomes. OVA loaded DSPC:Chol liposomes were produced at either a 1:1 FRR, 3:1 FRR or 5:1 FRR (at 15 mL/min speed) using microfluidics. The formulations were inspected visually (A) as well as by circular dichroism. The results are representative of the samples.

#### 5.4.1.7 Stability of OVA loaded liposomes

Whilst producing liposomes with high protein loading is needed, it is equally important that the formulations are stable and to determine how long the liposomes maintain their structural integrity. As these formulations contain protein, the stability assays are used which are reflective of the storage conditions that may be required by these formulations. The effect of thermal changes was explored in terms of liposomes size, PDI and zeta potential. A temperature of around 4°C was chosen in accordance to the International conference on harmonisation guidelines ((ICH) (Guideline, 2016)). According to the pharmaceutical guidelines, a cold temperature of 4°C was used to determine the long term stability of the liposomal formulations.

The results from Figure 5.13 show that all four formulations (PC:Chol, DMPC:Chol, DPPC:Chol and DSPC:Chol) are stable for up to seven days at 4°C. In terms of size, minimal increases in size were observed after seven days with the sizes below 140 nm. For instance, a 17 nm increase was calculated for OVA loaded PC:Chol liposomes and a 30 nm increase for OVA loaded DMPC:Chol liposomes (Figure 5.13A). The PDI for all formulations remains below 0.2 for up to 3 days, after which small increase in PDI is observed (Figure 5.13B). This is also shown by the intensity plots for the four formulations (Figure 5.14). The OVA loaded DSPC:Chol liposomes become more heterogeneous (with a recorded PDI of 0.4 after 7 days), whilst the zeta potential remains above -10 mV (and remains neutral) (Figure 5.13C).

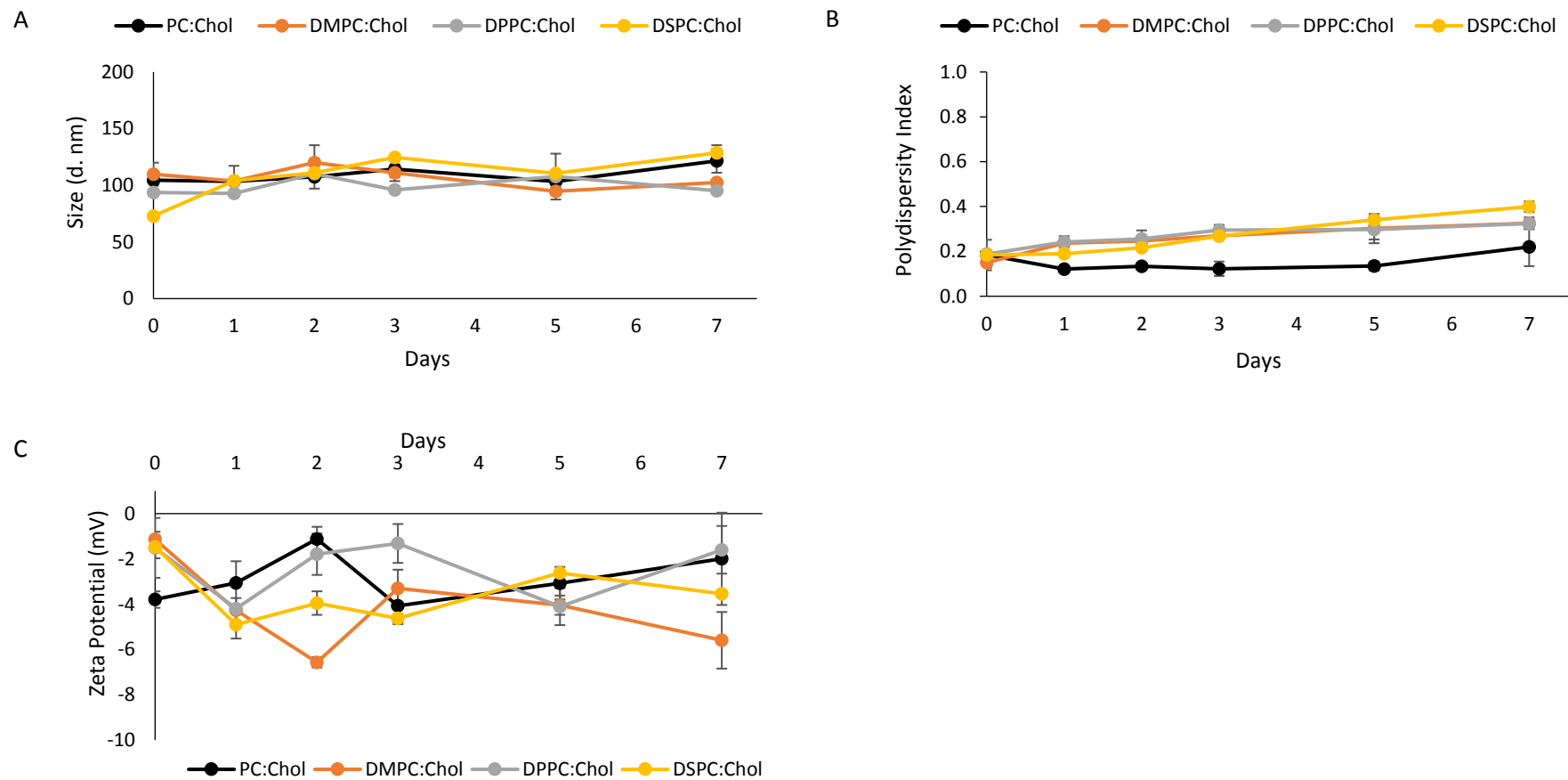


**Figure 5.13.** The stability of OVA loaded liposomes produced by microfluidics (at a 3:1 FRR and 15 mL/min TFR), with regards to liposome size (A), polydispersity index (B) and zeta potential (C). Four liposomal formulations (PC:Chol, DMPC:Chol, DPPC:Chol and DSPC:Chol) were produced and kept three different test conditions (5°C, 25°C and 37°C) to determine the stability. Measurements were taken at set time points over seven days using dynamic light scattering. The results represent mean  $\pm$  SD, n=3 independent batches.

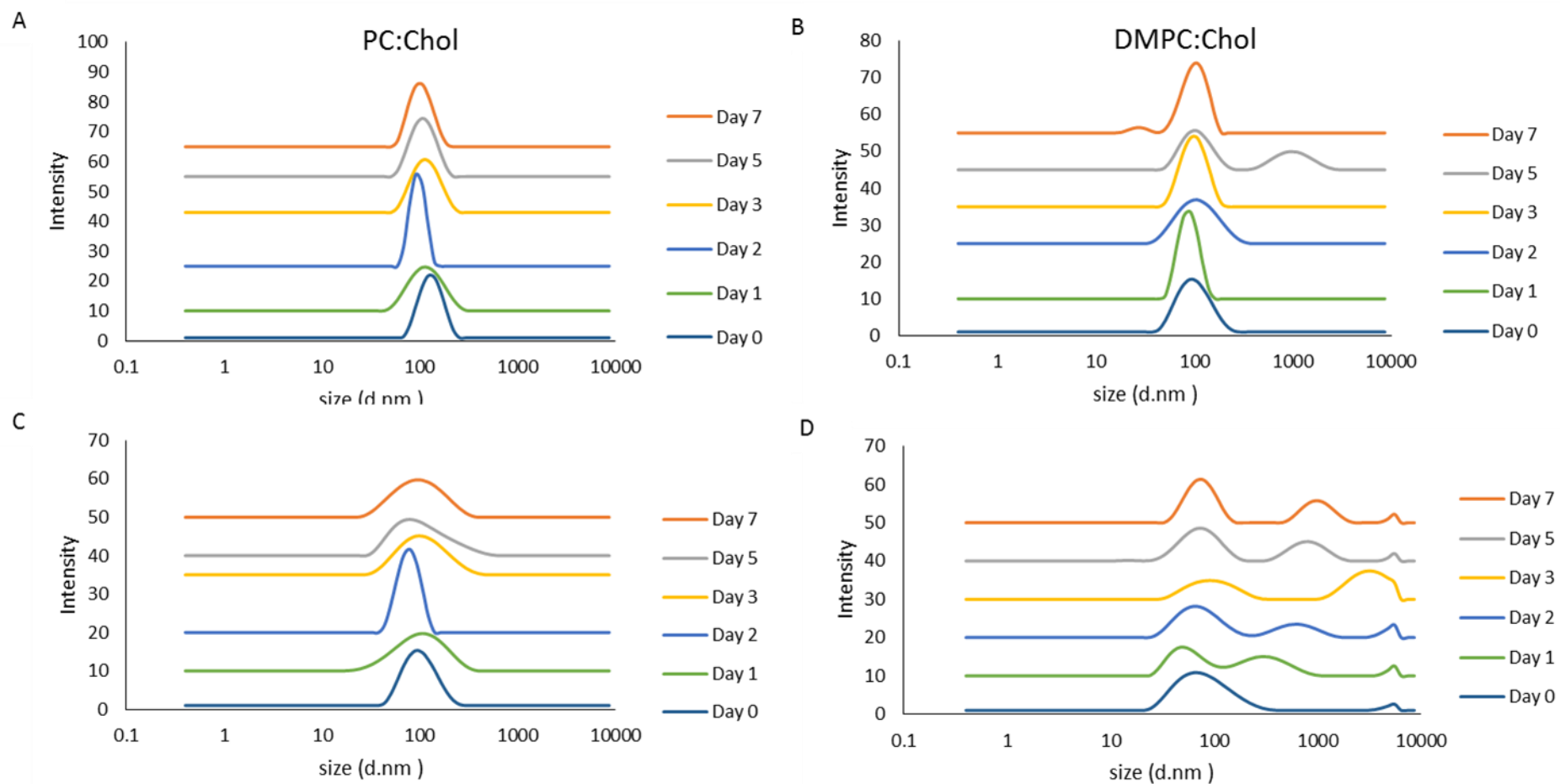


**Figure 5.14.** Peak intensity of OVA loaded PC:Chol (A), DMPC:Chol (B), DPPC:Chol (C) and DSPC:Chol made by microfluidics (3:1 FRR and 15 mL/ min TFR) and kept at 4°C for 7 days. The plots are representative of one measurement of the liposomal formulations.



#### 5.4.1.8 Release of ovalbumin from ovalbumin loaded liposomes

For liposomes to be successful, they must be able to retain, deliver and release protein as needed to meet therapeutic needs. Determining the release profile of liposomal formulations is needed, release in-vitro can be used to determine behaviour in vivo. The rate of release is dependent on many factors including the lipid composition, the presence of cholesterol, the type of drug or the nature of the proteins entrapped (Panagi et al., 1998). The effect of liposome composition was investigated using neutral liposomes containing varying carbon chain lengths lipids (PC, DMPC, DPPC, and DSPC) in addition to the presence of cholesterol. All four neutral formulations (PC:Chol, DMPC:Chol, DPPC:Chol and DSPC:Chol) were produced using microfluidics at a 3:1 FRR and 15 mL/min TFR, using 4 mg/mL initial lipid and 0.25 mg/mL initial OVA concentrations.

The results from Figure 5.15 show all four liposomal formulations (PC:Chol, DMPC:Chol, DPPC:Chol and DSPC:Chol) are capable of protein release (at 37°C in PBS buffer (pH 7.3)). The amount of OVA protein entrapped and released was measured directly by quantifying the amount of OVA remaining within the liposomes at set times. The most release is observed within 24 hours, with a sustained release observed thereafter. The general trend observed is that liposomal formulations produced with shorter hydrocarbon tails (such as PC:Chol and DSPC:Chol) release the most protein within 24 hours compared to the longer hydrocarbon tail liposomes (DPPC:Chol and DSPC:Chol). The burst release profiles for the formulations produced by microfluidics match previous studies whereby a burst release is observed within the first 12 hours, after which a slower rate of release is observed (Murao et al., 2002, Monteiro et al., 2014, Panagi et al., 1998).

Post 24 hours,  $29 \pm 9\%$  and  $42 \pm 6\%$  OVA protein remains within PC:Chol and DMPC:Chol liposomes respectively, compared to  $47 \pm 2\%$  and  $66 \pm 5\%$  OVA remaining within DPPC:Chol and DSPC:Chol liposomes. The results obtained from Figure 5.15 confirm previous studies that have shown DSPC liposomes are more stable; longer hydrocarbon tailed lipids release at slower rates (Panagi et al., 1998). For PC:Chol liposomes, all encapsulated OVA is released within 72 hours. Meanwhile, not all the encapsulated OVA is released by 120 hours for both DPPC:Chol and DSPC:Chol;  $14 \pm 5\%$  and  $30 \pm 10\%$  OVA remaining is quantified for DPPC:Chol and DSPC:Chol liposomes respectively. The notable difference in the release rates between the formulations can be attributed to the length of the lipid hydrocarbon tail. Previous

research has shown longer chain lipids have slower release rates due to their increased bilayer rigidity. The longer chained lipids are able to form more Van der Waals forces between the longer hydrocarbon tails, which improves membrane packing compared to shorter chained lipids (like PC) (Mohammed et al., 2004, Panagi et al., 1998).

Furthermore, as the flow rate ratio is known to impact the loading of the liposomal formulations, the release rate of OVA loaded DMPC:Chol liposomes produced at a 3:1 and 5:1 FRR was determined; the initial OVA concentration was matched for both FRRs. Using microfluidics, the encapsulation efficiency for OVA loaded DMPC:Chol liposomes produced at a 3:1 FRR is higher (at  $37 \pm 0.2 \%$ ) compared to DMPC:Chol formulations produced at a 5:1 FRR ( $29 \pm 0.6 \%$ ). The burst release of OVA within 24 hours is observed for OVA loaded DMPC:Chol liposomes produced at both 3:1 and 5:1 FRRs.

However, Figure 5.16 show there is a difference in release rate with OVA loaded DMPC:Chol liposomes produced at a 5:1 FRR released at a faster rate. To investigate this further, an  $F_2$  test was conducted with values of between 50- 100 suggesting similar release profiles. The  $F_2$  test determined a similarity factor ( $f_2$ ) of 24.6, which confirms the release profiles of the OVA loaded DMPC:Chol liposomes produced at a different FRR are different. The difference between the FRR can be attributed to the manufacturing process, where increasing the FRR causes a decrease in the alcohol concentration. In doing so, at a 5:1 FRR the solvent stream is reduced so at the solvent-aqueous liquid interface the lipids precipitate and form discs at a faster rate. There is less time for the lipid disc to expand and form liposomes (Zizzari et al., 2017); a shift in the position of the liquid interface position occurs when manufacturing at a 3:1 or a 5:1 FRR (Oellers et al., 2017). Both of these factors can impact the assembly and thus the release profiles of the respective formulations. Added to this, the shift in the position of the solvent- aqueous liquid or solvent concentration can cause small changes in the position of cholesterol intercalated within the bilayers. Previous research has shown a upright position of cholesterol is preferred when producing DMPC:Chol liposomes containing more than 30% cholesterol, as it is more aligned to the phospholipid bilayer (Khelashvili and Harries, 2013). Consequently, the position of the cholesterol, shift in the solvent-aqueous phase, and smaller solvent stream may all influence the release profile of the formulations. This knowledge can be used to formulate liposomes with differing release profile depending on whether a sustained release was required, further highlighting the versatility of the microfluidics manufacturing method.

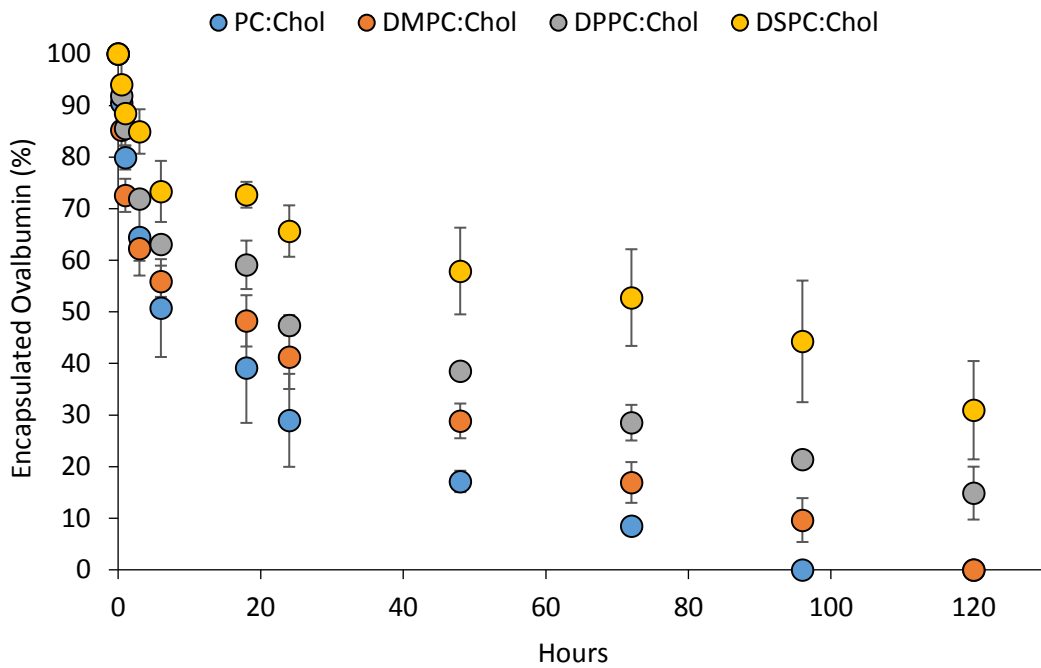


**Figure 5.15.** The release profile of ovalbumin from OVA loaded (PC:Chol, DMPC:Chol, DPPC:Chol and DSPC:Chol) liposomes produced by microfluidics (3:1 FRR and 15 mL/min TFR) and purified by TFF. The formulations were kept at 37°C in buffer, with samples collected at specific time points. Direct measurement of the encapsulated OVA was performed, to establish the release rate of the protein. The results represent mean  $\pm$  SD, n=3 independent batches.

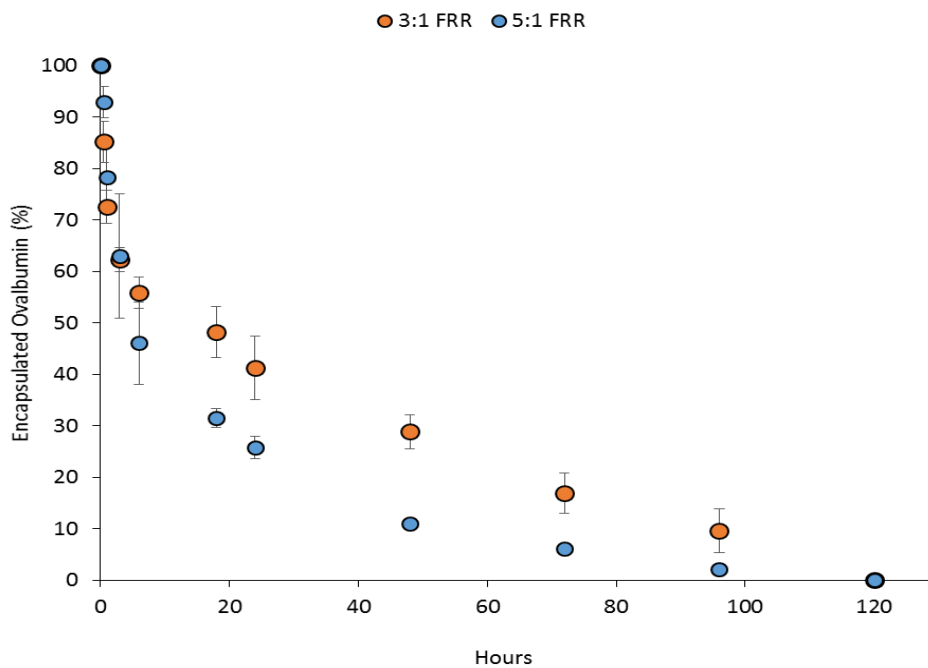


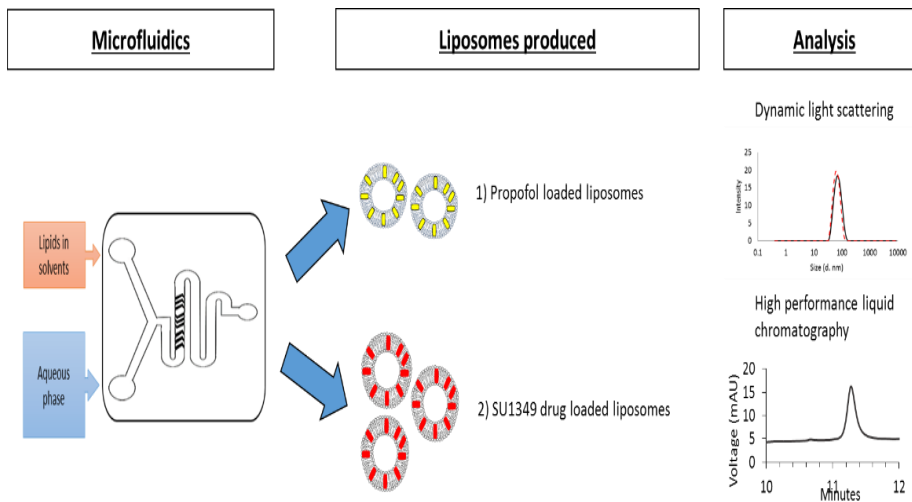
**Figure 5.16.** The release profile of OVA loaded DMPC:Chol liposomes produce at either a 3:1 or a 5:1 FRR (with a 15 mL/min TFR) and purified by TFF. The formulations were kept at 37°C in buffer, with samples collected at specific time points. Direct measurement of the encapsulated OVA was performed, to establish the release rate of the protein. The results represent mean  $\pm$  SD, n=3 independent batches.

## 5.5 Conclusion

In this chapter, the ability of microfluidics to achieve high loading of liposomal formulations was investigated. The encapsulation of protein within liposomal formulations using microfluidics was compared to traditional methods (thin film lipid hydration followed by sonication), with the results showing microfluidics enables a higher encapsulation rate. For instance, on average a 29% encapsulation efficiency difference was observed for the two methods for DSPC:Chol liposomal formulations. Furthermore, critical process parameters including the lipid concentration, protein concentration and microfluidics parameters (FRR) were investigated to identify ideal formulations parameters. The results show the lipid, protein and manufacturing parameters can all influence the physicochemical parameters of liposomes. Increasing the initial protein concentration had little impact on the liposomal physicochemical properties (such as size), whilst changing the initial lipid concentration did effect the physicochemical properties of the liposomes produced. The lipid concentration had no significant impact on protein loading. The manufacturing process plays a large role in determining the amount of encapsulated protein, with a FRR of 3:1 encapsulating more protein in comparison to a 5:1 FRR. Circular dichroism revealed the protein maintains its structure during the microfluidics manufacture; the exposure time of the protein to the solvent is short and does not cause denaturation. In addition, the release profiles of lower transition temperature lipid formulations (PC:Chol and DMPC:Chol) was quicker than with the use of higher transition lipids (DPPC:Chol and DSPC:Chol). Whilst all four formulations show an initial burst release, full release of the protein after 4 days was only observed for PC:Chol and DMPC:Chol liposomal formulations. The results indicate that although all four neutral formulations are equally capable of encapsulating liposomal formulations, the choice of lipids can be tailored to suit needs, particularly depending on whether a faster release of protein is required.

# Chapter 6

## High throughput microfluidics manufacture of liposomes loaded with small molecular drugs



Work presented in this chapter has been published in:

1. DIMOV, N., KASTNER, E., HUSSAIN, M., PERRIE, Y. & SZITA, N. 2017. Formation and purification of tailored liposomes for drug delivery using a module-based micro continuous-flow system. Scientific reports, 7, 12045.5.1 Introduction.

## 6.1 Introduction

### 6.1.1 Liposomal delivery systems for poorly soluble drugs

One of the major challenges impacting drug discovery and formulation development is the poor solubility of newly discovered chemical entities, with more than 90% of newly discovered drug having low solubility (Loftsson and Brewster, 2010, Savjani *et al.*, 2012, Muller and Keck, 2004). Whilst these drugs may have excellent stereochemistry and binding affinity to target sites, administering them therapeutically is incredibly difficult and is often associated with poor absorption (Savjani *et al.*, 2012). Administering these drugs via injection can lead to aggregate formation, local toxicity and poor bioavailability. There is also a risk of embolism formation that can be detrimental to the patient (Lukyanov and Torchilin, 2004), and so packaging these drugs into liposomal delivery systems is one way in which the adverse effects of poorly soluble drugs can be avoided. Incorporating the poorly soluble drugs into the bilayer of liposomes (as shown in Figure 6.1) offers a way in which to control the bio distribution and degradation of the drug. Previous research has shown formulation parameters (including the molecular weight of the drug, the lipophilicity, lipid concentration and type of lipids used) as well as the liposome manufacturing technique, all influence the incorporation and release profile of the drugs in the bilayer (Ali *et al.*, 2010, Ali *et al.*, 2013, Mohammed *et al.*, 2004, Dimov *et al.*, 2017).

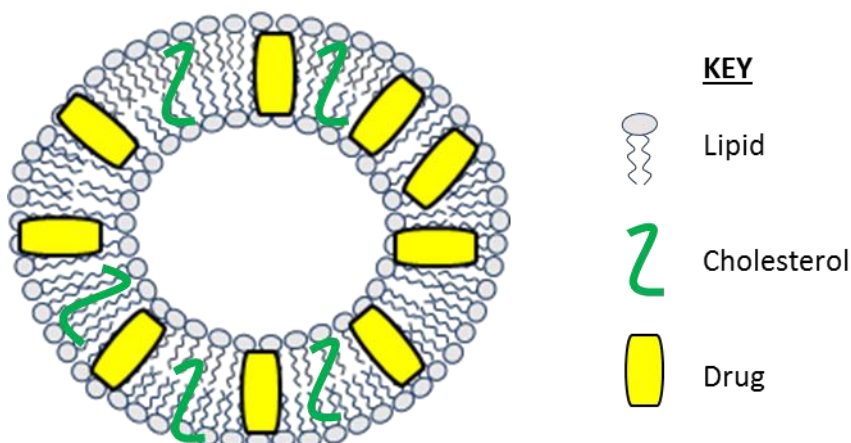


**Figure 6.1.** Representation of a liposomal formulation with cholesterol, and loaded with a lipophilic drug.

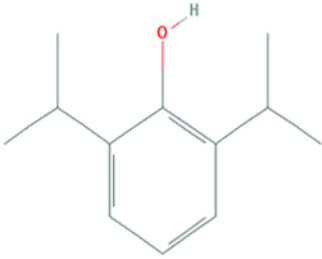
## 6.1.1 Manufacturing small molecular drug loaded liposomes using microfluidics

### 6.1.1.1. Manufacturing small drug loaded liposomes

Several studies have shown the potential of microfluidics to produce liposomes in a range of sizes, as well as encapsulate different materials including small interfering RNA (Belliveau et al., 2012; Chen et al., 2012), low solubility drugs (Kastner et al., 2015) and dual loaded liposomes (Joshi et al., 2016). Based on this, the ability to rapidly produce liposomal formulations with high loading of small molecule drugs was investigated. The ability of microfluidics to incorporate hydrophobic drugs into the lipid bilayer was tested.

Previous studies have shown the molecular weight of drugs can influence the drug loading, with larger molecules such as rifampicin (molecular weight (Mw) = 823 g/mol) have a low drug loading compared to propofol (Mw = 178 g/mol) and ibuprofen (Mw= 206 g/mol) (Ali et al., 2010; Ali et al., 2013). The characteristics of propofol, a general anaesthetic which is only partially soluble in an aqueous environment are shown in Table 6.1. Due to this, commercially available propofol are emulsions (marketed as Diprivan®, Propofol-Lipuro® , or Propofol-Lipuro®; (Formulary, 2018). As a result, the drug loading of propofol within liposomes was further investigated using microfluidics, as well as investigating the ability to scale-up the process.

**Table 6.1.** The characteristics of small molecule drug propofol (Formulary, 2018, Database, 2018).

DRUG	STRUCTURE	APPEARANCE	MOLECULAR WEIGHT (Mw)	WATER SOLUBILITY AT 25°C (mg/mL)
PROPOFOL		Yellow liquid	178	0.124

### **6.1.1.2 The manufacture of anticancer liposomes loaded with the novel SU1349 small drug molecule**

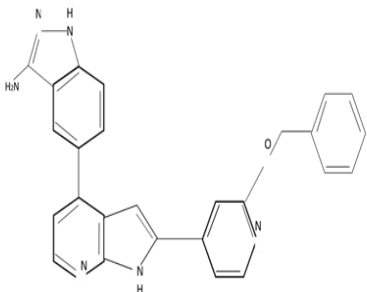
The shift in cancer treatment strategies from a general cytotoxic treatment to a more targeted approach has led to improvements in health care and cancer survival. A number of small drug molecules have been developed for interrupting pathways involved in cancer progression. For instance, patients with non-small cell lung cancer are treated with kinase inhibitors gefitinib and erlotinib, which potentially inhibit the epidermal growth factor receptor (EGFR) (Yap and Workman, 2012). The discovery and development of small molecular drugs to treat cancer has also been mirrored in protein and peptide research; monoclonal antibodies like trastuzumab are used to treat ERBB2- positive breast cancer (Slamon et al., 2001). Despite the advances in this field, the number of treatment options available to patients is often limited, with high failure rates associated with drug discovery and research (Kola and Landis, 2004). One major issue that withholds translation of small molecular drugs from research to a marketed product is the poor solubility of many small molecular drugs. According to ICH guidelines, a drug can be classified into one of four poorly soluble drug categories if the highest therapeutic dose is insoluble in 250 mL (or less) of aqueous media (at pH 1.2- 6.8, and temperature of  $37 \pm 1^\circ\text{C}$ ) (Kipp, 2004). Many cytotoxic drugs such as paclitaxel and etoposide are poorly soluble due to their structure (polycyclic nature), and since the 1990s the amount of new small molecular drugs discovered that are poorly soluble has risen (Ku, 2008).

In keeping with this, the SU1349 anti-cancer compound synthesised by Professor Simon MacKay's research group (University of Strathclyde) is a poorly water soluble small molecular drug. The SU1349 is a poorly soluble drug, with the characteristics of the drug shown in Table 6.2. The drug was designed for use as a nuclear factor kappa-B kinase subunit alpha (IKKA) inhibitor, to treat metastatic cancers associated with prostate and (or) pancreatic cancer. This drug is of particular importance as the IKKA subunit is associated with the nuclear factor kappa B (NFkB) pathway; it has been implicated in oncogenesis and is thought to be one compound that drives the metastatic pathway (Shukla et al., 2015). The poor solubility of the SU1349 drug can be improved by using liposomes as delivery vehicles. Previous papers have shown liposomes are able to encapsulate drugs, with the ability to dual load both hydrophobic and hydrophilic drugs (of metformin and glipizide) (Joshi et al., 2016). With this



in mind, it may be possible to improve the solubility of SU1349 drugs by loading into the liposomes.

**Table 6.2.** The characteristics of the novel small molecular drug SU1349.

DRUG	STRUCTURE	APPEARANCE	MOLECULAR WEIGHT (Mw)	WATER SOLUBILITY AT 25°C (mg/mL)
SU1349		Yellow powder	432	Very insoluble (permeability not known).

## 6.2 Aim and Objectives

The aim of this chapter is to determine the ability of microfluidics to encapsulate two small low solubility drug molecules in liposomal formulations. To do this the following objectives were considered:

4. Identification of the ideal manufacturing technique for the production of liposomes incorporating a large amount of drug.
5. Characterisation of small molecular propofol drug liposomal formulations.
6. Investigate the loading SU1349 drug into liposomes to improve solubility.

## **6.3 Materials and Methods**

### **6.3.1 Materials**

Phosphatidylcholine (PC) and 1,2-dimyristoyl-sn-glycero-3-phosphocholine (DMPC) from Avanti Polar Lipids Inc., Alabaster, USA. Cholesterol, Propofol (2,6-Bis(isopropyl)phenol), and, D9777-100ft dialysis tubing cellulose was obtained from Sigma Aldrich Company Ltd., Poole, UK. For purification of formulations by dialysis, a Biotech CE Tubing MWCO 300 kD was used (Spectrum Inc., Breda, The Netherlands). HPLC grade methanol, 2-propanol and dimethyl sulfoxide (DMSO) were purchased from Fisher Scientific, Loughborough, England, UK, in addition to the use of HPLC grade water. The SU149 drug was from Professor Simon MacKay (University of Strathclyde, Glasgow, UK).

### **6.3.2 Methods**

#### **6.3.2.1 Production of liposomes**

##### **6.3.2.1.1 Production of propofol loaded liposomes using thin film lipid hydration**

Multilamellar vesicles (MLVs) were produced using thin film lipid hydration. The PC:Chol lipids were dissolved in a chloroform/methanol (9:1 v/v) mixture, containing 1 mg/mL of propofol. The organic solvent was removed by rotary evaporation under vacuum followed by reconstitution with Tris buffer (10 mM, pH 7.3). The MLVs were down sized to SUVs using hand held extrusion Avanti Polar Lipids Inc., Alabaster, AL, US. Liposomes (1 mg/mL) were extruded using filters of various size; the pore size is incrementally decreased. Following this, the untrapped propofol was removed using cross flow filtration. The liposomes were characterised as previously described by dynamic light scattering (as described in chapter 2.3.2.4).

##### **6.3.2.1.2 Production of propofol loaded liposomes using microfluidics**

The propofol loaded liposomal formulations were produced using microfluidics at a 3:1 FRR and a 5 mL/min TFR. The lipids (PC and cholesterol) were dissolved in ethanol, with propofol added to the solvent phase, with Tris buffer (pH 7.4, 10 mM) used as the aqueous buffer.

The formulations were characterised by dynamic light scattering (as described in chapter 2.3.2.4).

#### **6.3.2.1.3 Production of SU1349 drug loaded liposomes**

DMPC:Chol liposomes were produced at 16:4  $\mu$ moles. Microfluidics was used to produce liposomes at a 3:1 and 5:1 Flow rate ratio (FRR) and a total flow rate (TFR) of 15 mL/ min. As the drug SU1349 is incorporated into the lipid bilayer, it was added into the solvent phase at a concentration of 0.5 and 0.05 mg/ mL. The DMPC lipid and cholesterol was dissolved in methanol, meanwhile the anti-cancer drug SU1349 was dissolved in Dimethyl sulfoxide (DMSO) as it is insoluble in methanol. Despite different solvents used this was not an issue as both solvents are miscible with one another. The samples were sized, polydispersity (PDI) and zeta potential measured before and after solvent removal using the Malvern Zeta sizer (method described in previous quarterly reports). Solvent was removed by dialysis; dialysis was performed for 1, 2 and 3 hours. The liposomes were characterised as previously described by dynamic light scattering (as described in chapter 2.3.2.4).

### **6.3.3 Removal of organic solvent**

#### **6.3.3.1 Removal of solvent and non- incorporated propofol using a syringe pump diafiltration system**

The liposomes produced by microfluidics and thin film lipid hydration followed by sonication were purified by a bespoke diafiltration system. Purification of the liposomes was performed as described by Dimov et al (Dimov et al., 2017). In brief, syringe pumps (Nemesys, Cetoni GmbH, Germany), connectors and capillaries were used to connect to the tangential flow filtration (TFF) system. Multiple diafiltration cycles were performed with the retentate replenished with buffer to compensate for the amount of liquid passing through the membrane to keep the volume the same. A speed of 2 mL/min was selected.

#### **6.3.3.2 Removal of solvent and non- incorporated SU1349 drug from DMPC:Chol liposomes**

The removal of solvent and non-incorporated DMPC:Chol liposomes using dialysis. The liposomal formulations (approximately 1 mL) was added into the dialysis tube and clipped at

the ends. The sample was then added to a beaker containing 200 mL of PBS and a stirrer bar. After 1, 2 and 3 hours of dialysis the liposomal sample was collected.

### 6.3.4 Quantification of protein and drugs encapsulated in liposomes

#### 6.3.4.1 Quantification of propofol drug loaded in PC:Chol liposomes

The loading of propofol in PC:Chol liposomes was calculated by RP-HPLC. First, the liposomes were solubilised by adding methanol to the liposome formulation (at a 1:1 v/v ratio). The Gemini C-18 5  $\mu$  110 A (150 $\times$ 4.60 mm) was used to detect propofol, using a flow rate of 1 mL/min and an injection volume of 20  $\mu$ L. A 23 minute elution gradient (ran at 268 nm), composed of solvent A (0.1% TFA in water) and solvent B (100% methanol) was used, with the elution gradient shown in Table 6.3. The propofol peak appeared at 6.8 minutes, a calibration curve was established to quantify the amount of propofol loaded in PC:Chol liposomes by comparing it to the standards.

**Table 6.3.** The high performance liquid chromatography elution gradient to quantify the amount of propofol drug.

TIME (MIN)	A%	B%
0	95	5
3	0	100
8	0	100
13	95	5
23	95	5

### 6.3.5 CryoTEM microscopy of propofol loaded liposomes

The structural integrity and morphology of liposomes was investigated using cryogenic transmission electron microscopy (CryoTEM). Samples were prepared using grids with lacey carbon and a 200 sized mesh; approximately 8  $\mu$ L of sample is added to a glow discharged

grid with blotting on both sides for approximately 5 seconds before plunging into nitrogen cooled ethane propane mix (70% ethane). Images were taken at a 15000x magnification using a Jeol 2011 with a 200kv beam (using a minimal dose protocol), scanned at a low magnification and jumping to a high magnification without exposing the sample to the beam first. The CryoTEM pictures were taken at Warwick University, UK by Dr Saskia Bakker, Advanced Bioimaging Platform, and University of Warwick.

### **6.3.6 Polyvar microscope images for SU1349 loaded DMPC:Chol liposomes**

A light microscope was used to determine the size of SU1349 DMPC:Chol liposomes. As the liposomes were around 1 micron or larger they could be imaged using a light microscope. Around 20  $\mu$ L of the liposome formulation was added to a light microscope slide. Using the software affinity analyse the liposomes seen under a x100 objective were captured and imaged.

### **6.3.7 Statistical analysis**

Results are represented as mean  $\pm$  SD with n=3 independent batches. ANOVA and T-tests were used to assess statistical significance, with a Tukey's post adhoc test (p value of less than 0.05).

## **6.4 Results and discussion**

### **6.4.1 Production of bilayer drug-loaded liposomes**

#### **6.4.1.1 Characterisation of Propofol loaded liposomes produced by microfluidics and post- extrusion**

The ability of microfluidics to produce high loading of small molecular drugs and heterogeneous formulations is well documented. For instance, the ability to produce high loaded liposomes by microfluidics has been shown by Kastner et al; using microfluidics 41% of propofol loading was achieved with the ability to produce liposomal formulations at a range of sizes (50 -450 nm). However, whilst high throughout production was achieved, research into the continuous manufacture the liposomal formulations was needed. To achieve this a bespoke tangential flow filtration system (TFF) was set up, whereby a syringe pump was coupled with a bespoke filtration system (as described by (Dimov et al., 2017)). In brief, the filtration system was made from two poly(methylmethacrylate) (PMMA) plates

with a straight channel to contain the filtration membrane in the middle. The two PMMA plates were used to seal and clamp filtration membranes in place, and connectors were used to join the syringe pump to the filtration system (Figure 6.2). The bespoke TFF system was set up, specifically to determine the ability to purify the model drug, propofol from PC:Chol liposomes by removing unloaded propofol and solvent. This was investigated using tangential flow filtration, whereby 1 mL of sample was injected into the diafiltration system. In total, three diafiltration cycles (with buffer replenishment) was require to remove the free propofol. Post purification, the propofol loaded PC:Chol liposomes produced by the microfluidics were measured for potential changes in physicochemical characteristics. The initial propofol concentration (1 mg/mL) was used to produce the PC:Chol liposomes.

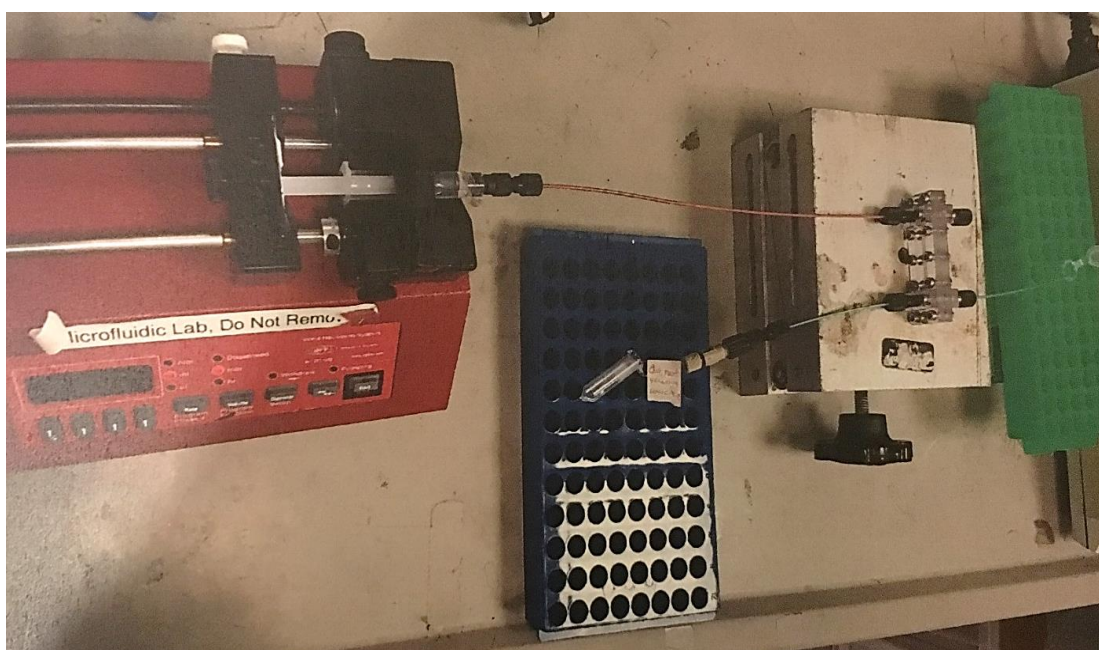


**Figure 6.2.** The bespoke TFF set up designed and built by Professor Nicolas Szita (University College London, UK).

The manufacturing technique for the production of propofol loaded PC:Chol liposomes (4:1 molar ratio) was investigated, comparing thin film lipid hydration followed by sonication to liposomes produced by microfluidics. The results from Table 6.4 shows propofol loaded MLVs are  $1801.1 \pm 228.2$  in size, with high PDI of  $0.42 \pm 0.146$ . The MLVs can be downsized to SUVs

using extrusion (10 passes through a 400 nm, 200 nm, 100 nm and final 50 nm pore size filters), producing SUVs sized  $107.9 \pm 14.1$  nm.

In contrast, producing propofol loaded liposomes using microfluidics is more efficient with the ability to produce SUVs in a single step process. The liposomes are around  $52.2 \pm 1.3$  nm in size, and are more heterogeneous with a PDI of  $0.18 \pm 0.016$  determined (Table 6.5). The results from Table 6.4 show that purification of SUVs (produced by thin film lipid hydration and downsized by extrusion) did not cause a change in size. The size of the liposomes produced remained at  $109.9 \pm 19.0$  from  $107.9 \pm 14.1$ . The PDI however, increases from  $0.17 \pm 0.104$  to  $0.34 \pm 0.064$ , suggesting the purification process may impact the liposomal physicochemical characteristics. Equally, the results from Table 6.5 show the size of liposomes produced by microfluidics remains the same as before purification ( $53.3 \pm 5.3$  and  $52.2 \pm 1.3$  nm respectively). Using this diafiltration system, the liposomal formulations become more heterogeneous as the PDI increased from  $0.18 \pm 0.016$  to  $0.29 \pm 0.053$  post purification. Compared to traditional manufacturing techniques, the results suggest microfluidics coupled with tangential flow filtration is the preferred manufacturing method for the ease of production of propofol loaded liposomes with a lower PDI.

Furthermore, both the traditional liposome production method (thin film lipid hydration followed by extrusion) and microfluidics was compared for the ability to achieve high protein loading (mol%). To quantify the amount of propofol loading, reverse phase-HPLC method was used. A calibration curve was established (Figure 6.3), where the correlation coefficient calculated is more than 0.99 and was used to determine the amount of propofol loading for PC:Chol liposomes. The results from production of propofol loading by the traditional method led to poor loading (mol%) of  $3.6 \pm 0.382\%$  compared to  $48.0 \pm 0.992\%$  produced by microfluidics.

**Table 6.4.** The physicochemical characteristics of propofol loaded PC:Chol liposomes manufactured as multilamellar vesicles (MLVs) by thin film lipid hydration, and downsized to small unilamellar vesicles (SUVs). The liposomes were purified by tangential flow filtration cycles, with the size and polydispersity index measured by dynamic light scattering. The amount of propofol loaded was calculated using HPLC. The results represent mean  $\pm$  SD, n=3 independent batches.

	<b>MLVS WITH DRUG</b>	<b>SUVS WITH DRUG</b>	<b>LIPOSOME WITH DRUG AFTER THREE PASSES THROUGH THE TFF*</b>
<b>SIZE (nm)</b>	1801.1 $\pm$ 228.2	107.9 $\pm$ 14.1	109.9 $\pm$ 19.0
<b>POLYDISPERSITY INDEX</b>	0.42 $\pm$ 0.146	0.17 $\pm$ 0.104	0.34 $\pm$ 0.064
<b>LOADING (mol%)</b>	N/A	N/A	3.6 $\pm$ 0.382

**Table 6.5.** The physicochemical characteristics of propofol loaded PC:Chol liposomes manufactured by microfluidics. The liposomes were purified by tangential flow filtration cycles (TFF), with the size and polydispersity index measured by dynamic light scattering. The amount of propofol loaded was calculated using HPLC. The results represent mean  $\pm$  SD, n=3 independent batches.

	<b>LIPOSOME WITH DRUG AFTER MICROFLUIDICS</b>	<b>LIPOSOME WITH DRUG AFTER THREE PASSES THROUGH THE TFF*</b>
<b>SIZE (nm)</b>	52.2 $\pm$ 1.3	53.3 $\pm$ 5.3
<b>POLYDISPERSITY INDEX</b>	0.18 $\pm$ 0.016	0.29 $\pm$ 0.053
<b>LOADING (mol%)</b>	N/A	48.0 $\pm$ 0.992



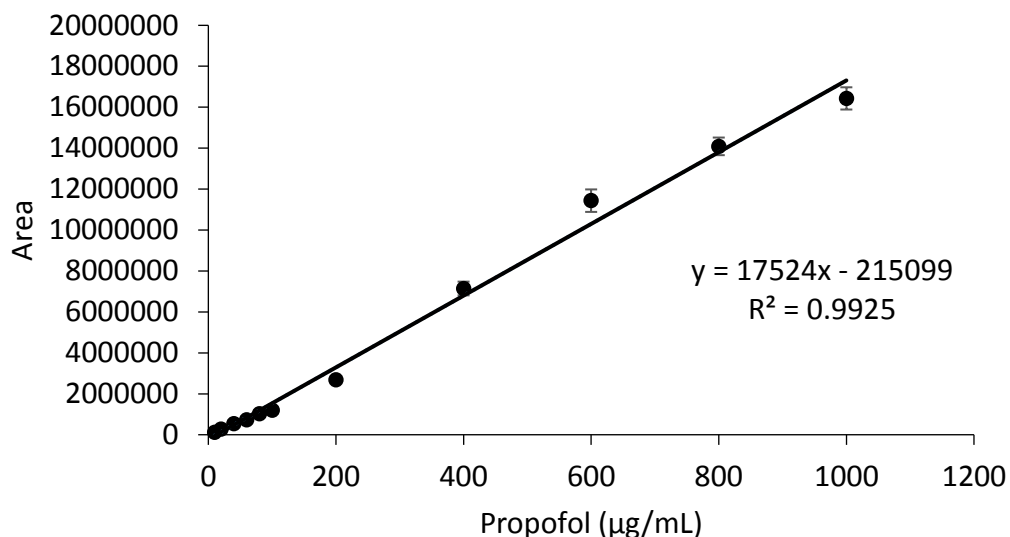


**Figure 6.3.** The calibration curve established to determine the amount of loading for propofol loaded PC:Chol liposomes. The results represent mean  $\pm$  SD, n=3 independent batches.

#### 6.4.2. Morphology of Propofol loaded liposomes

The physicochemical properties of propofol loaded PC:Chol liposomes was determined by dynamic light scattering (Table 6.5). To investigate the impact of microfluidics production and purification (using TFF), the morphology of the liposomal formulations was tested using CryoTEM. The image from Figure 6.4 show the liposomes are spherical in shape; no free propofol is observed showing the TFF system is efficient at removing free propofol. The liposomes have a distinct bilayer and a clear aqueous core can be observed. The liposomal formulations are also homogenous as observed by the similar sized liposomes observed, with the liposomes remaining below 100 nm. The liposomes do not aggregate and are disperse, as a result, the propofol loaded PC:Chol liposomes show that the TFF system is efficient at purification. It does not compromise the quality or physicochemical properties of the liposomal formulations. The results are in keeping with previous papers that have shown the ability to determine the morphology of SUVs using transmission electron microscopy. Research by Bibi et al has shown the ability to produce propofol loaded 1-palmitoyl-2-oleoyl-

sn-glycero-3-phosphocholine (POPC) and cholesterol liposomes, the morphology of which can be determined by transmission electron microscopy (Bibi *et al.*, 2011). This type of visual microscopy allows the inspection of the inner bilayers of liposomal formulations, in addition to the outer layer; therefore CryoTEM is a powerful analytical technique used to help characterise liposomal formulations.

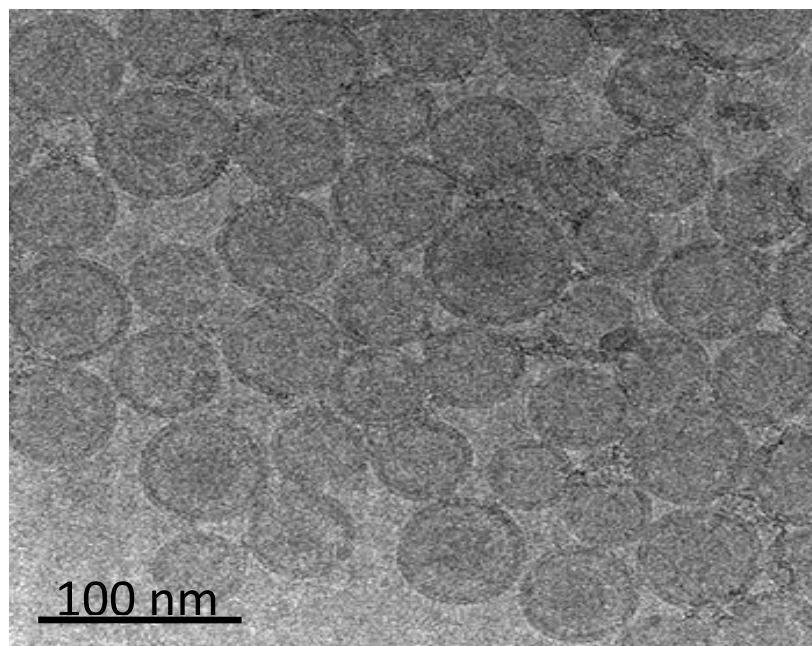


**Figure 6.4.** The morphology of Propofol loaded PC:Chol liposomes by cryoTEM. Images are taken by x1200 magnification.

#### **6.4.2 Production of SU149 incorporated liposomes**

Given that the microfluidics system had been shown as an effective method for the production of bilayer drug loaded liposomes, this method was also tested with the SU1349 drug. This small drug is a potential anti-cancer agent, but due to its insolubility it is hard to investigate the drug and determine its therapeutic benefits. Liposomes can improve this, so the production of SU1349 loaded liposomes by microfluidics was investigated. The first challenge on the production of the liposomes was finding a solvent in which the SU1349 drug was soluble; methanol, ethanol and acetyl nitrile were not compatible. As a result, dimethyl

sulfoxide (DMSO) was used to solubilise the SU1349 drug and in addition to the lipids (DMPC and cholesterol) made up the solvent component for microfluidics production.

DMSO is a class 3 solvent and has low toxicity (with more than 50 mg permitted daily exposure allowed) according to ICH guidelines, so this was used for the formulation of SU1349 loaded DMPC:Chol liposomes. As the drug is lipophilic, it was added into the solvent phase alongside the DMPC and cholesterol lipids (which was added to a 4:1 molar ratio). The amount of drug added to the formulations was 0.5 mg/mL, (producing an initial lipid to drug ratio of 24:1). The SU1349 loaded DMPC:Chol formulations were then produced using microfluidics at both the 3:1 and 5:1 FRR. The non- incorporated drug was removed by dialysis, with the length of dialysis varied to determine the minimal amount of time required for the removal of free propofol. Dialysis was performed for up to three hours for SU1349 loaded liposomes produced at either a 3:1 or 5:1 FRR, with aliquots taken every hour.

Results from Table 6.6 indicate large particle sizes; it is not clear if large liposomes are being formed or whether the results are due to aggregates because of precipitation. The size of the formulations produced at a varying FRR (3:1 and 5:1 FRR) was measured, with the 3:1 FRR producing particles smaller in size ( $1687 \pm 449.6$  nm) compared to the same formulation made at the 5:1 FRR ( $3930 \pm 151.2$  nm). After 1 hour dialysis, the size decreases to  $1358 \pm 328.9$  nm but become extremely heterogeneous (PDI=  $0.9 \pm 0.03$ ). Prolonged dialysis for 2 and 3 hours results in the size increasing back to before dialysis was performed;  $1780 \pm 125.2$  and  $1710 \pm 157.5$  nm respectively with fluctuations in the PDI. The zeta potential remains neutral and above -10 mV for up to 2 hours of dialysis, whilst after 3 hours the measured zeta potential for liposomes formulations produced at a 3:1 FRR is  $-18.6 \pm 0.87$  mV. Increased negative results would suggest changes in the formulation occur when dialysis is conducted for 3 hours.

In contrast, the SU1349 formulations produced at a 5:1 FRR are larger in size ( $3930 \pm 151.2$  nm) with the sizes fluctuating depending on the length of dialysis; the particle size decreases after 1 and 2 hours of dialysis but increases after 3 hours of dialysis. In correlation to this, the PDI also fluctuates with the most homogenous formulation produced after 1 hour of dialysis ( $0.1 \pm 0.09$ ). As observed for the 3:1 FRR, the SU1349 formulations produced at a 5:1 FRR whereby dialysis is performed for 3 hours, resulted in a more negative zeta potential ( $-20.5 \pm 0.73$  mV). Once again, it suggests 3 hours dialysis causes more aggregation and changes in the physicochemical properties of formulations irrespective of the FRR used. The longer

duration of dialysis, may encourage a greater amount of drug precipitation to occur which as a result impacts the size and PDI of the formulations (Edwards *et al.*, 2008). Based on these results, it is evident that producing liposomes smaller than 1000 nm (or 1 micron) is not possible with the current formulation and microfluidics parameters. It is not clear whether liposomes are being formed and so the formulations required further optimisation.

**Table 6.6.** Characterising SU1349 DMPC:Chol formulations in terms of size, PDI and zeta potential.

	SIZE (D. NM)		POLYDISPERSITY INDEX		ZETA POTENTIAL (MV)	
	3:1 FRR	5:1 FRR	3:1 FRR	5:1 FRR	3:1 FRR	5:1 FRR
<b>PRE- SOLVENT REMOVAL</b>	1687 ± 449.6	3930 ± 151.2	0.1 ± 0.06	0.3 ± 0.04	-0.1 ± 0.35	-0.5 ± 0.25
<b>1 HOUR DIALYSIS</b>	1358 ± 328.9	2478 ± 582.6	0.9 ± 0.03	0.1 ± 0.09	-4.9 ± 0.60	-4.6 ± 0.15
<b>2 HOURS OF DIALYSIS</b>	1780 ± 125.2	1049 ± 125.2	0.4 ± 0.18	0.7 ± 0.03	-7.0 ± 0.46	0.2 ± 0.30
<b>3 HOURS OF DIALYSIS</b>	1710 ± 157.5	1209 ± 94.7	0.7 ± 0.06	0.9 ± 0.06	-18.6 ± 0.87	-20.5 ± 0.73

#### 6.4.2.1 Morphology of SU1349 incorporated liposomes

The SU1349 formulations were further investigated with regards to the morphology, to try and determine the structure. As the structures were larger than 1000 nm, the formulations could be detected by light microscopy which is important for visual inspection of the particles. Light microscopy offers a quick and efficient method for the visualisation of samples in an aqueous medium. The use of a microscope slide and cover slip is sufficient for studying large particles, and pictures can be taken of the SU1349 loaded DMPC:Chol formulations (observed in Figure 6.5). The use of a 0.16 mm cover slip allows good resolution of the liposomal formulations (Bibi *et al.*, 2011). Although the particles are circular in nature, it is not clear if the particles have formed a bilayer structure or are aggregates (Figure 6.5). The particles appear heterogeneous in nature, with aggregation observed confirming the results obtained from dynamic light scattering used to measure the physicochemical properties of the liposomes. The thicker bilayer is suggestive that some of the SU1349 drug is encapsulated within the liposomal bilayer, but whether the drug has precipitated out and is not incorporated into the bilayer is not clear. As a result, the amount of drug loading needed to be quantified alongside the optimisation of the liposomal formulations.

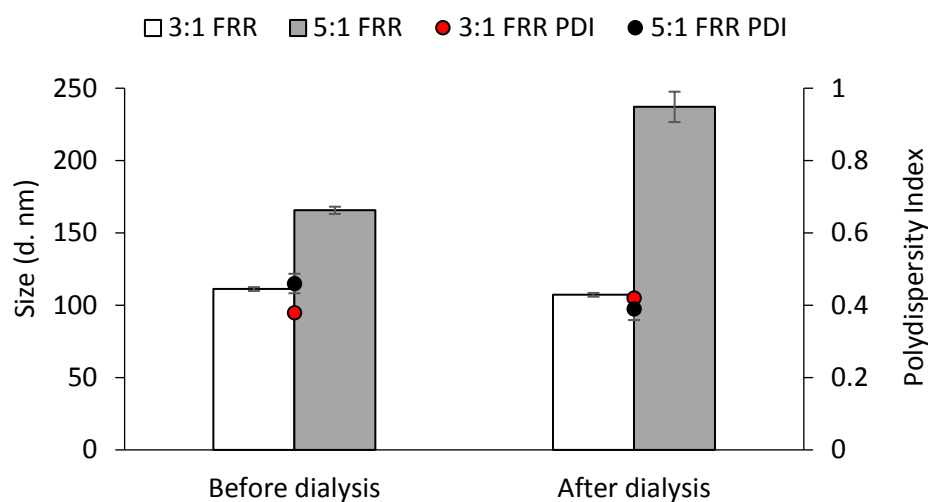


**Figure 6.5.** The morphology of SU1349 loaded DMPC:Chol liposomes. The images were taken by a light microscope.

#### 6.4.2.2 Optimisation of the SU1349 incorporated DMPC:Chol liposomes

Initial attempts to produce SU1349 DMPC:Chol liposomes produced particles that were too large to be used as an anticancer agent, the liposomes were in the micron range (Table 6.6). Based on earlier work, the system was scaled down with the use of 2 mg/mL lipid concentration, and 0.05 mg/mL initial SU1349 drug. As a result, the initial lipid to drug ratio was increased from 24:1 to 40:1, to determine if the SU1349 drug is influencing the size of the liposomes.

The results from Figure 6.6 show that reducing the initial drug concentration, significantly improves the size of the liposomal formulations produced. The liposomes produced using both the 3:1 FRR and 5:1 FRR are significantly smaller (below 300 nm) than those produced earlier. The formulations produced at a 3:1 FRR are more stable with the size remaining around 100 nm;  $112 \pm 1.3$  nm before and  $107 \pm 1.7$  nm after dialysis. The difference in size and stability, can once again be attributed to the production process of the liposomal formulations produced at the differing FRRs. Varying the FRR results in the amount of solvent stream differing, which consequently impacts the formation of liposomes. The PDI measured is less than 0.4 for SU1349 drug produced at both FRRs, with the formulations remaining neutral (shown by the zeta potentials of above -10 mV) pre and post dialysis. Manufacturing liposomal formulations around 100 nm is important, as at that size the liposomes are now clinically useable for intravenous injection (as an anti-cancer therapeutic). Liposomes larger than 100 nm are more likely to undergo clearance by the mononuclear phagocytic system, in comparison to smaller sized liposomes, therefore smaller liposomes (around 100 nm) are preferred. At 100 nm, the charge and the composition of the liposomes is a greater determining factor for the efficiency of the liposomal formulations (Senior et al., 1991, Senior and Gregoriadis, 1982).



<b>Zeta Pot (mV):</b>	<b>Before dialysis</b>	<b>After dialysis</b>
3:1 FRR	-2.6 ± 0.8	-4.6 ± 1.3
5:1 FRR	-4.6 ± 1.3	-5.7 ± 0.9

**Figure 6.6.** The physicochemical properties of SU1349 drug loaded DMPC:Chol liposomes. The size (d. nm), polydispersity index (PDI) and zeta potential (mV) is measured by dynamic light scattering. The results represent mean ± SD, n=3 independent batches.

Furthermore, whilst the size of the liposomes is important, it is necessary to quantify the amount of SU1349 drug loading for the SU1349 loaded DMPC:Chol liposomes. The drug loading was quantified by liquid chromatography coupled with mass spectroscopy. The analysis performed by Professor MacKay's research group, confirmed the presence of the SU1349 drug loaded into the liposomes by mass spectroscopy. Figure 6.7 displays the expected mass in both the positive (Figure 6.7A) and the negative (Figure 6.7B) mass spectroscopy confirming the presence of the drug. To quantify the amount loaded, liquid chromatography was used with an example of the SU1349 chromatogram shown in Figure 6.8. The SU1349 peak detected for the SU1349 loaded DMPC:Chol liposomes has a very low intensity, indicating poor loading. This is reflected in Table 6.7 whereby manufacture of the SU1349 loaded DMPC:Chol liposomes leads to poor loading ratio of 1.03% post-microfluidics production. The majority of the drug goes into the waste during the manufacturing process, this may be due the highly insoluble nature of the SU1349 drug. The majority of the drug is not incorporated into the lipid bilayer. Once SU1349 liposomal drugs have been formed, very little SU1349 drug is lost during the purification process, with the drug to lipid ratio quantified as 0.90% after dialysis. The poor loading is attributed to the very insoluble nature of the



SU1349 drug, therefore this particular anti-cancer drug was not researched further as the amount loaded is unable to meet therapeutic needs.

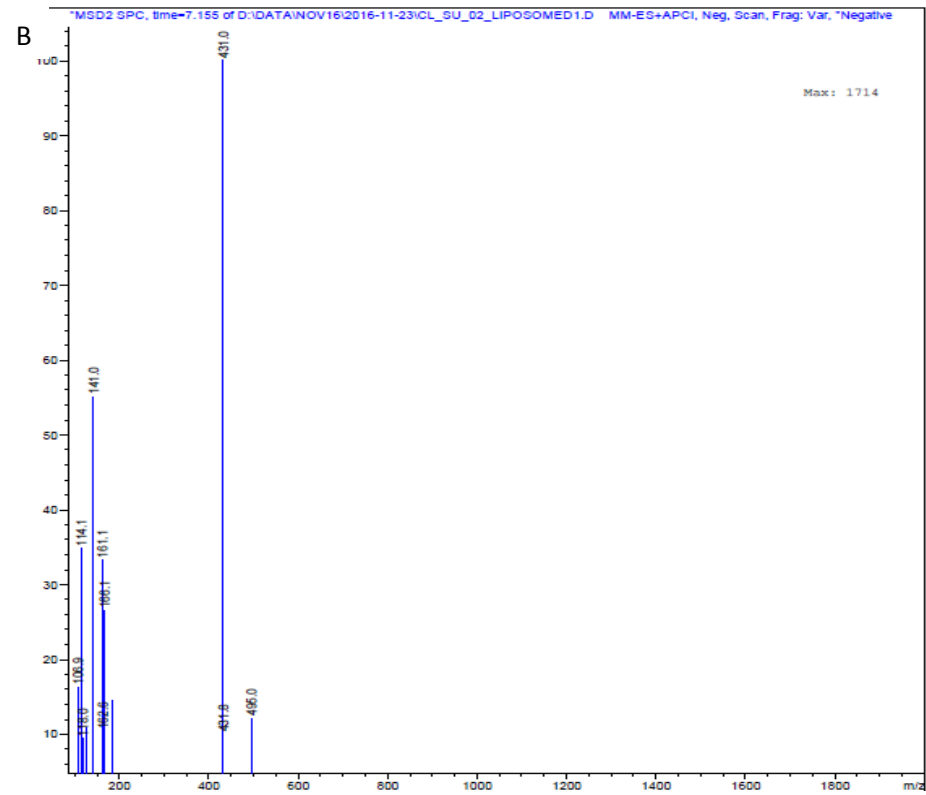
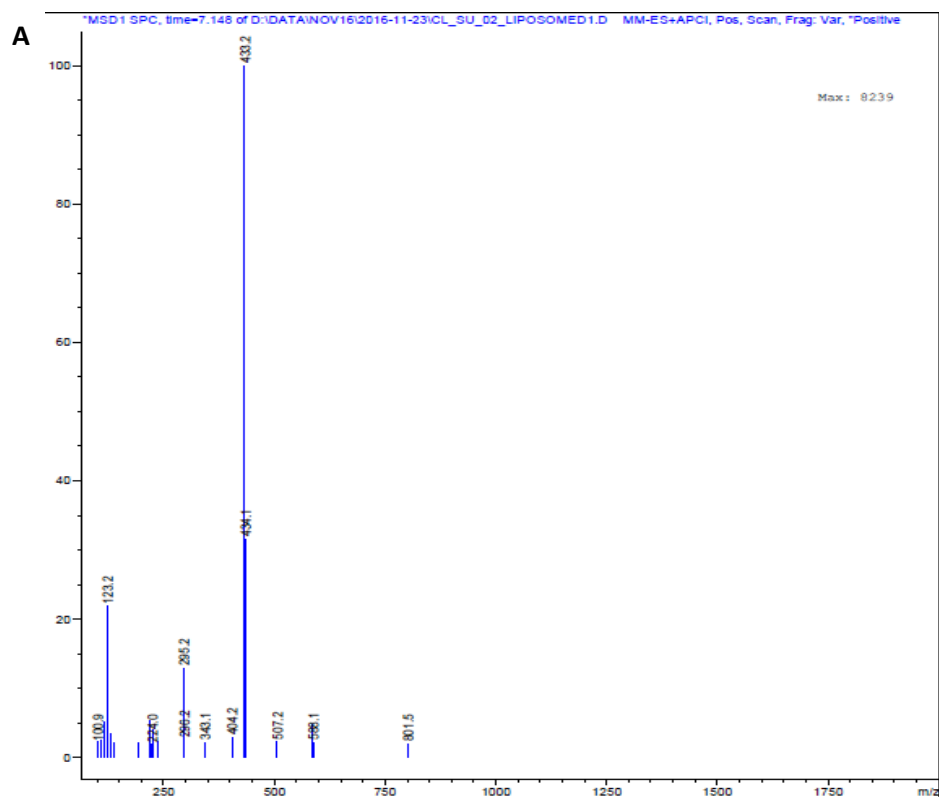


**Figure 6.7.** Identification of the SU1349 drug using mass spectroscopy ran at positive (A) and negative (B) parameters. The peaks are representative of one SU1349 loaded liposomal sample.

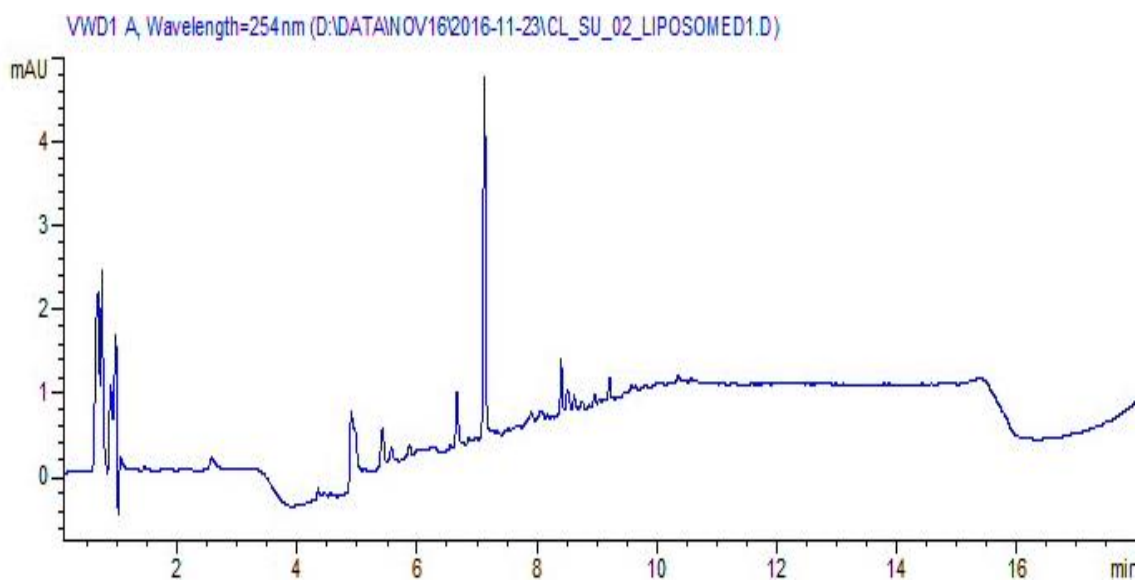


**Figure 6.8.** Quantifying the amount of SU1349 using liquid chromatography, with the chromatograph scan of the SU1349 drug loaded into the liposomes.

**Table 6.7.** The quantification of loading amount and ratio of SU1349 by DMPC:Chol liposomes produced by microfluidics.

SAMPLE	AMOUNT OF SU1349 DRUG ( $\mu\text{G}/\text{ML}$ )	DRUG LOADING (%)	DRUG TO LIPID LOADING (%)
BEFORE MICROFLUIDICS	50	100	-
POST MICROFLUIDICS PRODUCTION	16	32	1.03
POST PURIFICATION (BY DIALYSIS)	14	28	0.90

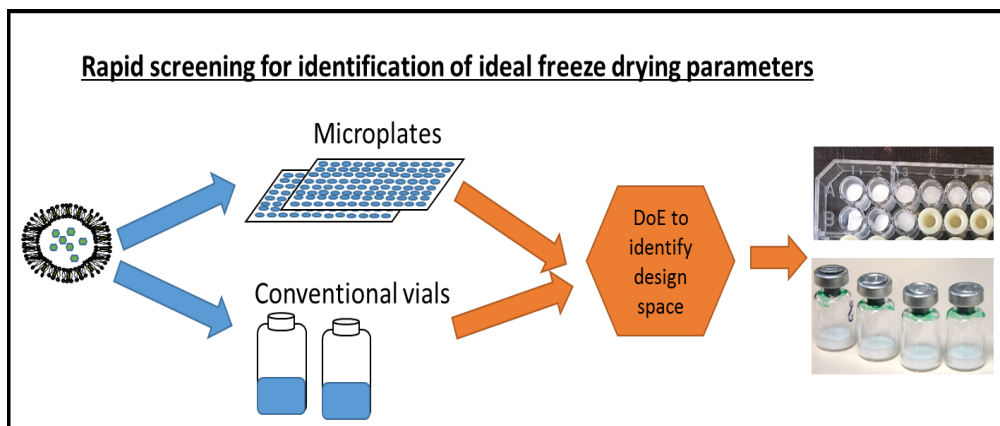
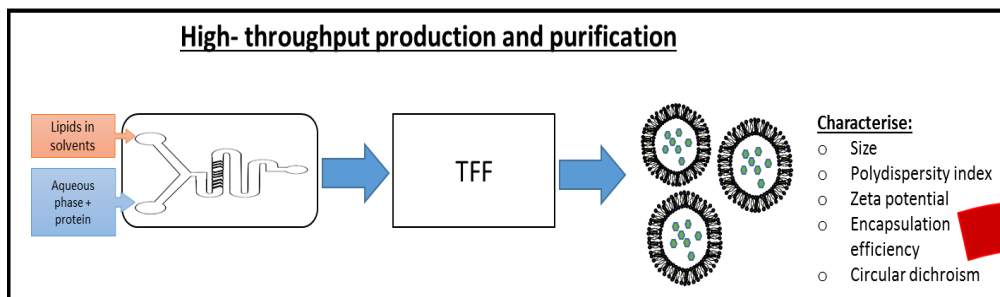
## 6.5 Conclusion

In this chapter, the loading of small molecular weight drugs with low solubility incorporated into liposomal formulations was investigated. The liposome manufacturing technique of thin film lipid hydration was compared alongside the production of liposomal formulations by microfluidics. The small molecular weight drug, propofol was used as a model drug to investigate loading. Results show both manufacturing techniques are able to produce drug loaded liposomal formulations around 100 nm or less (for microfluidics production). However, thin film lipid hydration resulted in heterogeneous liposomal formulations and a lower loading of less than 5 % compared to around 48 % achieved by microfluidics. Taking these results into consideration, the use of microfluidics to encapsulate the highly insoluble SU1349 drug was investigated. After process optimisation, particles around 100 nm in size were measured implying clinical relevancy, but it is unclear whether the particles are actually liposomes and further optimisation is required. However, due to the poor loading of the formulations due to the highly insoluble drug this was not investigated further.

Overall, the results from this chapter highlight the ability to fine-tune the formulation parameters to produce liposomal formulations within specification. The highly sensitive nature of the microfluidics technique to formulation changes illustrates the versatility of this microfluidics process. The quick and efficient manufacturing of microfluidics is ideal for the manufacture of novel liposomal formulations from bench to production.

# Chapter 7

## Strategies for the high throughput production of liposomes in a freeze-dried format.



## 7.1 Introduction

### 7.1.1 Stability of liposomes

Colloidal systems, such as liposomes, are increasingly used in pharmaceuticals due to their versatility. The amphiphilic nature enables the encapsulation of proteins and drugs, making them ideal delivery vehicles (Fenske and Cullis, 2008, Torchilin, 2005). Liposomes are complex multi-component systems, thus studying the stability of the formulations is equally as important as their applications. In particular, emphasis should be placed on ensuring lipids and the protein are chemically stable (Zuidam *et al.*, 1995), the protein remains encapsulated and, the desired therapeutic effect is not compromised due to changes in the physicochemical properties (Grit and Crommelin, 1993). The storage of formulations in an aqueous environment for long periods of time can develop instabilities that can be classified into two categories; chemical and physical degradation (Table 7.1). Formulations to be used as therapeutics are required to have a long shelf-life, although the time can vary as illustrated by Table 7.2. Furthermore, whilst many liposome products exist on the market in liquid form (**Error! Reference source not found.**), maintaining a cold chain for exporting worldwide is incredibly expensive. Alternative preservation and storage methods (discussed in section 7.1.2) can be used.

**Table 7.1.** Degradation mechanisms accounting for the reduced stability of liposome formulations.

CHEMICAL DEGRADATION	PHYSICAL DEGRADATION
Oxidation of lipids (by the free radical mechanism); unsaturated phospholipids are more prone to this due to the presence of double bonds (Grit and Crommelin, 1993, Mohammed <i>et al.</i> , 2006).	Aggregation and fusion of liposomes; particularly for neutral liposomes (Crommelin <i>et al.</i> , 1994, Nagase <i>et al.</i> , 1997).
Hydrolysis of lipids; caused by the hydrolysis of the ester bond at either the 1 or 2-acyl position. The process is pH driven and can occur in acidic and basic environments. Hydrolysis can lead to the formation of free fatty acids, lysophospholipids and phosphoglycerol compounds (Zuidam <i>et al.</i> , 1995).	Drug leakage (Asayama <i>et al.</i> , 1992).
	Changes to size distribution (Ingvarsson <i>et al.</i> , 2011).

**Table 7.2.** Liposome products currently on the market.

FORM	PRODUCT NAME	DRUG	LIPID COMPOSITION	STORAGE TIME (MONTHS)	REF
Powder	Ambisome	Amphotericin B	HSPC, DSPG, cholesterol	36	(Immordino <i>et al.</i> , 2006, Meunier <i>et al.</i> , 1991, Chang and Yeh, 2012)
	Myocet	Doxorubicin	PC, cholesterol	18	(Immordino <i>et al.</i> , 2006, Park, 2002, Gardikis <i>et al.</i> , 2010)
	Visudyne	Verteporfin	Egg PG, DMPC, ascorbyl palmitate	48	(Chowdhary <i>et al.</i> , 2003, Fahr <i>et al.</i> , 2005)
Suspension	Abelcet	Amphotericin B	DMPC, DMPG	24	(Immordino <i>et al.</i> , 2006, Meunier <i>et al.</i> , 1991, Chang and Yeh, 2012)
	Doxil/ Lipo-Dox	Doxorubicin	HSPC, cholesterol, PEG-2000-DSPE	20/ 36	(Immordino <i>et al.</i> , 2006, Park, 2002, Hoarau <i>et al.</i> , 2004)
	DepoCyt	Cytarabine	DOPC, DPPG, cholesterol, triolein	18	(Immordino <i>et al.</i> , 2006, Chang and Yeh, 2012)
	Epaxal	Inactivated hepatitis A virus	Lecithin, cephalin	36	(Usonis <i>et al.</i> , 2003, D'Acremont <i>et al.</i> , 2006)
	DaunoXome	Daunorubicin	DSPC, cholesterol	12	(Immordino <i>et al.</i> , 2006, Rivera, 2003, Tomkinson <i>et al.</i> , 2003)

### 7.1.2 Approaches for improving the storage stability of liposomes

There are a range of methods by which long term stability and longevity of liposomes can be improved, including freeze drying (FD), spray drying and spray-freeze drying. Freeze drying (otherwise known as lyophilisation) involves three stages; freezing, primary drying and secondary drying. The freezing phase is the point at which samples are cooled, with water separating from the liposomes and cryoprotectant, forming ice crystals and the non-volatile components are immobilised (Bedu-Addo, 2004). The main purpose of the primary drying phase is for the water present in the sample to undergo sublimation (transition from a solid to a gaseous state) under low pressure and elevated temperature. The secondary drying phase is important for the removal of any residual moisture which is important in improving the overall stability of the formulations (Bedu-Addo, 2004).

Alternatively, spray drying is another technique that can be utilised to stabilise and store liposome formulations for long periods of time by removing moisture. The process is multi-staged, requiring atomization and dehydration before the powder can be collected. This technique involves spraying the liposomes through a specific sized nozzle into a hot dry chamber. As the droplets pass through the nozzle, coming into contact with the heat, the moisture is removed (dehydration occurs) to form a powder (Masters, 2002, Maltesen and van de Weert, 2008, Grasmeyer, 2015). Similarly, freeze-spray drying is another technique which combines principles from both freeze-drying and spray-drying to form stable liposome powders (Mensink *et al.*, 2017). The atomised droplets are passed through a pre-cooled chamber (such as liquid nitrogen) rather than a hot chamber. The frozen droplets are then dispensed into vials, which are then freeze dried. Although all three techniques improve stability, there are advantages and disadvantages to all three techniques (Table 7.3), FD is the most commonly used (Ingvarsson *et al.*, 2011, Mensink *et al.*, 2017).



**Table 7.3.** Comparison of the three drying technologies available for the stabilisation of liposomes in a dry state.

	ADVANTAGES	DISADVANTAGES	REF
<b>FREEZE-DRYING</b>	<ul style="list-style-type: none"> <li>Improves storage stability of liposomes</li> </ul>	<ul style="list-style-type: none"> <li>Disruption of liposome structure due to stress</li> <li>Expensive process</li> <li>Time and energy consuming</li> </ul>	(Tang and Pikal, 2004, Chen <i>et al.</i> , 2010)
<b>SPRAY DRYING</b>	<ul style="list-style-type: none"> <li>Relatively cheap</li> <li>Quick process</li> </ul>	<ul style="list-style-type: none"> <li>Formulations exposed to excess heat</li> <li>High shear forces</li> <li>The process is not well studied with regards to liposomes</li> </ul>	(Patel <i>et al.</i> , 2009, Skalko-Basnet <i>et al.</i> , 2000, Kim, 2001)
<b>FREEZE-SPRAY DRYING</b>	<ul style="list-style-type: none"> <li>Avoids adverse effect caused by heat</li> </ul>	<ul style="list-style-type: none"> <li>Relatively little information is available</li> <li>Expose liposomes to shear stress</li> </ul>	(Sweeney <i>et al.</i> , 2005, Bi <i>et al.</i> , 2008)

Furthermore, the addition of stabilizers during freeze drying is used to protect samples from freezing and drying stresses induced during the freeze drying cycle. Cryoprotectants are often added to protect against freeze-induced damage, whilst lyoprotectants protect against damage caused by dehydration. The most popular excipients used for the freeze drying of liposomes are sugars (including sucrose, trehalose, glucose, lactose and mannitol) (Carpenter *et al.*, 1992, Lombrana *et al.*, 2001). For successful preservation of liposomes, the sugars chosen must undergo primary drying at a temperature below the collapse temperature, and the glass transition temperature of the sugar. The glass transition temperature for sugars differ depending on the type and concentration of sugar used. For instance, sucrose used between 5- 15% has a measured glass transition temperatures of between -33.8°C to -32.4°C in comparison to trehalose which has lower glass transition temperatures between -39.8°C to -38.5°C (Hua *et al.*, 2003). The disaccharide sugars trehalose and sucrose are well known to be effective cryoprotectants (Anchordoguy *et al.*, 1987), and so are routinely used for freeze drying samples. Despite the routine use of freeze drying, there are many theories as to how freeze-drying enables the preservation of fragile pharmaceutical products such as liposomes. The most common three theories are the water replacement theory (Golovina *et al.*, 2009, Mensink *et al.*, 2017), vitrification (Slade *et al.*, 1991) and kosmotropic effects (Mensink *et al.*, 2017) (Table 7.4).

**Table 7.4.** Theories of freeze drying.

THEORY	DESCRIPTION	DIAGRAM
Water replacement	<ul style="list-style-type: none"> <li>The most widely known and studied dehydration theory for freeze drying.</li> <li>Based on thermodynamic considerations.</li> <li>Cryoprotectants exert their effects by replacing the hydrogen bonds to the surrounding water molecules.</li> <li>The theory has been investigated by a multitude of techniques including Fourier transform infrared spectroscopy (FTIR), Langmuir studies, and differential scanning calorimetry (Golovina <i>et al.</i>, 2009, Chang and Pikal, 2009, Prestrelski <i>et al.</i>, 1993, Allison <i>et al.</i>, 1999).</li> </ul>	
Vitrification	<ul style="list-style-type: none"> <li>Stability is caused by changes in the reaction kinetics.</li> <li>Cryoprotectants surround each particle, essentially forming a mesh that separates one liposome from another. The liposomes are immobilized in an amorphous sugar matrix preventing aggregation and fusion.</li> <li>The sugars used to freeze dry liposomes have glass transition temperatures. Above this, the sugars lose their amorphous structure and fail to immobilise the product (Slade <i>et al.</i>, 1991, Chang <i>et al.</i>, 2005, Grasmeijer, 2015).</li> </ul>	
Kosmotropic effects	<ul style="list-style-type: none"> <li>The addition of some excipients to the formulation arranges the water from a disorderly state into a more orderly state.</li> <li>It also exerts its effects on proteins, adding to the stabilization of the liposomal formulations (Mensink <i>et al.</i>, 2017, Ingvarsson <i>et al.</i>, 2011).</li> </ul>	

## 7.2 Aim and Objectives

Given the limited knowledge supporting the freeze-drying of liposomes, the aim of the work in this chapter was to produce 1,2-dimyristoyl-sn-glycero-3-phosphocholine (DMPC) and 1,2-distearoyl-sn-glycero-3-phosphocholine (DSPC) liposomes with cholesterol (DMPC:Chol and DSPC:Chol liposomes), containing the protein OVA in a stable freeze-dried format. The objectives of this study were to:

- Consider the factors that influence freeze drying of liposomes.
- Develop methods to rapidly screen and identify suitable freeze dried formats.
- Identify the design space needed to produce stable freeze dried formulations

## 7.3 Materials and Methods

### 7.3.1 Materials

The lipids 1,2-dimyristoyl-sn-glycero-3-phosphocholine (DMPC) and 1,2-distearoyl-sn-glycero-3-phosphocholine (DSPC) were all obtained from Avanti Polar Lipids Inc., Alabaster, AL, US. Cholesterol, Ovalbumin (OVA), sucrose and trifluoroacetic acid was obtained from Sigma Aldrich Company Ltd., Poole, UK. For OVA purification by Tangential flow filtration (TFF), a modified polyethersulfone (mPES) 750 kD MWCO hollow fibre column was purchased from Spectrum Inc., Breda, The Netherlands. A Jupiter column (C18 (300 Å), 5 µm, dimensions 4.60 X 150 mm) was procured from Phenomenex, Macclesfield, UK. HPLC grade Methanol and 2-propanol were purchased from Fisher Scientific., Loughborough, England, UK. All water and solvents used were HPLC grade. The vials used to freeze dry liposomes were 2mL Fiolax clear glass 35mm x 16 mm diameter (Schott VCDIN2R) and, the accompanying lid closures (13mm halobutyl igloo closures) obtained from Adelphi healthcare packaging, (Haywards Heath, UK).

### 7.3.2 Methods

#### 7.3.2.1 Production and purification of Ovalbumin loaded liposomes using microfluidics

Lipids and cholesterol were dissolved in methanol at 4 mg/mL (2:1 W/W ratio) and injected through one of two inlets on the microfluidics herringbone micromixer chip. Ovalbumin (OVA) was solubilised in phosphate buffered saline (PBS) (10 mM, pH 7.3) at a concentration of 0.25 mg/mL and injected into the second inlet. Both empty and OVA loaded liposomes were produced at a 3:1 flow rate ratio (FRR) (the ratio between the organic and aqueous phase) and 15 mL/min total flow rate (TFR) (the speed that the two inlets are injected through the chip). The liposome formulations were purified by KrosFlo® Research 2i Tangential flow filtration system (TFF) (Spectrum labs, California, USA) as previously described. Briefly, the samples are flushed with phosphate buffered saline (PBS) (10 mM, pH= 7.3) at a speed of 27 mL/min to remove solvent and untrapped protein.

### **7.3.2.2 Dynamic light scattering**

Dynamic light scattering (DLS) was used to analyse the size of liposomes, (ideally between 25 - 1000 nm), with the Z-average and polydispersity index (PDI) given, using the Malvern Zetasizer Nano ZS (Malvern Instruments, Malvern, UK). Liposome sample was added to PBS and diluted to 1:300 to measure the size and PDI.

### **7.3.2.3 Quantification of encapsulated Ovalbumin**

The liposomal formulations were rehydrated with water, with the amount of OVA remaining quantified after the sample had been run through the TFF. Purification after rehydration was needed to ensure removal of all OVA which is no longer encapsulated. An Evaporative light scattering detector (ELSD) was used after high performance liquid chromatography (HPLC-ELSD) to quantify the amount of OVA encapsulated inside the liposomes. A Jupiter A100 column was used to detect the OVA protein. The flow rate used was 1 mL/ min, with a gain of 8 and an OVA peak appearing at 11.8 minutes. A standard calibration curve for OVA was established using various concentrations; the amount of encapsulated OVA in liposomes produced by microfluidics and sonication was calculated using the peak area of the sample in relation to the standards. The elution gradient is shown in Table 7.5.

**Table 7.5.** The HPLC gradient used to detect the OVA protein.

<b>TIME</b>	<b>SOLVENT A (0.1% TFA)</b>	<b>SOLVENT B (100% METHANOL)</b>
0	100	0
10	0	100
15	0	100
15.1	100	0
20	100	0

#### **7.3.2.4 Freeze- thawing of liposomes**

Liposomes composed of DMPC:Chol or DSPC:Chol (4 mg/mL) loaded with OVA (initial concentration of 0.25 mg/mL) were produced by microfluidics at a 3:1 FRR at a 15 mL/min TFR. The untrapped OVA and solvent were removed by TFF at a speed at 27 mL/min. Sucrose at 10% final (a 1:1 mix of 20% sucrose) was added to the liposome formulations at a 1:1 v/v ratio. The samples were then frozen at -20°C, -80°C and -80°C in the Thermo Scientific™ Mr. Frosty™ Freezing Container (TMF) (Thermo Scientific., Hamel Hampstead., England, UK). To assess the stability of the liposomes, the formulations were then thawed on three separate occasions with any changes in the liposomal characteristics measured by dynamic light scattering.

#### **7.3.2.5 Freeze dried microscopy**

The freeze dried microscope was used to determine the freeze, collapse and melt temperature of samples and cryoprotectants to optimize the freeze drying cycle. To do this, a Linkam FDCS 196 cryostage mounted on a BX51 Olympus optical microscope connected to a Linkam control unit (TMS 94, VC 94, LNP, Linkam Scientific Instruments Ltd, Tadworth, Surrey, UK) for visualisation was used. In these studies, 3 µL of sample (containing 7.5% sucrose to the liposome formulations at a 1:1 ratio (v/v)) onto a Quartz glass crucible with a coverslip then placed over the sample, enclosed by a thin metal shim. This was then fitted into the microscope and the sample temperature was adjusted using liquid nitrogen. The

samples were initially frozen at 10°C/ min until -50°C was reached (to determine the freezing point). The sample was then held for two minutes before drying was started by applying vacuum to a defined limit, then ramping the temperature to 20°C, to establish the collapse and melt of the samples. Images were taken every 20 seconds and were analysed using the 'Linksys' operating software.

#### **7.3.2.6 Modulated Differential scanning calorimetry (MDSC)**

Modulated differential scanning calorimetry was performed on the Q2000 DSC (TA Instruments, Elstree, Hertfordshire, UK). The unit was flushed with nitrogen gas and cooled using a RGA chiller unit (TA Instruments). Following loading sample and empty reference pan the unit was cooled to -90°C at 10°C/ min marking the end of cycle 1; the thermal changes were recorded from this point on. Cycle 2 consisted of holding the sample at isothermal conditions for eight minutes after which the sample was ramped up at 1.5°C/ min with modulation at 0.23°C/min until 25°C was reached.

Samples were prepared by pipetting 80 µL of sample containing 7.5% sucrose into a pre-weighed pan. The sample is sealed by placing an O- ring and lid on top of the pan and press sealing the pan so that the pan and lid are crimped together. The filled pan is weighed and the sample weight is calculated (difference between empty and filled pans), as this information is required by the MDSC software Thermal Advantage (TA Instruments). Post run the results can be analysed using the software with the graphs showing three data sets; heat flow, reversing heat flow and non-reversing heat flow. The reversing heat flow (blue line) was used to determine the glass transition values as it comes from the modulated analysis of the profile.

#### **7.3.2.7 Dynamic Mechanical Analysis (DMA)**

The dynamic mechanical analysis technique is used to detect rheological changes occurring in the sample as the temperature is changed and a stressing frequency between 1 and 100Hz is applied. The DMA Q8000 (TA Instruments) was connected to nitrogen gas and compressed air supplies. Prior to analysing a sample, the DMA machine had to be switched on so that a temperature of -70°C could be reached.

Sample preparation involved adding a final concentration of 7.5% sucrose to the liposome formulations to be analysed at a 1:1 ratio (v/v). The sample (100 µL) was loaded evenly onto a filter paper (ThermoFisher product number E1, 89 x 140 mm, Box/100) cut to size to fit the large steel sample holder. Once the product is added to the machine, the sample was held at that temperature for five minutes before the temperature was ramped to 5°C at 1°C/min, whilst 1 bar of gas pressure was applied and a stressing frequency applied and the strain in the sample measured. Successfully ran samples was analysed using the Universal Analysis software (TA Instruments).

#### **7.3.2.8 Freeze drying cycle**

The Telstar Lyobeta 15 (Telstar SPS, Terrassa, Spain) was used to freeze dry liposomes; three freeze dried cycles were tested (referred to as FDC1-3). The FDC1 cycle included pre-cooling the shelf to -45°C. The liposomes containing sucrose (at a 1:1 v/v ratio) were pipetted either into 2ml volume vials (total added volume of 500 µL) or 96-well microplates (200 µL per well) and then placed onto separate shelves. From the vials, two samples were selected to contain thermocouple probes inside so the temperature changes in the product could be monitored directly. The primary drying phase involved increasing the shelf temperature from -45°C to -30°C where it was held for 10 hours at 0.1 mBar vacuum. The second drying phase involved increasing the temperature to 20°C and holding the temperature for 5 hours. Excluding the pre-shelf freeze, the freeze dry cycle was 15 hours long, and a lyophilized cake was produced.

The FDC2 cycle (using a ramped freeze step FD cycle) was run for a total of 40 hours. The samples were frozen from 4°C to -45°C, over a 90 min period. Once the temperature had been achieved, the samples were held for 180 minutes at -45°C after which a vacuum of 0.1 mBar was applied. The primary drying involved ramping up the temperature to -30°C (the process taking 30 minutes); the temperature was maintained for a total of 22 hours. For the secondary drying phase, the temperature was increased from -30°C to 30°C then held for 6 hours under a vacuum of 0.1 mBar.

The FDC3 (snap freeze FD cycle) required snap freezing the samples before starting the cycle by dipping the samples in liquid nitrogen. The cycle involved a pre cooled shelf temperature of -45°C (which took 30 minutes to achieve) after which the samples were added and held for (90 minutes) before a pressure of 0.1mBar was applied. The first drying cycle involved

ramping the temperature up to -30°C (in 30 minutes at 0.1 mBar) after which it was held at this temperature for 10 hours. The secondary drying stage involved a temperature ramp from -30°C to 30°C then holding this temperature for 6 hours, whilst maintaining the pressure of 0.1 mBar.

At the end of the cycle both vials and microplates would be back-filled with dry nitrogen gas to atmospheric pressure and closures pushed into place (using 13mm diameter igloo-format bromobutyl closures, Adelphi Tubes, for the vials and 96-stopper LyoCapCluster mats, Micronics BV, Lelystad, Netherlands for the microplates).

### **7.3.2.9 Measuring moisture content using the automated Karl Fisher**

The coulometric Karl Fischer titration technique is used to calculate the moisture remaining in the sample after freeze drying. Iodine and sulphur dioxide react with water in a stoichiometric manner and the electrical current required to back titrate the iodide produced is measured and is proportional to the quantity of water present. Water can be quantified in the range of 10 µg to mg per sample. An automated robotic system (GX270 Gilson Robotic sampler) was connected to a coulometer and cell (CA200 Mitsubishi coulometer and cell) in a combined system from A1-Envirosciences, (Blyth, UK). Freeze dried samples were transferred into glass autosampler vials (ThermoFisher, Loughborough, UK) under an inert low moisture environment using a CaptAir pyramid Glove bag (Cole Parmer, London, UK) then placed in the autosampler alongside empty vial blanks to account for any moisture associated with the vial. The method comprised automated addition of 3 mL of anolyte reagent to each of the samples followed by robotic shaking for 15 minutes, after which 1 mL of the supernatant is removed and injected into the coulometer and the moisture content titrated.

### **7.3.2.10 Design of Experiments**

The statistical software package, MODDE11 (Umetrics, Sartorius-stedim Biotech, Sweden) was used to plan and implement the design of experiments looking at the ideal parameters (liposomes concentration, sucrose concentration and encapsulation of OVA) needed to successfully freeze dry liposomes. A full 2<sup>3</sup> factorial study was conducted at a 95% confidence



interval. The outputs of the experiments took into consideration changes in size, PDI and encapsulation efficiency when predicting the best freeze drying parameters.

## **7.4 Results and Discussion**

The main purpose of freeze drying (FD) liposomal formulations is to preserve physicochemical properties and ensure functionality upon storage. There are a number of factors that can influence the stability of the liposome formulations including lipid, protein and cryoprotectant concentrations. The quickest method to test the impact of these factors and to establish a design space for the freeze drying process is to carry out design of experiments (DoE) studies. A full factorial design experiment was set up; with eleven variants of each formulation (DMPC:Chol + OVA) and (DSPC:Chol + OVA) tested. After FD, these results were fed back into the DoE software to predict favourable outcomes and define the design space (section 7.4.5). As well as this, high throughput screening of formulations parameters is important so that the optimal conditions can be determined quickly. To achieve this, the use of 96 well plates to effectively FD liposomal formulations was investigated.

### **7.4.1 Characterization of liposomes before freeze drying**

The liposome formulations need to be characterised prior to testing FD conditions. The results shown in Table 7.6 and Table 7.7 illustrate the liposomal characteristics for DMPC:Chol and DSPC:Chol produced with and without OVA. All liposomes produced by microfluidics (and purified by TFF) are below 100 nm in size, with a low PDI (<0.25) and high encapsulation efficiency (35-50%) achieved (Table 7.6 and Table 7.7). The liposomes formulations made with an initial concentration of 7 mg/mL of lipid and 0.125 mg/mL of OVA, were used as centre point controls for the DoE studies.

As reported previously, using microfluidics in combination with TFF produced liposomes in the range expected. The quality of the liposomes produced was the same as that mentioned in previous chapters. Similar to previously reported research, whereby microfluidics was used to manufacture and encapsulate low solubility drugs (Dimov et al., 2017) and DNA (Kastner

et al., 2014) at high encapsulation efficiency, the high encapsulation efficiency of ovalbumin (OVA) protein is as demonstrated in Table 7.6 and Table 7.7. Reproducibility is highly important, especially for delivering manufacturability. The liposome physicochemical properties (Table 7.6 and Table 7.7) match previous chapters, illustrating the reproducibility of the microfluidics system, whereby liposomes within a specific range are consistently produced. Whilst the production of high quality liposomes is necessary, suitable preservation techniques post production are also required. This must be done without compromising liposome integrity, and so freeze drying of liposome formulations was investigated.

**Table 7.6.** The physicochemical properties of DMPC:Chol liposomes produced with and without ovalbumin.

FORMULATIONS	LIPID CONCENTRATION (mg/mL)	OVALBUMIN (mg/mL)	SIZE (d. nm)	POLYDISPERSITY INDEX	ZETA POTENTIAL (MV)	ENCAPSULATION EFFICIENCY (%)	AMOUNT ENTRAPPED ( $\mu$ G/ ML)
1	4	0	79 $\pm$ 0.5	0.12 $\pm$ 0.08	-5 $\pm$ 1.0	-	-
2	10	0	79 $\pm$ 0.5	0.09 $\pm$ 0.017	-2 $\pm$ 0.6	-	-
3	4	0.25	96 $\pm$ 1.2	0.21 $\pm$ 0.005	-2 $\pm$ 0.7	37	70
4	10	0.25	88 $\pm$ 0.2	0.22 $\pm$ 0.012	-2 $\pm$ 0.3	39	74
5	7	0.125	91 $\pm$ 0.1	0.25 $\pm$ 0.005	-1 $\pm$ 1.4	49	46

**Table 7.7.** The physicochemical properties of DSPC:Chol liposomes produced with and without ovalbumin.

FORMULATIONS	LIPID CONCENTRATION (mg/mL)	OVALBUMIN (mg/mL)	SIZE (d. nm)	POLYDISPERSITY INDEX	ZETA POTENTIAL (MV)	ENCAPSULATION EFFICIENCY (%)	AMOUNT ENTRAPPED ( $\mu$ G/ ML)
6	4	0	46 $\pm$ 0.1	0.15 $\pm$ 0.005	-2 $\pm$ 1.2	-	-
7	10	0	56 $\pm$ 3.0	0.21 $\pm$ 0.005	-1 $\pm$ 0.4	-	-
8	4	0.25	65 $\pm$ 3.7	0.27 $\pm$ 0.050	-2 $\pm$ 0.2	34	65
9	10	0.25	88 $\pm$ 0.2	0.23 $\pm$ 0.010	-4 $\pm$ 1.5	36	68
10	7	0.125	57 $\pm$ 4.0	0.22 $\pm$ 0.007	-2 $\pm$ 1.3	48	45

## 7.4.2 Analytical experiments to develop the freeze drying cycle

The cycle parameters used to FD liposome formulations are key to delivering good cakes and stable products. Tailor-made FD cycles (FDC) are used in the pharmaceutical industry to deliver consistent commercial products. To optimize the FD design, several preliminary analysis tools can be used to aid with designing the FD cycle. For instance, freeze drying microscopy (FDM) and modulated differential scanning calorimetry (MDSC) have traditionally been used to determine the critical temperatures to define parameters of the FD cycle, with DMA also being used in recent years (Gearing *et al.*, 2010). To design the best FD cycle (FDC) for the liposomes, previous research was used alongside the information obtained from the three aforementioned analytical techniques.

### 7.4.2.1 Freeze-thaw

The freezing stage of the FDC is essential for effective preservation of the samples. The freezing stage is important as it converts most of the water into ice; the ice crystals formed can be large or small and affect stability of the liposomes, potentially causing increases in liposome size due to aggregation as the liposomes concentrate. To investigate this, freeze-thaw experiments were conducted as a means to test this at  $-20^{\circ}\text{C}$ ,  $-80^{\circ}\text{C}$ , and using a ramped  $-80^{\circ}\text{C}$  controlled rate freezing at  $1^{\circ}\text{C}/\text{min}$  using a Thermo Scientific™ Mr. Frosty™ Freezing Container (TMF).

Overall, the results in Figure 7.1 show that freezing with cryoprotectant is necessary as without it the liposome size increases. For example, DMPC:Chol formulations frozen without cryoprotectant increased from  $88 \pm 4$  nm before freeze-thaw (FT) to  $369 \pm 58$  nm using the TMF (Figure 7.1). Similarly, DSPC:Chol formulations frozen without cryoprotectant using TMF increased from  $53 \pm 2$  nm to  $404 \pm 25$  nm (Figure 7.1). Furthermore, as the freezing temperature decrease from  $-20^{\circ}\text{C}$  to  $-80^{\circ}\text{C}$  the change in size becomes more prominent. This is shown for both DMPC:Chol and DSPC:Chol formulations, with a notable increase in size for DMPC:Chol formulations frozen at  $-20^{\circ}\text{C}$  ( $115 \pm 3$  nm) compared to a  $347 \pm 27$  nm and  $369 \pm 58$  nm increase in size at  $-80^{\circ}\text{C}$  and at TMF respectively (Figure 7.1). The increase in size (without cryoprotectant) for both formulations, is significantly larger for samples frozen using the TMF compared to snap freezing at  $-80^{\circ}\text{C}$  ( $p < 0.01$  for both DMPC:Chol and

DSPC:Chol formulations) (Figure 7.1A and B). The addition of cryoprotectant sucrose limits the increase in size; DMPC:Chol liposomes increase in size from  $88 \pm 4$  nm to  $92 \pm 3$  nm after freezing at  $-20^{\circ}\text{C}$ . The same is observed for DSPC:Chol liposomes, with the size increasing from  $112 \pm 2$  nm from  $53 \pm 2$  nm.

These results demonstrate that a slower rate of freezing (occurring when liposomes are frozen at  $-20^{\circ}\text{C}$ ) causes a smaller increase in vesicle size and PDI, with vesicle sizes similar to liposomes prior to the freeze-thaw cycle (Figure 7.1). Using the TMF to control the rate of freezing till  $-80^{\circ}\text{C}$  did not help. Due to the nature of the liposome formulations, which are in a liquid suspension and the liposomes consisting of an aqueous core, the formulations are extremely sensitive to the freezing process. Comparing the two formulations, the DMPC:Chol formulations appear more stable than the DSPC:Chol formulations. Freezing at  $-20^{\circ}\text{C}$  causes the DSPC:Chol size to double whilst the DMPC:Chol size does not change significantly. The influence of the freezing technique and bilayer composition has been investigated, with respect to carboxyfluorescein loaded liposomes (van Winden *et al.*, 1997, Fransen *et al.*, 1986). Research by van Winden and colleagues, found the freezing parameters play an important role in freeze drying liposomes. A slow freezing rate of  $0.5^{\circ}\text{C}/\text{min}$  for liposomes enables a maximum of 80% retention of carboxyfluorescein (for DPPC liposomes), in comparison to 40% retention achieved after quick freezing liposomes in liquid nitrogen. Despite this, the liposomes underwent changes in their physicochemical properties post FD. Rehydration of FD samples resulted in an increase in size, which is not ideal when trying to produce liposomes for pharmaceuticals. Given liposome integrity is influenced by freezing temperature; freezing at  $-80^{\circ}\text{C}$  causes an exponential increase in liposomes size attributed to aggregation and fusion of liposomes. The increase in osmotic pressure due to ice formation, is responsible for the damage to the bilayer. As mentioned earlier, the rate of freezing influences the size of ice crystals. Rapid freezing forms smaller ice crystals, which in turn have a greater influence on the bilayer; damaging and resulting in aggregation. Cryoprotectants combat this to some extent, therefore taking the freeze-thaw results into consideration the freeze temperature used to freeze the liposomes should be above  $-80^{\circ}\text{C}$ .

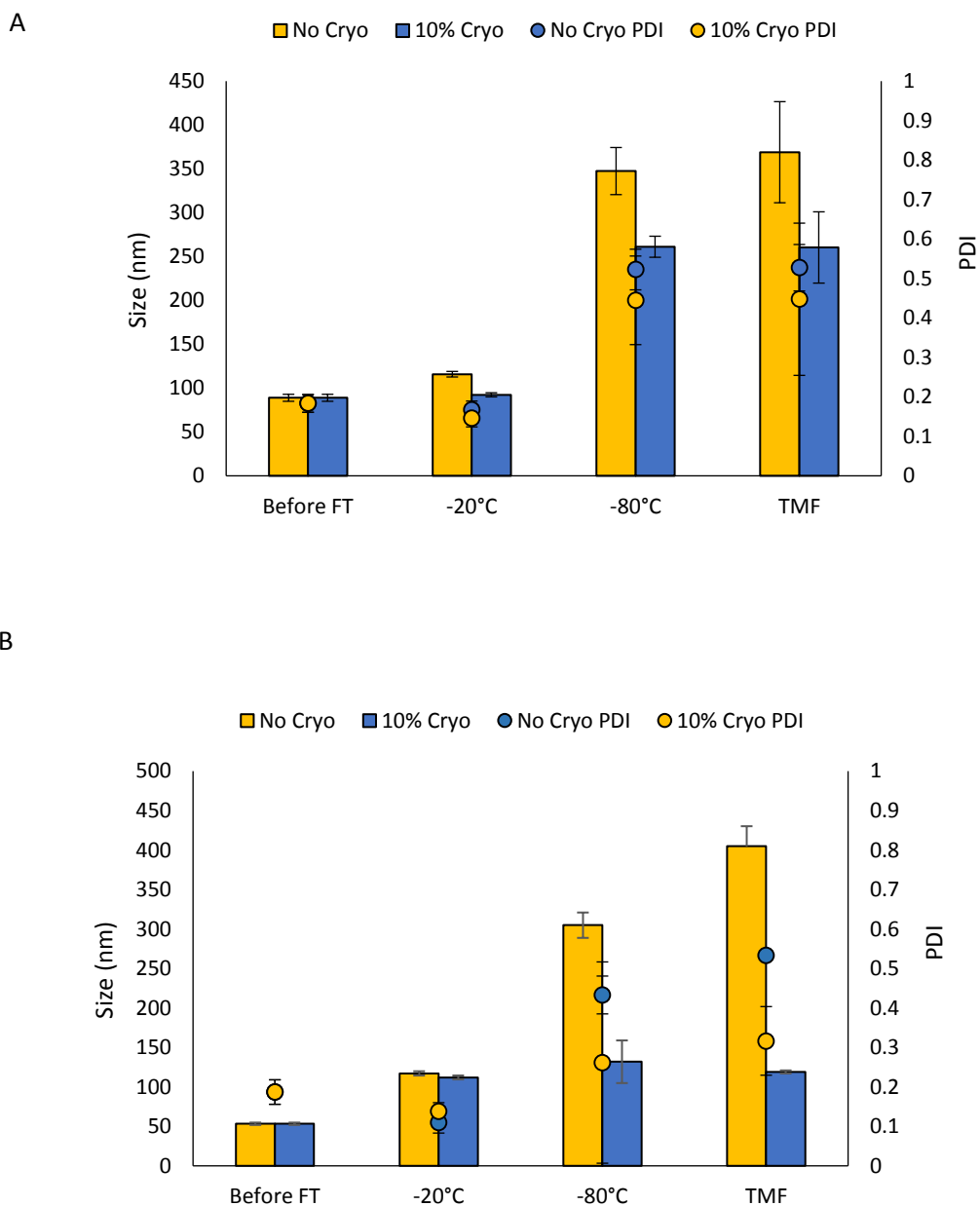


**Figure 7.1.** The effect of freezing and thawing on the size and PDI of ovalbumin loaded DMPC:Chol (A) and DSPC:Chol (B) liposomes. The physicochemical properties were measured after the samples were frozen at varying temperatures. Results represent three independent batches,  $\pm$  SD.

#### 7.4.2.2 Freeze drying microscopy

Freeze dried microscopy (FDM) is a technique used to predict the conditions for the FD cycle with respect to both the formulation and cryoprotectant. This technique allows an estimate of the freezing and collapse temperature of the formulations to be obtained. Physical changes to the sample can be observed in real time with all three formulations undergoing

FD. The temperature is ramped during FD until collapse occurs. The freezing temperature for the three liposomal formulations; DMPC:Chol, OVA loaded DMPC:Chol and OVA loaded DSPC:Chol are within a tight range between -23 and -19°C (Table 7.8). The collapse point for all three formulations is also between -39 and, -33°C, and changes in morphology of the liposome- cryoprotectant mixture can be observed (Figure 7.2, Figure 7.3 and Figure 7.4). The collapse temperatures identified is then used as a guide for the FD cycle; the collapse temperature is the temperature at which freezing must occur to ensure maximum solidification of the material. The temperature during primary drying must not exceed the collapse temperatures identified to prevent collapse of the liposome formulations.

Similar collapse temperatures are observed irrespective of the lipid used, the concentration or the presence of the protein OVA suggesting the cryoprotectant sucrose is dominating the FD process. The collapse values obtained are comparable to the collapse temperature of sucrose of -31°C shown by previous research (Crowe *et al.*, 1986a). The data suggests the ratio of carbohydrate to lipid is more important to the FD process than the concentration of lipid and protein present; the high amount of cryoprotectant is key in preventing leaking and aggregation (Crowe *et al.*, 1986a). The sucrose acts by forming hydrogen bonds with the lipid-phosphate head groups region of the liposomes, resulting in a mesh in which the liposomes are in. The mesh protects liposomes from mechanical damage, from ice crystals causing rupture of the lipid bilayer, as well as preventing leakage (Crowe *et al.*, 1997). From the FDM results, it is possible to infer the 7.5 % of sucrose used is sufficient for the FD of liposomes. The collapse temperature of the matrix determined by FDM was considered alongside the data from the MDSC and dynamic mechanical analysis (DMA), to develop a FD cycle for liposome formulations. It is important that the primary drying of the liposome-cryoprotectant mix is performed at a product temperature below the collapse temperature to ensure optimal FD conditions, whereby the liposomes are embedded into the cyroprotectant matrix.

**Table 7.8.** Determining the freezing and collapse temperatures of liposome formulations using freeze dried microscopy.

<b>FORMULATION</b>	<b>CONCENTRATION (MG/ML)</b>	<b>OVALBUMIN</b>	<b>FREEZING POINT (°C)</b>	<b>COLLAPSE (°C)</b>
<b>DSPC:CHOL</b>	4	Yes	-23	-34
<b>DMPC:CHOL</b>	10	No	-19	-33
<b>DMPC:CHOL</b>	10	Yes	-19	-39



**Freezing Phase:**

Freeze liposomes at 10°C/  
min till -50°C.

**Freezing Point:**

Liposomes froze at -18.6°C  
indicated by the colour change.

**Drying Phase:**

Ramp the temperature back to  
20°C and monitor the drying front

**Full Collapse:**

Full collapse of liposomes occurs

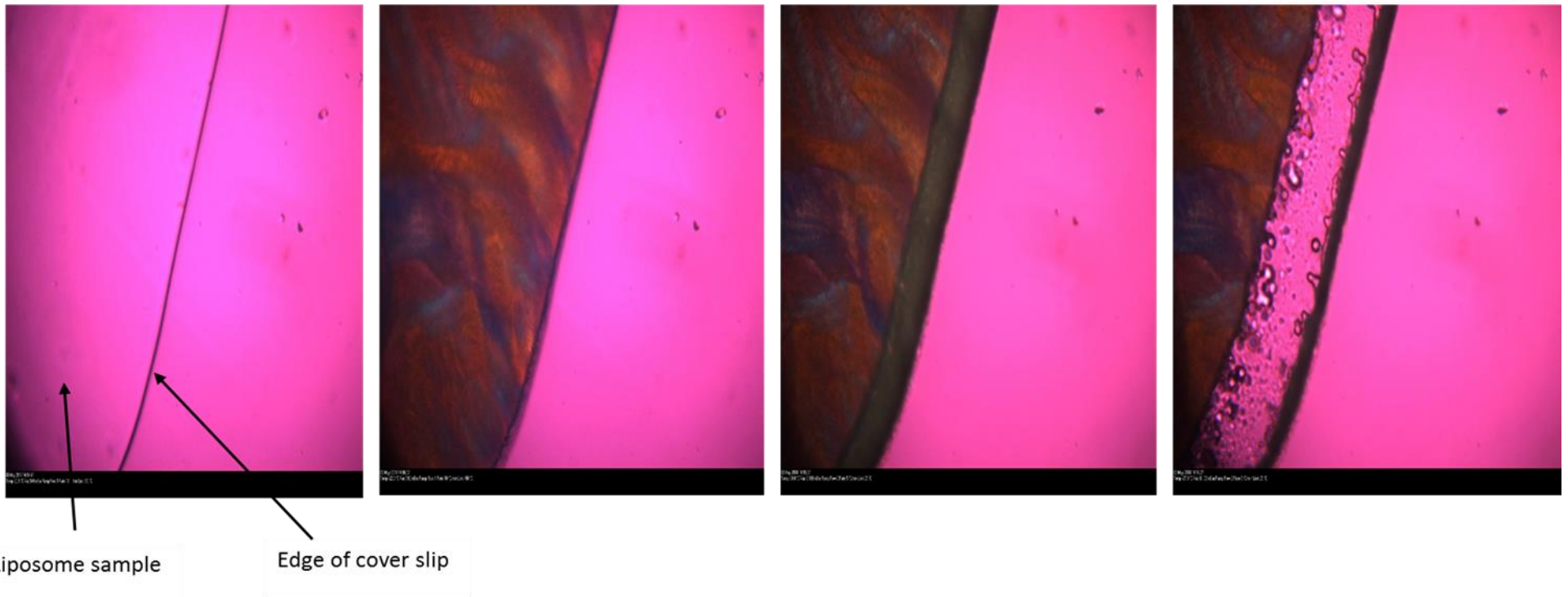


**Figure 7.2.** Freeze dried microscopy of DSPC:Chol (4 mg/ml initial) with an initial concentration of 0.25 mg/mL OVA entrapped inside. The formulation was added at a 1:1 v/v ratio to sucrose, producing a final concentration of 7.5% sucrose in the formulation.

**Freezing Phase:**

Freeze liposomes at 10°C/  
min till -50°C.

**Freezing Point:**

Liposomes froze at -18.6°C  
indicated by the colour change.

**Drying Phase:**

Ramp the temperature back to  
20°C and monitor the drying  
front

**Full Collapse:**

Full collapse of liposomes occurs

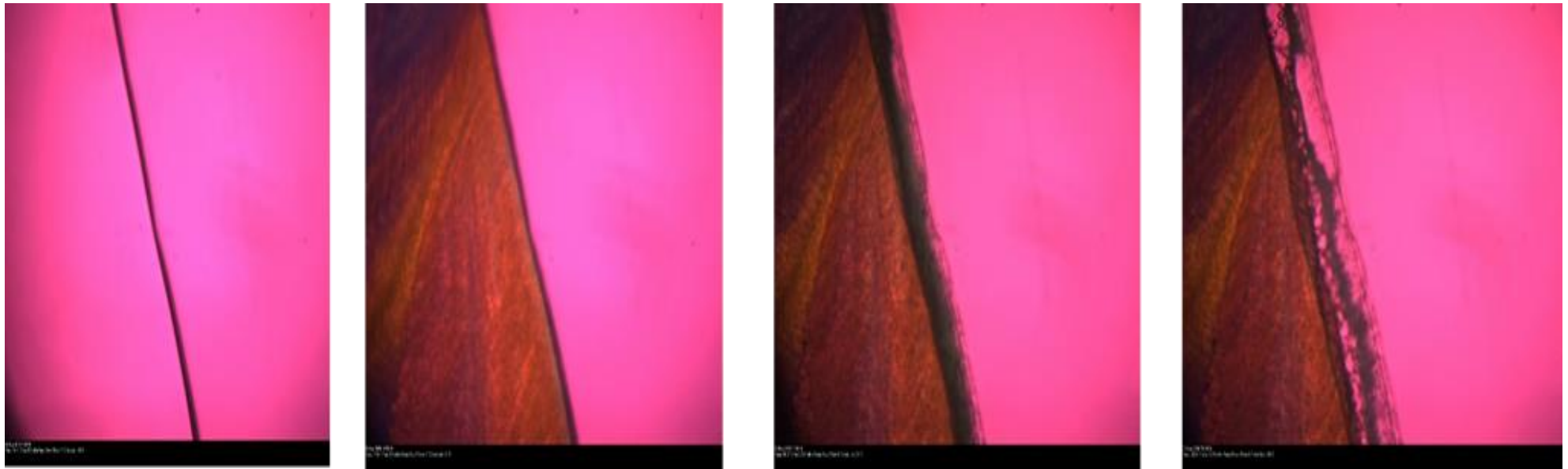


**Figure 7.3.** Freeze dried microscopy of empty DMPC:Chol (10 mg/mL initial). The formulation was added at a 1:1 v/v ratio to sucrose, producing a final concentration of 7.5% sucrose in the formulation.

**Freezing Phase:**

Freeze liposomes at 10°C/  
min till -50°C.

**Freezing Point:**

Liposomes froze at -18.6°C  
indicated by the colour change.

**Drying Phase:**

Ramp the temperature back to  
20°C and monitor the drying front

**Full Collapse:**

Full collapse of liposomes occurs

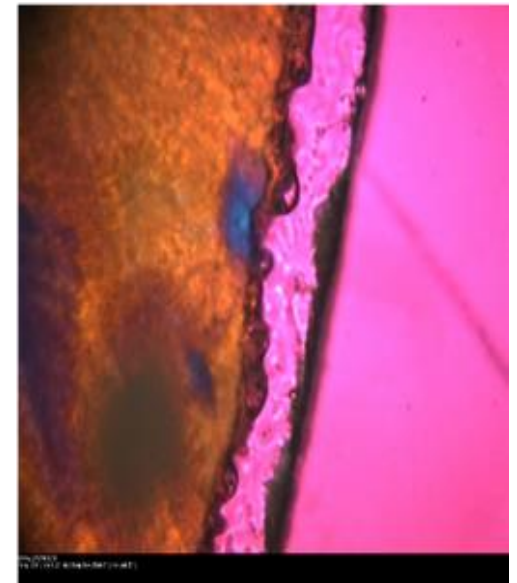
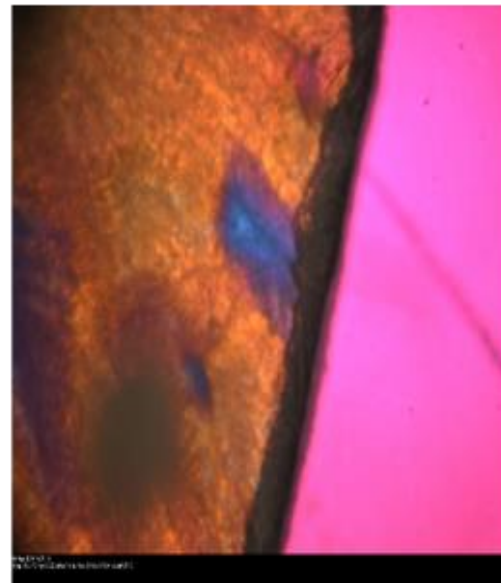


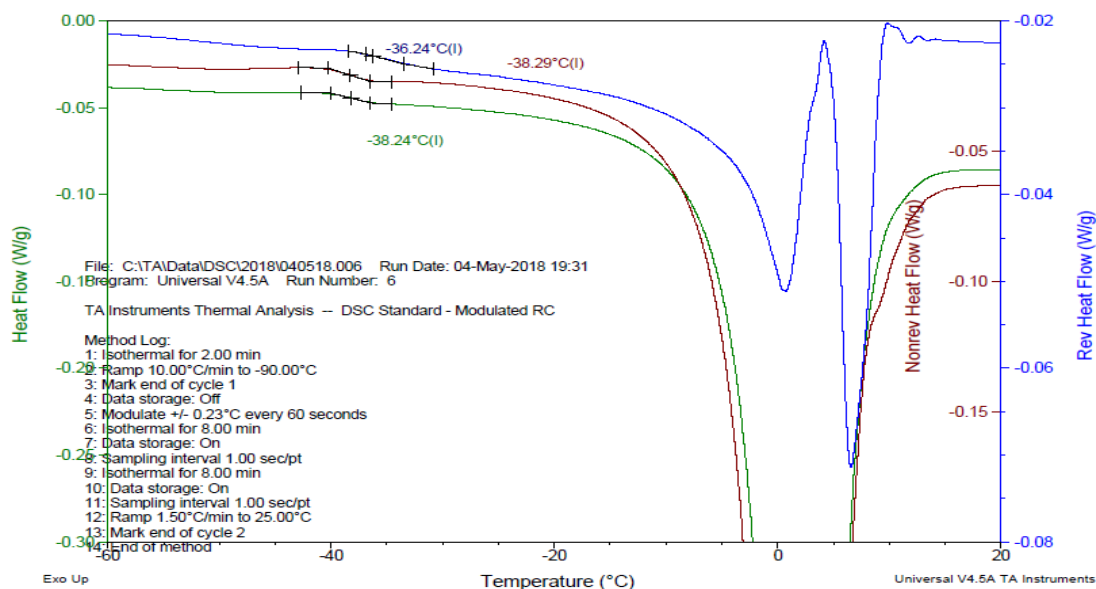
**Figure 7.4.** Freeze dried microscopy of DMPC:Chol (10 mg/mL initial) with an initial concentration of 0.25 mg/mL OVA entrapped inside. The formulation was added at a 1:1 v/v ratio to sucrose, producing a final concentration of 7.5% sucrose in the formulations.

### 7.4.2.3 Modulated Differential scanning calorimetry

To determine ideal FD conditions, it is important the glass transition temperature ( $T_g'$ ) in the frozen state is identified; this indicates when the sample becomes significantly more mobile as the amorphous state softens. The  $T_g'$  established for the sample should not be exceeded, (during primary drying) in order to produce an elegant cake and avoid collapse of the powder. Like FDM, modulated differential scanning calorimetry (MDSC) is a popular technique to determine ideal freeze drying parameters. MDSC is used to detect the thermal changes a product experiences when cooled and heated over a range of temperatures. For this experiment, three formulation-cryoprotectant mixtures were run in the MDSC to determine the  $T_g'$  values; empty DSPC:Chol (4 mg/mL), empty DMPC:Chol (10 mg/mL), and OVA loaded DMPC:Chol (10 mg/mL). As shown from Figure 7.5, there are three value sets obtained for each sample run. The reversing heat flow (blue curve in Figure 7.5) is quoted as the  $T_g'$ , as this value is taken from the modulated analysis of the profile. The  $T_g'$  value of all three formulations (empty DSPC:Chol, empty and OVA loaded DMPC:Chol) are the same irrespective of the lipids and the presence of the protein ovalbumin (Figure 7.5). The  $T_g'$  for cryoprotectant: OVA loaded DMPC:Chol liposome mixture is  $-36.2^\circ\text{C}$  (Figure 7.5A) and,  $36.2^\circ\text{C}$  for empty DMPC:Chol liposome mixture (Figure 7.5B). The concentration of the liposomes within the preparation also does not seem to make a difference, with DSPC:Chol formulations made with an initial lipid concentration of 4 mg/mL having a  $T_g'$  of  $-36.1^\circ\text{C}$  (Figure 7.5C). As seen with FD microscopy, the sucrose is dominating the  $T_g'$  of the formulation-cryoprotectant mixture to a large extent. The MDSC technique can be used to study the effect of cryoprotectant (in the liposomes mixture) as stabilizers. In the absence of cryoprotectants, a sharp increase in  $T_g'$  occurs as in the dehydration state the lipid head groups are in close proximity to one another. The closeness causes increased van der Waal's forces between the lipids resulting in increases  $T_g'$ , which can be mitigated with the use of cryoprotectants such as sucrose (Crowe et al., 1985, Ohtake et al., 2005). The cryoprotectant used can largely influence the MDSC results of liposome: cryoprotectant mixtures. Mixtures of soy PC:Chol liposomes with 10% trehalose have high  $T_g$  values of  $-30.7^\circ\text{C}$  compared to a  $T_g$  value of  $-38.7^\circ\text{C}$  in the presence of glucose (Hua et al., 2003). The MDSC thermograms also differ between the cryoprotectant used, the  $T_g'$  of glucose being around  $-41^\circ\text{C}$  and sucrose around  $-31^\circ\text{C}$ . From the results (**Error! Reference source not found.**A-C), all the thermograms are

imilar which is due to the presence of sucrose. In all three curves the  $T_g'$  is difficult to detect as it is a weak thermal event and the MDSC trace is dominated by the water melt peak at -20°C, therefore dynamic mechanical analysis (DMA), which is claimed to be more sensitive for determination of the  $T_g'$ , was also used to determine the  $T_g'$  of the liposome-cryoprotectant mixtures.

A



B

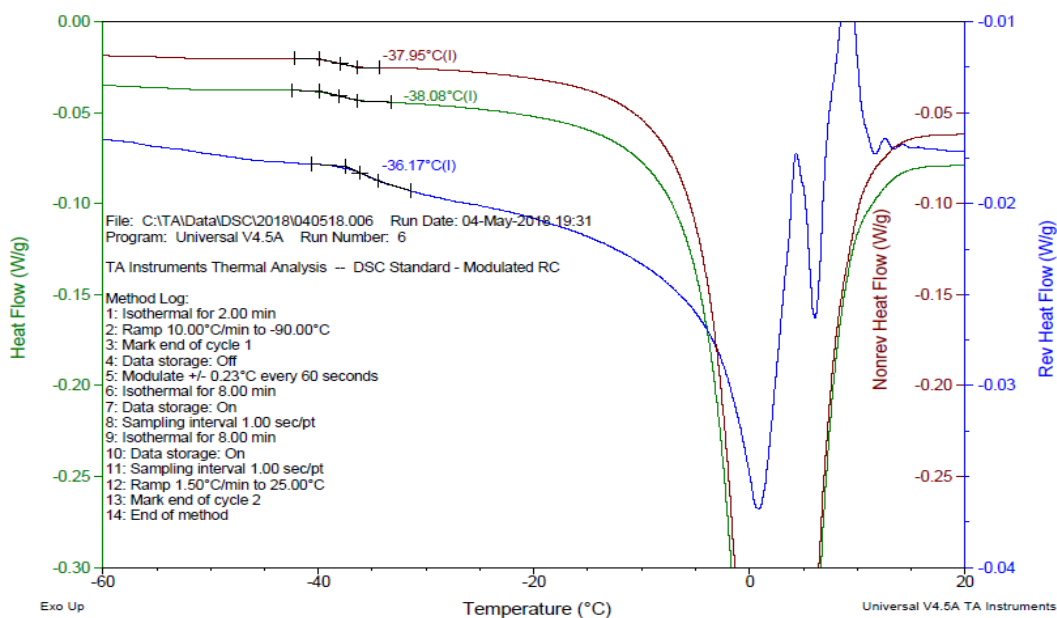
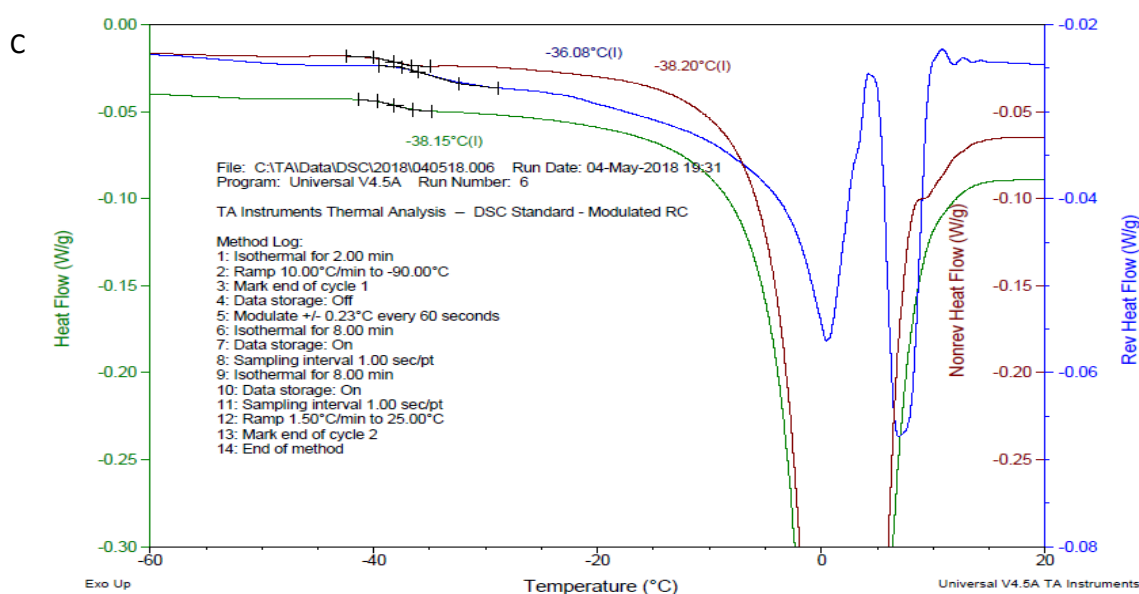


Figure continued onto the next page.



**Figure 7.5.** Modulated differential scanning calorimetry results for DMPC:Chol (10 mg/mL) with (A) and without (B) ovalbumin, and DSPC:Chol (4 mg/mL) liposomes with OVA (C) encapsulated inside the aqueous core (0.25 mg/mL initial). The sample contained a final concentration of 7.5% sucrose.

### 7.3.2.2 Dynamic mechanical analysis (DMA)

Dynamic mechanical analysis (DMA) is a rheological technique that can be used to predict the  $T_g'$  of liposome formulations. Whilst MDSC has been used for many years, the technique struggles to detect  $T_g'$  values due to eutectic events or higher melts dominating the profiles, thus DMA has been explored. DMA measures changes in morphology (namely melts, crystallisation, alpha and beta transitions) by applying stress to a sample and measuring the strain. From this, multiple sets of data can be obtained including the dynamic stiffness as well as damping (tan Delta) (Figure 7.6). The most frequently quoted value is tan Delta; the value for this increases significantly when a sample passes through its glass transition. This technique was used to determine the  $T_g'$  of liposomes as well as discerning whether this technique would give similar results to the MDSC.

As shown by Figure 7.6A-C and Table 7.9, the tan Delta values for the three formulations OVA loaded DSPC:Chol, DMPC:Chol, OVA loaded DMPC:Chol are all between -23 and -24°C. Like MDSC, there is little to no difference between the three formulations, once again highlighting the important role sucrose plays in the liposome- cryoprotectant mixture. The DMA peaks

are clearer in comparison to the MDSC graphs (Figure 7.5) with the Tg' more easily identifiable. Although there is minimal differences between all three formulations using both techniques, there is a noticeable difference in Tg' values (of ~10°C) between MDSC and DMA. The findings are in keeping with other studies, whereby a 10°C difference was determined for the Tg' of trehalose measured by either DMA and MDSC (Gearing et al., 2010). The difference in Tg' values between DMA and MDSC may be due to different basis of the techniques being used; DMA is thermomechanical whilst MDSC measures changes in thermal reaction change. For the DMA, adjusting the stressing frequency from 0.1 Hz to 1 Hz may results in Tg' value that match more closely to the MDSC data. It was argued that the difference in measurement between the DMA and MDSC does not significantly affect the FD parameters to be selected. Notably, the Tg' is not a single value but an interval range, so there is a degree of variability when measuring Tg' using DMA and MDSC, which uses minute volumes of the actual sample to be freeze dried.

In summary, the results obtained from the collapse temperature using FDM, and Tg' results obtained from MDSC and DMA were reviewed (Table 7.9). The collapse for all three samples was between -39 and -33°C, with a Tg' of -34°C determined by MDSC. Due to the complimentary results, the results from FD microscopy and MDSC were taken into consideration when designing the FD cycle.

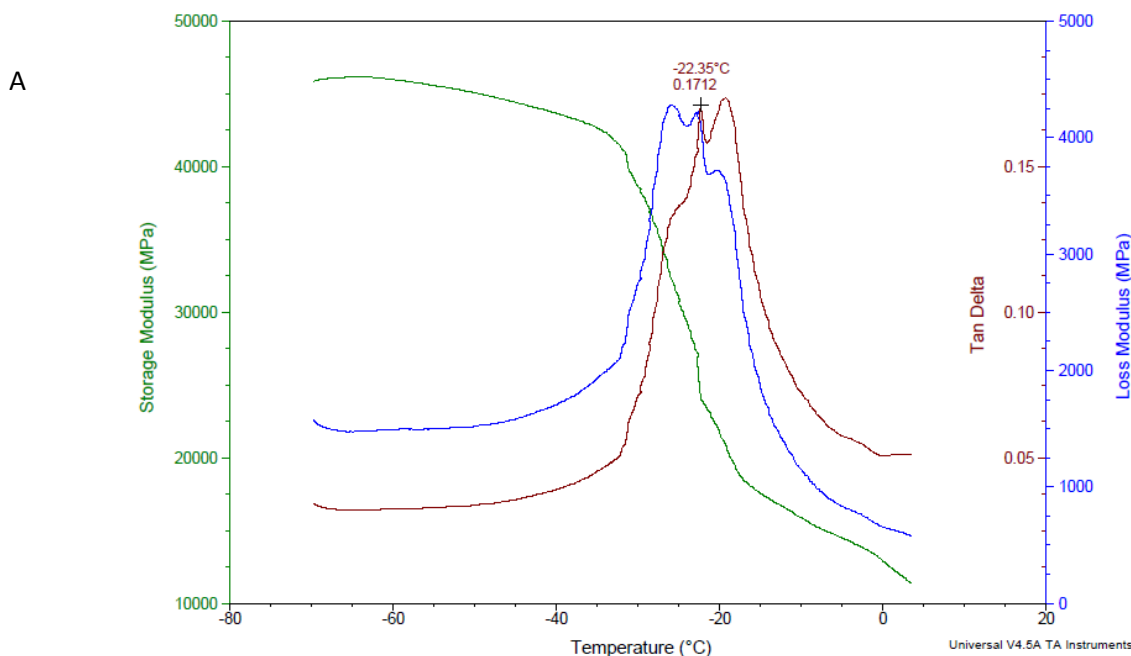
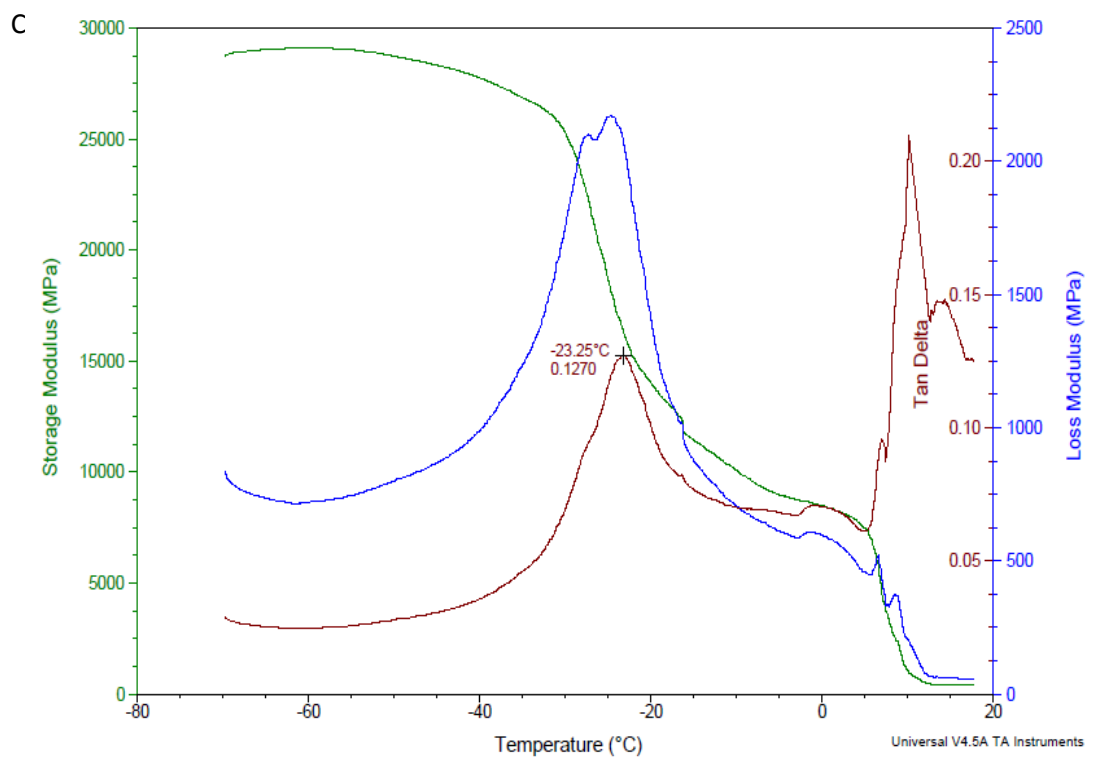
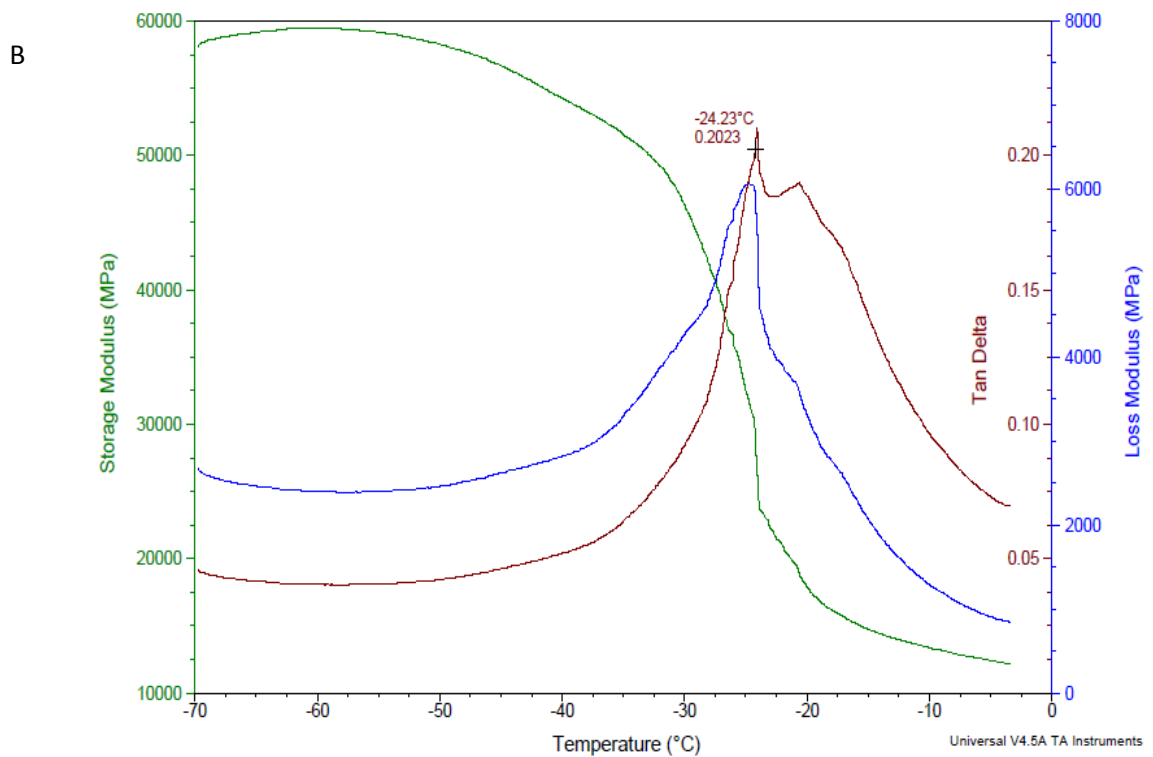


Figure continued on the next page.



**Figure 7.6.** Dynamic mechanical analysis results for DMPC:Chol (10 mg/mL) with (A) and without (B) ovalbumin, and DSPC:Chol (4 mg/mL) liposomes with OVA (C) encapsulated inside the aqueous core (0.25 mg/mL initial). The sample contained a final concentration of 7.5% sucrose.



**Table 7.9.** Comparing techniques used to determine the glass transition temperature for liquid samples.

FORMULATIONS	CONCENTRATION (MG/ML)	SUCROSE (%)	DMA RESULTS (TAN DELTA (°C))	MDSC (°C)
DSPC:CHOL + OVA	4	7.5	-23.4	-36.2
DMPC:CHOL	10	7.5	-23.3	-36.1
DMPC:CHOL + OVA	10	7.5	-24.2	-36.2

### 7.4.3 Freeze drying cycles

The FD cycle was designed taking into consideration the freezing and collapse temperature identified using FDM and MDSC. Using these results as well as reviewing literature, three freezing variations along with three FD cycles were investigated. As shown in section 7.4.2.1, the temperature used to freeze liposomes affects the physicochemical properties of the sample. Freezing is an important stage in the FD cycle, so three ways in which samples can be frozen (slow, intermediate and quick) were explored alongside three variants of the FD cycle. The process flow sheet below (Figure 7.7) summarises the three FD cycles tested; with FD cycle 1 (FDC1) based on the principles of DoE to predict ideal parameters for FD liposome samples. The FDC1 was used as a basis to design further FD cycles (FDC2 and FDC3).

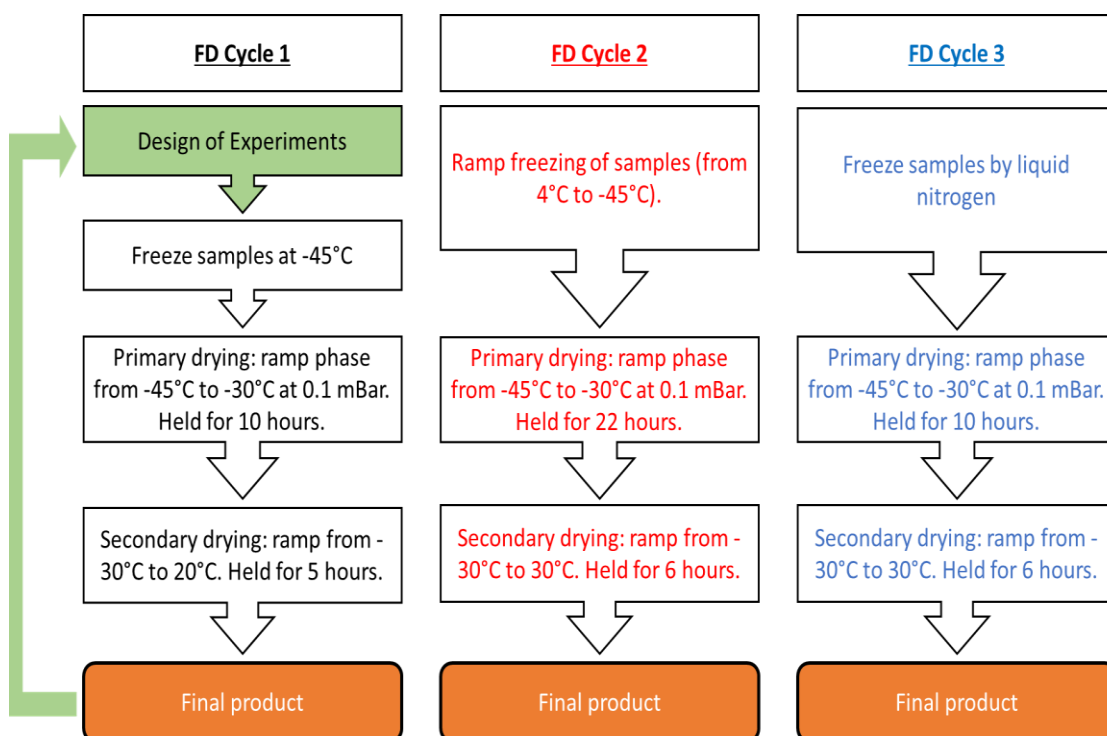


**Figure 7.7.** Process flow sheet for three freeze drying cycles including the freezing procedure for liposome formulations.

#### 7.4.3.1 Real time analysis of the freeze drying cycle 1

Real time monitoring of the FD process is possible by inserting thermocouple probes into vials. For FDC1, probes were inserted into DSPC:Chol (4 mg/mL) and DSPC:Chol (10 mg/mL) liposomes for monitoring. Figure 7.8 shows that the samples (Tc profiles in blue and black lines) lag behind the shelf temperature during the primary drying phase. Previous studies have shown this too, and so the cycle was designed to be held at -30°C (slightly higher than the collapse temperatures obtained) as it takes a while for the sample temperature to adjust in comparison to the actual shelf. In recent years, modern freeze drying cycles have been designed to maximise the sublimative cooling effect by operating at a shelf temperature as high as possible, without causing collapse. Throughout the progression of the FD cycle, the temperature of the product changes whilst the pressure and shelf temperature are kept constant. The FD process contains associated analytical tools to monitor and check the FD

process is running to the best efficiency. Change in product temperature can be monitored in several ways, including the use of thermocouples or by pressure rise measurements (pink and grey lines in Figure 7.8). For instance, the monometric temperature measurement (MTM) is a pressure rise test (shown by the pink line in Figure 7.8). The pink line measures changes in the water vapour; here the isolating valve between the chamber and condenser is closed for 30 seconds every hour. As sublimation nears completion, the amplitudes of the spikes decreases until negligible. The second technique (grey line in Figure 7.8) is a comparative barometric method, which is not influenced by changes in water vapour. As FD progresses, the water vapour decreases (caused by the completion of sublimation) the two profiles (pink and grey lines) converge.

Moreover, the results from both of these tests indicate the whole batch has not undergone complete sublimation; completion of sublimation is only achieved until ramping to the secondary stage occurred. The results from the pressure rise tests indicate the primary stage of the FD cycle should be extended for complete sublimation, however, this contrasts with the individual vials with thermocouples where the temperature inflections indicated that primary drying was sufficiently long to complete sublimation. The difference can be attributed to the site of measurements; the thermocouples measure product temperature at the bottom of the vial whilst the pressure rise test measure temperature at the interface (Tang and Pikal, 2004). The pressure rise tests are advantageous over the thermocouples given that minimal operator set-up is required. It also yield accurate product resistance, which can be used to characterise the heat and mass transfer in real time during primary drying (Tang *et al.*, 1999). As a result, the primary drying stage of the FD cycle was extended (FDC2 and FDC3) to determine if this influenced the freeze drying of the liposomal formulations.

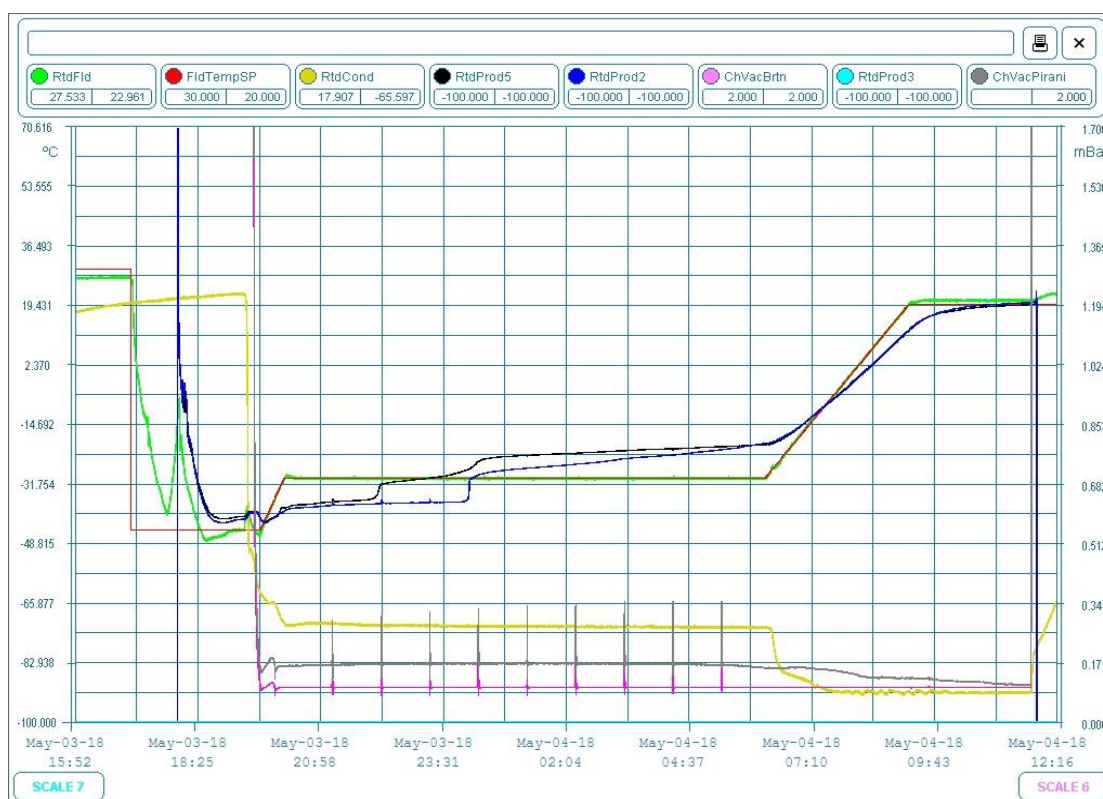


**Figure 7.8.** Real time analysis of liposomes frozen using freeze drying cycle 1.

#### 7.4.4 High throughput production of freeze dried liposomes

The use of microplates for FD, alongside DoE, allows understanding of the FD cycle and formulation optimisation to be gained more quickly by running conditions in parallel. The high-throughput process is also cost effective as very little material is needed, in comparison to conventional FD vials. Miniaturization of the FD process is possible using microplates. Previously, using microplates, successful screening was carried out for the enzyme lactic dehydrogenase to determine the ideal FD. The enzyme had been unstable during FD so optimisation was required (Grant *et al.*, 2009). Whilst a number of proteins have been tested in microplates, to the best of our knowledge nobody has investigated FD liposomes in microplates. The ability of microplates to successfully FD liposomes was tested, with vials used in parallel for comparison. Flat bottom microplates were selected with the edges of the microplate removed, to allow the bottom of the plate to contact the shelf directly for even FD to occur. This also mitigates the edge effect so water may not need to be added to the edge wells, freeing up more space for testing samples (Grant *et al.*, 2009, Grant *et al.*, 2012).

The results show liposomes-cryoprotectant mixtures are capable of undergoing FD in both microplates (Figure 7.9A) as well as vials (Figure 7.9B). This was observed irrespective of the lipid type (DMPC or DSPC lipid), lipid concentration, protein concentration and, the ratio of cryoprotectant added. Visual inspection of the samples show good quality freeze dried cakes have been produced (Figure 7.9), with a good degree of reproducibility achieved for samples across multiple wells. The geometry of the microplates, is a key consideration when FD samples. Flat bottom plates have the same diameter per well, therefore even and reproducible cakes (similar to the vials) are formed in comparison to using v-shaped microplates (Graberg and Gieseler, 2006). For high throughput FD screening, flat bottom plates are preferred as they are readily available and negate the need to use specialist equipment that would be required if using V-shaped microplates, as they enable good contact with the shelf without special adaptations (Grant *et al.*, 2012).

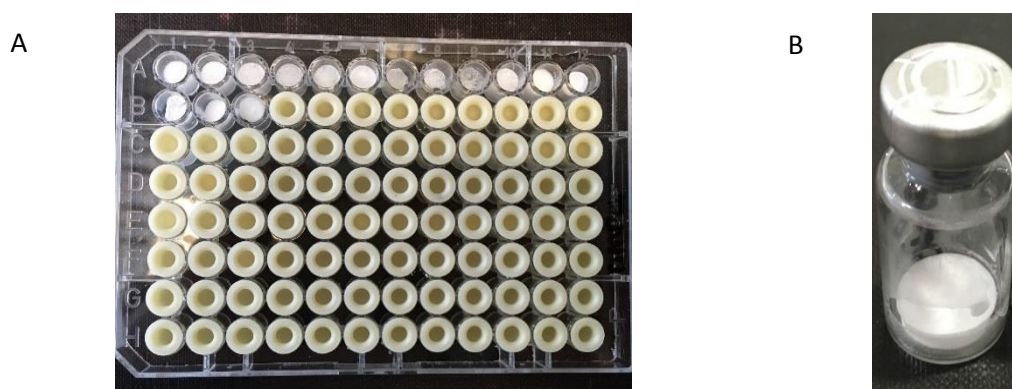


**Figure 7.9.** DMPC:Chol freeze dried in either a microplate (A) or a conventional vial (B).

Furthermore, reconstitution of the cakes in microplates and vials was quick and easy; the cake was rehydrated in less than 10 seconds using a hand held pipette and mixing the sample by pipetting up and down. Post rehydration with water, the samples were characterised for changes in the size and PDI of the liposomes. The medium in which the liposome formulations are FD did not make a difference in these experiments. Similar changes in DMPC:Chol physicochemical properties are observed for formulations FD in either vials (Figure 7.10A) or microplates (Figure 7.10B). Results from the samples dried in vials show a 30- 34% increase in size for empty DMPC:Chol liposomes (4 and 10 mg/mL) preserved in either 5 or 10%

sucrose (Figure 7.10). The DMPC:Chol formulations rehydrated in microplates, show an 20-25% increase for empty DMPC:Chol liposomes and, a 12- 21% increase in size for OVA loaded DMPC:Chol liposomes. The PDI remains less than 0.2, irrespective of the freezing medium, the formulation parameters or the concentration of sucrose used.

As with the DMPC:Chol formulations, changes in the DSPC:Chol physicochemical properties in vials (Figure 7.11A) or microplates (Figure 7.11B) are the same. For instance, empty DSPC:Chol liposomes (4 mg/mL) FD at 10% sucrose in vials and microplates, significantly increased in size to 114 and 112 nm respectively (from an original size of 47 nm). The increase in size occurs regardless of the lipid, protein and sucrose concentrations (Figure 7.11), and is greater than that observed for DMPC:Chol liposomes. Empty DSPC:Chol liposomes more than double in size at both 4 and 10 mg/mL (from 47- 56 nm to 113- 140nm), whilst OVA loaded DSPC:Chol liposomes double in size (65- 88 nm to 117- 132 nm) (Figure 7.11). The PDI for both formulations (DMPC:Chol and DSPC:Chol), with and without protein remains at 0.2 or less for all FD formulations. The results suggest despite a relatively high freezing temperature of -45°C chosen based on the freeze-thaw experiments (section 7.4.2.1), it may be possible that the freezing temperature and primary drying rate was not optimal for the FD of the samples. As shown in section 7.4.2.1, the freezing temperature is key in the FD process and getting this incorrect can result in increased liposomes size post thawing. The damage caused by the wrong temperature is irreversible and depending on the formulation, can compromise the pharmacokinetic activity. Previous researchers have also shown the rate of freezing has an effect on the size (Allison and Gregoriadis, 1974, Pikal-Cleland et al., 2000). Compared to DMPC:Chol liposomes, there is a greater increase in size for DSPC:Chol liposomes. The size increase for OVA loaded DMPC:Chol is not as pronounced, compared to empty liposomes, suggesting that OVA along with being the model antigen, has stabilising effects. This is in keeping with literature whereby the addition of protein to formulations improves stability (Ntimenou et al., 2006). The stabilising effect is more prominent at a higher liposomes concentration (10 mg/mL), where only a 30 nm increase was observed (10% sucrose) compared to a 50 nm increase for OVA loaded DSPC:Chol liposomes produced at 4 mg/mL (10% sucrose).

In addition, previous literature has shown some leakage of drugs after rehydration of FD liposome samples (Hua et al., 2003). To test for this, rehydrated samples were put through the TFF to remove any OVA that may have leaked out during the FD process. The amount of

OVA remaining post hydration was calculated by high pressure liquid chromatography (HPLC) -evaporative light scattering detector (HPLC-ELSD) and, compared to the original encapsulation efficiency. Under the FDC1 parameters, the DMPC:Chol liposomes show 100% retention of OVA suggesting the FD parameters are good for protein despite adjustments required to limit the increase in liposome size (Table 7.10).

Likewise, the amount of OVA retained after FD was the same as that prior to the FD of DSPC:Chol, suggesting the FD parameters are suitable to prevent leakage (Table 7.11). The absolute recovery of OVA after FD may be in part due to the high freezing temperature of -45°C. The high freezing temperature is ideal to prevent leakage; it causes the formation of large crystals and prevents leakage due to an osmotic pressure created (van Winden et al., 1997). At a slow rate of freezing, the water can diffuse across the bilayer reaching equilibrium, hence the number of ice crystals formed inside the aqueous core is decreased (Ingvarsson et al., 2011). The presence of cholesterol also helps prevent leakage by helping sublimation at the water lipid interface (Samuni et al., 2000). As a result, lipids are closer together forming van der Waal interactions between neighbouring lipids so the permeability of the liposomes is reduced preventing leakage of hydrophilic protein (Samuni et al., 2000, Barenholz, 2002, Krasnowska et al., 2001). The findings confirm the concentration of the formulation, along with protein have an effect on the stability of liposomes during freeze drying.

In summary, initial characterization of DMPC:Chol and DSPC:Chol formulations post FDC1 revealed interesting results. Importantly, the FDC1 was able to retain all the encapsulated protein, which is essential when producing pharmaceuticals. However, the physicochemical properties of the liposomes were affected adversely by the FDC1. The sucrose and lipid concentration have a small influence on the liposome size, whilst the addition of protein OVA adds stability to the formulation, minimizing the increase in size. To better understand the results from this initial experiments, the results were analysed by DoE to establish the FD design space. By doing this, the ideal parameters and design space for FD of liposomes can be determined.

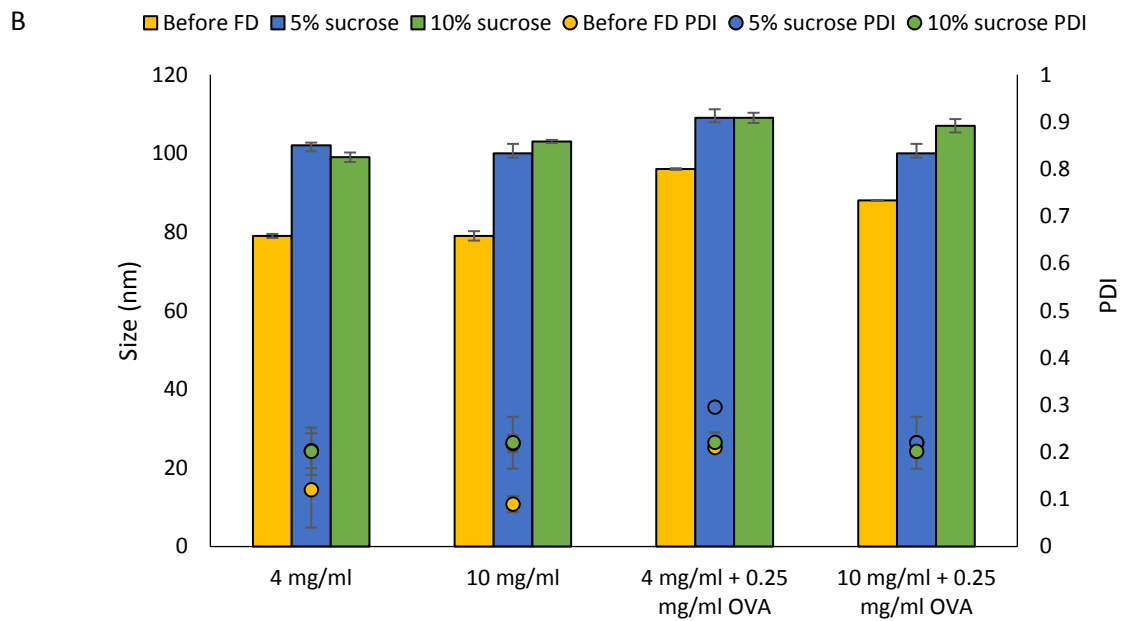
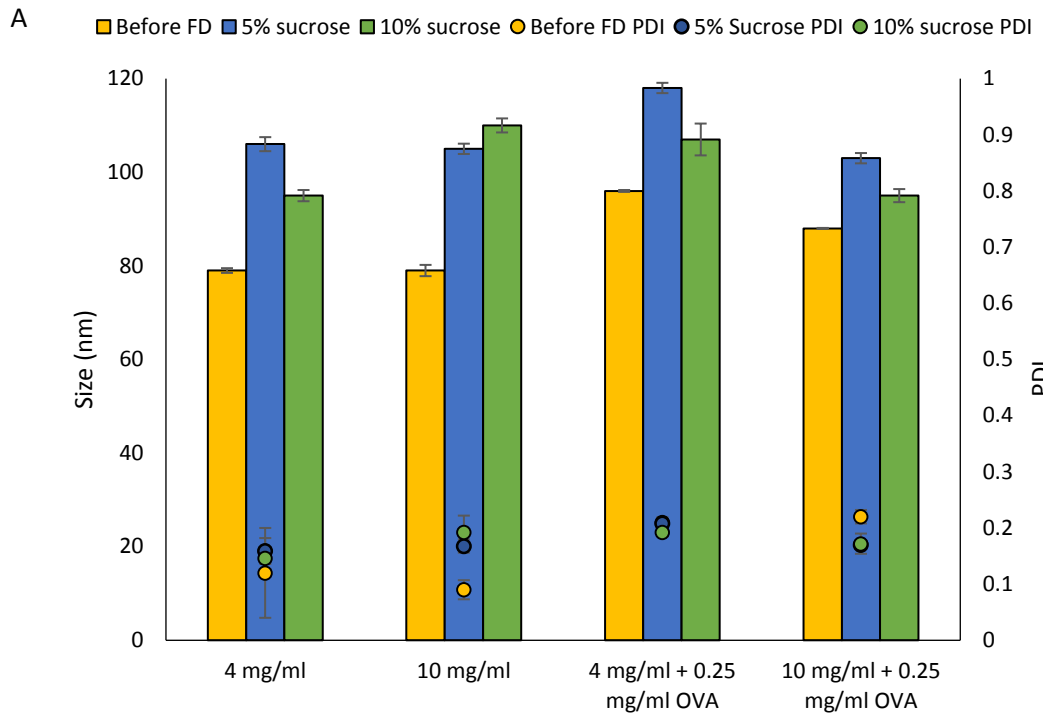


**Figure 7.10.** Characterising DMPC:Chol (4 and 10 mg/mL ) liposomes loaded with and without OVA (0.25 mg/mL) before and after freeze drying. The samples contained different amounts of sucrose and were freeze dried in either vials (A) or in microplates (B). Results represent three independent batches,  $\pm$  SD.



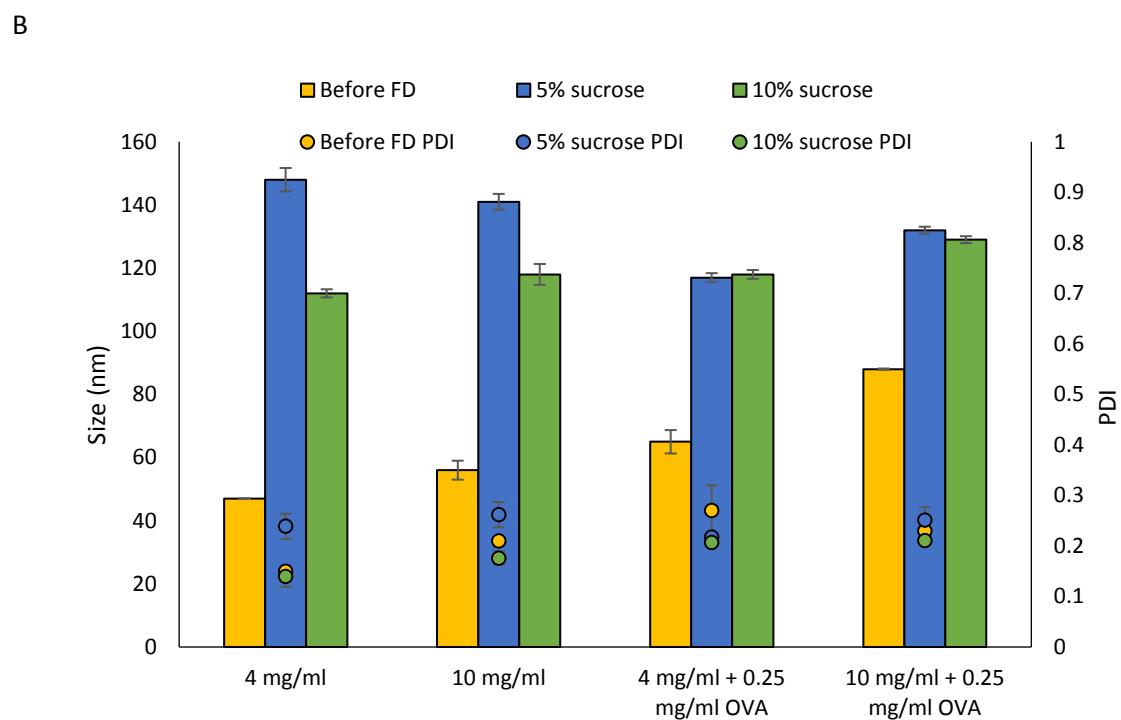
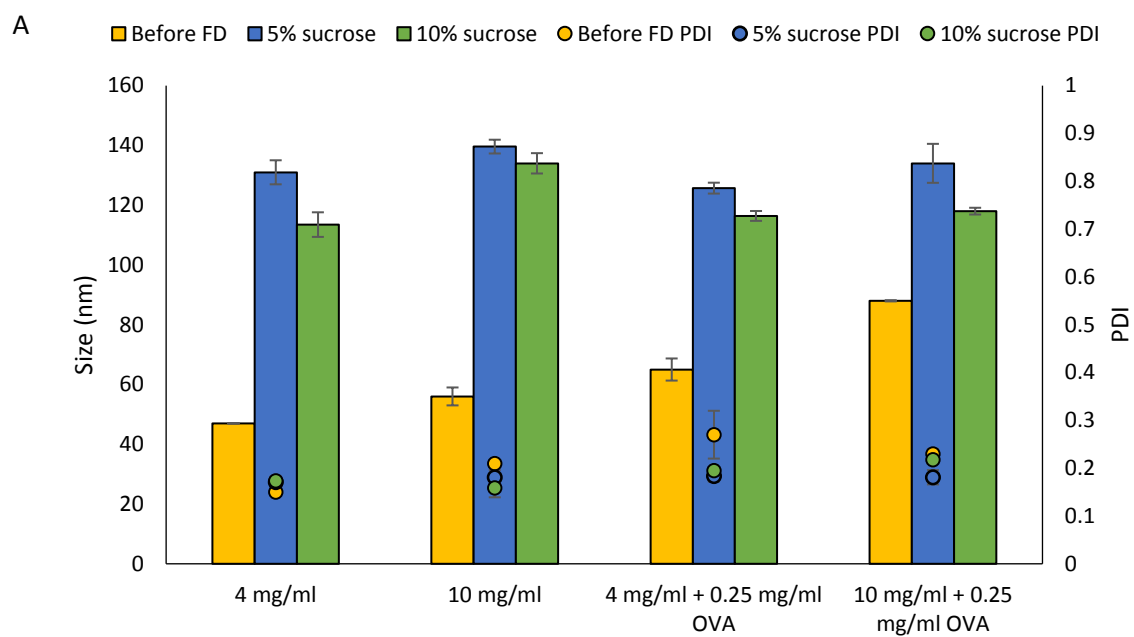


**Figure 7.11.** Characterising DSPC:Chol (4 and 10 mg/mL) liposomes loaded with and without OVA (0.25 mg/mL) before and after freeze drying. The samples contained different amounts of sucrose and were freeze dried in either vials (A) or in microplates (B). Results represent three independent batches,  $\pm$  SD.

**Table 7.10.** Ovalbumin encapsulation of DMPC:Chol liposomes before and after freeze drying with different sucrose concentrations. Results represent n of three independent batches,  $\pm$  SD.

LIPID CONCENTRATION (MG/ML)	OVALBUMIN (MG/ML)	SUCROSE (%)	EE BEFORE (%)	EE AFTER (%)
4	0.25	5	37 $\pm$ 0.2	36 $\pm$ 0.2
4	0.25	10	37 $\pm$ 0.2	37 $\pm$ 0.3
10	0.25	5	39 $\pm$ 0.3	33 $\pm$ 1.0
10	0.25	10	39 $\pm$ 0.3	40 $\pm$ 3.0

**Table 7.11.** Ovalbumin encapsulation of DSPC:Chol liposomes before and after freeze drying with different sucrose concentrations. Results represent n of three independent batches,  $\pm$  SD.

LIPID CONCENTRATION (MG/ML)	OVALBUMIN (MG/ML)	SUCROSE (%)	EE BEFORE (%)	EE AFTER (%)
4	0.25	5	34 $\pm$ 0.3	30 $\pm$ 0.7
4	0.25	10	34 $\pm$ 0.3	33 $\pm$ 0.2
10	0.25	5	36 $\pm$ 0.5	35 $\pm$ 1.1
10	0.25	10	36 $\pm$ 0.5	34 $\pm$ 0.4

#### 7.4.5 Design of Experiments

In the pharmaceutical industry, it is vital to have a well characterised manufacturing process, with established design spaces. The design of experiments (DoE) can be incorporated into FD cycle development to improve the quality of the product. To do this, a full factorial DoE was run investigating the effect of lipid concentration, presence of protein and sucrose concentration on the physicochemical properties of FD liposomes (size, PDI and encapsulation efficiency). Both formulations (DMPC:Chol and DSPC:Chol) had their own DoE set up with 11 parameters explored (including centre points in triplicate) for the design space to be established. The relationship between lipid, protein and sucrose was investigated for the best outcomes; minimal changes in size, PDI and encapsulation efficiency. Data values obtained after rehydrating FD cakes was fed back into the software which calculated a positive relationship between liposome concentration and protein.

The results from Figure 7.12 establishes the design space for DMPC:Chol liposomes. When considering the size as the variable outcome, the results show the higher lipid and sucrose concentration, the greater the possibility for the liposomes to be 100 nm in size (Figure 7.12A). Higher sucrose content also maintains the homogeneity of the liposomes (Figure 7.12B). The concentration of OVA present did not have a great impact (Figure 7.12C) but the presence of protein was necessary to maintain a liposome size below 100 nm.

Equally, a high sucrose and lipid concentration allows for smaller OVA loaded DSPC:Chol liposomes, with a low PDI to be produced (Figure 7.13A and B). The same conditions also delivers a high encapsulation efficiency (Figure 7.13C). Furthermore, the results from both formulations show the sweet spot to be at 10 mg/mL lipid, 0.25 mg/mL OVA with the addition of 10% sucrose, thus these parameters were selected for further FD of liposome formulations. The results are in keeping with previous research looking into the effect of cryoprotectants and concentration on liposomes. A 10% sucrose concentration was found by others to be ideal for FD liposomes, with less than 5% leakage of water soluble nucleobase uracil (Hua *et al.*, 2003). The type of cryoprotectant used also affected stability, with disaccharide sugars, such as trehalose and sucrose, retaining the most protein in comparison to glucose (Hua *et al.*, 2003). Whilst DoE was successfully used to predict the ideal formulation parameters, given the changes in liposome size by FDC1, further FD conditions were explored. Using the lipid and sucrose concentration predicted, the FD cycles conditions

were altered in comparison to FDC1 to improve liposome stability post FD. To do this, FDC1 was adjusted and two other cycles FDC2 and FDC3 were investigated.

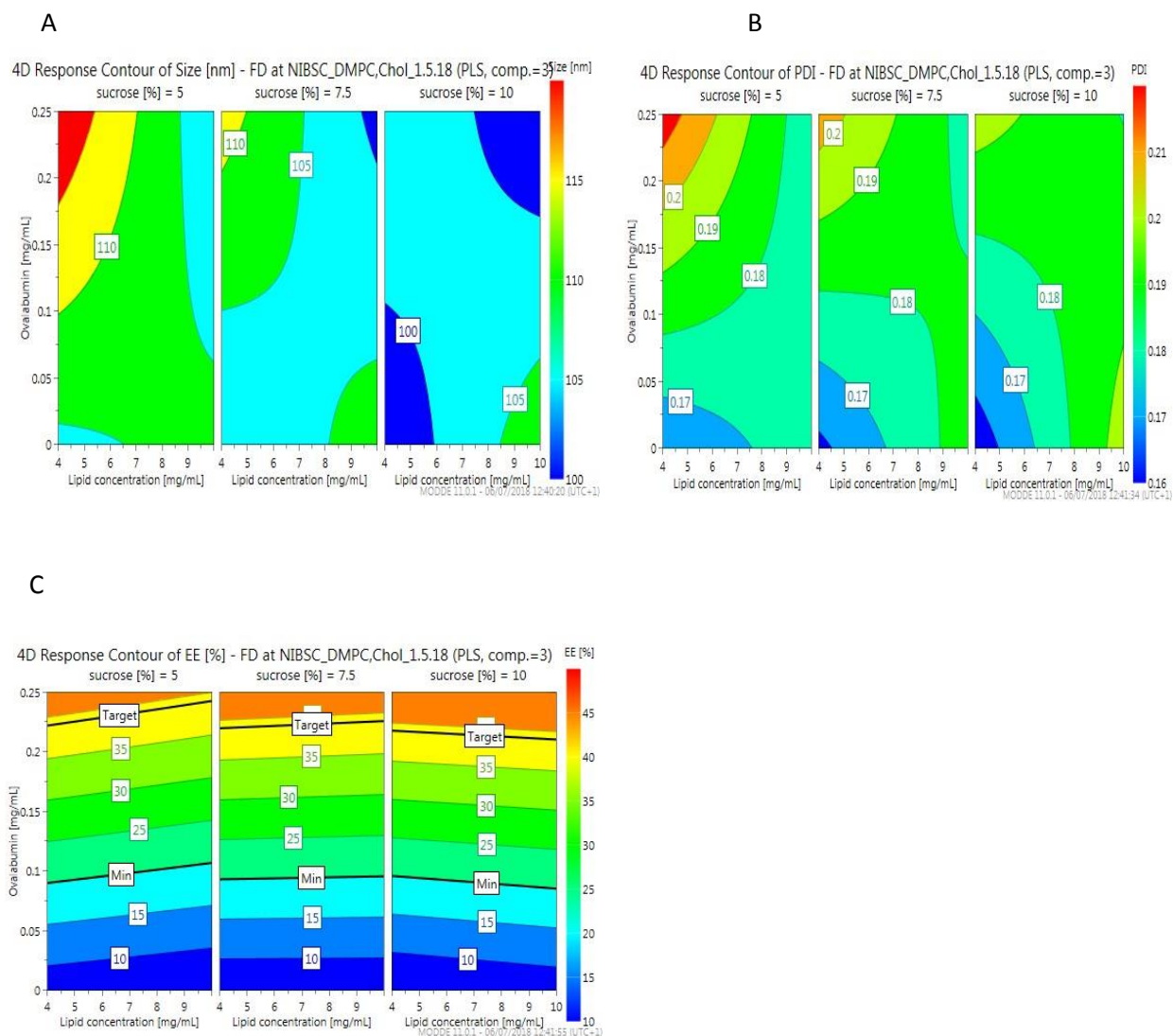


**Figure 7.12.** Design of experiments plots predicting the outcomes in terms of size (A), PDI (B) and encapsulation efficiency (C) of OVA loaded DMPC:Chol liposomes.

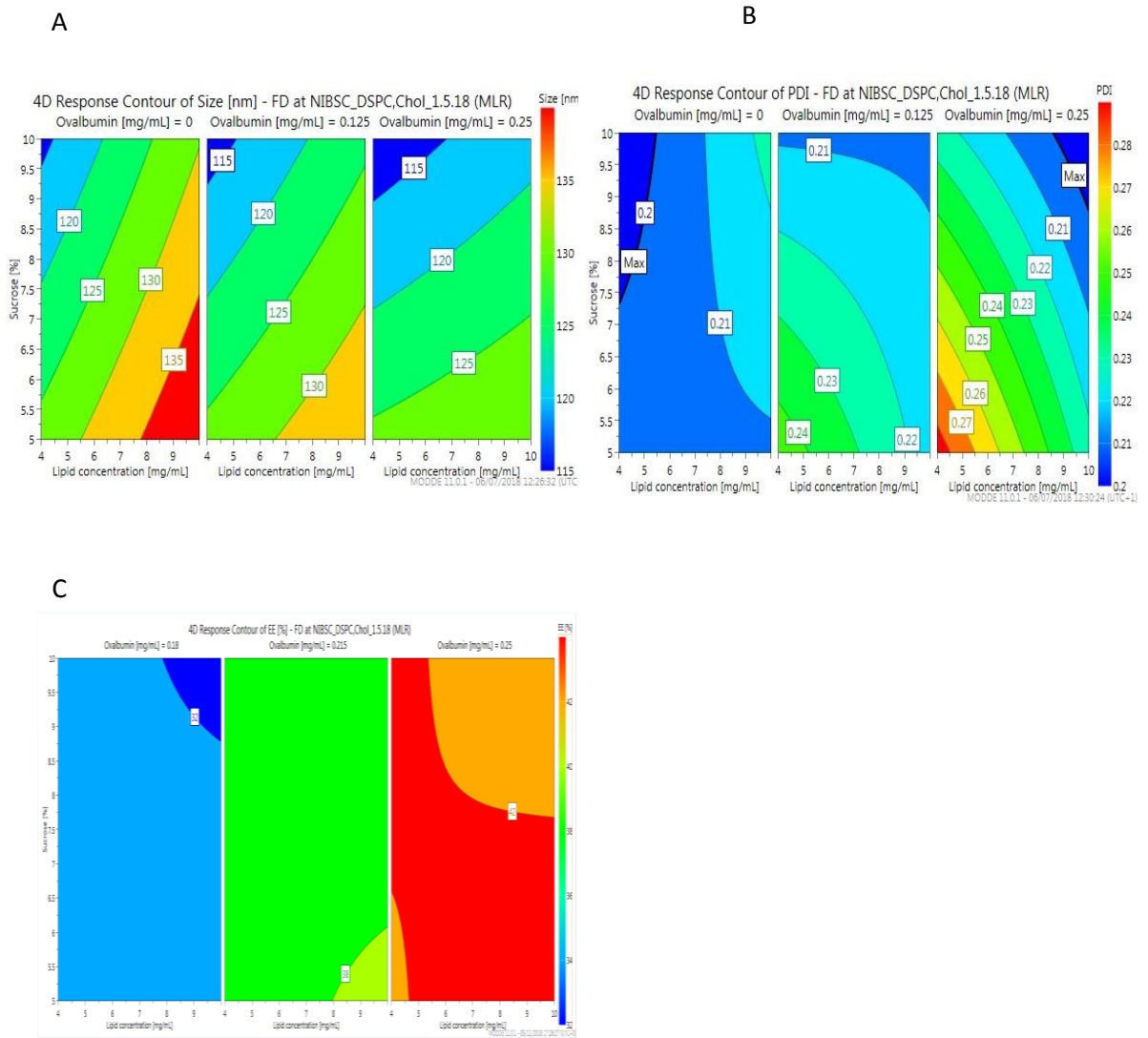


**Figure 7.13.** Design of experiments graphs predicting the outcomes in terms of size (A), PDI (B) and encapsulation efficiency (C) of OVA loaded DSPC:Chol liposomes.

### 7.4.6 Freeze dried cycle 2 and Freeze dried cycle 3

The results from FDC1, although encouraging, were not ideal due to the increase in liposome size. The changes can result in poor or even loss of liposome functionality. To improve this, the FD conditions were adjusted and two different freezing approaches (ramp freezing (FDC2) and snap freezing (FDC3)) were evaluated. Based on the previous results from the DoE experiments, OVA loaded DMPC:Chol and DSPC:Chol liposomes were produced at 10 mg/mL. Sucrose (10%) was added to the formulations at 1:1 v/v, with the samples either ramp (Figure 7.14A and B) or snap frozen (Figure 7.14C and D) before undergoing FD. Post FD the cakes were inspected visually; there is no difference in the cakes formed between the OVA loaded DMPC:Chol and OVA loaded DSPC:Chol formulations. Figure 7.14A and B show slow ramp freezing forms better cakes than those samples that were snap frozen in liquid nitrogen (Figure 7.14C and D). Snap freezing liposomes resulted in a poor appearance and quality of cakes, with some vials showing signs of partial collapse. This is observed for both DMPC:Chol and DSPC:Chol formulations.

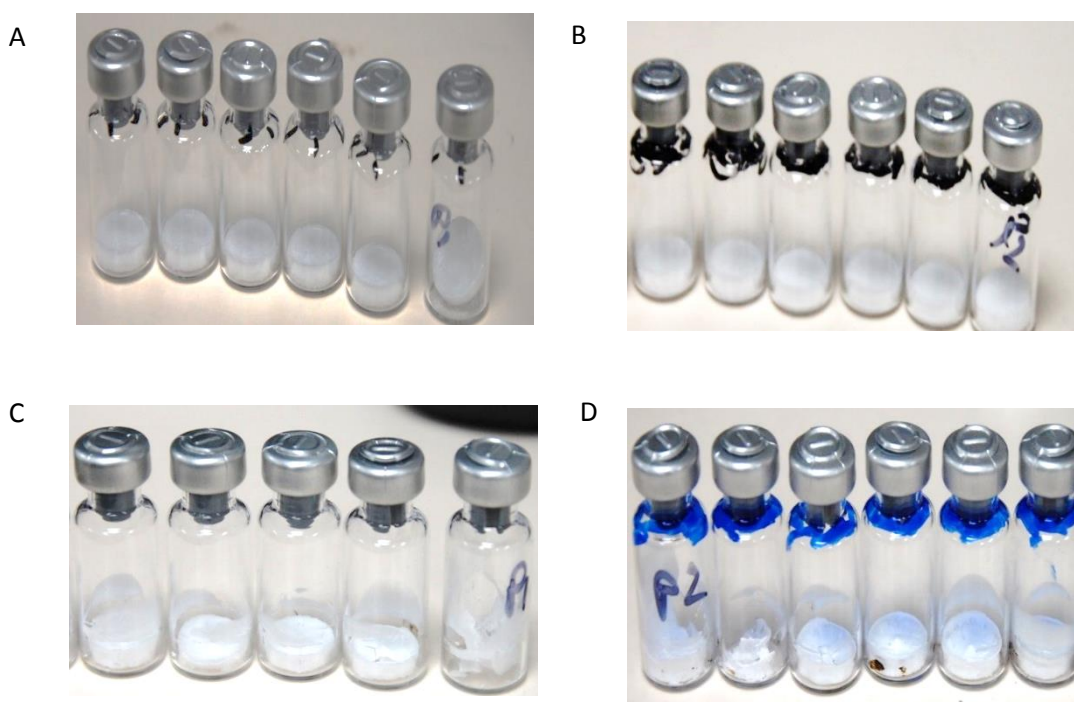


**Figure 7.14.** The cakes formed after testing different freezing and freeze drying conditions. The DMPC:Chol liposomes were either ramp frozen (A) or snap frozen (C). The DSPC:Chol formulations were also subjected to ramp (B) and snap freezing (D), after which the cakes were inspected visually for any deformations.

The rehydration of OVA loaded DMPC:Chol and DSPC:Chol liposomes having undergone FDC2 and FDC3 was quick. The FD samples were easy to reconstitute, with rehydration happening within seconds. Measuring the physicochemical properties of rehydrated samples indicate that the changes to the FD cycle improved stability of both DMPC:Chol and DSPC:Chol liposomes loaded with OVA (Figure 7.15). For the DMPC:Chol formulation both FDC2 and FDC3 performed better compared to FDC1. The snap freeze method (FDC3) caused a significant increase in size for DMPC:Chol and DSPC:Chol liposomes ( $p < 0.001$ ). For the DMPC:Chol liposomes, post hydration after FDC3 caused a 15 nm increase in size from  $85 \pm 0.8$  nm to  $100 \pm 0.3$  nm, whilst no change in size occurred ( $85 \pm 0.4$  nm) for DMPC:Chol liposomes frozen using the ramp freeze approach (FDC2). The DMPC:Chol formulations dried using FDC2 resulted in a homogenous population before and after FD, as indicated by the low PDI ( $< 0.2$ ).

In comparison, the size increases for DSPC:Chol formulations are much more pronounced. The size of DSPC:Chol liposomes increased significantly ( $p < 0.001$ ), doubling after FD using the snap freeze method (FDC3) from  $50 \pm 0.3$  nm to  $108 \pm 0.4$  nm (Figure 7.15). The increase in size resulting from the ramp method (FDC2) was not as large; an increase of 38 nm (from  $50 \pm 0.3$  to  $88 \pm 0.3$  nm) was observed using FDC2. The ability of the formulations to retain the encapsulated OVA under the new freezing and FD cycles was investigated (Table 7.12). Analysis of the samples showed that both FDC2 and FDC3 are capable of retaining more than 99% of the entrapped OVA, despite changes in size observed for FDC3, in particular the DSPC:Chol formulation. The results indicate this formulation is not as stable in a FD format in comparison to DMPC:Chol liposomes. The apparent difference in stability can be attributed to the difference in the initial liposome size. One reason for this may be due to the increased surface area. The DSPC:Chol liposomes are smaller and so have a higher surface area for the same amount of space (Hsu *et al.*, 1995). As a result, the sucrose may not be able to cover the whole area during freeze drying and so the space between neighbouring bilayers is reduced to around 1 nm (Wolfe and Bryant, 1992). This is problematic, as it can cause fusion between adjacent liposomes. Another reason for the increase in size could be caused by the increased surface tension experienced by smaller liposomes (Crowe and Crowe, 1988). When rehydration occurs, the inner bilayer wants to expand as a result of water entering the aqueous core, thus causing swelling and an increase in liposome size (Crowe and Crowe, 1988).

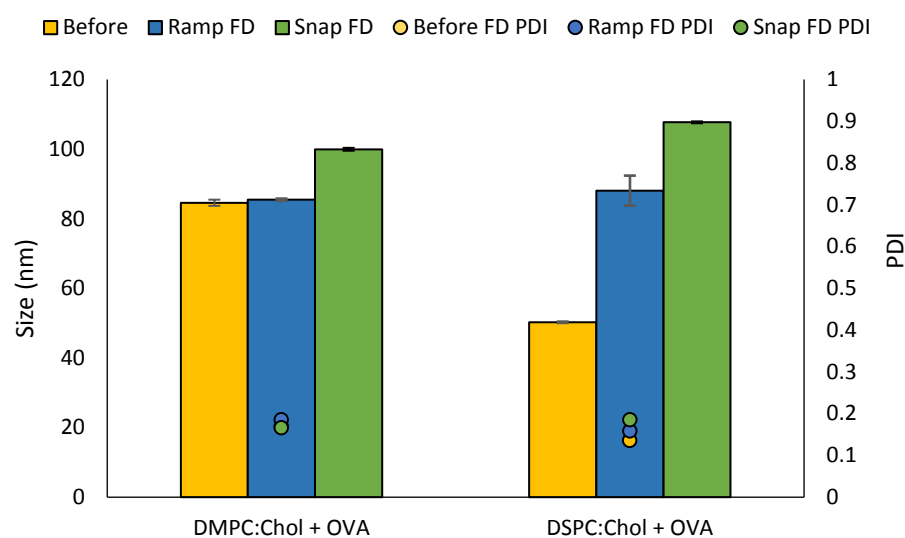


**Figure 7.15.** The physicochemical properties of OVA loaded DMPC:Chol and DSPC:Chol liposomes before and after freeze drying. The liposomes were subjected to two freeze drying options; a ramp freeze cycle or a snap freeze cycle, with liposome suspensions (before freeze drying) used as a control. All samples were freeze dried in the presence of the cryoprotectant sucrose (10% v/v at a 1:1 ratio). Results represent three independent batches,  $\pm$  SD.

**Table 7.12.** The encapsulation of OVA before and after freeze drying using two different cycles. Results represent three independent batches, mean  $\pm$  SD.

FORMULATION	Freeze drying cycle	SUCROSE (%)	EE BEFORE (%)	EE AFTER (%)
DMPC:CHOL + OVA	Snap Freeze (FDC2)	5	39 $\pm$ 1	38 $\pm$ 1
DMPC:CHOL + OVA	Snap Freeze (FDC2)	10	39 $\pm$ 1	38 $\pm$ 1
DSPC:CHOL + OVA	Ramp Freeze (FDC3)	5	36 $\pm$ 1	36 $\pm$ 2
DSPC:CHOL + OVA	Ramp Freeze (FDC3)	10	36 $\pm$ 1	36 $\pm$ 1



#### 7.4.7 Residual moisture content

The residual moisture present in FD samples is important; and it can be indicative of the long term stability of the pharmaceutical product. A high moisture content often correlates with poor product stability, so it is important to measure this. The most widely used approach to measure moisture is the use of the coulometric Karl Fischer method; a highly accurate method suitable for a wide range of pharmaceuticals and included in Pharmacopoeial monographs. The only drawback of this method is that the test sample is destroyed and can't be reused.

The residual moisture results for FDC1 were poor, in comparison to the residual moisture measured for FDC2 and FDC3 (Table 7.13). Although FDC1 experiment retained the entrapped OVA inside the liposomes, the increased size and high residual moisture content post FD is problematic. The measured moisture content for DMPC:Chol liposomes, with (4.15%) and without (4.23%) OVA was above 4% (Table 7.13). The residual moisture content measured is too high, with previous literature quoting a moisture content above 2% as contributing to the instability of the FD products, whereas product with a moisture content of less than 2% has been shown to be stable (Nagase et al., 1997); no chemical degradation is observed for lyophilised liposomes containing doxorubicin that have been in storage for 6 months at 30°C (Van Winden and Crommelin, 1997).

Taking the results from FDC1 into consideration, strategies were employed to reduce the moisture content for samples FD by FDC2 and FDC3. To achieve this, the FD cycle was tweaked; the primary drying temperature was raised to -25°C (up from -30°C) and the step length extended to 22 hours for FDC2. The secondary drying phase, which is instrumental in removing excess moisture, was extended by 1 hour (from 5 hours), with a new secondary drying temperature of 25°C set (raised by 5°C). OVA loaded liposomes were used, as moisture results from FDC1 showed no significant difference in residual moisture content between empty and OVA loaded liposomal formulations. The residual moisture content for liposomal formulations FD by FDC2 and FDC3 showed that changes in the drying conditions can improve residual moisture content. The residual moisture content for both FDC2 and FDC3 was around 2%, reiterating the importance of secondary drying to remove excess moisture (Franzé et al., 2018).

However, there is a difference in residual moisture content for formulations undergoing freeze drying by FDC2 (ramp) or FDC3 (snap frozen) (Table 7.13). The measured moisture content for OVA loaded DMPC:Chol and DSPC:Chol was 1.00% and 1.35% for FDC2, compared to 2.30% and 2.44% for OVA loaded DMPC:Chol and DSPC:Chol formulations using FDC3 (Table 7.13). No significant difference between the formulations was observed highlighting the freeze drying approach is the most important factor with regards to the residual moisture content of the sample (Table 7.13). Extension of the primary drying phase for FDC2 up to 22 hours compared to 10 hours for FDC3 has a beneficial effect on the residual moisture content. For freeze dried liposomal formulations to meet the standards specified, it is important the correct volume of cake and appearance is achieved. The amount of residual moisture content can vary depending on the liposome formulations; while formulations with high residual moisture content can be stable, the International Conference on Harmonisation (ICH) Q8 (R2) recommends producing freeze dried formulations with a residual moisture content of less than 2% (ICH Q8 (R2) (ICH, 2009)). For instance, freeze dried doxorubicin loaded liposomes with a residual moisture content of below 1% were stable for 6 months and did not undergo degradation (Tang and Pikal, 2004).

In addition, residual moisture content below 2% is not essential for protein loaded liposomes; proteins require some residual hydration for stability, with the residual level of hydration varying depending on the protein (Zheng et al., 2008, Luthra et al., 2007, Hubbard et al., 2007). The results obtained from FDC2 are optimal; out of FDC1-3 it is the preferred conditions for the production of high quality FD liposomes likely to demonstrate long-term stability. The ability to selectively screen, and efficiently FD and produce high quality FD liposomes has been shown using FDC2.

**Table 7.13.** The residual moisture content of liposomes freeze dried under different conditions, containing the cryoprotectant sucrose.

<b>FREEZE DRYING CONDITIONS</b>	<b>SAMPLE (CONTAINING 10% SUCROSE)</b>	<b>RESIDUAL MOISTURE CONTENT (%)</b>
<b>FDC1</b>	Empty liposomes	4.23
	OVA loaded liposomes	4.14
<b>FDC2</b>	OVA loaded DMPC:Chol	1.00
	OVA loaded DSPC:Chol	1.35
<b>FDC3</b>	OVA loaded DMPC:Chol	2.30
	OVA loaded DSPC:Chol	2.44

## 7.5 Conclusion

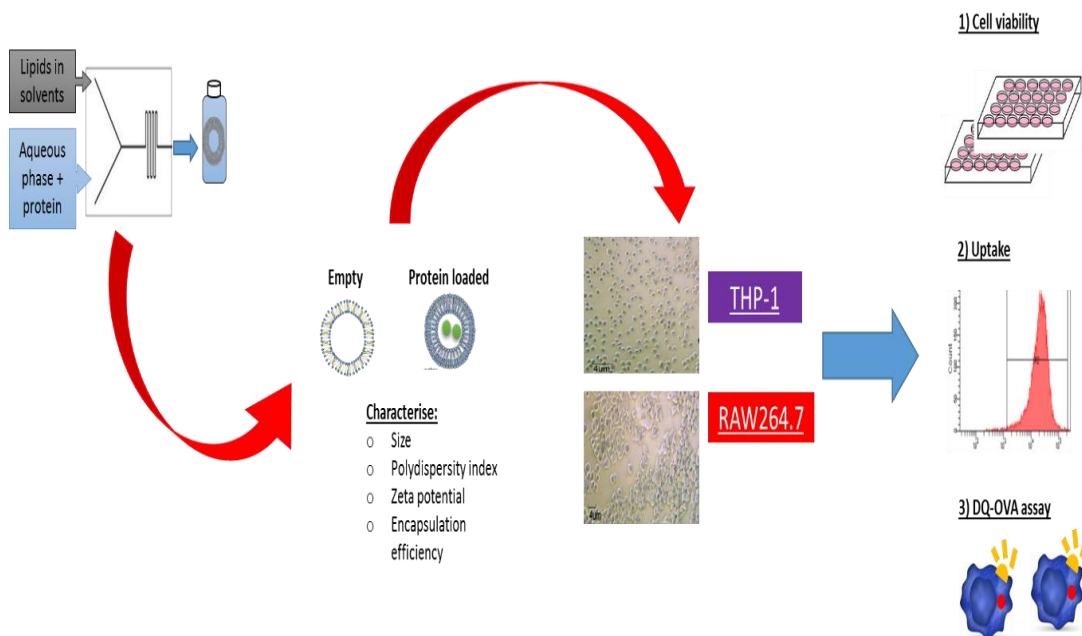
In conclusion, applying the DoE to microplate formats enables high throughput screening of formulations for freeze drying of liposomes. Microplates can rapidly and easily identify optimal parameters including cryoprotectant screening and concentration screening, with little material being consumed. The results from this chapter showed that the lipid type, the presence of protein, type of cryoprotectant and its concentration all play a role in the production of freeze dried stable liposomes. In line with previous literature, the disaccharide sugar sucrose is efficient in its role as a cryoprotectant (Crowe and Crowe, 1988). There is little to no leakage of the protein OVA during the whole manufacturing process. The availability of the cryoprotectant, and simplicity of the process make it ideal for the high throughput manufacturing and preservation of liposomal medicine. The ramp freezing coupled with the FDC2 parameters was the best cycle for the preservation of OVA loaded DMPC:Chol and DSPC:Chol liposomes. The liposome physicochemical properties and protein encapsulation remain the same, as well as producing FD cakes with low residual moisture content. The simple manufacturing process of liposomes by microfluidics alongside a straightforward FDC2 (Table 7.14) cycle, are promising options for manufacturing and overcoming previous challenges associated with the production of FD liposome formulations.

**Table 7.14.** The optimal freeze drying cycle for the preservation of protein loaded liposomes.

<b>FREEZE DRYING CYCLE 2 (FDC2)</b>	
<b>FREEZING</b>	Ramp freezing of samples (from 4°C to -45°C)
<b>PRIMARY DRYING</b>	Apply vacuum of 0.1 mBar Ramp the shelf temperature up from -45°C to -25°C Hold for 22 hours
<b>SECONDARY DRYING</b>	Ramp the shelf temperature up from -30°C to 30°C Hold for 6 hours
<b>FINAL PRODUCT</b>	Seal the vials

# Chapter 8

## Developing rapid in vitro screening tools to investigate liposomal formulations



## **8.1 Introduction**

### **8.1.1 Consideration of factors influencing the interactions between cells and liposomal formulations**

#### **8.1.1.1 Impact of liposomal formulation characteristics on cells**

When considering formulation development, it is important to be able to screen drug delivery formulations with regards to cellular delivery for understanding cell interactions, cytotoxicity and uptake amongst other things. There are a wide range of models and protocols available to consider these interactions but many of these are time-consuming and there is large variability in protocols used. Liposomes are well recognised for their versatility, biodegradability and low toxicity as well as the ability to protect the API of interest (Allen and Cullis, 2004). They have been explored as delivery systems, including for the use of vaccines by targeting phagocytic cells. The targeting of these cells including macrophages, dendritic cells and monocytes enables the manipulation of the immune system to treat a wide range of diseases and infections. However, there is a lack of in vitro models available to rapidly screen liposomal formulations in terms of vaccines efficacy. Such a tool would be particularly advantageous in the development of liposomal adjuvants, as liposomal formulations have physicochemical properties that can be manipulated and used to facilitate their uptake by cells, including monocytes and macrophages. Several factors influence the uptake of the formulations; the size and charge of formulations highly influence uptake. Yet, the mechanism and key quality attributes that control uptake are not well understood. Many studies have shown small sized liposomes (around 100 nm) can be taken up by a wide range of cells including phagocytes by non-receptor mediated processes (Ahsan *et al.*, 2002), whilst larger sized liposomal formulations are more likely to target phagocytic cells. As a result, the optimal size of the formulation can be tailored and adjusted according to the desired therapeutic effect and specific cell targeting.

The charge of the liposomal formulation can also impact uptake and functionality of the systems. Positively charged cationic liposomes are efficient at delivering APIs to the desired cells (Zuhorn *et al.*, 2007); however, the strong electrostatic attraction between positively

charged liposomal formulations and negatively charged cells (in particular phagocytic cells) can elicit a strong undesired immune reaction therefore limiting their use in therapy (Zhang *et al.*, 2005). Due to this, negatively charged or neutral liposomal formulations are more favoured. Negatively charged anionic liposomes containing lipids such as phosphatidylserine (PS) and phosphatidylglycerol (PG) are readily taken up by cells despite both cells and the anionic formulations having a negative electrostatic charge (Ahsan *et al.*, 2002). Although they are good at delivering cargo, the amount of protein they can encapsulate is less than what is achieved by neutral formulations. For instance, Forbes *et al.* (Forbes *et al.*, 2019) showed that DSPC:Chol formulations containing PS (DSPC:Chol:PS liposomes) resulted in a decrease in encapsulation efficiency to ~20% (10% lower encapsulation efficiency of the protein ovalbumin) in comparison to the neutral DSPC:Chol formulations (where around 34% encapsulation efficiency is achieved). Similar differences in encapsulation efficiency were also reported by Colletier *et al.*, whereby substituting the neutral lipid POPC for the anionic lipid POPS, lead to a 20% reduction in encapsulation efficiency of acetylcholinesterase from 40% encapsulation efficiency achieved by neutral formulations (Colletier *et al.*, 2002). The difference in encapsulation results show the electrostatic charge between proteins and lipids greatly impacts the encapsulation efficiency of the liposomal formulations, hence neutral liposomal formulations were considered for their ability to be taken up by cells.

#### **8.1.1.2 Consideration of cell lines for investigation of liposomal interactions**

Liposomes offer a means of therapeutic targeting, and naturally come into contact and target phagocytic cells. The role macrophages and monocytes play in control of disease and maintaining immunity is very important, therefore targeting these particular cells can be important. Unlike other non-phagocytic cells such as epithelial cells, macrophages (and other mononuclear phagocytic cells) are able to take up liposomes by phagocytosis in addition to other routes such as endocytosis. To aid with this receptor mediated uptake, mononuclear phagocytic system (MPS) cells express a range of ligands including; antibody receptors (Fc-receptors), mannose receptors, toll-like receptors, scavenger receptors and integrins. Targeting these allows for the delivery of the liposomal formulation to specific cells, therefore macrophages are widely used as model cells to study, characterise and optimise ideal liposomal formulation parameters in-vitro.

Based on this, macrophages were selected as model cells for understanding the liposomal formulation interactions, and identifying ideal and optimal delivery conditions. A suitable in-vitro model to represent biological conditions is required, which is easy to conduct and offers a simple and reliable method to study macrophage differentiation, interactions, functions and responses from external stimuli such as liposomal formulations. Despite primary cells being ideal for this, obtaining primary MPS cells (like macrophages and dendritic cells) is difficult. The correct identification and isolation of these cells is challenging; dendritic cells are sensitive to mechanical stress, which can result in alteration of their phenotypic markers (Marshall *et al.*, 2015). To overcome this, monocytes can be isolated from the buffy coat of blood and stimulated to differentiate into monocyte derived macrophages (MDMs) and monocyte derived dendritic cells (MDDCs) (Blank *et al.*, 2006). However, the cells are very small in number, therefore obtaining a sufficient amount for testing is yet another obstacle that limits research with primary cells. As a result, many research laboratories use cell lines for their research, due to their ease in culture, ready availability and transferability across groups, making them ideal for cell culture models. Table 8.1 reviews some of the monocyte/macrophage cell lines available for research, of which the THP-1 cells are the most popularly used for in-vitro cell cultures. The cell line is genetically homogenous, therefore minimizing the degree of variability of the cells over a number of passages (Chanput *et al.*, 2014, Chanput *et al.*, 2015). Stimulated macrophage-like THP-1 cells are often used in immunological studies, and are incredibly versatile. Studies can be performed on monocyte THP-1 cells as well as in their differentiated macrophage-like form, with the ability to co-culture these cells with others. Comparison of these THP-1 monocytes with human derived primary PBMC cells have been conducted, with similar results obtained for both the THP-1 cell line and the primary cells (Chanput *et al.*, 2014). For instance, upon stimulation of cells for three hours with lipopolysaccharide, both the THP-1 cell line and PBMCs showed upregulation of the toll-like receptors (Hijiya *et al.*, 2002). Based on this, the human derived THP-1 cell line along with the murine RAW264.7 cell line were used to investigate liposomal formulations.

**Table 8.1.** Comparison of monocyte/ macrophage cell lines.

ZCELLS	SOURCE	ADVANTAGES	DISADVANTAGES	REF
<b>THP-1</b>	Monocytic cells taken from 1 year old suffering from acute monocytic leukaemia.	Quick doubling time of 35- 50 hours. Has a low biosafety level (does not contain toxic products or virus components).  Homogenous genetic background therefore minimizing variability	Needs stimulating with PMA for 24 hours before they can be used as macrophages	(Chanput <i>et al.</i> , 2014, Chanput <i>et al.</i> , 2015)
<b>U937</b>	Myeloid cell taken from a 37 year old Caucasian male.	Quick doubling time.  Can use till a high passage number	Needs stimulating with PMA for 24 hours before they can be used as macrophages.	(Chanput <i>et al.</i> , 2014, Chanput <i>et al.</i> , 2015)
<b>RAW 264.7</b>	Macrophage obtained from an adult male BALB/c mouse.	Doesn't require stimulation and widely available.  Homogenous cells therefore less variants in results.	Mouse origin	(Xie and Calaycay, 1992)
<b>J774.2</b>	Mouse BALB/c monocyte macrophage	Cheaper.  Homogenous cells  No contamination risks from other cells.	Mouse origin.  May not fully represent the diversity found in primary cells	(Mukherjee <i>et al.</i> , 1996)



### 8.1.2 Cells on a chip

The use of microfluidics devices to study cells and cell culture is becoming more popular; the ability to control many process parameters whilst culturing cells, studying cell-cell interactions between individual cells, and investigating in real time offers a viable alternative to traditional cell culture methods. There have been many suggested uses for lab on the chip devices for example, 3D organ culturing, growing and priming T-cells for T-cell therapy and analysis (Sarkar *et al.*, 2015). There are pros and cons for both microfluidic and macroscopic levels of culture (Table 8.2). Unlike the traditional macroscopic methods of growing cells in a flask, the microfluidics devices offer the ability to automate, and rapidly run multiple parallel designs. Despite this, the use of microfluidics devices to study cells is in its early days and the full potential use remains to be seen (Halldorsson *et al.*, 2015). As a result, in this chapter, the potential to pass cells through the benchtop Nanoassemblr device was investigated. Using non adherent cells, the ability to pass THP-1 cells through the Nanoassemblr chip was tested (Figure 8.1).

**Table 8.2.** The advantages and disadvantages of microfluidics cell culture and macroscopic cell cultures.

	<i>ADVANTAGES</i>	<i>DISADVANTAGES</i>
<i>MICROFLUIDIC CELL CULTURE</i>	<ul style="list-style-type: none"> <li>• Flexibility of design</li> <li>• Automation and better experimental control</li> <li>• Lower number of cells required</li> <li>• Can study multiple parameters quickly</li> <li>• Ability to perform real time chip analysis</li> </ul>	<ul style="list-style-type: none"> <li>• Novel surface exposure (for example PDMS)</li> <li>• Transfer of knowledge is difficult</li> <li>• No known standard procedure</li> <li>• Chip design and operational set ups can be difficult</li> </ul>
<i>MACROSCOPIC CELL CULTURE</i>	<ul style="list-style-type: none"> <li>• Well known standardized procedures</li> <li>• Measurements in pH, CO<sub>2</sub> and O<sub>2</sub> levels are well recorded</li> <li>• Pre-existing knowledge and literature makes knowledge transfer easier</li> <li>• Materials, reagents and equipment are easily available</li> <li>• Easy to do</li> </ul>	<ul style="list-style-type: none"> <li>• High reagent consumption</li> <li>• Not as flexible; limited in the type of flasks that can be used</li> <li>• Hard to study one individual cell</li> <li>• Media is stagnant</li> </ul>

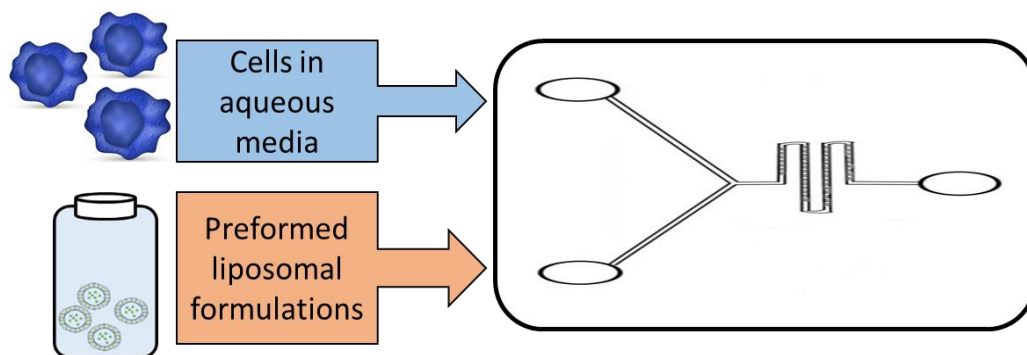


**Figure 8.1.** Exposing cells in aqueous media to pre-formed liposomes (produced by microfluidics) to encourage mixing, study uptake and interactions.

## 8.2 Aim and Objectives

The aim of the work in this chapter was to investigate the cellular interactions of empty and OVA loaded liposomes, and to explore the use of microfluidics for cell mixing. To determine this the following were objectives investigated:

1. Investigate the effect of lipid, OVA concentration and lipid concentration on cell viability and uptake.
2. Understand the efficiency and functionality of the liposomal formulations.
3. Investigating high throughput mixing and processing of cells by using microfluidics technology.

## 8.3 Materials and Methods

### 8.3.1 Materials

Phosphatidylcholine (PC), 1,2-dimyristoyl-sn-glycero-3-phosphocholine (DMPC), 1,2-dipalmitoyl-sn-glycero-3-phosphocholine (DPPC) and 1,2-distearoyl-sn-glycero-3-phosphocholine (DSPC) were all obtained from Avanti Polar Lipids Inc., Alabaster, AL, US. Cholesterol, Ovalbumin (OVA), D9777-100FT dialysis tubing cellulose membrane and trifluoroacetic acid was obtained from Sigma Aldrich Company Ltd., Poole, UK. For OVA purification and release studies the Biotech CE tubing (MWCO 300 kD) was used from Spectrum Inc., Breda, The Netherlands. For sample purification by Tangential flow filtration (TFF) a modified polyethersulfone (mPES) 750 kD MWCO hallow fibre column was purchased from Spectrum Inc., Breda, The Netherlands. The 2-mercaptoethanol (31350-010), RPMI medium 1640 (A10491-01), DQ-OVA (D12053), Dulbecco's modified eagle medium (42430-025), Trypsin-EDTA and Foetal bovine serum (FBS) was ordered from Life technologies, Thermo Scientific., Hamel Hampstead., England, UK. CellTiter-Blue® cell viability assay (G8080) was ordered from Promega. A Jupiter column (C18 (300 Å), 5 µm, dimensions 4.60 X 150 mm) was procured from Phenomenex., Macclesfield, UK. HPLC grade Methanol and 2-propanol were purchased from Fisher Scientific., Loughborough, England, UK. All water and solvents used were HPLC grade. THP-1 cells and RAW264.7 cells were gifts from Dr. Dino Rotondo and Dr. Andrew Paul respectively (SIPBS, University of Strathclyde, Glasgow). The MH-S (95090612) alveolar macrophage cells were purchased from the European collection of authenticated cell cultures (ECACC)., Salisbury, UK.

### 8.3.2 Methods

#### 8.3.2.1 THP-1 cells

THP-1 cells are a continuous cell line derived from human blood monocytes. When cultured this cell line grows in suspension with some cells displaying adherent properties. The cells are grown in complete RPMI media (containing 10% fetal bovine serum and penicillin streptomycin) and allowed to grow till 70- 80% confluency before being passaged. In order to use the cells as macrophages, the human monocytes need to be stimulated to undergo differentiation. To induce differentiation, Vitamin D3 (VD3) is added to the cells at 100 nM

(1:1000 dilution). The cells are then poured into a petri dish and left for 48 hours to undergo differentiation. The marker CD14 is used to confirm the cells have undergone differentiation into macrophages using flow cytometry.

### **8.3.2.2 RAW264.7 cells**

RAW264.7 cells are a continuous cell line derived from macrophages of mice origin. The cells are adherent and are grown in DMEM supplemented with 10% FBS and Pen/Strep allowed to grow till 60- 70% confluency before being passaged. The cells have a high turnover; cells are passaged every 3 days depending on the confluency. Cells from passage 5 to 32 were used.

### **8.3.2.3 Cell counting**

A light microscope was used to count the number of viable cells so that the correct seeding density could be calculated. Cells mixed with Tryphan blue are counted using a haemocytometer grid, with the average of from four squares (4x4 squares) counted. The dye stains dead cells blue and so consequently only live cells are accounted when calculating the seeding density for in- vitro studies. The equation 8.1 was used to calculate the cell density:

Equation 8.1

$$\text{Cell density} = \text{average no. of cells} \times \text{dilution factor} \times 10^4$$

*Whereby:*

- The average number of cells is the average number of cells taken from the 4x4 grid counted in the haemocytometer.
- The dilution factor is the ratio of the volume of cells to the Tryphan blue dye added. For example if 20  $\mu\text{l}$  of dye is added to 20  $\mu\text{l}$  of cells then the dilution factor is 2.

### **8.3.2.4 Cell imaging**

Pictures of cells were taken using a light microscope and the imaging software ImagePro2. Cells to be imaged were kept in the flasks and where placed on the microscope platform. The objective for the camera was x10 whilst the magnification lens could be changed but was kept at x10. The overall magnification for the cells was x100. Images were taken using a

randomized procedure with the images edited to measure the average size of cells using the editing software.

### 8.3.2.5 Viability assays

Cell titre-blue (Promega®) is an in-vitro colorimetric assays used to determine cell viability. It is a metabolic assay, whereby living cells are able to convert resazurin which is blue in colour into the fluorescent product resorufin (Figure 8.2). There is a visible colour change from blue to pink if living cells are present. The amount can be quantified by using a spectrophotometer at 590 nm. Confluent cells were plated on a 96 well plate at a density of  $1-2 \times 10^6$ /mL. For the cell viability assay, confluent THP-1 or RAW264.7 cells were plated on a 96 well plate at a density of  $1-2 \times 10^6$ /mL, with 100  $\mu$ L added to each well. They were left for 24 hours so the cells could settle from the handling. Liposomes were added at a concentration of 0.006- 0.2 mg/mL for 24 hours, after which they were removed. CellTitre blue (CBT) was added to these wells at a volume of 20  $\mu$ l per 100  $\mu$ l of media, and left for between 1- 5 hours (till a colour change occurred). The quantification of viable cells was determined by calculating the percentage difference between the positive cells (cells without exposure to liposomes) and the test wells. The following controls were used; a negative control of lysed cells that have previously been treated with liposomes before lysis, liposomes without the presence of cells and a positive control of untreated cells.

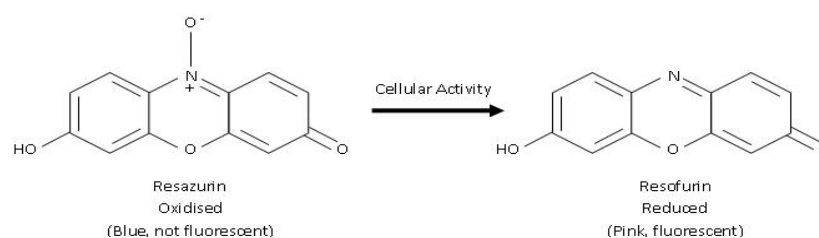


**Figure 8.2.** Metabolic reaction that causes a visual change in the cell culture solution allowing detection of cell viability.

### 8.3.2.6 Uptake studies

RAW264.7 and stimulated THP-1 were plated at a density of  $1-2 \times 10^6$  cells/mL, using 24 well plates. The DiIC labelled liposomes (100  $\mu$ g/mL) were added and left for up to three hours; the liposomes were removed after 30 minutes, 1, 2 and 3 hours respectively. The formulations were then removed and cells were washed with phosphate buffered saline

(PBS) three times. A parallel experiment was done with the cells kept at 4°C to stop endocytosis as a control experiment. The cells were detached from the plates by cells scraping (for RAW264.7 cells) or using trypsin (500 µL) for 10 minutes (for THP-1 cells). Post trypsin, 500 µL of fresh media was added. The cells were then centrifuged for 5 minutes at 300 xg, after which the supernatant was discarded. The cell pellets were suspended in PBS (500 µL). Uptake of liposomes was then measured by flow cytometry at 549/ 565 nm ex/em.

### **8.3.2.7 Determining THP-1 cell differentiation**

The differentiation of the THP-1 cells was determined by detection of CD14 expression using the BD FACS canto (BD Biosciences, UK). For this a fixative and flow wash buffer needed to be prepared. The fixative was made of 1% v/v Formaldehyde in PBS. The flow wash buffer consists of 1% w/v Bovine Serum Albumin in PBS (isotonic and buffered to neutrality, to cushion the cells against damage during centrifugation, block non-specific staining, and prevent capping of bound antibody). Stimulated and non-stimulated THP-1 cells were added at an equal volume at a concentration of  $1 \times 10^6$  cells into FACS tubes. After centrifugation at 300g for 5 minutes the suspension was removed and the cell pellets were suspended in 1 mL of 0.1% BSA/PBS per tube. This was repeated twice after which 100 µL of antibody (IgG specific from Cambridge Biosciences (319801)) was added. The samples were then incubated on ice and in the dark for 20 minutes. After incubation, 1 mL of 0.1% BSA/PBS was added to each tube and centrifuge at 1200 rpm for 5 minutes. The step was repeated three times with the supernatant discarded after each spin. After which 500 µL of 1% formaldehyde/PBS to each tube to fix the cells. The samples were then analysed using flow cytometry using 5000 events.

### **8.3.2.8 Investigating protein integrity using DQ-OVA**

Cells were grown on 24 well plates till confluent. Ovalbumin and DQ-OVA loaded liposomal formulations were exposed to the cells for three hours. The DQ™ovalbumin is a self-quenched conjugate of ovalbumin that was loaded into neutral DMPC:Chol and DSPC:Chol liposomes. The DQ-OVA is conjugated to the dye BODIPY FL and only fluoresces once the OVA undergoes enzymatic degradation by the cells. If degradation occurs the DQ-OVA goes on to exhibits bright green fluorescence. After three hours, the particles and liposomes were removed, and the cells were washed with PBS three times. The cells were then added to flow cytometer tubes and measured using the BD FACSCanto at 505/ 515 nm of ex/em. To

calculate the amount of DQ-OVA processing, the mean fluorescence intensity was compared to non-encapsulated DQ-OVA controls.

### **8.3.2.9 Statistical packages**

The results are represented as mean  $\pm$  SD with n=3 independent batches. T-tests and ANOVA tests were used to assess statistical significance, with a Tukey's post ad-hoc test.

## **8.4 Results**

### **8.4.1 Morphological analysis of cells**

The ability to use light microscopy provides an easy, non-invasive, and quick alternative (to fixing or freezing) for the visualisation of cells. The viewing of live cells, provides non-distorted images without the risk of missing components (Fiolka, 2014). Light microscopy allows images of the cells to be obtained as passing light directly through a cell culture causes the light wavelength to change. The changes in the wavelength are associated with the refractive index of cells, allowing for images to be obtained. Phase contrast, dark field microscopy and differential interference contrast all allow for cell morphology to be determined, as well as observations of processes like mitosis or changes in movement. Studying the cells in terms of their shape and appearance is important for confirming the cells are healthy. It allows identification of deterioration of cells including granularity around the nucleus and detachment from the surface if the cells are adherent. Figure 8.3 shows the morphology of non-stimulated THP-1 cells (Figure 8.3A) and RAW264.7 cells (Figure 8.3B). The THP-1 cells in media are round in morphology and semi-adherent, which is expected for non-differentiated THP-1 cells (Michée et al., 2013). The majority of the RAW264.7 cells are circular in shape with a few irregular shaped cells, which is similar to what is shown by the European Collection of Authorised Cell Culture (ECACC) (Culture, 2018).

Furthermore, the THP-1 cells were stimulated with vitamin D3 (VD3) for up to three days, with the THP-1 cells visualised each day (Figure 8.3C). The cells were observed for morphological changes, with the THP-1 cells losing the round shape. At 24 hours the cells become attached and become more elongated, this is more clearly observed after 48 hours where the majority of THP-1 cells have undergone differentiation. These results are in keeping with previously published reports, whereby differentiation causes THP-1 cells to become adherent (Michée et al., 2013), with changes in cellular shape observed regardless of

whether the cells are stimulated by VD3 or Phorbol-12-myristate-13-acetate (PMA). To quantify the amount of THP-1 cells that have undergone differentiation, flow cytometry was performed. The flow cytometry analysis (in Figure 8.4) show stimulating THP-1 cells with VD3 over two days results in more than 90% of THP-1 cells undergoing differentiation into macrophage like cells. There is a clear shift in the peaks whereby differentiated cells are shifted and so can be detected by the use of antibodies. These results are in keeping with previous research which has shown both VD3 and PMA are viable methods for THP-1 differentiation (Daigneault *et al.*, 2010). During macrophage differentiation, internal changes within the cells occur. For instance, macrophage differentiation causes an increase in granularity and cytoplasmic volume which is observed in both primary cells and for THP-1 cells differentiated by VD3 stimulation (Sokol *et al.*, 1987, Daigneault *et al.*, 2010). As both primary and cell line macrophages display similar characteristics, the RAW264.7 cell line and THP-1 cell line were used. The THP-1 cells are stimulated with VD3, as is not as sticky as phorbol 12-myristate 13-acetate (PMA) and is easier to remove post- differentiation of THP-1 cells.

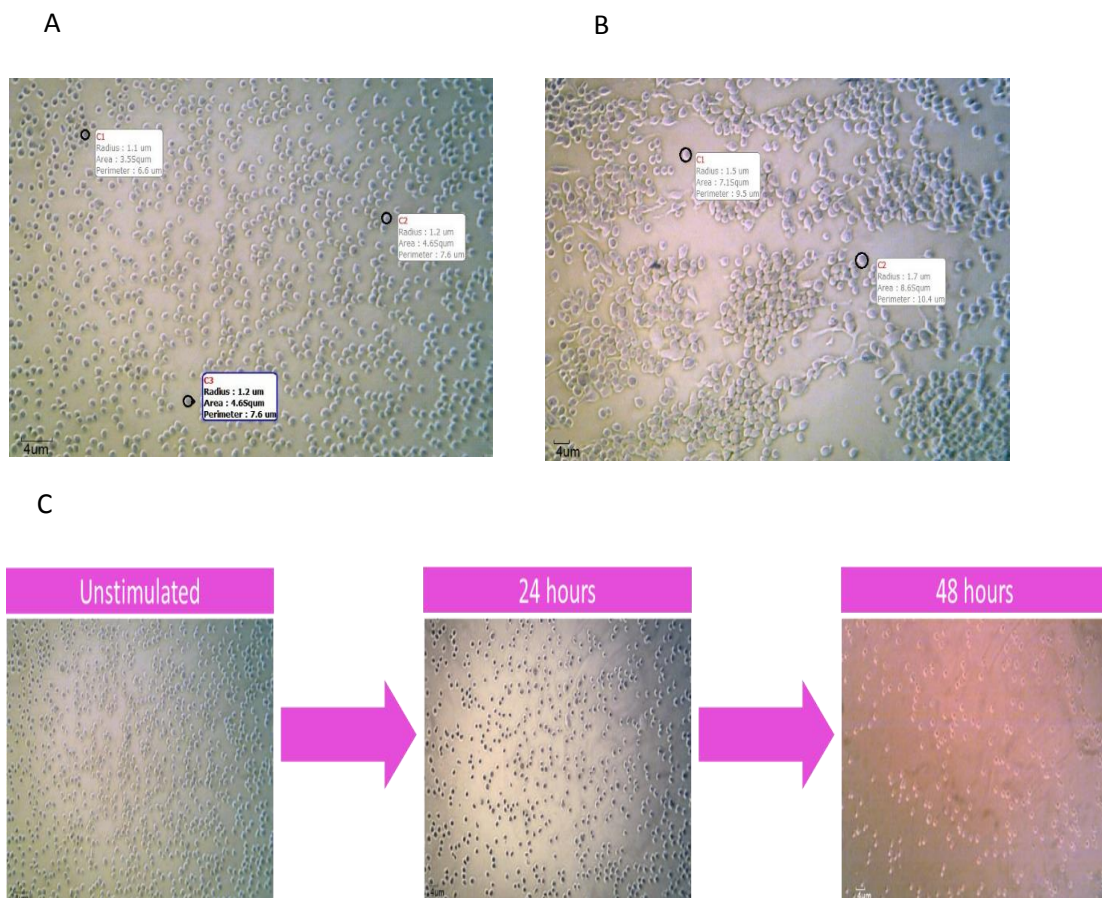




**Figure 8.3.** Morphology of undifferentiated THP-1 cells (A) and RAW264.7 cell line (B). After THP-1 cells are stimulated with Vitamin D3, images of the cells were taken every 24 hours for 2 days to observe any morphological change due to differentiation (C). The results are representative of the sample.

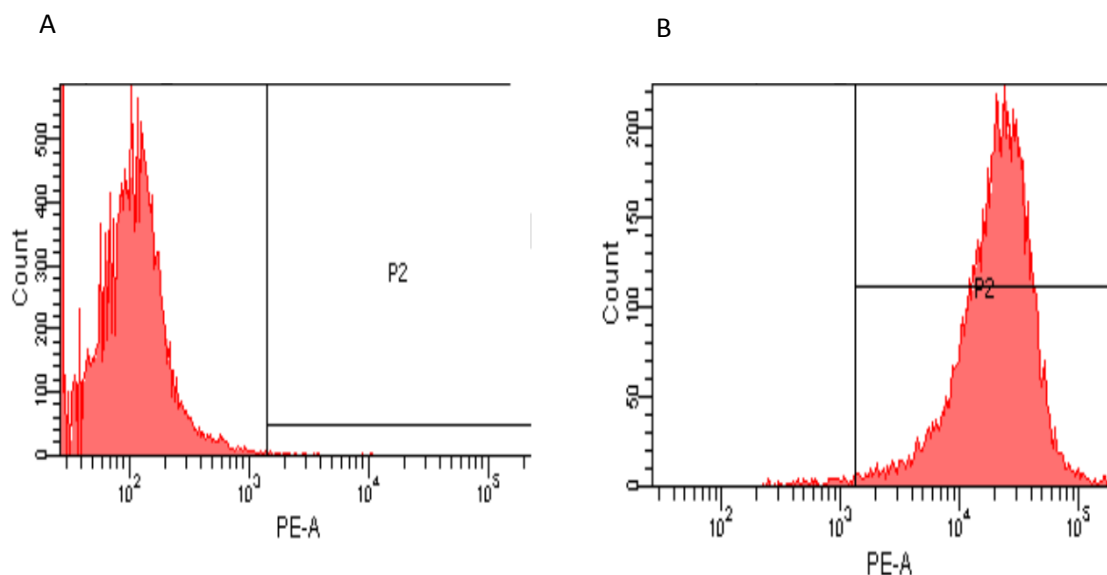


**Figure 8.4.** THP-1 cells that have not been differentiated are shown by the histogram (A), while the histogram on the right shows the positive cell population which had differentiated (B).

#### 8.4.2 Cell viability of cells exposed to liposomal formulations

In general, liposomal formulations are regarded as biodegradable and non-toxic. Cell viability of the neutral formulations were conducted to establish a working liposome concentration range and to confirm lack of toxicity. Formulations produced were conducted with and without the encapsulation of the protein ovalbumin (OVA). The formulations were tested on differentiated THP-1 cells and RAW264.7 cells. Initially, one liposomal formulation with low transition temperature (DMPC) and one with high transition temperature (DSPC) was selected and coupled with cholesterol (Chol) at a 2:1 wt/wt ratio. The concentration of empty DMPC:Chol and DSPC:Chol exposed to differentiated THP-1 cells and RAW264.7 cells was varied (between 6-200  $\mu\text{g}/\text{mL}$ ), with the cell viability tested. The formulations produced by

microfluidics (at a 3:1 FRR and 15 mL/min TFR) were less than 100 nm in size and a PDI of less than 0.2 illustrating homogeneity of the formulations.

The empty DMPC:Chol and DSPC:Chol liposomal formulations are non-toxic across a range of concentrations, with a cell viability of more than 90% determined across a range of concentrations (Figure 8.5). At a concentration of 200  $\mu\text{g}/\text{mL}$ , the RAW264.7 cell viability for DMPC:Chol is  $104 \pm 1.4\%$  and  $95 \pm 2\%$  for DSPC:Chol liposomes (Figure 8.5A). Similarly, the cell viability for THP-1 cells was  $99 \pm 4\%$  for DMPC:Chol liposomes and  $101 \pm 3\%$  for DSPC:Chol liposomes at a concentration of 200  $\mu\text{g}/\text{mL}$  (Figure 8.5B). The high cell viability observed irrespective of the liposomal formulation, suggests the neutral liposomal formulations are safe for exposure to both macrophage cell lines (THP-1 cells and RAW264.7 cells). This was further explored by exposing PC:Chol, DMPC:Chol, DPPC:Chol and DSPC:Chol liposomal formulations to RAW264.7 cells. The results from Figure 8.6 show that the lipid type does not impact the cell viability with a 95% cell viability calculated for all four lipids for both cell lines.

Furthermore, OVA encapsulated within the neutral liposomal formulations was investigated. Initially DMPC:Chol and DSPC:Chol liposomes were produced using microfluidics (at a 3:1 FRR and 15 mL/min TFR) with varying amount of OVA. The toxicity of these formulations was then tested using RAW264.7 cells; the results once again showing a cell viability of near 100% (Table 8.3), suggesting the combination of protein and neutral liposomes is non-toxic and biocompatible. Based on this, OVA loaded DMPC:Chol and OVA loaded DSPC:Chol liposomes were selected to test the cell viability for THP-1 cells. Empty and OVA loaded liposomes at a liposomal concentration of 100  $\mu\text{g}/\text{mL}$  were tested in parallel. A liposome concentration was selected as previous results have shown even at high concentrations, the liposomal formulations are non-toxic. The results from Table 8.3 show the presence of OVA protein having no impact on cell viability which remained near 100% for THP-1 cells. The biocompatibility of the liposomal formulations coupled with cells is essential for the therapeutic effects to be carried out. In general, neutral formulations are less toxic in comparison to positively charged cationic liposomal formulations. For instance, RAW264.7 cells exposed to positively charged liposomes containing stearylamine (SA) induce apoptosis. This is induced by the production of reactive oxygen species (ROS) and releasing cytochrome 3 amongst other things (Takano et al., 2003, Iwaoka et al., 2006), which is caused by the triggering of the mitochondrial pathway (Aramaki et al., 2001). As a result, neutral liposomal

formulations can be used as drug delivery vehicles as they don't induce a strong immune reaction, but can alternatively be used as vaccine adjuvants.

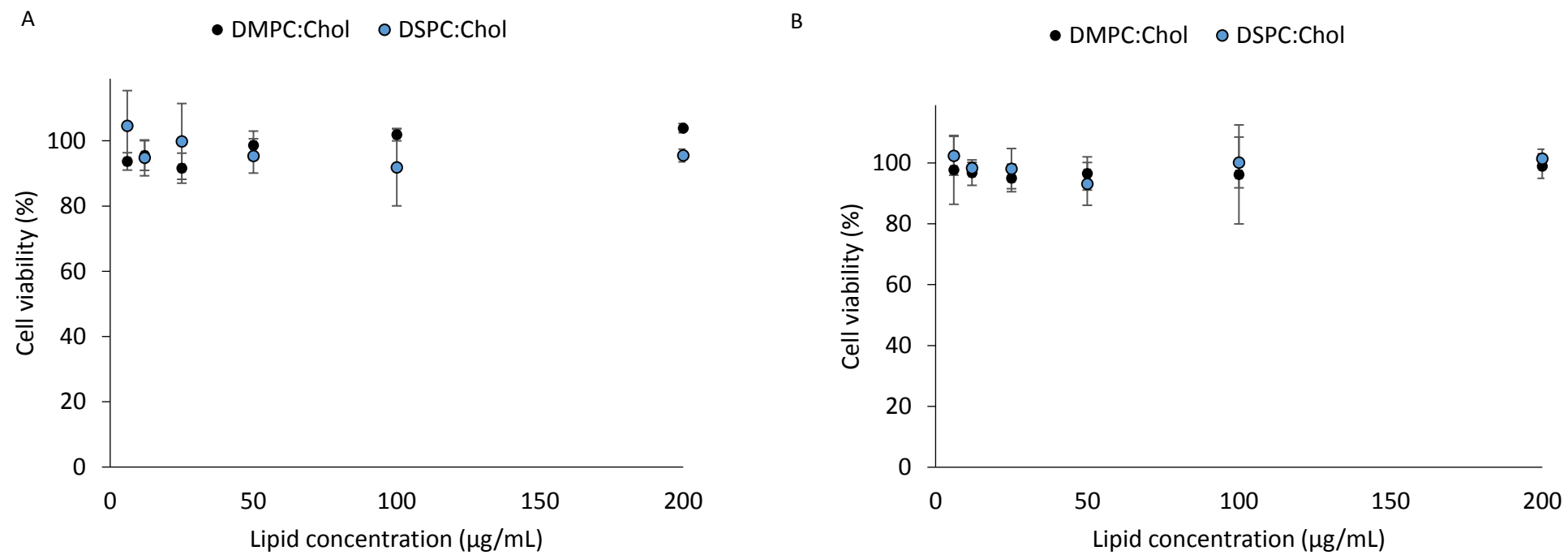


**Figure 8.5.** Cell viability of DMPC:Chol and DSPC:Chol liposomes exposed to RAW264.7 cells (A) and differentiated THP-1 cells (B). The DMPC:Chol and DSPC:Chol were produced by microfluidics at a 3:1 FRR and 15 mL/min TFR. Varying concentrations of the lipid were exposed to the cells plated in 96 well plates and left for 24 hours. The cell viability was then calculated using the cell titre blue assay. The results represent mean  $\pm$  SD, n=3 independent batches.

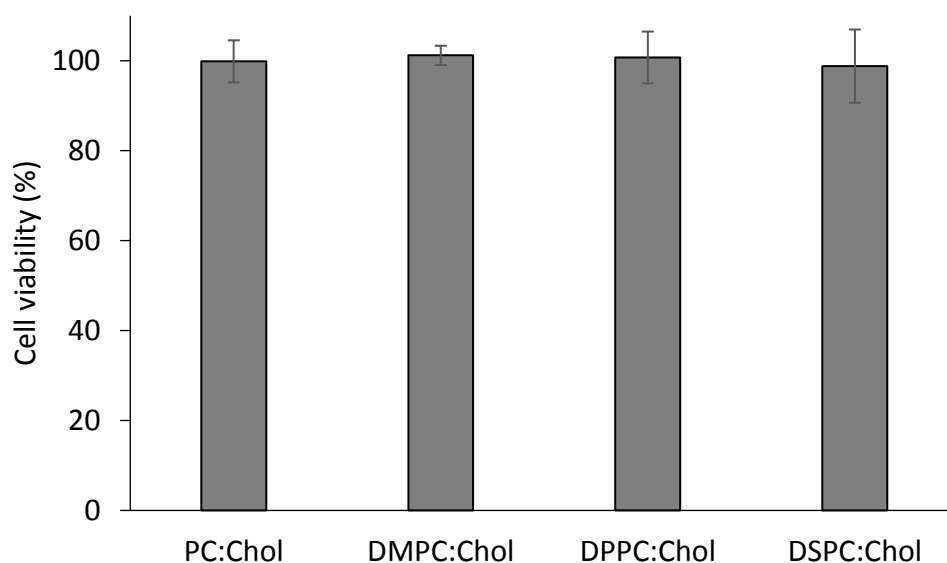


**Figure 8.6.** RAW264.7 cells were exposed to four neutral formulations containing OVA. The four formulations were made at a 3:1 FRR and 15 mL/min TFR. The aqueous phase contained 0.25 mg/ mL of OVA. The formulations were purified using TFF. The cells were exposed to 100 µg/ mL of each formulation and cell viability was determined using cell titre blue. Results represent mean ± SD, n=3 independent batches.

**Table 8.3.** Cell viability of RAW264.7 cells when exposed to empty and Ovalbumin (OVA) loaded DMPC:Chol and DSPC:Chol liposomes. The DMPC:Chol liposomes containing a different starting concentration of OVA were produced using microfluidics at a 3:1 FRR and 15 mL/min TFR. Similarly, empty and OVA loaded DSPC:Chol liposomes, using 0.25 mg/mL initial OVA were produced at a 3:1 FRR and 15 mL/min TFR. The liposomes were added to RAW264.7 cells and left for 24 hours, with the cell viability measured using the cell titre blue assay. The results represent mean ± SD, n=3 independent batches.

OVA CONCENTRATION (µG/ML)	0	100	250	500	750
DMPC:CHOL	100 ± 6.5%	101 ± 1.7%	103 ± 4.4%	101 ± 2.1%	98 ± 3.1%
DSPC:CHOL	97 ± 5.4%	-	95 ± 4.6%	-	-

### 8.4.3 Uptake of liposomal formulations by macrophage cells

The uptake of the liposomal formulations is necessary for the formulations to be therapeutically active. Liposomal physicochemical properties can influence the uptake of the formulations by cells with size playing an important role, which greatly impact the endocytosis of the formulations. The type of endocytosis undertaken by the cells can vary, with spherical shaped liposomes less than 200 nm more readily taken up by both MPS and non-MPS cells (Jiang et al., 2008, Rejman et al., 2004). To determine the efficiency of the liposomal formulations, the uptake of empty and OVA loaded DMPC:Chol and DSPC:Chol liposomes by macrophage cell lines (THP-1 and RAW264.7 cells) was investigated. The liposomal formulations produced by microfluidics were fluorescently labelled using DiIC to allow for quantification of uptake. The physicochemical properties of the formulations, summarised in Table 8.4 are below 100 nm in size, are homogenous as illustrated by a PDI of below 0.2 and neutral (with a zeta potential of above -10 mV). As the formulations were within specification, these formulations were used for cell culture. Uptake studies were conducted at two temperatures; both 37°C and 4°C with the study run at the colder temperature to confirm uptake by endocytosis.

The results from both RAW264.7 (Figure 8.7A and B) and differentiated THP-1 (Figure 8.7C and D) cells show uptake of empty and OVA loaded liposomes is possible, and occurs by endocytosis as little to no uptake is observed in the study run at 4°C (Figure 8.7B and D). Minimal uptake of less than 10% is observed which could be due to residual liposomes attached to the cells, or incomplete endocytosis (Figure 8.7B). For the assays conducted at 37°C using RAW264.7 cells, uptake of the liposomes is quick (Figure 8.7A). Liposomes are taken up at 30 minutes, and the amount increases as the cells are exposed to the liposomal formulations for a longer amount of time. For instance, at 30 minutes there is a 24% difference in uptake between empty and OVA loaded DMPC:Chol liposomes, meanwhile a 7% difference is observed for DSPC:Chol liposomes with and without OVA for RAW264.7 cells. The amount of liposomes taken up increases to a maximum of  $66 \pm 2.6\%$  uptake of DMPC:Chol liposomes observed after three hours. In contrast, the OVA loaded DMPC:Chol are taken up much slower with  $39 \pm 0.3\%$  uptake of OVA loaded DMPC:Chol liposomes observed after three hours.

In comparison, for THP-1 cells there is no significant difference between the uptake of empty liposomes compared to OVA loaded liposomal formulations (Figure 8.7A). The THP-1 cells are

better at taking up liposomal formulations in comparison to RAW264.7 cells, with  $80 \pm 7.5\%$  of DMPC:Chol liposomes taken up after 3 hours compared to  $66 \pm 2.6\%$ . This trend is observed for DSPC:Chol liposomes, as well as the OVA loaded versions of the formulations. Uptake of OVA loaded DMPC:Chol after three hours is  $65 \pm 4.5\%$  in comparison to  $39 \pm 0.3\%$  for RAW264.7 cells. The uptake of empty DSPC:Chol liposomes and OVA loaded formulations was  $70 \pm 4.5\%$  and  $65 \pm 2.0\%$  respectively, therefore suggesting the THP-1 cells are better at uptake.

Cell specific differences could be the reason for the difference in uptake between RAW264.7 and THP-1 cells. Whilst similar uptake rates are observed for empty and OVA loaded DMPC:Chol and DSPC:Chol liposomes, this was not observed for RAW264.7 cells. The differences in uptake of empty and protein loaded liposomes could be attributed to the membrane fluidity. Whilst cholesterol limits the fluidity of the lipids, empty liposomes may be more fluid and so are easily taken up compared to liposomes which contain protein within the aqueous core. As a result, the protein loaded liposomes are less malleable and so uptake is much slower. However, these differences are not notable for THP-1 cells; the differences in the endocytosis mechanisms may be responsible for this. It is well documented that uptake by endocytosis can be achieved by both clathrin and caveolin mediated pathways, to differing degrees. Previous research by Jiang and team has shown neutral nanoparticles are more likely to be taken up by the clathrin pathway (Jiang *et al.*, 2010), with others showing LAMP-1 uptake of particles by RAW264.7 cells (Migliore and Coppedè, 2009). The variability in the type of endocytosis utilised by the cells may impact the rate of formulation uptake, with THP-1 performing better than RAW264.7 cells. The results are encouraging as the THP-1 cells are more representative of human physiological behaviour, as the cell line is human derived whilst RAW264.7 cells are murine cells. The heterogeneity of the differentiated THP-1 cells is similar to what is observed in patients, therefore this cell line is more preferred (Forrester *et al.*, 2018).

**Table 8.4.** The physicochemical properties of empty and OVA loaded DMPC:Chol and DSPC:Chol formulations. The size, polydispersity and zeta potential was measured using dynamic light scattering. The results represent mean  $\pm$  SD, n=3 independent batches.

<b>Formulations</b>	<b>Size (nm)</b>	<b>PDI</b>	<b>Zeta Potential (mV)</b>
DMPC:Chol	69 $\pm$ 0.3	0.22 $\pm$ 0.011	-2.8 $\pm$ 0.9
DMPC:Chol + OVA	73 $\pm$ 2.0	0.18 $\pm$ 0.031	-4.6 $\pm$ 0.7
DSPC:Chol	57 $\pm$ 0.9	0.27 $\pm$ 0.002	-3.8 $\pm$ 1.0
DSPC:Chol + OVA	61 $\pm$ 3.7	0.20 $\pm$ 0.104	-6.5 $\pm$ 0.8



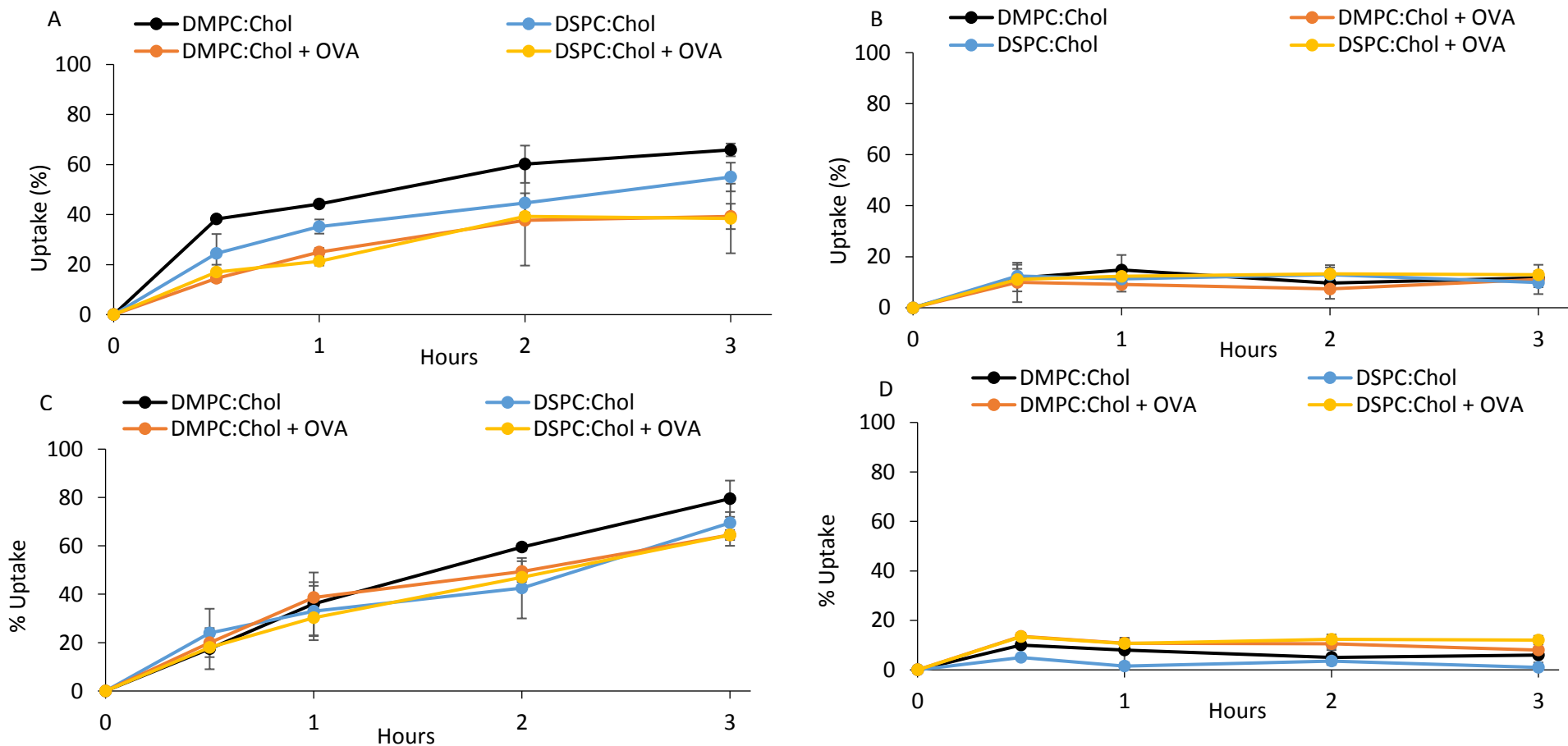


**Figure 8.7.** Uptake of empty and OVA loaded DMPC:Chol and DSPC:Chol formulations by RAW264.7 cells at 37°C (A) and 4°C (B) and stimulated THP-1 cells at 37°C (C) and 4°C (D). All formulations were made using microfluidics at a 3:1 FRR and 15mL/min TFR, with 0.25 mg/mL of OVA added into the aqueous phase. Removal of unentrapped OVA was by tangential flow filtration at 27 mL/min. The formulations were added to RAW264.7 cells for varying amounts of time after which uptake was determined using the BD FACSCanto. The results represent mean  $\pm$  SD, n=3.

## 8.6 DQ-OVA processing by macrophages

In chapter 5.4.1.5, the circular dichroism analysis of protein showed the structural integrity of OVA was maintained despite coming into brief contact with solvent during the microfluidics manufacturing process. Whilst, the OVA loaded formulations are readily taken up by macrophages, the ability for the cells to process the entrapped protein is not understood. To do this, DQ-OVA was used as a model protein to understand antigen processing. The THP-1 and RAW264.7 cells were exposed DMPC:Chol or DSPC:Chol liposomes loaded with DQ-OVA. This conjugated protein provides a good indication of the processing of the liposomal formulations; once the DQ-OVA has undergone proteolytic degradation it fluoresces green and can be readily analysed.

The results from Figure 8.8 show THP-1 and RAW264.7 cells are capable of taking up and processing both DMPC:Chol and DSPC:Chol loaded liposomal formulations within three hours. For RAW264.7 cells, of the 39% of OVA loaded DMPC:Chol liposomes taken up, around  $80 \pm 5 \%$  is degraded within three hours (Figure 8.8A). A similar amount ( $81 \pm 5 \%$ ) of DQ-OVA encapsulated within DSPC:Chol liposomes is degraded within three hours by THP-1 cells (Figure 8.8A). High levels of degradation of OVA loaded DMPC:Chol and DSPC:Chol levels are also observed for THP-1 cells (Figure 8.8B). Post three hours, the amount of DQ-OVA processed for both formulations becomes similar, with 100% of the DQ-OVA degraded after 48 hours for both DMPC:Chol and DSPC:Chol formulations (Table 8.5).

In order for liposomal formulation to be successful, the cells need to process the contents of the liposomes in addition to internalisation. The incorporation of DQ-OVA into the formulations is an excellent tool for determining cell- liposome interactions. The conjugated DQ-OVA confirms the cells ability to process the formulations, as well as allowing the quantification of degradation taking place. The results confirm both RAW264.7 and THP-1 cells are able to process and rapidly degrade the liposomal formulations, which is in keeping with previous qualitative reports. Previous research by Tanaka et al (Tanaka et al., 2010) using confocal microscopy, has shown primary murine macrophages can rapidly degrade encapsulated DQ-OVA within two hours irrespective of the lipid type used (saturated or unsaturated lipids). Also, the rate of processing is highly dependent on the cell type; research by Chiang et al (Chiang *et al.*, 2016) compared macrophage and dendritic cells ability to process non- encapsulated DQ-OVA. Macrophages were able to internalise and process DQ-

OVA in 15 minutes, whilst minimal degradation of the DQ-OVA by dendritic cells was observed (Chiang *et al.*, 2016). Similarly, the results from Figure 8.8 show rapid process for DQ-OVA incorporated into DMPC:Chol and DSPC:Chol formulations. The results from the in-vitro assay highlight the DQ-OVA model developed is a useful tool for rapidly testing processing and screening of various formulations. It offers the potential of being a useful when developing therapeutic liposomal formulations.

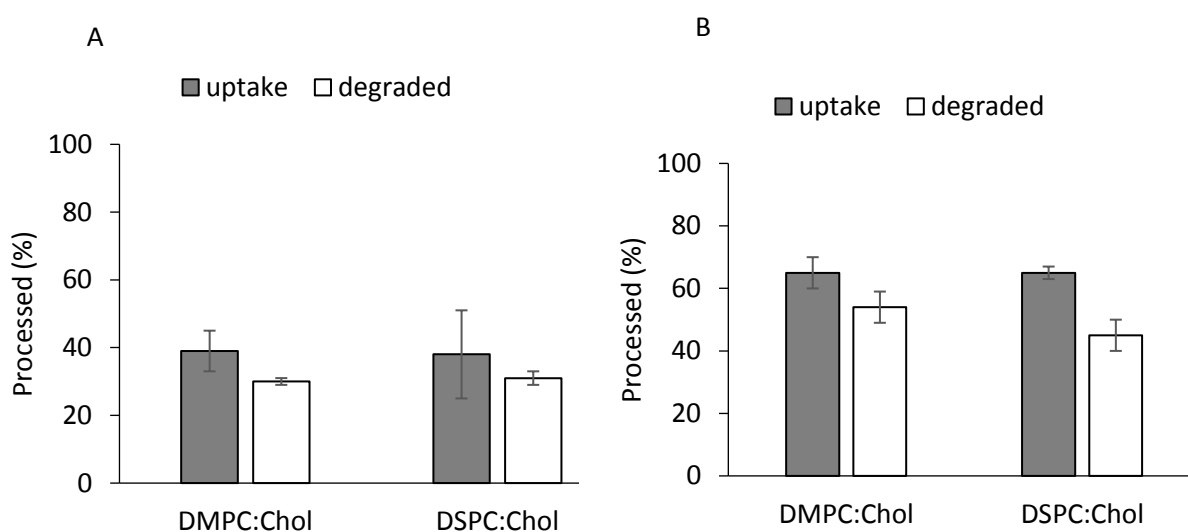


**Figure 8.8.** The percentage of DQ-OVA cleaved in three hours was compared to the amount of OVA loaded liposomes taken up by RAW264.7 (A) and THP-1 cells (B). Results represent three independent batches,  $\pm$  SD.

### 8.7 Passing THP-1 cells through a microfluidics cartridge.

The lab on the chip concept has been explored extensively from growing organs on a chip to microfluidics. Taking this into consideration, the ability to pass cells through the microfluidics chip alongside preformed liposomes (made by microfluidics) was explored. It was hoped this novel idea can encourage mixing, improving the uptake rate and even possibly translate to cell driven therapy. The first step required was to determine if the microfluidics chip, in particular the herringbone structure can harm the cells. The cells of choice were non stimulated THP-1 cells as they grow in suspension therefore, reducing the risk of the cells sticking to the chip when passing through. Also, as the THP-1 cell lines are human derived these monocytes more accurately mimic monocytes present in the blood.

Initially, a low cell density of 100 cells/mL were passed through the chip to avoid blockages or aggregation inside the chip. As the amount of cells was low, they were able to pass easily through the chip and so the cell number per mL was increased by 10 fold each time, till 10000 cells/mL was reached. The cells were passed through the chip at a 1:1 FRR; the solvent side contained the cells in cRPMI media whilst the aqueous phase contained complete RPMI media. The lowest flow rate of 2 mL/min was used to encourage mixing, after which cell viability assays were performed. The results from Table 8.5 show microfluidics did not result in cell death with a cell viability of above 95 % calculated for THP-1 cells passed through the chip compared to control THP-1 cells. The similarity between the control cells and THP-1 cells that went through the chip highlight the microfluidics chip structure does not cause mechanical damage to the cells.

Based on these results, a concentration of 10,000 cells/mL was selected to determine the effect of flow speed on cells (Table 8.5). The cells were passed through the chip from low to high speeds (2- 15 mL/min). The increase in speed from 2- 10 mL/min did not impact the cell viability which remained above 95 %. At 15 mL/min the cell viability decreased to  $88 \pm 2$  % suggesting this flow speed is too fast for the cells (Table 8.5). This is not problematic as speed is not the key factor here; to encourage mixing of cells with liposomes a slow speed is preferred so further experiments were run at 5 mL/min (Table 8.5). The cells were further analysed using light microscopy to confirm passing cells through the chip at varying speeds does not cause morphological changes. Figure 8.9 shows the morphology of the THP-1 cells does not change as a result of passing through the microfluidics chip.

**Table 8.5.** The percentage of viable cells after passing through the microfluidics chip at various speeds. The results represent three independent batches,  $\pm$  SD.

<i>Speed</i>	<i>Cell viability (%)</i>			
	mL/min	100 cells	1000 cells	10,000 cells
<b>2</b>		97 $\pm$ 3	98 $\pm$ 3	95 $\pm$ 2
<b>5</b>		-	-	96 $\pm$ 4
<b>10</b>		-	-	100 $\pm$ 9
<b>15</b>		-	-	88 $\pm$ 2

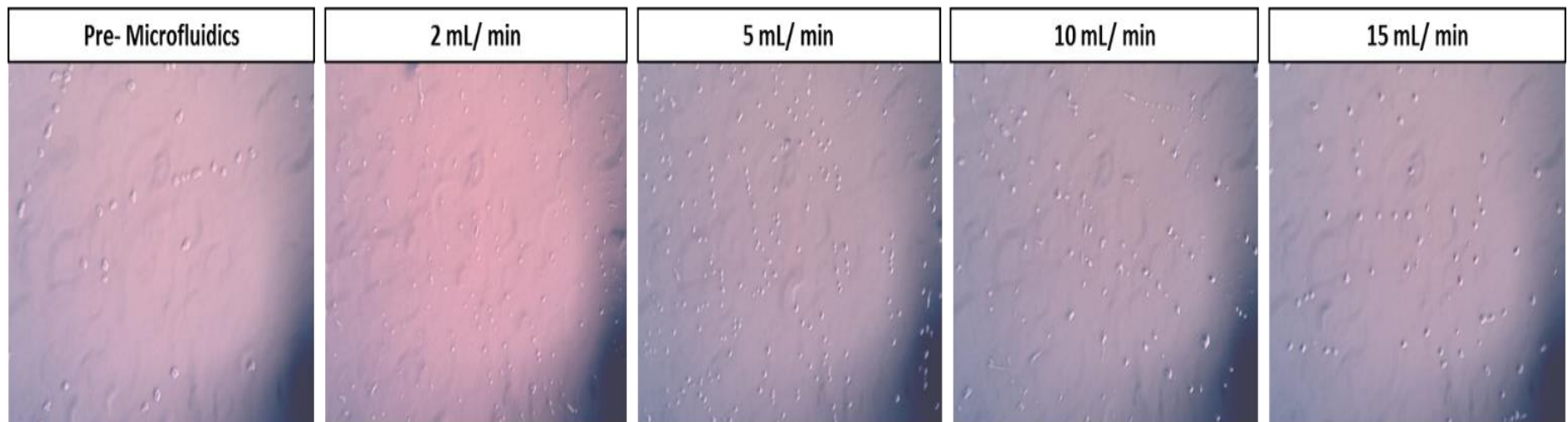


**Figure 8.9.** The morphology of THP-1 cells before after being passed through the microfluidics chip at varying flow rates. The cells were analysed using a light microscope using an x10 objective lens.

Furthermore, as the results confirmed THP-1 cells passed through the microfluidics chip are viable, liposomal formulations were introduced alongside the cells passing through the chip. THP-1 cells (at a cell density of 10 000 cells/mL) were exposed to 1 mg/mL of DiIC labelled DMPC:Chol liposomes at a 1:1 FRR and a flow speed of 5 mL/min. Due to the low cell density, uptake was measured using a fluorescence plate reader, but the fluorescence values were too low to give reliable measurements. Values of less than 2 % uptake were calculated with wide error margins (as shown in Figure 8.10), and so the process requires further optimisation. Previous work by Claudia et al has shown that while it is possible to measure uptake using a plate reader, it is tricky to get similar result to that obtained from flow cytometry. The process requires additional optimisation steps (Claudia *et al.*, 2017). For instance, Claudia et al, showed reliable uptake measurements of the amine-functionalized AMI20 polystyrene particles was not possible as the fluorescence signal was too low. As a result, a greater understanding of the particles and parameters is required for the measurement of liposomal uptake by the cells using a fluorescence reader, which is a versatile and cheaper alternative to flow cytometry.

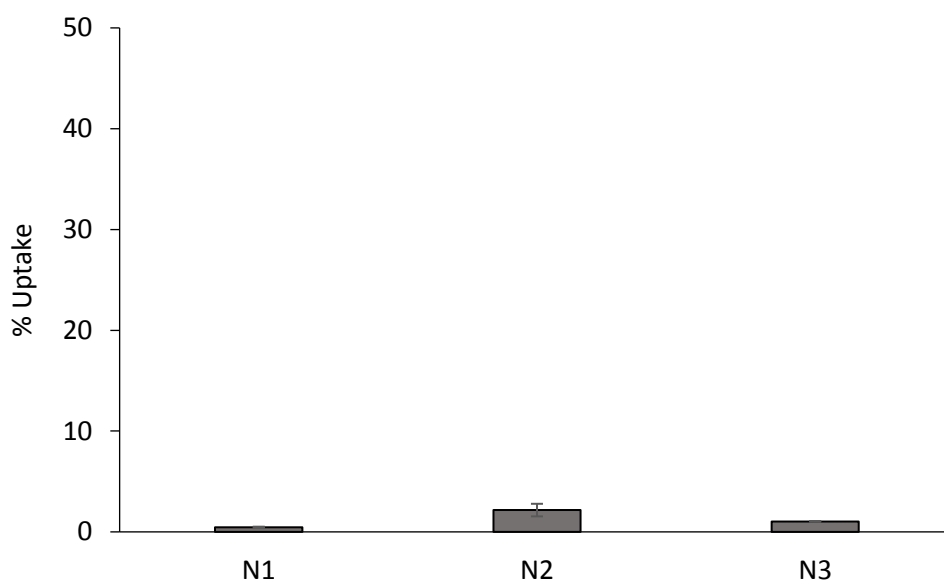


**Figure 8.10.** The uptake of DiIC labelled DMPC:Chol (1 mg/mL final concentration) by THP-1 monocytes. The pre-formed DiIC labelled liposomes were passed through the microfluidics chip alongside the THP-1 cells at a 1:1 FRR and 5 mL/ min. After this, the cells were then plated onto a 96 well plate and fluorescence was measured using a plate reader, to quantify the amount of liposome uptake. The results represent three independent batches, each shown individually  $\pm$  SD.

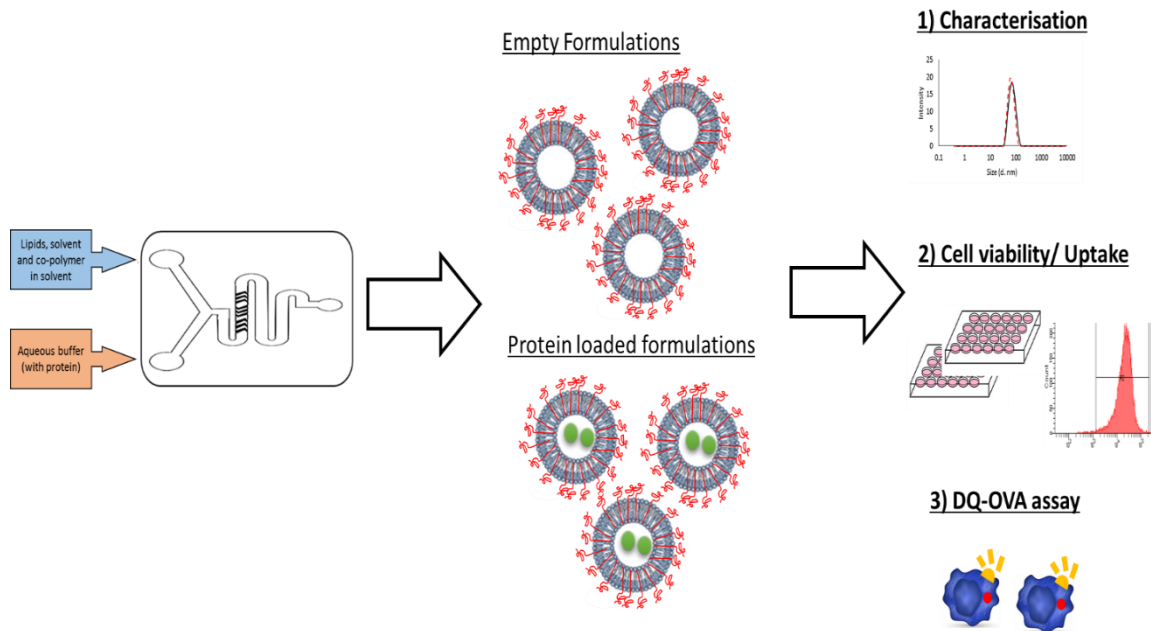
## 8.5 Conclusion

In this chapter, the use of liposomal formulations as therapeutics was further explored *in-vitro*, with particular attention paid to liposome- cell interactions. In keeping with previous research, the neutral formulations were non- toxic and readily taken up by both RAW264.7 and THP-1 cells, however little was known about the processing of the formulations once internalised. Many researchers use confocal microscopy to track liposomes internally and determine the fate of the formulations, however this method can be hard to replicate. It is also a qualitative approach, with quantification of the amount of formulations not possible and so a novel quantitative method was developed to determine the fate of internalised liposomes. The model involves using DQ-OVA to quantify the amount of processing and subsequent degradation of the conjugated DQ-OVA protein by RAW264.7 and THP-1 cells. The results from Figure 8.8 show that both cell lines are capable of the rapid processing of internalised liposomes. More than 50% of the liposomal formulations taken up by the cells were processed within three hours, with 100% degradation of DQ-OVA observed after 48 hours. As a result, this model is an ideal tool for screening various formulations (of different size, charge and lipid composition) for antigen processing.

Following on from this, the ability to enhance uptake and rapid screening for liposomal formulations was explored by passing cells through a chip device. It was hoped that the flow movement of cells alongside preformed liposomes in the Nanoassemblr cartridge would lead to rapid mixing, and quicker cell-liposome interactions resulting in faster uptake. Despite the cells remaining viable after passing through the microfluidics Nanoassemblr cartridge, uptake of the liposomal formulations was poor. This is probably due to the very short exposure time of seconds compared to a minimum of 30 minutes when investigating uptake using traditional well plates. Increasing the mixing time of cells with liposome may improve uptake and so further development and optimisation of this model is required. The ability to determine uptake using a fluorescent plate reader as highlighted by research by Claudia *et al* (Claudia *et al.*, 2017), coupled with this microfluidics mixing process is a promising alternative to flow cytometry. It has the possibility to allow for hundreds of formulations to be screening quickly and cost efficiently compared to existing approaches.

# Chapter 9

## Evaluating the addition of co-polymers to liposomal formulations produced by microfluidics





## 9.1 Introduction

### 9.1.1 Long circulating liposomes

There are many conventional liposomal drug formulations available on the market; with parameters such as size, fluidity and lipid type all influencing how stable the formulations are, and how they will act once administered (Chonn *et al.*, 1992, Oja *et al.*, 1996, Senior and Gregoriadis, 1982). For instance, adding cholesterol to the formulation improves lipid packing therefore, improving the stability of liposomes by decreasing the amount of phospholipid interactions with blood circulating high-density lipoproteins (HDLs). The susceptibility of conventional liposomal formulations to HDLs and coating from other plasma proteins (such as opsonins) results in rapid clearance from the blood circulation by the mononuclear phagocyte system (MPS) (Scherphof *et al.*, 1985). The opsonising proteins are recognised by immunoglobulins, amongst other proteins (such as beta-2 glycoproteins, beta-2-macroglobulin) (Chonn and Cullis, 1995, Patel, 1992, Murai *et al.*, 1995). The same is also observed for polymeric particles such as polylactic co-glycolic acid (PLGA) for controlled release of therapeutic agents (Kawashima *et al.*, 1999, Edwards *et al.*, 1997, Fu *et al.*, 2002, Learoyd *et al.*, 2010, Fiegel *et al.*, 2004), but these particles are typically associated with fast burst release which is unwanted for certain therapeutic targets (Kim and Martin, 2006). More recently, biodegradable co-polymers such as polyglycolide (PGA)-co- poly-D-lysine (PDL) have been investigated as an alternative delivery vehicle (for proteins, hydrophilic and hydrophobic drugs). Despite the synthesis of these co-polymers, they are rapidly phagocytosed by the MPS system. Whilst this fast rate of clearance is useful for delivery of antibacterial drugs to treat infections within the MPS system, it is not convenient for the delivery of drugs or protein beyond the MPS system (Alving *et al.*, 1978, Agrawal and Gupta, 2000, Basu and Lala, 2004).

The longevity and circulatory time of liposomal and polymer formulations administered intravenously can be improved by the addition of poly-(ethylene glycol) (PEG), which is used as a stabiliser. It is a polyether compound, which is non-toxic, biocompatible and has low

solubility and immunogenicity (Dreborg and Akerblom, 1990). The incorporation of PEG into the liposomal formulations can be achieved in many ways; by adding PEG into the liposome preparation, adsorbing onto the surface of preformed vesicles, or by covalently bonding PEG to the liposomal formulations. There has been some research showing the addition of PEG can improve the stability and solubility of proteins and peptides (Caliceti and Veronese, 2003). Inclusion of PEG into the liposomal formulations changes the pharmacokinetic profile of the formulations; the surface modification shields the liposomal formulation from plasma protein. Interactions with the plasma protein are limited, so formulations are protected from MPS cells for longer (Blume and Cevc, 1993, Vert and Domurado, 2000). The addition of PEG also prevents the aggregation of the liposomal formulations by increasing the hydrophilicity of the formulations. The presence of the PEG overcomes the van der Waal's forces, and causes a repulsion between the formulations preventing aggregation. Through the use of X-ray analysis, Needham et al (Needham *et al.*, 1992) showed the addition of the PEG1900 lipid to liposomal formulation causes the bilayer to increase about 50Å from the surface and is the reason for the repulsive forces between the particles. Despite the advantages of PEGylated liposomes there are some draw backs to using these formulations, with some research showing they can activate the immune system (by activation of the complement system) (Moghimi and Szebeni, 2003). In addition, covalently attaching PEG to phospholipids such as DPPC to create a lipid with a functionalised head group (for instance dipalmitoyl-sn-glycero-3-phosphoethanolamine-N-[mPEG-5000] is used due to the strong interactions. Due to the asymmetry of this functionalised co-polymer with respect to DPPC lipid, there is a chance micelles can be formed in addition to the production of stealth liposomal formulations (Shimada *et al.*, 2000). As a results, there has been an increase in the synthesis of co-polymers with the inclusion of mPEG to improve long circulating liposomal formulations.

In addition, while PEGylated liposomes avoid clearance by macrophages, recent research has shown adding PEG can help drainage to the lymph node. For instance, adding 1mol% DSPE-PEG2000 to cationic DOTAP liposomes results in drainage to the lymph node, in addition to prolonged retention and uptake of liposomes by antigen presenting cells (Zhuang *et al.*, 2012). The lipid variability and composition of PEGylated liposomes can impact lymph node distribution; longer length PEG results in faster drainage and are more favourably retained by scavengers of the respective lymph nodes (Oussoren and Storm, 1997, Moghimi, 2006). Based on this research, a new lipid based system containing PEG has been approved for the

delivery of siRNA. The formulation Onpattro™ (patisiran) was approved for therapeutic use in 2018 (by both the European medicines agency (EMA) and FDA) to treat polyneuropathy. It is composed of DSPC, Diln-MC3-DMA and PEG2000-DMG lipids (Onpattro (patisiran), 2018) and so there is a possibility for more PEGylated liposomal formulations with varying compositions to be approved for therapeutic use.

### 9.1.2 Co-polymers as delivery vehicles

Based on the growing and renewed interest in the use of PEG, the effect of adding PEGylated co-polymers was investigated as potential alternatives to current PEGylated lipids. These co-polymers were synthesised by Professor Casettari's research group (University of Urbino Carlo Bo, Italy). In total, five co-polymers varying in length were considered for their inclusion into the DMPC:Chol liposome, with their properties listed in Table 9.1. The synthesised co-polymers are non-toxic, biodegradable, odourless, but very poorly soluble.

**Table 9.1.** The properties of functionalised polyethylene glycol attached to varying lengths of polylysine.

<i>Co-polymers</i>	<i>Code</i>	<i>Chemical name</i>	<i>Mw</i> <i>(<sup>1</sup>H-NMR)</i>	<i>Form</i>
<i>CP1</i>	mPEG <sub>550</sub> - PDL <sub>9500</sub>	Methoxy Polyethylene Glycol 0.55 kDa-co-Poly (delta-decalactone) 9.5 kDa	10 kDa	White, waxy
<i>CP2</i>	mPEG <sub>550</sub> - PDL <sub>29500</sub>	Methoxy Polyethylene Glycol 1.9 kDa-co-Poly (delta-decalactone) 29.5 kDa	30 kDa	White, waxy
<i>CP3</i>	mPEG <sub>1900</sub> - PDL <sub>24000</sub>	Methoxy Polyethylene Glycol 1.9 kDa-co-Poly (delta-decalactone) 24 kDa	26 kDa	White, waxy
<i>CP4</i>	mPEG <sub>1900</sub> - PDL <sub>10000</sub>	Methoxy Polyethylene Glycol 1.9 kDa-co-Poly (delta-decalactone) 10 kDa	12 kDa	White, waxy

CP5	mPEG <sub>1900</sub> -	Methoxy Polyethylene Glycol 1.9	98	White, waxy
	PDL <sub>96000</sub>	kDa-co-Poly (delta-decalactone) 96 kDa	kDa	

## 9.2 Aim and Objectives

In this chapter, the ability of co-polymers to integrate into liposomal formulations was investigated. The objectives are:

- Determine whether varying sized co-polymers can be inserted into the bilayer.
- Characterise polymer-liposome hybrid formulations with and without protein, in relation to their physicochemical properties and stability.
- Investigate the difference in uptake and processing of co-polymer DMPC:Chol liposomal formulations compared to the neutral DMPC:Chol counterpart.

## 9.3 Materials and Methods

### 9.3.1 Materials

The 1,2-dimyristoyl-sn-glycero-3-phosphocholine (DMPC) lipid was obtained from Avanti Polar Lipids Inc., Alabaster, AL, US. The synthesised co-polymers were a gift from Professor Luca Casettari (*Department of Biomolecular Sciences, University of Urbino Carlo Bo, Italy*). Acetone, Cholesterol, Ovalbumin (OVA), D9777-100FT dialysis tubing cellulose membrane and trifluoroacetic acid was obtained from Sigma Aldrich Company Ltd., Poole, UK. For OVA purification and release studies the Biotech CE tubing (MWCO 300 kD) was used from Spectrum Inc., Breda, The Netherlands. For sample purification by Tangential flow filtration (TFF) a modified polyethersulfone (mPES) 750 kD MWCO hollow fibre column was purchased from Spectrum Inc., Breda, The Netherlands. The materials related to cell in-vitro studies were purchased as previously described in Chapter 8.4.1.

### 9.3.2 Methods

#### 9.3.2.1 Production of co-polymer liposomes using microfluidics

The co-polymers were dissolved in 100 % acetone, and mixed with DMPC and cholesterol lipids at the desired concentration (with each formulation containing 1-8% co-polymer). This was then injected alongside PBS buffer (pH 7.3) with and without OVA (at an initial OVA

concentration of 0.25 mg/mL). The co-polymer liposomes were purified as previously described, by tangential flow filtration and the physicochemical characteristics (size, polydispersity index and zeta potential) were determined using dynamic light scattering.

#### **9.3.2.2 Quantification of entrapped protein**

The amount of encapsulated protein OVA within the co-polymer liposomal formulations was calculated as previously described by HPLC-ELSD. In brief, the amount of OVA was quantified by a gradient method using solvent (A) of 0.1 % trifluoroacetic acid in water (HPLC grade) and solvent B of 100 % methanol. The peak appeared at 11.8 minutes with the amount calculated using a pre-established calibration curve.

#### **9.3.2.3 Stability of the co- polymer liposomal formulations**

The stability of empty and OVA loaded DMPC:Chol liposomal formulations was determined with respect to changes in the size, PDI and zeta potential. The liposomal formulations were stored at 4°C and 37°C respectively for seven days, with samples collected daily for seven days.

#### **9.3.2.4 In-vitro studies**

Differentiated THP-1 cells were used to determine the cell viability, uptake and DQ-OVA processing of co-polymer DMPC:Chol liposomes as described in chapter 8 (sections 8.3.2.5 - 8.3.2.8).

#### **9.3.2.5 Statistical analysis**

The results are represented as mean  $\pm$  SD with n=3 independent batches. T- tests and ANOVA tests were used to assess statistical significance, with a Tukey's post ad-hoc test (p value of less than 0.05).

## **9.4 Results and Discussion**

### **9.4.1 Evaluating the ideal amount of co-polymer required for stealth liposomal formulations**

The initial challenge when using co-polymers to synthesise stealth liposomes (using microfluidics at a 3:1 FRR and 15 mL/min TFR) was finding a solvent that can dissolve the co-polymers as they have low solubility. The co-polymers were insoluble in methanol, ethanol and acetonitrile respectively with the co-polymers only soluble in 100% acetone. Whilst

acetone is compatible with the microfluidics chip, the DMPC and cholesterol lipids are not soluble in acetone. As a result, the lipids were dissolved in 100% methanol which is miscible with acetone, and the lipid preparation was run through the microfluidics. The amount of co-polymer added to DMPC:Chol liposomal formulations was investigated in terms of changes to the physicochemical properties (size, and PDI). Two co-polymers, one low mPEG value ( $m\text{PEG}_{550}\text{-PDL}_{9500}$ , CP1) and one with high mPEG value ( $m\text{PEG}_{1900}\text{-PDL}_{96000}$ , CP5) was selected. The amount of co-polymer use was either 1% (wt/wt) or 4% (wt/wt) of co-polymer, with the results showing both amounts are able to form liposomal formulations (Figure 9.1). Statistical analysis of liposome size with and without co-polymer show there is a significant increase in size once co-polymer is added (Figure 9.1A). Although there is no concrete evidence to show the co-polymer is incorporated such as cryoTEM images, given the co-polymers are very insoluble and the increase in size upon addition it indicates the co-polymers are incorporated into the formulations. Analysis before and after purification revealed no significant difference post purification of the liposomal formulations, with measured sizes of around 150 nm (Figure 9.1A). The inclusion of Co-polymer 5 (CP5) into DMPC:Chol liposomal formulations at 4% produced the smallest liposomal formulation of around  $117 \pm 31$  nm, whilst adding CP1 at 4% produced DMPC:Chol liposomes similar in size (around 170 nm) to when 1% of CP1 was added. The results show adding co-polymers at a high percentage (4% in this case) is the preferred option, and does not drastically change the physicochemical properties of these empty co-polymer loaded DMPC:Chol liposomes (Figure 9.1A). The PDI of both co-polymers at different concentration remained below 0.2 after purification (Figure 9.1B), indicating a homogenous population of stealth liposomes are being produced. The zeta potential remained above -5 mV (data not shown), showing the DMPC:Chol formulations were still neutral formulations despite the addition of the co-polymers. The results are encouraging, as other research papers have shown using more than 4 % of PEG on liposomal formulation can cause micelle formation due to the increased curvature of the co-polymers (Photos et al., 2003). Thus, the ability to produce highly PEGylated liposomes without adversely impacting formulation characteristics is advantageous.

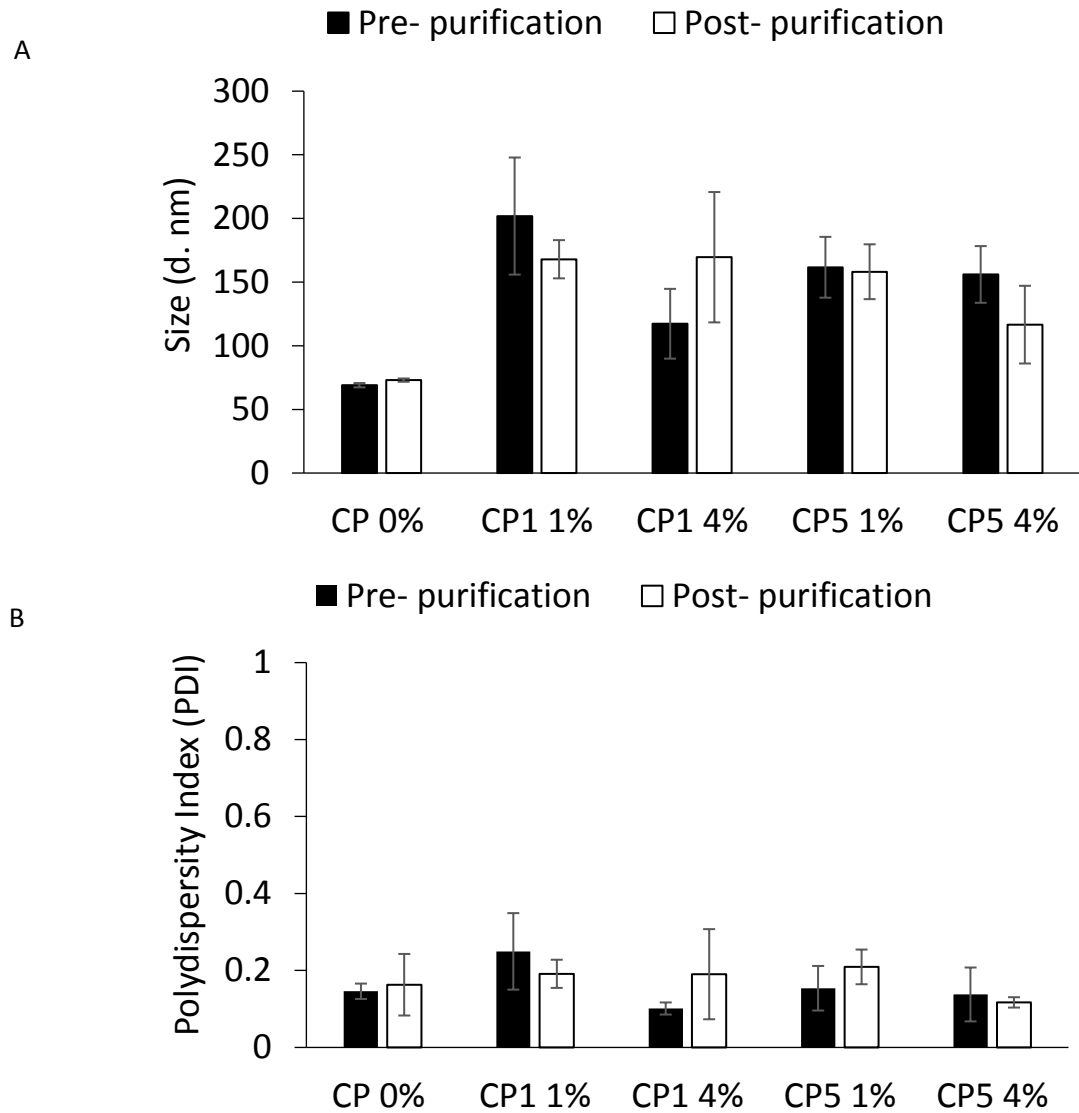


**Figure 9.1.** The size (A) and polydispersity index (B) measurements of empty and DMPC:Chol liposomes loaded with varying amounts of Co-polymer 1 (CP1) or Co-polymer 5 (CP5) before and after purification. The liposomal formulations were produced using microfluidics at a 3:1 FRR and 15 mL/min TFR. The results represent mean  $\pm$  SD, n=3 independent batches.

The stability of the co-polymer DMPC:Chol formulations was investigated at both 37°C (Figure 9.2 and 9.3) and 4°C for up to seven days (Figure 9.4). All formulations stored at 37°C, regardless of the type and amount of co-polymer used are stable over seven days with the sizes of the liposomal formulations remaining below 150 nm (Figure 9.2A). The PDI of the formulations remains below 0.2, with the size intensity plots for CP1 1 % DMPC:Chol liposomes (Figure 9.3A), CP1 4 % DMPC:Chol liposomes (Figure 9.3B), CP5 1 % DMPC:Chol liposomes (Figure 9.3C) and CP5 4% DMPC:Chol liposomes (Figure 9.3A) also reflecting this. Equally, the zeta potential of the formulations measured over seven days, shows the liposomal formulations remain neutral with values of above -10 mV measured. This shows that storage of the liposomal formulation at physiological temperature has no adverse effects on the liposomal formulation.

In addition, storage of the co-polymer DMPC:Chol liposomes at 4°C was also investigated (Figure 9.4). The sizes measured showed the formulations undergo much more changes in size compared to the formulations stored at 37°C (Figure 9.4A). For DMPC:Chol formulations containing 1% of CP1, a size increase of 97 nm was observed at day 5 from 170 nm. Minimal change in size is observed for 4 % CP1 DMPC:Chol at day 5 (from 169 nm to 144 nm), with a size of 137 nm measured at day 7. Equally, the DMPC:Chol liposomes produced with CP5 are also susceptible to changes in size over the course of 7 days. For liposomes produced with 1 % CP5 the size change from 158 nm to 80 nm is observed, whilst formulations produced using 4 % CP5 also show a similar decrease in size from 117 nm to 90 nm at day 7. In particular, the DMPC:Chol liposomes produced with 1 % of CP1 and CP5 are more unstable with large fluctuations in PDI observed. Meanwhile the PDI of DMPC:Chol formulations produced with 4% CP remains below 0.2, suggesting they are still homogenous formulations. This is observed from the size- intensity plots of the DMPC:Chol formulations produced using CP1 at 1 % (Figure 9.5A).

Overall, whilst the reason for the differences in size over time when stored at 4°C were unclear, based on the results from measurement of the liposome physicochemical properties and stability assays, the 4 % CP formulation was selected for further studies. Whilst the formulations are still larger than DMPC:Chol liposomes without CP (size of around 72 nm), the measured sizes of 4 % CP1 and CP5 are below 200 nm therefore uptake by endocytosis is possible (and is investigated in section 9.4.5). The stability assays highlight the liposomal formulations are more stable when 4 % of the co-polymer is included. The formulations are



not sensitive to heat and so the formulations could be kept at room temperature with minimal changes in liposomal physicochemical properties expected. Moreover, the stability of the hybrid co-polymer liposomal formulations is in keeping with previous research by Ruyschaert et al. It was shown incorporation of co-polymers (Amphiphilic ABA triblock copolymers, such as poly(2-methyloxazoline)-block-poly(dimethylsiloxan)-block-poly(2-methyloxazoline) (PMOXA-PDMS-PMOXA)) provides stability to PC liposomes. The hybrid formulations were 75 nm in size, compared to 112 nm in size of PC liposomal formulations, and did not collapse when undergoing dehydration (Ruyschaert *et al.*, 2005). As a result, all further work on the production of co-polymer liposomal formulation involved the use of 4% co-polymer.

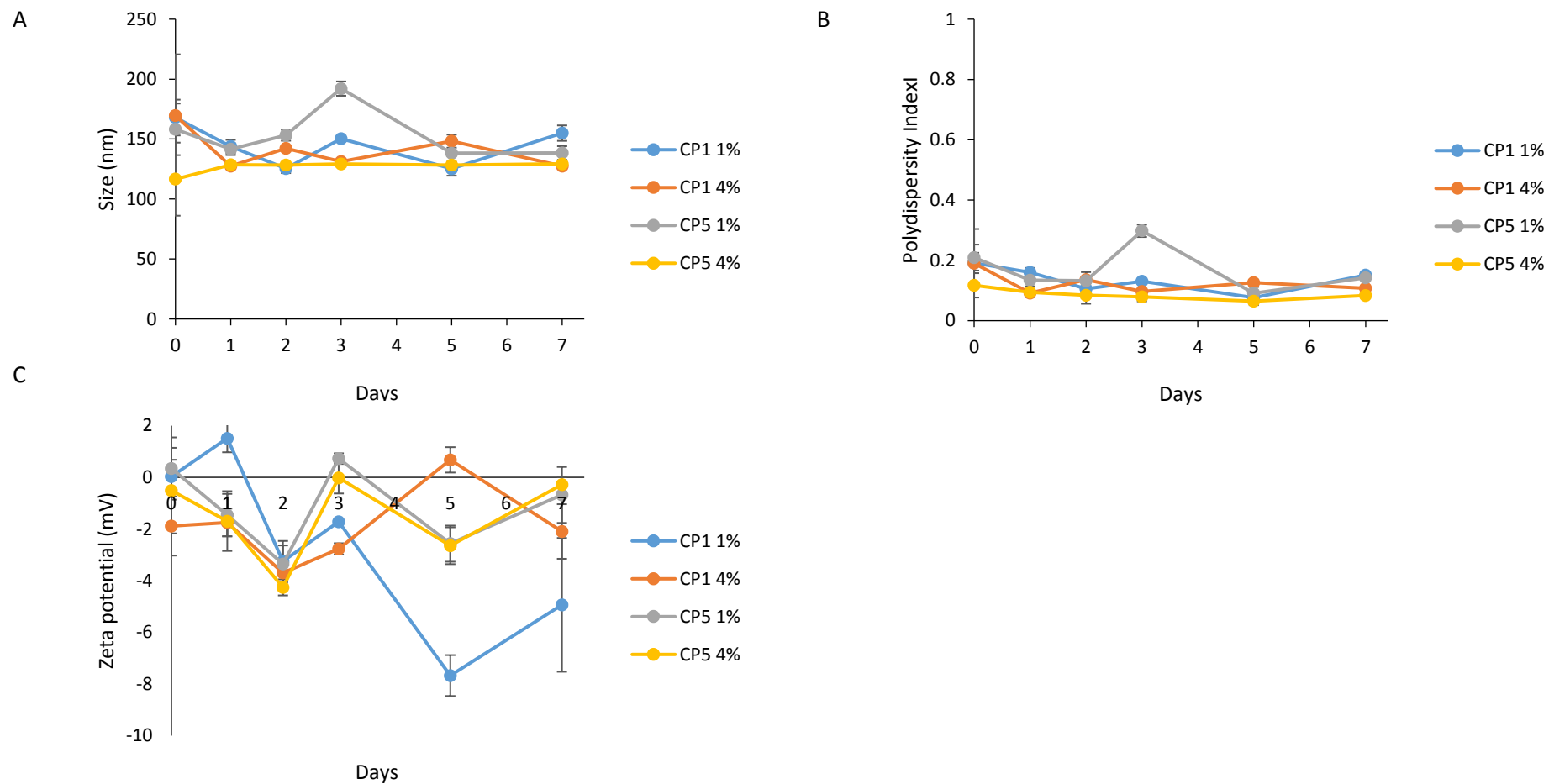


**Figure 9.2.** The stability of co-polymer loaded DMPC:Chol formulations kept at 37°C for seven days. The formulation were made using microfluidics (at a 3:1 FRR and 15 mL/min TFR) using either 1% or 4% co-polymer 1 or 5. Samples were taken every day for seven days with the size (A), polydispersity index (B) and zeta potential (mV) measured using dynamic light scattering. The results represent mean  $\pm$  SD, n=3 independent batches.

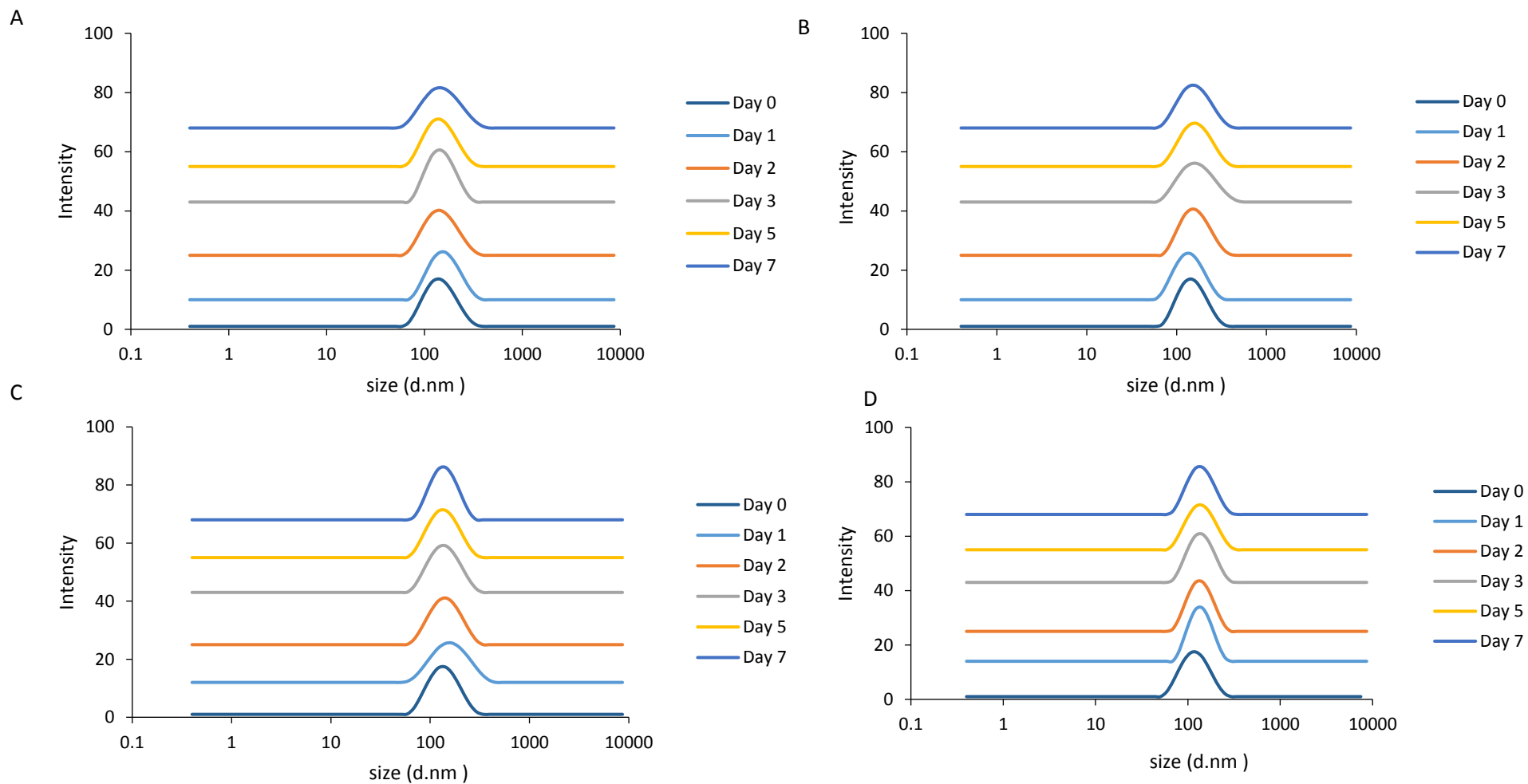


**Figure 9.3.** The size- intensity plots of co-polymer DMPC:Chol liposomes at 37°C. The co-polymer 1 was added to DMPC:Chol liposomes during production at 1 %(A) or 4 % (B), with co-polymer 5 also added at either 1 % (C) or 4 % (D). The size-intensity plots were analysed every day for up to seven days, with each plot representative of one measurement of the sample.

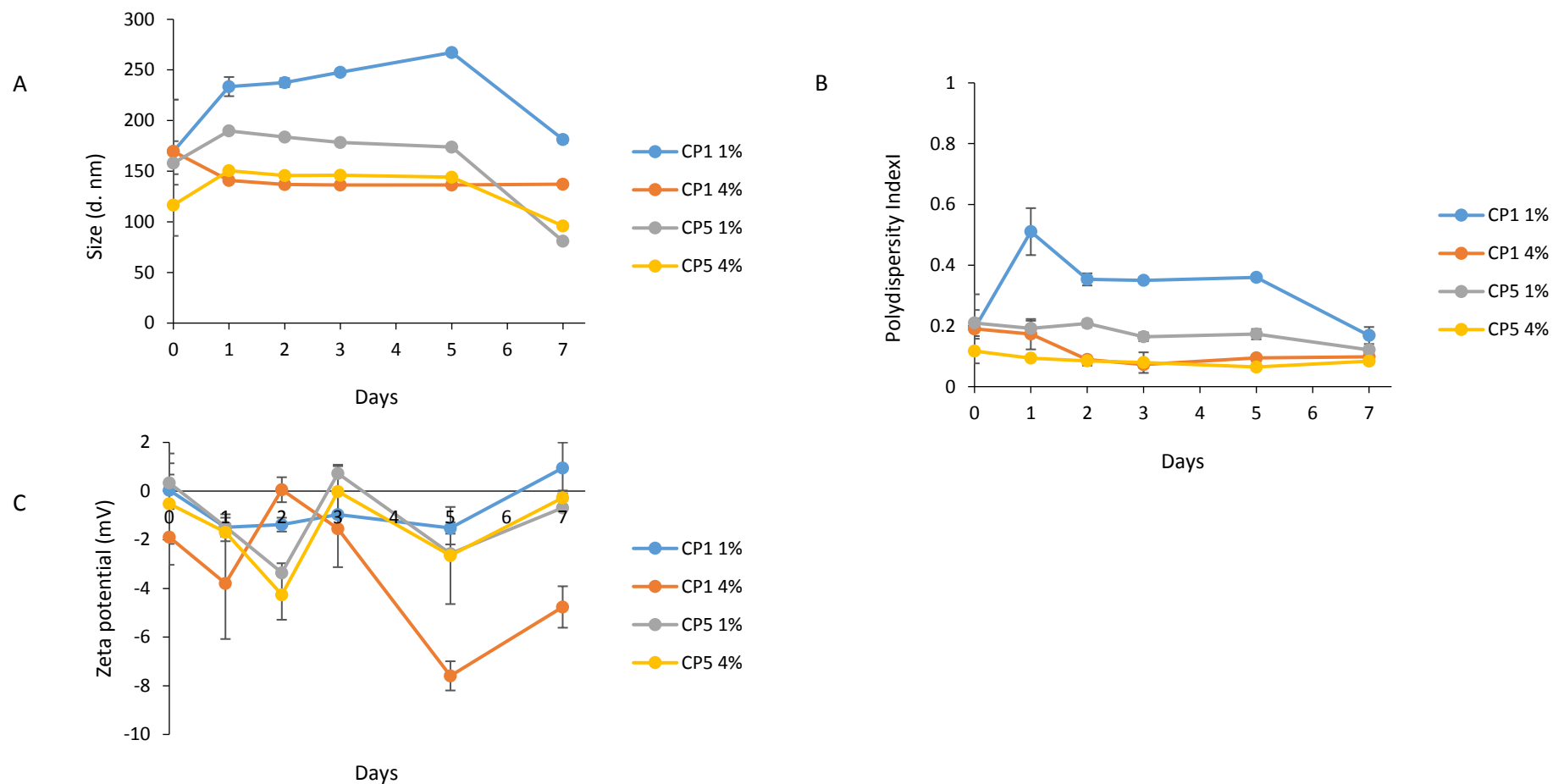


**Figure 9.4.** The stability of co-polymer loaded DMPC:Chol formulations kept at 4°C for seven days. The formulations were made using microfluidics (at a 3:1 FRR and 15 mL/min TFR) using either 1% or 4% co-polymer 1 or 5. Samples were taken every day for seven days with the size (A), polydispersity index (B) and zeta potential (mV) measured using dynamic light scattering. The results represent mean  $\pm$  SD, n=3 independent batches.

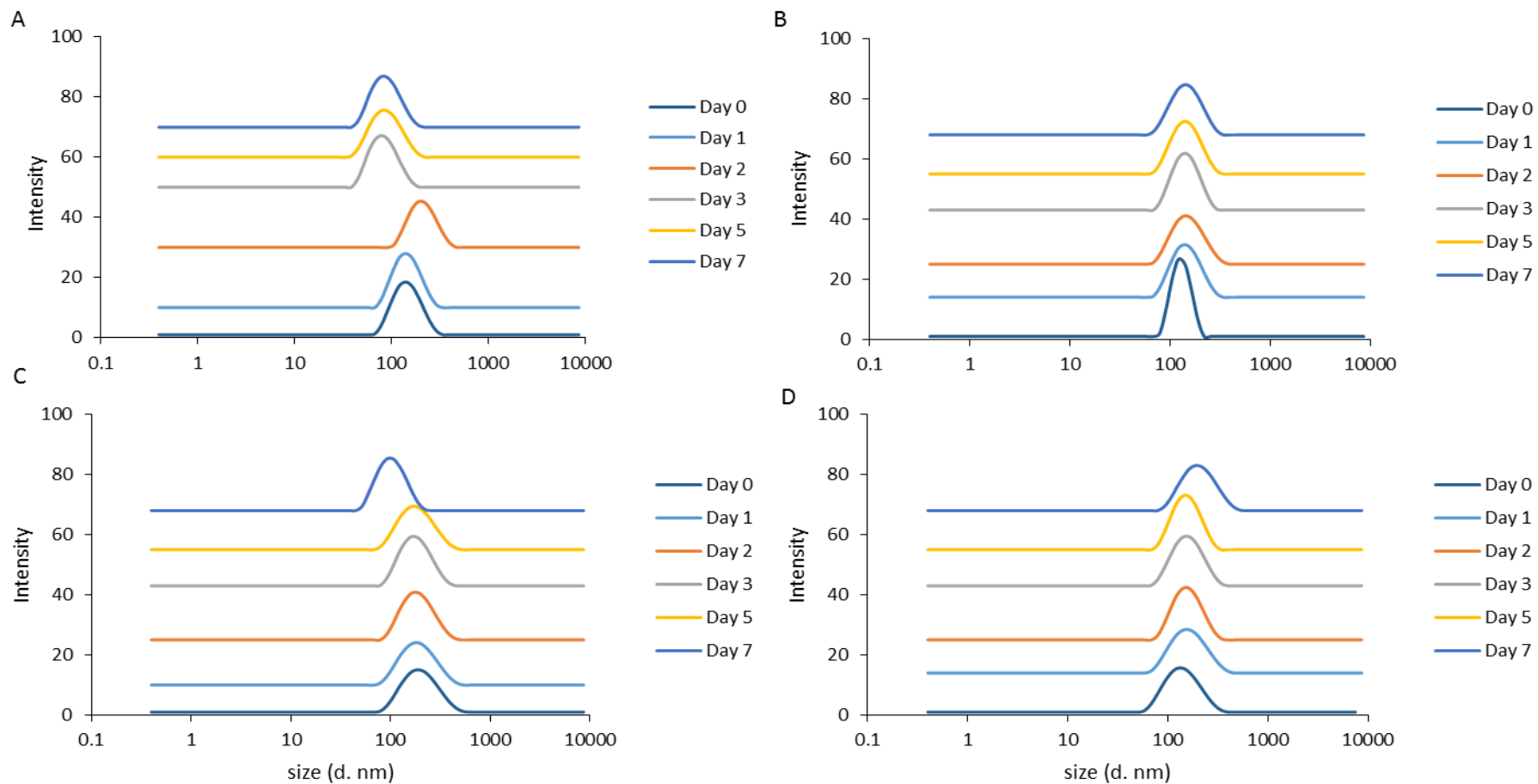


**Figure 9.5.** The size- intensity plots of co-polymer DMPC:Chol liposomes at 4°C. The co-polymer 1 was added to DMPC:Chol liposomes during production at 1 %(A) or 4 % (B), with co-polymer 5 also added at either 1 % (C) or 4 % (D). The size-intensity plots were analysed every day for up to seven days, with each plot representative of one measurement of the sample.

#### 9.4.2 The effect of varying co-polymer chain length on DMPC:Chol formulation characteristics

Based on the results from section 9.4.1, all five co-polymers were added to the DMPC:Chol liposomal formulation at 4 %. The results show the size of the co-polymers influence the physicochemical properties of liposomal formulations to some extent (Figure 9.6). For instance, despite the same amount of mPEG contained in CP1 and CP5, the difference in PDL length causes the CP1 to be smaller (10 kDa) than CP2 (30 kDa) (Figure 9.6A). The DMPC:Chol liposomes containing CP1 are 61 nm smaller than liposomes produced with CP2. Similarly, as the mPEG amount increases (for CP3-5), the DMPC:Chol liposomes made with CP3 are larger in size ( $207 \pm 42$  nm) due to it being 26 kDa in comparison to CP4 liposomes ( $187 \pm 7$  nm) which is 12 kDa (Figure 9.6A). Meanwhile, CP5 formulation is not impacted by size (98 kDa) with this formulation producing the smallest sized liposomes at  $117 \pm 31$  nm. All co-polymers produced homogenous liposomes with a PDI measurements of below 0.2 (Figure 9.6B), and a zeta potential above -10 mV indicating the liposomes are still neutral in charge (Figure 9.6C).

Previous studies have shown the amount of PEG that can be added to liposomal formulations varies; less than 10 % PEG-2000 can be stably incorporated into the formulations (Bradley *et al.*, 1998), compared to 1- 2% for PEG-500 (Montesano *et al.*, 2001). The co-polymers allow for a high amount of PEG incorporated into the particles, with formation of vesicles with only co-polymers also possible, therefore producing micelles (Photos *et al.*, 2003). With the increase in molecular weight of co-polymers, the bilayer membranes become thicker and more stable (Discher *et al.*, 2002, Bermudez *et al.*, 2002) and so the incorporation of co-polymers into liposomal formulations allows the benefits of both (Photos *et al.*, 2003). The mixed hybrid formulations allows for the stability of the mPEG component and increased encapsulation achievable from the lipid components, and so the encapsulation efficiency of the OVA by the synthesised co-polymer DMPC:Chol liposomes was determined (Ruyschaert *et al.*, 2005).

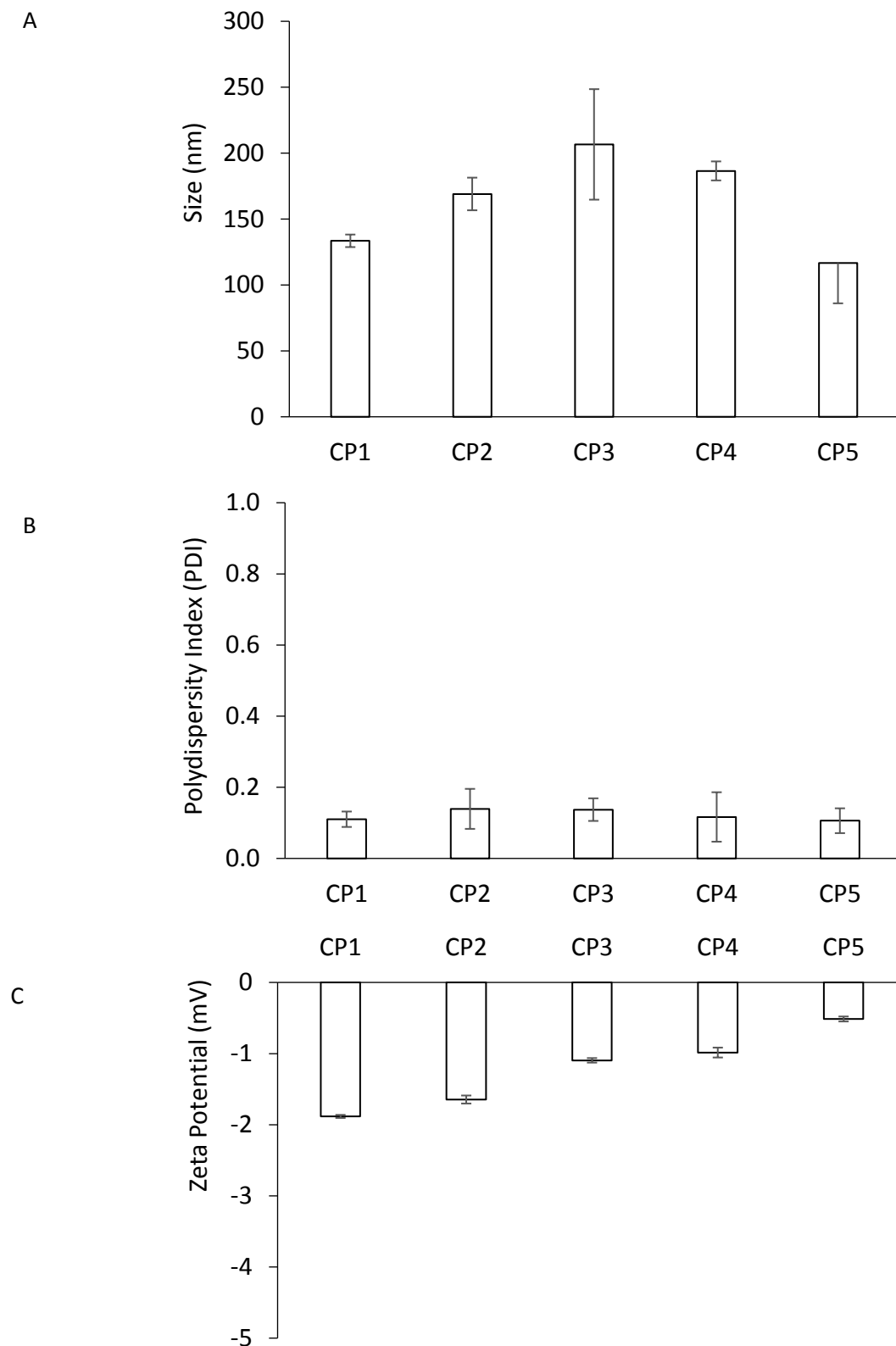


**Figure 9.6.** The physicochemical properties of DMPC:Chol liposomes containing varying lengths of copolymers chains. The liposomal formulations were produced using microfluidics at a 3:1 FRR and 15 mL/min TFR. The size (A), polydispersity index (B) and zeta potential (C) were measured using dynamic light scattering. The results represent mean  $\pm$  SD, n=3 independent batches.

### 9.4.3 Protein encapsulation of co-polymer DMPC:Chol liposomal formulations

The co-polymer DMPC:Chol liposomes were tested for their ability to encapsulate the protein ovalbumin. The formulations were produced by microfluidics using the optimised manufacturing process previously outlined in chapter 3 (3:1 FRR and 15 mL/min TFR). The co-polymer, DMPC lipid and cholesterol were injected into the solvent phase and the aqueous phase consisting of phosphate buffered saline (PBS, pH=7.3) containing 0.25 mg/mL initial ovalbumin (OVA). All five co-polymers were tested for their encapsulation ability, with similar encapsulation efficiencies of between 36- 41 % calculated for all five co-polymer liposomal formulations. There is no significant difference observed between the co-polymer liposomal formulations (Table 9.2).

In contrast, analysis of the physicochemical properties of these formulations (Table 9.2) show that some co-polymer formulations are greatly impacted by the presence of OVA. The presence of OVA has a stabilising effect on the formulation, which is particularly observed for CP3 liposomal formulations that are  $108 \pm 0.4$  nm, in comparison to empty CP3 DMPC:Chol liposomes that were measured to be  $207 \pm 42$  nm in size (Table 9.2). Whilst a smaller decrease in size was measured for DMPC:Chol liposomes formed with CP1, 2 and 4. A size increase from  $117 \pm 31$  nm to  $178 \pm 1$  nm was measured for OVA loaded CP5 DMPC:Chol liposomal formulation (Table 9.2). Once again, the PDI of the formulation was below 0.2 (Table 9.2) and the zeta potential of the formulations was above -10 mV (Table 9.2). The similar encapsulation efficiencies achieved by the co-polymer DSPC:Chol liposomal formulations can be attributed to the microfluidics manufacturing process, whereby the OVA is added during the liposomal production process rather than after. The results suggest the molecular weight of the co-polymer did not impact the amount of encapsulation. As all co-polymers were formulated with the same components (mPEG and PDL), similar encapsulation is achieved. Results by Ahmed and Discher (Ahmed and Discher, 2004) show swapping the PDL for polycaprolactone (PCL) results in a reduced amount of encapsulation. For instance, there is a significant difference in encapsulation between the co-polymers; 81 % encapsulation of indomethacin (IND) was achieved by mPEG-b-PeDL micelles, compared to 66 % encapsulation by mPEG-b-PCL (Kakde *et al.*, 2016). The results from Table 9.2 show loading achieved by these co-polymer DMPC:Chol liposomes is similar to DMPC:Chol liposomes manufactured by microfluidics, and thus the co-polymer DMPC:Chol liposomes were investigated further in terms of applicability (through in-vitro studies).



**Table 9.2.** Characterisation of ovalbumin loaded DMPC:Chol liposomes containing 4% of all five co-polymers. The size, polydispersity index and zeta potential was determined by dynamic light scattering. The amount and encapsulation efficiency of the protein ovalbumin by co-polymer DMPC:Chol liposomes of varying lengths. The formulations were produced by microfluidics (at a 3:1 FRR and 15 mL/min TFR). The results represent mean  $\pm$  SD, n=3 independent batches.

<b>FORMULATION</b>	<b>SIZE (D. NM)</b>	<b>POLYDISPERSITY INDEX</b>	<b>ZETA POTENTIAL (MV)</b>	<b>AMOUNT (<math>\mu</math>G/ML)</b>	<b>ENCAPSUALTION EFFICIENCY (%)</b>
<b>CP1</b>	126 $\pm$ 1	0.16 $\pm$ 0.012	-7 $\pm$ 0.6	68 $\pm$ 7	36 $\pm$ 4
<b>CP2</b>	115 $\pm$ 1	0.13 $\pm$ 0.008	-7 $\pm$ 0.5	67 $\pm$ 3	36 $\pm$ 1
<b>CP3</b>	108 $\pm$ 0.4	0.19 $\pm$ 0.006	-12 $\pm$ 0.9	67 $\pm$ 4	36 $\pm$ 2
<b>CP4</b>	94 $\pm$ 0.2	0.21 $\pm$ 0.010	-9 $\pm$ 0.9	77 $\pm$ 8	41 $\pm$ 4
<b>CP5</b>	178 $\pm$ 1.4	0.16 $\pm$ 0.008	-11 $\pm$ 1.3	73 $\pm$ 4	39 $\pm$ 2

#### 9.4.4 The viability of THP-1 cells exposed to co-polymer DMPC:Chol liposomal formulations

The synthesised co-polymers are thought to be non-toxic and biodegradable. To investigate this, cell viability assays were performed using THP-1 cells that were exposed to co-polymer liposomal formulations across a range of concentrations (6- 200 µg/mL) to determine the ideal concentration required (Figure 9.7). Both empty and OVA loaded liposomal formulations were investigated for the viability of the cells. The results from cell viability of empty CP1 and CP5 across a range of concentration shows the co-polymer formulations are non-toxic (Figure 9.7), with a cell viability of around 100 %.

In addition, OVA loaded DMPC:Chol added to THP-1 cells shows the addition of OVA is non-toxic (Figure 9.8). The cell viability of the co-polymers was measured to be around 100 %, confirming the reports that the PDL polymer is non-toxic. The PDL component is a viable alternative to PCL; it can be sourced sustainably from castor oil. It is currently used as flavourings and in the fragrance industry, thus the polymer is biodegradable. Also, given PEG is a hydrophilic polymer, with noted low toxicity it was predicted the PEG component of the co-polymer lipids were non-toxic (Harris *et al.*, 2001, Nakamura *et al.*, 2012). The addition of PEG is widely known to improve formulation stability and pharmacokinetics of drugs, along with PEGylated liposomes already existing on the market for therapeutic use (Harris *et al.*, 2001). One such example of a PEGylated liposomal formulation on the market is Doxil which has a low toxicity, and is used as a cancer treatment in more than 80 countries (Drummond *et al.*, 1999, Gabizon *et al.*, 2003). Results from the cell viability assays corroborate this, the results show co-polymer inclusion does not adversely impact cell viability, with more than 90% of cells viable after exposure to the co-polymer liposome formulations. The findings show the combination of PDL-PEG is non-toxic and the assays were used to pick a working concentration of 100 µg/mL.

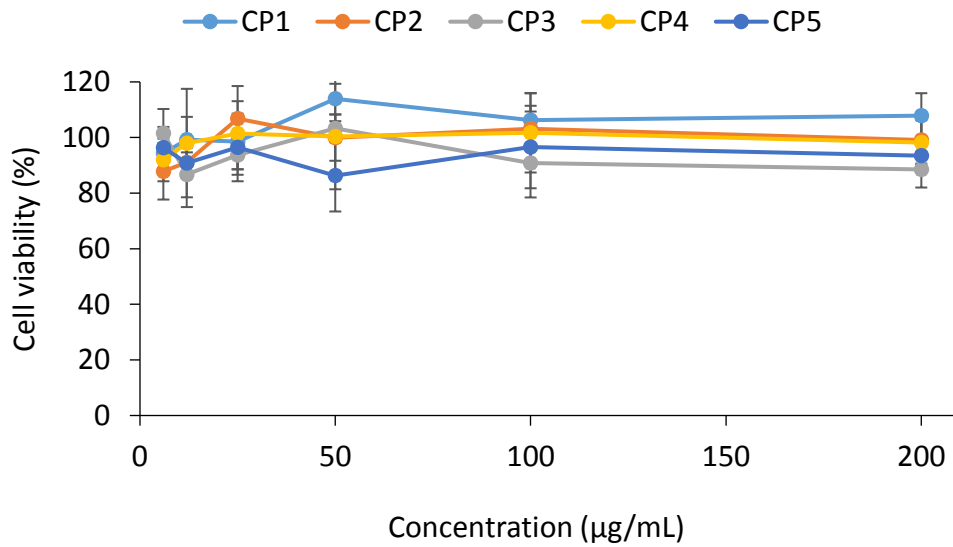


**Figure 9.7.** The cell viability of THP-1 cells exposed to empty DMPC:Chol liposomes with varying lengths of co-polymer (co-polymers 1-5). The THP-1 cells were exposed to 100 µg/mL of the formulations for 24 hours after which the viability was determined by cell titre blue assay. The results represent mean  $\pm$  SD, n=3 independent batches.

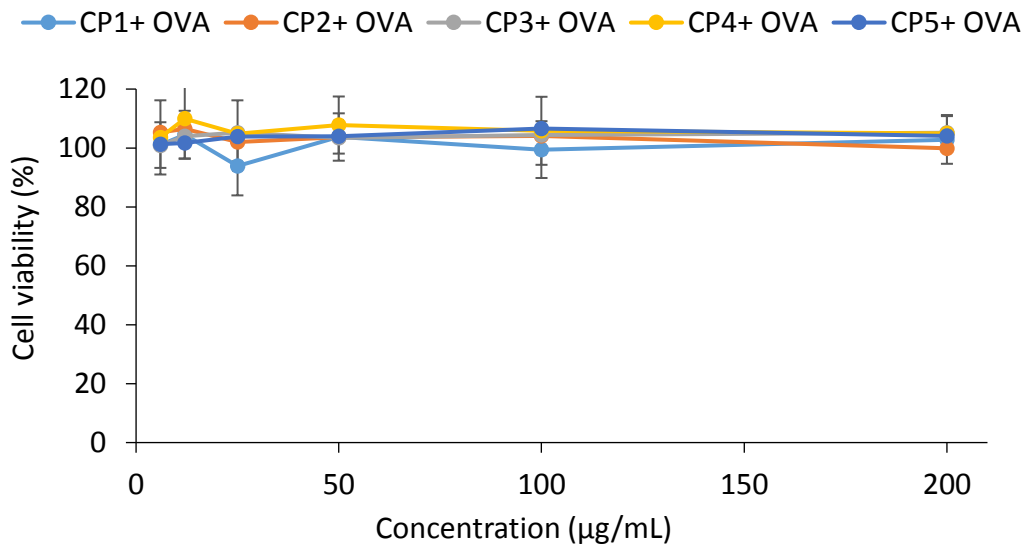


**Figure 9.8.** The cell viability of THP-1 cells exposed to OVA loaded DMPC:Chol liposomes with varying lengths of co-polymer (co-polymers 1-5). The THP-1 cells were exposed to 100 µg/mL of the formulations for 24 hours after which the viability was determined by cell titre blue assay. The results represent mean  $\pm$  SD, n=3 independent batches.

#### 9.4.5 The uptake of co-polymer DMPC:Chol liposomal formulations by THP-1 cells

The ability of THP-1 cells to take up the co-polymer liposomal formulations was investigated. Previous papers have shown that the addition of co-polymers can improve uptake of particles, therefore this was initially investigated using empty co-polymer DMPC:Chol liposomes. The uptake of these formulations was carried out at both 37°C and 4°C to determine if uptake was by endocytosis, with empty DMPC:Chol liposomes run in parallel for comparison. The results from Figure 9.9A show uptake of co-polymers occurs within 30 minutes, regardless of the co-polymer type used. The uptake of CP1 DMPC:Chol liposomes after 3 hours was  $90 \pm 4 \%$ , for CP2 uptake of  $76 \pm 4 \%$  was calculated,  $67 \pm 5 \%$  for CP3,  $76 \pm 2 \%$  for CP4 and  $86 \pm 3 \%$  for CP5 (Figure 9.9A). The DMPC:Chol formulations was run in parallel with  $76 \pm 8 \%$  uptake occurring within three hours (Figure 9.9A). Statistical analysis of the results revealed there is no significant increase in the uptake of CP2-5 in comparison to neutral DMPC:Chol liposomal formulations. Running the experiments in parallel at 4°C showed the uptake was by endocytosis with less than 10 % of uptake observed for all formulations (Figure 9.9B).

Furthermore, OVA was added to the CP liposomal formulations and the uptake was investigated. The uptake of CP1- 5 after three hours was  $80 \pm 4 \%$ ,  $77 \pm 6 \%$ ,  $89 \pm 5 \%$ ,  $89 \pm 4 \%$ , and  $71 \pm 5 \%$  respectively (Figure 9.10A). From Figure 9.10A it shows uptake of OVA loaded CP is similar to OVA loaded DMPC:Chol liposomal formulations, with an uptake of  $68 \pm 1 \%$  calculated after three hours. There is no significant difference between the uptake of liposome with or without co-polymers. Once again, running a parallel experiment at 4°C confirms uptake is by endocytosis as uptake is below 10 % across the three hours (Figure 9.10B). Results from the in-vitro assays show co-polymer liposomes do not cause adverse interactions, nor cause unwanted activation of the neutrophil liposomal formulations (Photos et al., 2003). The rapid uptake observed in Figure 9.9 and Figure 9.10 is encouraging, as previous in-vivo results have shown the addition of PEG can improve movement of formulations to the lymph node. Comparison of PEGylated and non-PEGylated cationic liposomes given intramuscularly has shown the addition of PEG enhances clearance rates from the site of injection (Kaur et al., 2012). Only 10% of the original amount of PEGylated liposomes remained at the site of injection after four days, compared to 60% of the non-PEGylated liposomes (Kaur et al., 2012). The formulations are more stable when given intravenously compared to their non-PEGylated counterparts (Kaur et al., 2012). The

enhanced migration of PEGylated formulations to the lymph node is good for antigen presenting and subsequently generating an immunisation response. Subsequently, the results from Figure 9.9 and 9.10 show co-polymers may be a viable option as liposomal vaccines. The inclusion of PEG may facilitate faster migration of the formulations to lymph nodes and therefore result in faster antigen processing and presentation.

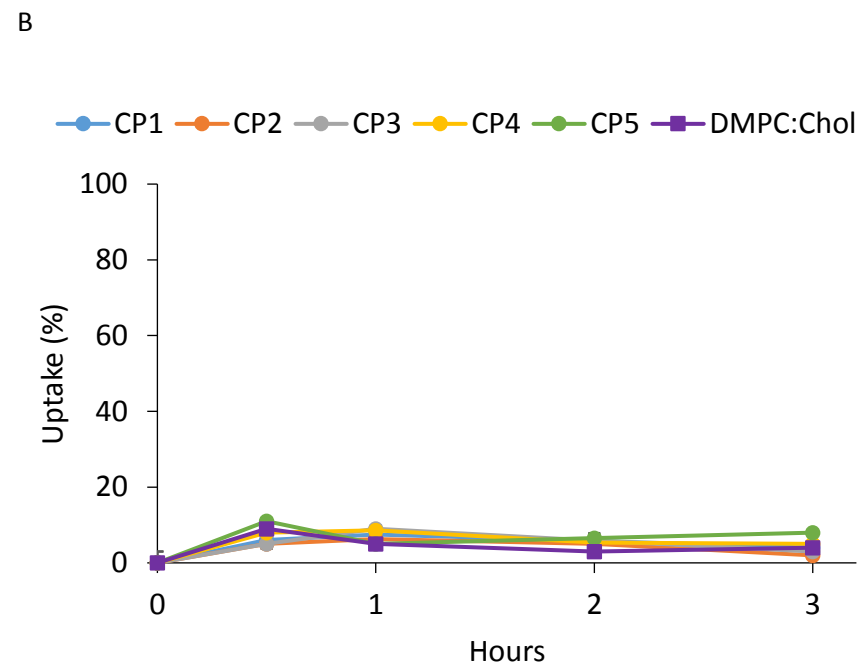
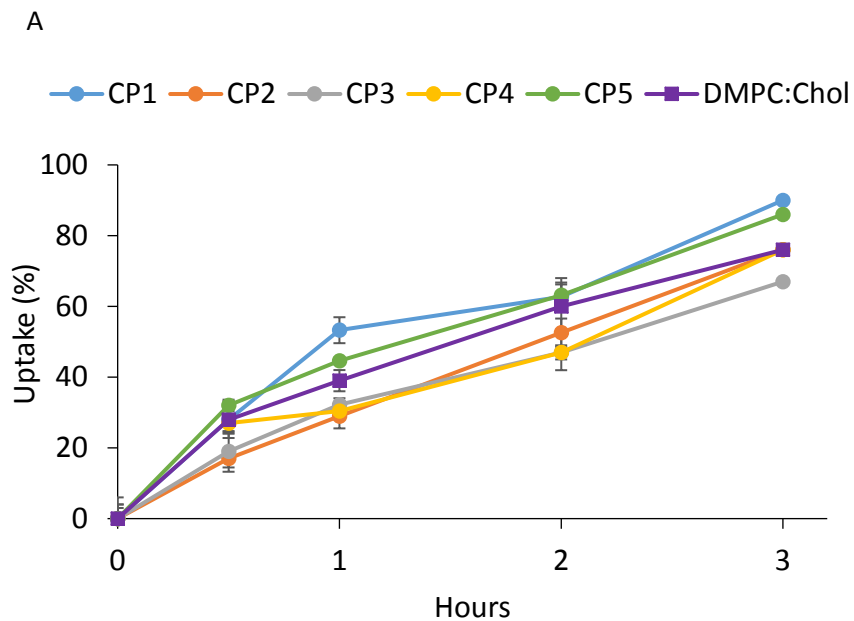
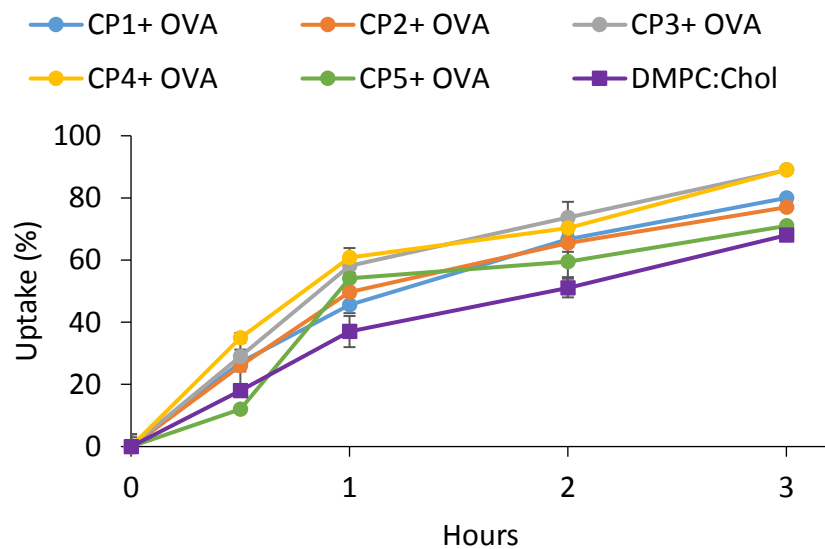


**Figure 9.9.** The uptake of empty co-polymer (CP1- 5) liposomal DMPC:Chol formulations compared to DMPC:Chol formulations. All formulations were produced by microfluidics at a 3:1 FRR and 15 mL/min TFR. The cells were exposed to the formulations for up to three hours (with samples collected at 0.5, 1 2, and 3 hours) at either 37°C or 4°C. After a set amount of time the formulations were removed and the uptake was measured using flow cytometry. The results represent mean  $\pm$  SD, n=3 independent batches.

A



B

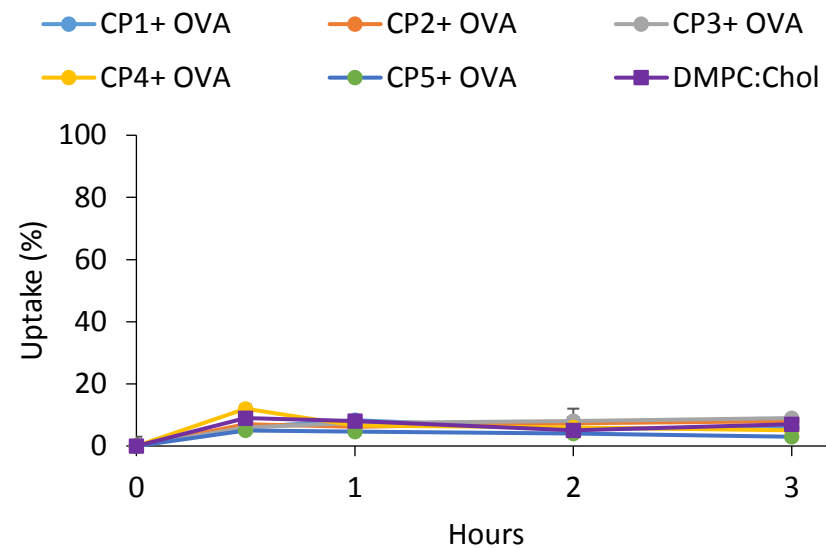


**Figure 9.10.** The uptake of ovalbumin (OVA) loaded co-polymer (CP1- 5) liposomal DMPC:Chol formulations compared to OVA loaded DMPC:Chol formulations. All formulations were produced by microfluidics at a 3:1 FRR and 15 mL/min TFR. The cells were exposed to the formulations for up to three hours (with samples collected at 0.5, 1 2, and 3 hours) at either 37°C or 4°C. After a set amount of time the formulations were removed and the uptake was measured using flow cytometry. The results represent mean  $\pm$  SD, n=3 independent batches.

#### 9.4.6 Processing of co-polymer DMPC:Chol formulations

As OVA loaded CP4 DMPC:Chol liposomes resulted in the most uptake by THP-1 cells ( $89 \pm 4$  %), this particular formulation was investigated for internal liposome processing of the formulations. The formulations were loaded with DQ-OVA, an OVA conjugate which when degraded in the cell fluoresces green. The results show DQ-OVA processing was quick (Figure 9.11); of the 89% of OVA loaded CP4 liposome taken up,  $47 \pm 8$  % was processed within three hours. The amount of DQ-OVA processing increases the longer the cells are left, with 100% processing of DQ-OVA observed after 48 hours. The results show the addition of co-polymers is not hindering uptake or processing of DQ-OVA, which indicates the co-polymers are biodegradable. The cells can easily and rapidly breakdown the formulations; the DQ-OVA is readily processed within three hours. Results from this assay highlight the usefulness of incorporating co-polymers into formulations, as it can improve stability of formulations in circulation as well as enhance vaccine adjuvant responses (Kaur *et al.*, 2012). The PEG component on the co-polymer is likely to improve migration to the lymph node, therefore these formulations may be useful therapeutics which need further exploring.

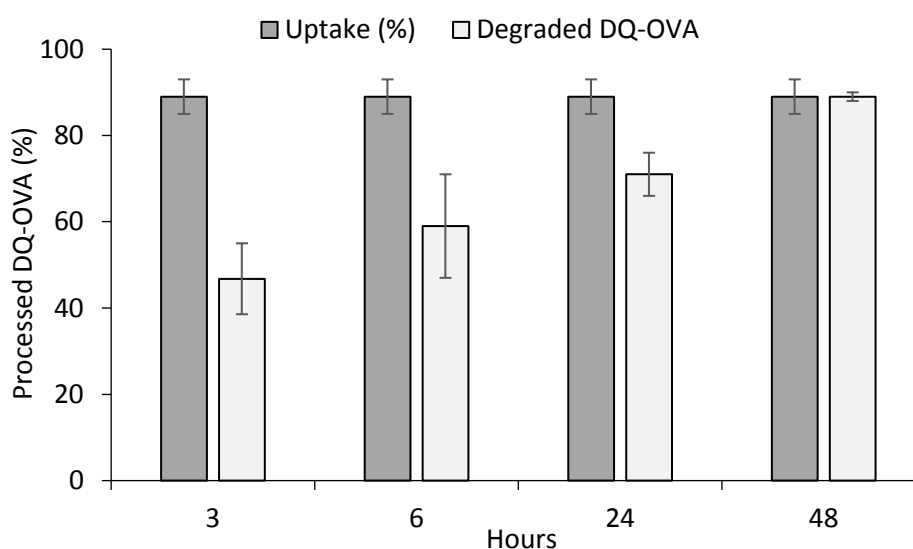


**Figure 9.11.** The processing of DQ-OVA in relation to uptake over 48 hours. THP-1 cells were exposed to OVA loaded CP4 (4%) DMPC:Chol liposomes for a set amount of hours (3- 48 hours), after which the formulations were removed and the amount of OVA processing was quantified by flow cytometry. The results represent mean  $\pm$  SD, n=3 independent batches.



## 9.5 Conclusion

In this chapter, the ability to produce co-polymer and liposome hybrid formulations using the synthetic polymers provided by Dr. Casterri was confirmed. The compatible solvents required to produce these formulations was discovered (methanol and acetone), along with testing the manufacturing capability with microfluidics. The results show that varying lengths of synthesised co-polymers can be added to the liposomal formulations, with varying increases in the size of DMPC:Chol formulations in comparison to conventional DMPC:Chol liposomes. The co-polymer liposomes were characterised (in terms of size, PDI and zeta potential), with microfluidics enabling the production of homogenous liposomal formulations that were also stable.

In addition, the co-polymer liposomes were also loaded with protein to determine the impact on the physicochemical properties and encapsulation. Results showed that the addition of protein had a stabilising effect, with smaller sized liposomes produced. Like the empty co-polymer liposomes the OVA loaded formulations were homogenous in nature. The amount of OVA loading achieved was similar to what is obtained for conventional OVA loaded DMPC:Chol liposomes, suggesting that the microfluidics manufacturing method may enable high loading irrespective of the formulation. The co-polymer liposomes are as equally capable of processing DQ-OVA when compared to conventional liposomes. As a result, the combination of co-polymer with lipids enables both the stability and high encapsulation efficiency attributed to the co-polymer and lipids respectively. The results are encouraging; the similar functional property of these co-polymer liposomes to conventional DMPC:Chol liposomes offers an alternative for when long circulating non-toxic formulations are required. It provides the foundation for further building collaborations and further exploring the use of co-polymers within liposomal research.

# **Chapter 10**

## **Conclusion**

## **10.1 Summary of the findings**

### **10.2 Characterisation of liposomal formulations produced by microfluidics**

Liposomal formulations are well defined as drug delivery vehicles with multiple manufacturing methods available. Initial studies compared the microfluidics production with traditional thin film lipid hydration methods followed by sonication. Microfluidics production was the preferred method as smaller sized and more homogenous formulations were produced. Unlike microfluidics, liposomal formulations containing protein can become denatured with the possibility of contamination (requiring further purification steps), when probe sonication is used for downsizing formulations (Philippot and Schuber, 2017). The ease of manufacturing by microfluidics and the better quality liposomes produced makes microfluidics the manufacturing method of choice.

In agreement with previous reports (Jahn *et al.*, 2010, Zook and Vreeland, 2010), the flow rate ratio (FRR) was one of the main manufacturing parameter impacting liposomal characteristics (in terms of size, PDI and loading ability). The manufacturing process parameters were further investigated with respect to the formulation composition (such as solvent choice, buffer choice and initial lipid concentration). The results show the formulation composition can influence the size of the formulations; with higher lipid concentrations (of above 4 mg/mL) producing smaller sized vesicles. The normal operating ranges and parameters were also identified with the use of design of experiments analysis, so a larger design space can be identified with the minimum amount of experiments required. Using the DoE software, the ideal operating ranges for producing small liposomal formulations was identified, with the results once again showing that a higher FRR of 3:1 is ideal for this. Based on these parameters, further liposomal formulations were investigated with respect to both the manufacturing technique as well as the liposomal products produced.

### **10.3 Continuous manufacturing and scale- out of liposomal formulations**

High throughput and streamlining of liposome manufacturing processes is essential if liposomal products are to be used more widely. Whilst current liposomal medicines do exist on the market, trouble with manufacturing means that these therapeutics are not ideal nor

cost effective. As a result, a manufacturing process using microfluidics technology for production have been investigated previously by Dimov et al (Dimov *et al.*, 2017). However, the model lacked the ability to measure the quality of liposomes during manufacturing in real time (at-line monitoring) so this was tested. Through use of commercially available equipment, a manufacturing process was developed which allowed for the production and purification of liposomal formulations, as well as the ability to measure the quality of the products at-line. The liposomal formulations produced by this technique were stable, and at-line measurements gave comparable results to off-line (manual) measurements.

In addition, the ability to screen formulations rapidly when working in a research setting is highly advantageous, and so this was investigated by using a high throughput dynamic light scattering plate reader. Measurements taken by the Zetasizer APS are comparable to the off-line measurement, thus suggesting the use of this equipment is ideal for when automated rapid screening of formulations is required. The smaller amount of sample required for testing is also advantageous as less money is spent on initial screening stages of formulation development, therefore a highly viable and practical alternative for the characterisation of liposomal formulations is shown.

#### **10.4 Rapid protein quantification techniques for determining the protein loading in liposomal formulations**

The nature of liposomal formulations makes them ideal as delivery vehicles and so it is important to develop viable methods to measure the amount of loading for the correct therapeutic dose to be achieved. Traditionally, most loading is calculated indirectly by mass balance (subtracting the non- entrapped from the original amount), however this is not very accurate. In this thesis, the use of a solubilising technique (Fatouros and Antimisariis, 2002) was implemented and multiple methods were developed to directly quantify the amount of entrapped protein. Direct measurement of the entrapped protein was possible, with two HPLC methods giving comparable loading results. The results suggest HPLC is a fast technique for the quantification of entrapped protein, making it ideal for a variety of uses (from developing formulations, to quality control checks). Both methods were thoroughly examined to ensure they both meet the ICH guidelines (Guideline, 2005b); with UV-HPLC and ELSD-HPLC able to quantify protein to a high degree of accuracy and repeatability. The HPLC

analytical methods were able to quantify protein at very low concentrations, highlighting the robustness of the procedures, with the HPLC-ELSD having the added bonus of being able to change the sensitivity of the system (referred to as gain). At high gains (above 5), the equipment was highly sensitive to small protein amounts with clear distinct peaks obtained. Hence we have developed easily adaptable protein quantification methods for the direct quantification of protein loaded formulations.

## **10.5 Rapid microfluidics manufacture of protein loaded liposomes**

The complexity of protein has often meant that entrapping antigen inside liposomes for therapeutics is challenging. The production of liposomal formulations often requires heat, mechanical movement (or agitation) as well as solvent (to dissolve lipids), all of which can cause protein denaturation (either chemical or physical) (Szoka and Papahadjopoulos, 1978, Tanford, 1968, Clark and Smith, 1989). Maintaining protein integrity is vital for therapeutic function, and so in this thesis it is shown that using microfluidics to produce ovalbumin loaded liposomes does not cause denaturation of the protein. Circular dichroism revealed the protein structural integrity is maintained during microfluidics production, with high encapsulation efficiency achieved in comparison to traditional techniques such as sonication. The poor loading of protein observed for traditional production techniques is in keeping with previous reports with less than 10 % encapsulation of protein achieved (Lapinski *et al.*, 2007). In this thesis, we show the ability of microfluidics technology to encapsulate significantly more protein (32- 38 %) in a rapid manner, which is an advantage of this system.

## **10.6 High throughput manufacture of liposomes loaded with small molecular drugs**

Liposomes provide a solution for delivery of insoluble compounds, by allowing drug interactions with the lipid bilayer. Using the small molecular drug propofol as a model drug, the ability of the microfluidics system to produce liposomal formulations containing insoluble drugs was explored. A high loading efficiency of around 42% was achieved which is in keeping with previous report, with poor loading observed using traditional production methods. For instance, Joshi *et al* (Joshi *et al.*, 2016) showed the ability to dual load drugs into liposomal formulations at a high loading capacity using microfluidics.

In addition, the ability for the SU1349 drug to be loaded into liposomal formulations using microfluidics was tested. The drug was poorly soluble and so achieving high loading was difficult. The formulations were larger in size (more than 500 nm), but adjusting the formulation composition produced formulations around 100 nm in size. Despite this, it is unclear whether liposomes are being formed or the sizes are due to aggregation. Further experiments such as cryoTEM images are needed for clarification.

Moreover, the insolubility of the SU1349, and lack of solvent compatibility means the drug is not ideal for therapeutic use. The results show that while microfluidics is able to achieve significantly more loading of protein and small molecular drug, the process is still impacted by the lipid formulation composition. Thus, despite the poor loading of the SU1349 the results highlight the usefulness and versatility of the microfluidics technology.

### **10.7 Strategies for the high throughput production of liposomes in a freeze dried format**

Freeze drying of liposomal formulations is a technique that can be used to preserve the physicochemical properties and stability of the liposomal formulations. A range of parameters that can influence the successful freeze drying of the formulations (including the lipid concentration, presence of protein or cryoprotectant concentration) were tested (Van Winden and Crommelin, 1997, Carpenter *et al.*, 1992, Lombrana *et al.*, 2001). Due to the number of experiments required, DoE was used to define the design space for the ideal freeze drying of the liposomal formulations. There was no significant difference in the cake appearance irrespective of whether the formulations underwent freeze drying in vials or microplates. In this thesis, the ideal freeze drying cycle for the liposomal formulations was identified; minimal changes in the liposomal characteristics (size and PDI) were observed, with no leakage of the encapsulated protein (Crowe *et al.*, 1986b, Crowe *et al.*, 1997). The results show the freeze drying method is ideal for the freeze drying of formulation, compared to previous existing methods whereby leakage of product was problematic. Here we identify a method that is not only simple to run, but allows for high throughput screening due to the ability to freeze dry small quantities in a 96 well plate.

### **10.8 Screening of cell cultures for liposomal formulation investigation**

The applicability of liposomal formulations produced by microfluidics was investigated using in-vitro cell assays. Two macrophage cell lines (RAW264.7 and THP-1 cells) were used as model cells, for rapid screening and processing of antigen using OVA loaded DMPC:Chol and DSPC:Chol liposomal formulations. In this thesis, a quick and efficient method for measuring antigen processing was developed using DQ-OVA. The formulations were readily taken up, with more than 50% of internalised liposomes processed within three hours. The studies provide a valuable tool for understanding antigen processing and can be readily applied to many formulations consisting of various lipid types.

In addition, microfluidics mixing was explored as a potential tool for the rapid screening of cell-liposome interactions. Passing cells through a microfluidics chip showed no adverse effects with the cells maintaining viability. However, liposomal formulations run alongside microfluidics showed minimal uptake with further experiments required to improve this.

### **10.9 Evaluating the addition of co-polymers to liposomal formulations produced by microfluidics**

The ability for liposomal formulations to reach the target site is important for the therapeutic effect to occur. While neutral liposomes are ideal due to their non-toxicity and high encapsulation rate, they are easily targeted by the MPS system because of their interactions with plasma proteins (Scherphof *et al.*, 1985). The addition of mPEG forms a protective shield around the liposomal formulation, preventing coating from plasma proteins and aggregation of the vesicles (Needham *et al.*, 1992). The inclusion of mPEG co-polymer lipids to DMPC:Chol liposomes improved the stability of the liposomal formulations. The uptake of neutral co-polymer DMPC:Chol liposomes was similar to that achieved by neutral DMPC:Chol liposomes, however uptake of OVA loaded formulations was increased for some co-polymer DMPC:Chol formulations in comparison to OVA loaded DMPC:Chol formulations. The formulations are equally functional, with the similar amount of OVA encapsulation achieved. As seen with neutral formulations, the DQ-OVA loaded co-polymer liposomes were processed quickly. The results present co-polymer formulations as a viable alternative for when longer circulation time and release profiles are required.

## 10.10 Overall conclusion

To conclude, the overall aim of this thesis (highlighted in Chapter 1) was to investigate microfluidics technology (with particular emphasis on defining optimal parameters) for the production of a range of formulations and applications. Based on the objectives highlighted in Chapter 1, the studies from this thesis have shown that:

1. The quality of liposomal formulations produced by microfluidics is better (with regards to homogeneity, size and higher encapsulation efficiency) in comparison to traditional methods (thin film lipid hydration followed by sonication).
2. Design of experiments was used to define the ideal microfluidics parameters for the production of neutral liposomal formulations. For instance, a FRR of 3:1 was identified as the ideal parameter for producing the smallest sized formulations, with the speed having little impact (so a TFR of 15 mL/min was used).
3. A manufacturing process was developed which enables monitoring of liposome quality in real-time. The process has potential to be used for future liposomal formulation production.
4. Rapid quantification methods for protein loaded liposomal formulations were developed using high-performance liquid chromatography. The methods developed are easily transferable and were highly accurate in addition to highly sensitive (as demonstrated with low LoD and LoQ values of less than 10 µg/mL).
5. The microfluidics manufacturing method is able to encapsulate more than 30 % of protein inside liposomal formulations, compared to less than 10% encapsulation reported by sonication. Similarly, the loading of small molecular drugs by microfluidics (approximately 40% for propofol) was significantly higher than the same formulations produced by traditional methods.
6. The liposomal formulations are readily taken up by macrophages by endocytosis, with uptake observed within 30 minutes for both empty and OVA loaded formulations, in addition to co-polymer loaded formulations. Around 60% uptake of empty liposomal formulations was observed within 3 hours, with uptake of OVA loaded formulations slightly lower (around 48%) by THP-1 cells. Once uptake has occurred, the DQ-OVA assays revealed the cells can quickly breakdown the



formulations, with OVA processing occurring within three hours. A similar trend is also observed for co-polymer liposomal formulations highlighting the usefulness of the liposomal formulations.

7. The ideal freeze drying cycle for freeze drying liposomal formulations was developed. The method preserved the characteristics of the liposomes (in particular the size and PDI) with no leakage of the encapsulated OVA.

# **Chapter 11**

## **References**

- ABRAHAM, S. A., WATERHOUSE, D. N., MAYER, L. D., CULLIS, P. R., MADDEN, T. D. & BALLY, M. B. 2005. The Liposomal Formulation of Doxorubicin. *Methods in Enzymology*. Academic Press.
- AGRAWAL, A. K. & GUPTA, C. 2000. Tuftsin-bearing liposomes in treatment of macrophage-based infections. *Advanced drug delivery reviews*, 41, 135-146.
- AGUILAR, M.-I. 2004. Reversed-Phase High-Performance Liquid Chromatography. In: AGUILAR, M.-I. (ed.) *HPLC of Peptides and Proteins: Methods and Protocols*. Totowa, NJ: Springer New York.
- AHMED, F. & DISCHER, D. E. 2004. Self-porating polymersomes of PEG–PLA and PEG–PCL: hydrolysis-triggered controlled release vesicles. *Journal of controlled release*, 96, 37-53.
- AHSAN, F., RIVAS, I. P., KHAN, M. A. & SUÁREZ, A. I. T. 2002. Targeting to macrophages: role of physicochemical properties of particulate carriers—liposomes and microspheres—on the phagocytosis by macrophages. *Journal of controlled release*, 79, 29-40.
- AHYAYAUCH, H., COLLADO, M. I., ALONSO, A. & GOÑI, F. M. 2012. Lipid bilayers in the gel phase become saturated by triton X-100 at lower surfactant concentrations than those in the fluid phase. *Biophysical journal*, 102, 2510-2516.
- AKBARZADEH, A., REZAEI-SADABADY, R., DAVARAN, S., JOO, S. W., ZARGHAMI, N., HANIFEHPOUR, Y., SAMIEI, M., KOUHI, M. & NEJATI-KOSHKI, K. 2013. Liposome: classification, preparation, and applications. *Nanoscale Res Lett*, 8, 102.
- ALI, M. H., KIRBY, D. J., MOHAMMED, A. R. & PERRIE, Y. 2010. Solubilisation of drugs within liposomal bilayers: alternatives to cholesterol as a membrane stabilising agent. *Journal of Pharmacy and Pharmacology*, 62, 1646-1655.
- ALI, M. H., MOGHADDAM, B., KIRBY, D. J., MOHAMMED, A. R. & PERRIE, Y. 2013. The role of lipid geometry in designing liposomes for the solubilisation of poorly water soluble drugs. *International journal of pharmaceutics*, 453, 225-232.
- ALLEN, T. M. & CULLIS, P. R. 2004. Drug delivery systems: entering the mainstream. *Science*, 303, 1818-1822.
- ALLEN, T. M. & CULLIS, P. R. 2013. Liposomal drug delivery systems: from concept to clinical applications. *Adv Drug Deliv Rev*, 65, 36-48.
- ALLISON, A. & GREGORIADIS, G. 1974. Liposomes as immunological adjuvants.
- ALONSO, A., URBANEJA, M.-A., GOÑI, F. M., CARMONA, F. G., CÁNOVAS, F. G. & GÓMEZ-FERNÁNDEZ, J. C. 1987. Kinetic studies on the interaction of phosphatidylcholine liposomes with Triton X-100. *Biochimica et Biophysica Acta (BBA)-Biomembranes*, 902, 237-246.
- ALTMAN, D. G. & BLAND, J. M. 1983. Measurement in medicine: the analysis of method comparison studies. *The statistician*, 307-317.
- ALVING, C. R., STECK, E. A., CHAPMAN, W. L., WAITS, V. B., HENDRICKS, L. D., SWARTZ, G. M. & HANSON, W. L. 1978. Therapy of leishmaniasis: superior efficacies of liposome-encapsulated drugs. *Proceedings of the National Academy of Sciences*, 75, 2959-2963.
- ANCHOROGUY, T. J., RUDOLPH, A. S., CARPENTER, J. F. & CROWE, J. H. 1987. Modes of interaction of cryoprotectants with membrane phospholipids during freezing. *Cryobiology*, 24, 324-331.
- ANDAR, A. U., HOOD, R. R., VREELAND, W. N., DEVOE, D. L. & SWAAN, P. W. 2014. Microfluidic preparation of liposomes to determine particle size influence on cellular uptake mechanisms. *Pharmaceutical research*, 31, 401-413.
- ANDERSON, M. & OMRI, A. 2004. The effect of different lipid components on the in vitro stability and release kinetics of liposome formulations. *Drug delivery*, 11, 33-39.

- ARAMAKI, Y., TAKANO, S. & TSUCHIYA, S. 2001. Cationic liposomes induce macrophage apoptosis through mitochondrial pathway. *Archives of biochemistry and biophysics*, 392, 245-250.
- ASAYAMA, K., ARAMAKI, Y., YOSHIDA, T. & TSUCHIYA, S. 1992. Permeability changes by peroxidation of unsaturated liposomes with ascorbic acid/Fe<sup>2+</sup>. *Journal of Liposome Research*, 2, 275-287.
- AWADE, A. C. & EFSTATHIOU, T. 1999. Comparison of three liquid chromatographic methods for egg-white protein analysis. *Journal of Chromatography B: Biomedical Sciences and Applications*, 723, 69-74.
- BALL, P. 2000. Scale-up and scale-down of membrane-based separation processes. *Membrane Technology*, 2000, 10-13.
- BANGHAM, A. D. & HORNE, R. W. 1964. Negative staining of phospholipids and their structural modification by surface-active agents as observed in the electron microscope. *Journal of Molecular Biology*, 8, 660-670.
- BARENHOLZ, Y. 2002. Cholesterol and other membrane active sterols: from membrane evolution to "rafts". *Progress in lipid research*, 41, 1-5.
- BARENHOLZ, Y. C. 2012. Doxil<sup>®</sup>—the first FDA-approved nano-drug: lessons learned. *Journal of controlled release*, 160, 117-134.
- BARTOLOMEO, M. P. & MAISANO, F. 2006. Validation of a reversed-phase HPLC method for quantitative amino acid analysis. *Journal of biomolecular techniques : JBT*, 17, 131-137.
- BASU, M. K. & LALA, S. 2004. Macrophage specific drug delivery in experimental leishmaniasis. *Current molecular medicine*, 4, 681-689.
- BAZAK, R., HOURI, M., EL ACHY, S., KAMEL, S. & REFAAT, T. 2015. Cancer active targeting by nanoparticles: a comprehensive review of literature. *Journal of cancer research and clinical oncology*, 141, 769-784.
- BEDU-ADDO, F. K. 2004. Understanding lyophilization formulation development. *Pharmaceutical Technology*, 20, 10-19.
- BERMUDEZ, H., BRANNAN, A. K., HAMMER, D. A., BATES, F. S. & DISCHER, D. E. 2002. Molecular weight dependence of polymersome membrane structure, elasticity, and stability. *Macromolecules*, 35, 8203-8208.
- BI, R., SHAO, W., WANG, Q. & ZHANG, N. 2008. Spray-freeze-dried dry powder inhalation of insulin-loaded liposomes for enhanced pulmonary delivery. *Journal of drug targeting*, 16, 639-648.
- BIBI, S., KAUR, R., HENRIKSEN-LACEY, M., MCNEIL, S. E., WILKHU, J., LATTMANN, E., CHRISTENSEN, D., MOHAMMED, A. R. & PERRIE, Y. 2011. Microscopy imaging of liposomes: From coverslips to environmental SEM. *International Journal of Pharmaceutics*, 417, 138-150.
- BIRNGRUBER, T., RAML, R., GLADDINES, W., GATSCHELHOFFER, C., GANDER, E., GHOSH, A., KROATH, T., GAILLARD, P. J., PIEBER, T. R. & SINNER, F. 2014. Enhanced Doxorubicin Delivery to the Brain Administered Through Glutathione PEG ylated Liposomal Doxorubicin (2 B 3-101) as Compared with Generic C aelyx,<sup>®</sup>/D oxil<sup>®</sup>—A Cerebral Open Flow Microperfusion Pilot Study. *Journal of pharmaceutical sciences*, 103, 1945-1948.
- BLANK, F., ROTHEN-RUTISHAUSER, B. M., SCHURCH, S. & GEHR, P. 2006. An optimized in vitro model of the respiratory tract wall to study particle cell interactions. *Journal of Aerosol Medicine*, 19, 392-405.
- BLUME, G. & CEVC, G. 1993. Molecular mechanism of the lipid vesicle longevity in vivo. *Biochimica et Biophysica Acta (BBA)-Biomembranes*, 1146, 157-168.

- BOSWELL, G., BUELL, D. & BEKERSKY, I. 1998. AmBisome (liposomal amphotericin B): a comparative review. *The Journal of Clinical Pharmacology*, 38, 583-592.
- BRADLEY, A. J., DEVINE, D. V., ANSELL, S. M., JANZEN, J. & BROOKS, D. E. 1998. Inhibition of liposome-induced complement activation by incorporated poly (ethylene glycol)-lipids. *Archives of biochemistry and biophysics*, 357, 185-194.
- BRIUGLIA, M.-L., ROTELLA, C., MCFARLANE, A. & LAMPROU, D. A. 2015. Influence of cholesterol on liposome stability and on in vitro drug release. *Drug delivery and translational research*, 5, 231-242.
- BURADE, V., BHOWMICK, S., MAITI, K., ZALAWADIA, R., RUAN, H. & THENNATI, R. 2017. Lipodox® (generic doxorubicin hydrochloride liposome injection): in vivo efficacy and bioequivalence versus Caelyx® (doxorubicin hydrochloride liposome injection) in human mammary carcinoma (MX-1) xenograft and syngeneic fibrosarcoma (WEHI 164) mouse models. *BMC cancer*, 17, 405-405.
- CALICETI, P. & VERONESE, F. M. 2003. Pharmacokinetic and biodistribution properties of poly (ethylene glycol)-protein conjugates. *Advanced drug delivery reviews*, 55, 1261-1277.
- CAPRETTO, L., CARUGO, D., MAZZITELLI, S., NASTRUZZI, C. & ZHANG, X. 2013. Microfluidic and lab-on-a-chip preparation routes for organic nanoparticles and vesicular systems for nanomedicine applications. *Advanced drug delivery reviews*, 65, 1496-1532.
- CAPRETTO, L., CHENG, W., HILL, M. & ZHANG, X. 2011. Micromixing Within Microfluidic Devices. In: LIN, B. (ed.) *Microfluidics: Technologies and Applications*. Berlin, Heidelberg: Springer Berlin Heidelberg.
- CARPENTER, J., ARAKAWA, T. & CROWE, J. 1992. Interactions of stabilizing additives with proteins during freeze-thawing and freeze-drying. *Developments in biological standardization*, 74, 225-38; discussion 238-9.
- CARTER, P. J. 2011. Introduction to current and future protein therapeutics: A protein engineering perspective. *Experimental Cell Research*, 317, 1261-1269.
- CARUGO, D., BOTTARO, E., OWEN, J., STRIDE, E. & NASTRUZZI, C. 2016. Liposome production by microfluidics: potential and limiting factors. *Scientific Reports*, 6, 25876.
- CHAN, Y.-H., CHEN, B.-H., CHIU, C. P. & LU, Y.-F. 2004. The influence of phytosterols on the encapsulation efficiency of cholesterol liposomes. *International Journal of Food Science & Technology*, 39, 985-995.
- CHANG, H.-I. & YE, M.-K. 2012. Clinical development of liposome-based drugs: formulation, characterization, and therapeutic efficacy. *International Journal of Nanomedicine*, 7, 49-60.
- CHANPUT, W., MES, J. J. & WICHERS, H. J. 2014. THP-1 cell line: an in vitro cell model for immune modulation approach. *International immunopharmacology*, 23, 37-45.
- CHANPUT, W., PETERS, V. & WICHERS, H. 2015. THP-1 and U937 cells. *The Impact of Food Bioactives on Health*. Springer.
- CHEN, C., HAN, D., CAI, C. & TANG, X. 2010. An overview of liposome lyophilization and its future potential. *Journal of Controlled Release*, 142, 299-311.
- CHIANG, M. C., TULLETT, K. M., LEE, Y. S., IDRIS, A., DING, Y., MCDONALD, K. J., KASSIANOS, A., LEAL ROJAS, I. M., JEET, V. & LAHOUD, M. H. 2016. Differential uptake and cross-presentation of soluble and necrotic cell antigen by human DC subsets. *European journal of immunology*, 46, 329-339.
- CHONN, A. & CULLIS, P. R. 1995. Recent advances in liposomal drug-delivery systems. *Current Opinion in Biotechnology*, 6, 698-708.

- CHONN, A., SEMPLE, S. & CULLIS, P. 1992. Association of blood proteins with large unilamellar liposomes in vivo. Relation to circulation lifetimes. *Journal of Biological Chemistry*, 267, 18759-18765.
- CHOWDHARY, R. K., SHARIFF, I. & DOLPHIN, D. 2003. Drug release characteristics of lipid based benzoporphyrin derivative. *J Pharm Pharm Sci*, 6, 13-9.
- CHRISTENSEN, D., HENRIKSEN-LACEY, M., KAMATH, A. T., LINDENSTRØM, T., KORSHOLM, K. S., CHRISTENSEN, J. P., ROCHAT, A.-F., LAMBERT, P.-H., ANDERSEN, P. & SIEGRIST, C.-A. 2012. A cationic vaccine adjuvant based on a saturated quaternary ammonium lipid have different in vivo distribution kinetics and display a distinct CD4 T cell-inducing capacity compared to its unsaturated analog. *Journal of controlled release*, 160, 468-476.
- CHRISTIE, W. W. 1985. Rapid separation and quantification of lipid classes by high performance liquid chromatography and mass (light-scattering) detection. *Journal of Lipid Research*, 26, 507-512.
- CLARK, D. C. & SMITH, L. J. 1989. Influence of alcohol-containing spreading solvents on the secondary structure of proteins: a circular dichroism investigation. *Journal of Agricultural and Food Chemistry*, 37, 627-633.
- CLAUDIA, M., KRISTIN, Ö., JENNIFER, O., EVA, R. & ELEONORE, F. 2017. Comparison of fluorescence-based methods to determine nanoparticle uptake by phagocytes and non-phagocytic cells in vitro. *Toxicology*, 378, 25-36.
- CLOGSTON, J. D. & PATRI, A. K. 2011. Zeta Potential Measurement. In: MCNEIL, S. E. (ed.) *Characterization of Nanoparticles Intended for Drug Delivery*. Totowa, NJ: Humana Press.
- COLLETIER, J.-P., CHAIZE, B., WINTERHALTER, M. & FOURNIER, D. 2002. Protein encapsulation in liposomes: efficiency depends on interactions between protein and phospholipid bilayer. *BMC biotechnology*, 2, 9.
- CROMMELIN, D. J. 2016. Formulation of biotech products, including biopharmaceutical considerations. *Pharmaceutical Biotechnology*. CRC Press.
- CROMMELIN, D. J., GRIT, M., TALSMA, H. & ZUIDAM, N. J. 1994. Liposomes as carriers for drugs and antigens: approaches to preserve their long term stability. *Drug development and industrial pharmacy*, 20, 547-556.
- CROWE, J. H. & CROWE, L. M. 1988. Factors affecting the stability of dry liposomes. *Biochimica et Biophysica Acta (BBA) - Biomembranes*, 939, 327-334.
- CROWE, J. H., OLIVER, A. E., HOEKSTRA, F. A. & CROWE, L. M. 1997. Stabilization of dry membranes by mixtures of hydroxyethyl starch and glucose: the role of vitrification. *Cryobiology*, 35, 20-30.
- CROWE, L. M., CROWE, J. H. & CHAPMAN, D. 1985. Interaction of carbohydrates with dry dipalmitoylphosphatidylcholine. *Archives of biochemistry and biophysics*, 236, 289-296.
- CROWE, L. M., WOMERSLEY, C., CROWE, J. H., REID, D., APPEL, L. & RUDOLPH, A. 1986a. Prevention of fusion and leakage in freeze-dried liposomes by carbohydrates. *Biochimica et Biophysica Acta (BBA) - Biomembranes*, 861, 131-140.
- CROWE, L. M., WOMERSLEY, C., CROWE, J. H., REID, D., APPEL, L. & RUDOLPH, A. 1986b. Prevention of fusion and leakage in freeze-dried liposomes by carbohydrates. *Biochimica et Biophysica Acta (BBA)-Biomembranes*, 861, 131-140.
- CULTURE, E. C. O. A. C. 2018. RAW264.7 cells [Online]. Available: [https://www.phe-culturecollections.org.uk/products/celllines/generalcell/detail.jsp?refId=91062702&collection=ecacc\\_gc](https://www.phe-culturecollections.org.uk/products/celllines/generalcell/detail.jsp?refId=91062702&collection=ecacc_gc) [Accessed 2018].

- D'ACREMONT, V., HERZOG, C. & GENTON, B. 2006. Immunogenicity and safety of a virosomal hepatitis A vaccine (Epaxal®) in the elderly. *Journal of travel medicine*, 13, 78-83.
- DAIGNEAULT, M., PRESTON, J. A., MARRIOTT, H. M., WHYTE, M. K. & DOCKRELL, D. H. 2010. The identification of markers of macrophage differentiation in PMA-stimulated THP-1 cells and monocyte-derived macrophages. *PloS one*, 5, e8668.
- DAMIATI, S., KOMPELLA, U., DAMIATI, S. & KODZIUS, R. 2018. Microfluidic devices for drug delivery systems and drug screening. *Genes*, 9, 103.
- DATABASE, P. C. 2018. *Propofol* (PubChem Compound Database; CID=4943) [Online]. National Center for Biotechnology Information. : National Center for Biotechnology Information. . Available: <https://pubchem.ncbi.nlm.nih.gov/compound/4943> [Accessed 13th Decemeber 2018 2018].
- DEVARAJ, G. N., PARAKH, S., DEVRAJ, R., APTE, S., RAO, B. R. & RAMBHAU, D. 2002. Release studies on niosomes containing fatty alcohols as bilayer stabilizers instead of cholesterol. *Journal of colloid and interface science*, 251, 360-365.
- DEVOTTA, I., BADIGER, M., RAJAMOCHANAN, P., GANAPATHY, S. & MASHELKAR, R. 1995. Unusual retardation and enhancement in polymer dissolution: role of disengagement dynamics. *Chemical engineering science*, 50, 2557-2569.
- DIMOV, N., KASTNER, E., HUSSAIN, M., PERRIE, Y. & SZITA, N. 2017. Formation and purification of tailored liposomes for drug delivery using a module-based micro continuous-flow system. *Scientific reports*, 7, 12045.
- DISCHER, B. M., BERMUDEZ, H., HAMMER, D. A., DISCHER, D. E., WON, Y.-Y. & BATES, F. S. 2002. Cross-linked polymersome membranes: vesicles with broadly adjustable properties. *The Journal of Physical Chemistry B*, 106, 2848-2854.
- DOUVILLE, V., LODI, A., MILLER, J., NICOLAS, A., CLAROT, I., PRILLEUX, B., MEGOULAS, N. & KOUPPARIS, M. 2006. *Evaporative light scattering detection (ELSD): a tool for improved quality control of drug substances*.
- DOZIER, J. K. & DISTEFANO, M. D. 2015. Site-Specific PEGylation of Therapeutic Proteins. *International journal of molecular sciences*, 16, 25831-25864.
- DREBORG, S. & AKERBLUM, E. 1990. Immunotherapy with monomethoxypolyethylene glycol modified allergens. *Critical reviews in therapeutic drug carrier systems*, 6, 315-365.
- DRUMMOND, D. C., MEYER, O., HONG, K., KIRPOTIN, D. B. & PAPAHAJDOPOULOS, D. 1999. Optimizing liposomes for delivery of chemotherapeutic agents to solid tumors. *Pharmacological reviews*, 51, 691-744.
- DUA, J., RANA, A. & BHANDARI, A. 2012. Liposome: methods of preparation and applications. *Int J Pharm Stud Res*, 3, 14-20.
- DULBECCO, R. & VOGT, M. 1954. Plaque formation and isolation of pure lines with poliomyelitis viruses. *Journal of Experimental Medicine*, 99, 167-182.
- EDWARDS, D. A., HANES, J., CAPONETTI, G., HRKACH, J., BEN-JEBRIA, A., ESKEW, M. L., MINTZES, J., DEEVER, D., LOTAN, N. & LANGER, R. 1997. Large porous particles for pulmonary drug delivery. *Science*, 276, 1868-1872.
- EDWARDS, K., KARLSSON, G. & CULLIS, P. R. 2008. Influence of Drug-to-Lipid Ratio on Drug Release Properties and Liposome Integrity in Liposomal Doxorubicin Formulations AU - Johnston, Michael J. W. *Journal of Liposome Research*, 18, 145-157.
- EKSBORG, S. 1981. Evaluation of method-comparison data. *Clinical chemistry*, 27, 1311-1312.
- ELOY, J. O., DE SOUZA, M. C., PETRILLI, R., BARCELLOS, J. P. A., LEE, R. J. & MARCHETTI, J. M. 2014. Liposomes as carriers of hydrophilic small molecule drugs: strategies to

- enhance encapsulation and delivery. *Colloids and Surfaces B: Biointerfaces*, 123, 345-363.
- EPAND, R. M., EPAND, R. F. & MAEKAWA, S. 2003. The arrangement of cholesterol in membranes and binding of NAP-22. *Chemistry and physics of lipids*, 122, 33-39.
- FAHR, A., VAN HOOGEVEST, P., MAY, S., BERGSTRAND, N. & LEIGH, M. L. 2005. Transfer of lipophilic drugs between liposomal membranes and biological interfaces: consequences for drug delivery. *European Journal of Pharmaceutical Sciences*, 26, 251-265.
- FANG, J., NAKAMURA, H. & MAEDA, H. 2011. The EPR effect: Unique features of tumor blood vessels for drug delivery, factors involved, and limitations and augmentation of the effect. *Advanced Drug Delivery Reviews*, 63, 136-151.
- FARZANEH, H., EBRAHIMI NIK, M., MASHREGHI, M., SABERI, Z., JAAFARI, M. R. & TEYMOURI, M. 2018. A study on the role of cholesterol and phosphatidylcholine in various features of liposomal doxorubicin: From liposomal preparation to therapy. *International Journal of Pharmaceutics*, 551, 300-308.
- FATOUROS, D. G. & ANTIMISIARIS, S. G. 2002. Effect of amphiphilic drugs on the stability and zeta-potential of their liposome formulations: a study with prednisolone, diazepam, and griseofulvin. *Journal of colloid and interface science*, 251, 271-277.
- FAYOLLE, D., FIORE, M., STANO, P. & STRAZEWSKI, P. 2018. Rapid purification of giant lipid vesicles by microfiltration. *PloS one*, 13, e0192975.
- FENSKE, D. B. & CULLIS, P. R. 2008. Liposomal nanomedicines. *Expert opinion on drug delivery*, 5, 25-44.
- FIEGEL, J., FU, J. & HANES, J. 2004. Poly (ether-anhydride) dry powder aerosols for sustained drug delivery in the lungs. *Journal of controlled release*, 96, 411-423.
- FIOLKA, R. 2014. Chapter 16 - Seeing more with structured illumination microscopy. In: WATERS, J. C. & WITTMAN, T. (eds.) *Methods in Cell Biology*. Academic Press.
- FORBES, N., HUSSAIN, M. T., BRIUGLIA, M. L., EDWARDS, D. P., HORST, J. H. T., SZITA, N. & PERRIE, Y. 2019. Rapid and scale-independent microfluidic manufacture of liposomes entrapping protein incorporating in-line purification and at-line size monitoring. *International Journal of Pharmaceutics*, 556, 68-81.
- FORMULARY, B. N. 2018. *Propofol* [Online]. National Institute for Health and Care Excellence
- National Institute for Health and Care Excellence. Available: <https://bnf.nice.org.uk/drug/propofol.html#medicinalForms> [Accessed 13th December 2018 2018].
- FORRESTER, M. A., WASSALL, H. J., HALL, L. S., CAO, H., WILSON, H. M., BARKER, R. N. & VICKERS, M. A. 2018. Similarities and differences in surface receptor expression by THP-1 monocytes and differentiated macrophages polarized using seven different conditioning regimens. *Cellular Immunology*, 332, 58-76.
- FORSSEN, E. A. 1997. The design and development of DaunoXome® for solid tumor targeting in vivo. *Advanced Drug Delivery Reviews*, 24, 133-150.
- FOSGERAU, K. & HOFFMANN, T. 2015. Peptide therapeutics: current status and future directions. *Drug Discovery Today*, 20, 122-128.
- FRANSEN, G. J., SALEMINK, P. J. M. & CROMMELIN, D. J. A. 1986. Critical parameters in freezing of liposomes. *International Journal of Pharmaceutics*, 33, 27-35.
- FRANZÉ, S., SELMIN, F., SAMARITANI, E., MINGHETTI, P. & CILURZO, F. 2018. Lyophilization of Liposomal Formulations: Still Necessary, Still Challenging. *Pharmaceutics*, 10, 139.



- FU, J., FIEGEL, J., KRAULAND, E. & HANES, J. 2002. New polymeric carriers for controlled drug delivery following inhalation or injection. *Biomaterials*, 23, 4425-4433.
- GABIZON, A., SHMEEDA, H. & BARENHOLZ, Y. 2003. Pharmacokinetics of pegylated liposomal doxorubicin. *Clinical pharmacokinetics*, 42, 419-436.
- GALL, D. 1966. The adjuvant activity of aliphatic nitrogenous bases. *Immunology*, 11, 369.
- GARDIKIS, K., TSIMPLOULI, C., DIMAS, K., MICHA-SCRETTAS, M. & DEMETZOS, C. 2010. New chimeric advanced Drug Delivery nano Systems (chi-aDDnSs) as doxorubicin carriers. *International journal of pharmaceuticals*, 402, 231-237.
- GEARING, J., MALIK, K. P. & MATEJTSCHUK, P. 2010. Use of dynamic mechanical analysis (DMA) to determine critical transition temperatures in frozen biomaterials intended for lyophilization. *Cryobiology*, 61, 27-32.
- GOBBY, D., ANGELI, P. & GAVRIILIDIS, A. 2001. Mixing characteristics of T-type microfluidic mixers. *Journal of Micromechanics and microengineering*, 11, 126.
- GOLOVINA, E. A., GOLOVIN, A. V., HOEKSTRA, F. A. & FALLER, R. 2009. Water replacement hypothesis in atomic detail—factors determining the structure of dehydrated bilayer stacks. *Biophysical journal*, 97, 490-499.
- GRABERG, S. & GIESELER, H. 2006. Freeze drying in non-vial container systems: evaluation of heat transfer coefficients of PCR-plates and correlation to freeze-drying cycle design. *CPPR Freeze-Drying of Pharmaceuticals and Biologicals. Garmisch-Partenkirchen, Germany*.
- GRANT, Y., DALBY, P. & MATEJTSCHUK, P. 2012. Use of design of experiment and microscale down strategies in formulation and cycle development for lyophilization. *American Pharmaceutical Review*, 15.
- GRANT, Y., MATEJTSCHUK, P. & DALBY, P. A. 2009. Rapid optimization of protein freeze-drying formulations using ultra scale-down and factorial design of experiment in microplates. *Biotechnology and bioengineering*, 104, 957-964.
- GRASMEIJER, N. 2015. Improving protein stabilization by spray drying. *Ridderprint, Groningen*.
- GREGORIADIS, G. 1973. Drug entrapment in liposomes. *FEBS Letters*, 36, 292-296.
- GREGORIADIS, G. & DAVIS, C. 1979. Stability of liposomes invivo and invitro is promoted by their cholesterol content and the presence of blood cells. *Biochemical and Biophysical Research Communications*, 89, 1287-1293.
- GREGORIADIS, G., LEATHWOOD, P. & RYMAN, B. E. 1971. Enzyme entrapment in liposomes. *FEBS letters*, 14, 95-99.
- GRIT, M. & CROMMELIN, D. J. 1993. Chemical stability of liposomes: implications for their physical stability. *Chemistry and physics of lipids*, 64, 3-18.
- GROTEFEND, S., KAMINSKI, L., WROBLEWITZ, S., DEEB, S. E., KÜHN, N., REICHL, S., LIMBERGER, M., WATT, S. & WÄTZIG, H. 2012. Protein quantitation using various modes of high performance liquid chromatography. *Journal of Pharmaceutical and Biomedical Analysis*, 71, 127-138.
- GUIDELINE, I. 2016. Impurity: guideline for residual solvents. *Q3C (R6), Step, 4, 20*.
- GUIDELINE, I. H. T. Validation of analytical procedures: text and methodology Q2 (R1). International Conference on Harmonization, Geneva, Switzerland, 2005a. 11-12.
- GUIDELINE, I. H. T. 2005b. *Validation of analytical procedures: Text and methodology Q2 (R1)*. [Online]. Available: [https://www.ich.org/fileadmin/Public\\_Web\\_Site/ICH\\_Products/Guidelines/Quality/Q2\\_R1/Step4/Q2\\_R1\\_Guideline.pdf](https://www.ich.org/fileadmin/Public_Web_Site/ICH_Products/Guidelines/Quality/Q2_R1/Step4/Q2_R1_Guideline.pdf) [Accessed 12th Januray 2019].
- GUPTA, S., JAIN, A., CHAKRABORTY, M., SAHNI, J. K., ALI, J. & DANG, S. 2013. Oral delivery of therapeutic proteins and peptides: a review on recent developments. *Drug Delivery*, 20, 237-246.

- HABJANEC, L., FRKANEC, R., HALASSY, B. & TOMAŠIĆ, J. 2006. Effect of liposomal formulations and immunostimulating peptidoglycan monomer (PGM) on the immune reaction to ovalbumin in mice. *Journal of liposome research*, 16, 1-16.
- HAIDAR, Z. S., HAMDY, R. C. & TABRIZIAN, M. 2008. Protein release kinetics for core-shell hybrid nanoparticles based on the layer-by-layer assembly of alginate and chitosan on liposomes. *Biomaterials*, 29, 1207-1215.
- HALLDORSSON, S., LUCUMI, E., GÓMEZ-SJÖBERG, R. & FLEMING, R. M. 2015. Advantages and challenges of microfluidic cell culture in polydimethylsiloxane devices. *Biosensors and Bioelectronics*, 63, 218-231.
- HARASHIMA, H. & KIWADA, H. 1996. Liposomal targeting and drug delivery: kinetic consideration. *Advanced drug delivery reviews*, 19, 425-444.
- HARRIS, J. M., MARTIN, N. E. & MODI, M. 2001. Pegylation. *Clinical pharmacokinetics*, 40, 539-551.
- HE, C., HU, Y., YIN, L., TANG, C. & YIN, C. 2010. Effects of particle size and surface charge on cellular uptake and biodistribution of polymeric nanoparticles. *Biomaterials*, 31, 3657-3666.
- HELENIUS, A. & SIMONS, K. 1975. Solubilization of membranes by detergents. *Biochimica et Biophysica Acta (BBA)-Reviews on Biomembranes*, 415, 29-79.
- HENRIKSEN-LACEY, M., BRAMWELL, V. W., CHRISTENSEN, D., AGGER, E.-M., ANDERSEN, P. & PERRIE, Y. 2010a. Liposomes based on dimethyldioctadecylammonium promote a depot effect and enhance immunogenicity of soluble antigen. *Journal of controlled release*, 142, 180-186.
- HENRIKSEN-LACEY, M., CHRISTENSEN, D., BRAMWELL, V. W., LINDENSTRØM, T., AGGER, E. M., ANDERSEN, P. & PERRIE, Y. 2010b. Liposomal cationic charge and antigen adsorption are important properties for the efficient deposition of antigen at the injection site and ability of the vaccine to induce a CMI response. *Journal of controlled release*, 145, 102-108.
- HESSEL, V., LÖWE, H. & SCHÖNFELD, F. 2005. Micromixers—a review on passive and active mixing principles. *Chemical Engineering Science*, 60, 2479-2501.
- HIJIYA, N., MIYAKE, K., AKASHI, S., MATSUURA, K., HIGUCHI, Y. & YAMAMOTO, S. 2002. Possible involvement of toll-like receptor 4 in endothelial cell activation of larger vessels in response to lipopolysaccharide. *Pathobiology*, 70, 18-25.
- HIROTA, K. & TERADA, H. 2012. *Endocytosis of particle formulations by macrophages and its application to clinical treatment*, INTECH Open Access Publisher.
- HOARAU, D., DELMAS, P., ROUX, E. & LEROUX, J.-C. 2004. Novel long-circulating lipid nanocapsules. *Pharmaceutical research*, 21, 1783-1789.
- HOLLAND, W. L., STAUTER, E. C. & STITH, B. J. 2003. Quantification of phosphatidic acid and lysophosphatidic acid by HPLC with evaporative light-scattering detection. *Journal of lipid research*, 44, 854-858.
- HOOD, R., VREELAND, W. & DEVOE, D. L. 2014. Microfluidic remote loading for rapid single-step liposomal drug preparation. *Lab on a Chip*, 14, 3359-3367.
- HSU, C. C., NGUYEN, H. M., YEUNG, D. A., BROOKS, D. A., KOE, G. S., BEWLEY, T. A. & PEARLMAN, R. 1995. Surface denaturation at solid-void interface—a possible pathway by which opalescent participates form during the storage of lyophilized tissue-type plasminogen activator at high temperatures. *Pharmaceutical research*, 12, 69-77.
- HUA, Z.-Z., LI, B.-G., LIU, Z.-J. & SUN, D.-W. 2003. Freeze-drying of liposomes with cryoprotectants and its effect on retention rate of encapsulated ftorafur and vitamin A. *Drying Technology*, 21, 1491-1505.

- HUANG, C. & MASON, J. 1978. Geometric packing constraints in egg phosphatidylcholine vesicles. *Proceedings of the National Academy of Sciences*, 75, 308-310.
- HUANG, J.-H., WU, C.-W., LIEN, S.-P., LENG, C.-H., HSIAO, K.-N., LIU, S.-J., CHEN, H.-W., SIU, L.-K. & CHONG, P. 2015. Recombinant lipoprotein-based vaccine candidates against *C. difficile* infections. *Journal of biomedical science*, 22, 1.
- HUANG, Y.-Y. & WANG, C.-H. 2006. Pulmonary delivery of insulin by liposomal carriers. *Journal of Controlled Release*, 113, 9-14.
- HUBBARD, A., BEVAN, S. & MATEJTSCHUK, P. 2007. Impact of residual moisture and formulation on Factor VIII and Factor V recovery in lyophilized plasma reference materials. *Analytical and bioanalytical chemistry*, 387, 2503-2507.
- HUNTINGTON, J. A., GETTINS, P. G. & PATSTON, P. A. 1995. S-ovalbumin, an ovalbumin conformer with properties analogous to those of loop-inserted serpins. *Protein Science*, 4, 613-621.
- ICH, I. Q3C (R6) Impurities: Guideline for Residual Solvents. 2016. *There is no corresponding record for this reference.*
- ICH, Q. R. ICH Harmonised Tripartite Guideline, Pharmaceutical Development: Q8 (R2). International Conference on Harmonization of Technical Requirements for Registration of Pharmaceuticals for Human Use, 2009.
- IMMORDINO, M. L., DOSIO, F. & CATTEL, L. 2006. Stealth liposomes: review of the basic science, rationale, and clinical applications, existing and potential. *International journal of nanomedicine*, 1, 297.
- INGVARSSON, P. T., YANG, M., NIELSEN, H. M., RANTANEN, J. & FOGED, C. 2011. Stabilization of liposomes during drying. *Expert opinion on drug delivery*, 8, 375-388.
- ISRAELACHVILI, J. N., MITCHELL, D. J. & NINHAM, B. W. 1977. Theory of self-assembly of lipid bilayers and vesicles. *Biochimica et Biophysica Acta (BBA) - Biomembranes*, 470, 185-201.
- IWAOKA, S., NAKAMURA, T., TAKANO, S., TSUCHIYA, S. & ARAMAKI, Y. 2006. Cationic liposomes induce apoptosis through p38 MAP kinase–caspase-8–Bid pathway in macrophage-like RAW264. 7 cells. *Journal of leukocyte biology*, 79, 184-191.
- JAAFAR-MAALEJ, C., ELAISSARI, A. & FESSI, H. 2012. Lipid-based carriers: manufacturing and applications for pulmonary route. *Expert opinion on drug delivery*, 9, 1111-1127.
- JAHN, A., STAVIS, S. M., HONG, J. S., VREELAND, W. N., DEVOE, D. L. & GAITAN, M. 2010. Microfluidic Mixing and the Formation of Nanoscale Lipid Vesicles. *ACS Nano*, 4, 2077-2087.
- JAHN, A., VREELAND, W. N., DEVOE, D. L., LOCASCIO, L. E. & GAITAN, M. 2007. Microfluidic directed formation of liposomes of controlled size. *Langmuir*, 23, 6289-6293.
- JAHN, A., VREELAND, W. N., GAITAN, M. & LOCASCIO, L. E. 2004. Controlled vesicle self-assembly in microfluidic channels with hydrodynamic focusing. *Journal of the American Chemical Society*, 126, 2674-2675.
- JANEWAY, C. A., TRAVERS, P., WALPORT, M. & CAPRA, J. D. 2005. Immunobiology: the immune system in health and disease.
- JIANG, W., KIM, B. Y., RUTKA, J. T. & CHAN, W. C. 2008. Nanoparticle-mediated cellular response is size-dependent. *Nature nanotechnology*, 3, 145-150.
- JIANG, X., DAUSEND, J., HAFNER, M., MUSYANOVYCH, A., RÖCKER, C., LANDFESTER, K., MAILÄNDER, V. & NIENHAUS, G. U. 2010. Specific Effects of Surface Amines on Polystyrene Nanoparticles in their Interactions with Mesenchymal Stem Cells. *Biomacromolecules*, 11, 748-753.
- JOSHI, S., HUSSAIN, M. T., ROCES, C. B., ANDERLUZZI, G., KASTNER, E., SALMASO, S., KIRBY, D. J. & PERRIE, Y. 2016. Microfluidics based manufacture of liposomes

- simultaneously entrapping hydrophilic and lipophilic drugs. *International journal of pharmaceutics*, 514, 160-168.
- KAKDE, D., TARESCO, V., BANSAL, K. K., MAGENNIS, E. P., HOWDLE, S. M., MANTOVANI, G., IRVINE, D. J. & ALEXANDER, C. 2016. Amphiphilic block copolymers from a renewable  $\epsilon$ -decalactone monomer: prediction and characterization of micellar core effects on drug encapsulation and release. *Journal of Materials Chemistry B*, 4, 7119-7129.
- KASTNER, E., KAUR, R., LOWRY, D., MOGHADDAM, B., WILKINSON, A. & PERRIE, Y. 2014. High-throughput manufacturing of size-tuned liposomes by a new microfluidics method using enhanced statistical tools for characterization. *International Journal of Pharmaceutics*, 477, 361-368.
- KASTNER, E., VERMA, V., LOWRY, D. & PERRIE, Y. 2015. Microfluidic-controlled manufacture of liposomes for the solubilisation of a poorly water soluble drug. *International journal of pharmaceutics*, 485, 122-130.
- KATO, A. & TAKAGI, T. 1988. Formation of intermolecular. beta.-sheet structure during heat denaturation of ovalbumin. *Journal of Agricultural and Food Chemistry*, 36, 1156-1159.
- KAUR, R., BRAMWELL, V. W., KIRBY, D. J. & PERRIE, Y. 2012. Manipulation of the surface pegylation in combination with reduced vesicle size of cationic liposomal adjuvants modifies their clearance kinetics from the injection site, and the rate and type of T cell response. *Journal of controlled release*, 164, 331-337.
- KAWASHIMA, Y., YAMAMOTO, H., TAKEUCHI, H., FUJIOKA, S. & HINO, T. 1999. Pulmonary delivery of insulin with nebulized DL-lactide/glycolide copolymer (PLGA) nanospheres to prolong hypoglycemic effect. *Journal of Controlled Release*, 62, 279-287.
- KESSLER, R. J. & FANESTIL, D. D. 1986. Interference by lipids in the determination of protein using bicinchoninic acid. *Analytical biochemistry*, 159, 138-142.
- KETTENES-VAN DEN BOSCH, J., VERNOOIJ, E., UNDERBERG, W. & CROMMELIN, D. 2000. Chemical stability of liposome components. *SÖFW-journal*, 126, 32-36.
- KHELASHVILI, G. & HARRIES, D. 2013. How sterol tilt regulates properties and organization of lipid membranes and membrane insertions. *Chemistry and Physics of Lipids*, 169, 113-123.
- KIM, D.-H. & MARTIN, D. C. 2006. Sustained release of dexamethasone from hydrophilic matrices using PLGA nanoparticles for neural drug delivery. *Biomaterials*, 27, 3031-3037.
- KIM, J.-C. K., JONG-DUK 2001. Preparation by spray drying of amphotericin B-phospholipid composite particles and their anticellular activity. *Drug delivery*, 8, 143-147.
- KIPP, J. 2004. The role of solid nanoparticle technology in the parenteral delivery of poorly water-soluble drugs. *International journal of pharmaceutics*, 284, 109-122.
- KIRBY, C., CLARKE, J. & GREGORIADIS, G. 1980. Effect of the cholesterol content of small unilamellar liposomes on their stability in vivo and in vitro. *Biochemical Journal*, 186, 591-598.
- KOLA, I. & LANDIS, J. 2004. Can the pharmaceutical industry reduce attrition rates? *Nature reviews Drug discovery*, 3, 711.
- KOMATSU, H., SAITO, H., OKADA, S., TANAKA, M., EGASHIRA, M. & HANDA, T. 2001. Effects of the acyl chain composition of phosphatidylcholines on the stability of freeze-dried small liposomes in the presence of maltose. *Chemistry and Physics of Lipids*, 113, 29-39.

- KOZLOV, M., LICHTENBERG, D. & ANDELMAN, D. 1997. Shape of phospholipid/surfactant mixed micelles: cylinders or disks? Theoretical analysis. *The Journal of Physical Chemistry B*, 101, 6600-6606.
- KRAFT, J. C., FREELING, J. P., WANG, Z. & HO, R. J. Y. 2014. Emerging Research and Clinical Development Trends of Liposome and Lipid Nanoparticle Drug Delivery Systems. *Journal of pharmaceutical sciences*, 103, 29-52.
- KRAGH-HANSEN, U., LE MAIRE, M. & MØLLER, J. V. 1998. The mechanism of detergent solubilization of liposomes and protein-containing membranes. *Biophysical Journal*, 75, 2932-2946.
- KRASNOWSKA, E. K., BAGATOLLI, L. A., GRATTON, E. & PARASASSI, T. 2001. Surface properties of cholesterol-containing membranes detected by Prodan fluorescence. *Biochimica et Biophysica Acta (BBA)-Biomembranes*, 1511, 330-340.
- KU, M. S. 2008. Use of the biopharmaceutical classification system in early drug development. *The AAPS journal*, 10, 208-212.
- KUČERKA, N., NIEH, M.-P. & KATSARAS, J. 2011. Fluid phase lipid areas and bilayer thicknesses of commonly used phosphatidylcholines as a function of temperature. *Biochimica et Biophysica Acta (BBA) - Biomembranes*, 1808, 2761-2771.
- LAOUI, A., JAAFAR-MAALEJ, C., LIMAYEM-BLOUZA, I., SFAR, S., CHARCOSSET, C. & FESSI, H. 2012. Preparation, Characterization and Applications of Liposomes: State of the Art. *Journal of Colloid Science and Biotechnology*, 1, 147-168.
- LAPINSKI, M. M., CASTRO-FORERO, A., GREINER, A. J., OFOLI, R. Y. & BLANCHARD, G. J. 2007. Comparison of liposomes formed by sonication and extrusion: rotational and translational diffusion of an embedded chromophore. *Langmuir*, 23, 11677-11683.
- LASIC, D. D. 1993. *Liposomes: from physics to applications*, Elsevier Science Ltd.
- LEADER, B., BACA, Q. J. & GOLAN, D. E. 2008. Protein therapeutics: a summary and pharmacological classification. *Nature Reviews Drug Discovery*, 7, 21.
- LEAROYD, T. P., BURROWS, J. L., FRENCH, E. & SEVILLE, P. C. 2010. Sustained delivery of salbutamol and beclometasone from spray-dried double emulsions. *Journal of microencapsulation*, 27, 162-170.
- LEE, J. N., PARK, C. & WHITESIDES, G. M. 2003. Solvent compatibility of poly (dimethylsiloxane)-based microfluidic devices. *Analytical chemistry*, 75, 6544-6554.
- LEE, K. Y. & YUK, S. H. 2007. Polymeric protein delivery systems. *Progress in Polymer Science*, 32, 669-697.
- LEONARD, R., WILLIAMS, S., TULPULU, A., LEVINE, A. & OLIVEROS, S. 2009. Improving the therapeutic index of anthracycline chemotherapy: Focus on liposomal doxorubicin (Myocet™). *The Breast*, 18, 218-224.
- LESNEFSKY, E. J., STOLL, M. S., MINKLER, P. E. & HOPPEL, C. L. 2000. Separation and quantitation of phospholipids and lysophospholipids by high-performance liquid chromatography. *Analytical biochemistry*, 285, 246-254.
- LEWIS, B. A. & ENGELMAN, D. M. 1983. Lipid bilayer thickness varies linearly with acyl chain length in fluid phosphatidylcholine vesicles. *Journal of Molecular Biology*, 166, 211-217.
- LI, N., PENG, L.-H., CHEN, X., NAKAGAWA, S. & GAO, J.-Q. 2011. Effective transcutaneous immunization by antigen-loaded flexible liposome in vivo. *International Journal of Nanomedicine*, 6, 3241-3250.
- LICHTENBERG, D., GOÑI, F. M. & HEERKLOTZ, H. 2005. Detergent-resistant membranes should not be identified with membrane rafts. *Trends in biochemical sciences*, 30, 430-436.

- LICHTENBERG, D., YEDGAR, S., COOPER, G. & GATT, S. 1979. Studies on the molecular packing of mixed dispersions of Triton X-100 and sphingomyelin and its dependence on temperature and cloud point. *Biochemistry*, 18, 2574-2582.
- LIN, J. & MCKEON, T. 2000. Separation of intact phosphatidylcholine molecular species by high performance liquid chromatography.
- LINDBLAD, E. B., ELHAY, M. J., SILVA, R., APPELBERG, R. & ANDERSEN, P. 1997. Adjuvant modulation of immune responses to tuberculosis subunit vaccines. *Infection and Immunity*, 65, 623-629.
- LITZINGER, D. C. & HUANG, L. 1992. Phosphatidylethanolamine liposomes: drug delivery, gene transfer and immunodiagnostic applications. *Biochimica et Biophysica Acta (BBA)-Reviews on Biomembranes*, 1113, 201-227.
- LIU, W., YE, A., LIU, W., LIU, C., HAN, J. & SINGH, H. 2015. Behaviour of liposomes loaded with bovine serum albumin during in vitro digestion. *Food Chemistry*, 175, 16-24.
- LOFTSSON, T. & BREWSTER, M. E. 2010. Pharmaceutical applications of cyclodextrins: basic science and product development. *Journal of pharmacy and pharmacology*, 62, 1607-1621.
- LOMBRANA, J., ZUAZO, I. & IKARA, J. 2001. Moisture diffusivity behavior during freeze drying under microwave heating power application. *Drying technology*, 19, 1613-1627.
- LU, Y., SUN, W. & GU, Z. 2014. Stimuli-Responsive Nanomaterials for Therapeutic Protein Delivery. *Journal of controlled release : official journal of the Controlled Release Society*, 194, 1-19.
- LU, Y., YANG, J. & SEGA, E. 2006. Issues related to targeted delivery of proteins and peptides. *The AAPS journal*, 8, E466-E478.
- LUKYANOV, A. N. & TORCHILIN, V. P. 2004. Micelles from lipid derivatives of water-soluble polymers as delivery systems for poorly soluble drugs. *Advanced Drug Delivery Reviews*, 56, 1273-1289.
- LUTHRA, S., OBERT, J. P., KALONIA, D. S. & PIKAL, M. J. 2007. Impact of critical process and formulation parameters affecting in-process stability of lactate dehydrogenase during the secondary drying stage of lyophilization: A mini freeze dryer study. *Journal of pharmaceutical sciences*, 96, 2242-2250.
- LUTSIK, M., KWON, G. S. & SAMUEL, J. 2002. Analysis of peptide and lipopeptide content in liposomes. *Journal of pharmacy & pharmaceutical sciences: a publication of the Canadian Society for Pharmaceutical Sciences, Societe canadienne des sciences pharmaceutiques*, 5, 279-84.
- MALTESEN, M. J. & VAN DE WEERT, M. 2008. Drying methods for protein pharmaceuticals. *Drug Discovery Today: Technologies*, 5, e81-e88.
- MAO, S., GERMERSHAUS, O., FISCHER, D., LINN, T., SCHNEPF, R. & KISSEL, T. 2005. Uptake and transport of PEG-graft-trimethyl-chitosan copolymer-insulin nanocomplexes by epithelial cells. *Pharmaceutical research*, 22, 2058-2068.
- MARQUARDT, D., HEBERLE, F. A., GREATHOUSE, D. V., KOEPPE, R. E., STANDAERT, R. F., VAN OOSTEN, B. J., HARROUN, T. A., KINNUN, J. J., WILLIAMS, J. A. & WASSALL, S. R. 2016. Lipid bilayer thickness determines cholesterol's location in model membranes. *Soft matter*, 12, 9417-9428.
- MARSHALL, L. J., OGUEJOFOR, W., WILLETTS, R. S., GRIFFITHS, H. R. & DEVITT, A. 2015. Developing accurate models of the human airways. *Journal of Pharmacy and Pharmacology*, 67, 464-472.
- MARTY, C. & SCHWENDENER, R. A. 2005. Cytotoxic tumor targeting with scFv antibody-modified liposomes. *Adoptive Immunotherapy: Methods and Protocols*, 389-401.

- MASSING, U., CICKO, S. & ZIROLI, V. 2008. Dual asymmetric centrifugation (DAC)—A new technique for liposome preparation. *Journal of Controlled Release*, 125, 16-24.
- MASTERS, K. 2002. *Spray drying in practice*, SprayDryConsul International ApS.
- MAZZELLA, N., MOLINET, J., SYAKTI, A. D., DODI, A., DOUMENQ, P., ARTAUD, J. & BERTRAND, J.-C. 2004. Bacterial phospholipid molecular species analysis by ion-pair reversed-phase HPLC/ESI/MS. *Journal of lipid research*, 45, 1355-1363.
- MCELHANEY, R. N. 1982. The use of differential scanning calorimetry and differential thermal analysis in studies of model and biological membranes. *Chemistry and Physics of Lipids*, 30, 229-259.
- MENDEZ, R. & BANERJEE, S. 2017. Sonication-based basic protocol for liposome synthesis. *Lipidomics: Methods and Protocols*, 255-260.
- MENSINK, M. A., FRIJLINK, H. W., VAN DER VOORT MAARSCHALK, K. & HINRICHS, W. L. 2017. How sugars protect proteins in the solid state and during drying (review): mechanisms of stabilization in relation to stress conditions. *European Journal of Pharmaceutics and Biopharmaceutics*, 114, 288-295.
- MEUNIER, F., PRENTICE, H. & RINGDEN, O. 1991. Liposomal amphotericin B (AmBisome): safety data from a phase II/III clinical trial. *Journal of Antimicrobial Chemotherapy*, 28, 83-91.
- MICHÉE, S., BRIGNOLE-BAUDOUIIN, F., RIANCHO, L., ROSTENE, W., BAUDOUIIN, C. & LABBÉ, A. 2013. Effects of benzalkonium chloride on THP-1 differentiated macrophages in vitro. *PLoS One*, 8, e72459.
- MIGLIORE, L. & COPPEDÈ, F. 2009. Environmental-induced oxidative stress in neurodegenerative disorders and aging. *Mutation Research/Genetic Toxicology and Environmental Mutagenesis*, 674, 73-84.
- MOGHADDAM, B., ALI, M. H., WILKHU, J., KIRBY, D. J., MOHAMMED, A. R., ZHENG, Q. & PERRIE, Y. 2011. The application of monolayer studies in the understanding of liposomal formulations. *International Journal of Pharmaceutics*, 417, 235-244.
- MOGHIMI, S. M. 2006. The effect of methoxy-PEG chain length and molecular architecture on lymph node targeting of immuno-PEG liposomes. *Biomaterials*, 27, 136-144.
- MOGHIMI, S. M. & SZEBENI, J. 2003. Stealth liposomes and long circulating nanoparticles: critical issues in pharmacokinetics, opsonization and protein-binding properties. *Progress in lipid research*, 42, 463-478.
- MOHAMMED, A., WESTON, N., COOMBES, A., FITZGERALD, M. & PERRIE, Y. 2004. Liposome formulation of poorly water soluble drugs: optimisation of drug loading and ESEM analysis of stability. *International journal of pharmaceutics*, 285, 23-34.
- MOHAMMED, A. R., BRAMWELL, V. W., COOMBES, A. G. & PERRIE, Y. 2006. Lyophilisation and sterilisation of liposomal vaccines to produce stable and sterile products. *Methods*, 40, 30-38.
- MONTEIRO, N., MARTINS, A., REIS, R. L. & NEVES, N. M. 2014. Liposomes in tissue engineering and regenerative medicine. *Journal of the Royal Society Interface*, 11, 20140459.
- MONTESANO, G., BARTUCCI, R., BELSITO, S., MARSH, D. & SPORTELLI, L. 2001. Lipid membrane expansion and micelle formation by polymer-grafted lipids: scaling with polymer length studied by spin-label electron spin resonance. *Biophysical journal*, 80, 1372-1383.
- MORRIS, M. C., DEPOLLIER, J., MERY, J., HEITZ, F. & DIVITA, G. 2001. A peptide carrier for the delivery of biologically active proteins into mammalian cells. *Nature biotechnology*, 19, 1173.
- MOUREY, T. H. & OPPENHEIMER, L. E. 1984. Principles of operation of an evaporative light-scattering detector for liquid chromatography. *Analytical Chemistry*, 56, 2427-2434.

- MOZAFARI, M. 2010. Nanoliposomes: preparation and analysis. *Liposomes*. Springer.
- MUKHERJEE, S., FELDMESSER, M. & CASADEVALL, A. 1996. J774 murine macrophage-like cell interactions with *Cryptococcus neoformans* in the presence and absence of opsonins. *Journal of Infectious Diseases*, 173, 1222-1231.
- MULLER, R. H. & KECK, C. M. 2004. Challenges and solutions for the delivery of biotech drugs – a review of drug nanocrystal technology and lipid nanoparticles. *Journal of Biotechnology*, 113, 151-170.
- MURAI, M., ARAMAKI, Y. & TSUCHIYA, S. 1995. Identification of the serum factor required for liposome-primed activation of mouse peritoneal macrophages. Modified alpha 2-macroglobulin enhances Fc gamma receptor-mediated phagocytosis of opsonized sheep red blood cells. *Immunology*, 86, 64.
- MURAO, A., NISHIKAWA, M., MANAGIT, C., WONG, J., KAWAKAMI, S., YAMASHITA, F. & HASHIDA, M. 2002. Targeting efficiency of galactosylated liposomes to hepatocytes in vivo: effect of lipid composition. *Pharmaceutical research*, 19, 1808-1814.
- NAGASE, H., UEDA, H. & NAKAGAKI, M. 1997. Effect of water on lamellar structure of DPPC/sugar systems. *Biochimica et Biophysica Acta (BBA)-Biomembranes*, 1328, 197-206.
- NAKAMURA, K., YAMASHITA, K., ITOH, Y., YOSHINO, K., NOZAWA, S. & KASUKAWA, H. 2012. Comparative studies of polyethylene glycol-modified liposomes prepared using different PEG-modification methods. *Biochimica et Biophysica Acta (BBA) - Biomembranes*, 1818, 2801-2807.
- NARANG, A., CHANG, R.-K. & HUSSAIN, M. A. 2013. Pharmaceutical development and regulatory considerations for nanoparticles and nanoparticulate drug delivery systems. *Journal of pharmaceutical sciences*, 102, 3867-3882.
- NEEDHAM, D., MCINTOSH, T. & LASIC, D. 1992. Repulsive interactions and mechanical stability of polymer-grafted lipid membranes. *Biochimica et Biophysica Acta (BBA)-Biomembranes*, 1108, 40-48.
- NEULASTA, E. M. C. E. September 2018. *Neulasta* [Online]. [Accessed Accessed on February 2019].
- NGUYEN, N.-T. & WU, Z. 2004. Micromixers—a review. *Journal of micromechanics and microengineering*, 15, R1.
- NTIMENOU, V., MOURTAS, S., CHRISTODOULAKIS, E. V., TSILIMBARIS, M. & ANTIMISIARIS, S. G. 2006. Stability of protein-encapsulating DRV liposomes after freeze-drying: a study with BSA and t-PA. *Journal of liposome research*, 16, 403-416.
- O'SULLIVAN, B., AL-BAHRANI, H., LAWRENCE, J., CAMPOS, M., CÁZARES, A., BAGANZ, F., WOHLGEMUTH, R., HAILES, H. C. & SZITA, N. 2012. Modular microfluidic reactor and inline filtration system for the biocatalytic synthesis of chiral metabolites. *Journal of Molecular Catalysis B: Enzymatic*, 77, 1-8.
- OELLERS, M., BUNGE, F., VINAYAKA, P., DRIESCHE, S. V. D. & VELLEKOOP, M. J. Flow-Ratio Monitoring in a Microchannel by Liquid-Liquid Interface Interferometry. Multidisciplinary Digital Publishing Institute Proceedings, 2017. 498.
- OHTAKE, S., SCHEBOR, C., PALECEK, S. P. & DE PABLO, J. J. 2005. Phase behavior of freeze-dried phospholipid–cholesterol mixtures stabilized with trehalose. *Biochimica et Biophysica Acta (BBA)-Biomembranes*, 1713, 57-64.
- OJA, C. D., SEMPLE, S. C., CHONN, A. & CULLIS, P. R. 1996. Influence of dose on liposome clearance: critical role of blood proteins. *Biochimica et Biophysica Acta (BBA)-Biomembranes*, 1281, 31-37.
- ONPATTRO (PATISIRAN), E. M. A. 2018. *Onpattro (patisiran)* [Online]. Available: <https://www.ema.europa.eu/en/medicines/human/EPAR/onpattro#product-information-section> [Accessed Accessed February 2019].



- OTAKE, K., IMURA, T., SAKAI, H. & ABE, M. 2001. Development of a New Preparation Method of Liposomes Using Supercritical Carbon Dioxide. *Langmuir*, 17, 3898-3901.
- OUSSOREN, C. & STORM, G. 1997. Lymphatic uptake and biodistribution of liposomes after subcutaneous injection: III. Influence of surface modification with poly (ethyleneglycol). *Pharmaceutical research*, 14, 1479-1484.
- PANAGI, Z., AVGOUSTAKIS, K., EVANGELATOS, G. & ITHAKISSIOS, D. 1998. Protein-induced CF release from liposomes in vitro and its correlation with the BLOOD/RES biodistribution of liposomes. *International journal of pharmaceuticals*, 163, 103-114.
- PANTALER, E., KAMP, D. & HAEST, C. W. 2000. Acceleration of phospholipid flip-flop in the erythrocyte membrane by detergents differing in polar head group and alkyl chain length. *Biochimica et Biophysica Acta (BBA)-Biomembranes*, 1509, 397-408.
- PAOLINELLI, C., BARTERI, M., BOFFI, F., FORASTIERI, F., GAUDIANO, M. C., DELLA LONGA, S. & CASTELLANO, A. C. 1997. Structural differences of ovalbumin and S-ovalbumin revealed by denaturing conditions. *Zeitschrift für Naturforschung C*, 52, 645-653.
- PARK, J. W. 2002. Liposome-based drug delivery in breast cancer treatment. *Breast Cancer Research*, 4, 95.
- PATEL, G., CHOUGULE, M., SINGH, M. & MISRA, A. 2009. Nanoliposomal dry powder formulations. *Methods in enzymology*, 464, 167-191.
- PATEL, H. 1992. Serum opsonins and liposomes: their interaction and opsonophagocytosis. *Critical reviews in therapeutic drug carrier systems*, 9, 39-90.
- PATTNAIK, T. R. P. 2009. Improving liposome integrity and easing bottlenecks to production.
- PATTNI, B. S., CHUPIN, V. V. & TORCHILIN, V. P. 2015. New Developments in Liposomal Drug Delivery. *Chem Rev*, 115, 10938-66.
- PERRIE, Y., MOHAMMED, A. R., KIRBY, D. J., MCNEIL, S. E. & BRAMWELL, V. W. 2008. Vaccine adjuvant systems: Enhancing the efficacy of sub-unit protein antigens. *International Journal of Pharmaceutics*, 364, 272-280.
- PESCHKA, R., PURMANN, T. & SCHUBERT, R. 1998. Cross-flow filtration—an improved detergent removal technique for the preparation of liposomes. *International Journal of Pharmaceutics*, 162, 177-183.
- PETERS, J., MARION, J., BECHER, F. J., TRAPP, M., GUTBERLET, T., BICOUT, D. J. & HEIMBURG, T. 2017. Thermodynamics of lipid multi-lamellar vesicles in presence of sterols at high hydrostatic pressure. *Scientific Reports*, 7, 15339.
- PHILIPPOT, J. R. & SCHUBER, F. 2017. *Liposomes as Tools in Basic Research and Industry (1994)*, CRC press.
- PHOTOS, P. J., BACAKOVA, L., DISCHER, B., BATES, F. S. & DISCHER, D. E. 2003. Polymer vesicles in vivo: correlations with PEG molecular weight. *Journal of Controlled Release*, 90, 323-334.
- PIKAL-CLELAND, K. A., RODRIGUEZ-HORNEDO, N., AMIDON, G. L. & CARPENTER, J. F. 2000. Protein denaturation during freezing and thawing in phosphate buffer systems: monomeric and tetrameric  $\beta$ -galactosidase. *Archives of Biochemistry and Biophysics*, 384, 398-406.
- QUEVEDO, E., STEINBACHER, J. & MCQUADE, D. T. 2005. Interfacial polymerization within a simplified microfluidic device: capturing capsules. *Journal of the American Chemical Society*, 127, 10498-10499.
- RAFFY, S. & TEISSIE, J. 1999. Control of lipid membrane stability by cholesterol content. *Biophysical journal*, 76, 2072-2080.
- RAMALDES, G. A., DEVERRE, J. R., GROGNET, J. M., PUISIEUX, F. & FATTAL, E. 1996. Use of an enzyme immunoassay for the evaluation of entrapment efficiency and in vitro stability in intestinal fluids of liposomal bovine serum albumin. *International Journal of Pharmaceutics*, 143, 1-11.

- RAMANA, L. N., SETHURAMAN, S., RANGA, U. & KRISHNAN, U. M. 2010. Development of a liposomal nanodelivery system for nevirapine. *Journal of Biomedical Science*, 17, 57-57.
- REJMAN, J., OBERLE, V., ZUHORN, I. S. & HOEKSTRA, D. 2004. Size-dependent internalization of particles via the pathways of clathrin-and caveolae-mediated endocytosis. *Biochemical Journal*, 377, 159-169.
- RIAHI, R., TAMAYOL, A., SHAEGH, S. A. M., GHAEMMAGHAMI, A. M., DOKMECI, M. R. & KHADEMHOSEINI, A. 2015. Microfluidics for advanced drug delivery systems. *Current Opinion in Chemical Engineering*, 7, 101-112.
- RIVERA, E. 2003. Liposomal anthracyclines in metastatic breast cancer: clinical update. *The oncologist*, 8, 3-9.
- ROCES, C. B., KASTNER, E., STONE, P., LOWRY, D. & PERRIE, Y. 2016. Rapid Quantification and Validation of Lipid Concentrations within Liposomes. *Pharmaceutics*, 8, 29.
- RUYSSCHAERT, T., SONNEN, A. F., HAEFELE, T., MEIER, W., WINTERHALTER, M. & FOURNIER, D. 2005. Hybrid nanocapsules: interactions of ABA block copolymers with liposomes. *Journal of the American Chemical Society*, 127, 6242-6247.
- SACKMANN, E. K., FULTON, A. L. & BEEBE, D. J. 2014. The present and future role of microfluidics in biomedical research. *Nature*, 507, 181.
- SAH, H. 1999. Stabilization of proteins against methylene chloride/water interface-induced denaturation and aggregation. *Journal of Controlled Release*, 58, 143-151.
- SALMASO, S., BERSANI, S., SEMENZATO, A. & CALICETI, P. 2006. Nanotechnologies in protein delivery. *Journal of nanoscience and nanotechnology*, 6, 2736-2753.
- SAMUNI, A. M., LIPMAN, A. & BARENHOLZ, Y. 2000. Damage to liposomal lipids: protection by antioxidants and cholesterol-mediated dehydration. *Chemistry and physics of lipids*, 105, 121-134.
- SARKAR, S., MOTWANI, V., SABHACHANDANI, P., COHEN, N. & KONRY, T. 2015. T cell dynamic activation and functional analysis in nanoliter droplet microarray. *Journal of clinical & cellular immunology*, 6.
- SAVJANI, K. T., GAJJAR, A. K. & SAVJANI, J. K. 2012. Drug solubility: importance and enhancement techniques. *ISRN pharmaceutics*, 2012, 195727-195727.
- SAWANT, R. R. & TORCHILIN, V. P. 2012. Multifunctional nanocarriers and intracellular drug delivery. *Current Opinion in Solid State and Materials Science*, 16, 269-275.
- SCHERPHOF, G. L., DIJKSTRA, J., SPANJER, H. H., DERKSEN, J. T. & ROERDINK, F. H. 1985. Uptake and Intracellular Processing of Targeted and Nontargeted Liposomes by Rat Kupffer Cells In Vivo and In Vitro. *Annals of the New York Academy of Sciences*, 446, 368-384.
- SCHILTZ, E., SCHNACKERZ, K. & GRACY, R. 1977. Comparison of ninhydrin, fluorescamine, and o-phthalaldehyde for the detection of amino acids and peptides and their effects on the recovery and composition of peptides from thin-layer fingerprints. *Analytical biochemistry*, 79, 33-41.
- SEMPLE, S. C., CHONN, A. & CULLIS, P. R. 1996. Influence of cholesterol on the association of plasma proteins with liposomes. *Biochemistry*, 35, 2521-2525.
- SENIOR, J., DELGADO, C., FISHER, D., TILCOCK, C. & GREGORIADIS, G. 1991. Influence of surface hydrophilicity of liposomes on their interaction with plasma protein and clearance from the circulation: studies with poly (ethylene glycol)-coated vesicles. *Biochimica et Biophysica Acta (BBA)-Biomembranes*, 1062, 77-82.
- SENIOR, J. & GREGORIADIS, G. 1982. Is half-life of circulating liposomes determined by changes in their permeability? *FEBS letters*, 145, 109-114.

- SERCOMBE, L., VEERATI, T., MOHEIMANI, F., WU, S. Y., SOOD, A. K. & HUA, S. 2015. Advances and challenges of liposome assisted drug delivery. *Frontiers in pharmacology*, 6, 286.
- SHIMADA, K., MATSUO, S., SADZUKA, Y., MIYAGISHIMA, A., NOZAWA, Y., HIROTA, S. & SONOBE, T. 2000. Determination of incorporated amounts of poly(ethylene glycol)-derivatized lipids in liposomes for the physicochemical characterization of stealth liposomes. *International Journal of Pharmaceutics*, 203, 255-263.
- SHUKLA, S., KANWAL, R., SHANKAR, E., DATT, M., CHANCE, M. R., FU, P., MACLENNAN, G. T. & GUPTA, S. 2015. Apigenin blocks IKK $\alpha$  activation and suppresses prostate cancer progression. *Oncotarget*, 6, 31216.
- SIMÕES, S., SLEPUSHKIN, V., DÜZGÜNES, N. & DE LIMA, M. C. P. 2001. On the mechanisms of internalization and intracellular delivery mediated by pH-sensitive liposomes. *Biochimica et Biophysica Acta (BBA)-Biomembranes*, 1515, 23-37.
- SKALKO-BASNET, N., PAVELIC, Z. & BECIREVIC-LACAN, M. 2000. Liposomes containing drug and cyclodextrin prepared by the one-step spray-drying method. *Drug development and industrial pharmacy*, 26, 1279-1284.
- SLADE, L., LEVINE, H. & REID, D. S. 1991. Beyond water activity: recent advances based on an alternative approach to the assessment of food quality and safety. *Critical Reviews in Food Science & Nutrition*, 30, 115-360.
- SLAMON, D. J., LEYLAND-JONES, B., SHAK, S., FUCHS, H., PATON, V., BAJAMONDE, A., FLEMING, T., EIERMANN, W., WOLTER, J. & PEGRAM, M. 2001. Use of chemotherapy plus a monoclonal antibody against HER2 for metastatic breast cancer that overexpresses HER2. *New England Journal of Medicine*, 344, 783-792.
- SOKOL, R., HUDSON, G., JAMES, N., FROST, I. & WALES, J. 1987. Human macrophage development: a morphometric study. *Journal of anatomy*, 151, 27.
- STEIN, P. E., LESLIE, A. G., FINCH, J. T. & CARRELL, R. W. 1991. Crystal structure of uncleaved ovalbumin at 1.95 Å resolution. *Journal of molecular biology*, 221, 941-959.
- STEIN, P. E., LESLIE, A. G., FINCH, J. T., TURNELL, W. G., MCLAUGHLIN, P. J. & CARRELL, R. W. 1990. Crystal structure of ovalbumin as a model for the reactive centre of serpins. *Nature*, 347, 99.
- STROOCK, A. D., DERTINGER, S. K. W., AJDARI, A., MEZIĆ, I., STONE, H. A. & WHITESIDES, G. M. 2002. Chaotic Mixer for Microchannels. *Science*, 295, 647-651.
- STUART, M. C. & BOEKEMA, E. J. 2007. Two distinct mechanisms of vesicle-to-micelle and micelle-to-vesicle transition are mediated by the packing parameter of phospholipid-detergent systems. *Biochimica et Biophysica Acta (BBA)-Biomembranes*, 1768, 2681-2689.
- SWEENEY, L. G., WANG, Z., LOEBENBERG, R., WONG, J. P., LANGE, C. F. & FINLAY, W. H. 2005. Spray-freeze-dried liposomal ciprofloxacin powder for inhaled aerosol drug delivery. *International journal of pharmaceutics*, 305, 180-185.
- SZOKA, F. & PAPAHDJOPOULOS, D. 1978. Procedure for preparation of liposomes with large internal aqueous space and high capture by reverse-phase evaporation. *Proceedings of the national academy of sciences*, 75, 4194-4198.
- SZOKA JR, F. & PAPAHDJOPOULOS, D. 1980. Comparative properties and methods of preparation of lipid vesicles (liposomes). *Annual review of biophysics and bioengineering*, 9, 467-508.
- TAKAHASHI, N. & HIROSE, M. 1992. Reversible denaturation of disulfide-reduced ovalbumin and its reoxidation generating the native cystine cross-link. *Journal of Biological Chemistry*, 267, 11565-11572.

- TAKANO, S., ARAMAKI, Y. & TSUCHIYA, S. 2003. Physicochemical properties of liposomes affecting apoptosis induced by cationic liposomes in macrophages. *Pharmaceutical research*, 20, 962-968.
- TANAKA, Y., TANEICHI, M., KASAI, M., KAKIUCHI, T. & UCHIDA, T. 2010. Liposome-Coupled Antigens Are Internalized by Antigen-Presenting Cells via Pinocytosis and Cross-Presented to CD8+ T Cells. *PLOS ONE*, 5, e15225.
- TANFORD, C. 1968. Protein denaturation. *Advances in protein chemistry*, 23, 121-282.
- TANG, X., NAIL, S. & PIKAL, M. 1999. Mass transfer in freeze drying: measurement of dry layer resistance by a non-steady state method (the MTM procedure). *AAPS PharmSci (supplement)*.
- TANG, X. C. & PIKAL, M. J. 2004. Design of freeze-drying processes for pharmaceuticals: practical advice. *Pharmaceutical research*, 21, 191-200.
- TOH, M.-R. & CHIU, G. N. C. 2013. Liposomes as sterile preparations and limitations of sterilisation techniques in liposomal manufacturing. *Asian Journal of Pharmaceutical Sciences*, 8, 88-95.
- TOMKINSON, B., BENDELE, R., GILES, F. J., BROWN, E., GRAY, A., HART, K., LERAY, J. D., MEYER, D., PELANNE, M. & EMERSON, D. L. 2003. OSI-211, a novel liposomal topoisomerase I inhibitor, is active in SCID mouse models of human AML and ALL. *Leukemia research*, 27, 1039-1050.
- TORCHILIN, V. P. 2005. Recent advances with liposomes as pharmaceutical carriers. *Nature reviews Drug discovery*, 4, 145.
- TORCHILIN, V. P. & LUKYANOV, A. N. 2003. Peptide and protein drug delivery to and into tumors: challenges and solutions. *Drug Discovery Today*, 8, 259-266.
- TORO, C., SANCHEZ, S., ZANOCCO, A., LEMP, E., GRATTON, E. & GUNTHER, G. 2009. Solubilization of lipid bilayers by myristyl sucrose ester: effect of cholesterol and phospholipid head group size. *Chemistry and physics of lipids*, 157, 104-112.
- TWOMEY, P. & KROLL, M. 2008. How to use linear regression and correlation in quantitative method comparison studies. *International journal of clinical practice*, 62, 529-538.
- UMRETHIA, M., KETT, V. L., ANDREWS, G. P., MALCOLM, R. K. & WOOLFSON, A. D. 2010. Selection of an analytical method for evaluating bovine serum albumin concentrations in pharmaceutical polymeric formulations. *Journal of pharmaceutical and biomedical analysis*, 51, 1175-1179.
- USMANI, S. S., BEDI, G., SAMUEL, J. S., SINGH, S., KALRA, S., KUMAR, P., AHUJA, A. A., SHARMA, M., GAUTAM, A. & RAGHAVA, G. P. S. 2017. THPdb: Database of FDA-approved peptide and protein therapeutics. *PLOS ONE*, 12, e0181748.
- USONIS, V., BAKASENAS, V., VALENTELIS, R., KATILIENE, G., VIDZENIENE, D. & HERZOG, C. 2003. Antibody titres after primary and booster vaccination of infants and young children with a virosomal hepatitis A vaccine (Epaxal®). *Vaccine*, 21, 4588-4592.
- VAN WINDEN, E. & CROMMELIN, D. 1997. Long term stability of freeze-dried, lyoprotected doxorubicin liposomes. *European journal of pharmaceuticals and biopharmaceutics*, 43, 295-307.
- VAN WINDEN, E. C., ZHANG, W. & CROMMELIN, D. J. 1997. Effect of freezing rate on the stability of liposomes during freeze-drying and rehydration. *Pharmaceutical research*, 14, 1151-1160.
- VERONESE, F. M. & MERO, A. 2008. The impact of PEGylation on biological therapies. *BioDrugs*, 22, 315-329.
- VERT, M. & DOMURADO, D. 2000. Poly (ethylene glycol): Protein-repulsive or albumin-compatible? *Journal of Biomaterials Science, Polymer Edition*, 11, 1307-1317.

- VERVOORT, N., DAEMEN, D. & TÖRÖK, G. 2008. Performance evaluation of evaporative light scattering detection and charged aerosol detection in reversed phase liquid chromatography. *Journal of Chromatography A*, 1189, 92-100.
- VILA-CABALLER, M., CODOLO, G., MUNARI, F., MALFANTI, A., FASSAN, M., RUGGE, M., BALASSO, A., DE BERNARD, M. & SALMASO, S. 2016. A pH-sensitive stearyl-PEG-poly(methacryloyl sulfadimethoxine)-decorated liposome system for protein delivery: An application for bladder cancer treatment. *Journal of Controlled Release*, 238, 31-42.
- WAGNER, A., VORAUER-UHL, K. & KATINGER, H. 2002. Liposomes produced in a pilot scale: production, purification and efficiency aspects. *European Journal of Pharmaceutics and Biopharmaceutics*, 54, 213-219.
- WALSH, T. J., YELDANDI, V., MCEVOY, M., GONZALEZ, C., CHANOCK, S., FREIFELD, A., SEIBEL, N. I., WHITCOMB, P. O., JAROSINSKI, P. & BOSWELL, G. 1998. Safety, tolerance, and pharmacokinetics of a small unilamellar liposomal formulation of amphotericin B (AmBisome) in neutropenic patients. *Antimicrobial agents and chemotherapy*, 42, 2391-2398.
- WERNINGHAUS, K., BABIAK, A., GROß, O., HÖLSCHER, C., DIETRICH, H., AGGER, E. M., MAGES, J., MOCSAI, A., SCHOENEN, H. & FINGER, K. 2009. Adjuvanticity of a synthetic cord factor analogue for subunit Mycobacterium tuberculosis vaccination requires FcR $\gamma$ -Syk-Card9-dependent innate immune activation. *The Journal of experimental medicine*, 206, 89-97.
- WHITESIDES, G. M. 2006. The origins and the future of microfluidics. *Nature*, 442, 368-373.
- WHITESIDES, G. M., OSTUNI, E., TAKAYAMA, S., JIANG, X. & INGBER, D. E. 2001. Soft lithography in biology and biochemistry. *Annual review of biomedical engineering*, 3, 335-373.
- WILKHU, J., MCNEIL, S. E., KIRBY, D. J. & PERRIE, Y. 2011. Formulation design considerations for oral vaccines. *Therapeutic delivery*, 2, 1141-1164.
- WITSCHI, C. & DOELKER, E. 1997. Residual solvents in pharmaceutical products: acceptable limits, influences on physicochemical properties, analytical methods and documented values. *European Journal of Pharmaceutics and Biopharmaceutics*, 43, 215-242.
- WOLFE, J. & BRYANT, G. 1992. Physical principles of membrane damage due to dehydration and freezing. *Mechanics of Swelling*. Springer.
- WORSHAM, R. D., THOMAS, V. & FARID, S. S. 2018. Potential of Continuous Manufacturing for Liposomal Drug Products. *Biotechnology Journal*.
- XIE, Q.-W. & CALAYCAY, J. 1992. Cloning and characterization of inducible nitric oxide synthase from mouse macrophages. *Science*, 256, 225.
- XU, X., COSTA, A. & BURGESS, D. J. 2012. Protein Encapsulation in Unilamellar Liposomes: High Encapsulation Efficiency and A Novel Technique to Assess Lipid-Protein Interaction. *Pharmaceutical Research*, 29, 1919-1931.
- YAMASAKI, M., TAKAHASHI, N. & HIROSE, M. 2003. Crystal structure of S-ovalbumin as a non-loop-inserted thermostabilized serpin form. *Journal of Biological Chemistry*, 278, 35524-35530.
- YAN, W. & HUANG, L. 2009. The effects of salt on the physicochemical properties and immunogenicity of protein based vaccine formulated in cationic liposome. *International journal of pharmaceutics*, 368, 56-62.
- YAP, T. A. & WORKMAN, P. 2012. Exploiting the cancer genome: strategies for the discovery and clinical development of targeted molecular therapeutics. *Annual review of pharmacology and toxicology*, 52, 549-573.

- ZHANG, J. A., ANYARAMBHATLA, G., MA, L., UGWU, S., XUAN, T., SARDONE, T. & AHMAD, I. 2005. Development and characterization of a novel Cremophor® EL free liposome-based paclitaxel (LEP-ETU) formulation. *European journal of pharmaceutics and biopharmaceutics*, 59, 177-187.
- ZHENG, Y., LAI, X., BRUUN, S. W., IPSEN, H., LARSEN, J. N., LØWENSTEIN, H., SØNDERGAARD, I. & JACOBSEN, S. 2008. Determination of moisture content of lyophilized allergen vaccines by NIR spectroscopy. *Journal of Pharmaceutical and Biomedical Analysis*, 46, 592-596.
- ZHIGALTSEV, I. V., BELLIVEAU, N., HAFEZ, I., LEUNG, A. K., HUFT, J., HANSEN, C. & CULLIS, P. R. 2012. Bottom-up design and synthesis of limit size lipid nanoparticle systems with aqueous and triglyceride cores using millisecond microfluidic mixing. *Langmuir*, 28, 3633-3640.
- ZHUANG, Y., MA, Y., WANG, C., HAI, L., YAN, C., ZHANG, Y., LIU, F. & CAI, L. 2012. PEGylated cationic liposomes robustly augment vaccine-induced immune responses: Role of lymphatic trafficking and biodistribution. *Journal of Controlled Release*, 159, 135-142.
- ZIZZARI, A., BIANCO, M., CARBONE, L., PERRONE, E., AMATO, F., MARUCCIO, G., RENDINA, F. & ARIMA, V. 2017. Continuous-Flow Production of Injectable Liposomes via a Microfluidic Approach. *Materials*, 10, 1411.
- ZOOK, J. M. & VREELAND, W. N. 2010. Effects of temperature, acyl chain length, and flow-rate ratio on liposome formation and size in a microfluidic hydrodynamic focusing device. *Soft Matter*, 6, 1352-1360.
- ZUHORN, I. S., ENGBERTS, J. B. & HOEKSTRA, D. 2007. Gene delivery by cationic lipid vectors: overcoming cellular barriers. *European Biophysics Journal*, 36, 349-362.
- ZUIDAM, N. J., GOUW, H. M. E., BARENHOLZ, Y. & CROMMELIN, D. J. 1995. Physical (in) stability of liposomes upon chemical hydrolysis: the role of lysophospholipids and fatty acids. *Biochimica et Biophysica Acta (BBA)-Biomembranes*, 1240, 101-110.

